ISSN 0971 - 6203

Journal of Medical Physics

Special Issue

Volume 42 | Supplement 1 | November 2017

Abstracts available at www.jmp.org.in

PubMed

AFOMP

Abstracts of AOCMP-AMPICON 2017
held at Jaipur, India during 4-7 November, 2017

Association of
Medical Physicists of India
An Affiliate of Indian National Science Academy
and
International Organization for Medical Physics
www.ampi.org.in

Medknow

Wolters Kluwer

Abstract Book

AOCMP AMPICON 2017

17th Asia-Oceania Congress of Medical Physics

&

38th Annual Conference of Association of Medical Physicists of India

AOCMP-AMPICON 2017

4th - 7th November 2017

Organised by

Department of Radiological Physics, SMS Medical College, Jaipur ,India

Under the auspices of

Asia - Oceania Federation of Organizations for Medical Physics (AFOMP)

&

Association of Medical Physicists of India (AMPI)

Print ISSN: 0971-6203, E-ISSN: 1998-3913

Journal of Medical Physics

(Incorporating AMPI Medical Physics Bulletin)

Association of Medical Physicists of India

(Regd. No. 421/1976 GBBSD, Public Trust F 4238)
(An affiliate of the Indian National Science Academy & The International Organization for Medical Physics)
C/o Radiological Physics & Advisory Division, BARC
CT & CRS Building, Anushaktinagar, Mumbai - 400094, ● Website: www.ampi.org.in

The Association of Medical Physicists of India (AMPI) is a professional but a non-profit making / non-governmental organization, devoted to serving the needs of the country in the field of Medical Physics. Its membership is open to science graduates, engineers and physicians interested in the application of physics to medical and biological sciences. Medical Radiation Physicists, Radiation Safety Officers, Radiological and Hospital Physicists, Radiation Oncologists and Radiologists form the main group of the association. It publishes this quarterly journal. The association is having about 1200 active members. The journal is provided to its members and also to the libraries of almost all leading Cancer Centres in the country on a very nominal subscription. Other than publishing Journal of Medical Physics, the association holds a national/ international conference every year to exchange information among its members. The association also supports advanced training of Medical Physicists by offering Travel Fellowships. For public awareness, publication of articles related to medical physics and radiation safety in newspapers and periodicals is encouraged. The association also works towards worldwide exchange of information on medical physics.

The College of Medical Physics of India (CMPI) is an autonomous wing of AMPI which was established to function as the certifying and accreditation body. Membership of AMPI is prerequisite to appear for CMPI certification examination. A member of AMPI can become member of CMPI only by passing the certification examination. CMPI certification indicates that the holder has acquired, demonstrated, and maintained a minimum standard of knowledge in medical physics and the competence to practice as clinical physicist in Diagnostic Radiology, Radiation Oncology and Nuclear Medicine.

Membership Fee Details
(w.e.f. February 07, 2015)

Annual Member	
Indian Resident	INR ₹ 1,280.00
Developing Countries	USD $ 50.00
Other Countries	USD $ 165.00
Life Member	
Indian Resident	INR ₹ 3,615.00
Developing Countries	USD $ 257.00
Other Countries	USD $ 970.00
Institution Member (India)	INR ₹ 4,780.00

Organizing and Endorsing Professional Bodies

AFOMP (Asia-Oceania Federation of Organizations for Medical Physics)

President	Dr. Tae-Suk Suh, S Korea
Vice President	Dr. Arun Chougule, India
Secretary General	Dr. Howell Round, New Zealand
Treasurer	Dr. Kwan-Hoong Ng, Malaysia

AMPI (Association of Medical Physicists of India)

President	Dr. Arun Chougule, Jaipur
Vice President	Mr. Balasubramanian Nagappan, Rohtak
Secretary	Dr. Vellaiyan Subramani, New Delhi
Treasurer	Dr. Varadharajan Ekambaram, Chennai

IOMP (International Organization for Medical Physics)

President	Dr.Slavik Tabakov, UK
Vice President	Dr. Madan Rehani, USA
Secretary General	Dr. Virginia Tsapaki, Greece
Treasurer	Dr. Anchali Krisanachinda, Thailand

Co-sponsoring: AAPM (American Association of Physicists in Medicine)

President	Dr. Melissa Carol Martin, USA
Chair of the Board	Dr. Bruce H Curran, USA
Secretary	Dr. Todd Pawlicki, USA
Treasurer	Dr. Mahadevappa Mahesh, USA

Endorsing: MEFOMP (Middle East Federation of Organizations of Medical Physics)

President	Dr Abdullah Al Hajj, KSA
Vice President	Dr Huda Al Naemi, Qatar
Secretary-General	Dr Laila Al Balooshi, UAE
Treasurer	Mr Rabih Hammoud, Lebanon

Scientific Committee:

Dr. Arun Chougule (Convenor), Scientific Committee AFOMP	
Dr. Lalit Aggarwal (Co-convenor), Varanasi	
Dr. Anatoly Rozenfeld, Australia	Dr. Monzen Hajime, Japan
Dr. Challapalli Srinivas, India	Dr. Pratik Kumar, India
Dr. D K Ray, India	Dr. R K Munjal, India
Dr. Dayanand Sharma, India	Dr. S D Sharma, India
Dr. Eva Bezak, Australia	Dr. Shinji Kawamura, Japan
Dr. Hasin Anupama Azhari, Bangladesh	Dr. Shobha Jayaprakash, India
Dr. Howell Round, New Zealand	Dr. Tomas Kron, Australia
Dr. Kinhikar Rajesh, India	Dr. V. Subramani, India
Dr. Koji Noda, Japan	Dr. G.A. Zakaria, Germany

Publication Committee:

Convenor: Dr. A.S. Pradhan, Mumbai	
Joint Convenor: Dr. S.D. Sharma, Mumbai	
Dr. Tae Suk Suh	South Korea
Dr. Howell Round	New Zealand
Dr. T. Ganesh	Delhi, India
Dr. Arun Chougule	Jaipur, India
Dr. Shigekazu Fukuda	Japan
Mrs. Philomina Akhilesh	Mumbai, India
Mr. Nitin Kakade	Mumbai, India
Mr. Gourav Kumar Jain	Jaipur, India

Journal of Medical Physics

Volume 42 - Supplement 1 - November 2017

Contents

Abstracts

17th Asia Oceania Congress of Medical Physics (AOCMP) and 38th Annual Conference of Association of Medical Physicists of India (AMPICON) 2017

4th -7th November, 2017

Jaipur, Rajasthan, India

Scientific Programme

Day 1: 4th November, 2017[Saturday]

Time	Programme		
08.00AM-09.00AM	Registration		
9.00AM-10.00AM	Inauguration of Conference		
10.00AM-10.30AM	High Tea and Inauguration of Trade Exhibitions		
	Hall A (Main Hall)	Hall B (JMA Hall)	Hall C (Bangur Basement CT/MRI Wing)
10.30AM-1.00PM	**Session I: Proton & Heavy ion Therapy** Chairpersons: Dr K Thayalan Dr Apurba Kabasi IS: Special talk- Particle therapy Prof Alejandro Mazal, France I-1: Production of carbon ions for heavy- ion radiotherapy Dr Atsushi Kitagawa, Japan I-2: Introduction to Proton therapy Prof Shigekazu Fukuda, Japan I-3: The present status of Boron Neutron Capture Therapy in Japan. Prof Yoshinori Sakurai, Japan O1-O4	**Session II: Modern Imaging (Courtesy: Siemens Healthineers)** Chairpersons: Dr Hafiz M Zin Dr Pratik Kumar I-4: Beginning of Computer-aided Diagnosis in Medical Imaging Prof Kunio Doi, USA I-5: Journey of Radiology in last over 120 years Dr Sunita Purohit, India I-6: What if Radiology was an art? Dr Robin Decoster, Belgium O5-O9	**Session III: Symposium 1/ IOMP School (60min)** MST-1: Practical application of Moodle for e-learning courses in Medical Physics Dr Vassilka Tabakova, UK **Session IV:** Symposium 2/ IOMP School (60min) Leadership and Entrepreneurship MST-2: Preparing Medical Physicists for future leadership roles Prof Carmel J. Caruana, Malta MST-3: Leadership and Entrepreneurship: A Medical Physicist's Perspective Dr A K Rath, India
01.00PM-02.00PM	Lunch		
02.00PM-04.00PM	**Session V: Medical Physics Education** Chairpersons: Dr R. Ravichandran Dr CS Sureka I-07: Codes of Conduct and Codes of Ethics in Medical Physics Dr Howell Round, NZ I-08: Resources to run an RT Department – Staffing and Materials. Prof Yakov Pipman, USA I-09: From IOMP to IMPCB - How a Decades Old Wish became Reality Prof Raymond Wu, USA I-10: Education trends after the official recognition of medical physics occupation in ISCO08 Prof Slavik Tabakov, UK	**Session VI: Symposium 3 (60min)** MST-4: The Evolving Posture Of Medical Physics As A Profession: Medical Physics 3.0 Dr Melissa Martin, USA **Session VII: Symposium 4/ IOMP School (60min)** MST-5: Future of Medical Physics and interaction with other science Prof Kiyonari Inamura, Japan	**Session VIII: Symposium 5 (120min)** Affordable therapy technologies MST-6: The need for affordable technologies based on CMC, Vellore Experience Prof Paul Ravindran, India MST-7: Project Introduction and a Compensator based IMRT for cobalt and Linac Prof Govinda Rajan, India MST-8: Principles of design for affordable technologies Prof Eric Ford, USA MST-9: Cobalt treatments are still relevant in a LINACs world A MR guided Co 60 machine perspective. Dr Lakshmi Santanam, USA MST-10: Programmatic Support for the develop of Indigenous technologies in cancer Dr D N Badodkar, India
4.00PM-4.15PM	Tea Break		

4.15PM-5.15PM	**Session IX: Advanced Medical Research** Chairpersons: Prof U Selvaraj Dr Raju Srivastava I-11: Processing of Medical Image Using Lattice Boltzmann Method Case Study – Cerebral aneurysm segmentation Dr D Datta, India I-12: Recent developments on Magnetic nano particle and their application in magnetic hyperthermia for cancer therapy and drug delivery. Dr Ambesh Dixit, India	**Session X: Monte Carlo & Special Algorithms** Chairpersons: Dr Raghuram Nair Dr Ramesh Desai I-13: Implementing EGSnrc Monte Carlo in a clinical setup and its potential applications Prof Paul Ravindran, India O10-O12	**Session XI: Symposium 6/ IOMP School (60min)** Latest CT Technologies in Japan MST-11: Latest performance evaluation of X-ray CT Dr Katsumi Tsujioka, Japan MST-12: Latest CT scanning technologies in Japan Dr Koichi Sugisawa, Japan
5.15PM-6.00PM	Dr Ramaiah Naidu Memorial Oration- Dr. PGG Kurup, India Chairpersons : Prof. Arun Chougule, President AMPI Dr. V. Subramani, Secretary AMPI		
6.00PM-7.00PM	Felicitation Programme		
7.00PM onwards	Cultural Programme		
9.00PM onwards	Dinner		

Day 2: 5th November 2017 [Sunday]

Time	Programme			
08.00AM-09.00AM	**Session XII: CMPI Teaching Programme** Chairpersons: Dr Suresh Pamidighantam, Dr KJ Maria Das TS-1: Technology of Advanced Radiotherapy equipment including Ion beam therapy equipment Dr SD Sharma, India TS-2: IGRT: Determining setup margins and correction methods Dr T Ganesh, India			
	Hall A(Main Hall)	Hall B(JMA Hall)	Hall C(Bangur Basement CT/MRI Wing)	Hall D(Radiological Physics Department upstairs)
9.00AM-10.30AM	**Session XIII : Electron Beam** Therapy & Special Procedures Chairpersons: Dr D.K. Ray Dr Satish Pelagade I-14: Clinical Electron Bram Dosimetry: Transition from AAPM TG-25 to AAPM TG-70. Dr Dimitris Mihailidis, USA I-15: New Approach to Managing Radiotherapy Patients with Cardiac Implanted Devices (CIEDs): Modern Technology RT and CIEDs. Dr Bipin Agarwal, USA I-16: Motion Management in Radiation Therapy Dr Lakshmi Santanam, USA	**Session XIV: High-tech** Radiotherapy: Challenges in the perspective of Radiation Oncologist, Medical Physicists and Radiotherapy technologists Chairpersons: Dr GV Giri Dr Ramakrishna Rao Dr Neeraj Jain I-17: Radiation Oncologist's perspective. Dr Nidhi Patni, India I-18: Medical Physicist's perspective Dr K. Krishna Murthy, India I-19: Radiation Technolgist's perspective Rakesh Kaul, India I-20: MR Guided Adaptive RT Prof Bhudatt Paliwal, USA	**Session XV: Symposium 7 / IOMP School (90min)** Radiation incidents and accidents in medicine MST-13: Incidents and accidents in CT and interventional Radiology Dr S D Sharma, India MST-14: Incidents and accidents in Nuclear Medicine. Dr Pankaj Tandon, India MST-15: Incidents and accidents in Radiotherapy Dr G A Zakaria, Germany	**Session XVI: Nuclear Medicine & Radiobiology** Chairpersons: Dr Kaliyappan P. Dr Aruna Kaushik I-21:Mitigation of consequential effects of Misadministration in Nuclear Medicine Prof A K Shukla, India O13-O17
10.30AM-11.00AM	Tea Break and Poster Presentations			

11.00AM-2.00PM	**Session XVII: Plenary Talk** I-22: Preparedness for Response to Radiological Emergencies Dr KS Pradeepkumar, India **Session XVIII: Brachytherapy** Chairpersons: Dr Kamlesh Passi, Dr Arumugham Balraj I-23:Advances in Brachytherapy Dr D D Deshpande, India O18-O28	**Session XIX: Modern RT techniques & Planning-I** Chairpersons: Poopati V Saji Oommen I-24: Image guided application in Medical Physics Prof. Tae Suk Suh, S Korea I-25: Do we need audit of Radiation Oncology facilities - internal or external or both? RK Munjal, India I-26:Management of CT image for obese patients in Radiotherapy treatment planning procedure SN Sinha, India O29-O32 **Session XX : Panel Discussion (60min)** Topic: Selection of Particle Therapy Technology: Should be based on capital costs or clinical needs. Moderator: Prof Alejando Mazal Panelists: PD1: Particle Therapy: Clinical Needs and Efficacy Dr DN Sharma, India PD2: Multi-Room Proton Therapy Technology Dr.Rajesh A. Kinhikar, India PD3: Compact Single Room Proton Therapy Facility Dr V Subramani, India PD4: Carbon Ion Therapy Technology Dr Atsushi Kitagawa, Japan	**Session XXI: Symposium 8 (60min)** New Developments in Photon Brachytherapy MST-16:Dosimetric Challenges of Photon Brachytherapy in Terms of Absorbed Dose to Water Prof G A Zakaria, Germany MST-17:New Developments in Image based Gynaecological Brachytherapy- Dr Hasin A Azhari, Bangladesh **Session XXII: Symposium 9 (120Min)** Radionuclide Imaging MST-18:Hybrid Imaging: Applications of PET-MRI in- Neurodegenerative Disorders- Dr Nand K Relan, USA MST-19:Importance of Quality Control in Nuclear Medicine Dr Subhash Kheruka, India MST-20: Optimization of Radiation Safety and Exposures in Nuclear Medicine Dr Pankaj Tandon, India MST-21:Role of Molecular Imaging in Oncology with special reference to radiation oncology Dr J K Bhagat, India	**Session XXIII : Dosimetry & QA** Chairpersons: Dr G Ramanathan Dr G Sahni I-27: In-vivo Dosimetry in Radiotherapy Prof M Ravikumar, India O39-O51
02.00PM-02.30PM	Lunch and Poster Presentations			
02.30PM-04.20PM	**Session XXIV: Materials and equipment for Research in Medical Physics** Chairpersons: Dr DS Dhote Dr Daxa Patel I-28: Advances in Medical Physics and Phantom development: A parallel Path. A review from historical to Computational phantoms Prof Franco Milano, Italy I-29: Revolutionary Role of Nanotechnology in Health Care Prof S H Pawar, India O52-O57	**Session XXV: Modern RT techniques & Planning-II** O33-O38 **Session XXVI : Symposium 10 (50min)** MST-22: Physics of Medical Isotope Production Prof R Chary, Canada	**Session XXVII: Symposium 11 (50min)** Radiobiophotonics & Normal Tissue Protection-A Firewall MST-23: Dr Rao V. L. Papineni, USA Dr Shahid Umar, USA	**Session XXVIII: Small Field** Dosimetry & Med Physics Educational Chairpersons: Dr Saraswati Chitra Dr Dayananda S O58-O68
04.20PM-04.30PM	Tea break and poster presentations			

04.30PM-6.00PM	**Session XXIX:** **AMPI best paper award session** Chairpersons: Mr Balasubramanian Dr E Vardharajan (BP1-BP9)	**Session XXX: Symposium 12 (60min)** Challenges of Advanced Quality Assurance in Radiotherapy: Treatment Planning and Delivery System MST-24: Moving from gamma passing rates to patient DVH-based online plan verification Dr Andreas Block, Germany MST-25: Monte Carlo methods as advanced quality assurance for special treatment situations Dr Wolfgang Baus, Germany	**Session XXXI: Symposium 13/ IOMP School (90Min)** Current status of the breast cancer and importance of the mammographic screening and quality control of the mammography MST-26: Overview of the breast cancer and mammographic status in Asia and in Japan. Dr Tokiko Endo, Japan MST-27: The guideline of quality control for Screening mammography in Japan. Dr Hiroko Nishide, Japan MST-28: Vision for mammography in the digital era. Prof Yoshie Kodera, Japan	
7.00PM onwards	Banquet and Cultural Programme by AFOMP countries			

Day 3: 6th November 2017 [Monday]

Time	**Programme**	
08.00AM-09.00AM	**Session XXXII :CMPI Teaching Session** Chairpersons: VK Sathiyanarayan, Dr V K Dangwal TS-3: Portal Dosimetry : Dr Raghavendra Holla, India TS-4: ICRU-89-Recent ICRU recommendation for Cervix Brachytherapy: Dr Jamema Swamidas, India	
	Hall A(Main Hall)	Hall B(JMA Hall)
9.00AM-10.30AM	**Session XXXIII : Radiobiology** Chairpersons: Dr Bharanidharan Ganesan, Dr K R Muralidhar I-30: Grid radiotherapy and its abs copal Effect: Radiation induced immunogenic response with immunotherapy Dr TS Kehwar, USA I-31: Results of the latest WHO BSS Workshop Dr Magdalena Stoeva, Bulgaria **Session XXXIV: Symposium 14 (40min)** MST-29: New Aspects of Medical Physics in Radiation Oncology and Imaging Prof G A Zakaria, Germany MST-30: Stereotactical treatment of liver tumours. Dr Wolfgang Baus Germany	**Session XXXV: Medical Physics Research & Biomedical Engg.-I** Chairpersons: Dr Brindha Subramanian , Dr. Kanchan Adhikari, Nepal I-32: Data Mining for Radiomics Prof Hidetaka Arimura, Japan I-33: FDG PET/CT simulation for radiotherapy planning Dr Kohei Hanaoka, Japan I-34: 4D in-silico stochastic spatio temporal model of tumor growth with angiogenesis Dr Eva Bezak, Australia O69
10.30AM-11.00AM	Tea Break	

11.00AM-01.30PM	**Session XXXVI: Trade Session** Chairpersons: Dr TS Elias, T1: Uncertainties in CTDI measurements on Axial Scans Mr Erik Wikstrom, Bergen India T2: Trade talk by Panacea expert T3:Trade talk by Siemens expert T1-T7	**Session XXXVII: Medical Physics Research & Biomedical Engg.-II** Chairpersons: Prof S Sowmya Narayan, Dr Sudesh Deshpande I-35: Development of video based mechanical quality assurance system for medical linear accelerator Dr Youngyih Han, S Korea I-36: Medical applications of 3D printing Dr Ramani Ramaseshan, Canada I-37: LA technology improves patients care-on 6 high theory Dr Yimin Hu, Republic of China
01.30PM-02.00PM	Lunch	
02.00PM-04.00PM	**Session XXXVIII: AOCMP best paper Award Session** Chairpersons: Dr. Tae Suk Suh, Dr. Howell Round 12 PAPERS (AB1-AB12)	**Session XXXIX: Symposium 15/ IOMP School (120Min)** The mini-symposium on DRLs MST-31: Establishing and monitoring DRLs MPS Mann, India MST-32: The current situation of dose and DRLs for radiographic and fluoroscopic examinations Dr Satish Uniyal, India MST-33: Radiation dose and DRLs for CT scanners in India Dr Roshan Livingstone, India
4.00PM-4.15Min	Tea Break	
04.15PM-5.45PM	**Session XXXX: Symposium 16/ IOMP School (90Min)** MDCT: Physics and Dosimetry MST-34: Physics and basic technology of CT Dr Mahesh Mahadevappa, USA MST-35: CT dosimetry Dr Ajai Srivastava, India MST-36: Techniques for dose optimization in CT Dr Roshan Livingstone, India	**Session XXXXI: Symposium 17 (90Min)** Medical Physics Training and Education Collaboration among both Regional Organizations MST-37: Advances of Radiation Therapy Treatment in MEFOMP Countries Dr Rabih Hammoud, Qatar MST-38: The Perspective in Development of Medical Physics in AFOMP Region Dr Tae Suk Suh, S Korea MST-39: Medical Physics Education and Training in MEFOMP Countries: Dr Ibrahim Duhaini, Lebanon MST-40: Radiation Safety and Regulatory Authorities in MEFOMP: Dr Laila Al Balooshi, UAE MST-41: A Brief History of Medical Physics in Asia-Oceania: Dr.Howell Round, NZ MST-42: The Status of Education and Training of Medical Physicists in the AFOMP Region Dr Kwan Hoong Ng, Malaysia
5.45PM onwards	AMPI GBM	Session XXXXII : Medical Physics Quiz
8.00PM onwards	Dinner	

Day 4: November 7th, 2017 (Tuesday, IDMP celebration Day)

Time	Programme	
	Hall A (Main Hall)	
09.00AM-09.30AM	IDMP INAUGURATION	
9.30AM-10.40AM	**SESSION 1: MEDICAL PHYSICS EDUCATION** Chairpersons: Dr J Velmurugan, Dr Muthuvel K	
9.30AM-10.00AM	History of Medical Physics – a new IOMP project	Dr. Slavik Tabakov, UK
10.00AM-10.20AM	Medical Physics Education & Profession perspective in AFOMP Region	Dr. Tae Suk Suh, S. Korea
10.20AM-10.40AM	Medical Physics perspective :INDIAN SCENARIO	Dr. S D Sharma, India
10.40AM-11.15AM	FLAGGING OFF OF IDMP RALLY AND HIGH TEA	
11.15AM-01.30PM	**SESSION 2: FEMALE MEDICAL PHYSICIST: GLOBAL& REGIONAL PERSPECTIVE** Chairpersons: Mrs Deboleena Mukherjee	
11.15AM-11.30AM	Pioneer Women Medical Physicists from MEFOMP Countries	Dr. Huda Al Naemi, Qatar
11.30AM-11.45AM	Medical Physicists Certification Process and Examination in the Middle East	Dr. Ibrahim Duhaini, Lebanon
11.45AM-11.55AM	Medical Physics World (MPW)	Dr. Magdalena Stoeva, Bulgaria
12.00PM-1.30PM	**SESSION 3: IOMP- IDMP PROGRAMME [LIVE TELECAST]**	
12.00PM-12.05PM	Introductory talk on IDMP	Dr. Slavik Tabakov, UK & Dr. John Damilakis, Greece
12.05PM-12.20PM	Medical Physics contributions to women's health and Radiation Safety	Dr. H. Anupama Azhari, Bagladesh
12.20PM-12.35PM	IOMP Women survey data	Dr. Virginia Tsapaki, Greece
12.35PM-12.50PM	MP Education, Profession and as a Career for women in Bangladesh: Problems and Perspective	Ms. Kazi Towmim Afrin, Bangladesh
12.50PM-1.05PM	Women Medical Physicists. Current status in India	Dr. Shobha Jayaprakash, India
01.05PM-01.20PM	Women and men in the Australasian college of physical scientists and engineers in medicine : Workforce survey	Dr. Eva Bezak, Australia
01.20PM-1.30PM	DISCUSSION	
01.30PM-02.30PM	Lunch	
02.30PM-04.00PM	**SESSION 4: RADIATION PROTECTION AND IMAGING OF WOMEN PATIENTS** Chairpersons: Dr Sushama P, Dr KM Ganesh	
2.30PM-3.00PM	Radiation safety aspects pertaining to female patients and staff	Dr. Nidhi Patni, India
3.00PM-3.30PM	Dose management of pregnant patients in Radiology	Dr. John Damilakis, Greece
3.30PM-4.00PM	Segmentation of Breast Masses using active contour modelling	Dr. William Rae, South Africa
04.00PM-05.00PM	VALEDICTORY FUNCTION AND AWARD DISTRIBUTION	
05.00PM-05.30PM	DUSK RELISH	

Invited Talks

I-1

PRODUCTION OF CARBON IONS FOR HEAVY-ION RADIOTHERAPY

Atsushi Kitagawa
National Institute of Radiological Sciences, National Institutes for Quantum and Radiological Science and Technology, Chiba, Japan. E-mail: a_kitagawa@nifty.com

Introduction: In order to treat a deep-seated tumor with the good localized dose distributions, carbon ion was predicted as a good candidate for heavy-ion radiotherapy by Rovert R. Willson in 1946. Based on physics, lighter ion species cause larger multiple scattering in the deep side, and heavier ion species give unexpected dose over the end-point due to the projectile fragmentation. In addition, the biological dose distribution depends on the depth and thickness of a tumor. In the case of ten and several cm depth and several cm thickness, the linear energy transfer of neon ions is too high than that of carbon ions shown by Lawrence Berkeley Laboratory, University of California in 1980's. Although heavier ions shows other biological advantages like oxygen enhancement ratio, the National Institute of Radiological Sciences (NIRS) chose carbon ions for the clinical trial at the Heavy-Ion Medical Accelerator in Chiba (HIMAC) in 1994. By HIMAC's success, the existing and almost all the planned heavy-ion radiotherapy facilities require a carbon beam.
Objectives: The requirement of carbon-beam intensity strongly depends on the facility design, i.e. the volume and shape of the target, the efficiency of the irradiation method, the transmission of the accelerator complex and so on. In order to obtain the biological dose rate of 5 GyE/min. (roughly equal to a physical dose of 2 Gy/min.), a few 10^8 particles per second are required at a typical present facility. The long-term stability and reproducibility are important for daily treatment. On the other hand, the short-term stability of the ion sources is not so sensitive. Because the existing facilities consist of a synchrotron and any injector and the fine structure of the beam pulse will almost disappear during the acceleration in the synchrotron. Moreover easy operation and maintenance are also important to reduce the operation cost. An ion source should satisfy these requirements.
Materials and Methods: An electron cyclotron resonance ion source (ECR) has been developed at HIMAC. An ECR ion source is a type of electron bombardment ion sources. The minimum B structure of magnetic field for the plasma confinement consists of a pair of mirror magnets and radial multipole magnet. The microwave is fed to maintain the plasma by ECR heating. The carbon ions are produced from a gaseous compound like CH_4 or CO_2. Since the ECR ion source has no consumptive or deteriorate parts, it is expected from view points of long lifetime, easy operation and maintenance. At present, ECR ion sources have been adopted at all existing facilities.
Results and Discussion: The existed ECR ion sources have been successfully operated in heavy-ion radiotherapy facilities. On the other hand, it seems that a present typical facility is still too large for a hospital. The size of facility is roughly 3000 m^2 and its initial construction cost will be a hundred and several million US dollars. At present the ECR ion source mainly supplies C^{4+} ions. If it's able to increase the charge state, it can help to reduce the cost of injector. The research and development for the higher charge-state production have been continued. The drastic innovation to change a present typical accelerator structure has been considered too. QST has started a new development project for the combination of a laser acceleration and superconducting magnets. A future ion source will face new requirements and technical problems.

I-2

INTRODUCTION TO PROTON THERAPY

Shigekazu Fukuda
Radiation Quality Control Section, National Institute of Radiological Sciences, National Institutes for Quantum and Radiological Science and Technology, Chiba, Japan. E-mail: fukuda.shigekazu@qst.go.jp

The aim of this lecture is to provide some introductory knowledge and the most recent status of proton therapy including leading-edge medical physics technology and facilities to medical physicists who are familiar with the radiation therapy using X-rays, electrons, but unfamiliar with proton therapy.
After tracing the history of the charged particle therapy including proton and other ions beam therapy briefly, we will concentrate on the way to make irradiation fields to realize the rationale of the radiotherapy, that is, the delivery of high dose of energy to the tumors while sparing normal tissue around it. High energy proton beams have good property, which is termed, Bragg curve and Bragg peak, to realize the rationale easily compared to X-rays. What makes the Bragg peak will be explained. In addition, we discuss issues related to interactions between charged particle beams and tissues such as linear energy transfer (LET), relative biological effectiveness (RBE) and oxygen enhancement ratio (OER).
We also review some proton beam facilities and their components including ion sources, accelerators, irradiation system, planning system and positioning system and so on. Furthermore, we delineate a picture of the future of proton beam therapy.
Proton therapy is expected to be a promising method for offering the superior quality of life to patients. The number of proton therapy facilities has been increasing over the world. However, there are some issues to be solved such as clinical performance compared to other methods such as IMRT and IGRT, reduction of building and maintenance costs and human resources. There are coming some new technologies and ideas to solve these problems.

I-3

THE PRESENT STATUS OF BORON NEUTRON CAPTURE THERAPY IN JAPAN

Yoshinori Sakurai

Division of Radiation Medical Physics, Research Reactor Institute, Kyoto University, Kyoto, Japan. E-mail: yosakura@rri.kyoto-u.ac.jp

The world's first clinical irradiation for boron neutron capture therapy (BNCT) was carried out using a neutron irradiation field for BNCT, installed at Brookhaven Graphite Research Reactor (BGRR) in USA in 1951. The first BNCT clinical irradiation in Japan was carried out at Hitachi Training Reactor (HTR) in 1968. Thereafter, BNCT clinical irradiation had been continuously performed at Musashi Institute of Technology research Reactor (MuITR), Kyoto University Reactor (KUR) and JAERI Research Reactor 2 (JRR-2) in Japan. In Kyoto University Research Reactor Institute (KURRI), BNCT clinical study using the Heavy Water Facility installed in KUR came to be regularly performed from February 1990. At first, BNCT in this institute was performed just for malignant brain tumor and melanoma. The application was extended for head and neck tumors in 2001, and for body tumors such as liver tumor, lung tumor, malignant pleural mesothelioma, etc. in 2005. It may be said that the development of current BNCT is supported by this wider application. There were the several interruption periods, but 510 clinical irradiations were carried out using KUR Heavy Water Facility as of August 2017. For the reactor-based BNCT, it is performed using only a few BNCT facilities at KURRI, National Tsing Hua University in Taiwan and so on, as of August 2017.

For accelerator-based neutron source for BNCT, the combination of Li-7 (p, n) Be-7 reaction and protons of nearly 2.5 MeV was the most reliable and the studies had been performed by some research groups in USA, UK, Russia, and so on, from the early 1980s. Spallation due to high-energy neutrons was expected for the larger neutron yield, and it had been studied by some research groups in Switzerland, and so on. In early 2009, the world's first accelerator-based system for BNCT clinical irradiation, "Cyclotron-Based Epi-thermal Neutron Source (C-BENS)" was completed at KURRI. For C-BENS, the combination of Be-9 (p, n) B-9 reaction and 30-MeV protons was selected. The clinical trial using C-BENS was started in 2012. At present, the development of the accelerator-based irradiation system for BNCT is energetically performed by various groups in the world. Especially in Japan, BNCT using various accelerator-based irradiation systems including C-BENS may be carried out at plural facilities in the near future.

Thus, it is the time when BNCT is shifting from a special particle therapy to a general therapy, now. In order to promote this shift, not only the development and improvement for the irradiation system but also the preparation and improvement in the physical engineering and medical physics, such as dosimetry system, etc., is important. The historical background for BNCT is introduced, and the present status of BNCT, especially in Japan, are reported focusing on the topics for physical engineering and medical physics.

I-4

BEGINNING OF COMPUTER-AIDED DIAGNOSIS IN MEDICAL IMAGING

Kunio Doi[1,2]

[1]Department of Radiology, The University of Chicago, Chicago, Illinois, USA, [2]Gunma Prefectural College of Health Sciences, Maebashi, Japan.
E-mail: k-doi@uchicago.edu

Computer-aided diagnosis (CAD) has become one of the major research subjects in medical physics and diagnostic radiology. Many different types of CAD schemes are being developed for detection and/or characterization of various lesions in medical imaging, including conventional projection radiography, computed tomography (CT), magnetic resonance imaging (MRI), and ultrasound imaging. Organs that are currently being subjected to research for CAD include the breast, chest, colon, brain, liver, kidney, and the vascular and skeletal systems. Commercial systems for detection of breast lesions on mammograms have been developed and have received FDA approval for clinical use. It has been reported that more than 10,000 commercial CAD systems have been used at many hospitals, clinics, and screening centers in the United States and in Europe for assisting radiologists in their task of detecting breast cancers. It has been reported also from prospective studies that CAD has provided a gain of approximately 10-20% in the early detection of breast cancers on mammograms.

CAD may be defined as a diagnosis made by a physician who takes into account the computer output as a "second opinion". The purpose of CAD is to improve the quality and productivity of physicians in their interpretation of radiologic images. The quality of their work can be improved in terms of the accuracy and consistency of their radiologic diagnoses. In addition, the productivity of radiologists is expected to be improved by a reduction in the time required for their image readings. The computer output is derived from quantitative analysis of radiologic images by use of various methods and techniques in computer vision, artificial intelligence, and artificial neural networks (ANNs), including machine learning and deep-learning convolution neural network. The computer output may indicate a number of important parameters, for example, the locations of potential lesions such as lung cancer and breast cancer, the likelihood of malignancy of detected lesions, and the likelihood of various diseases based on differential diagnosis in a given image and clinical parameters. Because the basic concept of CAD is broad and general, CAD is applicable to all imaging modalities, and to all kinds of examinations and images. In this lecture, the basic concept of CAD is first defined, and the current status of CAD research is then briefly described. In addition, the potential impact of CAD in the future is discussed and predicted.

I-5

JOURNEY OF RADIOLOGY IN LAST OVER 120 YEARS WHAT A DIFFERENCE 120 YEARS CAN MAKE!

Sunita Purohit

Department of Radio-Diagnosis, Santokba Durlabhji Memorial Hospital, Jaipur, Rajasthan, India.
E-mail: sdmhradiology@gmail.com

In November 1895, Wilhelm Conrad Rontgen first produced and detected X-rays.

Rontgen's discovery opened a window on the previously invisible interior of the human body and spawned the existence of an entirely new medical specialty, RADIOLOGY. Roentgen's discovery and its subsequent revolutionary impact represent one of sciences greatest stories. Since these early x-rays, there have been many milestones in the field of radiology including ultrasound, CT scan, MRI, mammography, nuclear imaging including position emission tomography [PET] which are used to diagnose and/or treat disease. In today's era, medical procedures are performed with the guidance of imaging technologies by Interventional Radiologists. While medical imaging technology has greatly advanced in last 120 years, the ways in which radiologists interact with these images has remained largely unchanged. Medical images can now be stored digitally in the picture archiving and communication system [PACS]. Patient can now easily store and share their medical images online. Patients and doctors all over the world can access these digital images any time. Direct access and control to digital medical images is the next evaluation in Radiology.

Despite the ever changing health care landscape, the future of Radiology on the 2017 horizon is bright. Radiologist will continue to play an important role in the journey to value based care from improving patient outcomes to cost efficient techniques. Through the adoption of innovative technologies and solutions, radiology will not only continue to make an impact, but will drastically improve overall quality of care.

I-6

WHAT IF RADIOLOGY WAS AN ART? WHEN RELATIONSHIPS DEFINE IMAGE QUALITY AND NOT THE PHYSICS

Robin Decoster

Hogeschool, Medical Imaging IMAGO, Universiteit
Brussel Health Sciences, Brussels, Belgium.
E-mail: robin.decoster@odisee.be

Loved by some, hated by others, the appreciation for art has always been a discussion in cultures and societies. What if a radiology department was just a small society? A society of different professions, collaborating to produce an acceptable radiography, with their background and ideas on the quality of a radiograph? Based on current research, the interaction between radiologists and radiographers will be analysed within the sociology framework. After outlining the cornerstones of this inter-professional culture, the influence of relationships on learning strategies and assessment of image quality will lead the reasoning to the conclusion of a common "gestalt" or the presence of a shared mental image of the ideal radiograph. In a "high tech" department, such as medical imaging, the role of technology and the interaction with the users cannot be neglected. After outlining the interpretative framework of current post-phenomenology, key points of human-machine interactions will be combined with the gestalt. The combination of sociology and phenomenology leads into a more philosophical approach to image quality, maybe unconventional, but therefore not less exciting.

I-7

CODES OF CONDUCT AND CODES OF ETHICS IN MEDICAL PHYSICS

W. Howell Round

School of Engineering, University of Waikato, Hamilton,
New Zealand. E-mail: secgenafomp@gmail.com

Purpose: Many organizations and societies that represent professional groups have a "Codes of Conduct" or "Codes of Ethics" document that their members commit to abide by. The Asia-Oceania Federation of Organizations for Medical Physics (AFOMP) has decided to produce a Code of Ethics to act as a model for its national member organizations to adopt.

Methods: A survey was made of a number of medical physics professional societies and organizations to obtain their codes of conduct or ethics. This was initially done by searching on-line for such statements, and later most of the IOMP member organizations were approached individually for copies of their codes of conduct or ethics.

Results: It was clear that very few such statements have been developed by medical physics professional societies or organizations. Those that had been developed ranged from short outlines that covered a couple of pages to in-depth statements running to a dozen pages that set out complaint and disciplinary procedures. In some countries, medical physicists are subject to codes of conduct or codes of ethics that have been developed by government agencies to apply to all medical disciplines and employees.

Medical physicists' codes tend to follow the same principles. These principles are commonly found in the codes of many professional bodies both within and outside of the medical based professions such as engineering and teaching. These are Professional Ethics, (1) Commitment to patients/society, (2) Accept responsibility for their work, (3) Work within limits of knowledge/experience, (4) Integrity, fairness and confidentiality, (5) Avoid conflicts of interest, (6) Stay up to date, (7) Report unethical behavior.

Research Ethics, (1) Fulfill legal/regulatory relations, (2) Get approval from relevant ethics committee, (3) Welfare of patients and animals, (4) Fully inform patients, (5) Don't misrepresent results, (6) Appropriate acknowledgement in publication.

Education Ethics, (1) Respect students/safe environment, (2) Equal opportunity/no discrimination, (3) Commit to students' completion, (4) Fair evaluation, (5) Confidentiality, (6) Students' right to review records/evaluation, (7) Avoid consensual relationships.

It must be noted, though, that many codes of ethics focus only on the professional ethics listed above. However, as medical physicists are often involved in research and development and in education and training, then ethical behaviour in research and education are also important.

Conclusions: As AFOMP is an umbrella organization for approximately 20 medical physics national member organizations from different countries, it needs to develop a code of ethics that is acceptable to all of its members taking into consideration the different cultures involved. This does not mean that it should set low expectations for the ethical conduct of the medical physicists in those countries, but it must still specify standards that are internationally acceptable.

I-8

RESOURCES TO RUN AN RT DEPARTMENT - STAFFING AND MATERIALS

Yakov Pipman

Chair, International Educational Activities Committee (AAPM), Chair, Professional Relations Committee (IOMP), New York, USA. E-mail: ypipman@gmail.com

I-9

FROM IOMP TO IMPCB: HOW A DECADES OLD WISH BECAME REALITY

Raymond K. Wu

Chief Executive Officer, International Medical Physics Certification Board, Phoenix, Arizona, Professor in Radiation Oncology (Retired), Eastern Virginia Medical School, Norfolk, Virginia, USA.
E-mail: raykwu@gmail.com

The International Labour Office in 2008 published the International Standard Classification of Occupations ISCO-08. In which the occupation of Medical Physicist is recognized with other professions under Group 2111 Physicists and Astronomers. A note was included on page 111 "medical physicists are considered to be an integral part of the health workforce alongside those occupations classified in Group 22: Health Professionals". IOMP subsequently published the Policy Statements 1 and 2, which outlined the role and responsibilities of Medical Physicists, the academic qualifications, and training requirements. In May 23rd 2010, the International Medical Physics Certification Board (IMPCB) was officially formed with help from IOMP and the IOMP Professional Relations Committee. At present there are fifteen Supporting Organizations of which IOMP is the Principal Supporting Organization. With the support of IOMP and other organizations, IMPCB can focus on standardization and accreditation of certification programs in accordance with IOMP guidelines. IOMP also provides supports through the scientific and educational programs for the benefit of certified individuals for continuing professional development purposes. In 2014 IMPCB began its accreditation program for local certification programs. Two programs had been fully accredited and the third one is being evaluated. In 2017, the first direct certification examinations session was offered in Trieste Italy in May for Part I and Part II, followed by other examination sessions in December (please refer to www.IMPCB.org). Only the specialty of Radiation Oncology Physics is offered for 2017 examinations. It is expected that in 2018 the specialty of Diagnostic Imaging and Interventional Radiological Physics will be included in examination sessions in Prague during the World Congress and elsewhere. In this special symposium the author will present the background and missions of IMPCB. He will make a report of the progress of IMPCB in the past twelve months. He will then announce the IMPCB near term plans, and explore the potential long term evolution as driven by the changes in the field and in the society. Requirements for accreditation of local certification boards will be described in the perspectives of US, Asian Oceania, and European medical physicists. Finally the author will explain how IMPCB upholds the policy statements of IOMP to achieve the goal of identifying those meeting the minimum requirements and confers the Board Certificates. Time will be reserved for open discussions with a panel of IMPCB officeholders.

I-10

EDUCATION TRENDS AFTER THE OFFICIAL RECOGNITION OF MEDICAL PHYSICS OCCUPATION IN ISCO08

Slavik Tabakov

President, International Organisation for Medical Physics (IOMP), Department of Medical Engineering and Physics, King's College London, UK.
E-mail: slavik.tabakov@kcl.ac.uk

One of the main achievements of the International Organisation for Medical Physics (IOMP) during 2011 was the inclusion of Medical Physics in the International Standard Classification of Occupations (ISCO). This was a result of many years hard work of the IUPESM, IOMP and IFMBE. This recognition of the profession by the International Labour Organisation opens new horizons and presents new challenges in front of us.
A specific horizon is the growing need of medical physicists in hospitals, as our profession is already an important part of the infrastructure of healthcare provision. This reflects in the need of opening new university courses in medical physics. To help with this IOMP published in 2011 a Guide for establishing such courses– the Model Curriculum and recently started Accreditation activities. This is related to the double growth of our profession in the past 20 years and the expected triple growth of the profession in the future 20 years.
One of the challenges in front of our Education is how to accommodate the constantly increasing volume of the professional knowledge in the limited space available in a post-graduate (MSc) teaching programme. A number of medical physics courses already cut parts of the teaching programme in order to include newer methods. This is expected to be topped-up during the practical training, following the university education, but such training is not offered in all places. At the same time some universities are offering introductory medical physics modules at BSc level, which are very attractive for students. This has led to the beginning of formation of new under-graduate (BSc) programmes in Medical Physics. The lecture will present several successful examples of such BSc-level programme.

I-11

PROCESSING OF MEDICAL IMAGE USING LATTICE BOLTZMANN METHOD CASE STUDY: CEREBRAL ANEURYSM SEGMENTATION

Debabrata Datta

Radiological Physics and Advisory Division, Bhabha Atomic Research Centre, Homi Bhabha National Institute, Mumbai, Maharashtra, India.
E-mail: ddatta@barc.gov.in

Recent advancement of multiscale multiphysics solution in the field of medical imaging invites mesoscopic mathematical tool for solving macroscopic fluid dynamics problems generally described by partial differential equations (e.g., Navier-Stokes equations in case of fluid mechanics problems). The Lattice Boltzmann Method (LBM) is an appropriate technique to achieve this target. The idea of the LBM is to construct or simulate a simplified discrete dynamics of macroscopic behaviours at mesoscopic scales by implementing distributions of particles on a lattice. Literature study on several research papers suggest that LBM is a promising tool to image processing. The LBM to image processing, especially to nonlinear anisotropic diffusion of images is first time applied by Jawerth *et al*.,[1] Zhao[2] proposed the GPU-accelerated LBM to solve the diffusion lattice problems[3] including volume smoothing, surface fairing and image editing. LBM for image denoising was mentioned in.[4] It can be proved that LBM based anisotropic diffusion model makes medical images smooth. Also Wang *et al*.[5] proposed a LBM-based anisotropic diffusion model to segment the lumen and the thrombus of aneurysm. An aneurysm is an abnormal bulging outward of an artery.[6] Because of certain histopathologic and hemodynamic factors, aneurysms most commonly occur in arteries that supply blood to the brain. Cerebral aneurysm is a fragile area on the wall of a blood vessel in the brain, which can rupture and cause major bleeding and cerebrovascular accidents. The segmentation of cerebral aneurysm is a primordial step for diagnosis assistance, treatment and surgery planning. Unfortunately, manual segmentation is still an important part in clinical angiography but has become a burden given the huge amount of data generated by medical imaging systems. Automatic image segmentation techniques such as partial differential equation based segmentation provides an essential way to simplify and speed up clinical examinations, reduce the amount of manual interaction and lower inter operator variability. The central idea of partial differential equation based methods is to evolve an initial curve towards to the lowest potential of a cost function, where its definition reflects the task to be addressed. Mostly, the minimization of the cost functional can be expressed as geometrical constraints on the evolving curve. One of the partial differential equation based aneurysm image segmentation technique known as lattice Boltzmann based geodesic active contour method (LBGACM) has been applied for segmentation of cerebral aneurysm image. Mathematical and computational details of LBGACM are beyond scope in the abstract, however, in this method, LBM applies to solve the GAC evolution equation. Cerebral aneurysm is one of the most serious diseases forming part of the stroke, and it is estimated to occur in 1 to 6 percent of the population. Also, up to 85 percent of subarachnoid haemorrhages, which are potentially lethal events with mortality rate as high as 50 percent are caused by the rupture of cerebral aneurysms. Computed tomography angiography (CTA) plays an essential role in the diagnosis, treatment evaluation, and monitoring of cerebral aneurysms. It allows us to detect narrowing or obstruction of blood vessels in time so that corrective therapy can be done, and it can also detect the minute changes in the vessel structure and anatomy. In addition, CTA images may give more precise anatomical details than either ultrasound or magnetic resonance images (MRI), particularly for small blood vessels. Now, CTA is becoming the radiological examination of choice for blood vessels diseases.

The lumen appearing as a focal object of giant aneurysms and thrombus part of the same having a low contrast compared to neighbouring tissues makes it difficult to obtain the manual or automatic segmentation reasoning the segmentation of giant aneurysms of the brain from CTA imaging remains a challenge. In this talk, an innovative segmentation methodology based on the combined use of the LBM and the level set method is proposed. The first methodology consists in extracting the group consisting of lumen and thrombus using a procedure in two steps, then refining the shape of the thrombus using the level set method. A typical experiments are performed on 258 slices of 8 patients CTAs with different types of giant aneurysms. The results on real images showed that the proposed method is comparable to manual segmentation, and quantitatively, the matching factors obtained using the proposed method are high, demonstrating good accuracy of the segmentation. The computational scheme of LBGACM based segmentation technique will be presented in detail.

References

1. Jawerth B, Lin P, Sinzinger E. Lattice Boltzmann models for anisotropic diffusion of images. J Math Imaging Vis1999;11:231-7.
2. Zhao Y. Lattice Boltzmann based PDE solver on the GPU. Vis Comput 2008;24:323-33.
3. Wolf-Gladrow D. A lattice Boltzmann equation for diffusion. J Stat Phys1995;79:1023-32.
4. Chang Q, Yang T. A lattice Boltzmann method for image denoising. IEEE Trans Image Process 2009;18:2797-802.
5. Wang Y, Courbebaisse G, Zhu YM. Segmentation of Giant Cerebral Aneurysms using a Multilevel Object Detection Scheme Based on Lattice Boltzmann Method. In Signal Processing, Communications and Computing (ICSPCC), 2011 IEEE International Conference on, IEEE. 2011. p. 1-4.
6. Seibert B, Tummala RP, Chow R, Faridar A, Mousavi SA, Divani AA, *et al.* Intracranial aneurysms: Review of current treatment options and outcomes. Front Neurol 2011;2:45.

I-12

RECENT DEVELOPMENTS ON MAGNETIC NANOPARTICLES AND THEIR APPLICATIONS IN MAGNETIC HYPERTHERMIA AND DRUG DELIVERY

Ambesh Dixit[1,2], Suvra Laha[1,2], Humeshkar[2]

[1]Department of Physics and Center for Solar Energy, Indian Institute of Technology, Jodhpur, Rajasthan, India, [2]Department of Physics and Astronomy, Wayne State University, Detroit, Michigan, USA.

E-mail: ambesh@iitj.ac.in

Magnetic nanoparticles (MNP) are attracting attention due to their potential for numerous applications including spin electronics, magnetic storage, ferrofluids, and microfluidics in conjunction with biomedical applications. MNPs provide a multifunctional platform for magnetic hyperthermia treatments acting as a localized source of heat, magnetically guided targeted drug delivery, magnetic resonance imaging (MRI) contrast agents and magnetic separation. MNPs are beneficial due to their (i) small crystallite size (few nanometer), which provides easy intravenous injection and externally controlled delivery via bloodstream to the malignant tumor that is not possible with other means; (ii) high surface to volume ratio for MNPs allows for surface engineering with few or multiple recognition molecules, which can assure targeting toward specific tumor tissues; and (iii) the remote heating of MNPs by the externally applied magnetic field allows the heat action only to the zone of accumulation of nanoparticles.

The magnetic hyperthermia is used in treating cancer using magnetically mediated localized heating with the aid of external oscillating magnetic field as malignant cancers cells start dying at or above 41°C. The onset of heating is either from the hysteresis losses or from Neel or Brown relaxation process and depends on geometry, composition, and magnetic moment of the MNPs in conjunction with the applied frequency and magnetic field strength. In addition, MNPs can be integrated/functionalized for loading and releasing drug, magnetically targeted to a specific site and activated for drug release. The discussion will cover the impact of magnetic nanoparticle anisotropy on magnetic properties leading to efficient magnetic hyperthermia and drug delivery. The associated physics and challenges will be covered in realizing the in vivo clinical trials for both magnetic hyperthermia and drug delivery.

I-13

IMPLEMENTING EGSNRC MONTE CARLO IN A CLINICAL SETUP AND ITS POTENTIAL APPLICATIONS

B. Paul Ravindran

Professor of Radiation Physics, Department of Radiation Oncology, Christian Medical College, Vellore, India.
E-mail: paul@cmcvellore.ac.in

Introduction: Radiation dose calculation plays a very important role in radiotherapy treatment planning and quality assurance. Though there are several algorithms that have been developed to get accurate dose calculation, Monte Carlo (MC) simulation is known to be the most accurate method for radiotherapy. In MC simulation, one computes how a particle propagates step by step according to fundamental physics principles. A number of MC algorithms have been developed, viz., as EGS4/5, EGSnrc, MCNP, PENELOPE, and GEANT4. In this work we describe the implementation of EGSnrc in our clinic.

Materials and Methods: EGSnrc Monte Carlo: The history of the EGSnrc system and underlying codes date back to the 1970s, called the Electron Gamma Shower (EGS), but we have now implemented the one of recent versions of EGSnrc (2016). The system is owned and maintained by the National Research Council (NRC) of Canada. The EGSnrc has two main modules; the BEAMnrc a general purpose user code for simulating radiation sources and DOSXYZnrc a general purpose EGSnrc user code to score an absorbed dose in a rectilinear voxelised phantom geometry. For the use of CT dataset, another user code, *ctcreate*, has been provided, that allows the user to build a DOSXYZnrc phantom from a CT dataset. Modelling linac for EGSnrc: BEAMnrc is a general purpose EGSnrc user code for simulating radiation sources and modelling radiation transport through various structures, such as alinac treatment head. In the case of linac, the simulation is based on the geometry model of the treatment head. The user specifies the various parts of the treatment head using the component modules (CMs) where each structure of the linac head is entered as a CM and the accelerator model thus built with various input parameters and cross-section data is compiled prior to simulation. The output data of the EGSnrc is collected on a user-specified plane, to a phase space file, in which the energy, position, direction, weight and charge of each particle are recorded which serves as an input for the DOSXYZnrc for generating the dose distribution in the phantom. For IX models linacs, the treatment head geometry and material information are provided by Varian, but for TrueBeam, the IAEA phase space files at the level of the collimator is provided which could be used as input to obtain the phase space file at the phantom surface. DOSXYZnrc: This is a user code provided to generate the phantom and the dose deposition in the phantom. The output phase space file from the EGSnrc is used as the input file and the phantom geometry is defined in DOSXYZnrc to obtain the dose distribution. The calculated dose deposition is written in an output file with ‘3ddose’ extension by the DOSXYZnrc. An in-house Matlab routine was developed to read the 3Ddose file, the output file of the DOSXYZnrc. The depth dose, beam profile and the output factor data could be derived using the Matlab code.

Conclusion: Implementation of Monte Carlo: One of the issues in MC simulation is the long computational time and porting MC packages onto parallel computing architectures is a direct way for increasing their efficiency. To address this a multi core (16 core) processor is used in our clinic and a bash script that splits an EGSnrc command over “n” independent processes was used where “n” is the number of cores in the CPU. The other method to further increase the processing speed is to distribute jobs over a number of computers in a cluster and we hope to implement this in future.

I-14

CLINICAL ELECTRON BRAM DOSIMETRY: TRANSITION FROM AAPM TG-25 TO AAPM TG-70

Dimitris Mihailidis

Radiation Physics Division, Department of Radiation Oncology, Perelman Center for Advanced Medicine, University of Pennsylvania, Philadelphia, PA, USA.
E-mail: dimitris.mihailidis@uphs.upenn.edu

The absolute calibration of clinical electron beams is increasingly based on TG-51 protocol. In addition, recently published dosimetry data on electrons beams bring up the question of how would one need to modify the widely used TG-25 that originally was based on TG-21 calibration protocol? The answer to the question is given by the recently published TG-70. This new protocol operates as supplement and update to TG-25 on issues that need to be modified because of TG-51 approach to electron dosimetry and because of newer data on clinical electron beams. It describes in detail the procedure of converting measured depth-ionization curves with ion chambers into depth-dose curves, making use of recently published stopping-power ratios and other conversion factors. It also describes the use of water equivalent phantoms to perform relative electron dosimetry based on recently published conversions factors. The report discusses small and irregularly shaped electron field dosimetry using the concept of lateral buildup ratio (LBR) as an avenue to evaluate electronic equilibrium and compute dose per MU for those fields. Finally, it gives some common clinical examples where electron beam dosimetry are applied.

This presentation will try to provide assistance to better understanding the methods and recommendations in TG-70. In addition, how to link the absolute dose calibration recommendations of TG-51 to the relative dose measurements of TG-71.

Educational Objectives: (1) Understand how TG-70 is a modification of TG-25. (2) Understand the methodologies presented in TG-70 for relative electron beam dosimetry. (3) Understand the practical use of clinical electron beams via clinical examples. (4) Outline the major recommendations of TG-70.

I-15

NEW APPROACH TO MANAGING RADIOTHERAPY PATIENTS WITH CARDIAC IMPLANTED DEVICES: MODERN TECHNOLOGY RT AND CIEDS

Dimitris Mihailidis, Bipin Agarwal[1], Moyed Miften[2]

Radiation Physics Division, Department of Radiation Oncology, Perelman Center for Advanced Medicine, University of Pennsylvania, Philadelphia, PA, USA, [1]Chief Physicist, Department of Radiation Oncology, Phoebe Putney Memorial Hospital, Albany, GA, [2]School of Medicine, University of Colorado, Denver, CO, USA. E-mail: bagarwal@phoebehealth.com

It has been twenty years since the AAPM published TG-34 on cardiac pacemakers of older technology, which has been the standard document for clinical use, even today, for managing patients with pacemakers (ICPs). Management of radiotherapy patients with modern technology cardiac implantable electronic devices (CIEDs) has been widely published in literature without the provision of a new comprehensive and concise set of recommendations. This need is clearly supported by the numerous publications in literature on effects of different irradiation modalities on pacemakers and defibrillators, the last 10 years. As treatment delivery technologies (IMRT, SBRT, dose escalations, proton beams, etc.,) and CIED technology advance, the need to address the management of patients with such devices receiving radiation treatment becomes increasingly important. As such, this session will provide updated guidance for caring for radiotherapy patients with CIEDs.

Learning Objectives: (1) Review the purpose and function of CIEDs. (2) Provide a review on sources of potential malfunctions of modern CIEDs, including malfunction mechanisms from high-LET radiation and transient effects attributed to medical imaging for radiotherapy. (3) Review the management of radiotherapy patients with cardiac devices. (4) Utilize recently available data and computation methods of out-of-field/peripheral dose by scattered photons and secondary neutrons estimate cumulative doses to CIEDs during treatment. Risk of failure associated with these doses will be discussed. (5) Provide comprehensive recommendations for management of radiotherapy patients with implanted cardiac devices from initial patient consultation to treatment delivery.

I-16

MOTION MANAGEMENT IN RADIATION THERAPY

Lakshmi Santanam

School of Medicine, Washington University in St. Louis, St. Louis, Missouri, USA. E-mail: lsantan@gmail.com

Motion management in Radiation Therapy (MMRT) is important for tumors that move. Intra fraction motion is an issue that needs to be addressed during simulation, planning and treatment delivery. During simulation, a surrogate device is used that correlates the position of the tumor to the respiratory cycle to generate a 4DCT. Various methodologies in 4DCT, namely phase and amplitude based binning and generation of Maximum intensity projections (MIP), Minimum intensity projections (minIP), or Average Intensity projections (AI) will be reviewed. Depending on the method chosen for treatment delivery, the target delineation can be restricted to individual phases like exhale, inhale or part or entire tumor motion envelope (Internal Tumor Volume (ITV). Average or Helical CT can be used for treatment planning. Treatment Delivery during tumor motion causes blurring of the dose distribution. Using respiratory synchronized techniques can reduce this blurring by turning the beam ON/OFF during the selected period of the breathing cycle or by moving the Multileaf collimators (MLCs) to track the tumor motion. Various motion management techniques like breath hold, active breathing control (ABC), self-controlled breathing, forced shallow breathing or automated respiratory synchronized techniques like gating or tracking and the quality assurance recommendations from TG76 and TG142 will be discussed.

Learning Objectives: (1) Understand the methods to acquire a 4D CT scan and its use in treatment planning and treatment delivery. (2) Discuss commissioning and QA Methods. (3) Discuss which clinical tumor sites would benefit from Motion Management.

I-17

CHALLENGES OF HIGH TECH RADIOTHERAPY: A RADIATION ONCOLOGIST'S PERSPECTIVE

Nidhi Patni

Department of Radiation Oncology, Bhagwan Mahaveer Cancer Hospital & Research Centre, Jaipur, Rajasthan, India. E-mail: nidhionco@gmail.com

Ongoing innovations in radiation oncology pose a challenge to the radiation oncologist to develop the beneficial and safe treatments for patients as well as to integrate them effectively in to the multimodality treatment. The revolution in radiation therapy has made the results comparable to standard surgical techniques in some cases. With the newer technologies like Intensity Modulated Radiation therapy (IMRT), Image Guided radiation Therapy (IGRT), Volumetric Modulated Arc Therapy (VMAT), Stereotactic Body RT (SBRT) therapeutic window is widening. But every leap and progress in science has to pay some price and so have the technological advances in RT. These challenges could be technical, psychological, economical and ethical.

Technical challenges include lack of experience and training in using the high precision radiation techniques. One has to constantly keep abreast not only about the sophisticated RT techniques but has to keep pace with the evolving sister modalities-chemotherapy and surgery. With the advent of volumetric RT planning the knowledge of anatomy has become very pertinent.

Contouring, verification of plans and QA checks consume lot of time but they have become an integral part of life of a modern radiation oncologist. In high tech RT, the margins

around targets have tightened and there is a gradual shift from conventional fractionation to hypo fractionation. Dose escalation is being experimented because of sub millimeter precision. Radiation oncologists have to be more vigilant than ever before about geographic miss of target and dose to OARS because with high doses per fraction and tight margins these lapses could be hazardous.

With the easy access to technology we are now dealing with more educated and aware patients and their families. Their expectations have gone up. One has to customize treatment for every patient. Counseling has become even more important as one has to explain the patient and family why a particular modality (which may not necessarily be the most expensive one) will be optimum.

Availability and access to high tech facility, trained personnel and funds for above remain an unmet need in ever growing cancer population in a developing country like ours. The cancer treatment is becoming expensive day by day as there is a cost for high tech RT, newer chemotherapeutic and targeted drugs and advanced surgical procedures. Often we face dilemma of choosing a better modality which is more apt or the modality the one which the patient can afford. Though health insurance is coming up but still it has a long way to go. With the existing market forces, pressure from the employees who have invested huge sum in high tech RT equipments, colleagues who may advertise that a particular technique is the only way to cure, the pressure to overuse the high tech RT is tremendous. To follow evidence based treatment and maintain ethnical practice is a tough task for a radiation oncologist in high tech RT era.

In a world of constant progress the driving force for changing our perspective must arise from within if we wish to be a part of the mainstream.

I-18

HIGH TECH RADIOTHERAPY: CHALLENGES IN THE PERSPECTIVE OF MEDICAL PHYSICISTS

K. Krishna Murthy, P. B. L. D. Prasad, K. Kaviarasu, T. Pratap Reddy

Department of Radiation Oncology, Krishna Institute of Medical Sciences, Secunderabad, Telangana, India.
E-mail: kammarikm@yahoo.co.in

The aim of high tech radiotherapy is to reduce radiation damage in healthy tissue while delivering desired optimal dose to the cancerous tissues (target volume). This principle has evolved many technical advances in the field and is achieved by integrating image modalities for contouring, numerical algorithms for planning, IGRT systems for delivery verification and software and networking systems to manage quality assurance of the treatments.

Exploiting the integration of these advances has led to the current high tech therapeutic approaches such as IMRT, VMAT, SRS, SBRT, IGRT, Heavy ion and proton therapy etc. Technological innovations continue to progress and improve the accuracy and precision both in the delivery and quality assurance of RT. The increasing complexity of radiation therapy planning and delivery posing many challenges to Medical Physicists in quality management of high tech radiation therapy. To meet the challenges a Medical Physicist must understand the complexity of using new and emerging technologies and implement thorough QA protocols, possibly driven by increased regulations. The challenges in the perspective of Medical Physicists are;

Perspective-I: Imaging Related Challenges: (a) Image registration, fusion of various types of images for planning, (b) Verification and IGRT related images.

Perspective-II: Planning Related Challenges: (a) Thorough knowledge about beam data configuration and various softwares, (b) IMRT, VMAT, SRS, SBRT related planning techniques.

Perspective-III: Machine Specific QA Challenges: (a) QA related to Linacs with MLCs, OBI, Exactrac system, RPM- gating, FFF etc., (b) QA related to cyber knife, Tomotherapy, Gamma knife, Linacs with MRI, Heavy ion and Proton therapy units.

Perspective-IV: Patient Specific QA Challenges; (a) Various dosimetric systems and (b) Small field dosimetry.

Action Plans Needed to Meet the Challenges: The AMPI and CMPI should look for the: (a) Preparation of need based protocols such as TG100 and Auditing like NABH, (b) Planning of need based training programmes such as providing more in-depth training (for example, establishing a website and give QM recommendations regarding various radiation therapy procedures and technologies. Provide web based training and focused workshops on quality and safety in radiation). In this talk, the challenges posed to a Medical Physicist in high tech radiotherapy planning, delivery, implementation of QA and need for the changes required to meet them are discussed.

I-19

THE EMERGING TECHNOLOGICAL DEVELOPMENT CHALLENGES AND WAYS TO ADDRESS THEM: RTT PERSPECTIVE

Rakesh Kaul, R. K. Munjal

Department of Radiation Oncology, Max Super Speciality Hospital, New Delhi, India.
E-mail: kaul.rakesh8@gmail.com

The Radiation Delivery method plays a critical role in achieving primary goal that is improving cure and control of malignant tumors through the use of emerging technologies in Radiation Oncology. Technological development in Radiation Therapy such as 3D-CRT, Intensity Modulated Radiation Therapy, SRS, SBRT and Gating all are non-invasive treatments that precisely deliver high doses of focused Radiation beams to tumors.

In addition to technological developments there has been a parallel advances in imaging technology and computer software that has led to significant improvement in the Radiation Therapy treatment accuracy. These technological development have provided improved outcomes and better quality of life for cancer patients. However there are chances which may result in unintended harm if not used properly. It is, therefore essential that adoption of these new Technologies be evidence based and should be implemented in clinical practice cautiously.

The main Health professionals involved in the delivery and execution of Radiation treatment are Radiation Oncologist, Medical Physicist and Radiotherapy Technologist. Each of the disciplines work through an integral process to plan, execute and deliver quality radiotherapy treatment to patients.

The potential or actual use of new technologies raises questions about cost, efficacy and ethics. The increased capital and operating costs and economic burden of increased QA is a challenging. Advanced technologies have many advantages but it requires well qualified professional and excellent QA/QC programs, as there is a little chance of adjustment once the treatment has been initiated.

With the development of emerging technology the professional role of Radiotherapy Technologists (RTT's) has changed tremendously over the last two decades. Presently RTT's task include, Mould room procedures, simulator planning, patient positioning and image verification to treatment delivery. But with the emerging technological development the RTT's role should be wider and should open more advance scope for practice. From the RTT's perspective there are various challenges while adopting and implementing new techniques and technology which needs to address in a professional way (1) Active participation in professional growth through training and continuing education, research and development and improving and delivering high quality patient cancer care. (2) Involvement in developing protocols, work instructions and training and reviewing current practice. (3) Extensive training and how to use the diagnostic image modalities effectively such as CT, MRI, PET and ultrasound based images in Radiotherapy planning. (4) To have an important role during on (On line / Off Line) image verification on Medical linear accelerator and involvement in decision making for re-planning. (5) Machine QA - Patient specific QA for all patients and dosimetric procedures. (6) Use knowledge, skills and compassion to attend to normal and emergency patient needs. (7) Demonstrate effective communication skills with patient and their relatives.

I-20

REAL-TIME MR GUIDED ADVANCEMENTS IN RT

Bhudatt Paliwal, K. Mittauer, P. Yadav, D. Tewatia, J. Bayouth, M. L. Bassetti

Departments of Human Oncology and Medical Physics, School of Medicine & Public Health, University of Wisconsin, Madison, WI, USA.
E-mail: paliwal@humonc.wisc.edu

With the advent of MR integrated radiation therapy systems there has been a significant advancement in the delivery of radiation therapy. Real-time MR imaging provides high quality MRI images, with superior soft-tissue contrast. This ability has contributed to innovative approach to manage respiratory and cardiac motionas well as the impact of gastrointestinal processes. New MR acquisition techniques reduce imaging times to about 12 seconds, providing 3D MRI sequence for motion artifact-free images with a large field of view (FOV) for short breath hold. Image based breathold management for gating is relatively superior to operator guidance.

Real-time MR guidance, on-table adaptive therapy, allows to incorporate anatomical changes that can take place within a short period of time. Treatment plan can be re-optimized to escalate or de-escalate dose based upon the proximity of nearby critical structures while the patient is on the treatment table. A seamless workflow permits re-planning to reduce dose to organs at risk while giving a greater dose to the target. Clinical examples of lung, liver, pancreas and duodenum cases will be used to illustrate the above advances and the adaptive capability of an MR integrated radiation therapy system. The benefits of real-time adaptive therapy applied to previously untreatable targets will be highlighted.

Further transition from a Cobalt to Linac systems will be described.

I-21

MITIGATION OF CONSEQUENTIAL EFFECTS OF MISADMINISTRATION IN NUCLEAR MEDICINE

A. K. Shukla

Department of Nuclear Medicine, Sanjay Gandhi Postgraduate Institute of Medical Sciences, Lucknow, Uttar Pradesh, India. E-mail: akshukla@sgpgi.ac.in

Misadministration as such includes the practices in nuclear medicine where wrong radiopharmaceutical or excess/inadequate radioactivity is administered to a patient causing undesirable radiation doses or repeat procedure in a patient. Misadministration is also said to have been caused if unjustified procedure involving use of radioactivity/radiopharmaceuticals is conducted either in pregnant or lactating female patients. Incorrect route of activity administration can also cause misadministration and may lead to repeat of the procedure apart fro undesirable radiation doses to patients. As a matter of fact each centre should establish its own guidance levels and protocols for diagnostic and therapeutic procedures in Nuclear Medicine. In general any deviation of administered activity of more than twenty five per cent from the prescribed activity in the guidance level would be regarded as misadministration. The absence of local rules to deal with abnormal situations can also lead to misadministration.

Causative Factors: The causative factors for misadministration include (1) Miscommunications, invisible labeling of vials/syringes containing activity, (2) Distraction due to increased patient load or ahy other stressful conditions, (30 Unawareness about the emergency procedures/absence of safety protocols, (4) Inefficient quality assurance and audit to detect inadequacies.

In addition to above listed factors it is also important to record the initiating events and contributing factors identified in cases of emergencies so as to ensure prevention of the similar incidents and potential radiation exposures in future.

Mitigational Initiatives: (1) Minimize and contain adverse effects by using all safety related protocols/devices, (2) Inform patient, referring physician and the nuclear physician, (3) Calculate radiation dose and institute corrective measures with prompt implementation, (4) A comprehensive event report to be prepared for submission to regulatory authority, (5) Concerned staff to be notified about the accident/misadministration, (6) Removal of orally administered radiopharmaceutical by use of laxatives, enemas, emesis and gastric lavage, (7) Induced and rapid excretion of administered radiopharmaceuticals by hydration or dieresis, (8) In case of serious patients removal of urine by catheterization, (9) Appropriate use of blocking agents to reduce radiation dose to thyroid, salivary gland and stomach etc.

Illustrative Example: A middle aged female patient scheduled for thyroid scan reported the department and informed the concerned technologist that she has no evidence of pregnancy but she was trying to get pregnant. The patient, however, was curious to know about the associated radiation risks if any and justification of the diagnostic examination. Technologist due to distracting factors misunderstood the patient and got an impression that patient is not interested in getting the examination done. The patient was persuaded to get the examination done and later it was found that the patient was in her early stages of pregnancy.

In a usual course the local rules of the department would have stated that a female patient to be considered as pregnant unless proven otherwise. However the absence of any local rules this could not be ascertained.

It can therefore be contemplated that precise guidelines in concordance with regulatory requirements need to be evolved specifically including the common factors that might lead to adverse effects from patient safety viewpoint and are attributable to therapeutic and diagnostic procedures involving use of radiopharmaceuticals/radioisotopes.

I-22

PREPAREDNESS FOR RESPONSE TO RADIOLOGICAL EMERGENCIES

K S Pradeep Kumar

Outstanding Scientist(OS), Associate Director, HS&E Group, Head, Radiation Safety Systems Division, Bbhabha Atomic Research Centre, Trombay, Mumbai, Maharashtra, India. E-mail: pradeepdrks@gmail.com

I-23

RECENT ADVANCES IN BRACHYTHERAPY

D. D. Deshpande

Department of Medical Physics, Tata Memorial Hospital, Parel, Mumbai, Maharashtra, India.
E-mail: deshpandedd@rediffmail.com

Introduction: The advantage of brachytherapy is the ability to deliver very high dose to the tumour while sparing the surrounding critical organs. The brachytherapy has evolved tremendously over past few decades. High Dose Rate (HDR) remote after-loading coupled with advances in treatment planning systems has ensured well defined protocols and methods for brachytherapy dose analysis. Recently use of imaging techniques for 3-D data acquisition for brachytherapy application, contouring and treatment planning hasmade significant contribution for better brachytherapy dose delivery.

Imaging in Brachytherapy: Orthogonal radiographs generally are used widely to feed the source positions and applicator geometry to obtain the brachytherapy plan. The CT and MRI are also being used for contouring various volumes like target and clinical organs which coupled with 3-D planning algorithms gives direct doses to critical organs with volume analysis. In case of intracavitary application MRI gives better visualization of soft tissue so that we can more clearly see the critical organs like bladder and rectum

Axial, sagittal and coronal images of MRI are being used for ICA planning. Delineation of GTV, HRCTV and OARs were performed. Reconstruction of applicators can be done with special dummy markers (water/gadolinium) inserted in the applicators.

Target and Other Volume Definitions: Treatment planning aims that the tumor receives the maximum dose and Organs At Risk (OAR's) receive the minimum.

International Commission on Radiation units and measurements (ICRU) through its various reports has standardized the brachytherapy treatments to a great extent. The most important was ICRU 38 (1985) which has given guidelines for reporting intracavitary therapy in Gynecology. American Brachytherapy Society (ABS) Image guided Brachytherapy working group (IGBWG) have provided guidelines in reporting the image based brachytherapy, which recommends the prescription of dose to a volume rather than a point. Later GEC ESTRO published guidelines for the practice and reporting of image based ICA, which has been widely accepted so that a unified approach is formed among the users of image based brachytherapy.

3D Planning in Interstitial Brachyterapy: The interstitial brachytherapy is carried out extensively in H and N, soft tissue, prostate etc. The CT images taken with dummies in the catheters and are directly transferred to planning system. The catheters are input by tracking algorithm and dose distribution is analyzed in 3D view. The target volume and surrounding critical organs are also marked, which helps in evaluation of dose to these volumes by DVH analysis and dose volume indices.

With stepping source dosimetry system (SSDS) with HDR brachytherapy use of wide variations of source positions inside the catheters and different dwell times for each position is possible. Also various optimization techniques like Geometric optimization, Dose point optimization, polynomial optimization etc. can be adopted after visualizing 3-D images of the target volume, implanted needles and dose distribution.

Imaging in Brachytherapy Application: The imaging also plays important role in actual application of brachytherapy in operation theatre. Ultrasound guided prostate I-125 seed implants are commonly performed. Also needle (template) prostate implant under the guidance of Transrectal Ultrasound probe (TRUS) is widely used. US guided intracavitary application is also performed so as to avoid perforation of uterine wall.

I-24

IMAGE GUIDED APPLICATION IN MEDICAL PHYSICS

Tae Suk Suh

Department of Biomedical Engineering, Research Institute of Biomedical Engineering, College of Medicine, The Catholic University of Korea, Seoul, South Korea.
E-mail: suhsanta@catholic.ac.kr

Recently, advances in medical imaging technology have accelerated the development of medical physics: the utilization of images in diagnosis and radiation therapy such as intensity modulated radiation therapy (IMRT), image guided radiation therapy (IGRT), Tomotherapy and Robot-guided RT. Single or multi-modality imaging for static or dynamic target has been applied in the field of medical physics to determine the local tumor volume and location of the tumor. While all radiation therapy are more or less image guided traditionally, imaging technology has primarily been used in producing 3D information of patient anatomy to identify the location of the tumor to treatment. New radiation treatment technique derived from the image guided technique has been developed to optimize the accuracy of radiotherapy. Especially, image guided applications are classified into two major aspects: (1) multi-modality imaging for better definition of tumor volume, (2) time-resolved imaging for modeling the intrafraction organ motion. In this presentation, two available imaging techniques will be highlighted, with emphasis on the principle and quality control of multi-modality imaging and moving organ.

Multi-modality imaging involves the incorporation of two or more the following imaging modalities: single photon emission computed tomography (SPECT), positron emission tomography (PET), magnetic resonance imaging (MRI), computed tomography (CT) and optical imaging. The incorporation of multi-modality imaging provides functional and anatomic information. Multi-modality imaging is essential for a primary diagnosis and determining the most suitable treatment plan, and can help us to reduce errors. In addition, it has attracted interest in the fields of molecular and functional imaging for primary-to-metastatic cancer screening and functional neuroimaging. Therefore, the application of multi-modality imaging should lead to a better and more reliable diagnosis and treatment.

Intrafraction motion has been an issue that is becoming increasingly important in the era of IGRT. Estimation of surrogated respiration motion through breathing cycle and 4D images is the biggest focus to correlate with actual organ motion. If target is moving, we need to use larger beam field, which delivers extra radiation dose to normal tissue. The solutions to avoid this extra dose to normal tissue by moving organ are to utilize respiratory motion control techniques. Therefore, we are studying common methods used in the management of respiration motion in radiation therapy: breath-hold, gating, and tumor tracking techniques. These techniques are generally implemented through four steps: (1) localization consisted of respiratory signal control and image guidance, (2) planning (3) verification, and (4) delivery.

The analysis of the multi-modality images and image registration provide useful information in delineating the target volume for radiation treatment planning (RTP). In addition, we need more accurate time-resolved 4D localization technique for modeling the intrafraction organ motion.

I-25

DO WE NEED AUDIT OF RADIATION ONCOLOGY FACILITIES - INTERNAL OR EXTERNAL OR BOTH?

R K Munjal

Head, Department of Medical Physics, Max Healthcare, New Delhi, India.
E-mail: ram.munjal@maxhealthcare.com

I-26

MANAGEMENT OF CT IMAGE FOR OBESE PATIENTS IN RADIOTHERAPY TREATMENT PLANNING PROCEDURE

S. N. Sinha

Chief Medical Physicist, Department of Radiation Oncology, Nayati Medicity, Mathura, Uttar Pradesh, India.
E-mail: sujitnathsinha@gmail.com

In radiotherapy treatment planning accurate CT data is essential. Computer tomography imaging has become mandatory for treatment planning in Radiotherapy. For obese patients when imaged with Diagnostic CT or even sometimes with large bore CT in the range 80 to 85 cm, corresponding image reconstruction FOV ranges between 50 cm to 65 cm. This implies that even if an obese patient is accommodated in the scanner, the CT data may have truncated image due to limitation in FOV size. The complete CT data is not available creating missing tissues laterally/obliquely where radiation beam path cannot be accurately derived due to lack of CT data and thereby giving error in monitor unit dose calculation. Such incomplete data also brings in beam angulation constraints during IMRT, VMAT type planning. Some vendors have options for extended Field of View (eFOV) of 82 cm but is reported in literature to have degradation of Hounsfield units (HU) observed beyond nominal FOV. We have developed different modules in Matlab to tackle imaging obese patients and take appropriate measures for use in treatment planning system. The main module was developed using a line profile template match method to produce a composite CT image series for obese patients from two partial CT – one taken with patient left sided and the other with patient right sided on the CT couch. The software was implemented and tested on images with bony structures in phantom and also in actual patients with good results. Further practical pitfalls were observed during CT imaging with some heavy weight patients. Since patient treatment couch in Linear Accelerator are flat, it is mandatory to have flat couch top externally fitted on CT couch for imaging. Obese patients when scanned in CT shifted on one side many a times, a tilt of the image is observed. Such tilts due to patient weight were overcome by utilizing in-house built modules in Matlab. Module “Dicom image rotation” was developed where the user can specify the known rotational angle of the image in pitch (coronal plane) and roll (transverse plane) direction for any dicom image. Further modules like “point by point Orthogonal Planar image registration” was developed to be used with fiducial markers which helped in aligning the images before obtaining composite CT data. The different tools used for obese patients to acquire complete CT data sets gave good results to be used for radiotherapy treatment planning.

I-27

IN-VIVO DOSIMETRY IN RADIOTHERAPY

M. Ravikumar

Department of Radiation Physics, Kidwai Cancer Institute, Bengaluru, Karnataka, India. E-mail: drmravi59@yahoo.com

The modern radiation treatment delivery techniques minimizes dose to the normal tissue and thereby increasing the prescribed dose to the tumor volume. Though there is an increase in the tumor control probability (TCP), the real advantage may be restricted by the probable raise in the normal tissue complication probability (NTCP). This necessitates the need for an accurate treatment delivery and measurement of dose delivered. The in-vivo dosimetry has become an integral part of verifying the treatment delivery to the patient. In-vivo dosimetry (IVD) is a vital component used to identify major deviations in treatment delivery as a part of quality assurance process thereby improving the quality of patient care in radiation therapy and is highly recommended by many international guidelines. The IVD does not imply that the dosimeter should necessarily be placed inside the living object. In EBRT, a dosimeter is normally placed on or near the surface of the patient, inside or in the neighborhood of the external beam.

There are different commercially available in-vivo dosimeters in practice. The current use of ionization chamber is mostly limited to phantom measurements though a few sealed chambers are used for in vivo measurements. Radiographic x-ray film performs several important functions in radiation therapy and can serve as relative radiation dosimeter and archival medium. Film provides excellent 2D spatial resolution and it gives information about the spatial distribution in the area of interest in a single exposure. Radiochromic film has a special dye and instantaneous colour change would occur after irradiation due to polymerization reaction. These films are used in the dosimetric verification of patient specific IMRT QA, stereotactic radiation and brachytherapy.

Thermoluminescence dosimeters (TLDs) are used in radiation therapy frequently as they can be placed on the skin or inside the patient body without the inconvenience of measuring cables. Also, they have wide applicable dose range, small dependence on energy, temperature and dose rate in the therapeutic range, very high sensitivity and no requirement to apply bias voltage and easy to transport. Plastic scintillator system offers excellent tissue equivalence, but their design makes it difficult to eliminate the noise signal produced from the actual plastic scintillator chip in the light-guide of the dosimetry system.

Diodes have been widely accepted in radiation dosimetry due to its robustness. Several correction factors have to be applied due to their energy dependence (Z =14), dose rate dependence, temperature dependence and angular dependence. The characteristics such as instantaneous read-out, small size, good linearity of the response and permanent storage of the dose demonstrated the efficacy of MOSFET as an in-vivo dosimeter in radiotherapeutic treatments for photon, electron and proton beams.

Diamond detectors have been considered suitable for clinical purposes due to their small size, good tissue equivalency and resistant to radiation damage. Diamond detectors exhibit high resolution and high sensitivity, however their advantage over semiconductor diodes is debated except for very small fields. It was reported in literatures that diamond detectors have less angular dependency than diodes in electron beams. Presently, EPIDs have largely replaced radioagraphic film as a tool for patient position verification during external beam radiation therapy. Since EPID images give dose information, their use in radiotherapy dose measurements was investigated by many groups. With the recent introduction of amorphous-silicon (a-Si) detectors, the interest in EPID dosimetry has been increased because of the favorable characteristics such as fast high resolution, image acquisition, digital format, and potential for IVD measurements.

The use of optically stimulated luminescence (OSL) as a dosimetry tool was recognized in the year 1950. The carbon–doped aluminium oxide Al_2O_3:C has become the dominant OSL material for dosimetric measurements due to its high sensitivity and other desirable properties. At present, OSLDs are available in various physical forms intended for different applications.

The presentation will focus on the need for IVD in radiotherapy practice, the advantages and limitations of various in-vivo dosimeters. Special attention will be given in highlighting the characteristics and practical advantages of OSL system which was implemented at our Institute recently.

I-28

ADVANCES IN MEDICAL PHYSICS AND PHANTOM DEVELOPMENT: A PARARALLEL PATH. A REVIEW FROM HISTORICAL TO COMPUTATIONAL PHANTOMS

Franco Milano

Department of Experimental and Clinical Medicine,
University of Florence, Florence, Italy.
E-mail: franco.milano.unifi@gmail.com

There are many origins of Medical Physics, deriving from the many scientific intersections between physics and medicine but probably modern Medical Physics (MP) initiates with the discover of X-rays by W. C. Röntgen W. C. awarded in 1901 by the Nobel Prize in Physics. Now a day MP encompass Medical Radiation Physics and embraces all medical specialities in diagnosis and therapy. Over the last few years MP has experienced tremendous technical and scientific advances in any application. Also methods of imaging and treatment procedures have become very sophisticated and complex. At any time Medical Physicists developed phantoms to mimic patient or human body characteristics in a given medical procedure either therapeutic or diagnostic. The complexity of a phantom is linked with the complexity of the medical procedure including the use of highly sophisticated equipment. The goal of the presentation is to review all types of phantom used in MP, from simple to complex, following the parallel development of advanced medical applications and phantoms. A short analysis and impact of the use of phantoms in Quality Control in modern equipment is also performed together with the necessity to give an adequate education to Medical Physicists in the aware use of complex phantoms.

I-29

NANOTECHNOLOGY AND ITS APPLICATIONS IN HEALTH CARE

S. H. Pawar[1,2]

[1]Centre for Research and Technology Developments,
Sinhgad Institutes, Solapur, [2]Centre for Interdisciplinary
Research, D.Y. Patil University, Kolhapur, Maharashtra,
India. E-mail: shpawar1946@gmail.com

The use of magnetic nanoparticles for biological and clinical applications is undoubtedly one of the most challenging research areas in the field of nano-biotechnology. The use of magnetic nanoparticles (MNPs) has witnessed noteworthy advances and holds great potential for biological applications. Magnetic nanoparticle-based biological research has rapidly advanced to a point where the research focus is shifting away from synthesis and characterization to the development and investigation of multifunctional MNPs. MNPs, specifically super paramagnetic nanoparticles, based upon their unique physical, chemical and thermal properties, offer high potential and have been proposed extensively for nano-bio applications. MNPs are eligible for various biomedical applications, such as magnetic hyperthermia, magnetic resonance imaging, target drug delivery, bacteria detection, cell labeling, magnetic separation, and enrichment of DNA. In recent years, major attention has been focused on the development of MNPs due to their fundamental properties. Firstly, their size, which generally ranges from a few nanometers to tens of nanometers, places them at dimensions that are smaller than or comparable to those of a cell (10–100 mm), a virus (20–450 nm), a protein (5–50 nm) or a gene (2 nm wide and 10–100 nm long). This means that they can 'get closer 'to a biological entity of interest. Certainly, they can be coated with biomolecules to make them interact with or bind to a biological entity, thereby providing a controllable means of 'tagging' or addressing it. Secondly, MNPs exhibit interesting size-dependent superparamagnetism. Such MNPs are highly preferred due to their ability to be magnetized upon exposure to a magnetic field, but they have no permanent magnetization (remanence) once the field is turned off. Thirdly, MNPs can be manipulated by using an external magnetic field, which provides a huge advantage and opens up many nano-bio applications in vivo. This can be achieved by functionalization of MNPs, which can be defined as, "The addition of a chemical functional group on the surface of MNPs in order to achieve surface modification that enables their self-organization, renders them compatible and make them potential for various kinds of applications" Specific group of applications discussed here for this audience is in the area of health care.

Health care is prime importance to every human being. It is well known that healthy mind lies in healthy body. Hence, every nation provides great importance for the provision of sufficient funds in its annual budget. The world health organization (WHO) keeps an eye on health care globally. It conducts the survey of diseases. Recent survey reveals that out of every 10 deaths in India, 8 are caused by non communicable diseases (NCDs) which include cardio vascular diseases, cancers, chronic respiratory diseases and diabetes. In light of these facts, our research group has focused the major thrust on the applications of nanotechnology in health care, specifically on atherosclerosis and nanotechnology, cancer nanotechnology, stem cells and regenerative medicine, wound healing and nanotechnology, and invitro fertilization. Our group has published considerable amount of research papers in highly reputed international research journals and reality available on website www.shpawar.com. In the present talk, attempts have been focused on right form synthesis and characterization of variety of nano materials, as per the requirements of diseases. Specifically, magnetic nanoparticles (MNPs) are of great interest for use in medicine for example, for targeted drug delivery, for enhancing the contrast of magnetic resonance images and in magnetic hyperthermia treatment. The role of magnetic NPs will be discussed at length in cancer nanotechnology, as it is a painless curing of cancer.

I-30

GRID RADIOTHERAPY AND ITS ABSCOPAL EFFECT: RADIATION INDUCED IMMUNOGENIC RESPONSE WITH IMMUNOTHERAPY

T. S. Kehwar

Eastern Virginia Medical School, Sentara Obici Hospital, Suffolk, Virginia, USA. E-mail: drkehwar@gmail.com

Purpose: This study investigates immunogenic antitumor response of GRID radiotherapy and effect of immunotherapy in combination.

Introduction: GRID radiotherapy, also known as Spatially Fractionated Radiation Therapy (SFRT), is a radiation treatment modality in which radiation is delivered through a matrix of equally spaced beamlets. At present GRID radiotherapy is given as a precursor to standard fractionation schemes with single or parallel opposed fields. In GRID radiotherapy, GTV is covered by single or parallel opposed fields without any margin and dose to the critical organs is kept minimum by avoiding direct entry or exit of the beamlet. Dose distribution in GRID radiotherapy has peaks and valleys, i.e. high and low dose beamlets. Many mechanisms of action of GRID radiotherapy has been proposed by various researchers. In this paper, a bystander effect of GRID therapy on immunogenic cells is highlighted with possibility to boost with immunotherapy.

Materials and Methods: In the GRID radiotherapy, the high dose in peak region damages DNA molecules within the tumor cells, normal tissue cells and immune cells results in producing a number of small fragments of different organelles, including genetic material (DNA molecules) within the nucleus, of tumor, normal and immune cells, and are released into the extracellular matrix that diffuse to low dose region (valley), where naïve cells of innate and adoptive immunity system, such as dendritic (DC), T and natural killer (NK) cells, are activated. The fragments from tumor cells released from the dying tumor cells are TAA and potentially can provide antigenic stimulation that induces antitumor- specific immune responses. DC cell uptake TAA from extracellular matrix and cross-presented on MHC-I molecules. The cross-presentation permit DC cells to elicit CD8+ T as well as CD4+ T cell responses to exogenous antigens. GRID radiotherapy induced DC, T and NK cells can migrate to the distally located metastatic site and be able to cause deleterious effect to the tumor cells results in regression of metastatic cancers, which are away from the irradiation field. This phenomenon is called abscopal effect. Abscopal effect appears to be a result of enhanced immune response directed to tumor cells. This response is sometimes not effective, hence need to combine immunotherapy to enhance DCs, T and NK cells.

Results and Discussion: The GRID radiotherapy can be performed either by custom made tungsten or Cerrobend equally spaced grids or MLCs can be used to create beamlets. In the GRID radiotherapy, dose is prescribed either at the dmax or at a depth in the peak of the beamlet. To enhance immunogenic effect of GRID radiotherapy, any one or combination of (1) monoclonal antibodies, (2) immune checkpoint inhibitors, (3) cancer vaccines, or (4) other non-specific immunotherapies, can be used. Many clinical trials reports increased survival rate compared to other cancer therapies.

Conclusions: Manipulation of the immune response may enhance the effects of radiation therapy both local or systemic levels through abscopal effect and immunotherapy combination may shape the future of radiotherapy.

I-31

IMPLEMENTATION OF INTERNATIONAL BASIC SAFETY STANDARDS FOR THE USE OF RADIOLOGICAL MEDICAL IMAGING DEVICES

Magdalena Stoeva, Jitendra Sharma[1], Maria Del Rosario Perez[2], Emilie Van Deventer[2], Pablo Jimemez[3], Miriam Mikhail[4], Ola Holmberg[5], Stewart Whitley[6], Jacques Abramowicz[7]

Medical Imaging Department Medical University, Plovdiv, Bulgaria, [1]Andhra Pradesh MedTech Zone, Visakhapatnam, Andhra Pradesh, India, [3]Pan American Health Organization (PAHO), Washington, [4]RAD-AID International, Maryland, [7]WFUMB, USA, [2]WHO, Switzerland, [5]IAEA, Wien, Austria, [6]ISRRT, UK. E-mail: ms_stoeva@yahoo.com

Introduction: The International Basic Safety Standards (BSS) for Protection against Ionizing Radiation and for the Safety of Radiation Sources represent a global benchmark for setting national regulations in the field of radiation protection. Co-sponsored by eight international organizations (IAEA, WHO, PAHO, FAO, ILO, EC, FAO and UNEP), the BSS include a robust set of safety requirements for medical use of ionizing radiation. BSS implementation in the health sector targets an improvementin radiation protection in medicine.

Results and Discussion: A Continuous collaboration between UN organizations, professional societies, patient advocates, manufacturers' associations, regulators and other relevant stakeholders is essential in ensuring that all patients at the global level are safe from undue excess amounts of ionizing radiation, and have access to safe medical imaging for diagnostic purposes.

Advanced technologies have opened new horizons for the use of radiation medical devices in diagnostic imaging and image-guided interventions, including the use of ionizing and non-ionizing radiation. Although safety and efficacy of procedures have improved, incorrect or inappropriate handling of these technologies can introduce potential hazards for patients and staff.

Among the major challenges are the justification of medical radiation exposure for new technologies, procedures or devices and of screening programs; the lack of radiation safety officers in medical facilities to ensure procurement of appropriate and safe devices; the need for increased number of medical physicists, for integration of radiation protection into HTA and for promotion of clinical audit programmes to ensure that clinical benefit outweighs radiation detriment.

This article presents the outcomes of a workshop on BSS implementation held as part of the 3rd WHO Global Forum on Medical Devices (Geneva, Switzerland, 10-12 May 2017). Presenters from the WHO, IOMP, ISRRT, RAD-AID International and WFUMB discussed their respective roles as medical physicists, radiologists and radiographers, and the actions conducted to promote the BSS as part of their missions and global outreach programs. Presenters from Norway and India shared their experiences indicating that implementation of the BSS requires an administrative framework involving dialogue and cooperation between relevant authorities and professional societies, beyond revising national laws and regulations. It was noted that similar BSS for non-ionizing radiation are lacking and some international organizations are joining efforts to bridge this gap. The upcoming ICRPM in Vienna in December 2017 will be influential in setting the stage for future handlings of radiation safety issues and improving implementation of BSS around the world.

Conclusion: The BSS Workshop at the WHO 3rd Global Forum on Medical Devices brought together comments from various national and international organizations, on how radiation safety in medical imaging is promoted globally. Continued collaboration leadership by each of these organizations will be essential to furthering the optimization of radiation safety alongside medical imaging for patients around the world.

I-32

DATA MINING FOR RADIOMICS

Hidetaka Arimura

Division of Quantum Science, Kyushu University, Fukuoka, JAPAN. E-mail: arimurah@med.kyushu-u.ac.jp

I-33

FDG PET/CT SIMULATION FOR RADIATION THERAPY PLANNING

Kohei Hanaoka[1,2]

[1]Division of Positron Emission Tomography, Institute of Advanced Clinical Medicine, Kindai University, [2]Department of Medical Physics Graduate, School of Medical Science, Kindai University, Osaka, Japan. E-mail: h@naoka.name

^{18}F-FDG PET/CT has an important role in radiation therapy planning. FDG PET/CT parameters such as standard uptake value and metabolic tumor volume provide important prognostic and predictive information. Importantly, FDG PET/CT for radiation planning has added biological information in defining the gross tumor volume (GTV) as well as involved nodal disease. Several studies have shown that PET has an impact on radiation therapy planning in an important proportion of patients.

On the other hands, FDG PET/CT for radiation therapy planning has several limitations. First of all, the method to determine the optimal threshold of FDG PET/CT images that generates the best volumetric match to GTV is not established. The size of the GTV derived from FDG accumulation changes significantly depending on the threshold value, the threshold value can affect the clinical target delineation. Secondly, FDG is not a cancer-specific agent, and false positive findings in benign diseases have been reported.

Successful radiation therapy planning requires cooperation of other professions and sufficient physical assessment.

The contents of this presentation are as follows. (1) QA and QC of the PET/CT system for radiation therapy planning. (2) Potential impact of metal artifact caused by patient immobilizers on PET/CT image. (3) 4-dimentional PET/CT system for radiation therapy planning. (4) Other PET tracers for radiation therapy planning. (a) Fluoromisonidazole (^{18}F-FMISO) as a tracer for detecting hypoxic tumor cells. (b) Carbon-11-methionine (^{11}C-MET) as a tracer for imaging brain tumor cells. (c) 4-borono-2-(18)F-fluoro-phenylalanine (^{18}F-FBPA) on the boron neutron capture therapy.

I-34

DEVELOPMENT OF 4D IN-SILICO STOCHASTIC SPATIO TEMPORALMODEL OF TUMOR GROWTH WITH ANGIOGENESIS

Eva Bezak[1,2], Jake Forster[2,3], Michael Douglass[2,3], Wendy Phillips[2,3]

[1]Sansom Institute for Health Research, School of Health Sciences, University of South Australia, [2]Department of Physics, University of Adelaide, [3]Department of Medical Physics, Royal Adelaide Hospital, Adelaide, Australia. E-mail: eva.bezak@adelaide.edu.au

Introduction: Mathematical and computational models, describing the complex biophysical processes associated with radiation induced cell death, have been used since the early 1960s. In 1973, Chadwick first presented a mathematical formula which accurately fit experimental data of cell survival as a function of absorbed dose. It was the first model that attempted to consolidate theories of *macroscopic* dose deposition and *micro/nanoscopic* damages caused by ionising radiation. In macroscopic radiobiological models (such as Chadwick's) small scale behaviour is consolidated into a set of analytical equations representing the large scale behaviour of the system. While these models are fast in terms of computation time, they are not robust enough in order to predict outcomes for a wide range of input parameters. As physical, chemical and biological interactions of radiation within an organic medium are stochastic processes, a stochastic type model is required for their accurate description. As a result, with improvements to the speed and general availability of computer hardware, a transition is occurring from simple analytical models to more physically realistic stochastic (Monte Carlo) models. At our institution, we developed a 4D integrated radiobiological model by combining "in-house" generated models with an existing Monte Carlo particle tracking toolkit (GEANT4). The result is a 4D simulation that can: grow a tumour composed of individual cells (with realistic chemical composition/geometry/cell cycle time) and blood vessels, irradiate the tumour, record the microdosimetric track structure in each cell, cluster spatially correlated ionisation events into DNA double strand breaks and then predict the likelihood that any given cell will survive.
Methods: In this work, a head neck squamous cell carcinoma (i.e. cells and blood vessels) is modelled using Matlab. Tumour cell oxygenation is a function of distance to the nearest blood vessel and hypoxic cells have an increased cell cycle time. Cell quiescence is simulated at low oxygen tensions. Cells may also become necrotic and be resorbed. To simulate head and neck cancers, a cell hierarchy of stem cells, transit cells and differentiated cells is considered and differentiated cell loss is included. Simulations were performed on the Phoenix supercomputer, University of Adelaide, using as many as 32 cores to observe the effects of hypoxia and necrosis on the rate of tumour growth.
Results: A semi-realistic 4D tumour model with angiogenesis for head and neck cancer has been developed. In accordance with clinical data reported in literature for head and neck cancers, values of relative vascular volume between 0.7-14%, blood oxygenation between 20-100 mmHg and vessel-to-necrosis distance between 80-300 μm were considered. This resulted in values of HF10 (fraction of cells with oxygenation <10 mmHg) ranging from 0-0.91, values of HF2 (fraction with oxygenation <2 mmHg) from 0-0.54, mean oxygenation from 2.0-67 mmHg and relative necrotic volume from 0-38%. With a probability for stem cell symmetric division of 0.02 and 80% loss of differentiated cells, the doubling time increased from 47 ± 4 days to 209 ± 10 days with increasing amounts of hypoxia and necrosis.
Conclusion: On going work includes growing tumours which are then finely voxelised and imported into Geant4 for irradiation using track structure methods, calculating both direct and indirect radiation damage. By taking into account cellular oxygenation and the formation of hydroxyl radicals, tumour response to photon radiotherapy is explored using this 4D tumour model for hypoxic tumours versus well oxygenated tumours. The novelty of this model is in its ability to predict both the microscopic and macroscopic outcome of radiobiology experiments while varying input parameters; e.g. cell type and its biological properties (including repopulation), radiation type, tumour geometry, dose, degree of hypoxia, oxygenation, effects of direct and indirect (i.e. free radical production) damageand others.

I-35

DEVELOPMENT OF VIDEO BASED MECHANICAL QUALITY ASSURANCE SYSTEM FOR MEDICAL LINEAR ACCELERATOR

Youngyih Han, Eun Hyuk Shin, Jung Suk Shin, Hee Chul Park, Doo Ho Choi, Jun Sang Cho

Department of Radiation Oncology, Samsung Medical Center, School of Medicine, Sungkyunkwan University, Seoul, Korea. E-mail: youngyihhan@gmail.com

In state-of-the art radiation therapy, one of the most important factors is to focus radiation to a tumor while minimizing radiation to peripheral normal tissues. In particular, SBRT, SRS, IMRT, IMPT require much higher precision and accuracy than the conventional treatment techniques, due to highly conformal dose distribution to a tumor.
Accordingly, quality assurance (QA) of the medical linear accelerator and subordinated equipment should be able to measure the degree of required accuracy which are less than 1 mm and 1 degree for angle for mechanical function of the treatment system. In addition the quality assurance measures need to be objective, precise and analyzed automatically to be efficient QA procedure. Therefore, we have developed video based mechanical quality assurance system which can meet the aforementioned requirements.
The developed system composed of three components, which are an indicator for marker, image capturing camera

and image analysis software. The indicator provides the reference position for measuring an isocentor of gantry rotation, collimator rotation, couch rotation as well as light field sizes. The camera is designed to be positioned at block slot of the linear accelerator and captures images which are transferred to a computer for analysis. The analysis software was coded using Labviewand it measured the track of the marker for rotation of the linac, couch and fidld sizes analyzed using the pixel calibration data. The performance of the developed system was verified against the false positive tests for light field sizes, isocenter offsets and couch movements. The developed system meets the all the required level of accuracy and precision which were less than 0.2 mm of accuracy for isoceter offset and couch movement and 0.23 mm for light field size measurement, thereby providing objective and efficient quality assurance of the high performance linacs.

I-36

MEDICAL APPLICATIONS OF 3D PRINTING

R. Ramaseshan[1,2,3,4], A. Chiang[1], J. Awotwi-Pratt[1,2], L Mathew[1], B. Vangenderen[1], C. Appeldoorn[1]

[1]Department of Medical Physics, BC Cancer Agency-Abbotsford, [2]Department of Medical Physics, University of the Fraser Valley, Abbotsford, [3]Department of Medical Physics, Simon Fraser University, Surrey, [4]Department of Medical Physics, University of British Columbia, Vancouver, British Columbia, Canada.
E-mail: rramaseshan@bccancer.bc.ca

Purpose: Utilization of 3D printing methodology in radiotherapy and other medical applications.

Background: There are a number of medical applications that use 3D printing technology solutions, for e.g. dentistry and plastic surgery reconstruction modelling. Applications of 3D printing in radiation therapy have not been widely reported in the literature. The selection of 3D printing technology is critical and can heavily impact its efficiency and functionality in the radiotherapy clinic. We are evaluating 3D printing technology in our Radiation Therapy Department for conformal patient bolus with application in external beam treatment, brachytherapy surface molds, patient weight loss management, patient cervix model obtained from CT data for interstitial HDR treatment validation, eye shields, and custom special locking collets for interstitial implants, MRI accessories, lung breathing phantom, room laser self-alignment, 3D surgical print evaluation, and MLC guide blocks.

Materials and Methods: The particular technology we are currently using is called Multi Jet Printing (MJP) which delivers professional print quality, with high precision (0.003”) and is simple to use. All 3D printed parts removed from the print platform will contain support material to fill up spaces within the printed material. The supporting material has to be removed and cleaned completely for a perfect print. With a typical 3D printer removing supporting material is a complex process. Our post process for cleaning the parts is easy and hand free. Our printer’s easy clean system uses steam to melt away the wax support material from even the most challenging print without compromising the part quality and functionality and is 4 times faster than the other similar methods used in the industry.

Applications and Results: For clinical applications, such as 3D printing of conformal bolus or brachytherapy surface molds the choice of material for tissue equivalency is an important consideration. Our printer is able to print 2 types of material; the first one is a UV Curable hard plastic and can be printed in Opaque White, Opaque Black and Translucent Clear. The second one is UV curable elastomeric material which is a rubber-like material similar to commonly used radiotherapy bolus and has 2 different colors, translucent Natural and Opaque Black. The wax support material is in white color, but gets removed completely by post processing. Dosimetrically, for 6 and 15 MV photon beams UV curable elastomeric bolus equivalent material has water equivalency within 1.5% on an average and the UV curable hard plastic has water equivalency of within 2% on average. The 3D printing of patient surface conformed bolus for external beam, Brachy surface mold, and patient weight loss management, patient cervix model obtained from CT data for interstitial HDR treatment validation and custom special locking collets for interstitial implants, MRI accessories, MLC guide block have been printed for validation and/or clinical use to date. Finally, workflow between the clinical treatment planning system (Eclipse) and 3D Printing software is straightforward. 3D custom bolus structure files exported from Eclipse and printed show excellent conformity with an anthropomorphic phantom.

Conclusion: 3D printing is a useful technology in a busy radiotherapy clinic and has a wider application in radiotherapy.

I-37

LA TECHNOLOGY IMPROVES PATIENTS CARE ON 6 HIGH THEORY

Yimin Hu

Cancer Institute and Hospital, Chinese Academy of Medical Sciences and Peking Union Medical College, Beijing, China. E-mail: yiminhu888@163.com

The big and fast development of the medical linear accelerator (LA) technology in the last 10 years, that brings a great clinical achievements by using SBRT (SRS), especially for NSCLC treatment. The modern medical LA has offered us very advanced technologies such as 5 highs:high output dose rate, high speed delivery, high resolution MLC leaves, high dose gradience on the edge of target, and high precision isocenter. Comparison on the modern single beam LA (such as C-arm and Ring based LA) with the ϒ-knife, the key difference between them is the dose rate in the target during the treatment delivery: for the former as the single beam is delivered at the sequential bases that results in the dose rate in target (tumor) is always lower than that in the tissue passing by, but for the later as it uses multi-converging beams which are delivered simultaneously that results in the dose rate in target is always higher than in the tissue passing by. Therefore a next generation LA will logically be using multi-beams instead of one beam that will add an extra sixth high dose rate in target to the present modern single beam C-arm based LA, namely that will integrate the functions of both modern single beam LA and modern ϒ-knife with 6 high beam characteristics. A next generation LA called TCFB (three 120° angled crossing firing beam) unit being developed in China now which will not only integrate all functions of the current single beam LA and γ-knife, but also offer us to do real-time IGRT and DGRT without bringing any extradoses to the patients.

I-38

Alejandro Mazal
Medical Physics Department, Institute Curie Proton Therapy Centre, Orsay, Paris, France.
E-mail: alejandro_mazal@hotmail.com

RNMO-2017

DR. RAMAIAH NAIDU MEMORIAL ORATION-2017

P Gopalakrishna Kurup
Ex-President, Association of Medical Physicists of India (AMPI). E-mail: pgg_kurup@yahoo.com

PD1

MULTI-ROOM PROTON THERAPY FACILITY

Rajesh A. Kinhikar
Medical Physicist, Dept. of Medical Physics, Tata Memorial Hospital, Mumbai, Maharashtra, India.
E-mail: rkinhikar@gmail.com

PD2

CLINICAL NEEDS AND EFFICACY

D.N.Sharma
Associate Professor, Department of Radiation Oncology, AIIMS, Delhi, India.
E-mail: sharmadn@hotmail.com

PD3

COMPACT SINGLE ROOM PROTON THERAPY FACILITY

Vellaiyan Subramani
Senior Medical Physics & Head of Medical Physics Unit, Department of Radiotherapy, Dr. B. R. A. IRCH, AIIMS, New Delhi-29. India.
E-mail: vsampisecretary@gmail.com

PD4

CARBON ION THERAPY FACILITY

Atsushi Kitagawa
National Institute of Radiological Sciences, National Institutes for Quantum and Radiological Science and Technology (NIRS-QST), Chiba, Japan. E-mail: a_kitagawa@nifty.com

Minisymposium Talks

MST-1

PRACTICAL APPLICATION OF MOODLE FOR E-LEARNING COURSES IN MEDICAL PHYSICS

V. Tabakova
Department of Medical Engineering and Physics, King's College, London, UK.
E-mail: vassilka.tabakova@kcl.ac.uk

E-Learning is quickly establishing itself as the environment most suitable for education and training in a dynamic profession such as Medical Physics.
This Mini-Symposium will give a brief overview of e-Learning and will deal with practical aspects of e-Learning in the profession.
It will be delivered in two parts and will demonstrate the free e-Learning platform Moodle.
The first part will deal with: (1) Types and effectiveness of e-Learning, (2) Our contributions in e-Learning in Medical Physics (e-Learning projects and products EMERALD, EMIT, etc.), (3) Features of some majore-Learning platforms in Higher Education, (4) Introduction to the Moodle platform.
The second part will look at the development of an educational e-module on Moodle – Step by Step (based on the example of the moduleon Physics of Medical Imaging). The roles and functions on Moodle will be discussed (Manager, Teacher, Student). The symposium will deal also with Formatting and settings and an illustration of building a complete module will be given (with lectures, coursework, quizzes etc.). It will be discussed how to gather effectively information from Moodle (student participation, grade information, etc.).
Throughout the Symposium the advantages of e-Learning in general and of Moodle in particular will be highlighted and the prerequisites for successful introduction of e-Learning will be discussed.
The symposium is expected to be of interest to educators in all fields related to Medical Physics. No prior knowledge of Moodle is required and no advance preparation is necessary.
The e-Learning platform Moodle has been used continuously for the past 6 years in the MSc Medical Engineering and Physics at King's College London, UK with great success. All users – students and lecturers alike, are finding it very useful, easy to use and intuitive.

MST-2

PREPARING MEDICAL PHYSICISTS FOR FUTURE LEADERSHIP ROLES

Carmel J. Caruana
Department of Medical Physics, Faculty of Health Sciences, University of Malta, Msida, Malta.
E-mail: carmel.j.caruana@um.edu.mt

In today's rapidly changing and highly competitive world, being a good scientist is not sufficient for a professional to prosper; good leadership, managerial and strategic planning skills have become essential. The issue of authentic leadership has become of central concern to all healthcare professions, but it is even more crucial for small professions such as Medical Physics. Preparing future leaders should be done in two ways: first by direct interaction with established and successful leaders who would share their experiences (role modelling) and secondly through a formal leadership course in Medical Physics leadership. This presentation will provide an example of both. The author of the presentation will present his own experiences of leadership and present a practical 'to do' list for successful leadership. This will be followed by a description of the leadership module of the EUTEMPE network in Europe (MPE01 Leadership in Medical Physics - Development of the profession and the challenges for the Medical Physics Expert http://eutempe-net.eu/modules/) which is presently the most comprehensive module available in Medical Physics leadership worldwide. It has been described by participants as a 'Mini MBA for Medical Physicists'. The module achieves its learning objectives using a combination of online and face-to-face phases. The online component consists of a series of sets of compulsory readings, each followed by online discussions targeting real world case studies. The online phase is asynchronous so that participants would not need to take time off their clinical duties and there will not be a problem with time zones. This is followed by an onsite phase (one week long, first two runs of the module held in Prague). Presentation during the onsite are by established leaders and followed by a discussion involving a panel made up of leaders of the profession. Total learning time (readings, presentations etc) is 80 hours.
Examples of recent case studies discussed are:
Case Study 1: Up to now there have only been Medical Physics Expertsin Radiation Oncology and Nuclear Medicine in your country. However, EU Directive 2013/59/EURATOM has recognized the importance of establishing Medical Physics also in Diagnostic and Interventional Radiology. You are having discussions about this issue with your healthcare authorities. Onerepresentative from the Ministry of Health tells you: "I can't understandwhy Medical Physicists are required in Diagnostic and Interventional Radiology. You don't have the high doses you have in Radiation Oncology" How would you tackle it?
Case Study 2: There are 5 chest radiography rooms in your hospital eachrun by a different team of radiographers. You have noticed that one ofthe rooms is repeatedly exceeding the local DRLs which you have established. How would you tackle it? You know that the team of radiographers doesn't like people investigating their techniques.
Case Study 3: Consider your particular Medical Physics department: (a) Describe the present situation of the department (b) Describe a desired future vision: how should the department be in 10 years time? (c) List 3 - 5 gaps between the present situation and future vision (d) List the Strengths and Weaknesses of the department, the Opportunities available and Threats it faces with respect to the achievement of the vison (SWOT analysis) (e) discuss means of reducing each gap using the results of the SWOT analysis.

MST-3

LEADERSHIP AND ENTREPRENEURSHIP: A MEDICAL PHYSICISTS PERSPECTIVE

Arabinda Kumar Rath
Hemalata Hospitals and Research Centre, Bhubaneswar, Odisha, India. E-mail: akrath.dr@gmail.com

Medical Physics as profession has grown leaps and bound in last few decades and continues to play significant role in clinical, research and academic activities in healthcare. The profession is witnessing new challenges due to fast growth of automation of technology that is compounded by new areas of innovations in the ever changing healthcare dynamics. Quality assurance in therapy and diagnostics continue to be the primary job description of the Medical Physicists. With the automation of many of these processes the man hour requirement of Medical Physicists is ever shrinking and many of these tasks are now relegated to other professionals with lesser academic qualifications like dosimetrists and technologists. Ability to remotely access data at high speed at significantly lower cost and in a more safe and secure environment has further reduced the need for physical presence of Medical Physicist in the hospitals. The corporatisation of healthcare and ability to bill services along with cost cutting by healthcare service providers, both Government and private, has added to the stress that Medical Physics as a profession is witnessing.

Being a Medical Physicist turned entrepreneur, I will try throwing light on the road ahead for our profession with examples from my personal journey till date. Standardisation of the academic qualification that remains a challenge has to be addressed by all of us at organisational level if Medical Physicists have to continue making impact in the healthcare continuum. Physicists have to learn the basics of management skills and have to get exposed to healthcare process holistically. These changes need to be included into the curriculum and for those who are already in the profession need to acquire these skills to keep themselves relevant.

Entrepreneurs create jobs and wealth. Our profession has been able to produce only a few entrepreneuers. Innovations using the domain expertise will help consolidate our professional growth as well as keep the cycle of scientific research and product development at a pace that will ensure financial growth and stability. Every speciality undergoes challenges of redundancy and what Medical Physics is witnessing is not different. Course correction and optimal resource management is the call of the day and we need to respond to it quickly.

MST-4

MEDICAL PHYSICS 3.0

Melissa Martin
President, American Association of Physicists in Medicine, Alexandria, Virginia, USA. E-mail: melissa@therapyphysics.com

Medical Physics is at a crossroads. Broad and profound changes in the delivery of healthcare are underway and accelerating. While reimbursements are diminishing, healthcare is faced with new mandates to deliver value-based, personalized, and evidence-based medicine. Grounded in science, innovation, and quantitation, the medical physicist has a noteworthy ability and calling to contribute directly to these challenges. A full realization of this potential, however, necessitates certain changes and a renewed commitment to the practice of physics in medicine. Quality healthcare requires such a progressive perspective; using the best that science and innovation can offer to human health is not only an economic mandate, but also an ethical and a professional one. In any progression of this nature, it is crucial to understand the goals and proactively set a standard that can clarify, unify, and motivate the advancement.

Medical Physics 3.0 (MP3.0) is an initiative to define and practice sustainable excellence in medical physics. MP3.0 re-visits the roots of medical physics and the calling of physicists to use their expertise to contribute to quality healthcare. MP3.0 is based on the core premise that medical physics has a unique position to be a scientific agency and catalyst for safety, precision, and innovation in the development and practice of medicine. MP3.0 aims to foster a culture within medical physics of seizing this opportunity, engaging proactively and meaningfully in patient care, and growing and building upon the unique skills of medical physicists. The initiative is devised as a road map focused on four key areas of progression: expertise, expansion, sustainability, and visibility.

In terms of expertise, MP3.0 is grounded on the global attributes of excellence for medical physics: We consider these unique attributes to be scholarship, innovation, care, and context-awareness. These attributes take unique forms as they are practiced in the four professional contexts of the discipline: clinical, scientific, educational, and administrative. Clinically, MP3.0 encourages medical physicists to gain competence beyond those required for conformance-based practice. The focus is extended to scientific, quality-bound care. Scientifically, MP3.0 sets the model of scientific excellence and innovation in all sub-fields of medical physics in clear distinctiveness from and interplay with associated disciplines of engineering, biomedicine, and informatics. Educationally, MP3.0 encourages updated and enhanced teaching skills to empower trainees and professionals to be at their best to improve human health, nationally and globally. And administratively, MP3.0 encourages leadership and management competence for confident and effective contribution to care.

The above goals of expertise apply to the current domains where physics is currently practiced in medicine. However, the current practice falls short of the notable potential that physics and physical sciences can have in medicine beyond the current practice. Clinically, there are underexplored areas of contribution where care can be enhanced with new physics contributions. These include clinical translation of science that currently remain within academic circles only. Scientifically, physics can be more systematically invoked in broad practice of medicine, including those beyond radiation medicine, the mainstay of medical physics thus far. Educational expansion includes incorporating MP3.0 into the canon of medical physics curriculum. Administratively, encouraging participation of medical physicists in upper administration of healthcare and academic institutions empowers the practice of evidence-based medicine.

The above objectives are effective only if they are enabled within a sustainable model. Towards that goal, MP3.0 aims to seek and model practices that can be achieved and maintained in practical terms using robust pathways, pragmatic hardware and software resources, new manpower models, and justification for resources.

MST-5

NEW HORIZON OF MEDICAL PHYSICS AND SYNERGETIC EFFECT WITH MEDICAL ENGINEERING AND INFORMATION SCIENCE

Kiyonari Inamura
Department of Medical Physics and Engineering, Osaka University, Suita, Osaka Prefecture, Japan.
E-mail: ina-kiyo@mue.biglobe.ne.jp

Purpose: To bring young investigators good opportunity for acquiring result of research and development in three areas of medical physics, medical engineering and medical informatics. Also to get rich harvest by synergetic effect between them.
Materials and Methods: Survey was done by collecting recent information and finding new horizons from international conferences such as AAPM, IOMP, ICBME, MEDINFO, CARS and others. My personal experience of 55 years in both areas of medical physics research in Osaka University and medical engineering in NEC Corporation is considered.
Examples of the Surveyresults: (1) New horizon of medical physics, (a) Knowledge based treatment planningutilizing a learninghealthsystemwithstrongerlinkagesbetweengenomic, pathology and clinical databases employing cloud-based global collaboration for radiotherapy, (b) Decisionmaking in adaptive radiotherapy, (c) Boron neutron capture therapy employing accelerators, (i) Compact MRI linac that works with a split MRI and fits in the vault, (ii) MRI-guided focused ultrasound thermal ablation. (d) Biomechanical modeling of anatomical response over the course of therapy. Example: deformable image registration, (e) Nanometer-scale Monte Carlo simulations and mechanistic biological modeling, (f) Computational biology: computational methods for dose-response modeling at the molecular, cellular and tissue levels, (g) Computer aided surgery for assisting minimally invasive therapies, (i) MBIR Model-Based Image Reconstruction for image guided interventions, (ii) Multiscale digital patient, (h) PPPM Predictive, Preventive and Personalized Medicine by data science models that can convert the knowledge to clinical predictions, (i) Microfluidics and nanofluidics, (j) DNA repair genes and radiation sensitivity, (k) Quantitative imaging biomarkers, (l) Digital breast tomosynthesis as a new mammographic modality separate from full field digital mammography, (m) Portable CT for disaster ambulance in earthquake, (n) Open source hardware: Publicly available hardware for anyone can study, modify, distribute, sell the design or hardware based on that design making modifications to it, sharing knowledge and encouraging commerce through the open exchange of designs. (2) New horizon of biomedical engineering, (a) Tissue mechanics, (b) Collaborative cancer research, (c) Intraoperative imaging, (d) Surgical robotics and navigation, (e) Vivo photoacoustic tomography and vivo photoacoustic microscopy of the human skin, (3) Stimulation from information sciences, (a) Artificial intelligence, (b) Big data application, (c) Cloud computing, (d) Optical flow technology application, (e) Multi-dimensional data-driven research, (f) Radiogenomics studies, (g) Sharing common ontology.
Why Medical Physics is Required for Medical Research?: (a) To avoid mistake/misleading, (b) To avoid abuse/waste of time, (c) To get capability/flexibility to remodeling and redesign in cycles mentioned below, (d) To get both accuracy and robustness, (e) Good chance is brought by physicist’s approach: Serendipity and abduction.
Cycles of Engineering Approach: Correction of unexpended performance at every node of a cycle chain: Materials check, device check, configuration check, system optimization, simulation, statistics, and performance check
Interaction between Physics and Engineering: (a) From different methodological approach, (b) From different pathways, definite truth and achievable pursuit, (c) From common field of approach for the same clinical target, (d) By common definition of ontology.
Synergetic Effect by Remodeling: High level of clinical attainment isrearized by rapid feedback and remodelling in cycles mentioned above.
Conclusion: The new strength is brought by sharing of results of investigation of medical physics, engineering and information science.
Truth finding, performance check and optimization are key issues all the time.
Common sharing of solution, goal and different methodology brings new stimulation to step forward.
Synergetic effect with high level of clinical result is brought by rapid feedback and remodeling in cycles of engineering approach.

MST-6

THE NEED FOR AFFORDABLE TECHNOLOGIES BASED ON CMC, VELLORE EXPERIENCE

Paul Ravindran
Professor of Radiation Physics, Department of Radiation Oncology, Christian Medical College, Vellore, India.
E-mail: paul@cmcvellore.ac.in

Introduction: Cobalt-60 was first used for treating cancer at the London Regional Cancer Centre, London, Ontario, Canada on 27th October 1951 and since then telecobalt units have been the main radiotherapy treatment modality in most cancer centres in the middle and low income countries. The last two to three decades have seen considerable advancements in linear accelerator technology, which has enabled delivery of high doses precisely to the target volume thus increasing the tumour control probability and reducing the normal tissue complication probability. The Radiotherapy department in Christian Medical College, Vellore has a Telecobalt unit as well as Linear Accelerators. Patients are treated based on their preference. However patients requiring specialized techniques for tumour control and reduced toxicity are treated on the Linear Accelerator.
Materials and Methods: Our institution has two Varian linear accelerators, a Clinac 2100C/D and a TrueBeam STX, both capable of delivering IMRT, Rapid Arc and IGRT and an

Equinox Cobalt unit. About 1/3rd of the patients in our clinic are treated with the Cobalt unit and of which nearly 50% are brain and head and neck cancer patients. Apart from the initial low investment and low maintenance cost, the down time of the cobalt unit is very low thus keeping the total cost per treatment affordable for the low income group. It would be deal and cost effective if precise treatment delivery methods such as 3D Conformal Radiotherapy (3D CRT) and Intensity Modulated Radiotherapy (IMRT) could be delivered with the cobalt units.

A feasibility study to develop prototype multi-leaf collimator for delivery of 3D CRT with the cobalt unit was performed in our institute, though this was not used clinically, the dosimetric study performed on this provided encouraging results.[1] Narrow beam collimators and couch mount for stereotactic patient fixation were developed to study the use of telecobalt units for stereotactic delivery of radiation. The dosimetry performed with the narrow beam collimators and the 'end to end' tests with in-house stereotactic phantom showed that it is feasible to deliver Stereotactic Radiotherapy (SRT) with the telecobalt units. The study concluded that in centres where linear accelerator is not available, cobalt is a viable alternative for stereotactic radiotherapy procedures.[2]

Conclusion: Telecobalt provides an acceptable megavoltage photon beam for clinical applications having energy equivalent to the effective energy of a 4 MV linear accelerator. If the 5 mm build-up thickness is preserved by proper understanding of physics, there will be no problem of skin morbidities.[3] Implementing the multi-leaf collimator and the intensity modulated delivery techniques in telecobalt units would enable providing advanced treatment techniques at relatively low cost. A recent study has predicted increased cancer burden in India due the increase in life expectancy and the changing life style.[4] The availability of radiotherapy treatment facilities is less than half of the requirement and this is likely to increase with the increase in cancer burden. Providing affordable high precision treatment facility with telecobalt units would certainly bridge this gap.

References

1. Singh IR, Ravindran BP, Ayyangar KM. Design and development of motorized multileaf collimator for telecobalt unit. Technol Cancer Res Treat 2006;5:597-605.
2. Singh RR, Ravindran P, Nizin PS, Ayyangar K. Dosimetric study of the narrow beams of 60Co teletherapy unit for stereotactic radiosurgery. Med Dosim 2000;25:163-9.
3. Ravichandran R. Has the time come for doing away with cobalt-60 teletherapy for cancer treatments. J Med Phys 2009;34:63-5.
4. Research Communication Burden of Cancer and Projections for 2016. Indian Scenario: Gaps in the Availability of Radiotherapy Trea. Available from: http://www.scholar.googleusercontent.com/scholar?q=cache:Os1Wx0J4ESUJ:scholar.google.com/+Cancer+control+program+in+india+radiotherapy+units&hl=en&as_sdt=0,5&as_vis=1. [Last accessed on 2017 Sep 09].

MST-7

PROJECT INTRODUCTION AND A COMPENSATOR BASED IMRT FOR COBALT

K. N. Govinda Rajan

Department of Medical Physics, PSG Hospitals, Coimbatore, Tamil Nadu, India.

E-mail: kngrajan@gmail.com

The main workhorse for cancer treatment in the low income countries is still a teletherapy Cobalt machine and according to WHO this situation is likely to continue for another 6 to 7 years. With the result, poorer patients in these countries are deprived of technologies for treating advanced stages of the disease, that are available only on linacs or other expensive treatment delivery equipment (like Tomotherapy etc.). The availability of advanced technologies (e.g. linac) were often superior to telecobalt machine causing a drastic decline in the demand for telecobalt equipment. Linac technology is, however, very expensive (and unaffordable to poorer patients) and also has high operation cost and complexity.

Developing advanced treatment delivery technologies like IMRT/IGRT for a telecobalt machine, on a cost effective basis, would offer the poorer patients advanced cancer treatment on a telecobalt machine. Using the simplest of delivery technologies would make treatment verifications a lot simpler. This would give a new lease of life to telecobalt equipment which can coexist with linac and offer the same level of cancer care for poorer sections of the population and for cases that can be adequately treated with telecobalt.

With the above objective Dr. Eric Ford, Professor of Radiation Oncology, University of Washington, Seattle, USA and I assembled a team with Panacea Medical Technologies Pvt. Ltd., Bangalore as the commercial partner and Paterson Cancer Center, Chennai as a clinical partner to develop the advanced IMRT technology for the Indian Telecobalt unit Bhabhatron, in India, since it was the least expensive system in the market. The team also includes a full time research fellow and other experts as well who would contribute towards research, Education and Training, administration activities etc.

The team prepared a grant proposal "A cost-effective radiation treatment delivery system for low- and middle-income countries" and after several revisions submitted the final version to the National Cancer Institute (NCI), USA for competitive funding. NCI approved the proposal and granted US $2.9 million for the implementation of the project. The duration of the project is for 5 years starting from May 2017. The commitment is for developing and constructing an IMRT capable telecobalt machine and in the second phase an IGRT telecobalt machine. The team has also solicited the cooperation and participation of BARC in this project.

A key component of the system being designed is the use of compensators for IMRT modulation. While there are different ways of implementing the IMRT technology, compensator based IMRT technology has many advantages in addition to being less QA intensive, less time consuming and less expensive. On successful completion of the prototype phase of the project, the team will initiate clinical trials at the partner site.

The presentations of other speakers in the mini-symposium namely Dr. Eric Ford, Dr. Lakshmi Santanam and Dr. Paul Ravindran would reinforce the belief that telecobalt still has lot of relevance in radiation therapy for many cancer patients and what we need today is increased sophistication in the telecobalt treatment delivery techniques and technologies that is the subject of this symposium.

MST-8

PRINCIPLES OF DESIGN FOR AFFORDABLE TECHNOLOGIES

Eric Ford
Department of Radiation Oncology, University of Washington, Seattle, Washington, USA.
E-mail: eford@uw.edu

Radiotherapy (RT) will see strong growth in the coming decades, driven both by the healthcare needs and the economic benefits. The Global Task Force on Radiotherapy for Cancer Control, for example, suggests that scaling up RT will result in a net economic benefit of US$11 to $280 Billion per country over the next 20 years. However, the technologies developed for industrialized countries are often challenging to implement in some settings due to cost, complexity, safety, staffing requirements, and infrastructure needs. We will review the implications of this drawing on recent surveys of the performance of linear accelerators in sub-Saharan Africa where resources are often extremely limited and yet growth and demand are strong.
All of this calls for new solutions to RT technologies which are more cost-effective and less complex. Any such solution must be capable of intensity modulated radiotherapy (IMRT), whose use is justified even in a resource-limited setting due to the decreased treatment-related morbidity and thereby reduction in the overall burden on the health care system during and following cancer therapy. Useful principles from design and human factors engineering will be reviewed including: (1) Automation of key tasks, which improves efficiency, reduces the reliance on highly-trained staff and improves safety, (2) Training and education which are key components in the rollout of new technologies, (3) A risk-based approach to development. A useful benchmark for this is AAPM Task Group 275, concurrently in completion with AAPM, (4) The reduction or elimination of inspection (QA) as the primary method for ensuring safe and accurate delivery, (5) Design approaches which are inherently fail-safe and/or prevent the user from making mistakes. Several examples will be reviewed.
Through best-practices in design cost and complexity can be greatly reduced and reliability and safety can be improved. This will make RT more widely available for patients in need.

MST-9

COBALT TREATMENTS ARE STILL RELEVANT IN A LINACS WORLD: A MR GUIDED CO 60 MACHINE PERSPECTIVE

Lakshmi Santanam
Department of Radiation Oncology, Washington University School of Medicine, Louis, Missouri, USA.
E-mail: lsantanam@wustl.edu

An MR-IGRT system consisting of a 0.35T magnetic resonance scanner with 3 Co^{60} heads has been in clinical use for around 3 years. Patients with treatment sites that included breast, head and neck, pelvis, thorax, abdomen and others are currently being treated. An integrated Monte Carlo treatment planning system is used for planning with 3D and IMRT techniques. In addition to using the MR for IGRT, online Adaptive Radiotherapy (ART) and motion management (Gating) can also be performed. Before the clinical implementation of the system, treatment plans were done to compare Co^{60} IMRT and LINAC plans for various sites and it was found to be comparable with respect to PTV coverage and OAR sparing. In addition the performance of the planning and delivery systems was evaluated using the AAPM TG119 benchmark plans. Trials to evaluate the use of online adaptive MR-SBRT for oligometastatic cancers and treatment of early stage breast cancers using Accelerated Partial Breast Irradiation (APBI) are currently being done. Multi institutional clinical trials are currently being developed to evaluate the benefits of this new technology. Results from these studies and our clinical experience with the system and its limitations will be discussed.

MST 10

PROGRAMMATIC SUPPORT FOR THE DEVELOP OF INDIGENOUS TECHNOLOGIES IN CANCER CARE

D N Badodkar
Bhabha Atomic Research Centre, Department of Atomic Energy, Mumbai , Maharashtra, INDIA.
E-mail: badodkar@barc.gov.in

MST-11

LATEST PERFORMANCE EVALUATION OF X-RAY CT

Katsumi Tsujioka
School of Health Sciences, Fujita Health University, Toyoake, Japan. E-mail: tsujioka@fujita-hu.ac.jp

It is important that we evaluate performance of the MDCT. The performance evaluation of the MDCT cannot often support by the conventional method. Particularly, a wrong evaluation result may be given by the conventional rating system by the new iterative reconstruction. This presentation describes a new performance rating system for MDCT and iterative reconstruction. (1) Spatial resolution (modulation transfer function: MTF, slice sensitivity profile: SSP), (2) Contrast resolution (image noise, contrast to noise ratio: CNR, noise power spectrum: NPS), (3) Temporal resolution (time sensitivity profile: TSP).
MPR display using multi-slice CT is very useful in current diagnosis. And isotropic resolution is important for good MPR display images. In this lecture, I will introduce the evaluation technique of MPR display.

MST-12

LATEST CT SCANNING TECHNOLOGIES IN JAPAN

Koichi Sugisawa
Department of Radiology, Keio University Hospital, Tokyo, Japan. E-mail: tsujioka@fujita-hu.ac.jp

Keio University Hospital is a large hospital in Tokyo. The latest CT apparatus is in operation in the radiological department. Even with the latest CT, CT technology is important for providing a good CT image. In addition to CT scan parameter setting technique, CT injection technique is also important

for CT examination. In this lecture, I will introduce the CT examination at Keio University Hospital.
Also I will give a lecture on education and academic activities of Japanese radiological technologists. These lecture contents will be important reference for radiological technologists other than Japan.

MST-13

INCIDENTS AND ACCIDENTS IN CT AND INTERVENTIONAL RADIOLOGY

S. D. Sharma
Radiological Physics and Advisory Division, Bhabha Atomic Research Centre, Mumbai, Maharashtra, India.
E-mail: sdsbarc@gmail.com

Computed tomography (CT) scanning and fluoroscopically guided interventional procedures are well accepted and acknowledged considering their clinical importance. CT scanning is used for a number of diagnostic procedures. The radiation dose to the patient in CT scanning is higher in comparison to patient dose in x-ray radiography. However, this is not a question of concern considering the medical value of the diagnostic information acquired from the CT scanning. Interventional radiology (IR) is a well-established procedure which is considered as an alternative to invasive surgery. With the advancement of robotics and specialized catheters, doctors are attempting increasingly complex IR procedures. The time of IR procedure ranges from a few minutes to a few hours depending on the type of clinical case and hence dose to the patient is relatively higher in this process. In fact, CT and IR are generally classified as high dose radiology procedures. Both CT scanning and IR procedures are used in several clinical conditions. CT scanners are used mainly for diagnosis. However, CT guidance is also used in many interventional procedures. In routine CT examinations, dose to the skin and other organs of the patient are not very high to cause any immediate radiation damage. But for complex CT guided interventional procedures skin dose may be of the order of a Gy. Even though, it is well known that radiation dose received by the patients in these radiological procedures are relatively high but practiced due to the requirements of the given clinical conditions. Radiation incidents/accidents in these procedures are not very common but in some situations the dose to patient reaches the threshold limit for deterministic effects such as hair loss, skin erythema, and cataract. The skin injuries can vary from mild erythema to deep skin ulceration. The incidental/accidental situations in these radiology procedures arises due to several contributing factors including poor knowledge of equipment, faulty computer software, lack of periodic quality assurance programme, improper training to operating personnel, lack of knowledge of radiation protection, high workload, insufficient staffing level, and use of inappropriate protocols.
A number of incidents/accidents concerning patients that showed signs of deterministic effects after diagnostic CT examinations and interventional radiology procedures have been reported. Very recently in India, we have come across two clinical cases of IR where dose to the patient is very high. In the first case, the patient underwent endovascular embolization. On investigation, it was noted that the procedure was complex which took more than 3 hours with a beam on time of about 90 minutes. The dose estimate indicated that the patient received skin dose in excess of 10 Gy and hence the severe skin reactions. The second case was related to ventricular pacemaker implantation which took about five hours including fluoro-time of about 100 minutes. The dose to the patient was more than 5 Gy and hence the patient had severe skin injuries.

MST-14

ACCIDENTS AND UNUSUAL INCIDENTS IN NUCLEAR MEDICINE

Pankaj Tandon, Ashish Ramteke
Radiological Safety Division, Atomic Energy Regulatory Board, Mumbai, Maharashtra, India.
E-mail: pantan@gmail.com

Nuclear medicine is a branch of medical science that uses unsealed radionuclide to diagnose and determine the severity of or treat a variety of diseases, including many types of cancers, heart disease, gastrointestinal, endocrine, neurological disorders and other abnormalities within the body. The use of unsealed radioisotopes in itself is vulnerable for different kinds of radiological implications, if not handled with proper precautions. In dealing with the nuclear medicine procedures, one has to be able to identify hazardous situations which can result in accidental exposure. A safety culture is required to be inculcated in the facility so that the collection of information on unusual events and accidents is available. The information so collected provides material that can be used to prevent recurrence of such unintended incidents.
The assurance of all practicable measures to minimize the likelihood of unintended or accidental medical exposures is important. In case, such exposures occur, prompt investigation should be carried out and corrective actions should be implemented then and there itself. There is a wide range of radiation incident that can occur in hospitals like; overexposures of patients, failure in management of radioactive materials, contamination etc. The safety assessment in the conquest of foreseeing the possible causes of radiation incident can be envisaged by investigating the interface of procedures in NM with i) the patient, ii) the radiation worker, iii) the public and iv) the environment at large. During i) Investigating the patients' interface with NM procedures, the possible radiation incidents can be related to referrals/prescription of the physicians, identification of patients information, administration of radiopharmaceutical, discharge from department etc. ii) On investigating the worker's interface with activities in NM, it can be envisaged that the possible radiation incidents can be in conjunction with ordering of radiopharmaceutical, its transport, receipt and unpacking, storage, preparation and administration of radiopharmaceutical, radioactive waste management etc. iii) whilethe public related incident can be envisaged in conjunction with transport in public domain, storage of radioactive material, handling of sources, radioactive patient etc. and iv) whereas, the environmentgets contaminatedduetoradioactive waste disposal, etc.
Literature review indicates that despite administrative and procedural systems being in place for checking requests for patient examinations and other activities in NM departments, mishaps have been reported worldwide. It is therefore need

of the hour that emphasise is given on robust procedures and training for all staff working in departments where radioactive material is handled. Alongside, there is a need to establish a local incident reporting and investigation system in order to create awareness among the staff of the potential for things to go wrong and at the same time promote the review and improvement of systems based on experience. The newly launched system e-LORA of AERB, India has this provision of incident reporting. Unless a culture of openness in reporting the smallest of incident is adopted by us, a strong and radiation incident proof working environment cannot be achieved.

MST-15

RADIATION INCIDENTS AND ACCIDENTS IN RADIOTHERAPY

Golam Abu Zakaria

Department of Medical Radiation Physics, Gummersbach Hospital, Academic Teaching Hospital of the University of Cologne, Gummersbach, Germany.
E-mail: g.zakaria@emw.hs-anhalt.de

The main application of radiotherapy is in the treatment of cancer. The aim in radiotherapy is to deliver a precisely predetermined dose to the malignant target region without causing injury to surrounding healthy tissue. An accident or a misadministration in radiotherapy is significant if it results in either an underdose or overdose, whereas in conventional radiation protection only overdoses are generally of concern. Therefore all procedures should be performed in such a way as to optimize the dose to tumor volume and to minimize the dose to healthy tissue. According to ICRU Publication 86, a Quality Assurance Program should be established considering the following important points for an overall preventive measure. (1) Organization, (2) Education and training, (3) Accepting testing and commissioning, (4) Follow up of equipment faults, (5) Communication, (6) Patient identification and patient charts, (7) Specific recommendation for External Beam Radiotherapy, (8) Specific recommendation for Brachytherapy.

In this presentation, some case histories of major accidental exposures in radiotherapy will be shown in the beginning, after that clinical consequence of accidental exposures will be described and finally recommendations for prevention will be given.

MST-16

DOSIMETRIC CHALLENGES OF PHOTON BRACHYTHERAPY IN TERMS OF ABSORBED DOSE TO WATER

Golam Abu Zakaria, Ulrich Quast[1], Theodor Kaulich[2]

Department of Medical Radiation Physics, Gummersbach Hospital, Academic Teaching Hospital of the University of Cologne, Gummersbach, [1]Radiology Center, University Hospital, Essen, [2]Department of Medical Physics, University Hospital for Radiooncology, Tuebingen, Germany. E-mail: g.zakaria@emw.hs-anhalt.de

In radiation therapy the dose to be applied is prescribed in terms of the absorbed dose to water. In photon brachytherapy (BT), however, radiation sources are still calibrated in terms of the reference air kerma rate or the air kerma strength. The clinical medical physicist has to convert the data needed for patient treatment by calculations. Brachytherapy treatment planning systems mostly use the AAPM TG-43 algorithm, assuming to have only one source, an infinite water medium and no heterogeneities e.g. no applicator. Thus, regarding these uncertainties, the measurement of distributions of absorbed dose to water in the vicinity of BT sources is necessary for new BT treatment techniques prior to clinical application.

For experimental dosimetry, the response R of a dosimetry detector has to be known at the position of measurement (r, θ). The response can be described as a product approach of two independent, energy dependent components, the extrinsic response and the intrinsic response: $(\bar{E}_{mean}) = R_{ext}(E)\ R_{int}(E) = ((D_{Det})/(D_w))\ (M - M_0)/D_{Det}$. The mean photon energy $\bar{E}_{mean}$ can be derived from Monte Carlo calculations, but only a few centres have the possibility of MC-simulations. The recently published photon BT quality index Q^{BT} characterizes the penetration power and the potential of producing scatter-radiation and allows to determine $\bar{E}_{mean}$. Being defined as $Q^{BT}(E) = D_{prim}\ (r = 2cm)/D_{prim}\ (r = 2cm) \cong (1/4)e^{-\mu\ 1cm}$, Q^{BT} can be received easily from internet available primary and scatter separated (PSS-) dose data for all commercially available BT photon sources yielding the effective mean energy at the AAPM TG-43 reference position ($r = 1$ cm, $\theta = 90°$) via tabulated $\mu\ \bar{E}_{eff}$ data. Further published data allow to derive $\bar{E}_{mean}(r,\theta)$ for any position of interest in the vicinity of BT-photon sources for typical BT dosimetry detectors.

MST-17

NEW DEVELOPMENTS IN IMAGE BASED GYNAECOLOGICAL BRACHYTHERAPY

Hasin Anupama Azhari

Department of Medical Physics and Biomedical Engineering, Gono Bishwabidyalay (University), Savar, Dhaka, Bangladesh. E-mail: ahasinanupama@gmail.com

The use of 3D imaging for Brachytherapy (BT) treatment planning has dramatically increased over past decade. Image guidance in Brachytherapy generally refers to both imaging needed for treatment planning and treatment verification. The rapid development in imaging techniques has aided the brachytherapist accurate delineation of structures of interest as it is moving from reference dosimetry to clinical target volume. For many decades, the fundamental system (Manchester system) based on extensive clinical experience, have been developed for the treatment of gynaecologic carcinoma according to ICRU report 38. Treatment planning based on 3D imaging, in combination with remote afterloader BT delivery, promises opportunity to improve patient outcome. 3D based image planning uses anatomical and functional information to conform the dose distribution to the target volume. Guidelines have been formulated to adapt image guided Gynaecological BT to the previously used technique and to plan and report the new technique. However the intrinsically inhomogenous dose distributions in BT make the production of reproducible treatments from patient to patient or even from fraction to fraction an issue. Therefore at least during a transition phase, the standard systems and applicator loading (with which one has gathered experience) should still be used as a starting point for treatment planning from which the closer adaptation of DD can follow.

Recently the second part of the GYN GEC ESTRO working group recommendations is focused on 3D dose-volume parameters for brachytherapy of cervical carcinoma. Methods and parameters have been developed and validated from dosimetric, imaging and clinical experience from different institutions. Cumulative dose volume histograms (DVH) are recommended for evaluation of the complex dose heterogeneity. Dose volume parameters derived from the DVH such as D90 and D100, the minimum dose delivered to 90 and 100% of the volumes of GTV, HR CTV and IR CTV, should be checked. The volume, which is enclosed by 150 or 200% of the prescribed dose (V150, V200), is favored for overall assessment of high dose volumes. V100 is recommended for quality assessment only within a given treatment schedule. For Organs at Risk (OAR) the minimum dose in the most irradiated tissue volume of 0.1, 1, and 2 cm^3; optional 5 and 10 cm^3 must be studied. Also in ICRU 89, it is recommended to keep D98% as the primary parameter and D90% in the case of research-oriented analysis. The minimum dose values for reporting OAR is $D_{0,1cm}{}^{3}$ and D_{2cm3} as in case of OAR due to heterogeneity of absorbed-dose within the organ walls, OAR. Applying these recommendations to 3D image guided Gynaecological Brachytherapy, treatment dose prescription to traditional reference points such as ICRU point A becomes less mandatory and however reporting dose to point A should be continued.

MST-18

HYBRID IMAGING: APPLICATIONS OF PET-MRI IN NEURODEGENERATIVE DISORDERS

Nand K. Relan

Stony Brook University Medical
Center, Stony Brook, New York, USA.
E-mail: nand.relan@stonybrookmedicine.edu

Clinical techniques are limited in its evaluation of neurodegenerative disorders due to its low clinical accuracy in the early diagnosis of these disorders. Nuclear imaging has the advantage via SPECT, SPECT-CT or PET-CT imaging to detect functional changes in the brain before they are fully manifested clinically. However, these modalities have limited anatomical details that can easily miss contributing or underlying pathology that may underwrite to patient presentation. The simultaneous acquisition of Fluorodeoxyglucose Positron Emission Tomography together with Magnetic Resonance Imaging (FDG PET-MRI) localizes pathological areas of interest adding significant anatomical and structural detail, and improves diagnostic accuracy. In addition, PET-MRI may show an underlying tumor, epileptic focus, inflammatory processes, or vascular causes of patient symptoms such as multi infarct dementia. Overall FDG PET-MRI of the brain demonstrates additive value in evaluating patients with suspected dementia by increasing diagnostic confidence, limiting radiation compared to CT, and providing more comprehensive information not normally obtained on PET-CT. PET-CT can be used to distinguish the myriad of comorbidities contributing to patient symptoms and incidental findings in which further follow up is warranted. The focus of this talk will be to discuss principles, techniques and clinical applications of simultaneous FDG PET-MRI in evaluating neurodegenerative conditions. Furthermore, key imaging findings resulting from neurodegenerative disorders and inflammatory conditions will be presented.

MST-19

IMPORTANCE OF QUALITY CONTROL IN NUCLEAR MEDICINE

Subhash Chand Kheruka

Department of Nuclear Medicine, SGPGIMS, Lucknow,
Uttar Pradesh, India. E-mail: skheruka@gmail.com

Nuclear medicine is critically dependent on the accurate, reproducible performance of clinical radionuclide counting and imaging instrumentation. Quality control (QC), which may be defined as an established set of ongoing measurements and analyses designed to ensure that the performance of a procedure or instrument is within a predefined acceptable range, is thus a critical component of routine nuclear medicine practice. An extensive series of parameters has been developed over the years for acceptance testing and performance characterization of □-cameras, SPECT and PET scanners, and other nuclear medicine instrumentation. And detailed data acquisition and analysis protocols for this purpose have been promulgated by the National Electrical Manufacturers Association (NEMA), the American Association of Physicists in Medicine (AAPM), IAEA, IEC and other regulatory, advisory, and professional organizations.

Proper record keeping greatly facilitates detection of gradual deterioration of performance over an extended period of time, by analyzing the results for degradation and initiating corrective action when necessary.

A baseline set of quality control results should be recorded, after a thorough evaluation of the system at installation and acceptance testing, to serve as a reference for the life of the equipment. These can be used as a basis for developing detailed protocols for individual systems and models of equipment.

As advances in medicine occur at a rapid rate, the review and update of guidelines, such as these, should take place at regular intervals and should be considered to be part of the quality assurance process.

MST-20

OPTIMIZATION OF RADIATION SAFETY AND EXPOSURES IN NUCLEAR MEDICINE

Pankaj Tandon

Radiological Safety Division, Atomic Energy
Regulatory Board, Mumbai, Maharashtra, India.
E-mail: drpankaj@aerb.gov.in

The ultimate goal of any type of medical imaging procedure is to obtain the best image quality while delivering the smallest radiation dose possible to the patient. The best image quality though, does not necessarily give the correct diagnosis for a given medical condition at the lowest possible dose to the patient. Additionally the vast number of alternative diagnostic modalities available today and their rapid evolution make the choice of the most suitable modality for a particular medical condition very difficult, if dose to the patient is to be considered as a major constraint. It is therefore very important to know the dose received by the patient from the different modalities to arrive at the same diagnostic result. This is especially important in Nuclear Medicine where the different modalities produce images of the metabolic function of the human body and they are more likely to arrive at the same diagnostic outcome. The aim of this article is to give an overview of the methods used to optimise the diagnostic value of the images produced by Nuclear Medicine diagnostic modalities.

Nuclear medicine is a rapidly growing discipline that employs advanced novel hybrid techniques that provide unique anatomical and functional information, as well as targets for molecular therapy. Concomitantly, there has been an increase in the attention paid to medical radiation exposure. A radiological justification for the practice of nuclear medicine has been implemented mainly through referral guidelines based on research results such as prospective randomized clinical trials. The International Commission on Radiological Protection (ICRP) recommends diagnostic reference levels as a practical mechanism to optimize medical radiation exposure in order to be commensurate with the medical purpose. In many countries, various societies of Nuclear Medicine have been implementing radiological optimization through a survey of the protocols on how each hospital determines the dose of administration of each radiopharmaceutical. In the case of nuclear medicine, radiation exposure of caregivers and comforters of patients discharged after administration of therapeutic radiopharmaceuticals can occur; therefore, optimization has been implemented through written instructions for patients, based on national recommendations. The assessment of occupational exposure in Nuclear Medicine (NM) is constant and mandatory process. Radiation protection safety culture, quality assurance programme, different protective measures and acquired automated infusion systems, which affect the doses of optimization, were implemented in NM department. It is important to evaluate NM staff doses and influencing factors in all the modalities being used in nuclear medicine facilities. The Nuclear Medicine Specialist is responsible for the clinical management of the patient undergoing a diagnostic or therapeutic nuclear medicine procedure. This includes the decision to proceed with a Nuclear Medicine procedure based on the specialist's knowledge of the potential risks and benefits of the procedure, taking into account the clinical information, and the sensitivity and specificity of the procedure. When considering the justification for a medical exposure, the benefit is weighed against the detriment, including radiation effects. For diagnostic procedures the potential detriment is the risk of inducing cancer. This risk is greater in children and decreases with age. For effective doses greater than 100mSv, the overall lifetime risk of fatal cancer is estimated to be 5% per Sv. Whilst there is no epidemiological evidence of an increased risk below about 100 mSv, using the LNT hypothesis it is possible to extrapolate the risk to lower doses although thereis uncertainty in such estimates. An approximate guide is given by age-specific mortality risk factors in a general population. For an effective dose of 20 mSv, the nominal risk is about 1 in 1200 for adults aged 30 to 60 years at the time of exposure. For adults aged 70 or more the risk falls to less than 1 in 3000. However, for children up to 10 years old the risk is about 1 in 450.

MST 21

ROLE OF MOLECULAR IMAGING IN ONCOLOGY WITH SPECIAL REFERENCE TO RADIATION ONCOLOGY

J K Bhagat

Sr. Consultant & Head, Department of Nuclear Medicine, Bhagwan Mahaveer Cancer Hospital & Research Centre, Jaipur, Rajasthan, India.

E-mail: drjkbhagat@yahoo.co.uk

MST-22

PHYSICS OF MEDICAL ISOTOPE PRODUCTION

C. Rangacharyulu

Department of Physics & Engineering Physics, University of Saskatchewan, Saskatoon, Saskatchewan, Canada.

E-mail: chary.r@usask.ca

Radioactive isotopes are playing increasingly important roles in medical diagnostics and therapeutic applications. These isotopes are produced either at nuclear reactors or particle accelerators. The reactions are induced either by charged particles or neutral beams of neutrons or photons. There are some basic physics principles at work to help determine the production channels and to optimize the irradiation protocols for both economic reasons and also to ensure the quality of the product and minimize interfering channels of other isotopes.

The first criterion is the energetics of the nuclear reaction which yields the isotope of interest. This is represented by a single physics parameter known as the Q value of the reaction. If the Q-value is negative, the process does not occur below a threshold energy of the projectile. By choosing the kinetic energies of the projectiles or the energies of photons above the threshold for the process, one can induce the production. The second criterion is to maximize the rate of production. In this regard, there are at least two considerations. First is to the find the projectile energies where the yield is maximum. The second is to minimize the production of interfering isotopes, if any. These details are characterized by the "cross section" of the process. The task is to make a judicious choice of projectile energies to strike a balance between the two criteria. The Brookhaven Laboratory website[1] and its mirror sites have all the available data, a compilation of the worldwide research carried out in the last few decades. This is a public domain website accessible to anyone interested and needs this information.

As medical isotopes are radioactive, they decay while being produced. As the decay rate at any instance is proportional to a) the number of atoms of the species and b) inversely related to the lifetime of the isotope, the isotope production shows an exponential growth. Thus the continuous irradiation with a constant flux of projectiles on a target material of fixed quantity results in a saturation activity.[2] This phenomenon means an enterprise of decreasing returns for prolonged irradiations.

This symposium will present the audience the physics reasonings and introduce them to the website so that they

can become familiar and use them for their applications. I will also go over the radioactive decay details of the parent-daughter equilibrium activities so that the participants will appreciate the intricacies of isotopes production whether it is at a nuclear reactor or a particle accelerator facility.
I will illustrate these aspects of physics with concrete examples of most commonly used isotopes such as the production of FDG, ^{99m}Tc and other fission products. Time permitting, the participants will be encouraged to address the isotopes of their personal interest, if any.

MST-23

RADIOBIOPHOTONICS & NORMAL TISSUE TOXICITY

Dr. Rao V. L. Papineni, Dr. Shahid Umar.
School of Medicine, University of Kansas Medical Center,
PXI. Inc, and PACT & Health USA.
Email: docpapineni@gmail.com

Visualization via "light" coupled with "ionizing radiation" has made a profound impact both in understanding the disease mechanism and its treatment. Rapid advances in photonics also aided in bridging the physics and medicine towards the new front in Cancer Radiation Therapy. This Session brings to forefront "Radiobiophotonics" bringing to fold the rapidly growing fields pertaining to biophotonics in relation to radiobiology and Radiation Therapy. These fields, Molecular Image Guided Radiation Therapy (MIGRT), X-Ray Luminescence, Radiobioluminescence, Microscopy, Cherenkov Luminescence and it's role in microdosimetry, metastatic tumor phototherapy, activated nanodelivery and particle therapy beam tracking will be discussed. The normal tissue toxicity assessment during radiation therapy or Nuclear Accidents using Radiobiophotonics will be elaborated. Epithelial regeneration model will be used to describe the use of photonics in assessing Normal tissue injury and pharmacological intervention. Epithelial regeneration is critical for barrier maintenance and organ function after intestinal injury. The intestinal stem cell (ISC) niche provides Wnt, Notch and epidermal growth factor (EGF) signals supporting Lgr5(+) crypt base columnar ISCs for normal epithelial maintenance. Little is known about the regulation of the ISC compartment after tissue damage. Exposure to high doses of radiation triggers a number of potentially lethal effects. Among the most severe is the gastrointestinal (GI) toxicity syndrome caused by the destruction of the intestinal barrier, resulting in bacterial translocation, systemic bacteremia, sepsis and death. The pathophysiological downstream events and the search of effective radioprotective agents by Papineni and Umar Labs will be highlighted. Further this symposia will describe the significance of such radiation pharma interventions as effective emergency nuclear countermeasures not only for patients undergoing abdominal irradiation for GI malignancies but to promote survival and delay mortality for victims of radiation exposure and nuclear disasters.

MST-24

MOVING FROM GAMMA PASSING RATES TO PATIENT DVH-BASED ONLINE PLAN VERIFICATION

Andreas Block
Institute of Medical Radiation Physics and
Radiation Protection, Klinikum Dortmund, Germany.
E-mail: andreas.block@klinikumdo.de

Modern radiotherapy techniques such as intensity modulated radiation therapy (IMRT) and volumetric arc therapy (VMAT) are requiring appropriate efforts for comprehensive quality assurance. Each treatment field can be highly complex and justifies quality assurance (QA) to verify (1) the treatment planning system's (TPS) ability to calculate the dose accurately and (2) the delivery system's ability to deliver the dose accurately. For IMRT verification 2D detector arrays equipped with ionization chambers or semiconductor detectors play a major role.
A significant percentage of radiotherapy institutions use the single-gantry-angle composite method for IMRT QA analysis instead of field-by-field analysis. Almost universally is the use of some quantitative comparison between TPS planar dose and measured dose with generating statistics of calculations such as percentage difference, distance to agreement (DTA) and gamma analysis.
The gamma analysis based on the multidimensional distance between the measurement and calculation points in both the dose and the physical distance. For the gamma analysis an ellipsoid surface whose major axes are determined by the individual acceptance criteria and the center of which is located at the measurement point in question is stretched in the dose-distance space. The minimum radial distance between the measurement point and the calculation points (expressed as a surface in the dose-distance space) is termed the γ-index. Regions where $\gamma<1$ correspond to locations where the calculation does not meet the acceptance criteria. The most prevalent standard for acceptance testing is the combined 3% dose difference criterion and the 3 mm criterion for distance-to-agreement.
However, one the one hand recent experimental studies have been carried out revealing the limited sensitivity of gamma analysis to patient dose deviation under different IMRT errors. On the other hand farther studies shown that per-beam planar gamma passing rates do not predict the clinical impact on the patient in terms of the changes in DVH values for the CTV and organs at risk (OAR). This gap try to close different software solutions such as the 3DVH (Sun Nuclear, USA), the Delta^{4DVH} (SandiDos, Sweden) and the COMPASS system (IBA Dosimetry, Germany). Using such patient-DVH-based metrics IMRT QA allows per-patient dose QA to be based on metrics that are both sensitive and specific.
However, pre-treatment plan verification are typically performed only once prior to the first treatment session assuming that there are no changes or errors in all sub-sequent treatment sessions. Moreover, adaptive radiotherapy approaches demand for on-line verification of dose delivery. A common feature of the transmission detectors is that they are placed in the photon beam between the MLC and the patient. Various online beam monitoring systems were described in the literature, such as the DAVID system (PTW, Germany), the integral quality monitor (IQM) detector (iRT Systems, Germany) or the Dolphin detector with the COMPASS verification software (IBA).
The DAVID system consists of a flat, multi-wire transmission-type ionization chamber. Each of the parallel wires is positioned exactly in the projection of the midline of a MLC leaf pair, so that the signal from each wire is proportional to the line integral of

ionization density over its length and thereby to the opening width of the associated leaf pair. The sum of all wire signals is a measure of the total radiant energy transferred to the patient. The IQM system consists of an area integrating energy fluence monitoring sensor and a calculation module. The measured signal from the sensor for each beam segment is compared on-line to the precalculated value to verify the accuracy of the treatment delivery. The expected signal is calculated based on the field information derived directly from the treatment planning system (TPS).

The COMPASS quality assurance system consists of a software which is used for dose computation and measurement based dose reconstruction and a 2D detector array. The new Dolphin detector (DD) is a transmission detector and will provide fluence measurements of IMRT plans. It is a pixel-segmented ionization chamber system with 1513 air. Vented plane parallel chambers (diameter 3.2 mm) with an active area of 240 x 240 mm^2. The DD is suitable for daily online treatment plane verification using patient-DVH-based metrics.

MST-25

MONTE CARLO METHODS AS ADVANCED QUALITY ASSURANCE FOR SPECIAL TREATMENT SITUATIONS

Wolfgang Baus
Department of Radiation Oncology, University Hospital of Cologne, Cologne, Germany.
E-mail: wolfgang.baus@uk-koeln.de

Introduction: Every now and again there are situations in treatment planning or application which cannot be simulated by the department's treatment planning system or, similarly, where the calculation algorithm available is not to be trusted. In these situations dose measurements might be advised. However, using a real Monte Carlo (MC) package could be an alternative to time-consuming measurements and in many cases could even provide a deeper insight. The MC code comes free of charge in many cases (e.g. EGSnrc[1]) and with published so-called phase spaces as source (e.g. from the IAEA[2]) we have versatile starting points for many interesting investigations of clinical relevance. With the graphical user interfaces (GUI) or user codes provided with the EGSnrc package it is easy to translate clinical questions into simple setups which nevertheless are often sufficient to provide the relevant answers. To achieve this it is not generally necessary to be a specialist in MC methods. However, though MC in itself is thoroughly benchmarked, it is always required to check the results for plausibility. Besides a short overview of the method the talk will give three examples of its use. First, MC simulation models the usage of bolus in conjunction with large air gaps, motivated by a patient treatment. Second, starting with a clinical case the physics of individual electron cutouts will be investigated. As a third example, MC in the support of advanced linac QA will be presented.

Materials and Methods: The MC simulations were performed using the DOSRZnrcusercode (Rev. 1.55) of EGSnrc MC[3] running within a virtual linux machine. The radiation source used ('source 21') wereeither a 10 x 10 cm^2 linac phase space (example 1) or CyberKnife Iris-Collimator phase spaces (example 3). The second example was carried out by means of an early PC implementation of the EGS code, EGSray.[4] The simulations were verified by measurement a white polystyrene (PS) slab phantom with a Roos-type (PTW 34001) ion chamber (case 1).

Results: For case 1, there is good agreement between MC simulation and the ion chamber measurement. Both methods agree that at least for about 4 cm of air gap or less between bolus and surface there remains still about 90 % of the bolus effect. Even for an air gap of 8 cm the surface dose is about twice as high with bolus compared to the dose without bolus. Regarding case 2, the MC simulation could explain the clinical evidence and by the same token gave a greater insight into the physics of electron irradiation. For the third example, correction factors for advanced linac quality assurance (QA) could be produced by MC which otherwise would be hard to get at.

Conclusions: The examples given of MC simulations demonstrated that they can be used as a versatile easy-to-use tool to answer questions in treatment delivery and advanced QA in cases which might not always be answered easily by measurements.

References

1. Kawrakow I. Accurate condensed history Monte Carlo simulation of electron transport. I. EGSnrc, the new EGS4 version. Med Phys 2000;27:485-98.
2. Available from: https://www.nds.iaea.org/phsp/phsp.htmlx. [Last accessed on 2017 Jul 24].
3. Available from: https://www.nrc-cnrc.github.io/EGSnrc/. [Last accessed on 2017 Jul 24].
4. Kleinschmidt C. EGs-ray, a program for visualization of Monte Carlo calculations in radiation physics. Z Med Phys 2001;11:119-23.

MST-26

OVERVIEW OF THE BREAST CANCER AND MAMMOGRAPHIC STATUS IN ASIA AND IN JAPAN

Tokiko Endo
Department of Radiology, National Hospital Organization Higashi Nagoya National Hospital, Nagoya, Japan.
E-mail: endot@e-nagoya.hosp.go.jp

Breast cancer is the top cancer in women both in the most Western and Asian countries. The incidence of the breast cancer is lower in Asia than in the western countries, but, is increasing due to increase life expectancy, increase urbanization and adoption of western life styles.

Mammography screening is the only method that has proved to be effective and cost-effective. In Japan, the mammographic breast cancer screening was started in 2004, and quality control has been done by the Japan Central Organization on Quality Assurance of Breast Cancer Screening, which is consisted with nine major societies concerning the breast cancer diagnosis and treatment. The Japanese Society of Radiological Technology and the Japan Society of Medical Physics are the members of this organization and play impotent roles in mammographic quality control.

The main activities of this organization are the education for radiological technicians and interpreters and the insurance the mammographic facilities meet radiation dose and image quality standard.

I'll introduce the state of the breast cancer and the efforts for breast cancer screening in Asian countries and in Japan.

MST-27

THE GUIDELINE OF QUALITY CONTROL FOR SCREENING MAMMOGRAPHY IN JAPAN

Hiroko Nishide
Radiological Technology, Gifu University of Medical Science, Seki, Japan. E-mail: hnishide@u-gifu-ms.ac.jp

Mammographic image used for breast cancer screening is required to produce high quality images at the lowest radiation dose possible, consistently. In Japan, the quality control manual of the physical and technical aspects for mammography was published by Japan Society of Radiological Technology (JSRT). The manual provides guidance on conducting and evaluating quality control (QC) tests. QC tests are based on recommendations from several organizations. Test Items for quality control are image quality evaluation, kVp accuracy and reproducibility, beam quality assessment (half-value layer measurement), AEC reproducibility, average glandular dose, evaluation of system resolution, etc. In Japan, the Central Committee on Quality Control of Mammographic Screening was established in 1997 for QC of screening mammography. Medical facilities are evaluated with regard to three items: inspection of documents, image evaluation (phantom images and clinical images), and exposure dose evaluation using a glass dosimeter. I'll introduce the quality control system for imaging quality and dose in Japan.

MST-28

VISION FOR MAMMOGRAPHY IN THE DIGITAL ERA

Yoshie Kodera
Department of Radiological Technology, School of Health Sciences, Nagoya University, Graduate School of Medicine, Nagoya, Japan.
E-mail: kodera@met.nagoya-u.ac.jp

Mammography has characteristics of high sharpness and high contrast to detect the micro-calcifications and masses. In the era when using the intensifying screen film systems, sharpness could be secured but the contrast rise was limited. Low energy x-rays were used to obtain high contrast. However, this choice has led to excessive radiation dose to the breast. Even when the mammography system shifted to the digital system, the energy of the X-rays used remained low. Was this choice correct? The light and shade of the analog system could be evaluated by contrast value, but in the digital system the contrast is variable by image processing and cannot be used an index of evaluation. Therefore, the signal-to-noise ratio (SNR) has been proposed instead of the index of contrast for digital systems. In recent years, we are studying for the purpose of developing new digital mammography. One of the studies is to develop determine a newly high-definition direct-type complementary metal-oxide semiconductor (CMOS) digital x-ray imager under conditions applicable to mammography. We compare the physical image properties of this CMOS digital x-ray imager with those of the conventional mammography systems. The other one is to reduce exposure dose, we have proposed a new mammography system that uses a Cadmium Telluride (CdTe) series photon counting detector. This system uses higher energy than the typical mammographic energy, using a tungsten target. The purpose of the latter study was to assess the possibility of dose reduction when using our proposed system. Through development of these systems, we consider the possible appearance of mammography in the new digital age.

MST-29

NEW ASPECTS OF MEDICAL PHYSICS IN RADIATION ONCOLOGY AND IMAGING

Golam Abu Zakaria
Department of Medical Radiation Physics, Klinikum Oberberg, Gummersbach Hospital, Academic Teaching Hospital of the University of Cologne, Gummersbach, Germany. E-mail: g.zakaria@emw.hs-anhalt.de

Medical Physics is the application of physics concepts, theories and methods to medicine and health care. Medical physicists play a vital and often leading role for any medical research team. Their activities cover some key areas such as cancer, heart diseases and mental illnesses. In cancer treatment, they primarily work on issues involving imaging and radiation oncology. Thus the medical physicists play a mandatory role in every radiation oncology team.

The capability of controlling the growth of any cancer with radiation dose is always associated with the unavoidable normal tissue damage. Accordingly, many physical-technical developments in radiotherapy facilities are aimed to give a maximum radiation dose to tumour cells and – at the same time – minimize the dose to the surrounding normal tissue.

For that reason, after the development of the 60-Co Irradiation Units in the 50ties medical Linear Accelerators were developed in the following decades. Advanced Linear Accelerators, Helical Tomotherapy and Cyber Knife Machines have been developed over the past two decades. Last but not least, Neutrons, Protons and even heavier Ions have also been applied. At the same time, treatment calculation and delivery methods have been continuously improved from conventional multi-beam techniques to tumour shape conformal methods such as 3D- Conformal Radiotherapy (3DCRT), Radio Surgery, Intensity Modulated Radiotherapy (IMRT), Image Guided Radiotherapy (IGRT), Stereotactic Body Radiation Therapy (SBRT) and Adaptive Radiotherapy (ART).

The concentration of dose to tumour requires precise information on the shape and the anatomical geometry of the tumour within the body. The techniques providing such pieces of information in a visible form is summarized by the term of "Imaging". X-ray has played a dominant role almost from the time of its discovery in 1895. Up to now, the use of x-rays has been extended to tomographic imaging with Computer Tomography (CT) and other imaging modalities like Ultrasound (US), Magnetic Resonance Imaging (MRI) or Positron Emission Tomography (PET) which have been developed over the last decades. By their combined use, the required information level on the clinical tumour target volume for radiotherapy has been tremendously raised.

The physical and technical development of radiation oncology and imaging are discussed in this talk covering aspects in biology as well.

MST-30

STEREOTACTICAL TREATMENT OF LIVER TUMORS

Wolfgang Baus
Department of Radiation Oncology, University
Hospital of Cologne, Cologne, Germany.
E-mail: wolfgang.baus@uk-koeln.de

Scope: Stereotactic body radiotherapy (SBRT) is a method of percutaneous radiotherapy which allows precise irradiation of tumors mainly of the torso in one or a few fractions with a fraction dose of considerably more than 2 Gy (Hypofractionation). The most important indications for SBRT are today lesions of the lung and liver and tumors of the spinal column near the spinal cord besides small volume re-irradiation of pretreated regions. Additional indications are tumors of the pancreas or the kidneys. SBRT of the prostate is – at least in Germany – still experimental. Liver lesionscan be metastases (e.g. of colorectal tumors or breast cancer) or primary liver tumors such as the hepatocellular carcinoma (HCC) or, more rarely, the cholangiocarcinoma. Generally, surgical resection or liver transplantation are the methods of choice. However, only the smaller part of the lesions is eligible for surgery and there is a broad range of alternatives when operation is not possible or not desired. This is foremost radiofrequency ablation (RFA) or transarterial chemoembolization (TACE). SBRT as an additional method is today mostly second line when other methods are not feasible or without success. The working group on stereotaxy of the German society of radiooncology (DEGRO) has recently summarized in a guideline the status of SBRT for liver tumors, together with recommendations for the implementation.[1] This guideline is basis for the talk, enriched by some more physical aspects.

Materials and Methods: The guideline[1] gives an overview of the existing evidence for SBRT of liver tumors in comparison to alternative methods. Recommendations for the practical implementation are given according to the literature and to the experience within the DEGRO working group. Liver irradiation at the University Hospital of Cologne is carried out with a robotic linac (CyberKnife) of which the experiences are presented.

Result: Only about a quarter of all liver lesions can be tackled by surgery therefore there is need for alternative treatments. Despite that randomized comparisons of the different therapy options are mostly missing, SBRT is within the existing evidence comparable with the other methods (e.g. local control of metastases SBRT vs. RFA 67-92% vs. 79-93%, 2-year overall survival 30-62% vs. 42-77%). Dose prescription for RT is varying both in total dose and in how to prescribe (e.g. reference point, encompassing isodose line), therefore the guideline does not include a unique recommendation. However, a biologically equivalent dose (BED) of at least 80, better 100 Gy, should be aimed at. In respect of the acceptable dose constraints for the organs at risk (healthy liver, duodenum, stomach, heart etc.) the guideline also merely states the literature. For liver treatment, management of the respiratory motion is mandatory. This could be done by using an internal target volume (ITV) concept which takes the movement into account by enlarged margins, preferably on the basis of a 4D-CT. On the other hand the movement itself could be minimized by applying an abdominal press or motion could be tackled by respiratory controlled irradiation using gating or tracking. For treatment planning, generally an algorithm should be used which also works reliably in regions of disturbed secondary electron equilibrium (however, as long as the tumor is not in the vicinity of the diaphragm the differences to a so-called pencil beam algorithm are in most cases negligible). Three dimensional conformal techniques as well as fluency modulation (IMRT) and rotational methods (VMAT) are possible. Using 6 MV photons and an MLC with not more than 5 mm leaf width seems appropriate. Flattening filter free (FFF) beam qualities might be advantageous in respect to the longer beam-on times connected with hypofractionation. Suitable imaging, maybe depending on the choice of motion management, is also mandatory. Lastly, compared to non-stereotactical radiotherapy, SBRT demands enhanced efforts in terms of quality assurance. For that, one can draw on the existing standards for cranial stereotaxyor on specialized publication such as the report of Task Group 101 and 135 of the AAPM[2,3] and the upcoming ICRU report 91.[4]

Conclusion: The guideline in regard to liver SBRT of the German DEGRO working group was presented together with practical experience in liver SBRT, with special attention to physical aspects.

References

1. Sterzing F, Brunner TB, Ernst I, Baus WW, Greve B, Herfarth K, *et al.* Stereotactic body radiotherapy for liver tumors: Principles and practical guidelines of the DEGRO working group on stereotactic radiotherapy. Strahlenther Onkol 2014;190:872-81.
2. Benedict SH, Yenice KM, Followill D, Galvin JM, Hinson W, Kavanagh B, *et al.* Stereotactic body radiation therapy: The report of AAPM task group 101. Med Phys 2010;37:4078-101.
3. Dieterich S, Cavedon C, Chuang CF, Cohen AB, Garrett JA, Lee CL, *et al.* Report of AAPM TG 135: Quality assurance for robotic radiosurgery. Med Phys 2011;38:2914-36.
4. ICRU Report 91. Prescribing, Recording, and Reporting of Stereotactic Treatments with Small Photon Beams. In Press; 2017.

MST-31

DIAGNOSTIC REFERENCE LEVELS AND THEIR NEED IN 21ST CENTURY

MPS Mann
Consultant Medical Physicist & RSO, Pan
Maxhealthcare, Delhi, India.
Email: mpsingh.mann@gmail.com

The need to implement Diagnostic Reference Levels is paramount. So far no one has even tried in India. The Indian Radiological and Imaging Association has not undertaken any project with intention to implement it. Individually, we have very little work done in this direction in India.

According to International Journal of Radiation Biology, Low exposure to doses of around 0.5 Gy is associated with a significantly increased risk of cardiovascular damage, up to decades after exposure. This raises questions about the nature of long-term alterations in the heart's vascular system caused by such doses. Hence the need to have a control on the exposure to the patients.

Soile Tapio, M.D. and Omid Azimzadeh, M.D. of Helmholtz Zentrum München, German Research Center for Environmental Healthstudied how human coronary artery endothelial cells respond to a relatively low radiation dose of 0.5 Gy and found several permanent alterations in the cells that had the potential to adversely affect their essential functions

Diagnostic reference levels were first mentioned by the International Commission on Radiological Protection (ICRP) in 1990.[1]

From the 1996 Report: The Commission now recommends the use of diagnostic reference levels for patients. These levels, which are a form of investigation level, apply to an easily measured quantity, usually the absorbed dose in air, or in a tissue equivalent material at the surface of a simple standard phantom or representative patient.

The use of diagnostic reference levels as an important dose optimization tool is endorsed by many professional and regulatory organizations, including the ICRP, American College of Radiology (ACR), American Association of Physicists in Medicine (AAPM), United Kingdom (U.K.) Health Protection Agency, International Atomic Energy Agency (IAEA), and European Commission (EC).

The diagnostic reference level are used for as a simple test for identifying procedures where the level of patient dose or administered activity is high. If it is found that the procedures are consistently giving high dose and the diagnostic reference level are being exceeded, a review of the procedure and the equipment is ordered.

It is inappropriate to use them for regulatory or other punitive purposes. Diagnostic reference levels apply to medical exposure, not to occupational and public exposure. Thus, they have no link to dose limits or constraints. Ideally, they indicate the generic optimization of protection. In practice, this is unrealistically difficult and it is simpler to choose the initial values as a percentile point on the observed distribution of doses to patients. The values should be selected by professional medical bodies and reviewed at intervals that represent a compromise between the necessary stability and the long-term changes in the observed dose distributions.

The selected values of DRLs will be specific to a particular region or a country. These levels are not suggestive of an ideal dose for a particular procedure or an absolute upper limit for dose. Rather, the the DRLs combine the three important elements: the dose level at which an procedure is done, with appropriate Radiation safety and good diagnostic value imaging is achieved. In conjunction with an image quality assessment, a qualified medical physicist should work with the radiologist and technologist to titrate the exposure Factors downwards, if possibleto seewhether or not the required image quality was possible at lower dose levels. Thus, reference levels act as “trigger levels” to initiate quality improvement. Their primary value lies in identifying dose levels that may be unnecessarily high – that is, to identify those situations where it may be possible to reduce dose without compromising the required level of image quality.

Reference levels are typically set at the 75th percentile of the dose distribution. The survey must be from a conducted across a broad user base (i.e., large, small facilities, public and private hospitals and OPDs) using a specified dose measurement protocol and phantom. They are established both regionally and nationally, and considerable variations have been seen across both regions and countries3. Dose surveys should be repeated periodically to establish new reference levels, which can demonstrate changes in both the mean and standard deviation of the dose distribution.

The use of diagnostic reference levels has been shown to reduce the overall dose and the range of doses observed in clinical practice. For example, U.K. national dose surveys demonstrated a 30% decrease in typical radiographic doses from 1984 to 1995 and an average drop of about 50% between 1985 and 20004,5. While improvements in equipment dose efficiency may be reflected in these dose reductions, investigations triggered when a reference dose is exceeded can often determine dose reduction strategies that do not negatively impact the overall quality of the specific diagnostic exam. Thus, data points above the 75th percentile are, over time, moved below the 75th percentile – with the net effect of a narrower dose distribution and a lower mean dose.

CT Diagnostic Reference Levels from Other Countries: Diagnostic reference levels must be defined in terms of an easily and reproducibly measured dose metric using technique parameters that reflect those used in a site’s clinical practice. In radiographic and fluoroscopic imaging, typically measured quantities are entrance skin dose for radiography and dose area product for fluoroscopy. Dose can be measured directly with TLD or derived from exposure measurements. Some authors survey typical technique factors and model the dose metric of interest.

In CT, published diagnostic reference levels use CTDI-based metrics such as CTDIw, CTDIvol, and DLP. Normalized CTDI values (CTDI per mAs) can be used by multiplying them by typical technique factors, or CTDI values can be measured at the typical clinical technique factors. Tables 1 and 2 below provide a summary of CT reference levels from a variety of national dose surveys.

Diagnostic Reference Levels: CT Diagnostic Reference Levels From the ACR CT Accreditation Program.

Beginning in 2002, the ACR CT Accreditation Program has required sites undergoing the accreditation process to measure and report CTDIw and CTDIvol for the head and body CTDI phantoms. The typical acquisition parameters for a site's adult head (head), pediatric abdomen (ped), and adult abdomen (body) examinations were used to calculate CTDIw and CTDIvol. For the pediatric exam, sites were instructed to assume the size and weight of a typical 5-year-old child, and doses were measured using the 16-cm phantom. The average and standard deviation of these doses were calculated by year. Summary data for CTDIvol are shown in Table 3 below.

In every case except adult abdomen exams in 2003, both the average dose and the standard deviation fell for each consecutive year. Thus, the establishment of CT reference levels in the United States appears to have helped reduce both the mean dose and the range of doses for these common CT examinations.

Although dose reduction was observed for adult head CT examinations, feedback from sites undergoing accreditation indicated that sites were systematically reducing dose to below the 60 mGy level, even though complaints with regard to head image quality at this dose level were common. The purpose of reference levels is to decrease dose levels only when doing so does not compromise image quality or patient care. Changes in technology (multi-detector-row CT) and practice (3-5 mm image widths) have occurred since the U.K. dose survey that gave rise to the 60 mGy level for the adult head.

Table 1: Adult diagnostic reference levels for weighted computed tomography dose index (mGy) and dose length product (mGy/cm)

	Whole exam				*Abdomen and pelvis*			
	Head		*Abdomen*		*Pelvis*		*Whole exam*	
	CTDIw	*DLP*	*CTDIw*	*DLP*	*CTDIw*	*DLP*	*CTDIw*	*DLP*
EC, 1999-2006	60	1050	35	900	-	-	35	780
ACR, 2002-2007	60	-	35	-	-	-	-	-
UK, 2003-2008	-	930	20	470	-	-	20	560
Germany, 2003-2009	60	1050	25	770	-	-	24	1500
Switzer-land, 2004-2010	60	800	20	710	30	540	-	-
Taiwan, 2007-2011	72	850	31	680	28	520	-	-

EC: European commission, ACR: American College of Radiology, UK: United Kingdom, CTDIW: Weighted computed tomography dose index, DLP: Dose length product

Table 2: Adult diagnostic reference levels for volume computed tomography dose index (mGy) and dose length product (mGy/cm)

	Whole exam				*Abdomen and pelvis*			
	Head		*Abdomen*		*Pelvis*		*Whole exam*	
	CTDIvol	*DLP*	*CTDIvol*	*DLP*	*CTDIvol*	*DLP*	*CTDIvol*	*DLP*
Sweden, 2002-2012	75	1200	25	-	-	-	-	-
UK, 2003-2008	65-100	930	14	470	-	-	14	560
Netherlands, 2008-2013	-	-	-	-	-	-	15	700
EC, 2004-2014	60	-	25	-	-	-	15	700
ACR, 2008-2015	75	-	25	-	-	-	-	-

EC: European commission, ACR: American College of Radiology, UK: United Kingdom, CTDIvol: Volume computed tomography dose index, DLP: Dose length product

Table 3: Volume computed tomography dose index (mGy) statistics from the first 3 years of the American College of Radiology computed tomography Accreditation Program

	Adult head			*Adult abdomen*			*Pediatric abdomen*		
	2002	*2003*	*2004*	*2002*	*2003*	*2004*	*2002*	*2003*	*2004*
Mean	66.7	58.5	55.8	18.7	19.2	17.0	17.2	15.9	14.0
SD	23.5	17.5	15.7	8.0	8.7	7.6	9.7	8.6	7.0
75 percentile	76.8	63.9	60.0	22.6	23.4	21.1	20.6	20.5	18.4
90 percentile	99.0	82.2	74.0	29.5	30.6	25.8	26.6	25.6	23.4

SD: Standard deviation

As can be seen in Tables 1 and 2, these changes have resulted in an increase in the diagnostic reference level for head CT (U.K. 2003 data now specifies CTDIvol reference levels of 65 mGy for the cerebrum and 100 mGy for the posterior fossa). Thus, the ACR CT Accreditation Program used survey data from the inception of the program to establish the most current U.S. reference levels for head CT (i.e., 2002 data were used to avoid including dose values that were thought to yield inadequate image quality). Beginning January 1, 2008, the ACR CT reference levels were changed to a CTDIvol of 75 mGy (adult head), 25 mGy (adult abdomen) and 20 mGy (pediatric abdomen)15. These values will be reassessed periodically.

CT Diagnostic Reference Levels for Other CT Applications: Because the practice of CT encompasses many more exam types than routine head and body exams, reference levels for many common CT examinations are important for continuing dose optimization efforts in CT. To this end, several national surveys have begun to assess a broader range of exam types. Additionally, the ACR has begun a project to automatically collect CTDIvol data directly from the DICOM header, thus allowing considerably faster accumulation of data sufficient to establish reference levels for additional exam types. This information will extend the value of the diagnostic reference level concept to the majority of CT applications, enabling individual CT users and the community at large to answer the question, "What doses are typical and what doses are too much?"

In conclusion DRLs havebeen proven to be an effective tool that aids in optimisation of protection in the medicalexposure of patients for diagnostic and interventional procedures. However, with time it hasbecome evident that additional advice is needed. There are issues related to definitions of theterms used in previous guidance, determination of the values for DRLs, the appropriate interval for re-evaluating and updating these values, appropriate use of DRLs in clinicalpractice, methods for practical application of this tool, and application of the DRL concept tonewer imaging technologies. This has attained special significance in view of the dose for children must be less.

MST-32

THE CURRENT SITUATION OF DOSE AND DRLS FOR RADIOGRAPHIC AND FLUOROSCOPIC EXAMINATIONS

Satish Uniyal
Department of Radiology, Swami Rama Himalayan University, Dehradun, Uttarakhand, India.
E-mail: dr.suniyal@gmail.com

Medical radiation is the largest contributor of human-made radiation exposure today and the majority of this exposure is from diagnostic X-rays (UNSCEAR 2010). Due to advancing imaging technology and increasing investments in healthcare worldwide, a continuous growth in the use of diagnostic X-rays has been recorded in recent times and raised serious concerns about higher patient doses. For effective optimization of the diagnostic exposures, the International Commission on Radiological Protection (ICRP) introduced the concept of diagnostic reference level (DRL) in 1996 which was subsequently recommended by the International Atomic Energy Agency (IAEA) (1996), European Commission (EC) (1999) and many other organizations. The objective of a DRL is to help avoid radiation dose to the patient that does not contribute to the clinical purpose of the image. It provides a means for practices to compare their radiation dose data to benchmarks derived from aggregated dose data collected on a local, regional, or national level. Patient dose for radiographic examinations is commonly expressed in units of air kerma-area product (P_{KA}) or entrance surface air kerma (Ka,e) or an assessment of both, whereas, the most appropriate dose descriptor for fluoroscopy examinations is P_{KA}. In general, the 75th percentile of the distribution of the dose quantity is considered an appropriate level for the DRL.
The DRL process has been popularized in Europe and applied with good results. In 2008, the European Commission published a review of recent national surveys of population exposure from medical X-rays in 10 countries of Europe. An update of this project came in 2014 that included the dose data from 36 European countries, on the basis of which DRLs for X-ray examinations in terms of Ka,e and P_{KA} and for fluoroscopy procedures in terms of P_{KA} were established in most of these countries. As per records of the United Kingdom, periodic dose surveys and five-early reviews since1980 to date have greatly reduced doses delivered to patients (HPA-CRCE-034). In the United States, DRLs presented by organizations such as the American College of Radiology (ACR), American Association of Physicists in Medicine (AAPM) and National Council for Radiation Protection and Measurements (NCRP) have been adopted as actual standards. NCRP published report 172 which defined DRLs and achievable doses for radiographic and fluoroscopic examinations. National DRLs in India were proposed for radiographic examinations in 2001 and subsequently in 2010, but no study is available on dose and DRLs for fluoroscopy procedures. Japan national DRLs have been established in 2015 for general radiography and fluoroscopically guided interventional procedures. Australian government has implemented national DRLs for computed tomography, but radiography and fluoroscopy procedures currently lack established national DRLs. In addition of nation-wide surveys, local DRLs have been reported from countries like Canada, India, Sudan, Iran, China etc.
Although the country specific regulators have emphasized upon the requirement of periodic quality control of the X-ray systems and regular reporting of their operating status, proper implementation of the prescribed DRLs is still required at different levels. Currently, patient dose levels are in a state of flux due to the introduction of digital technology both in radiography and fluoroscopy. In this perspective, a more proactive approach would be to continuously capture all radiation dose data to evaluate compliance and reformulate DRLs for further optimization of radiation dose.

MST-33

RADIATION DOSE AND DRLS FOR CT SCANNERS IN INDIA

Roshan S. Livingstone
Department of Radiology, CMC, Vellore, Tamil Nadu, India. E-mail: roshanlivingstone@gmail.com

Purpose: Radiation safety in CT scanners is of concern due its increased radiation dose to patients. Though CT imparts a substantial amount of manmade radiation to the human population, the clinical benefits with the appropriate use of this modality far exceed the risks associated with exposures to ionizing radiation. This study intends to evaluate radiation doses and establish regional Diagnostic Reference Levels (DRL) for CT scannersin India.
Materials and Methods: In-site CT dose measurement was performed for 127 CT scanners in Tamil Nadu as a part of Atomic Energy Regulatory Board (AERB) funded project. These studies were done 5 years ago, however this information sets the trend for establishing DRLs in India. CT dose index (CTDI) was measured using a 32 cm polymethyl methacrylate (PMMA) body phantom and 10-cc ion chamber in each CT scanner. Dose Length Product (DLP) was obtained using scan length and volume CTDI ($CTDI_{vol}$) values calculated from measured weighted CTDI ($CTDI_w$) values. The effective doses were estimated by multiplying the DLP values by normalized coefficients found in the European guidelines on quality criteria of CT. The exposure parameters used in the study was based on routine practices from each installation. The CT numbers and image noise expressed as standard deviation of measured density values for the 32 cm body phantom were measured from the software of each CT scanner.
Results: Out of the 127 CT scanners, 13 were conventional, 53 helical single-section, 44 multidetector (MDCT) and 17 refurbished machines. An average of 2080 CT examinations is performed each day in the region, out of which 2.8% are pediatrics. Out of the 2080 examinations, 1065 were head scans, 409 thorax, 429 abdomen and 177 extremities. Twenty seven scanners were installed in residential area, 86 in hospitals and 44 in commercial centres. The Table 1 shows the regional DRLs for CT abdomen and thorax scans. Twenty seven CT scanners had deranged CT numbers and this could be attributed to irregular calibration of machines.
Discussion and Conclusion: This study reveals that the regional DRLs are within the international reference level for CT scanners except for a few centres. These studies are valuable

Table 1: Regional diagnostic reference levels for computed tomography of abdomen and thorax as practiced in India

CT examination (scan length)	Effective doses in mSv				
	Mean±SD	Range	25th percentile	50th percentile	3rd quartile
Abdomen (33.8 cm)	6.66±2.7	1.6–20.6	5.03	6.4	7.8
Thorax (36.1 cm)	8.04±3.3	1.9–24.9	6.1	7.7	9.4

SD: Standard deviation, CT: Computed tomography

and can be periodically conducted as a part of National reference studies in order to keep doses as low as reasonably achievable and to develop optimization strategies. Therefore, it is important to audit examinations carried on patients and to ensure that doses do not deviate from the regional levels. In light of this study, it is advisable to have dose descriptives such as $CTDI_{vol}$, DLP or effective dose values available on the CT console. Users should be encouraged to monitor displayed dose descriptors to monitor trends in patient doses.

MST-34

PHYSICS AND BASIC TECHNOLOGY OF CT

Mahadevappa Mahesh

The Russell H. Morgan Department of Radiology and Radiological Science, Johns Hopkins University School of Medicine, Baltimore, Maryland, USA.
E-mail: mmahesh@jhmi.edu

Computed Tomography is one of the prime imaging modalities in any hospital around the globe. From its inception in 1973, CT technology have advanced leaps and bounds in medical diagnosis. Advances in x-ray tubes, detection technologies and image reconstruction methods led to the development of multiple-row detector CT (MDCT) technologies in early 2000, that has been the impetus for new fields such as Cardiovascular CT, Hybrid CT (PET-CT and SPECT-CT), CT Perfusion, Cone Beam CT, etc. It is now possible to image the entire organ (such as heart) in less than 0.3 seconds providing isotropic resolution images with high temporal resolution. With all x-ray imaging modalities, including CT, the concern is the radiation dose. Since CT procedures are one of the major imaging procedures performed in any hospital, it is important to optimize CT protocols in order to provide quality images at optimal radiation dose.
As part of the mini-symposium on CT, this lecture will discuss the basics of physics and technology of MDCT.
Educational Objectives: (1) To understand basic principles of multiple-row detector CT scanners, (2) To become familiar techniques that impact image quality and radiation dose, (3) To learn more about the CT technology currently on the horizon.

MST-35

CT DOSIMETRY

Ajai K. Srivastava

Department of Radiology, UCMS, GTB Hospital, New Delhi, India. E-mail: drajai.india08@gmail.com

Doses from CT have become of wide spread interest particularly with regards to the chest and abdominal CT among children and young adults. CT has entered in to a new dimension includes vascular and cardiac exams. Spectral CT, a newer innovation in CT Technology, provide more diagnostic information as compared to traditional CT scanner by knowing tissue composition. Each of these exams prompts the need of measuring dose and estimating risk and dose optimization for the dose reduction in CT. Effective dose is best used dose descriptor to optimize exams and to compare risks between proposed examinations. The quantities used for expression of CT doses are weighted computed tomography dose index ($CTDI_{w)}$) and dose length product (DLP) that takes into account 'beam collimation and number of rotation in a complete examination.
Weighted computed tomography dose index ($CTDI_{w)}$) can be defined as

$$CTDI_w = (1/3)\ (CTDI_{100})_{center} + (2/3)\ (CTDI_{100})_{periphery}$$

$$CTDI_{100} = \frac{1}{nT}\int_{-50}^{+50} D(z)dz$$

Where, N is the number of *acquired* slices per scan – also referred to as the number of data channels used during acquisition, and T is the nominal width of each *acquired* slice (which is not necessarily the same as the nominal width of the *reconstructed* slice width).
D(z) is the dose at point z on any line parallel to the z (rotational) axis for a single axial scan along 100 mm (-50 mm to + 50 mm).
DLP = $CTDI_{vol}$* scan length in cm; units are mGy*cm.
$CTDI_{vol}$ represent, however, only CT scanner output and therefore this approach obviously does not take into account any patient-specific or even examination specific factors. Moreover in the measure of 32 cm diameter phantom, for same technical factors, will underestimate the actual doses in thin patients. In the light of this limitation, size specific dose estimation (SSDE) has been reported by researcher and AAMP Report no 204, in which conversion factors may be used to convert $CTDI_{vol}$ into size specific dose estimate and these conversion factors are independent of scanner manufacture and tube voltage. However, some CT scanner manufacturer use $CTDI_{vol}$ value measured using 16 cm diameter phantom. And caution needed to ensure that correction factors specific to reference phantoms are used. To account for scattered does distribution, AAPM Task group 111 (TG111) has proposed that instead of using a 100 mm pencil chamber and measuring dose to a partially irradiated chamber, a smaller chamber can be used and helical mode is used to scan a given scan length of the scanner. A series of such measurement on scan of different length can be measured with the integrating ion chamber located at the centre of each scan. Dose profile obtained through this measurement can be used to derive the rise to dose equilibrium curve.
Effective dose can be estimated from the DLP using conversion factors.
Effective Dose from DLP is calculated as =

$$E_{DLP} \text{ x DLP mSv} \quad (9)$$

However, effective dose alone does not give a complete picture of estimated radiation risk to specific radiation sensitive organs or patients of a specific age or gender. For a complete picture, specific organ doses and age, gender, and organ specific risk estimates are needed using current International Commission on Radiation Protection (ICRP) recommendations taking in to considerations of relative radiation sensitivities of various organs and tissues. Another way of obtaining the pattern of energy deposition in patients undergoing CT examination is by calculation using Monte Carlo simulation techniques. This type of calculation assumes that the patient resembles the phantom used for measurements or Monte-Carlo simulation. The most direct way of estimating doses to patients undergoing CT examination is to measure point organ doses in patients like phantom using TLD or OSL dosimeter.

MST-36

TECHNIQUES FOR DOSE OPTIMIZATION IN CT

Roshan S. Livingstone
Department of Radiology, Christian Medical College, Vellore, Tamil Nadu, India.
E-mail: roshanlivingstone@gmail.com

Radiation dose from Computed Tomography (CT) is of concern as the amount of dose imparted to the patient is significantly high when compared to conventional radiography investigations. The optimization of CT imaging protocols involve a collaborative effort between radiologists, medical physicists, and technologists in order to obtain acceptable image quality with reduced radiation dose. In this context, it is important to be aware of various optimisation methods used in CT. Earlier, in the conventional CT scanners, operator had to adjust tube potential (kV) and tube current (mA) based on the patient habitus and this may be performed using weight based protocols which are different for pediatric and adult population. The recent advances in CT has introduced automated tube current modulation (ATCM), optimized x-ray tube potential, iterative image reconstruction and dual energy in order to reduce radiation dose and maintain adequate image quality. Though all the CT vendors provide presetexposure parameters in all CT protocols, optimisation is required depending upon the study being performed. The ATCM technique varies tube current while scanning in order to account for differences in patient attenuation and ensures more homogeneous image quality resulting in a reduction of radiation dose. In the z axis (longitudinal) modulation, the tube current is varied along longitudinal axis of the patient such that the lower attenuation part of the body will be acquired at with low tube current than the ones with higher attenuation. In the x-y axis (angular) modulation, the tube current is varied in the anteroposterior and lateral projections such that it is reduced in the direction of lower attenuation projection. Another technique is to reduce the x-ray tube voltage for certain CT protocols. For evaluating iodinated structures, the effective energy of the x-ray beam closer to the k-edge of iodine can be selected. Hence selection of optimal kV for a CT study on the basis of imaging task and patient habitus will reduce dose. It is known that reduction in radiation dose increases noise in the image thus affecting diagnostic value. Iterative reconstruction technique (statistical method) identifies factors contributing to noise from CT images and use statistical models to selectively remove noise and improve image quality thus reducing radiation dose. The level of noise suppression using iterative reconstruction technique can be customized to minimize the effect of altered image quality on CT images. All three dose reduction techniques – ATCM, selection of appropriate tube potential and use of iterative image reconstruction can be combined for effective dose reduction.

Reduction of radiation dose is also achieved using dual energy CT (DECT). Using ultrafast kilovoltage switching with a few millisecond delay between readings, the DECT scanner acquires different sets of images. These acquired data set can be reconstructed into different set of images at various keV. During a multiphasic abdominal CT, virtual unenhanced (non-contrast) images can be reconstructed from a contrast-enhanced DECT dataset, thus eliminating the need for prior unenhanced scanning leading to substantial reduction on the overall radiation dose associated with the examination. These newer radiation dose reduction techniques can be effectively implemented in clinical CT scanning to keep doses as low as reasonably practicable.

MST 37

RADIATION ONCOLOGY FACILITIES: CURRENT STATUS AND FUTURE PERSPECTIVES IN THE COUNTRIES MEMBERS OF THE MEFOMP

Rabih Hammoud
Chief of Medical Physics Radiation Oncology, Hamad Medical Corporation, Wayne State University, Michigan.
E-mail: rhammoud2@hamad.qa

MST-38

THE PERSPECTIVE IN DEVELOPMENT OF MEDICAL PHYSICS IN AFOMP REGION

Tae Suk Suh
President, Asia-Oceania Federation of Organizations for Medical Physics (AFOMP), Professor of Medical Physics, Department of Biomedical Engineering, College of Medicine, The Catholic University of Korea, Seocho-gu, Seoul, Korea. E-mail: suhsanta@catholic.ac.kr

Asia–Oceania has a diverse cultural, social, educational, and economical background. Some 60% of the world's population reside in Asia who speak hundreds of languages and dialects. The Asia–Oceania Federation of Organization for Medical Physics (AFOMP) was formed to act as one of the regional branches of the International Organization of Medical Physics (IOMP), similar to the EFOMP announced in July 2000 during the Chicago World Congress on Medical Physics and Biomedical Engineering (WC 2000). The formation of AFOMP aims to provide a solid platform for closer and mutual support among its member organizations, particularly in the promotion of education and training, standard of practice, and professional status of the medical physicists in its affiliated regions. Furthermore, AFOMP aims to facilitate and encourage cross-regional collaboration and interaction on every aspect of medical physics. In this presentation, we will review current activities and roles of AFOMP and discuss future development of medical physics in the AFOMP region.

One major role of AFOMP is to hold the Asia–Oceania Congress of Medical Physics (AOCMP) every year. The AOCMP has been held 16 times since the first one, which was held in Bangkok, Thailand in 2001. Many activities have been organized by AFOMP. One of the main activities has been to develop the AFOMP policy statement. Five AFOMP policy statements have been developed thus far. Some of them were published in the Australasian Journal of Physics and Engineering Science in Medicine (APESM), which is one of the AFOMP official journals. The first issue of the AFOMP newsletter was published as an e-version in December 2007. The format and contents of the AFOMP newsletter have been improved by a new editor, who has been in appointment since 2013. The AFOMP website was initially developed in 2007, improved several times, and, recently, newly designed by a professional company, making it ready for use. There are three journals, which were officially endorsed by AFOMP: the Biomedical Imaging and Interventional Journal (BIIJ), Australasian Physics and Engineering Science in Medicine (APESM), and Radiological Physics and Technology (RPT). In addition, AFOMP have activities in collaboration with IAEA, WHO, UNDP, IOMP, etc.

The role and status of medical physicists in the AFOMP region have gradually improved and is being recognized by related societies. However, the importance of medical physics and necessity of accreditation have not been recognized by government or the general public yet. A considered strategy supported by a strong action plan is crucial for AFOMP to move forward.

MST-39

MEDICAL PHYSICS EDUCATION AND TRAINING IN MEFOMP COUNTRIES

Ibrahim Duhaini, Nabil Iquillan[1], Laila Al Balooshi[2]

Chief Medical Physicist & RSO, Rafik Hariri University Hospital, Beirut, Lebanon, [1]Departments of Occupational Health and Safety, Hamad Medical Corporation, Doha, Qatar, [2]Medical Physics section, Dubai Health Authority, Dubai Health Authority, Dubai, UAE. E-mail: duhaini@yahoo.com

The Education and Training of medical Physics in MEFOMP countries have been evolved since the last decade to better suit the demand and fulfill the market need of physicists in our region. The programs of Medical Physics will be reviled for some countries in our region.

The mission of MEFOMP Educational and Training Committee (ETC) is to promote activities related to education and training of medical physicists for the purpose of improving the quality of medical services for patients in the region through advancement in the practice of physics in medicine. ETC helps and provides support for all medical physics trainee in all member countries to understanding of different levels of learning, and the types of knowledge required for higher level functions such as problem solving, creative innovations, and applied clinical applications.

Medical physics education can be much more effective and efficient when all regional chapters of IOMP share their knowledge and experience to enhance the outcome with coordination of highly qualified experts of medical physics professionals.

MST 40

RADIATION SAFETY AND REGULATORY AUTHORITIES IN MEFOMP

Laila Al Baloushi

Head of Medical Physics section & Specialist Medical Physicist, Senior Medical Physicist & Chief RPO, Dubai Health Authority, UAE. E-mail: LgAlBalooshi@dha.gov.ae

MST-41

A BRIEF HISTORY OF MEDICAL PHYSICS IN ASIA-OCEANIA

W. Howell Round

Secretary General, Asia-Oceania Federation of Organizations for Medical Physics (AFOMP), School of Engineering, University of Waikato, Hamilton, New Zealand. E-mail: secgenafomp@gmail.com

The history of medical physics in Asia-Oceania goes back to the late nineteenth century when X-ray imaging was introduced. The first X-ray images in the region were taken in Australia and New Zealand in 1896, just a year after the discovery of X-rays was reported by Roentgen. Shortly after images were being obtained in Japan, India and the People's Republic of China. The Japanese industry started to produce X-ray units very quickly with units being introduced into hospitals by 1900.

Medical physicists were not employed by the medical systems until much later. The first medical physicists were appointed in Australia, New Zealand and India in the mid-1930s and in the People's Republic of China in the 1940s. Training in those days was basically non-existent with the first physicists not even having access to experienced medical physicists to learn from. Some had the opportunity to travel overseas to get on-the-job experience, but the opportunities quickly disappeared once World War II started.

Over the following decades as radiotherapy units were introduced in other countries in Asia-Oceania, more physicists were appointed to provide the required scientific expertise to provide a safe and effective service.

Medical physics professional societies started to form in the 1970s as the number of physicists in some countries became sufficiently large to warrant such a development. Prior to this, in Australia and New Zealand, a lot of the physicists were members of the UK Hospital Physicists Association until the Australasian College of Physical and Engineering Scientists in Medicine was formed. About this time MSc degrees in medical physics started to be established in some countries and later some certification systems for medical physicists appeared. Formal training schemes requiring an MSc, clinical training and examinations finally appeared after 2000.

Some of the professional societies became members of the

International Organization of Medical Physics after it was established in 1960. The need for regional organizations was met by the establishment of the Asia-Oceania Federation of Organizations for Medical Physics and the South East Asian Organization for Medical Physics in 2000.
Medical physics is now established as a profession in almost all countries in Asia-Oceania with excellent training schemes being available in an increasing number of countries.

MST 42

THE STATUS OF EDUCATION AND TRAINING OF MEDICAL PHYSICISTS IN THE AFOMP REGION

Kwan Hoong Ng
Department of Radiology, University of Malaya Medical Centre, Kualalampur, Malaysia.
E-mail: ngkh@ummc.edu.my

IDMP

IDMP-1

HISTORY OF MEDICAL PHYSICS: A NEW IOMP PROJECT

Slavik Tabakov

President, International Organisation for Medical Physics (IOMP), Department of Medical Engineering and Physics, King's College London, UK. E-mail: slavik.tabakov@kcl.ac.uk

Medical Physics is relatively young profession and very dynamic profession. This creates a need for a reference source showing the development of the profession and the progression of ideas. Such source is naturally a project describing the history of the profession. Recently IOMP launched such project aiming to show the creation and the evolution of different equipment and methods, as well as their clinical application; the overall development of the profession and the main contributors in the various topics in medical physics.

The project will create a Compendium of independent Volumes/Parts, which will reflect the main areas of development of medical physics, including: Diagnostic Radiology (X-ray) Imaging; Computed Tomography; Radiotherapy (External beam); Radiotherapy (Brachytherapy); Nuclear Medicine Imaging; Ultrasound Imaging; Magnetic Resonance Imaging; Optical Systems and NIR in Medicine; Medical Informatics; Radiation Measurement and Protection in Medicine; Professional Development; Education&Training Development. Other fields can also be added during the development of this large project, which is expected to attract a large international team and to take several years.

Each Volume of the Compendium will be relatively independent and will have its own Leads/Editors, who will prepare the internal structure of the Volume (its Chapters/Sub-chapters) and will invite colleagues to write these Chapters. Each Chapter will refer to specific types of equipment and/or method(s). The methodology of the projects will roughly follow the methodology of development of the Encyclopedia of Medical Physics project (www.emitel2.eu). The project volumes will be printed as Annex to the issues of the free online Journal of IOMP Medical Physics International (MPI).

The project results will be a very useful source of information for future new developments and will provide a canvas for future updates. Very importantly, the project results will be a written proof of the significant role played by medical physicists in contemporary medicine.

IDMP-2

MEDICAL PHYSICS EDUCATION & PROFESSION PERSPECTIVE IN AFOMP REGION

Tae Suk Suh, Ph.D.

Department of Biomedical Engineering, College of Medicine, The Catholic University of Korea, Seoul, South Korea. Email: suhsanta@catholic.ac.kr

Asia-Oceania has a diverse cultural, social, educational, and economical background. Around 60% of the world's population resides in Asia and Oceania and speak hundreds of languages and dialects. Geographically, Asia comprises five sub-regions: North East, South East, Central, South, and Middle East.

There is a shortage of medical physicists worldwide, especially in the Asia region. The reason for this is there are fewer education and training programs for medical physicists in Asia. The most difficult part of medical physics is in the area of clinical training. Therefore, there are fewer qualified medical physicists and more transfer of qualified medical physicists to advanced countries.The lack of recognition of medical physics standards of practice is a common issue in many Asian countries. Most of the Asian countries do not have accreditation or certification systems for medical physicists.The IAEA data for Asian countries with education, clinical training, and proper accreditation process in the field of medical physics show that most parts of Asia do not have clinical trainings or accreditation programs.

Education in medical physics in the Asian region has been supported by the IAEA or the IOMP.Most clinical centers in the Asian region cannot afford the time and investment in the clinical training of physicists. A joint approach with regional professional bodies has fostered clinical and scientific meetings to encourage clinical practice and to transfer skills and maintain communication among professionals. An example of was the UNDP project supported by the Korean FDA. The UNDP project provided a one-month clinical training opportunity in Korea for medical physicists in developing countries in Asia. The IAEA also provided many clinical training programs for medical physicists in Asia through various projects.

The role and status of medical physicists in the AFOMP region has gradually improved as can be seen by its increasing recognition in societies. However, neither the governments nor the public has yet recognized the importance of medical physics and the necessity for accreditation. A well-prepared strategy and a strong action plan are crucial for the AFOMP to move forward.

IDMP-3

MEDICAL PHYSICS EDUCATION: INDIAN SCENARIO

S. D. Sharma

Radiological Physics and Advisory Division, Bhabha Atomic Research Centre, CT and CRS, Mumbai, Maharashtra, India. E-mail: sdsbarc@gmail.com

Medical Physics is a new and important discipline of science which deals with the application of physical principles and methods to the diagnosis and treatment of diseases. About three decades ago, medical physics activities were restricted primarily to the dosimetry of ionizing radiation. In the recent past, this concept has changed considerably and now the medical physicists are involved in all the aspects of medical application of radiation including radiation safety and play

vital roles both in diagnosis and therapy diseases. Foreseeing the requirements of medical physicists and radiation safety officers (RSOs) well in advance, the Radiological Physics and Advisory Division (erstwhile Division of Radiological Protection), Bhabha Atomic Research Centre (BARC) started a regular training programme in Radiological Physics in 1962, in collaboration with World Health Organization. This course was later converted as Diploma in Radiological Physics (DipRP). The DipRP course of BARC is a prestigious multidisciplinary education and training programme which is well recognised both in India and abroad.

Considering the increased demand of medical physicists/ RSOs in the country, a few universities/institutions also started education and training programme in medical physics. Currently, fourteen universities/institutions are conducting courses in medical physics in India. As far as course modality is concerned, two different types of medical physics courses are conducted in India, namely (i) Post MSc Diploma in Radiological/Medical Physics (DipRP/DipMP), and (ii) MSc Degree in Medical Physics [MSc (Medical Physics)]. In DipRP/ DipMP course, the entry level qualification of the candidate is MSc Degree in Physics whereas in MSc (MedicalPhysics) course the entry level qualification is Bachelor of Science Degree majoring in physics. As most of the medical physicists trained in India work in the discipline of radiation oncology medical physics (ROMP), the entry level qualifications are based on the eligibility criteria prescribed by the Atomic Energy Regulatory Board (AERB) for medical physicist and RSO. The curriculum of the DipRP course, conducted by BARC, has been adopted by the AERB indicating it to be one of the best courses in the country with its well-organized modality.

A qualified medical physicist is a professional with education and specialist training who is competent to practice unsupervised in one or more subfields of medical physics. An ROMP is involved in many clinical activities including performance evaluation of imaging and therapy equipment, physical and patient dosimetry, treatment planning, research and development, and teaching related to medical use of ionizing radiation and associated radiation protection and safety. Advanced technology therapy and imaging equipments are now-a-days commonly used for treating the cancer patients by highly advanced clinical techniques such as intensity modulated radiotherapy, image guided radiotherapy, stereotactic radiosurgery/radiotherapy, and volumetric modulation arc therapy. Providing physics support in these high precision and highly conformal clinical techniques are also the routine responsibilities of the medical physicists. It will be challenging for a medical physicist without supervised clinical experience to provide physics support in such cases. Due to the complexity of recent radiotherapy equipment and clinical techniques and to ensure the effective and safe treatment for the patient, medical physics internship at a well-equipped radiotherapy centre for at least one year duration on successful completion of academic component has recently been incorporated in the medical physics education in India. A structured competency based medical physics internship programme was developed and implemented from July 2013. As on today, more than 100 radiotherapy centres are conducting medical physics internship in India.

In addition, efforts were made to harmonize academic part of the medical physics programme. In this context, a process of assessment of medical physics courses were initiated to ensure that the syllabus and infrastructure are adequate to conduct the programme effectively. Further, competency certification process of clinical medical physicists has also been started way back in 2009 and by now about 50 candidates has been certified by the College of Medical Physics of India. Competency testing and certification for RSOs are also conducted since early days of medical physics programme in India. Now, this process has been revised and re-structured with effect from 2007.

In summary, medical physics education in India is well-structured. However, there is always scope of improving the quality of teaching and training which is being initiated by incorporating training for trainers. Now, it is required to initiate the process of revalidation of certification both for clinical competency and radiological safety.

IDMP-4

PIONEER WOMEN MEDICAL PHYSICISTS FROM MEFOMP COUNTRIES

Huda M. Al Naemi

Chief Medical Physicist & RSO, Hamad Medical Corporation, Doha, Qatar. E-mail: halnaomi@hamad.qa

Establishment of Middle East Federation of Medical Physics (MEFOMP) in 2009 was part of the International Organization for Medical Physics (IOMP) efforts to organize regional medical physics societies under its umbrella and to further enhance and improve the status of medical physics across the Globe.

The main Goals of MEFOMP are; to Promote advancement of medical physics in the Middle East (ME), Educate and train local society members on new procedures and technologies, Encourage exchange of expertise and information among societies and to organize regional conferences and symposia.

The number of Female medical physicists obtained from the MEFOMP countries medical physicssocieties (in Lebanon, Syria, Jordan, Iraq, Palestine, King Saudi Arabia (KSA), United Arab Emirates (UAE), Kuwait, Qatar, Bahrain, Oman and Yemen) was found to be 243. Whereas the total number of medical physicists in these countries is 700 working in radiology, oncology, nuclear medicine and all other medical physics fields. This means that 35% of the medical physicists in the Middle East are women. The highest number of female medical physicists was found to be in Kingdom of Saudi Arabia 84 (35 % of the total MEFOMP females). The highest percentage of the female medical physicist in MEFOMP counties is in the UAE as 70% of medical physicists are females.

Some of the women in MEFOMP countries are pioneers in their field, their creativity and achievements have contributed to medical physics and that is sure to inspire a new generation of young women to pursue their highest ambitions in medical physics and other fields.

IDMP-5

MEDICAL PHYSICISTS CERTIFICATION PROCESS AND EXAMINATION IN THE MIDDLE EAST

Ibrahim Duhaini

Chief Medical Physicist and RSO, Rafik Hariri University Hospital, Beirut, Lebanon. E-mail: duhaini@yahoo.com

Certifying medical physics is becoming an essential part in recruiting medical physicists in hospitals across the Middle East region. Due to the lack of a comprehensive post graduate programs in MP in most of ME countries; hospitals find it very difficult to hire MP without the proper credentials and clinical experiences. Also, MP in the region find it very difficult to apply and travel for certification in Europe or North America due to visa and other related issues. So, if these certifying bodies are welling to cooperate with MEFOMP and/or similar organizations in the ME region so that certifications will be offered in the region for the region in a way to ease the process and save efforts and resources from the burdens of MP.

Certifying Medical Physicist requires an individual to obtain a university degree at the level of Master degree in Medical Physics, this is followed with at least a one year of clinical residency program in the Medical Physics fields applied in a Hospital.

The existing local/national certifying organization exam models are utilized as reference to design the final exam structure which can be customized for the medical physicists that will be working in the Middle East.

Three Exam Model proposals will be discussed here, all of which aim to evaluate the competencies of the individual medical physicist knowledge and skills by following various examination approaches.

IDMP-6

INTRODUCTORY TALK ON IDMP

John Damilakis

Department of Medical Physics, Faculty of Medicine, University of Crete, Heraklion, Greece. E-mail: john.damilakis@med.uoc.gr

The International Organization for Medical Physics (IOMP) celebrates every year the International Day for Medical Physics (IDMP) on November the 7th. The day was chosen by IOMP in recognition of the pioneering research work on radioactivity of Marie Sklodowska-Curie who, on that day in 1867, was born in Poland. This year we celebrate the 150th birthday of Marie Sklodowska-Curie and the theme is 'Medical Physics: Providing a Holistic Approach to Women Patients and Women Staff Safety in Radiation Medicine'. IDMP is an excellent opportunity to promote the role of medical physicists in the worldwide medical scene.

Medical Physics enables healthier lives for women. There are health problems that are more prevalent in women than in men such as breast cancer and osteoporosis. Medical physicists not only develop methods to diagnose and treat breast cancer but also play a fundamental role in their application ensuring the quality of procedures while minimizing radiation risks to women patients. X-ray mammography was developed in the 60s. In 1965, Charles Gros, a French medical physicist developed the first X-ray unit dedicated to mammography called 'Sonographe'. X-ray mammography has been considered as a 'gold standard' for screening of asymptomatic women. Dedicated CT systems have also been developed by medical physicists for the three-dimensional high-resolution imaging of the breast. In 1963, J. Cameron and James Sorenson, medical physicists from the USA developed the first non-invasive technique to assess bone mineral. They introduced single photon absorptiometry to measure peripheral bone mineral density. This had tremendous implications in healthcare, especially for the early diagnosis of osteoporosis.

Globally, women have fewer opportunities than men and less representation in the workplace. Increasing the number of women medical physicists should be a priority for our profession. IDMP 2017 is an excellent opportunity to discuss and try to address work challenges for women medical physicists. IOMP 'Women Subcommittee' is working with IOMP national member organizations to address gender inequality and empower women medical physicists. I would like to congratulate the Subcommittee for these activities.

IDMP-7

MEDICAL PHYSICS CONTRIBUTION TO WOMEN'S HEALTH AND RADIATION SAFETY CONSIDERATIONS IN MEDICAL PHYSICS TOWARDS WOMEN'S HEALTH AND RADIATION SAFETY

Hasin Anupama Azhari

Department of Medical Physics and Biomedical Engineering, Gono Bishwabidyalay, Savar, Bangladesh. E-mail: ahasinanupama@gmail.com

The discovery of X-rays, natural radioactivity and ionizing radiation has played an important role in numerous fields in modern scientific and technological developments radically influencing the entire modern civilization spanning fields like atomic and nuclear physics, agriculture, industry and in medicine providing an impetus for development of radiology and radiotherapy as medical specialties and medical physics. In this article contributions of medical physics for the occupational workers especially for women, s health in terms of radiation safety have been described. Continuous technological advancements in all areas of medical physics are significantly increasing the risk of potential exposure to ionizing radiation. General acceptance of risks of radiation is a matter of consensus, and therefore, international safety standards are needed to provide the justification of the use of any radiation with standardization, optimization and limitation of exposure. International consensus was achieved for the IAEA safety standards (BSS) through the IAEA SAFETY SERIES, which adopted and documented for medical public and occupational exposures as well as the special needs for the safety of women medical physicists with child bearing incidence. Participants of these initiatives are six major relevant international organizations: FAO, IAEA, ILO, the OECD Nuclear Energy Agency (OECD/NEA), Pan American Health Organization (PAHO) and WHO. The purpose of the standards is to establish basic requirements for protection against the risks associated with exposure to ionizing radiation and for the safety from the radiation sources.

Radiation sources and installations should be provided with the best available protection and safety measures under the prevailing circumstances, so that the magnitudes and likelihood of exposures and the numbers of individuals exposed should be As Low As Reasonably Achievable

(ALARA). For the establishment of dose limitation (DLs), the National Council on Radiation Protection and Measurements (NCRP) assessed risk on the basis of data from reports of the National Academy of Sciences (Biologic Effects of Ionizing Radiation [BEIR]. NCRP 116 and ICRP 60 recommend a limit of radiation exposure to a member of the general public as 1 mSv per year and the limit for the fetus of an occupationally exposed individual to 0.5 mSv per month (NCRP) and 2 mSv during the gestation period (ICRP).

When a radiologic worker becomes pregnant, she should notify her supervisor. The main risk is that of abortion if the radiation exposure results in death of the conceptus. Response of fetus to radiation is non threshold in nature and ten times more susceptible than maximum permissible dose (MPD) and thus special considerations are required. It requires a foetal dose of more than 100 mGy for this to occur. Based on this, it was suggested to do away with the 10-day rule and replace it with a 28-day rule postulated by ICRP for woman of reproductive age. The pregnant worker should be provided with a second personnel monitoring device at waist level as well as counseling. No alteration in work schedule is required normally.

A safety culture should be developed that governs the attitudes and behavior in relation to protection and safety of all individuals and organizations dealing with sources of radiation with special consideration to pregnant women. In-depth defensive measures should be incorporated into the design and operating procedures for radiation sources to compensate for potential failures in protection or safety measures; and also protection and safety should be ensured by sound management and good engineering, quality assurance, training and qualification of personnel, comprehensive safety assessments and attention to lessons learned from experience and research.

IDMP-8

IOMP WOMEN SURVEY DATA

Virginia Tsapaki

Department of Medical Physics, Konstantopoulio General Hospital, Athens, Greece. E-mail: virginia@otenet.gr

According to the latest International Organization for Medical physics (IOMP) survey, which was published in the year 2015, women represent approximately 28% of the total medical physicist (MP) workforce globally (4807 women out of the 17024 medical physicists). In more detail, women percentages in different regions of the world are 47% in Europe, 21% in USA, 33% in Africa, 35% in Asia and 50% in Middle East. Despite the fact that the number of women MP is increasing over the years, surveys in Australia and Canada showed that they still are under-represented in leadership roles. A European survey concluded in 2012 concluded that women researchers constituted less than 40% in most countries of European Union. The European Commission makes a great effort to identify and quantify the remaining inequalities between the two genders, as gender equality is a fundamental value for the European Union. Many European policies have been introduced in the attempt to reach this gender balance. Although long-term gender equality trends seem to be encouraging, there are still steps to do. As reported in the recent literature, USA data suggest that around one quarter of deans and department heads are women; in science this drops to nearly 1 in 20. Part of this problem of under representation stems from the population pool: only 33% of science and engineering doctorate holders employed in academia are women. Other issues include well known problems of women's participation in science, technology, engineering, and mathematics (STEM) fields such as 1) lack of role models, 2) unconscious biases, 3) discrimination 4) unwelcoming climates, etc.

In order to investigate if all this is actually true in the medical physics filed, IOMP decided to run a detailed survey. It was thought that the results of the survey could provide an opportunity for countries as well as IOMP, for a more in-depth analysis and deliberate on further actions. An online questionnaire was created, prepared as a Google Forms survey asking the country a number of simple questions relating not only on the total number of MPs and women MPs, but also on issues related to leadership or high level professional or scientific roles. The questionnaire was sent to all national member organizations of IOMP. In the attempt to have as much data as possible, even non-IOMP member countries were included in the survey. The results will be presented.

IDMP-9

MP EDUCATION, PROFFESSION AND AS ACAREER FOR WOMEN IN BANGLADESH: PROBLEMS AND PERSPECTIVE

K. T. Afrin, N. Karmaker, H. A. Anupama

Department of Medical Physics and Biomedical Engineering, Gono Bishwabidyalay, Savar, Bangladesh. E-mail: towmimzaman@gmail.com

Introduction: Medical physics is among the fastest progressing scientific and practical areas in Bangladesh. Historically women had played an important role in the field of physics, contributing to the leading achievements in the area. Our world is dominated by men but women have made significant contributions to the development of medical physics study and practice. According to survey of IOMP 2015, Sixty-six countries answered the survey, with 52% of responses provided by women. The total number of medical physicists cited was 17024, representing more than three quarters of the worldwide medical physics workforce. This included 4807 women – just 28% of the total.

Objectives: The main objective of this study is to find out the educational, career and professionals status of medical physics for women in Bangladesh existing or opportunity.

In Bangladesh three universitiesare offering M.Sc program in medical physics (MP); Gono Bishwabidyalay (University) is the pioneer one, offering degree since 2001, Dhaka University and Khwaja Yunus Ali University, offering since 2014. Female students areonly 20% in these universities, due to challenge of balancing family life, childcare support, gender inequality, social class, caste, religion, ethnicity, early marriage and house hold work. Also for economical constraint, normally after bachelor course, the femalestudents are unable to admit in M.Sc course as educations in private University areexpensive for poor students. Another reason is traditionally women are underrepresented in those fields based on mathematics and physical science.

Medical physics study is a new subject with a little exposure to common people so our people are unawareabout itsprospective career. Lack of job availability, dreadful of radiation hazards for the females discontinues their careers. Also in Bangladesh jobs are available after four years honors' program. In this field for career in medical physics minimum requirement is M.Sc in MP, which is one of cause for discontinuing to develop career in this field. Most of the female students in science are always pressurized from their family for early marriage. It seems tobe difficult to succeed as a medical physicist.

As a profession medical physics in Bangladesh is now at the beginning stage because of the lack of governmental position in hospital. Bangladesh Medical Physics Society (BMPS) is working with the government for recruitment rules for the MP. On the other hand private hospitals are recruiting MP with the advent of diagnostic and therapeutic treatment modalities based on medical physics.

Discussion and Conclusion: According to WHO report, we need total 160 radiotherapycenters, 320 LINACS, 640 Medical Physicists only in cancer treatment. Bangladesh government is purchasing recent updated technology for radiotherapy and radiology. The importance and necessity of this manpower is needed to be circulated in media and newspapers for public awareness. In the mean time, BMPS is working hard to popularize this subject, make awareness in public sector and to create position in the hospitals and continuous professional development for the graduates. The experiment to establish a department in Gono University is a successful story. Through German collaboration since its inception and help of other countries like India and China, Gono University is trying hard to maintain international standard. IOMP is working towards strengthening of the role of the women in our professional society.

Two years training program for certificationwill be started through national and international collaboration. BMPSalso trying best to involvefemale participants specially in AAPM, IAEA, AFOMP, IOMP conference for their career. A step towards achieving this objective is the formation of IOMP-W (IOMP women medical physics group). We certainly believe this group will encourage our Female medical physics community in education, profession and career.

IDMP-10

CONTRIBUTION OF WOMEN TO MEDICAL PHYSICS AND STATUS OF WOMEN MEDICAL PHYSICISTS AN INDIAN PERSPECTIVE

Shobha Jayaprakash

Chief Medical Physicist & RSO, B.Y.L. Nair Ch. Hospital, Mumbai, Maharashtra, India.

E-mail: shobhajp@hotmail.com

Today Medical Physics is among the fastest progressing in scientific and medical areas. Historically women played an important role in the creation, advancement and application of medical physics. In the last World Congress of Medical Physics and Bio medical engineering at Toronto, they had a special session for discussing problems faced by Women Physicists as well as their achievements. There has also been some discussion on the gender issues in Medical Physics community in the recent past. It is not always easy being a woman and a professional, as they have to balance between the family life and professional duties, but women have been proven to excel in multitasking.

Marie Curie, a pioneer in the field of radioactivity was the first woman to be awarded two Nobel Prizes in different sciences (Physics and Chemistry). One of Marie Curie's most famous citations: "We must have perseverance and above all confidence in ourselves. We must believe that we are gifted for something and that this thing must be attained". Marie Curie had opened the doors of her lab to many women for which she was an icon and represented an example to follow. Large number of women was found to be working her scientific research laboratory.

First international study on number of women Medical Physicists globally was performed by IOMP in 2013. 66 countries had participated and the survey results showed that out of the total number of Medical Physicists only 28% were females. The latest study on Women in Medical Physics performed in Australia/New Zealand and published in 2016 showed a considerable increase in the number of Women Medical Physicists. The rising number was contributed to women both deserving and passionate in their chosen fields

A survey was conducted in order to document the total number of Medical Physicists in India and the percentage of Women Medical Physicists. The data collection was done with the help of all the AMPI Chapters, AERB, seniors and colleagues. This is the first survey carried out in India. (1) To document the number and percentage of Women Medical Physicists. (2) Their contribution to Medical Physics -Status of Women Medical Physicists. The total number of Registered Medical Physicists in India as of today is 1042. This includes 361 women – which is just 35% of the total (which is slightly below the target (40% female) set by European countries. We have many female Physicists in faculty positions, involved in teaching and research. Many of them have national and international publications to their credit and also represent the country in International conferences. Even though not many Women Physicists are occupying eminent positions in various national and international forums and associations, they have still made significant impact wherever they have been chosen to officiate.

In India, many female Physicists face employment issues, as most of the hospitals are not in favour of employing female physicists, the reason provided was the late working hours which many Employers felt women were not capable of. Facilities such as formation of online group of Women Medical Physicists of India are a step towards recognition and help required by such individuals. This is an easy means to discuss and ask for advice without any inhibitions. Hence we have started an Online Indian Womens' Medical Physicist Group to discuss common issues and problems. The initial response has been overwhelming. It's really encouraging to see the camaraderie among our co-workers who have mailed their valuable opinions and suggestions. This has been an eye opener which needs to be addressed and dealt with. The facility can be made more accessible by forming Zonal Groups with a Zonal Representative who can co-ordinate with the Central Body.

It is also planned to organize, on a regular basis, seminars, workshops, refresher courses including hands on training etc. which will be beneficial for working Physicists and trainees to enhance and improve their working skills. A concept like this will bring to forefront the profession of Medical Physics among women thus increasing the sorry percentile of the Women Physicist statistics. Overall this will also help us to popularize the role of women in medical physics and encourage Female medical physicists to advance in the profession.

IDMP-11

WOMEN AND MEN IN THE AUSTRALASIAN COLLEGE OF PHYSICAL SCIENTISTS AND ENGINEERS IN MEDICINE: WORKFORCE SURVEY

Eva Bezak[1,2], Roksolana Suchowerska[3], Elizabeth Claridge Mackonis[4], Heath Pillen[5], Anna Ralston[6], Annette Haworth[7], Natalka Suchowerska[4,7]

[1]Sansom Institute for Health Research and the School of Health Sciences, University of South Australia, [2]School of Physical Sciences, University of Adelaide, Adelaide, [3]Centre for Social Impact, Swinburne University, Melbourne, Victoria, [4]Chris O'Brien Lifehouse, [6]St George Hospital Cancer Care Centre, [7]Faculty of Science, University of Sydney, New South Wales, [5]International Centre for Allied Health Evidence, UniSA , Australia. E-mail: eva.bezak@adelaide.edu.au

Introduction: A survey was designed to determine the aspirations, motivations and workplace experiences of members of the Australasian College of Physical Scientists and Engineers in Medicine (ACPSEM). The survey collected both quantitate and qualitative data, including open ended questions. This presentation reports the survey's qualitative results. The qualitative data analysis was in part funded by the ACPSEM.

Methods: The research was approved by Ethics at University of South Australia and endorsed by ACPSEM.

All 205 female members (30% of total membership) and 440 males were invited to complete the survey online.

The data for the qualitative analysis were responses to open-ended questions within the Survey. The data was thematically analysed by twice. First, by the survey authors and secondly by a single researcher, who was a male allied health researcher not involved in the development of the survey or data collection. Open codes were assigned to key categories in the data on a first reading of the survey responses and refined to 24 codes on a second reading. Codes were arranged into themes inductively by examining the relationship between them. Analysis of responses continued until no new themes emerged from the data, despite further analysis. Since the number of females in a senior managerial role was limited, further analysis was performed for this subgroup to account for any relevant variations in the data.

Results: 102 female and 150 male completed surveys were received, with 66 surveys analysed, before data saturation was reached.

The survey revealed a number of themes that reflect concerns and opportunities identifying the direction for improving work-life balance and gender equity within the medical physics profession in Australasia. Issues around managing challenging workloads and professional development were amplified for women with children and child-rearing responsibilities, directly contributing to a reduction in work capacity and a reorientation of work-life priorities. Some evidence of gender inequities in the professional context were reported. Female respondents, in particular those assuming a carers role, perceived these inequities to be the entrenched attitudes and structures that act to favour one group over another. For some women, this gender bias meant that it was difficult to engage fully in the profession when indicators of success (e.g. meeting the inflexible needs of organisations through working long hours, work hour flexibility and travel) favoured those without carer responsibilities. Inefficient management practices contributed to an environment where unreasonable time demands are placed on staff with carer responsibilities, limiting opportunities to engage in career development activities. In contrast, male (and some female) respondents perceived the workplace to offer equal treatment of individuals irrespective of gender and that individuals are responsible for their own success and advancement within the profession.

Conclusions: The survey provides direction for strategies to improve work-life balance and enable equitable engagement in the profession. The first is to identify and develop role models that actively model successful work-life balance and flexibility in gender roles and in professional conduct. The second is to improve the management skills of current and emerging administrators, advocating for improved work conditions for medical physics professionals at an organisation level. Finally, efforts need to be made to establish flexible professional development and career progression opportunities amongst those that are unable to commit to large workloads, which is common for those with child-rearing responsibilities. The realisation of these strategic goals will reduce the identified barriers to full female participation in the workforce, and shift gender-based subcultures within the workplace.

IDMP-12

RADIATION SAFETY ASPECTS PERTAINING TO FEMALE PATIENTS AND STAFF

Nidhi Patni

Department of Radiation Oncology, BMCHRC, Jaipur, Rajasthan, India. E-mail: nidhionco@gmail.com

Many organizations in the world are committed to gender parity. Increasing number of women is working in the fields of radiation medicine and in industries dealing with radiation. Women patients may be exposed to radiation in radiology, radiation oncology, nuclear medicine, interventional cardiology, dentistry etc. Radiation safety of women staff and women patients is different from their male counterparts because of conception and pregnancy. So, fetal health is a matter of concern in the above. Also, the excess relative risk of radiation induced cancers in females relates to higher risk of thyroid cancer and high radiosensitivity as compared to males.

With the advances in technology radiation equipment are safer than ever. Highly sophisticated radiation safety, QA and measurement gadgets are a norm. Strict personal radiation exposure monitoring is being done on a regular basis. According to the latest recommendations from Atomic Energy Regulatory Board (AERB), the maximum permissible effective dose for radiation workers 20 mSv annually averaged

over five consecutive years. For pregnant radiation workers, the dose to embryo or fetus should not exceed 1 mSv, after declaration of pregnancy.
Best possible measures are taken to achieve ALARA. “Rule of ten” is a safe practice while going for an elective radiological investigation in a female in reproductive age group. Fetus is most sensitive to radiation effects between 8 and 15 weeks of pregnancy. If the mother has been given a radioisotope, depending upon its half life, breast feeding should be avoided. In a multidisciplinary approach, lesser amount of radiation dose is required and lesser volume of tissue is irradiated, especially since more effective systemic therapy is available now. Same stands true for patients undergoing radiation therapy. Modern radiation treatment has reduced the irradiated volumes on one hand but high precision treatments like IMRT, IGRT and SBRT have increased the integral dose. The stochastic effects of integral dose are of concern. Radiations safety of women staff and women patients needs special consideration.

IDMP-13

DOSE MANAGEMENT OF PREGNANT PATIENTS IN RADIOLOGY

John Damilakis
Department of Medical Physics, Faculty of Medicine, University of Crete, Heraklion, Greece.
E-mail: john.damilakis@med.uoc.gr

Conceptus dose and risk assessment is of great importance whenever a diagnostic or interventional X-ray examination of a pregnant patient is necessary. Estimation of conceptus radiation dose and associated risks is also needed in cases of accidental exposure of pregnant patients from X-ray procedures. This presentation will provide information about methods to estimate radiation dose absorbed by the unborn child from x-ray examinations and strategies to manage pregnant patients so that radiation doses to the mother and child are kept as low as reasonably achievable.
When the uterus is remote from the directly exposed anatomical area, the embryo/fetus is exposed to scattered radiation and its dose is negligible (dose lower than 1 mGy). Normally, a detailed embryo/fetus dose evaluation is not needed for such studies. Radiologic examinations involving the abdomen and/or pelvis may deliver relatively high radiation dose to the unborn child. For abdominal examinations, maternal body size and uterus position should be taken into consideration to obtain accurate dose estimation. Patient-specific Monte Carlo simulations have been used to accurately estimate radiation dose from an abdominal CT examination. A standard CT examination for appendicitis or ureteral stones performed on the mother would result in an embryo/fetus dose of about 10-25 mGy. Multi-phase abdominal CT examinations may deliver relatively high doses to the unborn child. Doses to the unborn child below 100 mGy should not be considered a reason for therapeutic abortion.
The risk to the embryo/fetus for stochastic effects is assessed on the basis of radiation dose using appropriate risk factors. CoDE (Conceptus Dose Estimation) online software tool allows a) calculation of conceptus radiation dose and associated risk from X-ray examinations performed on the expectant mother and b) anticipation of conceptus dose for the pregnant employee who participates in fluoroscopically-guided interventional procedures. CoDE is available free of charge. For more information please visitembryodose.med.uoc.gr

IDMP-14

SEGMENTATION OF BREAST MASSES USING ACTIVE CONTOUR MODELLING

W. I. D. Rae, S. N. Acho
Department of Medical Physics, University of the Free State, Bloemfontein, South Africa. E-mail: raewid@ufs.ac.za

Introduction: Breast disease is widespread and is a major cause of morbidity and mortality worldwide. Imaging of the breast is a widely used standard for assessment of pathology and screening of asymptomatic people who may have some increased risk of cancer, or in some countries screening if available to all women over some predefined age (usually 40 years). Imaged tumours often infiltrate surrounding normal tissues and thus delineation of the tumour to define a focal area for treatment, or to assess change in the tumour over time, is difficult and often not unanimous. Reliable and reproducible metrics describing the tumour morphology are thus difficult to obtain and to quantify. To achieve reliable quantitative measures of lesions within the breast it is necessary to have a reliable segmentation method to define objects seen in the image. Active contours are useful in defining boundaries around masses by defining a contour which expands and contracts over the edge of a mass until it reaches a minimum energy state dependent upon the statistical information inherent in the digital image. It has been shown that segmentation outcomes for active contours which are driven by local statistical information depend upon the placement of the initial level set contour. This is limiting. A more robust and generalised method to determine mass specific boundaries would facilitate the automated or assisted analysis of mammograms to allow wider utilisation in computer aided diagnostic and detection systems.
Aim: To develop a mass segmentation technique which is reliable and can lead to more meaningful segmentation of breast pathology by providing a mass-specific threshold value, which requires minimal intervention from the user, and which minimises the energy functional of the segmentation contour for individual masses.
Materials and Methods: Problems with segmentation using convex active contour model masses have all sizes, shapes, locations and more often embedded in the complex matrix of the breast parenchyma tissue therefore a single threshold value for a database of masses is not practical, therefore we propose a mass-specific threshold value for convex energy functional of each massdriven by global stats. Images were smoothed prior to segmentation. This mathematical method is applied to a series of test masses with a range of pathologies as a proof of concept.
Results: The proposed model performed well when compared to other standard techniques of mass segmentation and was independent of the initial position of the initial contour.
Discussion: Each mass lesion is unique and using a

smoothed image was shown to be useful in defining its best representation. Using the probability matrix (interactive process) derived from random walk algorithm acted as a confidence map to guide the segmentation process. Such stable boundaries can be useful as they define the “inside” and “outside” of masses thus effectively using statistical measures to see how the mass characteristics change over the area of overlap of, or invasion by, the mass and the surrounding normal tissues. This may be able to give insight into the behaviour of masses at their boundary and allow modelling of masses according to their pathological origin.

Conclusion: Active contour modelling is a reliable segmentation method. The results are independent of the initial level set contours and require a minimal level of intervention from the user. It allows interrogation of the statistical character of the junction between masses and their surrounds, thus potentially allowing better characterisation of imaged tumours.

Teaching Session

TS-1

TECHNOLOGY OF ADVANCED RADIOTHERAPY EQUIPMENT INCLUDING ION BEAM THERAPY EQUIPMENT

S. D. Sharma
Radiological Physics and Advisory Division, Bhabha Atomic Research Centre, CT and CRS, Mumbai, Maharashtra, India. E-mail: sdsbarc@gmail.com

In recent years, several technological developments have taken place in the design and capabilities of radiotherapy equipment especially beam delivery devices. Radiotherapy beam delivery devices can in general be classified as teleisotope machines, medical electron linear accelerators and ion beam accelerators (proton and heavy ion). Among teleisotope machines, we have conventional telecobalt unit which has recently been equipped with multileaf collimator (MLC), specialised telecobalt machine such as Gamma Knife (various variates) and super specialised machine such as View Ray. The conventional telecobalt machine, which contains a single high activity source, is still the work horse of middle and lower income countries. Gamma knife, which contains multiple cobalt sources (ranging from 30 to 201) and specialised narrow field collimators, is also being used popularly for treatment of mainly intracranial tumours. Many versions of this equipment are available globally. Super specialised teleisotope machine (the View Ray) is the new addition in the armamentarium of external beam therapy. This device contains three source heads at 120 degree apart and diverging multileaf collimators plus an on-board magnetic resonance (MR) imaging device. This super specialised teleisotope machine can be used for treating varieties of cancer cases by applying the techniues of intensity modulated radiotherapy, stereotactic body radiotherapy and on-couch adaptive radiotherapy.

Various versions of technologically advanced medical electron linear accelerators (LINACs) are also available in the radiotherapy departments globally. Medical electron linear accelerators can be classified in two general categories, namely standard LINAC and specialised LINAC. Technological changes have been incorporated in both the categories of the LINACs. For example, advanced medical LINAC with flattening filter free photon beams as well as on-board magnetic resonance imaging system have been introduced recently. The MR-LINAC is the most recent development. The MR-LINAC can be used for treating various cancer cases. It has the capability of simultaneous dose delivery and fast acquisition of diagnostic quality MR images. This helps in tracking the tumour and visualising the anatomy of the patient during treatment. The constant monitoring of the patient during treatment enables the precise targeting of the tumour and help in minimising the dose to normal tissues/organs at risk. A few unitsof MR-LINAC are in use clinically and short term outcome of the treatment is curiously awaited.

Ion beam (mainly proton and carbon) therapy equipment are also in clinical use at a few radiotherapy centres. Proton beam accelerator (energy in the range of 80 to 250 MeV) is in clinical use from last few decades. This is a highly specialised beam delivery device which contains a cyclotron, beam transport system and treatment gantries. Pristine proton beam curve is hardly used rather Spread Out Bragg Peak (SOBP) is created to match the tumour size in the beams eye view and the dose is delivered. The proton beam accelerators are also equipped with precise beam shaping and beam modulating devices plus x-ray imaging system. However, the radiobiological advantage of proton beam is slightly over photon beam and hence heavy ions (e.g. carbon ion) are thought to be a relatively better option as far as the use of high LET radiation is concerned in radiotherapy. Carbon ion accelerators are used at a few centres to generate the clinical data. The technological details of these accelerators will be discussed in detail.

TS-2

IGRT: DETERMINING SETUP MARGINS AND CORRECTION METHODS

Tharmarnadar Ganesh
Department of Radiation Oncology, Fortis Memorial Research Institute, Gurgaon, Haryana, India.
E-mail: sptgnadar@yahoo.com

The International Commission on Radiation Units and Measurements (ICRU) in its report number 50 defines clinical target volume (CTV) as a tissue volume that contains a GTV and/or subclinical microscopic malignant disease, which has to be eliminated. Going by this definition, CTV is thus an anatomical-clinical concept, that has to be defined before a choice of treatment modality and technique is made. ICRU further adds that margins will have to be added around the CTV to compensate for the effects of organ and patient movements and inaccuracies in beam and patient set up leading to the concept of Planning Target Volume (PTV). The margin is called as CTV-to-PTV margin.

The ICRU Report 62, a supplement to the Report 50, refined the concept of CTV-to-PTV margin. Instead of arriving at PTV from CTV through a single margin that accounts for organ movements and setup inaccuracies, ICRU 62 defines a new process wherein expanding of CTV to PTV is achieved in two steps: first from CTV-to-internal target volume (ITV) through adding of internal margin (IM) and then in the second step from ITV-to-PTV through adding of setup margin (SM). While the IM accounts for the effects of internal organ movements, the setup margin accounts for inaccuracies in patient setup. The need for the splitting of CTV-to-PTV margin into IM and SM arises from the differences between the factors that control these margins. Since the IM is to account for the movements of internal organ, one has practically no, or very little, control over its magnitude. On the other hand the setup margin accounts for uncertainties in setup which are largely controllable and in a carefully designed workflow its magnitude can be significantly reduced. Thus, the two margins have to be viewed from different perspectives if the overall margin is to be kept low.

The setup margin, calculated from van Herk formula, is given as SM = 2.5Σ + 0.7σ, where Σ is the systematic error and σ is the random error. The systematic error is repeated in every treatment fraction and the random error, as the name suggests, randomly affects individual fractions. The errors are computed from the measurements of translational positional shifts in the three directions. They can be computed for a single patient and for a population of patients. While the former helps in alleviating the SM required for an individual patient, the latter helps in deducing a SM required for the concerned treatment site in that clinic that can be incorporated at the time of contouring. The SM is thus a department specific parameter and cannot be and shall not be taken from text books or literature.

After determining the SMs for different sites in a clinic, the next challenge is their meaningful implementation to make the workflow smooth and efficient. This is a crucial step for every department. Each department should carefully design its image guidance protocols for different sites that shall be driven by the SMs determined. The protocols shall clearly define the roles and responsibilities of every team member involved in the process. Action levels, and what actions should be taken if these are exceeded, shall be made known to everyone in the team. Online and offline imaging protocols are the commonly practiced. If these are not practiced correctly, due to failure in understanding them, it can severely hamper the department's workflow efficiency.

The presentation would cover in depth two important *practical* aspects: (i) determining the SM for a population of patients and (ii) how to clinically implement that SM in a manner improving the efficiency.

TS-3

PORTAL DOSIMETRY

Raghavendra Holla

Department of Medical Physics and Radiation Safety, Amrita Institute of Medical Science and Research Center, Kochi, Kerala, India. E-mail: raghavendra.holla@gmail.com

Introduction: Electronic Portal Imaging Device (EPID) is a flat-panel radiation detector, mounted on a linear accelerator (linac). EPID originally designed for geometric verification of patient set-up during treatment, can also be used to obtain dosimetric information about the radiation delivered because of the favourable characteristics such as fast image acquisition, high resolution and digital format. The most common EPID available today is an array of photodiode detectors on an amorphous silicon (a-Si) glass substrate.

EPID dosimetry also know as portal dosimetry is the method of acquiring images and then using these images to determine the dose delivered to a known point (1D), plane (2D) or volume (3D) within a patient. This is achieved via calibration of the EPID using an absorbed dose standard, image processing and knowledge of the patient anatomy.

Application of EPID for dosimetry can be classified according to whether they are performed during treatment time (i.e. with the patient) or outside of treatment time (i.e. without the patient).

EPID can be used for pre-treatment verification, a procedure comparing the whole or part of the intended treatment plan with measurements of corresponding radiation beams delivered by the linear accelerator without patient with open fields or a phantom. This comparison can focus on different aspects of the planned treatment: e.g. predicted and measured leaf positions, dose delivered to the detector or phantom, or incident energy fluence extracted from measurements.

Use of EPID is demonstrated by many researchers for Treatment verification. In this process comparison of all or part of the planned and the delivered dose distribution based on measurements acquired during radiotherapy of the patient is done. These measurements can be used to determine the dose delivered to the detector or patient, or incident energy fluence obtained from measurements.

If the determination of the dose in the detector (EPID), patient or phantom, or determination of the incident energy fluence, based on measurements without an attenuating medium between the source and the detector is performed then it is termed as Non-transmission (or non-transit) dosimetry.

In Transmission (or transit) dosimetry, determination of the dose at the position of the detector (EPID), patient or phantom, or determination of the incident energy fluence, based on radiation transmitted through the patient or phantom is performed. The measurement or determination of the dose inside a phantom is performed with EPID including the dose at points, lines, planes or volumes within the phantom at In-Phantom Dosimetry.

Ex-vivo dosimetry refers to the measurement or determination of the dose inside the patient using EPID transmitted images acquired during the treatment. The acquired images are used either to predict the dose delivered to the patient in 2D or 3D reconstruction of the dose for the entire volume of treatment.

To use of EPID for dose measurements requires calibration and corrections of EPID images to account for the various detector characteristics. Many studies have been performed to study the dosimetric response of EPIDs. For the flat panel detectors, studies have demonstrated a stable dose response that is independent of dose rate and linear with integrated dose. However, the flat panel response is also dependent on the incident photon energy and is affected by radiation scattered in the detector's many layers. The EPID also exhibits ghosting and image lag effect, an exponential memory effect with sequentially acquired frames. A global calibration model for calibrating EPID images to dose includes correction factors for, (1) Absolute dose calibration, (2) Image lag and Ghosting effect, (3) Field size dependence and beam profile Correction, (4) Buildup and energy spectrum correction.

A calibration model developed using these parameters are SSD dependent and hence a correction model has to be developed for a fixed SSD.

Conclusion: Portal dosimetry is evolving now to an integrated part in the total chain of verification procedures that are implemented in a radiotherapy department. It provides a safety net for advanced treatments as well as a full account of the dose delivered to specific volumes, allowing adaptation of the treatment from the original plan if necessary. The combination of an accurate EPID dosimetric calibration and a reliable interpretation of this EPID dose in terms of patient dose would provide a powerful new form of treatment verification for external beam therapies.

TS-4

ICRU REPORT 89: PRESCRIBING, RECORDING, AND REPORTING BRACHYTHERAPY FOR CANCER OF THE CERVIX

Jamema Swamidas, Umesh Mahantshetty[1]

Departments of Medical Physics and [1]Radiation Oncology, Tata Memorial Centre, Mumbai, Maharashtra, India. E-mail: svjamema@gmail.com

The objective of this talk is to summarize the recently published ICRU report-89 for Prescribing Recording and Reporting Brachytherapy (BT) for cancer of the cervix. This ICRU report which was published in 2016, deals with the radiation therapy treatment with special emphasis on BT for cervical cancer. It took more than 3 decades to revise the ICRU 38 published in 1985. The report provides definitions, concepts and terms to enable, valid and a reliable exchange of information regarding radiation therapy methods including external radiation and BT. It contains 234 pages, 13 chapters, an appendix of 9 clinical examples, a five page summary and a concise two page summary of the recommendations at the end.

The report starts with a comprehensive information about the epidemiology, incidence, work-up, basic treatment principles and historical outcomes with radio(chemo)therapy. A comprehensive overview of various BT systems including the historical roots linking with the current practices and recent advances in BT. Subsequent chapters include in detail all the processes involved in BT planning including various imaging modalities, modern BT applicators, adaptive target for external and BT, radiobiology considerations, and advanced BT treatment planning process, reporting of dose volume parameters for uniform prescribing, recording and reporting. The highlight of the report is summary and key messages at the end of each chapter which can be implemented in various environments. Tumor can be precisely assessed and delineated in three dimensions taking into account tumor growth pattern at BT and the topography of the adjacent OAR which has been addressed very well in chapter 5. Chapter-6 introduces radiotherapy related morbidity endpoints and sub volumes of OARs, based on the morbidity profiles as known from the clinical experience. For OARs, two reference volumes D_{2cm3}, $D_{0.1cm3}$, characterizing maximum exposed region in the adjacent organ walls were considered.

Chapters 9-12 are dedicated to treatment planning aspects from physics point of view which include applicator reconstruction, treatment planning and absorbed dose calculation, especially chapter-10 is dedicated to radiographic dose assessment, which emphasises that a common terminology needs to be established, such that progress in 3D BT can influence further developments in institutions with limited resources. Some of the recommended reference points are taken from the previous ICRU report -38, (bladder, rectum, pelvic wall and lymphatic trapezoid) in addition to the vaginal points. More specifically, this report has adopted the definition of point A as a reference point. This geometrical definition is recommended in order to provide a clear distinction with the anatomically defined target dose volume that has been introduced as a new concept. Chapter-11 describes the dose calculation formalism, includes the source strength specification. For absorbed dose calculation, AAPM TG 43 has been recommended. Further, correlation between TRAK and point A dose irradiated volumes is also indicated.

At the end of the report a short summary in tabular form gives a quick and complete overview of all the recommendations. The reporting is structured at different levels, Level 1 describes the minimum requirements, which should be followed in all centers, for all patients, and represents the minimum standard of treatment; level 2 indicates advanced standards that allow a more complete exchange of information between centers; level 3 is related to research and development for which reporting criteria cannot yet be established.

Appendix A consists of nine clinical examples describing in detail the various clinical, imaging, technical, and biological scenarios. The major recommendations as outlined in this report are applied and specified in these examples. On the website http://icru.org/content/reports/spreadsheets for calculating EQD2 doses are provided. This site also contains a printable form for reproducible clinical drawings as used in this report.

Trade Talks

TR-1

PRECISION AND UNCERTAINTIES IN CTDI MEASUREMENTS ON AXIAL COMPUTED TOMOGRAPHY SCANS

Erik Wikstrom, Soren Sören Sturesson
RTI Group AB, Mölndal, Sweden.
E-mail: erik.wikstrom@rtigroup.com

Introduction: The Computed Tomography Dose Index (CTDI) formalism has been used for quality controls on computed tomography (CT) systems for many years. Concerns has been raised weather the CTDI formalism is a relevant parameter for today's CT technology such as wider beams, helical scans etc, when the CTDI formalism is based on measurements on Axial scans and relatively narrow beam widths.

A 100 mm pencil ion chamber have been used to evaluate uncertainties in traditional CTDI measurements, and it's use for comparison to CTDI values for helical scans. E.g. can the $CTDI_{vol}$ value that is displayed on the CT console for a helical scan be validated by measure on an Axial scan?

Methods: A 100 mm long pencil ionization chamber were used to measure the $CTDI_{100,c}$ and $CTDI_{100,p}$ in a PMMA CD dose phantom. The variation in measured results were studied to evaluate different influence parameters that contributes to the CTDI calculations.

Result: Major variations in $CTDI_{100,p}$ were found. The reason for the variation is that the detector, when paced in a peripheral position of the phantom, may randomly become irradiated twice during one axial scan. This is due to that the radiation may be present for more than 360° of rotation. The CT machine that was used in this study had the radiation present for 380° at a one second axial scan.

Table attenuation when placing the phantom on the patient table is a major influence parameter when measured CTDI values is compared to the the console values.

$CTDI_{vol}$ values that were shown on the console for helical scans could not be directly compared to CTDI values measured in Axial scan, due to that the same technical parameters were not selectable, such as collimation. Also the presence of "over-rotation" in axial scans makes the comparison difficult.

Discussion: There are many factors that effects the measurement uncertainty when measure CTDI on axial scans using a pencil ion chamber. Measurement errors and uncertainties can be reduced by making a lot of exposures followed by careful evaluation of measured data. Then compensation for various generator characteristics can be applied. The measured CTDI value on an Axial scan has a limited relevance when used to evaluate the $CTDI_{vol}$ for a helical scan.

By once carefully establishing the relation between the $CTDI_{100,c}$ and $CTDI_{100,p}$, the $CTDI_w$ can be estimated with sufficient precision saving a lot of time, by significantly reducing number of exposures.

Conclusions: New methods for evaluating CT doses are of importance. Not only for wide beams and helical scans, but also for Axial scans.

AFOMP Best Paper

AB-1

PROTOTYPE DEVELOPMENT OF ARTIFICIAL INTELLIGENCE-BASED PROTON THERAPY PLANNING SYSTEM

Yong-Jin Kim, Do-kun Yoon, Sunmi Kim, Han-Back Shin, Moo-Sub Kim, Tae Suk Suh
Department of Biomedical Engineering, College of Medicine, The Catholic University of Korea, Seoul, Republic of Korea. E-mail: deseitn@gmail.com

Introduction: People are being helped of an artificial intelligence (AI) in many areas of life. And the AI is also can be used to progress a radiation therapy, It helps to establish a more accurate and faster treatment plan. In this study, we have studied the application of the AI to treatment planning acquisition for proton therapy, which requires more accuracy in dose calculation, to establish the treatment plan faster and accurately.
Objectives: The purpose of this study is to develop and operate an artificial neural network system of AI based radiation treatment planning system for proton therapy.
Materials and Methods: For a design of an artificial neural network, we establish the radiation treatment planning method by using convolution neural network model with some modifications. When a new input (patient data) data has been uploaded, it assigns a proper treatment plan through a supervised learning technique from a database. And it progresses the optimization for treatment plan through weight decay process. This mechanism leads to faster and more correct treatment plan creation than the conventional dose planning based on the either algorithm or Monte Carlo. This database was constructed by using a lot of results from Monte Carlo simulation operation. And it was interlocked with the deep learning algorithm.
Results and Discussion: In this study, we confirmed the target volume from convenient image using the developed algorithm. We successfully created the treatment plan by accessing the Monte Carlo database. In comparison with the treatment plan generation through direct Monte Carlo simulation, we deducted faster and equivalent therapeutic performance analysis results from the study. In terms of time, we succeed greatly fast acquisition of the proton therapy plan. For the aspect of accuracy, we have to improve the performance through the additional development of better optimization algorithms. In the future, we will progress the study to develop a complete engine.

AB-2

GRAPHICS PROCESSING UNIT-BASED FAST IMAGING TECHNIQUE DURING BORON NEUTRON CAPTURE THERAPY: MONTE CARLO SIMULATION STUDY FOR SINGLE-POSITRON EMISSION TOMOGRAPHY OPERATION

Hye Jeong Yang, Do-Kun Yoon, Han-Back Shin, Moo-Sub Kim, Sunmi Kim, Tae Suk Suh
Department of Biomedical Engineering, College of Medicine, The Catholic University of Korea, Seoul, South Korea. E-mail: suhsanta@catholic.ac.kr

Introduction: Boron neutron capture therapy (BNCT) is an effective radiation treatment technique based on the nuclear reaction between an epi-thermal neutron beam and boron particles. An alpha particle which is main therapeutic factor is emitted from the boron neutron capture reaction. Simultaneously as the boron neutron capture reaction was progressed, the prompt gamma ray of 478 keV is emitted from the same reaction point. The emitted prompt gamma ray can be used to gauge tumor status during the radiation treatment. However, it is difficult to monitor the therapeutic effect of BNCT in real time.
Purpose: Purpose of this study was to show the graphics processing unit (GPU) based fast prompt gamma ray imaging technique during BNCT using the Monte Carlo simulation.
Materials and Methods: To acquire the 478 keV prompt gamma ray image in a single step, positron emission tomography (PET) with an insertable specific collimator for single photon detection (S-PET) was simulated as shown in Figure 1. And then in order to perform a fast prompt gamma ray imaging, we were attempted to reconstruct the prompt gamma ray image using a modified reconstruction algorithm with GPU computation during BNCT [Figure 1].
Results and Discussion: Single photon detection from PET gantry with the insertable collimator was available during BNCT and prompt gamma ray of 478 keV had a capacity to obtain a tomographic image as shown in Figure 2. Moreover, prompt gamma ray images according to the treatment fraction were acquired almost immediately after the acquisition of projection data owing to GPU based image reconstruction. As a result, we could confirm the application feasibility of the fast prompt gamma ray technique for BNCT.
Conclusion: Due to the fast GPU computation, GPU application for BNCT S-PET has a large effect on reduction of reconstruction time. Therefore, it was possible to reconstruct GPU-based fast prompt gamma ray image during BNCT.

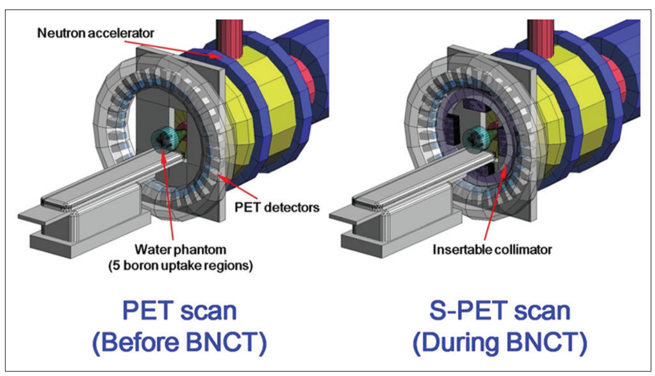

Figure 1: Simulation configuration of the acquisition of both the prompt gamma ray image and the positron emission tomography image. Neutron accelerator, water phantom including boron uptake regions, and positron emission tomography detector were simulated. In the right figure, the insertable collimator has been added (circular violet structure)

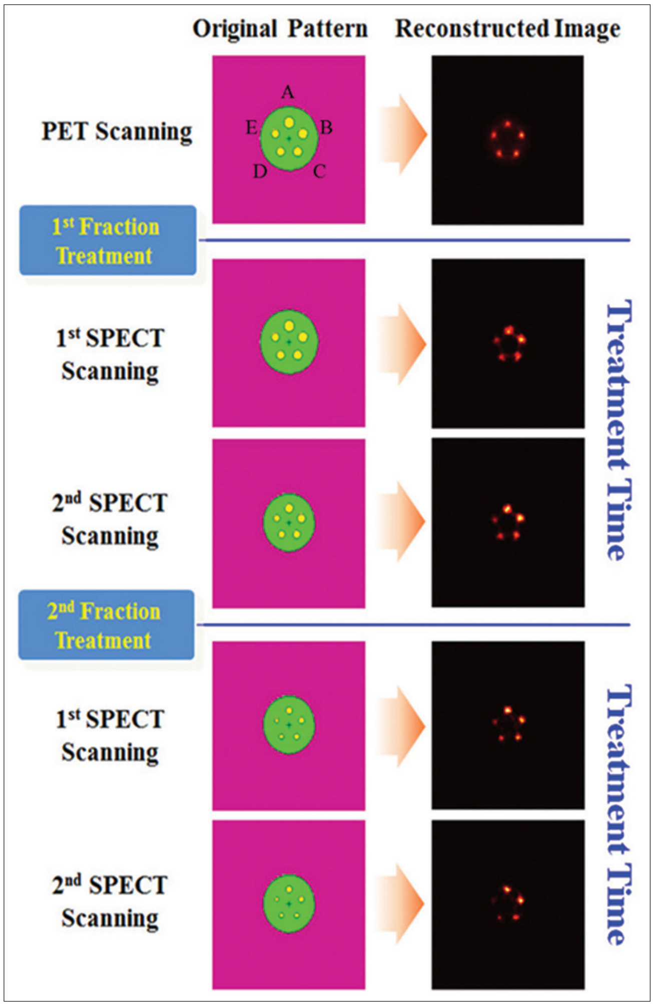

Figure 2: Diagram of the original pattern and reconstructed image depending on boron neutron capture therapy procedure. The original pattern shows the tomographic of the virtual water phantom. The BURs are labeled clockwise as A-E. On the right column, the positron emission tomography and prompt gamma ray images were reconstructed with a modified reconstruction algorithm

AB-3

TLD CORRECTION FACTORS FOR FIELD SIZES USED IN LUNG STEREOTACTIC BODY RADIATION THERAPY DOSIMETRIC MEASUREMENTS

Roger Cai Xiang Soh[1,2], Guan Heng Tay[3], Wen Siang Lew[1], Shaun Baggarley[2], James Cheow Lei Lee[1,3]

[1]Division of Physics and Applied Physics, School of Physical and Mathematical Sciences, Nanyang Technological University, [2]Department of Radiation Oncology, National University Cancer Institute Singapore, National University Hospital, [3]Division of Radiation Oncology, National Cancer Centre Singapore, Singapore. E-mail: roger_cai_xiang_soh@nuhs.edu.sg

Introduction: TLD dosimetric verification for Lung Stereotactic Body Radiation Therapy (SBRT) may be a challenge due to small field TLD dose perturbation within the low-density lung medium. Accurate measurement can be achieved by correcting the perturbed dose using TLD correction factors calculated by Monte Carlo (MC) methods. The current study investigates the MC calculated TLD correction factors against depth and field size within a proposed lung phantom.

Materials and Methods: 14 TLD-100 measurements were done along the central axis within a lung phantom, which consists of CIRS plastic water slabs sandwiching 14 pieces of composite cork slabs. TLD correction for the positions in composite cork was determined by taking the ratio of the Monte Carlo simulated dose response of TLD in cork to the Monte Carlo simulated dose response of TLD in water. BEAMnrc and DOSXYZnrc user codes were used for simulation (EGSnrc, National Research Council of Canada, Ottawa, ON).

Results: It was found that the greatest TLD correction was for the smallest field size investigated, 2 x 2cm^2, where electronic disequilibrium was found to be the greatest as shown in Figure 1. Corrections at inhomogeneous interfaces were dependent on the medium before the interface. In addition, MC corrected TLD measurements agree with Acuros External Beam (AXB) 2 x 2 cm^2 predicted depth doses to within 2% as shown in Figure 2.

Discussion: TLD perturbation is dependent on three main aspects, namely, lateral charge particle disequilibrium, over response of TLD in broad beam and partial volume averaging. Due to the small physical size of TLD-100, partial volume averaging was deemed negligible in this study. Lateral charge particle disequilibrium was found to be dependent on field size, the TLD material, and the density of the phantom. The electron range in low-density materials, such as composite cork, is longer than the range in water. Hence, lateral electronic disequilibrium occurs predominantly in composite cork. Furthermore, under small field conditions, the Compton electronic range is greater than the distance between the point of measurement to the field edge, increasing the probability for an electron to transfer its energy outside the field, resulting in greater electronic disequilibrium.

Lastly, the over response of TLD in broad beam was due to TLDs having a higher atomic number than that of water. 6 MV photon beam consists of an extensive amount of low-energy photons as compared to higher energies photon beam. Due to larger cross-section for photoelectric effect in high atomic

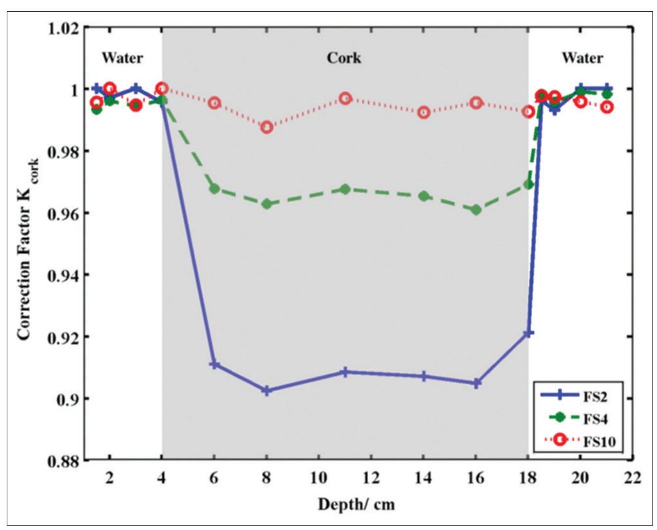

Figure 1: Monte Carlo simulated TLD correction factors with respect to depth

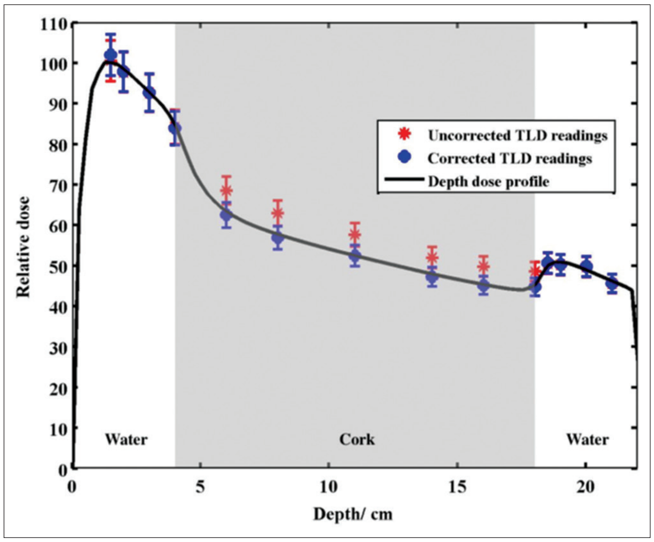

Figure 2: Monte Carlo TLD corrected measurements against AXB 2 x 2 cm^2 predicted dose profile

number materials within TLDs, low-energy photons will be absorbed to a high extent. This low energy photon absorption increases with increasing field sizes.

Conclusion: The results presented in this study indicate that corrections will be required for in-vivo TLD measurements in the proposed lung phantom for Lung SBRT dosimetry measurements. Monte Carlo simulated TLD correction factors calculated were dependent on the depth of measurement and field sizes. The greatest TLD correction was for the smallest field size investigated, 2 x 2cm^2. Further studies may include the effect of TLD angular dependence on TLD correction factors.

AB-4

INVESTIGATION OF OPTIMAL SHUTTER SCAN ACQUISITION PARAMETERS IN DIGITAL TOMOSYNTHESIS SYSTEM

Dohyeon Kim[1], Byungdu Jo[2], Haenghwa Lee[2], Donghoon Lee[1], Sunghoon Choi[2], Hyemi Kim[2], Zhen Chao[1], Seungyeon Choi[1], Hee-Joung Kim[1,2]

Departments of [1]Radiation Convergence Engineering and [2]Radiological Science, Yonsei University, Seoul, South Korea. E-mail: hjk1@yonsei.ac.kr

Introduction: Digital tomosynthesis system has been studied to reduce the exposure dose. Nevertheless, many studies have suggested that it is still needed to reduce the exposure dose in digital tomosynthesis system. Diagnostically important information is often concentrated on a region of interest (ROI) in a reconstructed 3D image. For this reason, ROI imaging techniques are considered to be a reasonable dose reduction method. If the ROI reconstruction method is applied to digital tomosynthesis system, it could expect a better dose reduction effect. But most studies do not focus on improving the image quality of the overall anatomy particularly in the outside ROI. Therefore, we proposed shutter scan acquisition for region of interest (ROI) imaging to reduce the patient exposure dose in digital tomosynthesis system. The purpose of this study was to investigate the effect of composition ratio of truncated and non-truncated projections and to determine the optimal set of acquisition parameters for the proposed shutter scan acquisition in digital tomosynthesis system.

Materials and Methods: Projections obtained by shutter scan acquisition consist of truncated and non-truncated projections as shown in Figure 1. A prototype chest digital tomosynthesis (CDT) system (LISTEM, Korea) and the LUNGMAN phantom (Kyoto Kagaku, Japan) with 8 mm lung nodule were used for this study. In this study, we call the number of truncated projections divided by the number of non-truncated projections as shutter weighting factor. The shutter scan acquisition parameters were optimized using 5 different acquisition sets with the shutter weighting factor (0.1, 0.3, 1, 3 and 7). A total of 81 projections with shutter scan acquisition were obtained in 5 sets according to shutter weighting factor. The image quality was investigated using the contrast noise ratio (CNR). We also calculated figure of merit (FOM) to determine optimal acquisition conditions for the shutter scan acquisition. The total effective dose was used as the dose value for calculating the FOM.

Results: The ROI of the reconstructed image with shutter scan acquisition showed enhanced contrast as shown in Figure 2. The CNR value was highest when the shutter weighting factor was 1. The highest CNR value, shutter weighting factor 1, is the acquisition set consisting of 41 truncated projections and 40 non-truncated projections. On the other hand, the result of the FOM value was the highest value when the shutter weighting factor was 3. The highest FOM value, shutter weighting factor

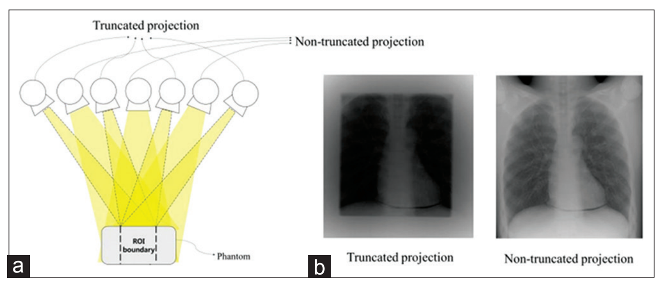

Figure 1: (a) Schematic diagram of the shutter scan acquisition, (b) obtained projections in shutter scan acquisition

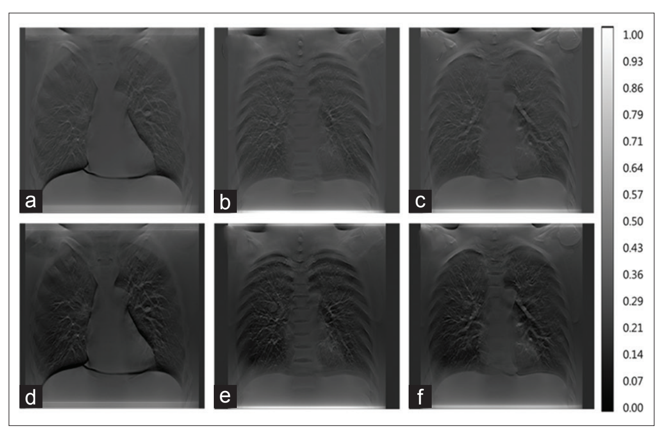

Figure 2: Reconstructed images: (a) conventional acquisition in 37th slice, (b) conventional acquisition in 25th slice, (c) conventional acquisition in 28th slice, (d) shutter scan in 37th slice, (e) shutter scan in 25th slice, (f) shutter scan in 28th slice

3, is the acquisition set consisting of 61 truncated projections and 20 non-truncated projections.

Discussion: It is expected that the patient exposure dose can be reduced by limiting field of view (FOV) to focus on region of interest in proposed shutter scan acquisition. We investigated the effects of composition ratio of the truncated and non-truncated projections on reconstructed images through the shutter scan acquisition.

Conclusion: The optimal acquisition conditions for the shutter scan acquisition were determined by deriving the figure of merit (FOM) values. Our results suggest possible directions for further improvements in digital tomosynthesis system for shutter scan acquisition method.

AB-5

STUDY OF FEASIBILITY OF USING A COMPLEMENTARY METAL OXIDE SEMICONDUCTOR BASED MOBILE PHONE CAMERA AS A RADIATION DOSIMETER

Josmi Joseph, I. Rabi Raja Singh, S. Amalan, E. Winfred Michael Raj, B. Paul Ravindran

Department of Radiotherapy, Christian Medical College, Vellore, Tamil Nadu, India.
E-mail: 95.josmijoseph@gmail.com

Introduction: Complementary metal oxide semiconductor (CMOS), is the fundamental sensor used in almost all digital imaging devices including smartphones. Some of the studies show that this sensor responds to ionizing radiation also and it is directly proportional to the exposure of incident radiation. There are already some downloadable applications (apps) available for detecting the stray ionizing radiation but not for measuring the radiation. To use CMOS as a radiation dosimeter which is not fully energy independent, individual calibration is necessary to account for the variation in response for different energies of radiation and also for different sensor. As a preliminary study, a separate Android application was developed and with the same, the characteristics such as buildup effect, energy dependence, dose linearity, consistency, angular dependence and relative dose factor measurement were examined and analyzed to check whether this sensor can be used as radiation dosimeter.

Objectives:
1. To develop an android application to use the CMOS sensor as radiation dosimeter
2. To study the following characteristics using the developed app, And to compare the same with the standard ion chamber values, Thermoluminescent dosimeter (TLD), Optically stimulated luminescence dosimeter (OSL) and semiconductor diodes.
   - Percentage Depth Dose
   - Dose linearity
   - Consistency
   - Energy dependence
   - Angular dependence
   - Relative dose factor measurement

Materials and Methods: When a CMOS is exposed to ionizing radiation, specks proportional to the number of incident photons will be formed on the frame. An android application has been developed to quantify the specks. It includes,
1. Calibration - to determine the threshold pixel value above which the pixel is to be considered as a radiation signal
2. Noise filtration - by high-delta method which will also help in determining the signal from each frame.

Using the developed app the above mentioned characteristics were studied and compared with that of standard ion chamber data.

Results and Discussion: It has been proved that the CMOS based smartphone have shown good linear response to the dose in the clinical range (100 cGy to 500 cGy). There is no need for an additional buildup material to be added to achieve the maximum ionization as the sensor has got inherent buildup due to its fabrication. It also shows good consistency. Even though the orientation of phone didn't affect the measured value, significant energy dependence was observed. This can be eliminated by performing individual calibration. The measured values from the for 100 to 500 cGy is found to be comparable with the data measured with other dosimeters such as Ionization chamber, Thermoluminescent dosimeter (TLD), Optically stimulated luminescence dosimeter (OSL) and semiconductor diodes. It is promising, that the smartphone with CMOS sensor can be used as a dosimeter for relative dose measurement even though it is found to be energy dependent.

AB-6

IMPROVING IMAGE QUALITY IN CONTRAST ENHANCED DUAL ENERGY MAMMOGRAPHY BY NOISE COMPENSATION TECHNIQUES

Minjae Lee, Donghoon Lee, Seungyeon Choi Junyoung Son, H. J. Kim

Department of Radiation Convergence Engineering, Yonsei University, Seoul, South Korea.
E-mail: hjk1@yonsei.ac.kr

Introduction: The incidence and the number of death due to breast cancer are continuously increasing. Conventional mammography (CM) is generally used for diagnosing breast, but it is well known that diagnosing in the dense breast with CM is difficult. Contrast enhanced dual energy mammography (CEDM) is one of the latest developments in breast diagnosis, and it is especially effective in dense breast. However, CEDM has inherent risk of side effects due to iodine contrast agents, and there is serious quantum noise problem due to dual energy imaging techniques. The purpose of this study was to confirm the feasibility of CEDM imaging using a diluted iodine contrast agent to reduce the possibility of adverse effects. In addition, various denoising algorithms were applied to CEDM in order to improve image quality.

Materials and Methods: We used a Mammographic x-ray system (SOUL, MEDI-FUTURE, Inc. South Korea) and, soft tissue equivalent slab phantom with 5cm thickness and 70% glandularity, and diluted iodine contrast agent with 5% and 10% Ioversol (320 mg iodine per milliliter). To acquire CEDM images, we used energy weighted log subtraction algorithms with low and high energy projection which were acquired with 26 kVp and 40 kVp, respectively. In addition, to reduce quantum noise in dual energy images we applied total variation denoising and non-local means (NLM) algorithms to CEDM images. We also measured the average glandular dose (AGD) of both CM and CEDM. To quantitatively evaluate the results, contrast to noise ratio (CNR) and figure of merit (FOM) were measured.

Results: The CM and CEDM images are shown in Figure 1. The CNR and FOM of the CM and the CEDM images were measured as shown in Table 1. Despite the use of a diluted iodine contrast agent, the signal of iodine was relatively well detected in CEDM compared to CM. Also, the results of using the denoising algorithms showed improved results. For example, CNR of CEDM with TV and NLM were about 2.4 times higher than CEDM without denoising algorithm. Although, AGD of CEDM was slightly higher than CM due to double exposures of different X-ray spectra, FOM, which considers both patient dose and image quality, was high in following order CEDM with NLM, CEDM with TV, CEDM without denoising and CM.
Discussion: The CNR and FOM of CEDMusing dual energy subtraction technique are higher than that of CM, but the image quality is reduced by increasing quantum noise. The image quality of CEDM using TV and NLM is improved because the CNR and FOM are increased by reducing quantum noise.
Conclusion: We confirmed the possibility of acquiring CEDM images using a diluted iodine contrast agent. With a diluted iodine contrast agent, CEDM images combined with denoising algorithm proved to obtain relatively superior iodine signal than CM.
Acknowledgment: This research was supported by Basic Science Research Program through the National Research Foundation of Korea (NRF) funded by the Ministry of Science, ICT & Future Planning (NRF-2017R1A2B2001818).

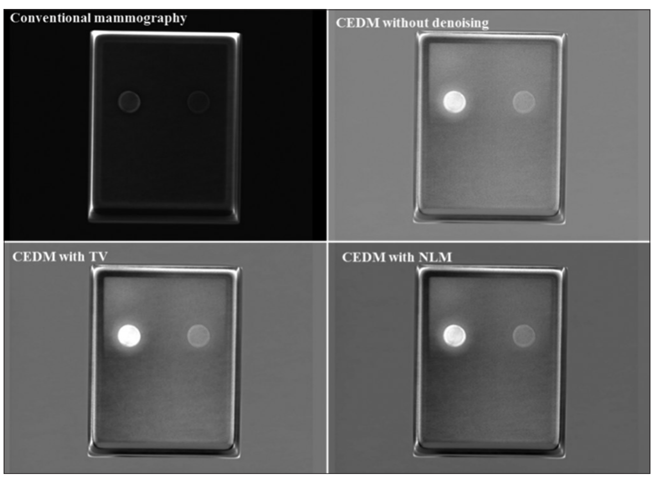

Figure 1: The conventional mammography image and contrast enhanced dual energy mammography without denoising and contrast enhanced dual energy mammography images with total variation, non-local means

Table 1: The contrast to noise ratio and figure of merit of the conventional mammography image and contrast enhanced dual energy mammography images without denoising and with denoising

	Contrast to noise ratio (CNR)	Figure of Merit (FOM)
Conventional mammography	2.1	2.2
Contrast enhanced dual energy mammography (CEDM) without denosing	4.7	8.2
CEDM with total variation (TV)	11.1	47.0
CEDM with non-local mean (NLM)	11.4	49.5

AB-7

MULTI-MODALITY IMAGE FUSION BASED ON IMPROVED FUZZY NEURAL NETWORK METHOD

Z. Chao[1], H. Lee[2], S. Choi[2], D. Kim[1], P. Jeon[1], H. J. Kim[1,2]
Departments of [1]Radiation Convergence Engineering and [2]Radiological Science, Yonsei University, Seoul, South Korea. E-mail: hjk1@yonsei.ac.kr

Introduction: In clinical applications, single modality images do not often provide enough diagnostic information. For instance, CT images clearly show bone tissue information, but for soft tissue, especially invasive tumors, CT images cannot correctly display boundaries. On the contrary, MRI images are more sensitive in soft tissue, which are helpful to determine the range of lesions, but the effects on bone tissue are not obvious. Thus it is necessary to correlate one modality of medical images to another to obtain more useful information. In recent years, neural network technique has been applied to medical image fusion by various researchers, meanwhile, many training methods for neural networks have been implemented, but the effects are not obvious. Therefore we produced a new system that based on fuzzy theory and Radial Basis Function Neural Network (RBFNN), then we proposed a new method (the combination of gravity search algorithm (GSA) and error back propagation algorithm (EBPA)) to train neural network to correct the parameters of the network.
Materials and Methods: New fuzzy-RBFNN system includes 5 layers: input layer, fuzzy partition layer, front combination layer, inference layer and output layer. In input layer, the neurons represent the images that need to be fused; In fuzzy partition layer, the membership functions are used to represent the neurons in this layer; In front combination layer and inference layer, the neurons represent the formulation of fuzzy rules and the output of fuzzy rules respectively; In output layer, the neuron represents fused image. Through this system, we firstly obtained actual output data after inputting two images to be fused. Ideal output data (training samples of fuzzy neural network) were then obtained by maximum value method. Next we trained the system by the combination of gravity search algorithm and error back propagation algorithm: original data required by GSA were obtained through EBPA and trained through GSA (we took the parameters of membership functions and the weighted factors between inference layer and output layer as original data). Finally we acquired fused images by the trained system. In this experiment, we used two sets of head images (CT, MRI and CT, SPECT). Entropy (H: the richness of image information) and Mutual Information (MI: the degree of correlation with the original variables) were used to quantitatively compare error backpropagation and particle swarm method.
Results: The results showed that error backpropagation method and particle swarm method generated worse results by showing lower H and MI values. On the contrary, medical image fusion based on our new method presented much better results with the highest performance H and MI.
Discussion: In this study, by adding more hidden layers, our improved fuzzy-RBFNN system can more clearly express the structure of input data and the function of neural network

compared with conventional Radial Basis Function neural network. In addition, we adopted a new method to train the neural network.

Conclusion: The experiments of image fusion prove that our new system can fuse medical images better than the other two methods, and a new training method can effectively improve the function of fuzzy-RBFNN system.

AB-8

ESTIMATION OF VIRTUAL SOURCE POSITION FOR ELECTRONS WITH REGULAR AND IRREGULAR FIELDS FROM A MEDICAL LINEAR ACCELERATOR

Doke Hanuman Bajirao, K. M. Ganesh, M. Ravikumar
Department of Radiation Physics, Kidwai Memorial Institute of Oncology, Bengaluru, Karnataka, India.
E-mail: hbdoke321@gmail.com

Introduction: The superficial and shallow tumors are usually treated with cerrobend shielded electron beams. The irregular field defining inserts are placed at the distal end of the electron applicators. When the treatment is delivered at an extended distance, the electron output and the percentage depth dose needs to be corrected based on inverse square law from the electron source position. As the electron beam emerging from an accelerator exit window undergoes complex multiple scattering in the scattering foil, the beam monitor chambers, the X-ray collimators, electron applicators, field defining inserts and air column. The position of scattering foil cannot be considered as a nominal source position and the output need to be corrected accordingly. In such cases the output can be predicted accurately assuming the effective or virtual source position.

Objectives: This study determines the virtual source position for different energies using different field sizes in Clinac DHX linear accelerator. This study also attempts to find the difference between the virtual source positions of regular and irregular field sizes for different energies using 10×10 cm^2, 15×15 cm^2 and 20×20 cm^2.

Materials: Dual energy linear accelerator Clinac DHX (Varian Medical Systems) with electron cones for different electron energy (6, 9, 12, 16, 20 MeV) and secondary standard ionization chamber, Electrometer, solid phantom used in this study.

Methods: Measurement of Virtual source position (VSP) for regular fields-For this study, electron energies ranging from 6-20 MeV in Clinac DHX linear accelerator with water equivalent solid phantom, parallel plate type chamber and Dose1 Electrometer.VSP for Electron cones of 4×4 cm^2, 6×6 cm^2, 10×10 cm^2, 15×15 cm^2, 20×20 cm^2 and 25×25 cm^2 of regular fields sizes were evaluated. The VSP were derived by acquiring the reading at central axis at Dmax depth for each electron energy. The readings were taken for four different SSDs such as 100cm, 105 cm, 110 cm and 120 cm in each radiation field. The measurements were repeated for all the available electron cones. The readings were taken with 100 monitor unit (MU) at Dmax with dose rate of 400 MU/min. Measurement of virtual source position for irregular fields-To measure the VSP using cut out blocks with different sizes and shapes was the VSP at each electron beam energy (6, 9, 12, 16 and 20 MeV) was used. In addition, the VSP obtaining using the method used in experiment when each cut out block (10×10, 15×15, 20×20) was used.

Results and Discussion: It is observed that the virtual source distance increases with increase in energy and field size. The estimation of virtual source distance for irregular field size using electron cones of 10x10 cm^2, 15x15 cm^2 and 20x20 cm^2 showed larger deviation with that of regular field for lower energies and subsequently narrows down with increase in electron energy. The results indicate that actual estimation of virtual source position for particular energy and field size is necessary when irregular field is used for treatment and in calculating the accurate doses. The diffusion phenomenon made with uniform dose distribution at the depth of the reference points significantly reduces the lateral scattering effect with the thickness of the cut-out block when compared to regular field. Due to the scattering of electron beam in its path by the scattering foils, collimator, and applicator, etc. Hence, for dose calculation with electron beams by direct SSD should not be used for dose estimation which will lead to error in dose estimation.

AB-9

DEVELOPMENT OF VOXEL BASED METHOD FOR EVALUATION OF THE RADIOTHERAPY TREATMENT PLANS: A NOVEL APPROACH

Gaganpreet Singh, Arun S. Oinam[1], Vivek Kumar
Centre for Medical Physics, Panjab University,
[1]Department of Radiation Therapy, Regional Cancer Center, Postgraduate Institute of Medical Education and Research, Chandigarh, India.
E-mail: gaganpreetsingh@live.com

Introduction: Radiotherapy treatment plans are evaluated by different methods i.e. slice by slice evaluation, DVH based evaluation and plan metrics methods etc. All the methods involves the three dimensional (3D) dose matrices which contain voxels having different information tagged with them. In this study, information of the location of voxel of different 3D dataset of computed tomography (CT) images, RT structures set and RT dose are used for the evaluation of the plan and further this approach is used for the radiobiological evaluation of the treatment plan.

Objectives: Development and implementation of the voxel based method for evaluation of the radiotherapy treatment plan incorporating radiobiological parameters.

Materials and Methods: In this study, Digital imaging and communication in medicine in radiotherapy (DICOM-RT) standard files are used to extract the CT Images, RT Structures set (RTSS), RT Dose and RT Plan information. Patient's plan is exported from the Eclipse TPS of Varian Medical System, Palo Alto, USA and imported into the in-house build program which is written in Matlab® software (Mathworks Inc.). In this program, Dose Cube and Structure set Cube are constructed by interpolating with respect to CT Cube in such a way that resultant structure Cube and Dose Cube are of the same dimensions. Voxels mapping have been used to reconstruct dose volume histograms (DVH) of different organs and target volumes of the plan. Further, Voxel based biologically equivalent dose (BED) and equivalent dose of 2 Gy (EQD_2) have been calculated using the standard mathematical formulism of BED and

EQD_2 doses. BED and EQD_2 based colorwash and isoeffect dose curves have also been constructed incorporating linear quadratic (LQ) model parameter alpha by beta ratios of assigned values of different normal tissues and tumor.

Results and Discussion: This study shows the reconstruction of the patient plan on an independently developed program based on DICOMRT standard files. It provides the visualization of contours and dose colorwash over the CT images same as that of represented by Eclipse TPS. Reconstructed DVH depends on the grid size of the CT-, Structure set-.and Dose – Cube. Change in the voxel size effect the DVH. In this study, DVH and colorwash construct from the voxel based approach compared with the Eclipse TPS. Results have shown a good agreement between the DVH and colorwash obtained from the TPS and from the developed program. BED and EQD_2 doses at different voxel locations have been calculated and used for the display of radiobiologically equivalent dose colorwash and isoeffective dose curves for the evaluation of the plans which provides better understanding of the radiobiological equivalent doses.

Conclusion: This study shows voxel based novel approach for evaluation of patient treatment plan which can be further extended for the radiobiological evaluation of treatment plans which incorporate radiosensitivity of different organs and target organs. This study can be further extended for the evaluation of complex radiotherapy treatment plan of the patients.

AB-10

3D SILICON MICRODOSIMETRY FOR BORON NEUTRON CAPTURE THERAPY: A SIMULATION STUDY

N. Hu, R. Uchida, L. T. Tran[1], A. Rosenfeld[1], Y. Sakurai[2]
Division of Nuclear Engineering, Graduate School of Engineering, Kyoto University, Kyoto, [2]Kyoto University Research Reactor Institute, Osaka, Japan, [1]Centre for Medical Radiation Physics, University of Wollongong, Wollongong, Australia.
E-mail: ko.naonori.25r@st.kyoto-u.ac.jp

Introduction: Boron neutron capture therapy (BNCT) is an emerging radiotherapy modality using a neutron beam collectively with boron-10 containing pharmaceutical to treat patients with cancer. In contrast to conventional radiotherapy, the types of radiation present in BNCT consists of many distinct radiation components, each having a different biological weighting factor. Microdosimetry is an effective dosimetry technique in a mixed radiation environment. Using this technique, it is possible to derive the relative contributions of different radiation modalities. This paper presents the feasibility study of a novel 3D mesa bridge microdosimeter in BNCT, developed by University of Wollongong (UOW).

Materials and Methods: This bridge microdosimeter is comprised of an array of 4248 individual silicon cells fabricated on a 10 μm thick n-type silicon-on-insulator substrate. The performance of the microdosimeter was studied using Monte Carlo simulation. Different boron converter and silicon-on-insulator substrate thickness was modelled and the energy deposition within the detector was simulated using the Particle and Heavy Ions Transport Code System (PHITS). The T-Deposit tally in PHITS was used to calculate the energy deposited per event inside the sensitive volume of the bridge microdosimeter. The lineal energy was calculated by dividing the deposited energy per event by the average chord length of the detector. The clinical BNCT field at Kyoto University Reactor (KUR) using both thermal and epithermal irradiation modes were used in this study.

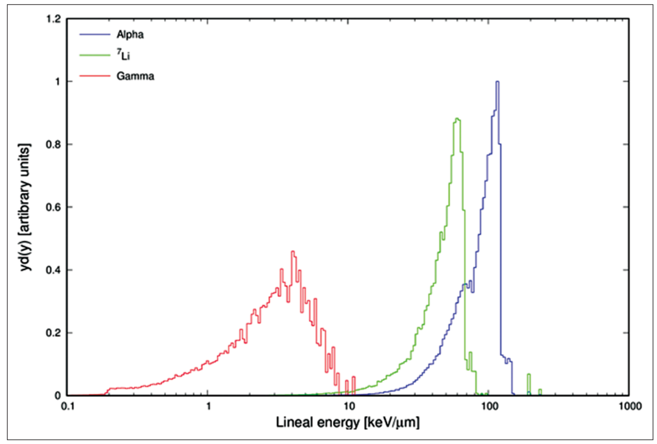

Figure 1: Microdosimetric spectrum of the Kyoto University Reactor epithermal beam generated by Particle and Heavy Ions Transport Code System

Results: A thinner boron converter resulted in more reaction particles reaching the sensitive volume of the detector. Approximately double the number of particles reached the detector for a 1 μm thick boron converter as compared to a 0.5 mm thick boron converter. For the alpha particle, a peak at 120 keV/μm was observed with both the 0.5 mm and 1 μm boron converter and a peak at 200 keV/μm was observed with no boron converter. A peak in the no boron converter spectrum arises from the boron p+ dopant in the device. Figure 1 shows the microdosimetric spectrum obtained from the bridge microdosimeter for the KUR epithermal beam.

Discussion: The range of the alpha particles produced during BNCT is approximately 5 μm. For a 10 μm thick detector, the alpha particle will come to a full stop inside the sensitive volume, resulting in an inaccurate lineal energy deposition. To account for this, a 2 μm thick detector was simulated and tested. Results showed the lineal energy deposition was improved with the use of the 2 μm thick sensitive volume detector. Simulation results showed that the thermal irradiation mode seemed the most appropriate mode to perform the measurements, because of the high thermal neutron flux, which resulted in high production of reaction particles, and lower epithermal and fast neutron flux, which resulted in lower recoil silicon particles produced.

Conclusion: The microdosimetric spectrum showed each particle can be separated by calculating the lineal energy. The simulation results show that this microdosimeter can be utilised as an effective tool for dosimetry in BNCT field and experimental validation will follow once KUR is operational.

AB-11

PERIPHERAL DOSE MEASUREMENTS WITH FFF BEAMS FROM LINEAR ACCELERATOR AND TOMOTHERAPY FOR SBRT OF CA PROSTATE - PHANTOM STUDY

Pragya Shree, R. A. Kinhikar, A. Dheera, C. M. Tambe, D. D. Deshpande

Department of Medical Physics, Tata Memorial Hospital, Mumbai, Maharashtra, India.
E-mail: pragyashree1991@gmail.com

Purpose: To quantify the relative peripheral doses (PD) for the unflattened beams for advanced treatment techniques with SBRT for Ca Prostate cases delivered with linear accelerator and tomotherapy machines.

Materials and Methods: Varian Truebeam linear accelerator was used to provide 6 and 10MV unflattened photon beams and Accuray Tomotherapy Hi-ArtII was used to provide 6MV unflattened photon beam. SBRT (for Ca prostate) treatment plans were generated for 6FFF and 10FFF photon beams using Eclipse and Tomo TPS (five patients for each). All treatment plans were delivered to the relevant anatomical region of a body phantom ($30\times90\times20$ cm^3, width $\times$ length $\times$ depth, stack of solid water slabs). Dosimetric measurements were performed with TLD-100 (LiF:MgTi) which were placed on surfaceat 5, 10, 15, 20 and 25cm from the field edge and at depth (5 and 10 cm) as well. The TLDs were read using Rexon reader and the readings at the respective distance and depth were recorded. The Peripheral Doses were normalized to the prescribed dose (14Gy in 2 fractions). The measured values of peripheral doses for Tomotherapy 6FFF photon beams was compared with the Truebeam 6FFF photon beam and the values for Truebeam 10FFF and 6FFF photon beams were also compared with each other.

Results: The measured mean peripheral doses (PDs) at 20cm beyond the field edge at surface (depth=0) with linac 10FFF and 6FFF was 0.32%±0.16 (ranging from 0.16% to 0.52%) and 0.30%±0.14 (0.17% to 0.49%) respectively and at a distance of 25 cm, 0.23%±0.1 (0.11% to 0.36%) and 0.22%±0.1 (0.12% to 0.35%) respectively. And at the depth of 10 cm, the measured mean PDs at 20 cm beyond the field edge with linac 10FFF and 6FFF was 0.23%±0.08 (0.13% to 0.33%) and 0.25%±0.1 (0.14% to 0.38%) respectively and at a distance of 25 cm, 0.17%±0.07 (0.1% to 0.27%) and 0.17%±0.07 (0.11% to 0.27%) respectively. The measured mean PDs at 20 cm beyond the field edge at surface with tomotherapy 6FFF was 0.38%±0.06 (0.30% to 0.46%) and at a distance of 25 cm, 0.25%±0.03 (0.22% to 0.29%). And at the depth of 10 cm, the measured mean PDs at 20 cm beyond the field edge with tomotherapy 6FFF was 0.33%±0.13 (0.22% to 0.56%) and at a distance of 25 cm, 0.22%±0.07 (0.17% to 0.34%).

Conclusions: The PDs for both the 6 FFF and 10 FFF photon beams were found to decrease with increasing distance from the radiation field edge. The relative deviation between PDs of 6FFF and 10FFF was found to decrease with increasing distance from the field edge and this deviation became almost negligible beyond 20 cm distance from the field edge. The measured PD from Tomotherapy 6FFF was found higher than Linac 6FFF by the maximum factor of 2.26.

AB-12

GPU-ACCELERATED 4D IMAGE RECONSTRUCTION USING ON-BOARD KV CONE-BEAM CT

Sunghoon Choi, Chang-Woo Seo, Hee-Joung Kim
Department of Radiological Science, Yonsei University, Wonju, Korea. E-mail: choi.sh@yonsei.ac.kr

Introduction: On-board kV cone-beam CT (CBCT) imaging has recently become available based on a flat-panel detector mounted in a linear accelerator (LINAC) for radiotherapy guidance. Respiration induces motion artifacts which could be reduced by retrospectively sorting projection images and reconstructing multiple three-dimensional (3D) CT dataset at different respiratory phases. Unfortunately, multiple breathing phases over a full gantry rotation involve huge number of projections to reduce aliasing artifact at each phase. Therefore, a real-time patient monitoring in treatment planning using 4D CBCT is quite challenging because it demands high computation time during image reconstruction.

Objectives: The main focus of this work is to present a GPU-accelerated 4D CBCT image reconstruction technique in order to diagnose a patient with a fast speed, thereby provides a real-time patient monitoring in treatment planning.

Materials and Methods: For a respiratory-correlated 4D CBCT reconstruction, the authors acquired total 1,262 projections of a moving phantom (QUASAR Programmable Respiratory Motion Phantom [Figure 1], Modus Medical Device Inc., London, ON) using a flat-panel based on-board imager (Varian Medical Systems, Palo Alto, CA). The breathing signal for determining respiratory correlation was directly measured from a real-time position management (RPM) respiratory gating system. Projection data of the phantom moving with simulated sinusoidal motion were acquired and reconstructed into 3D and 4D CBCT datasets. The number of retrospectively rearranged projection images in four respiratory phase bins was 445, 235, 236, and 413 for peak-exhale (PE), mid-exhale (ME), mid-inhale (MI), and peak-inhale (PI) state, respectively, while total of 335 projection images with equally spaced angle step around full 360 gantry rotation was involved in 3D reconstruction. All image reconstructions were conducted by using the filtered back-projection scheme. For image quality analysis, the reconstructed axial images of 3D and 4D data were visually compared with each other. The authors also verified the GPU-accelerated computing power over CPU

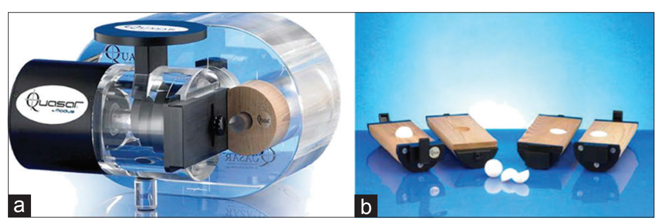

Figure 1: (a) The programmable motion phantom used in this study and (b) its cylindrical inserts with sphere target

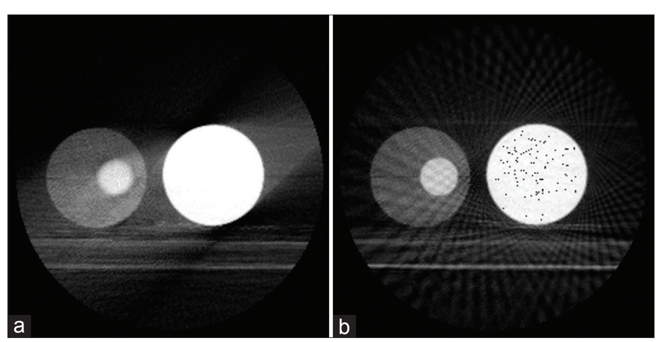

Figure 2: The reconstructed axial images of (a) conventional 3D dataset and (b) peak-exhale phase bin

programming by checking the elapsed time required for reconstructing both 3D and 4D volumetric data.

Results and Discussion: The reconstructed axial images in each respiratory phase of 4D data provided little geometric error of moving structure (e.g., little blurring artifact) compared to 3D data [Figure 2]. However, aliasing artifacts represented by the streaking lines were substantially highlighted in 4D images due to small angular coverage over full gantry rotation. The reconstruction times for producing 4D dataset were 2.69, 0.91, 0.94, and 1.56 sec (total 6.14 sec) for PE, ME, MI, and PI phase bin, respectively, on GPU programming, whereas the elapsed times on CPU programming were 287.70, 155.03, 147.08, and 256.69 sec (total 846.53 sec). This could demonstrate that GPU computing time shows an enhanced speed of ~137 times than CPU programming, which could match-up a clinically feasible time. In conclusion, the authors observed reasonable outcomes of GPU-accelerated 4D CBCT image reconstruction scheme for real-time patient monitoring through GPU-acceleration in the current work.

AMPI Best Paper

BP-1

APPLICATOR COMMISSIONING FOR IMAGE BASED BRACHYTHERAPY

N. Siji, K. Joshi, S. Dheera[1], U. Mahantshetty[1], S. Chopra, A. Laishram, Swati Kumari, D. D. Deshpande[1], S. V. Jamema

Advanced Centre for Treatment, Research and Education in Cancer (ACTREC), TMC, Navi Mumbai, [1]Tata Memorial Hospital, TMC, Parel, Mumbai, Maharashtra, India. E-mail: siji.menachery@gmail.com

Aim: In 3D image based brachytherapy, it is highly recommended to commission brachytherapy applicators to minimize the uncertainties during applicator reconstruction. The commercially available CT/MR compatible applicators are generally made up of two materials viz polymer and titanium. It has been reported that titanium applicators cause susceptibility artifacts especially in 3T MRI. The manufacturer specification of the magnetic field strength to be used with these applicators are 0.3-0.5T, however we have been using these applicators in 1.5T with proper commissioning. We are in the process of starting MR image based BT using 3T MRI. Hence, we carried out some QA tests using 3T MRI using both plastic and titanium applicators. The aim of this study is to report the results of the commissioning of brachytherapy applicators for MR image based Brachytherapy.

Materials and Methods: Two commercial brachytherapy applicators were evaluated viz Vienna applicator made of polymer with Ti needles (Elekta) and Fletcher- suit (Varian) applicator made of titanium. A CT/MR compatible phantom of size 30 cm x 20 cm x 12 cm was fabricated such that the applicator can be positioned in a reproducible geometry. The phantom was filled with the gel (3% Agarose + 1% Copper Sulphate) to closely resemble the tissue density in MRI. CT and MRI (1.5T and 3.0T) images of the phantom with the applicator were obtained followed by rigid registration and image analysis. CT slice thickness was 0.625 mm (GE DISCOVERY). The MR images obtained for 1.5T were as per the institutional protocol established already; however a new protocol for 3T was attempted. The MR sequences for 3T were as follows: T1 weighted FRFSE, T2 weighted FRFSE, T2 weighted SSFSE and T2 weighted FSE, all with a band width of 125 and of equal matrix of 256 x 256 pixels. The MR slice thickness was 3mm with 0.5 mm spacing. Various combination of TE (echo time), TR (repetition time), and Echo Train length were also used. The images were imported and co-registered with the CT series in Eclipse Treatment Planning System (Version 13.4) using rigid registration. Mutual Information with limited ROI method was used for the rigid registration. Manual visual correction of translation and rotation was carried out such that the registration is accurate. The MR images were analyzed for image quality and geometry.

Result: Vienna applicator did not show much difference in the image quality between 1.5 and 3.0T, however the titanium Fletcher-suit applicator resulted in artifacts which were larger in 3T as compared to 1.5T. For Titanium needles, T2 images had a better contrast between gel and the needle as compared to T1, however the needle tip could be more easily located in T1. In both the series the lumen of the needle could be identified as a void signal. When compared between T2 weighted FRFSE and FSE sequence, the former one had a grainy appearance but the needle body and tip could be well identified in both. The T2 weighted FSE sequence had a distinct artifact at the tip with a signal void region extending up to 0.8 cm but when fused with CT the needle tip was found to lie beyond the artifact at 0.5 cm in the signal void region, while in the T1 image the susceptibility artifact matched the CT tip. SSFSE series images were not of good quality. We have found that T1 weighted images with 100 kHz bandwidth, TR= 1160, TE min, Echo train length=6, slice thickness=3 mm and spacing of 0.5 mm, are best for titanium needle reconstruction with 3T.

Conclusion: The commissioning of the applicators was successfully carried out, as a part of prerequisite for the clinical implantation of MR image based Brachytherapy.

BP-2

RADIOBIOLOGICAL AND SECOND CANCER RISK ESTIMATES FOR INSTITUTIONAL THREE DIMENSIONAL CONFORMAL PLANNING METHOD: COMPARISON WITH TRADITIONAL GAP JUNCTION AND INVERSE IMRT PLANS OF PEDIATRIC MEDULLOBLASTOMA

A. Hemalatha, M. Athiyaman, Arun Chougule[1], H. S. Kumar[2]

Departments of Radiological Physics and [2]Radiotherapy, Sardar Patel Medical College, Bikaner, [1]Department of Radiological Physics, Sawai Man Singh Medical College, Jaipur, Rajasthan, India. E-mail: mailtohemathi@gmail.com

Introduction: The use of Radiation Therapy (RT) is associated with better outcome in many pediatric cancer patients but it is also associated with significant long term side effects and the risk of Second Cancers (SC). The present study is an attempt to analyze the radiobiological and SC risk associated with institutional Three Dimensional Conformal Radiotherapy Technique (3D CRT) in comparison with traditional 3DCRT gap junction and inverse Intensity Modulated RT (IMRT) for Cranio Spinal Irradiation (CSI).

Materials and Methods: The three different planning methods were created for ten pediatric medulloblastoma patients retrospectively in the eclipse treatment planning system (V13.7). The dose calculation was performed based on Anisotropic Analytical Algorithm (AAA) for 6 MV linac photon beam. The prescribed dose was 23.4Gy, 1.8Gy/fraction.

Planning Methods: The half beam blocked cranial and cervicothoracic spine field was created in both institutional and gap junction planning method. In the planning method 1 and 2 the diverging planes of the both spine field were matched using field alignment option and junction was shifted after seven fractions to reduce dose uncertainty created by error in setup. In the gap junction method the both diverging

planes were separated by distance S=S1+S2.S1 = 0.5 x L1 x (d/SSD1), Where L, SSD-Length and Source to Surface Distance of the corresponding fields, d-depth of spine. For the inverse IMRT plan the symmetrical bilateral cranial fields were matched with posterior spine field and inverse optimization was performed.

The Organ Equivalent Dose (OED) was calculated by plateau dose response model using equation A:

$$OED = \frac{1}{V}\sum_{i} Vi \left(1 - exp\left(-\delta_{org} D_i\right)\right) \quad (A)$$

where V is the whole organ volume, Vi & Di - volume and dose elements, which was extracted from differential dose volume histogram. And δorg is the organ specific model parameter taken from Schneider et al. The Lifetime Attribute Risk (LAR) of SC for age and sex dependent, site specific estimation was performed using Biological Effects of Ionizing Radiation VII parameters (R)

LAR=OED x R

Results and Discussion: There is no significant difference between planning methods in case of pneumonitis. The probability of heart failure is significantly lower for IMRT compared to planning method 1 [Figure 1]. The LAR estimation from Figure 2 shows that SC in lung, thyroid and colon cotributed most to the overall risk in all compared modalities.

Conclusion: From this study it concluded that with respect to sparing organ at risk during CSI the both institutional planning method and IMRT were found to have advantages compared to gap junction method. The LAR of SC is lower for all the organs with institutional planning method compared to IMRT and gap junction method.

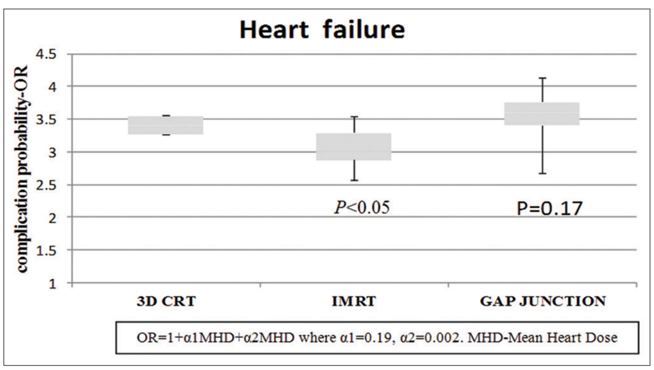

Figure 1: Box whisker plot for heart failure. *P* value compares significant difference between method 1 and 2, 1 and 3

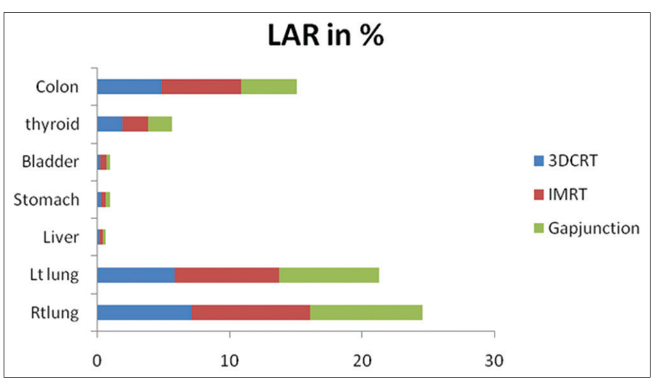

Figure 2: Lifetime attribute risk of second cancer for various organs

BP-3

RETROSPECTIVE ANALYSIS OF GEOMETRICAL INFORMATION ABOUT PAROTID AND PLANNING TARGET VOLUME TO PREDICT THE PAROTID MEAN DOSE

Amit Nirhali, V. K. Sathiyanarayanan, M. Pooja, S. Mithun, Basu Sumit, Bhooshan Zade

Department of Radiation Oncology, Ruby Hall Clinic, Pune, Maharashtra, India.

E-mail: amitnirhali@gmail.com

Introduction: Intensity Modulated Radiotherapy (IMRT) is the widely used technique in Head and Neck cancer cases, in which PTV is surrounded by OAR structures, so IMRT planning has a challenge of reducing the OAR Doses. Mainly salvaging parotid, as many times parotid overlaps with the PTV. It's very difficult to know the level to which parotid dose can be reduced maintaining the PTV Coverage. The purpose of this study is to develop a planning tool to improve the plan quality by generating a parotid mean dose predictive model based on the retrospective analysis of geometrical information database about parotid and planning target volume (PTV), just before the planning is done.

Materials and Methods: We randomly studied 60 HN IMRT cases (115 Parotid structures) 80-training data and 35-test, data planned on Pinnacle[9.8] TPS with DMPO optimization with 6MV photon beam and 7 to 9 beam directions and planned by different physicist and treated on Siemens ONCOR impression during the year of 2011 to 2016.

For each selected patient we tried further to reduce mean dose of Parotid without compromising PTV coverage and hot dose and extracted the total Parotid volume (V_p), parotid volume overlapped with PTV($V_{p'}$), Mean dose of Parotid (D_{mean}) and Dose Prescribed to the PTV with which parotid is overlapping (D_{pd}). A retrospective analysis of data extracted from each patient has shown a correlation between the fractions of parotid overlapping the PTV and the D_{mean}/D_{pd}. Exponential regression was done on plotted graph between the fractional overlap of parotid and D_{mean}/D_{pd}. A mathematical model as shown in equation (1) was generated for predicting D_{mean} based upon the fractional OAR-PTV overlap ($V_{p'}/V_p$),

$$\frac{D_{mean}}{D_{pd}} = A - (B \times e)^{-C \times \left(\frac{V_{p'}}{V_p}\right)} \quad (1)$$

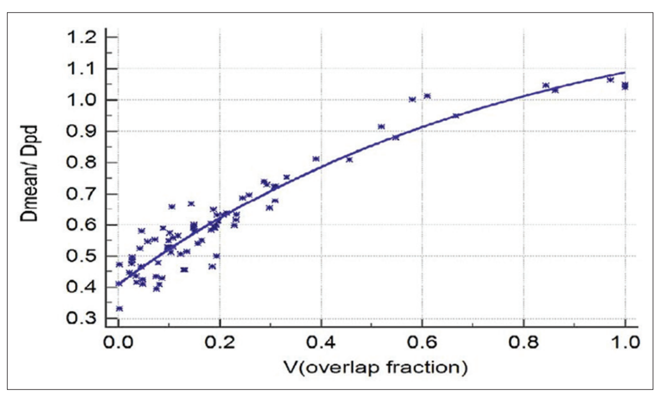

Figure 1: Regression plot between the fractional overlap of parotid and D_{mean}/D_{pd}

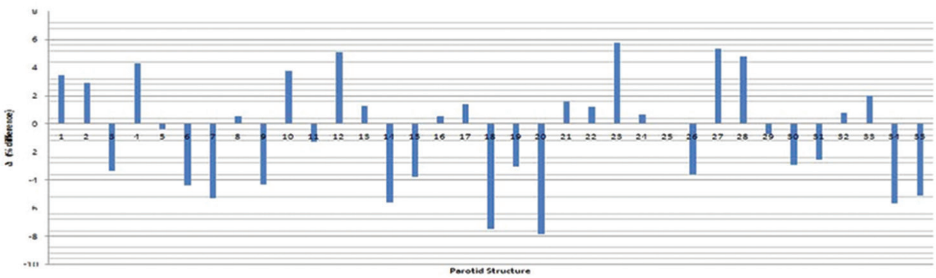

Figure 2: % deviation of D_{pred} from D_{plan}

Where A, B, C are model parameter selected to best fit the data.

To validate this model we used the above equation to predict the mean dose of 35 parotid volumes (D_{pred}) compared with the planned mean dose (D_{plan}) of the parotid. The difference between the predicted and planned mean dose (Δ) was calculated,

$$\Delta = \frac{D_{plan} - D_{pred}}{D_{plan}}$$

Result and Discussion: The Data analysis of fraction overlap of parotid Vs D_{mean}/D_{pd} showed correlation of 94.7% (p value <0.0001).

The exponential regression is done with mathematical modeled Parameter adjusted to A=1.35, B=0.9409 and C=1.2828 to provide an best fit the mathematical model to the local plot of D_{mean}/D_{Pd} versus $V_{p'}/V_p$ [Figure 1], the R^2 value for the above regression was 0.9545 (P value<0.0001). Thus equation below was derived to predict the parotid mean dose,

$$D_{pred} = D_{pd}\,[1.35 - (0.9409 \times e^{-1.2828 \times \left(\frac{V_{p'}}{V_p}\right)} \qquad (2)$$

In all the cases, data under test category showed smaller deviation (Δ) between predicted and planned parotid mean dose dose [Figure 2].

Conclusion: This tool helped the planner to decide the lower level of parotid dose that can be achieved and for oncologist to alter the overdrawn CTV without compromising treatment area which reduces the overlap of parotid with PTV.

BP-4

PREDICTING THE IMPACTS OF DAILY TRANSLATIONAL COUCH SHIFTS ON DOSE VOLUME HISTOGRAM AND RADIO BIOLOGICAL PARAMETERS OF VMAT PLANS USING CURVE FITTING METHOD

M. P. Noufal, K. K. Abdullah[1], P. Niyas, P. Subha[1]

Department of Medical Physics and Radiotherapy, Baby Memorial Hospital, [1]Department of Physics, Farook College, Kozhikode, Kerala, India.

E-mail: noufalsh@gmail.com

Introduction: Dose volume histogram (DVH) plays a vital role in evaluating the treatment plans. But patient set up errors introduces variations in the daily DVH and radiobiological parameters. Our study aims to check the feasibility of predicting daily DVH by incorporating random translational couch shifts, using curve fitting method, and using this to monitor changes in the radio biological parameters on a daily basis.

Materials and Methods: Let $D_j(x_0, y_0, z_0)$ be the dose received by Vjth volume of a structure in the DVH of the base plan, planned with an iso-center (IC) co-ordinate (x_0, y_0, z_0) [Figure 1a]. When there is a translational couch shift of 'i' on either side of the IC position (x_{0+i} in the right or positive x direction and x_{0-i} in the left or negative x direction), the dose received by Vjth volume due to translational couch shift now becomes $D_j(x_{0+i}, y_0, z_0)$ and $D_j(x_{0-i}, y_0, z_0)$ provided, there are no shifts in the y and z axis. Thus variations in $D_j(x_0, y_0, z_0)$ along the x direction can be represented by the fitted function $f(x, v_j)$ [Figure 1b]. Similarly variation in $D_j(x_0, y_0, z_0)$ along the y and z axis can be represented by functions $f(y, v_j)$ and $f(z, v_j)$ respectively. For each point on V_j, corresponding functions can be calculated and it can be used to predict effect of daily random couch shifts on DVH by the mathematical modeling of the base plan DVH without using any further dose computation on CT. To demonstrate this, we have selected 10 prostate patients treated with VMAT technology. Systematic couch translation shifts were introduced in the clinically accepted base plans with an increment of 1 mm and up to 5 mm from the IC in both positive and negative directions of each of the three axis, x (right–left), y (superior–inferior) and z (anterior–posterior). The DVHs of the base plan and the error plans were imported into the MATLAB software (2009b, The MathWorks, Natick, MA) and in-house MATLAB code was generated to find the best curve fitted functions $f(x, v_j)$, $f(y, v_j)$ and f(z, vj) for each points on the DVH and there by generating predicted DVH for PTV, CTV and OARs. It is then used to find the daily radio biological parameters such as the EUD (Equivalent uniform dose), tumor control probability (TCP) and normal tissue complication probability (NTCP). The EUD was calculated using the Niemierko model and NTCP values were calculated using the Lyman–Kutcher–Burman model . Finally, the MATLAB predicted and the T.P.S calculated DVH was compared to validate our method and percentage of variation between the two was evaluated.

Results and Discussion: When T.P.S calculated and MATLAB predicted DVHs were compared, both curves almost overlapped with each other and the maximum variation between the two curves at any point was less than 0.5% in targets and OARs [Figure 2a]. The mean and standard deviations of the variations in the DVH and radio biological parameters due to daily shifts, calculated by T.P.S and MATLAB predicted methods also showed a good correlation [Figure 2b].

Conclusion: Our method of predicting the effect of couch shifts on DVH and radiobiological parameters using curve fitting method is found effective to determine the uncertainties

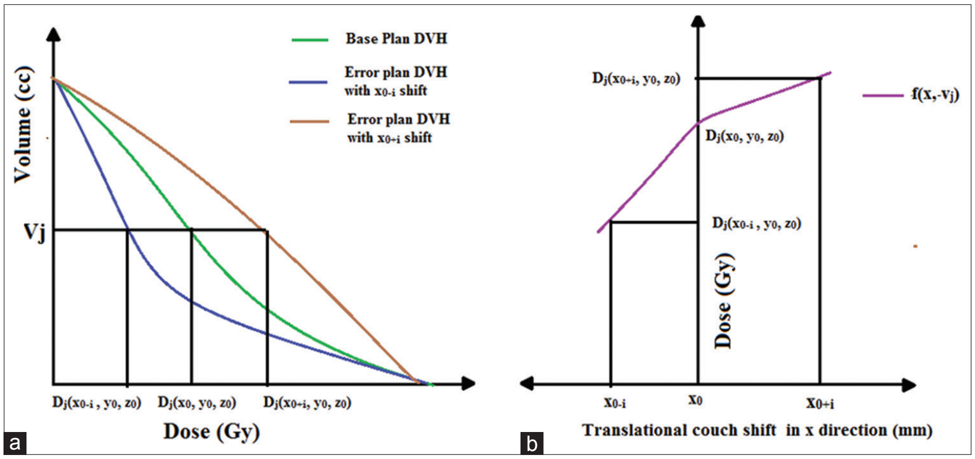

Figure 1: (a) Plot of cumulative dose volume histogram showing the dose received by V_j^{th} volume when planned at iso-centre (x_0, y_0, z_0) and with shifts of x_{0+i} and x_{0-i}. (b) Plot of the variations in $D_j(x_0, y_0, z_0)$ due to couch translation shifts along the x direction and the corresponding fitted function f(x, v_j)

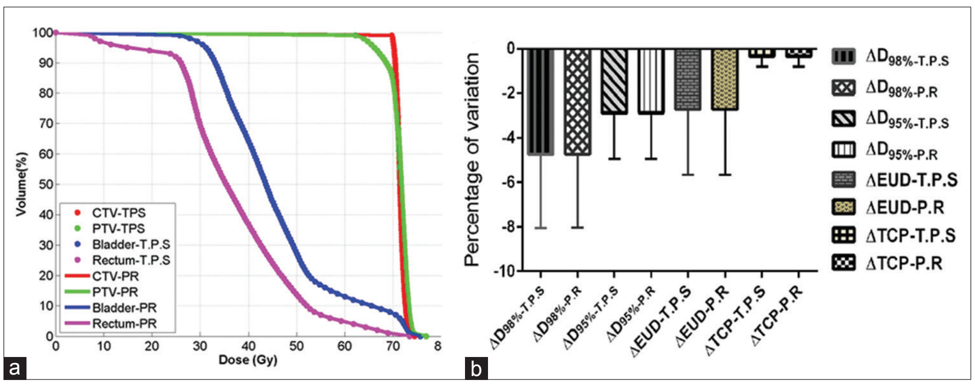

Figure 2: (a) Dose volume histograms calculated by the treatment planning system and predicted (PR) by the MATLAB for the CTV, PTV, bladder and the rectum when daily random translation couch shifts were applied. (b) The comparisons of T.P.S calculated and MATLAB predicted (PR) values for mean percentage of variation of the dose volume histogram and radio biological parameters between the base plans and the random couch shifted plans

in dose delivery on a daily basis, and to enhance the quality of treatment.

BP-5

STUDY OF THE EFFECTS OF DWELL TIME DEVIATION CONSTRAINT ON INVERSE PLANNING SIMULATED ANNEALING OPTIMISED PLANS OF INTRACAVITARY BRACHYTHERAPY OF CANCER CERVIX

Saurabh Roy[1,2], V. Subramani[3], Kishore Singh[1], A. K. Rathi[1]

[1]Department of Radiotherapy, Lok Nayak Hospital, [3]Department of Radiotherapy, Dr BRA IRCH, AIIMS, New Delhi, [2]Research and Development Center, Bharathiar University, Coimbatore, Tamil Nadu, India.
E-mail: saurabhroy86@gmail.com

Introduction: High Dose Rate (HDR) remote after loading brachytherapy machine and advanced treatment planning system have made it possible to make variations in individual dwell times across a catheter according to tumour density and for sparing normal structures. There is also the development of several inverse optimization methods such as Inverse Planning Simulated Annealing (IPSA) and Hybrid Inverse Planning Optimization (HIPO). But their actual application is not so frequent for treatment of cervical cancer with Intracavitary brachytherapy. One of the several reasons of it, is the limited research of inverse planning optimization for volume based intracavitary brachytherapy. Therefore very few institutions are venturing towards volume based IPSA optimised intracavitary brachytherapy. This study focuses on dwell time deviation constraint (DTDC) feature of IPSA based optimization which restricts the large variation of dwell time across the catheter. The aim to investigate the dosimetric variations in IPSA optimised intracavitary brachytherapy plans with the gradual change in DTDC values.

Materials and Methods: For this retrospective study we have generated IPSA optimised intracavitary brachytherapy plans for 20 cancer cervix patients using Oncentra Brachytherapy treatment planning system (version 4.3). The initial DTDC value of each IPSA plan was kept 0.0. Later on gradual increment was made in DTDC values in step of 0.2. The variations in dose volume histogram parameters D90%, V100%, V150%, V200%, for PTV were studied. For dose analysis of bladder and rectum, their D2cc parameters were investigated. Plan modulation index (M) defined by Ryan L. Smith *et al*. was used for characterising the variation of dwell time modulation with respect to gradual increase in DTDC parameter.

Results: Plan modulation index gradually decreases with increasing value of DTDC from 0.0 to 1.0. There was the 83%

decrease in M value from IPSA of DTDC 0.0 to fully constrained IPSA of DTDC 1.0. Number of activated dwell positions decreases for DTDC value of 0.0 to 0.2, but then gradually increases for increasing DTDC values. Total treatment time of IPSA plan decreases with increase in DTDC value. There was 6.89 % and 18.13 % decrease in average D90% value for DTDC 0.4 and 1.0 respectively compared to average D90% for IPSA plan of DTDC 0.0. The average value of V100% decreases with increasing DTDC and rate of decrement decreases from DTDC value 0.0 to 0.6 and then increases till 1.0. It was observed that both the values decreased with increasing DTDC value for IPSA plans. There was 4.37 % and 11.23% decrease in average PTV V150% values for DTDC 0.4 and DTDC 1.0 respectively compared to DTDC 0.0. Average D2cc values for rectum and bladder decrease with increasing DTDC values. There is reduction of 8.26% and 6.95% for D2cc values of rectum and bladder respectively for DTDC 1.0 compared to DTDC 0.0.

Discussion: Increase in DTDC value restricts the deviation of dwell time from average dwell time of every catheter. A higher value of DTDC in IPSA plan removes the larger of the dwell time in isolated dwell positions and also reduces overall treatment time, but this is at the cost of decreasing D90% and V100% value which indicate lower PTV coverage.

Conclusion: The benefits of applying DTDC values in IPSA plan for intracavitary brachytherapy are that, it removes local hot spots and reduces rectum and bladder doses.

BP-6

VOLUME MIS-ESTIMATION BY CT SCAN: IMPORTANCE OF CT PERFORMANCE IN PRECISION LUNG CANCER RADIOTHERAPY

Teerthraj Verma, Nirmal K. Painuly, Surendra P. Mishra[1], M. L. B. Bhatt, Anoop K. Srivastava[1], Ranjit Singh[2], Dipak Shrotia[3], Shraddha Srivastava, Navin Singh

King George's Medical University, [1]Dr. Ram Manohar Lohia Institute of Medical Sciences, Lucknow, [3]J.K. Cancer Institute, Kanpur, Uttar Pradesh, [2]Postgraduate Institute of Medical Education and Research, Chandigarh, India. E-mail: teerth05kashi@gmail.com

Introduction: Accuracy of radiation delivery to a moving target found directly related with the breathing motion as well as information provided by CT acquisition. The radiation treatments are becoming increasingly conformal and the pinpoint accuracy of modern radiation treatments would be worthless if the tumor was not in the spot where the radiation beams were aimed. Any geographic miss or incorrect isodose coverage of the region of interest (tumor) may lead to significant deviation of the planned dose, which could produce catastrophic results.

Objective: The purpose of present study was to quantify the volume mis-etimation by CT of target that underwent 3D motions placed inside the CIRS 3D phantom.

Materials and Methods: First validation of wood cylinder of diameter 6.4 cm as lung equivalent inhomogeneity was performed by measuring linear attenuation coefficient and HU value of wood slabs. A cavity of dimension 2x2x2 cm^3 was created in the wood cylinder. Then this cavity was filled with dental material to create the tumor of dimension 2x2x2 cm^3. It was ensured that center of this tumor was lying at the line joining the two lateral external surface markers on the CIRS phantom at the depth of 7.5 cm. This position of tumor was considered rest position and various movements (AP-PA, SI & lateral) were given with respect to rest position. CT images of CIRS phantom containing tumor model were acquired after proper alignment with three lasers similar to real patient simulation. Subsequently the tumor was shifted ± 5 mm, ± 15 mm and ± 25 mm with respect to "Rest Position" along superior and inferior directions. CT images were acquired after each movement. In total, 15 movements were given to the tumor to implement 1 D, 2D and 3D motions similar to real lung movements with the amplitude(s) as reported in various literatures.

Results and Discussion: To understand the impact of three dimensional displacement of tumor on delivered dose, a clinically relevant target having dimension 2 cm X 2 cm X 2 cm sandwiched between two wood slabs of wood cylinder (lung equivalent inhomogeneity) were put in the hollow space provided in CIRS phantom. The resulting scans showed that object shape was significantly distorted. Generally, it is the CT data that provides the tumor information (localization, volume of the target and its extension etc.) for the diagnosis as well as more importantly for radiotherapy treatment planning purposes. Therefore results of radiotherapy are affected directly by the performance of CT. In this study, the variations in tumor volume with target movements given by CT were recorded and the same was compared with its true physical volume. Trend of increase in overestimation of target volume (by CT imaging) with 3 directional movements range was found. The volume of the target was 7.8 cm^3 (rest position) however variation up to 9.5 cm^3 was observed in CT volume of the target with different movements. The irradiation of target with overestimated volume compared to true physical volume causes unnecessarily normal tissue irradiation.

BP-7

MONTECARLO BASED CORRECTION FACTORS FOR SMALL FIELD DETECTORS

P. S. Renil Mon, Sneha S. Nair, Raghavendra Holla, C. O. Clinto, M. K. Ashitha, E. Sreedevi, Bhaskaran K. Pillai

Department of Medical Physics and Radiation Safety, Amrita Institute of Medical Sciences and Research Centre, Kochi, Kerala, India. E-mail: ps.renil@gmail.com

Introduction: A radiation field is considered as small if the field dimension is less than the range of secondary electrons and the collimating devices are partially occluding the source. There are different types of detectors proposed for small field measurement, which includes unshielded diode, diamond detector, and small volume ion chambers. Even though the active volumes of these detectors are small, the non-water equivalent material of the detector will cause response variations. To overcome this uncertainty Alphonso *et al* introduce a new formalism for small field reference dosimetry. According to this formalism the relative output factor (ROF) which converts the absorbed dose to water by the standard reference field size to the given field size has to be corrected by the factor $k^{f_{clin},f_{msr}}_{Q_{clin},Q_{msr}}$. f_{msr} and f_{clin} are the machine specific reference field and the given clinical field. Q_{msr} and Q_{clin} are the corresponding beam qualities.

Objectives: Aim of our study is to calculate the $k^{f_{clin},f_{msr}}_{Q_{clin},Q_{msr}}$ factors for our clinical detectors, Edge detector (Sun Nuclear), 60017 diode (PTW), CC01 ion chamber (IBA) for SRS cones of diameter 5 mm to 15 mm in Elekta Synergy linear accelerator using Monte Carlo simulation.

Materials and Methods: Elekta Synergy Linear accelerator treatment head was simulated using BEAMnrc Monte Carlo code as per manufactures specification. All the three detectors we used were simulated as per the manufacture's specification. Three EGSnrc user codes were used for the detector simulation based on the detector geometry. Since PTW T60017 has a cylindrical geometry DOSRZnrc was used. Because of the rectangular geometry DOSXYZnrc was used to model the Sun Nuclear Edge diode and CC01 chamber was modelled with EGSchamber user code.

The Mote Carlo model of the treatment head was validated against the measured data for standard field size of 10x10cm2. Off axis profile, PDD and were verified as validation procedure. All measurements were done in 50X50X50 cm^3 water phantom (PTW RFA). PDD curves and profiles of cone fields were taken in 1mm resolution with PTW T60017 unshielded diode in integrated mode. Profiles were taken at the depth of maximum dose, at 5 cm and at 10 cm in SSD setup. ROF were also measured at the depth of maximum dose with reference field size f_{msr} (10X10 cm^2) for all the three detectors.

Results and Discussions: Measured and Monte Carlo calculated ROF were not in agreement. Edge and PTW 60017 diodes overestimated the ROF in the smaller field sizes 5 mm and 7.5 mm. In 5 mm field size edge diode over estimated by 9.5% while 60017 diode to 6.7%. In 7.5 mm field size variation was 7.8% and 4% for edge and 60017 diode respectively. 1% to 3% variation were observed for other field size of 10 to 15 mm in both the diode detectors. This variation is mainly due to the over response of silicon and the presence of other high density material. Even though the active volume of the silicon chip of edge diode is less, its response is more than that of 60017 diode because of the presence of copper plate and brass covering. CC01 ion chamber under responded up to 10% because of its low density active volume. When applying the Monte Carlo calculated correction factor on the measured ROF it is in good agreement with the Monte Carlo calculated ROF.

BP-8

DEVELOPMENT AND VALIDATION OF A MATLAB SOFTWARE PROGRAM FOR REAL TIME AND POSITIONING MANAGEMENT GATING GENERATED BREATHING TRACE

Naveen Kumawat, Anil Kumar Shrotriya[1], H. Malhotra Singh, Kartikeswar Patro, Anil K. Bansal, R. K. Munjal, A. K. Anand

Department of Radiation Oncology, Max Super Speciality Hospital, Saket, New Delhi, [1]Department of Physics, S.P.S.B. Government P.G. College, Shahpura, Bhilwara, Rajasthan, India. E-mail: ninunaveen@gmail.com

Introduction: In radiotherapy, the goal is to kill cancerous tumour while sparing surrounding normal tissues. This is more difficult when the target is moving with patient's breathing, so either take large PTV margin or to miss the target during treatment. To overcome this problem, AAPM TG 76 recommends, if the target displacement is more than 5 mm, motion management techniques should be considered. RPM is one of the motion management technique, provides facility to treat patients in amplitude based and phase based breathing cycles.

Objective: RPM version 1.7.5 has a limitation with its clinical application, it provides the facility to deliver radiation with either phase or amplitude based gating, but 4D-CT images are sorted only with respiratory phase. In regular breathing cycles, there is no significant difference between phase and amplitude based treatment, but in irregular breathing the performance of RPM is not robust with phase based gating and does not provide an easy way to change phase to equivalent amplitude based gating parameter. So, we developed a MATLAB Software program to calculate parameters for amplitude based treatment and analyse a RPM gating generated breathing profile.

Materials and Methods: For conversion of phase based gating window to amplitude based gating threshold, a program was designed using MATLAB (Matrix Laboratory, Math Work, R2016a) software. With this program, we analysed phase based gating profile as well as amplitude based gating profile using reference profile. Using this software program, we got predicted amplitude window for treatment, actual treated amplitude window, treatment range in terms of amplitude, duty cycle, errors in phase and amplitude. For validation of this program, we took a Varian Gating Phantom generated regular breathing trace of reference scan and found predicted amplitude parameters, and irradiated the phantom retrospectively with predicted parameters on phase and amplitude based gating. We selected 85% to 15% phases window for treatment, the phase window selection criteria were random.

Results: From reference profile, the predicted lower and upper window level was 1cm and 1.8 cm respectively from fitted trace. For phase based and amplitude treatment the actual lower amplitude was 0.99 and 1.02 cm and higher amplitude was 1.65 and 1.64 cm respectively, Treatment range was 0.65 and 0.62 cm respectively, duty cycle was 28.51% and 30.37% respectively. "Beam on" error with phase based treatment in term of phase was 1.4% and in term of amplitude was 0.98% and with amplitude based treatment the "beam on" error was 0.85%. in amplitude based treatment the treated phase window was 83.59% to 15.83%.

Discussion: The selected phase gating window in reference profile and treated phase window in amplitude based treatment was almost equal. If we set asymmetric phase window for treatment like 90% to 20% then the treated phase window may not match with set one, but it does not have significance because treatment was done with amplitude mode. The treatment range was almost equal in both mode. The "beam on" error in both modality was ~ 1%, which was due to machine lag time. The duty cycle in both modality is almost same but may vary with window section.

Conclusion: The results are encouraging and comparable for both modes of treatment under ideal breathing cycles so the developed program can be used for irregular breathing patterns to find errors and duty cycle and other parameters. This program is capable to observe inter fraction errors and variations in breathing trace.

BP-9

HIPPOCAMPAL SPARING WHOLE BRAIN RADIOTHERAPY: A PLANNING STUDY COMPARING COPLANAR AND NONCOPLANAR VOLUMETRIC MODULATED ARC THERAPY PLANS

C. A. Muthuselvi, K. Malathi, T. K. Bijina, A. Pichandi, S. Yuvarajan[1], B. Subbulakshmi

HCG Enterprises Ltd, [1]HCG-MSR Centre of Oncology, Bengaluru, Karnataka, India.
E-mail: muthuselvi.ca@gmail.com

Introduction: Whole Brain Radiotherapy (WBRT) is the most commonly used treatment option for patients with multiple brain metastases. WBRT provides rapid palliation of neurologic symptoms and improves local control as an adjuvant to resection or reduce surgery, but it also causes neurocognitive decline after therapy. Hippocampus sparing whole brain radiotherapy (HS-WBRT) can reduce neurocognitive deficits caused by radiation. Although avoiding hippocampus during whole brain irradiation is desirable, it is important to deliver a uniform dose to the rest of the brain for reducing the probability of cancer growth. The central location and unique anatomic shape of hippocampus shows great challenge in contouring and planning.

Objectives: The purpose of the study was to evaluate the feasibility of HS-WBRT using volumetric modulated arc therapy (VMAT). We performed this planning study comparing the PTV coverage, hippocampal dose as well as the unspecified tissue dose of VMAT using non- coplanar arcs and VMAT employed coplanar arcs for HS-WBRT.

Materials and Methods: Ten patients diagnosed with brain metastases underwent repeated planning of HS-WBRT. CT scan with 1.25 mm slice thickness was fused with MRI T1 & T2 weighted sequences of 1.25 mm slice thickness prior to the delineation of hippocampus, optic nerve, lens and chiasm. Hippocampal avoidance region was generated by three dimensionally expanding hippocampal contour by 5 mm. As per RTOG0933 recommendation, PTV was created by excluding the hippocampal avoidance region from CTV and prescribed to 30Gy in 10 fractions. Three VMAT plans, Coplanar VMAT (coVMAT) with three full arcs, Non-coplanar VMAT (1ncVMAT) with one coplanar full arc and two vertex arcs (150°arc, couch 90°), Non-coplanar VMAT (2ncVMAT) with one coplanar full arc and two oblique arcs (140°arc, couch 30°, 330°) were created for all ten patients using Monaco Treatment Planning System (TPS) v.5.1 for an Elekta synergy machine with agility MLC [Figure 1]. All three plans were normalized such that to meet RTOG acceptable compliance criteria for PTV and OAR's. Plans were evaluated using dosimetric indices such as $D_{2\%}$, $D_{98\%}$, V_{30Gy}, HI to the target, D_{min}, D_{mean}, D_{max} to the hippocampus and V_{5Gy}, V_{10Gy} of unspecified tissue, excluding the target volume.

Result and Discussion: All three VMAT plans achieved the RTOG0933 planning criteria [Figure 2]. Comparing the target doses in terms of $D_{2\%}$, $D_{98\%}$, V_{30Gy}, HI there were no significant differences among the three plans. Comparing the hippocampus, the mean hippocampal dose was 8.3% higher in coVMAT than the non coplanar plans. Hippocampus minimum and maximum dose also lesser in non coplanar plans by 6.9% & 7.2% than the coVMAT plans. The maximum and minimum hippocampus dose+ SD were 16.64 ± 0.7Gy, 14.48 ± 0.9Gy, 14.95 ± 0.8Gy and 9.42 ± 0.3Gy, 7.34 ± 0.4Gy, 7.31 ± 0.4Gy for the coVMAT, 1ncVMAT and 2ncVMAT respectively. We thus found that the non-coplanar VMAT is better than the coplanar VMAT in hippocampal sparing. The optic nerve, chiasm and lens dose were within the tolerance limit and similar in all three plans. To quantify the normal tissue dose because of non-coplanar beams we compared V_{10Gy} and V_{5Gy} of unspecified tissue (body-target). V_{5Gy} of unspecified tissue, excluding the target volume was 1174 ± 324cc, 1790 ± 274cc, 1294 ± 249cc for the coVMAT, 1ncVMAT, 2ncVMAT respectively. Unspecified tissue dose were higher in 1ncVMAT plan comparing with coVMAT and 2ncVMAT, because of the vertex field. The 2ncVMAT plan showed slightly higher unspecified tissue dose than the coVMAT plan.

Conclusions: From our results, we conclude that 2ncVMAT significantly reduced the hippocampus dose without increasing the normal tissue dose. Thus, non-coplanar VMAT with oblique arcs (2ncVMAT) was better than coplanar VMAT plan (coVMAT) and non-coplanar VMAT with vertex arc (1ncVMAT) for hippocampal sparring in whole brain radiotherapy.

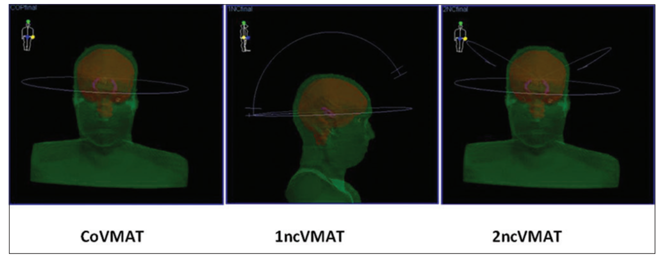

Figure 1: Beam arrangement of three volumetric modulated arc therapy plans

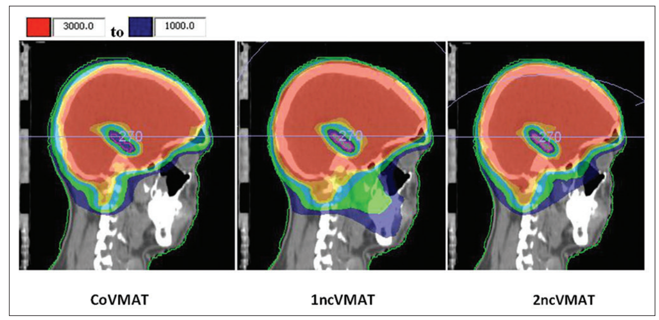

Figure 2: Dose distribution in cGy showing the hippocampal sparing as well as the unspecified tissue dose

Oral

O-1

RADIATION SAFETY ASSESSMENT OF PROTON THERAPY FACILITY IN INDIA

G. Sahani, Pankaj Tandon, A. U. Sonawane
Radiological Safety Division, Atomic Energy Regulatory Board, Mumbai, Maharashtra, India.
E-mail: gsahani@aerb.gov.in

Introduction: The concept of proton therapy was given first by the Robert R. Wilson in 1946. The first treatments were carried out with proton at Berkeley Radiation Laboratory in 1954. The world's first hospital-based proton therapy center was started in 1989 for ocular tumours at the Clatterbridge Centre for Oncology in the UK. At present, there are 73 particle therapy facilities which are operational and 15 under construction all over the world. Atomic Energy Regulatory Board (AERB), the organization which is responsible for enforcing provisions of radiation safety requirements in India in accordance with Atomic Energy Act, 1962 and Atomic Energy Radiation Protection Rules, 2004. AERB had received first application from the local supplier i.e. M/s IBA India Pvt Ltd., Chennai for obtaining no objection certificate (NOC) for their proton therapy accelerator model Proteus 235 having deliverable proton beam energies between 70 to 230 MeV for its to supply to M/s Apollo Hospitals Enterprises Pvt. Ltd, Chennai. Aim of this paper is to discuss the rationale ad process followed for the radiation safety assessment of the proton therapy accelerator facility and other safety review for issuance of various regulatory consents involved.
Materials and Methods: Though proton therapy facility is not new to the world but its first of its kind for India and the present safety code does not have stipulation on regulatory requirements for proton therapy facility. Accordingly, Chairman, AERB constituted Safety Committee for Hadron Therapy Facilities comprising experts from BARC, IGCAR, AERB and TMH for carrying out radiation safety review of Hadron Therapy Accelerator (for proton, carbon ion etc.), evaluation of radiation shielding for Hadron therapy facilities, to develop acceptance/quality assurance tests for such facilities for performance evaluation. Radiation safety and dosimetric parameters of Proton therapy Accelerators are different from that of medical linear accelerator. Hence for safety assessment of proton therapy accelerator, regulatory forms with relevant parameters for such facilities were developed after gathering information from manufacturer (M/s. IBA, Belgium) and literature available. Radiation safety assessment were completed by the above safety committee in four meetings after satisfaction from the submitted information and technical presentation by the manufacturer. Further, shielding calculation is very complex for proton therapy facilities due to its complex design. Analytical calculation method for the bunker overestimates at many locations depending upon the thickness of the walls/ceiling. Therefore, a working group comprising of Monte Carlo experts were formed for validation of the radiation shielding as proposed by the manufacturer for the user institution. This working group submitted its recommendation to the safety committee on the shielding adequacy of the layout plan.
Results and Discussion: Based on the safety review and recommendation of the safety committee, AERB has issued the site and layout approval to house 230 MeV Proteus 235 proton therapy accelerator and NOC to the M/s IBA India Pvt. Ltd, Chennai to supply this model to the M/s Apollo Enterprises Pvt. Ltd, Chennai. Construction of the facility is expected to be completed soon and further stage of regulatory review process will be completed once AERB receives application. Further, two more institutions have submitted their application for seeking regulatory clearances from AERB for establishing their proton therapy facilities. AERB is also in process of carrying out radiation safety review of proton therapy facilities of other two institutions.
Conclusion: AERB has followed rigorous review process for safety assessment of the proton therapy accelerator by constituting the safety committee comprising experts. As regulatory clearances for site & layout approval, import permission for proton therapy model Proteus 235 has already been granted by AERB, review of the performance test results will be reviewed by AERB for granting licence to operate the facility finally which will be the first proton therapy facility in the country.

O-2

EFFECT OF DELIVERABILITY CONSTRAINTS ON THE IMPT PLAN QUALITY

Bojarajan Perumal, R. Vaitheeswaran[1], Mohamad Nawaz Ahamad, Thajudeen Basha, Prajwal Kumar
Philips Radiation Oncology Systems, [1]Philips ICAP Applications, Philips Innovation Campus, Bengaluru, Karnataka, India. E-mail: bojarajan.perumal@philips.com

Purpose: The purpose of this study is to investigate the effect of deliverable constraints (Spot spacing and Minimum deliverable MU) in IMPT plan quality. Each IMPT delivery machine has their own limitations in terms of MU delivery just like LINAC's. Therefore after each optimization, there is a process called spot processing to be carried out in order to ensure that obtained MU's are deliverable by applying deliverable MU constraint. The spot processing can result in significant distortion in optimized dose distribution. In this paper the impact of applying deliverable MU constraint and the relation between spot spacing and deliverable MU constraint is studied.
Materials and Methods: Pinnacle IMPT non clinical version was used for IMPT Planning. Multiple treatment plans were generated for Prostate, Thorax, and H&N cases with varying spot spacing (2 –10 mm). Spot processing was done for all the plans and Dose Volume Histograms (DVH) were compared to evaluate OAR sparing and target dose homogeneity. DVH statistics were also compared before and after spot

processing to study the impact of applying deliverable MU constraint to the optimizer with variable spot spacing.

Results and Discussion: In this paper, DVH for multiple plans were evaluated to study the effect of spot spacing and use of applying deliverable MU constraint to the optimizer. In our study, we found that, when spot spacing decreases, there is a significant improvement in plan homogeneity and OAR sparing. But many spots are observed with low intensity which may affect the plan robustness. OAR doses decreases when spot spacing increases. But also observed that significant difference in final dose distribution between pre and post processing of planned spots. This is because, when smaller spot spacing (2 mm and 3 mm) is used, number of spots increased dramatically which causes the MU of the each spots to be lesser than or close to the minimum deliverable MU constraint of the delivery system. Many of these spots are eliminated during post processing which causes deterioration in the final plan quality. This deterioration effect decreases above 4mm spot spacing roughly.

Conclusion: Out study demonstrate that, Spot spacing must be chosen to balance target dose homogeneity and OAR sparing. While decreased spot spacing increases target dose homogeneity, it also causes decrease in plan robustness as number of low intensity spots exists. This study shows that spot spacing of around 5 mm can be an optimal size to balance the homogeneity and OAR sparing to retain plan robustness. Also the effect of incorporating delivery MU constraint decreases when spot spacing is around 5 mm or above.

O-3

RADIATION PROTECTION ASPECTS IN A MEDICAL CYCLOTRON FACILITY FOR PRODUCTION OF POSITRON EMITTERS

Aruna Kaushik, Swatantra, Nitin Kumar, Sachin Sony, Puja Panwar, Pradeep Goswami, Sukhvir Singh, Anil K. Mishra

Institute of Nuclear Medicine and Allied Sciences, New Delhi, India. E-mail: kaushik_aruna@rediffmail.com

Medical cyclotron dedicated for the production of positron emitting radioisotopes is operational at our Centre for the last ten years. It has an attached external beam facility that makes it unique in terms of research and radioisotope production. This is coupled to a radiochemistry laboratory wherein the positron emitting radioisotopes are labelled to pharmaceuticals to synthesize molecular imaging probes for Positron Emission Tomography (PET). Since the radioisotopes produced and handled in a medical cyclotron facility may be in solid, liquid and gaseous form, special precaution and care needs to be taken during production, synthesis and disposal of generated radioactive waste. Although the half-lives of positron emitters used for PET are short (few minutes to few hours), the amount of activity produced and handled during synthesis and dispensing is quite large. The objective of the present study is to address the radiation protection issues associated with production and synthesis of PET radiopharmaceuticals.

The medical cyclotron at our Centre (PETtrace System, M/s GE Medical Systems) is an unshielded type that accelerates negatively charged hydrogen ions (H^-) to 16.5 MeV or negatively charged deuterium ions (D^-) to 8.4 MeV energy. Positron emitting isotopes produced in the cyclotron are ^{18}F, ^{11}C, ^{13}N and ^{15}O. The synthesis of PET radiopharmaceuticals is carried out in hot laboratory that has chemistry modules housed in adequately shielded hot cells (M/s Comecer, Italy). The synthesis of PET radiopharmaceuticals may result in release of radioactivity in liquid or gaseous forms and generate solid waste. The radioactive gases from the synthesis modules are not released directly to the atmosphere but are compressed in the waste gas system till it decays to background level. It is subsequently released through exhaust system.

The radiation levels were monitored using area monitors (gamma and neutron) installed in the cyclotron vault, control console and beam extension facility. The gamma area monitor installed in the hot laboratory and the exhaust pipe was used to monitor the radiation levels during synthesis of PET radiopharmaceuticals. The exhaust pipe was also monitored by a gamma area monitor to measure the release of activity in air. The data from all the installed area monitors was displayed on the control console using ROTEM's Medismarts comprehensive monitoring system. Portable radiation survey cum contamination monitor ((Ramgene, M/s ROTEM, Israel) was used for contamination check and monitoring radiation levels at work benches, dustbins etc. The personnel were monitored using pocket dosimeters and thermoluminescent badges.

The gamma radiation levels in the vicinity of vault and in the hot laboratory ranged from 1 - 4 microsieverts per hour during isotope production. However, the radiation level during the transfer of ^{11}C in the form of ^{11}C labelled carbon dioxide from the cyclotron vault to the chemistry module was observed to increase to 10 – 20 microsieverts per hour. The radiation level near targets in the cyclotron vault ranged from 200 microsieverts per hour to 2 millisieverts per hour as monitored before every production. The havar foils removed from the target during maintenance were stored in the lead pit in the vault. However, the disposal of these foils need special attention and regulatory approval since these foils have long lived isotopes because of induced activity and the number of foils stored in the pit increase with time. The personnel involved in synthesis received whole body radiation dose of 2 – 3 microsieverts and wrist dose of 50 – 150 microsieverts per synthesis. The major contribution to personnel radiation dose was from dispensing of PET radiopharmaceuticals manually.

O-4

SMALL PHOTON FIELD DOSIMETRY WITH RADIOCHROMIC FILM USING AN INDIGENOUSLY DEVELOPED PROGRAM

Ankur Mourya, Chhape Ram, Abhijit Mandal, Satyajit Pradhan, Uday P. Shahi, Sunil Choudhary, Lalit M. Aggarwal

Department of Radiotherapy and Radiation Medicine, Institute of Medical Sciences, Banaras Hindu University, Varanasi, Uttar Pradesh, India. E-mail: lmaggarwal@yahoo.com

Introduction: The measurement of the dose distributions for smalls fields are quite different from the reference conditions stated in the dosimetry protocols. Accurate dosimetry of small fields is complicated due to the electron disequilibrium, steep dose gradients, perturbation due to different density of the detector and the medium. Due to these challenges, the suitable detector for small field dosimetry should have high spatial resolution, small volume, linearity, and reproducibility, independent of energy and dose rate. Because of low energy dependence and high spatial resolution, Radiochromic Film is an appropriate dosimeter for dose measurement in small radiation fields having regions of high dose gradient. EBT3 film has been studied and accepted as a two dimensional detector especially for small Field dosimetry.

Objective: To investigate the capability of GafchromicEBT3 (External beam therapy, Gafchromic™) Film for dosimetry of small rectangular photon beam delivered with MLC and jaws.

Materials and Methods: EBT3 radiochromic film was used for measurement of dose. To calibrate Radiochromic film, we have cut the film into several small pieces and irradiated for various known doses with 6MV photon beam from a Varian Unique linear accelerator (Varian, Palo Alto, CA). The doses delivered to these cut films were 25, 50, 75, 100, 150, 200, 250, 300 cGy and film samples were handled according to AAPM TG 55 Report. Epson expression 11000XL desktop flatbed document scanner was used for film scanning that has maximum scanning spatial resolution of 1600 by 3200 dpi. Film were scanned in 48 bit RGB mode (16 bit per color) with resolution of 72 dpi (0.353 mm per pixel) and saved in tagged image file format (tiff). We have written a program in MATLAB 2013a (Math Works, Natick, MA) to analyze the scan film data by converting intensity into Dose. Red color channel of image was used and these images were imported in our program written in MATLAB. All film were read before irradiation and 48 hours after irradiation for most precise determination of netOD (net Optical density). Film dose response is usually expressed as measured netOD against the dose delivered to the film. However, when using film for dose measurement, dose is more conveniently plotted as a function of the measured netOD so that the data can be fitted to a curve (least square method). Scanner does not read OD directly, therefore, we defined following formula.

$netOD = \log_{10} [(I_{unex} - I_{bkg})/ (I_{exp} - I_{bkg})]$

Where I_{unex} = reading of ROI (region of interest) for unexposed film I_{exp} = reading of ROI for exposed film

I_{bkg} = zero light transmitted intensity

For measurement of doses from Jaws and MLC (Varian millennium 120), 6 films of sizes 6 x 6 cm^2 were irradiated for 100MU, field sizes range from 1 x 1 cm^2 to 5 x 5 cm^2 within the solid water phantom at 5cm depth in SAD (SSD =95cm) setup. To read these films same procedure was used as used for film calibration. After that netOD was calculated and from this netOD, doses were calculated from our calibrated film data and doses obtained with gafchromic film was compared with doses obtained with other available dosimeters in the department.

Results and Discussion: With the help of film calibration data, doses for five different field sizes with MLC and Jaws were calculated. Dose for field sizes (1 x 1 cm^2 to 5 x 5 cm^2) defined by the jaws were 69.86, 83.31, 86.11, 88.12, 89.55 cGy and MLC were 70.91, 83.91, 86.96, 87.10, 90.41 cGy respectively. The variation in dose as compared to other dosimetric systems available in the department was within 3%. Percentage dose variation for MLC as compared to jaw were less than -1.48, -0.71, -0.98, 1.16, -0.95. It shows that with different field sizes dose delivered by MLC and jaws are same within 2% variation. Ionization chambers are usually used for calibration and beam measurements in conventional radiotherapy because of their high sensitivity, reproducibility and ease of use.

O-5

DUAL-ENERGY HIGH-RATE X-RAY COMPUTED TOMOGRAPHY SCANNER USING A YAP-PHOTOMULTIPLIER DETECTOR

Tsukuru Sato, Eiichi Sato, Yasuyuki Oda, Yuichi Sato[1], Satoshi Yamaguchi[2], Osahiko Hagiwara[3], Hiroshi Matsukiyo[3], Toshiyuki Enomoto[3], Manabu Watanabe[3], Shinya Kusachi[3]

Department of Physics, Iwate Medical University, [1]Department of Central Radiation, Iwate Medical University Hospital, [2]Department of Radiology, School of Medicine, Iwate Medical University, Morioka, [3]Department of Surgery, Toho University Ohashi Medical Center, Tokyo, Japan. E-mail: eclipsesato@gmail.com

Introduction: To perform quasi-monochromatic X-ray computed tomography (CT), we have developed several energy-dispersive CT scanners using cadmium telluride detectors. However, it is not easy to improve image quality owing to low count rates. Therefore, we have developed high-count-rate detectors using a small photomultiplier tube (PMT), a PMT, a multipixel photon counter, and short-decay-time scintillators.

In our research, major objectives are as follows: to develop a dual-energy (DE) counter using three comparators, to increase the minimum count rate after penetrating the object, to perform DE-CT for fundamental studies using a detector consisting of a cerium-doped yttrium aluminum perovskite [YAP(Ce)] and a PMT, to improve both the spatial and energy resolutions, and to obtain two different energy tomograms simultaneously at the two energy ranges. Therefore, we constructed a DE-CT scanner with two different energy selectors operated at a tube voltage of 100 kV to carry out K-edge CT using iodine (I) and gadolinium (Gd) media.

Methods: To obtain two kinds of tomograms at two different X-ray energy ranges simultaneously, we have constructed the DE X-ray photon counter with a YAP-PMT detector, three comparators, and two microcomputers (MCs). X-ray photons are detected using the YAP-PMT detector, and the event pulses produced using amplifiers are sent to three comparators simultaneously to regulate three threshold energies of 33, 50 and 55 keV. Using this counter, the energy ranges are 33-55 and 50-100 keV; the maximum energy corresponds to the tube voltage. We performed DE-CT at a tube voltage of 100 kV.

Results and Discussion: Using a 0.5-mm-diam lead pinhole, two tomograms were obtained simultaneously at two energy ranges. K-edge CT using I and Gd media was carried out utilizing the two energy ranges. At a tube voltage of 100 kV, the count rate was approximately 100 kilocounts per second (kcps), and the minimum count rate after penetrating objects in DE-CT was regulated to approximately 10 kcps by the tube current.

O-6

PRE-PROCESSING OF BREAST IMAGE FOR PERIPHERAL AREA CORRECTION

Hyemi Kim[1], Haeng-hwa Lee[1], Byungdu Jo[1], Dohyeon Kim[2], Donghoon Lee[2], Hee-Joung Kim[1,2]
Departments of [1]Radiological Science and [2]Radiation Convergence Engineering, College of Health Science, Yonsei University, Seoul, Korea.
E-mail: sisiisiii20@gmail.com

During breast image acquisition from the mammography, a compression paddle is used to make the breast thickness evenly. When the breast is compressed, the peripheral areas may not be fully compressed according to the breast thickness and composition. The inner regions of the breast are relatively thicker and denser than the peripheral areas, which can lead to overexposure to the periphery. Some images show low visibility of tissue structures in the breast peripheral areas due to the intensity change. It has a negative effect on diagnosis for breast cancer detection.
To improve image quality for analysis, we have proposed pre-processing technique based on distance transformation to enhance the visibility of peripheral areas. Since the results after image processing (segmentation, feature extraction) depend on the quality of the original image, the pre-processing is a necessary step.
As the initial step of the pre-processing, the breast region is separated from the background of the original image. In the case of MLO (Medio-lateral oblique) view image, the pectoral muscle is segmented by using the region-based segmentation method before pre-processing. Since the pectoral muscle shows a high intensity values in the image, it is removed at first and integrated after the image processing. The seeded region growing method initially specifies one seed pixel and extends the size of the region to neighboring pixels based on the intensity of the seed pixel. Also, only the pectoral muscle should be segmented by specifying the maximum distance from the seed pixel.
The peripheral areas of breast are determined by using the Otsu thresholding method to separate the peripheral and inner region based on the optimal threshold value. And the morphological processes are applied to peripheral areas to fill small holes and remove the small objects.
Before the correction of peripheral areas, the distance transform of breast region is performed by computing the distance from each pixel to the breast skin-line. This method aims to calculate the distance between each zero pixel and the nearest nonzero pixel in the binary images. For each pixel with the distance to the skin-line, the intensity of pixel is iteratively corrected by multiplying a propagation ratio. It is calculated as the ratio of the mean intensity of pixels at distances 1 and 2 steps from the furthest pixel of the peripheral areas to the skin-line. Finally, to evaluate the quality of processed images, the breast density is quantitatively calculated.
According to the results, the structure of breast tissues in the overexposed peripheral areas was well observed. By improving the intensity of the peripheral areas, we obtained a profile of uniform intensity from the inner region of breast to the skin-line. The pixel values of peripheral areas were normalized without losing information and weighted to reduce the intensity distribution variation. The histogram also showed that the low intensity parts of the peripheral areas were significantly reduced.
In addition, after applying the peripheral area correction, we applied the contrast enhancement method to calculate the breast density more accurately. Compared to the original image, the breast density calculated from the processed image obtained similar results with the actual density of breast image. These results suggest that appropriate pre-processing techniques are useful for improving image quality and more accurate density assessment.
In this study, the pre-processing technique based on distance transformation was used to overcome the problem of overexposed peripheral areas in the breast images. The results demonstrated that peripheral area correction method combined with contrast enhancement improved the visualization of the breast peripheral areas and the accuracy of the breast density assessment can be further improved.

O-7

MAMMOGRAPHY IMAGING STUDY USING SYNCHROTRONRADIATION

Reena Sharma[1], J. Shramika[1], S. D. Sharma[1,2], D. Datta[1,2]
[1]Radiological Physics and Advisory Division, Bhabha Atomic Research Center, [2]Homi Bhabha National Institute, Mumbai, Maharashtra, India.
E-mail: rmks_sharma@yahoo.com

Recent advancements of medical x-ray imaging techniques are based on differential absorption of x-ray intensity. However, the technology has its own limitation due to subject contrast in soft tissues. To overcome such limitations, an emerging technology called X-ray Phase Contrast Imaging (XPCI) algorithm has been employed in many medical imaging areas including mammography. Further XPCI has shown the potential improvement with respect to visibility contrast while examining soft tissues found within the breast. XPCI utilizes the refraction of x-rays at the boundary defined by two different density regions. This refracted and the direct waves propagate a finite distance and interfere due to a path difference to produce bright and dark fringes. This is manifested in terms of edge enhancement along the boundary of interest. Complex index of refraction is represented by $n=1-\delta-i\beta$, where δ is the refractive index decrement that is responsible for the phase shift, and β is the absorption index. Phase retrieval seems impossible with conventional x-ray sources (e.g conventional mammography x-rays) due to their low spatial coherence.
The aim of the study was to establish the suitability of XPCI for its diagnostic capability in terms of quantitative image quality parameter called contrast to noise ratio (CNR) as it plays an important role in deciding the image quality of any x-ray based imaging systems.
Present study utilizes the monochromatic 20 keV synchrotron x-ray with high degree of spatial coherence available at imaging beam line-4 (BL-4) of the synchrotron facility, Indus-II. Indus II is a 2.5 GeV, 300 mA third generation synchrotron radiation source located at Raja Ramanna Centre of Advanced Technology, Indore, India. We have carried out all the experiments using imaging camera system of Photonic Science VHR-1 which contains a 1:2 fibre-optic plate coated with Gadox Scintillator

and high resolution charged couple devices (pixels 4007 x 2678, pixel size 4.5 μm and field of view 18 mm x 12 mm).

Microcalcifications (MCs) in the breast are considered as indirect signs of pathological process and detecting these on mammograms are difficult task due to its small size which is less than 1 mm. In conventional mammography, aluminium (Al) is often used as a substitute material for calcification simulation and in the same line we have fabricated a microcalcification phantom using 'Al' with diameter of 5 mm and different thickness ranging from 50 -500 μm. These 'Al' discs were sandwiched between two polymethyl methacrylate (PMMA) sheets each having 1 mm thickness. Images of each 'Al' disc were acquired and CNR was measured for every disc using equation 1.

$$CNR = \frac{MPV_{signal} - MPV_{BKG}}{\sqrt{\frac{(SD_{signal})^2 + (SD_{BKG})^2}{2}}} \quad (1)$$

where, MPV_{signal} is the mean signal pixel value, MPV_{bkg} is the mean background pixel value, SD_{signal} is the standard deviation (SD) in the signal area, and SD_{bkg} is the standard deviations in the background area. CNR was calculated for each 'Al' disc image using Image J software (Image J -IJ 1.46).

Results of the present study show that measured CNR values for 'Al' discs with thicknesses 50, 100, 170, 400 and 500 μm are 6.24, 14.2, 21.5, 44.9, and 56.7 respectively. For 100 μm thick 'Al' disc, measured CNR values along with (PMMA) attenuator of thicknesses 1 to 8 mm are found to be 14, 13.4, 12.7, 11, 10.7, 10.4, 10.1, and 8.16 respectively. This condition was simulated to show how CNR for 100 micron 'Al' discs decreases with respect to its depth position in a soft tissue substitute material (e.g PMMA). Also edge line profile investigated for 100 μm thick 'Al' disc shows the improvement in visibility contrast at the boundary of disc under XPCI technique.

O-8

TRIPLE-ENERGY HIGH-RATE X-RAY COMPUTED TOMOGRAPHY SCANNER USING A CADMIUM TELLURIDE DETECTOR

Eiichi Sato, Yasuyuki Oda, Yuichi Sato[1], Satoshi Yamaguchi[2], Osahiko Hagiwara[3], Hiroshi Matsukiyo[3], Toshiyuki Enomoto[3], Manabu Watanabe[3], Shinya Kusachi[3]

Department of Physics, Iwate Medical University, [1]Department of Central Radiation, Iwate Medical University Hospital, [2]Department of Radiology, School of Medicine, Iwate Medical University, Morioka, [3]Department of Surgery, Toho University Ohashi Medical Center, Tokyo, Japan. E-mail: dresato@iwate-med.ac.jp

Introduction: Without pileup of the event pulses, the maximum count rate of a high-energy-resolution cadmium telluride (CdTe) detector is approximately 5 kilocounts per second (kcps). In energy-dispersive computed tomography (ED-CT), the photon count rate substantially decreases while penetrating the objects. The image quality improves with increasing minimum count rate after penetrating the object, and the incident count rate to the object should be increased with increases in the object thickness to maintain the minimum count rate for CT.

In our research, major objectives are as follows: to develop a triple-energy (TE) counter using three comparators, to keep the minimum count rate after penetrating the object, to perform TE-CT for fundamental studies using a readily available CdTe detector, and to obtain three different energy tomograms simultaneously at the three energy ranges. Therefore, we constructed a TE-CT scanner with three comparators operated at a tube voltage of 100 kV to carry out K-edge CT using iodine (I) and gadolinium (Gd) media.

Methods: To obtain three kinds of tomograms at three different X-ray energy ranges simultaneously, we have constructed a TE X-ray photon counter with a CdTe detector and three sets of comparators and microcomputers (MCs). X-ray photons are detected using the CdTe detector, and the event pulses produced using amplifiers are sent to three comparators simultaneously to regulate three threshold energies of 20, 33 and 50 keV. Using this counter, the energy ranges are 20-33, 33-50 and 50-100 keV; the maximum energy corresponds to the tube voltage. We performed TE-CT at a tube voltage of 100 kV.

Results and Discussion: Using a 0.5-mm-diam lead pinhole, three tomograms were obtained simultaneously at three energy ranges. K-edge CT using I and Gd media was carried out utilizing two energy ranges of 33-50 and 50-100 keV, respectively. At a tube voltage of 100 kV and a current of 60 A, the count rate was 15.2 kilocounts per second (kcps), and the minimum count rates after penetrating objects in TE-CT were regulated to approximately 2 kcps by the tube current.

O-9

HIGH-SENSITIVITY NEAR-INFRARED-RAY COMPUTED TOMOGRAPHY SCANNER

Yuichi Sato, Eiichi Sato[1], Yasuyuki Oda[1], Osahiko Hagiwara[2], Hiroshi Matsukiyo[2], Toshiyuki Enomoto[2], Manabu Watanabe[2], Shinya Kusachi[2]

Department of Central Radiation, School of Medicine, Iwate Medical University, [1]Department of Physics, Iwate Medical University, Morioka, [2]Department of Surgery, Toho University Ohashi Medical Center, Tokyo, Japan. E-mail: iwateidai@live.jp

Introduction: Recently, we have developed several energy-dispersive X-ray computed tomography (CT) scanners and performed K-edge imaging using iodine and gadolinium media. Using these scanners, blood vessels are observed at high contrasts. Subsequently, a 950-nm near-infrared-ray (NIR) CT scanner has been developed to observe hemoglobins in biomedical objects. However, it was difficult to penetrate the objects, since the NIRs in the living-body (LB) window range from 700 to 900 nm.

In our research, major objectives are follows: to develop an NIR-CT, to increase detection sensitivity, to produce LB-window NIRs, and to improve spatial resolutions. Therefore, we developed an 850-nm NIR-CT scanner and imaged biomedical objects.

Methods: In the NIR-CT, NIR rays are produced from a light-emitting diode (LED), and the penetrating rays are detected using an NIR phototransistor (PT) in conjunction with a long graphite collimator. The wavelengths of maximum LED intensity and high PT sensitivity are 850 and 940 nm, respectively. The photocurrents flowing through the PT are converted into voltages using an emitter-follower circuit, and the NIR sensitivity increases with increasing resistance between the emitter and the ground. The output voltages are sent to a personal computer through an analog digital converter. The projection curves for tomography are obtained by repeated linear scans and rotations of the object. The object rotates on the turn table, and the NIR scanning is conducted in both directions of its movement.

Results and Discussion: We performed NIR-CT using a set of LED and PT driven in the LB-window NIR range. The NIR photons easily penetrate a transparent object at a small incident angle, and the photons reflect around the objects at a large incident angle to the object. In addition, the photons also refracted, and only penetrating photons should be detected using a small-diam long collimator for the PT.

The pixel dimensions of the reconstructed CT image were 0.5 × 0.5 mm^2 because the scan step was 0.5 mm. However, the original spatial resolution was primarily determined by both the collimator diameter (1.0 mm) and length (10 mm), and the spatial resolutions were approximately 2 × 2 mm^2.

O-10

HIGH RESOLUTION CT LUNG PATIENT SKIN DOSE MEASUREMENT USING METAL OXIDE SEMICONDUCTOR FIELD EFFECT TRANSISTOR

A. Saravana Kumar, K. N. Govindarajan, B. Devanand[1], N. Elango[1], R. Rajakumar[1]

PSG Centre of Radiological Physics, PSG Institute of Medical Sciences Research, [1]Department of Radiology, PSG Institute of Medical Sciences Research, Coimbatore, Tamil Nadu, India.

E-mail: sarava87@gmail.com

Introduction: High-resolution computed tomography (HRCT) is computed tomography (CT) with high resolution. It is used in the diagnosis of various health problems, though most frequently for lung disease. It involves the use of special computed tomography scanning techniques to assess the lung parenchyma. The advent of MDCT has resulted in improved spatial resolution and faster scans acquisitions. Consequently, MDCT has become a more widely used diagnostic procedure, responsible for a greater proportion of medical Radiation exposure to patients. Although CT represents 11% of all radiographic examinations, it accounts for 67% of medically induced radiation exposure. A judicial practice of CT procedure has to be ensured for patient's safety. An understanding of patient CT radiation doses requires the assessment of organ and effective dose in patients undergoing CT procedures. The universal method for measuring organ and effective radiation doses is dose estimate from the CTDI or DLP, which is both used as readily accessible dose indicators of radiation dose in CT procedures. In this research study, patient skin dose were measured and compared with the console $CTDI_v$. Using these values, correlation can be found between CTDI vol and skin dose, the later can be used to infer the order of CTDIvol values.

Objective: The objective of our study was to measure radiation skin dose during HRCT lung using a novel dosimeter system and compared with the displayed console value.

Materials and Methods: A solid-state metal oxide semiconductor field effect transistor (MOSFET) was used to obtain real-time skin dose for HRCT lung procedures in 128 slice Siemens Somatom definition edge scanner. 50 HRCT lung cases have been selected, then two Mosfet sensors namely S1D and S2D were used and both have been placed on the patient with different points without affecting examination.

Results and Discussion: The console CT dose indices have been noted and the range and mean value of CTDIv is 4.8 mGy to 12.7 mGy, and 10.22 mGy respectively. The dose response to the Mosfet probes to exposure ranging and mean values are 2.51 cGy to 8.54 cGy, 4.8 cGy for S1D, and 2.83 cGy to 9.21 cGy, 4.7 cGy for S2D respectively. The sample measured data have been presented in Table 1. From this result, we observed that there is correlation between the measured CT skin doses and theoretically calculated console value.

Conclusion: On whole, this research work gives the substantial overview of HRCT lung practice in our hospital. From this study, it is recommended that it is very essential to justify CT procedures in advance and once the choice for CT scan is taken, it is compulsory to adopt the ALARA and dose reduction principle strictly. MOSFET technology can be used for protocol development in the rapidly changing MDCT scanner environment in which organ dose data are extremely limited. The data of such study is essential so as to reduce the time considerably for optimization of machine output and average patient doses.

Table 1: Comparison of console computed tomography dose index volume and measured skin dose using metal oxide semiconductor field effect transistor technology

Procedure	*kV*	*Total mAs*	*Pitch*	*Tube rotation time (s)*	*Exposure time (s)*	*Total $CTDI_v$ (mGy)*	*Mean skin dose (cGy)*	*Correlation factor*
HRCT lungs	120	1230	1.2	0.55	12.26	9.34	4.57	0.20
HRCT lungs	120	1818	1.2	0.28	5.27	12.71	4.66	0.27
HRCT lungs	120	583	1.2	0.28	5.67	4.86	2.43	0.20
HRCT lungs	120	890	1.2	0.28	8.33	5.64	2.67	0.21
HRCT lungs	120	1327	1.2	0.28	13.76	10.78	4.65	0.23
HRCT lungs	120	1822	1.2	0.28	12.99	11.13	5.41	0.20
HRCT lungs	120	1216	1.2	0.28	13.14	7.5	3.21	0.23
HRCT lungs	120	1846	1.2	0.28	12.91	10.54	4.71	0.22
HRCT lungs	120	1189	1.2	0.28	13.14	11.22	5.57	0.20
HRCT lungs	120	842	1.2	0.28	12.54	11.98	5.80	0.20

$CTDI_v$: Computed tomography dose index volume, HRCT: High-resolution computed tomography

O-11

KNOWLEDGE BASED PLANNING FOR STEREOTACTIC RADIOSURGERY: STANDARDISATION OF VOLUMETRIC MODULATED ARC THERAPY BASED FRAMELESS STEREOTACTIC TECHNIQUE USING A MULTIDIMENSIONAL ENSEMBLE MAPPING

Sarkar Biplab, Ganesh Tharmar, Satheeshkumar Anbazhagan, Kaur Harpreet, Jassal Kanan, Giri Upendra Kumar, R. Sashikumar, Saneg Kirshnankutty, S. P. Jeen, Munshi Anushhel, Mohanti Bidhu Kalyan

Department of Radiation Oncology, Fortis Memorial Research Institute, Gurgaon, Haryana, India.
E-mail: biplabphy@gmail.com

Aim: Knowledge based planning (KBP) is an emerging technique in a radiation therapy planning. It helps to standardise the radiotherapy planning as variations in knowledge and experience of the planner can lead to large differences in the quality of radiation therapy treatment plans. This may compromise the gains achieved through modern technologies such as IMRT or VMAT. This study is attributed to standardisation of brain SRS/SRT plans in our institution. The aim of this study is standardisation of the treatment plans by minimization of the influence of individual's skill and knowledge, based on a very large library of treatment plans. Further effort will be made to reduce the planning time.

Materials and Methods: 171 SRS/SRT patients treated in our clinic were considered in this study. An ensemble library was established using first 120 patients, further the KBP algorithm was validated for 29 library patients and tested for 51 new patients. Ensemble library was categorised against 8 different parameters (1) PTV dose coverage challenged by presence of organ at risk (OAR) or not (2) Prescription dose (3) Number of PTVs (4) laterality (left/right) (5) tumour volume (6) shortest distance between OAR and PTV (7) centre to centre distance between OARs and PTV (8) lateral dimension of external contour (brain). Further, on arrival of a new patient most appropriate library plan was chosen on the basis of above categorisation using an ensemble mapping technique. Further for new patient knowledge based planning (KBP) was created by associating most appropriate library plan with all parameters unchanged to the default isocentre. Optimization and dose calculation was carried out in MONACO with no or very minimal changes in the optimization constrain and arc length. Another independent treatment plan (IP) was generated by an experience medical physicist for comparison. IP and KBP were evaluated for PTV dose coverage (V98%), Paddick conformity index (PCI), dose spillage of (volume of 50% and 20% isodose lines; I50%, I20%) and OAR doses.

Result: For 43.3% (52 out of 120) patients it was observed that PTV dose was not challenged by the presence of any OAR. Validation result for ensemble mapping technique shows that for an OAR challenged PTV dose patient it is appropriately picking up the library plan. Independent plan (IP) was better than the knowledge based plans (KBP) in PTV coverage and dose conformity. PTV volume receiving 98% prescription dose (V98%) was 98.7 ± 1.1% and 97.5 ± 1.3% for IP and KBP respectively. For OAR challenged PTV's conformity was slightly high in IP (0.712) than KB plans (0.693). PTV V98% and PCI were not statistically different between two sets. If collimator angle optimization is not done for the OAR unchallenged cases PTV conformity is higher than KBP in IP and variation was statistically significant ($p<0.04$). Collimator angle optimization equalise the Conformity between IP and KBP. For the largest prescription dose group (12Gy in 1#, 64 patients) brainstem 0.5 cc Volume exhibit a mean dose of 873.1 ± 134.2 cGy and 854.5 ± 122.4 cGy for IP and KBP respectively. All other OAR doses were comparable between IP and KBP. MU difference was very nominal with IP shows a mean excess MU of 67.3 (3.7%) over KBP. IP requires on average 3.5 optimization/dose calculation which is about 3.5-5 hrs, where KBP does not require more than 1.5 runs (1.5-2) hrs.

Conclusion: KBP plans validation result indicate multidimensional ensemble mapping mechanism can pick up the library plan accurately. KBP plans, although marginally inferior in the dosimetric quality, they fulfil all the required clinical condition and dose constraints. KBP plans save a considerable planning time and almost independent of the treatment planner skill and knowledge. KBP works well with Monte Carlo planning system like MONACO.

O-12

MONTE CARLO MODELLING OF INDIGENOUSLY DEVELOPED MEDICAL LINEAR ACCELERATOR

P. K. Dixit, Subhalaxmi Mishra[1], T. Palani Selvam[1], Sanket S. Yavalkar[2], D. D. Deshpande[3]

Radiological Safety Division, Atomic Energy Regulatory Board, [1]Radiological Physics and Advisory Division, Bhabha Atomic Research Centre, [2]Department of Technology Innovation, Society for Applied Microwave Electronics Engineering and Research, [3]Department of Medical Physics, Tata Memorial Hospital, Mumbai, Maharashtra, India. E-mail: dixit.pk@gmail.com

Introduction and Objective: The objective of the present study is to simulate the 6 MV LINAC (model Siddharth), indigenously developed by SAMEER (Society for Applied Microwave Electronics Engineering and Research) using the

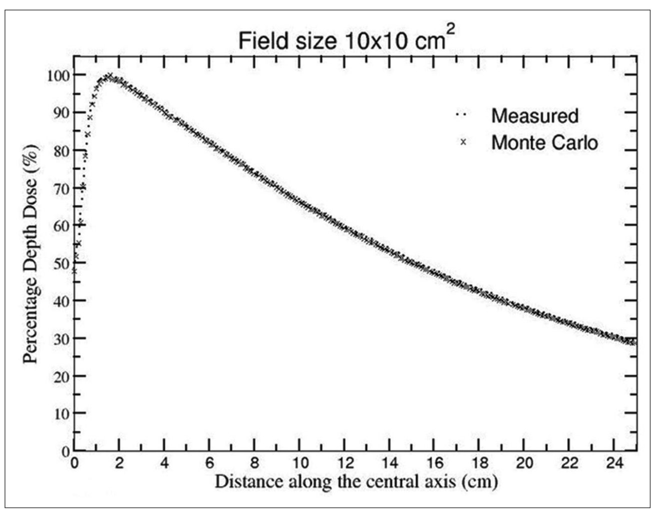

Figure 1: Comparison of measured and Monte Carlo calculated Percentage Depth Dose (%) variation with distance along the central axis for Field size of 10 x 10 cm²

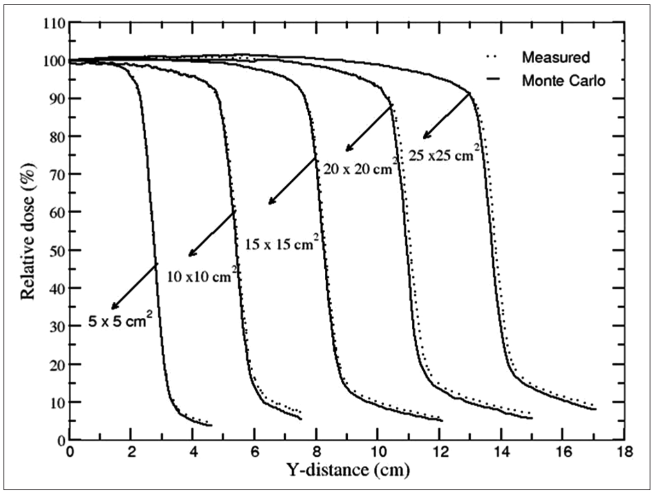

Figure 2: Comparison of measured and Monte Carlo calculated Relative dose variation with Y-distance for Field size of ranging from 5 x 5 cm^2 to 25 x 25 cm^2

BEAMnrc user-code of the EGSnrc Monte Carlo Code system. This study also includes identification of initial electron parameters and comparison of calculated dose distributions with the measured data.

Materials and Methods: Different components of the LINAC such as target, primary collimator, flattening filter, monitor chamber, mirror, and secondary collimator were modelled using the BEAMnrc user-code as per the technical design data provided by the manufacturer. In order to identify the initial electron parameters, phase space data at Source-to-Surface Distance (SSD) of 100 cm for the field size of 10 x 10 cm^2 was scored for different initial electron parameters. Using the phase space data, lateral dose distribution at 10 cm depth in a water phantom of dimensions 50 x 50 x 50 cm^3 was calculated using the DOSXYZnrc user-code. The investigation revealed that dose distribution corresponding to the initial electron energy 6.2 MeV with a Gaussian spread (FWHM of 1 mm) matched with the measured data. Further simulations involving various filed sizes (5 x 5 cm^2 – 25 x 25 cm^2) utilized the above electron parameters. Dose measurements in water phantom were carried out by PTW MP3 Water Scanning System and ionization chamber (Semiflex 0.125 cm^3). These measurements were performed with 1 mm resolution for both PDD curves and beam profiles.

Result and Discussion: The depth and lateral dose distributions for all the investigated field sizes agree to the measured data as well as with international reference data within about 2%. PDD for field size 10 x 10 cm^2 is shown Figure 1. Penumbra, field sizes, beam flatness and beam symmetry are found to be within the tolerance values. The calculated and the measured dose profiles for different field sizes are shown in Figure 2. The study suggests that Monte Carlo model of the Siddharth LINAC is accurate.

O-13

IMPACT OF PRECLINICAL PET GEOMETRICAL ARRANGEMENT ON PERFORMANCE PARAMETERS

Kajal Aggarwal, Fredéric Boisson, David Brasse

Hubert Curien Pluridisciplinary Institute, University of Strasbourg, Strasbourg, France.
E-mail: kajal792@gmail.com

Introduction: Preclinical Positron Emission Tomography (PET) is a nuclear imaging modality used to image animal models of human disease. Several groups proposed different geometrical arrangements, to push current limits of spatial resolution and system detection efficiency. Due to the different design choices each configuration has its own advantages and limitations.
While pixelated scintillators provide an advantage of improved spatial resolution, the depth of the crystal creates an imbalance between the detection efficiency and the spatial resolution. This arrangement leads to parallax error due to radially longer crystals, thus degrading the spatial resolution. This tradeoff can be overcome by introducing multi layers of crystals coupled in the radial direction. A geometrical arrangement having axially oriented pixelated crystals is also a promising concept to avoid parallax error. Similarly, other geometrical arrangements such as scanners with monolithic crystal slabs have their own benefits and drawbacks.

Objective: The objective of this study is to investigate the impact of four different preclinical PET scanner geometries using the figure of merit proposed by the National Electrical Manufacturers Association (NEMA) NU 4 - 2008 standards through Monte-Carlo simulations.

Materials and Methods: We propose to investigate four different geometries including a), pixelated crystal matrix coupled to Silicon Photomultiplier (SiPM) detector, b), dual layer of crystal matrices, c), crystal axially oriented with dual side readout and d), monolithic crystal slabs. The transverse field of views of the four systems are ranging from 5 to 6 cm according to the arrangement of the different PET modules. The average axial extent is set to 10 cm to cover the whole body of a mouse.

Result and Discussion: The figures of merit investigated according to NEMA procedure include scatter event rate, Noise Equivalent Count Rate (NECR), detection efficiency and spatial resolution. The preliminary results obtained using the GATE simulation platform show that the axial PET arrangement has the highest sensitivity along with higher NECR values, followed by dual layer arrangement and scanner employing monolithic scintillator, as predicted theoretically.
Those results will be compared to a state of the art preclinical scanner installed in our facility.

O-14

DEVELOPMENT OF F18-FDG PET/CT DATABASE OF LUNG MASSES FOR IMAGING RESEARCH

Mukesh Kumar, A. K. Pandey, Kartik Saroha, C. S. Bal, Rakesh Kumar

Department of Nuclear Medicine, AIIMS, New Delhi, India. E-mail: mukeshaiims2012@gmail.com

Introduction: Image processing algorithms have potential to assist in lesion (e.g. nodule) detection on PET/CT studies and to assess the stability or change in size of lesion on serial PET/CT studies. Comparison and evaluation of image processing techniques against each other require common data sets and standardized methods for evaluation. Creating a computer based tumor classifier system that can classify malignant versus benign lungs mass, inflammation versus malignancy, and responder versus non-responder to chemotherapy based on lungs PET/CT images can be of immense value. In order to validate the accuracy of such classifier we need large image database of the patients.

Objectives: The aim of this study was to develop the F18-FDG PET/CT images database of lung masses for imaging research.

Materials and Methods: Two hundred sixty four lungs cancer patients who underwent F18-FDG PET/CT scan from November 2015 to December 2016 for detection of early treatment response, for measurement of response to neo-adjuvant chemotherapy, chemo-radiotherapy or novel biologic therapies were included in this study. Their general information (patient's history, gender, age, no of Chemo/RT, identification number, final report issued by our department) and clinical history, biopsy reports of the lungs mass if available were recorded. Whole body F18-FDG PET/CT scans of all 264 selected patients (250 patients having lung cancer and 14 patients having normal lungs) were exported in DICOM format.

The PET and CT image series of all patients were reviewed in MeVisLab. The PET/CT fused axial section image which shows the maximum dimension of lung tumor was selected as representative image of lung mass of the patient. These images were also included in the database so that this database can be used as clinical teaching tool for postgraduate students.

The database was developed using Microsoft Access on Windows 7 Home Basic Copyright © 2009 Microsoft Corporation and Microsoft Access installed on the processor Intel® Core™ i3-2120 CPU @ 3.30 GHz, 2.0GB RAM and 64-bit operating system on the computer (Hewlett-Packard Company).

Results and Discussion: The database has information of 264 patients (adenocarcinoma: 34 %, NSCLC: 9%, SCC: 27%, and normal lungs: 5%) and some other details are given in Table 1. The demographic information, clinical history, lungs PET and CT images of each patient can be accessed with the help of mouse and push buttons available on the user interface of the database [Figure 1]. This image database can be used for standardization, evaluation and comparison of many digital image processing methods such as image enhancement, image registration, image fusion, and texture analysis etc. This image database can also be used as for teaching postgraduate students as it consists of the PET/CT images of different types of lung cancer at one place. Three types of PET/CT lung mass (Adenocarcinoma, NSCLC and SCC) and PET/CT normal lungs images can be accessed through this database for demonstration during the lecture. For example, a list of all PET/CT images of adenocarcinoma can be accessed and displayed to explain to the postgraduate students regarding the spatial pattern of the tumor appearance on the PET/CT images. Our future plan is to determine the size of the tumor on PET/CT images, and assign a label to each image based on the location, size, and stage of the disease. This will make the image database more valuable while teaching postgraduate nuclear medicine students.

Table 1: Patient demographic and clinical characteristics

Patient characteristics	*Value (%)*
Sex	
Male	203 (76.89)
Female	61 (23.10)
Histology	
Adenocarcinoma	90 (34.09)
NSCLC	23 (8.71)
SCLC	72 (27.27)
Not specified*	64 (24.24)
Fibrocarcinoma	1 (0.38)
Prechemo/RT	
For staging	71 (26.89)
Initial diagnosis	46 (17.42)
Postchemo	
Response evaluation	133 (50.38)
Normal lungs patients	14 (5.30)
Total number of patients in database	264

*64 patients have lung mass but not proven by Biopsy. NSCLC: Nonsmall-cell lung cancer, SCLC: Small cell lung cancer, RT: Radiotherapy

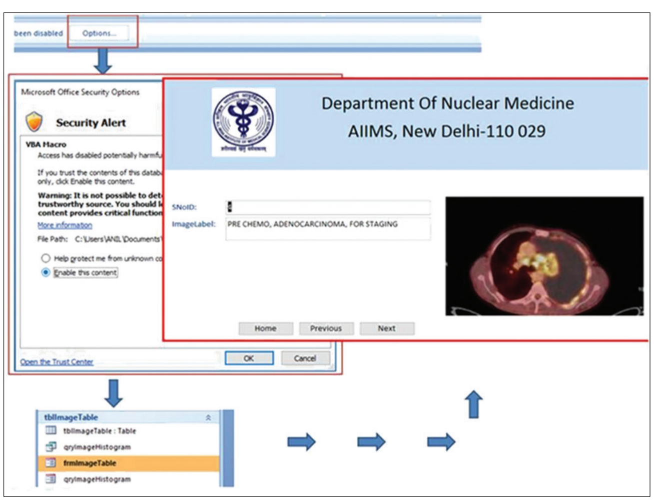

Figure 1: When user press Option button then Microsoft office Security Options appears. Now user can select to enable the content and then select *frmImageTable* to view the PET/CT images. *frmImagesTable* have command button for navigation (Home, Previous and Next)

O-15

OPTIMISATION OF THE MOVING AVERAGE FILTER PARAMETER FOR PROCESSING ^{99M}TC-MDP-BONE SCAN IMAGE

Anil Kumar Pandey, Chandan Singh Bisht, Averilicia Passah, Ravi Kant Gupta, Chetan Patel, Chandrashekhar Bal, Rakesh Kumar

Department of Nuclear Medicine, All India Institute of Medical sciences, New Delhi, India.
E-mail: bisht.chandan42@gmail.com

Introduction: ^{99m}Tc- Methylene diphosphonate (MDP) bone scan is corrupted with noise during image acquisition. Moving average filter can recover the original image signal from its noise-corrupted version. However, the user needs an optimized value of window size to obtain the best result. In this study we have optimised the value of window size for 99mTc-Methylene diphosphonate bone scan for best possible image quality.

Objective: The aim of the study was to find the optimum value of window size for mean filter to be applied on ^{99m}Tc-MDP bone scan for best possible image quality.

Materials and Methods: Seventy six ^{99m}Tc- MDP whole body bone scan (32 normal and 44 abnormal, total counts: 739,000 to 1783, 855 per image) images were included in this study. A *matlab* script was written to process these images using moving average filter with window sizes 3, 5, 7, 9, 11, 13 and 15 pixel widths. The experiment was conducted on personal computer having a 3.30 GHz i3-2120 CPU, 2 GB RAM memory, and 64-bit Windows operating system. The image quality of processed images (N = 456) were evaluated subjectively by two nuclear medicine physician to select the best image.

Results and Discussion: Nuclear medicine physicians preferred original images 73.61% times, and processed image with window size 3-pixel widths 26.39% times. Approximately 26% of whole body ^{99m}Tc- MDP bone scans required noise removal operation, and in those cases, the optimized window size of moving average filter for processing ^{99m}Tc- MDP bone scans was found to be 3-pixel widths.

O-16

RADIATION DOSE FROM ^{18}F-FDG PET/CT PROCEDURES: INFLUENCE OF SPECIFIC CT MODEL AND PROTOCOLS

Oluwabamise Adeleye, Naven Chetty

School of Chemistry and Physics, University of KwaZulu-Natal, Pietermaritzburg, South Africa. E-mail: hadebam001@gmail.com

Integrated PET/CT imaging has proven to be a valuable tool for the diagnosis, staging, and monitoring of therapy response of a broad range of malignancies due to the combined metabolic and morphological information provided. The increasing use of this imaging modality in the management of tubercular lesions has raised concerns regarding the associated radiation exposure, because of the additional exposure from CT acquisition with the internally administered radiopharmaceuticals. This work aimed to study the effects of CT model and study protocols on the overall radiation dose from a PET/CT scan.

Two PET/CT systems and five CT exposure protocols routinely applied for clinical patients in PET/CT imaging were retrospectively evaluated. CT doses were calculated using the CT-Expo dosimetry software, while doses from the PET component were estimated applying the International Commission on Radiological Protection (ICRP) 106 dose coefficients. Effective dose was calculated using the ICRP 103 and for comparison the ICRP 60 tissue weighting factors. The total effective dose for each system was compared in terms of percentages and the difference in CT component contribution to the total dose for all protocols were determined using two-sample t-test with $p < 0.05$ considered as significant.

Effective dose ranged from 8.0-24.05 mSv for the system I and 8.35-26.85 mSv for system II, resulting in differences of 4.3%-15% for the Low-dose scan and 4.1%-11% for standard dose scans. The contribution of CT component to the total dose was between 32-77% for the system I and 35-79% for system II; however, the contributions were not significantly different ($p > 0.05$) for all protocols.

Although the overall radiation dose was similar with both types of system, the observed variation in CT contribution represents a requisite pedestal on the need for a nation-wide dose assessment for further optimization of the imaging procedure to maximize benefit to patients.

O-17

ANALYSIS OF THERAPEUTIC EFFECTIVENESS BY GENERATION OF THREE ALPHA PARTICLES IN PROTON-BORON FUSION REACTION BASED ON MONTE CARLO SIMULATION CODE

Sunmi Kim, Han-Back Shin, Moo-Sub Kim, Do-Kun Yoon, Tae Suk Suh

Department of Biomedical Engineering, College of Medicine, Research Institute of Biomedical Engineering, Catholic University of Korea, Seoul, Korea. E-mail: sunmikim@catholic.ac.kr

Introduction: In previous reports, proton-boron fusion therapy (PBFT) induces tumor cell death through three alpha particles of triggered by one proton based on proton-boron fusion reaction. A major advantage of proton irradiation is a characteristic distribution of dose with depth. The dose deposited increases at first very slowly with depth and then very sharply near the end of a range, before dropping to almost zero. Protons deposit energy far more selectively than X-rays, improving long-term local control of the tumor, lower probability of damage to healthy tissue, low risk of complications, and the chance for rapid recovery after therapy. Theoretically, PBFT is a novel and desirable therapy for malignant tumors with advantages over conventional proton therapy and boron-neutron capture therapy (BNCT). In the case of BNCT, after the compound containing boron is accumulated at the tumor site, only one alpha particle resulting from the reaction between the epi-thermal neutron and the boron causes tumor cell death. If it could be matched the deposition of three alpha particles in the tumor regions and the proton's maximum dose point (Bragg peak), the therapy results can be more effective than in BNCT. However, a more quantitative evaluation for PBFT is needed for clinical application.

Objectives: The purpose of this research is to analysis the effectiveness by generation of three alpha particles in proton-boron fusion therapy (PBFT) based on a Monte Carlo simulation code.

Materials and Methods: Dosimetry using Monte Carlo simulation is a suitable technique to describe the energy deposition by alpha particle. A proton beam relevant to Bragg-peak was simulated using a Monte Carlo simulation code. After computed tomography (CT) scanning of a virtual water phantom including air cavities, the acquired CT images were converted as the simulation source code. We set boron uptake regions (BURs) in the simulated water phantom to achieve proton-boron fusion reaction. A rectangular 20(W) × 20(D) × 8.5(H) cm^3 water phantom (Water region density: 1 g/cm^3) with air cavities was used. The 1 phantom was comprised of two air cavities, each with a different size (2 × 20 × 2 cm^3, 4 × 20 × 4 cm^3) and location (6 cm, 11 cm away from the phantom surface). The proton emission in the simulation was directed toward the phantom. On the simulations, a boron concentration in the tumor and the adjacent healthy tissue to the tumor were incorporated to the virtual phantom, resulting in a concentration ratio of healthy tissue:tumor of 1:5. This ratio is approximately the concentration ratio found in some pharmacokinectic experimental studies of boron carries, mainly for the boronophenylalanine compound, known as BPA-fructose.

Results and Discussion: Results show clearly that three alpha particles affected the energy deposition. Thus, high therapy efficiency can be achieved by using smaller flux than that of conventional proton therapy or BNCT. We exploited the p + 11B $\rightarrow 3\alpha$ reaction to generate high-LET alpha particles with a proton beam. The results described the intrinsic strong points of PBFT. Although additional study needs to further verify the effectiveness of PBFT, we confirmed the greater therapeutic effectiveness of proton boron fusion reaction by generation of alpha particles over either conventional proton therapy or BNCT. We will proceed with further study on verification and quantification to move towards implementation of clinical treatment.

O-18

COMMISSIONING AND VALIDATION OF COMMERCIAL DEFORMABLE IMAGE REGISTRATION SOFTWARE

Jamema Swamidas, Reena Phurailatpam, Siji N. Paul, Kishore Joshi, D. D. Deshpande[1]

Department of Radiation Oncology, Advanced Centre for Treatment Research and Education in Cancer, [1]Department of Medical Physics, Tata Memorial Centre, Mumbai, Maharashtra, India.
E-mail: svjamema@gmail.com

Introduction: Validation/commissioning of Deformable Image Registration (DIR) is complex and still evolving. The objective of this study is to report the results of the validation tests carried out as part of commissioning of the commercially procured DIR algorithm before clinical implementation for adaptive contouring.

Materials and Methods: The DIR software tested was SmartAdapt® in Eclipse™ treatment planning system v13.6 (Varian Medical Systems Inc., Palo Alto, CA). The tests were carried out using physical and virtual phantoms in addition to the clinical test images. Physical Phantoms: Five phantoms made in-house with various known deformations with landmark points were used. The known deformations were ranged from simple to complex as shown in Figure 1. Contours were delineated for each phantom set which were propagated to the registered images. Synthetic/virtual phantoms: A set of 10 virtual phantoms were used (https://sites.google.com/site/dirphantoms/virtual-phantom-download). For each phantom, the magnitude of displacement in lateral, AP and SI direction were evaluated for various organs such as brainstem, spinal cord, mandible, parotids and external contours were compared with the ground truth. The results were obtained by comparing the DVF of the specified ROI to the ground-truth DVF. Clinical images for contour propagation: Four clinical sites namely, brain (n=5), HN (n=9), cervix (n=18) and prostate (23) patients were validated. A planning CT and a subsequent CT taken after 2-3 weeks (CT/CBCT), were considered retrospectively. OARs were manually delineated by a radiation oncologist (RO), followed by DIR and propagation of contours, which were compared with the RO drawn contours. Evaluation: Dice similarity co-efficient (DSC), shift in centre of mass (COM) and Hausdorff distances $Hf_{95\%}$ and Hf_{avg} were evaluated (3D slicer v 4.5.0.1).

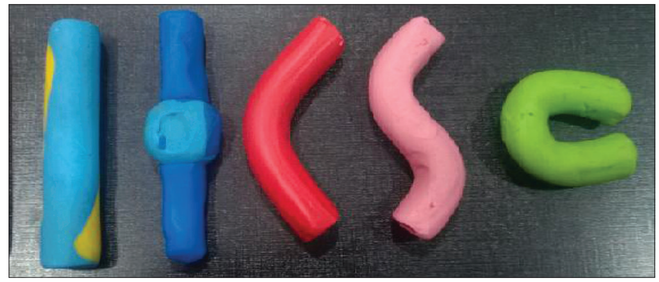

Figure 1: Physical phantoms-Clay model of different shapes

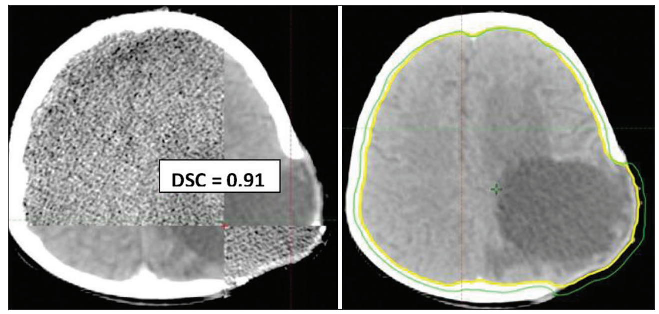

Figure 2: CBCT registered with CT of a brain cancer patient with post operative edema. Green: DIR generated contour, Yellow: RO drawn contour

Result: Physical phantoms: Mean (SD) DSC, $Hf_{95\%}$ (mm), Hf_{avg} (mm) and COM of all the phantoms 1-5 were, 0.84 (0.2), 5.1 (7.4) mm, 1.6 (2.2) mm, 1.6 (0.2) mm respectively. Phantom 5 had the largest deformation as compared to phantom 1-4, and hence had resulted in suboptimal indices, 0.5 (0.8) vs 0.9 (0.03), 18.3 (3.5) vs 1.8 (0.4), 5.7 (1.2) vs 0.64 (0.1) and 14.2 (1.8) vs 0.83 (0.3) mm.

Virtual phantoms: Several commercial DIR algorithms were investigated in this project, and our results (Institution -18) were consistent for all the ROIs. More specifically, our results were in good agreement with that of the institution -9 which also had used a similar algorithm as ours.

Clinical images: The contours propagated for brain patients resulted in a high DSC score (0.91 (0.04)) as shown in Figure 2, as compared to other sites (HN: 0.84, prostate: 0.81 and cervix 0.77). A similar trend was seen in other indices too.

In HN, the DSC was in the range of 0.81-0.87, with mandible scoring the highest with 0.87 (0.03). The less deformed structures like eyes and thyroid scored a mean (SD) DSC of 0.84 (0.06) as compared to parotids with relatively large deformations scoring 0.81 (0.03).

In cervix and prostate, DIR resulted in better results, when the small bladder was registered with large bladder and not vice versa. In other words the expansion of the bladder was handled well by DIR than the shrinkage. When the change in the bladder volume was about 50-150cc, the propagated contours were acceptable, however when the change in the bladder volume is of the order of 200-300cc, the contour propagation was unacceptable. Unlike bladder, rectum is more complex due to the presence of gas pocket and the complexity in shape.

Conclusion: DIR algorithm investigated works well in sites such as brain, HN, prostate and cervix for adaptive contouring purpose. However, the accuracy of the propagated contours is limited for some situations involving complex deformations that include large change in the volume of bladder, shape change in recto-sigmoid. Visual validation of the propagated contours is recommended for clinical implementation.

O-19

DEVELOPMENT OF REAL TIME ON-LINE QUALITY ASSURANCE DEVICE FOR AFTERLOADING HDR BRACHYTHERAPY

S. Senthilkumar

Department of Radiotherapy, Madurai Medical College, Govt. Rajaji Hospital, Madurai, Tamil Nadu, India. E-mail: senthilgh@gmail.com

Introduction: Accurate delivery of dose in HDR brachytherapy depends on the positioning accuracy of the Ir-192 source at the proper dwell position inside the applicator. Incorrect implementation of either of these parameters can potentially lead to insufficient tumour control and high dose being delivered to the incorrect treatment volume. Consequently, accurate positioning verification of the HDR source is a fundamental part of quality assurance (QA) procedure. A number of methods have been used to check the positional accuracy like mechanical rulers, autoradiography and video cameras. However, these methods are time consuming for a routine QA program and they cannot furnish information on the actual source locations, So these techniques may not enough to verify the accuracy of the HDR source position. I have developed a new real time On-line quality assurance device for testing and verification of source positioning and dwell time for HDR brachytherapy.

Objective: The objective of this study was to develop in-house software based real time On-line quality assurance device that can autonomously perform the source positioning and dwell time of HDR brachytherapy.

Materials and Methods: The in-house HDR QA device consisted of light tight box, PMMA block, a fluorescent screen, a webcamera and in-house software. The webcamera was placed on the top of the light tight box. The HDR source transferring tube was connected in the bottom of the light tight box. Ir-192 source would be loaded was put on the fluorescent screen and a sheet of PMMA was placed below the fluorescent screen. When the Ir-192 radioactive source moving on the fluorescent screen the gamma photons converted into light photon by the fluorescent screen. The visible lights indicates the real time positioning of the source. The visible light signal was recorded by the web camera, which was placed in the top of the light tight box. The web camera video signals was fed into a computer in-house software. In the software automatically calculate to determine the distance between successive dwell positions. Step intervals ranging from 5mm to 25mm were set while 5mm interval. The differences between two dwell positions were compared with the assigned values. For timing measurements, individual images from the video signal were similarly processed to identify the location of the source. Source actual dwell time was calculated from number of images, which indicated the source at the corresponding position. The total transit time was measured by subtracting source stationary time from total dwell time. Simultaneously Gafchromic EBT film autoradiography was also used for comparing the positioning accuracy.

Results and Discussion: In source positioning accuracy test, for assigned intervals of 5mm, 10mm, 15mm, 20mm and 25mm, average measured interval by the in-house software were 4.9mm, 9.9mm,14.9mm, 19.9mm and 24.5mm respectively. The result from autoradiography was also compared. The system achieved a time resolution of 10 ms and determined the dwell time to be 1.05 sec, with a standard deviation of 0.03 sec. The system was able to successfully perform positioning and timing QA measurements automatically and the movement of the source can be seen in the computer screen in the control console area during the procedure. It can provide fast and precise positional verification of a treatment plan. Advantages of our technique is its fast and precise positional verification, ability to visually check source treatment for safety checks and eliminating confusion distance between physical end of the catheter and center of the source. We can have the softcopy & hardcopy results for the further evaluation and comparison.

O-20

DOSIMETRIC IMPACT OF TWO METHODS OF POINT A DEFINITION IN HIGH DOSE RATE INTRACAVITARY BRACHYTHERAPY FOR CERVICAL CANCERS

Arpana Siwach, Shivakumar Gudi[1], Kevezo Zango Chuzho, Yogesh Ghadi, Jamema Swamidas, D. D. Deshpande, Umesh Mahantshetty[1]

Departments of Medical Physics and [1]Radiation Oncology, Tata Memorial Centre, Mumbai, Maharashtra, India. E-mail: siwach.arpana@gmail.com

Introduction: Intracavitary brachytherapy is an integral component of curative treatment for locally advanced cervical cancers. For many decades point A has been the surrogate for target definition and dose prescription in cervical brachytherapy and its still the most widely used method. Because of the geometric uncertainties related to the point A defined by the Manchester System (1953), some modifications to the definition has been suggested by American Brachytherapy Society (ABS) in 2011, which is adopted by the recently published ICRU 89 (2016). The dosimetric impact of such modifications needs to be evaluated.

Purpose: To investigate the dosimetric variations between two different methods of Point A definition and the impact of such variations on the ICRU surrogate points for rectum and bladder as well as 3D Dose volume parameters of these structures.

Materials and Methods: Twenty one patients who underwent CT based HDR Intracavitary brachytherapy using the standard stainless steel or CT/MR compatible Fletcher-Suit applicators (Nucletron- Elekta, Netherlands) were included in the study. Treatment planning was done using the “Oncentra” treatment planning system (version 4.3, Elekta) which works on TG43 calculation algorithm. Two treatment plans were generated each normalized to point A as per two different definitions: (i) The Revised Manchester point A which is defined 2 cm superior to the flange (surrogate for the external cervical os) and 2 cm lateral from the center of tandem and (ii) ABS /ICRU-89 point A definition which defines the point A from the midpoint of line joining the center of ovoid channels and then superiorly (R+2) cm along the tandem, where R is the radius of the ovoid and 2 cm lateral to it. Standard loading pattern was used for both the plans. Doses to point A in both the plans, ICRU Bladder and rectal points and 3D dose volume parameters 2cc for bladder and rectum were documented and compared using paired t test.

Results and Discussions: The plans normalized to point A defined according to the ICRU89/ABS recommendations, recorded higher doses at the point A defined by the Manchester system, bladder and rectal dose parameters. The mean differences standard deviations between the doses recorded at right and left Point A in two plans were 11.1 11.4 cGy ($p<0.005$) and 10.7 11.1cGy ($p<0.005$) respectively. Similarly the mean dose differences to ICRU Bladder point, ICRU Rectum point, Bladder 2cc and Rectum 2cc were 6.1 7.7cGy ($p=0.002$), 6.6 7.4 cGy ($p=0.001$), 9.7 10.1cGy ($p=0.000$) and 6.2 6.9 cGy ($p=0.001$) respectively. Also, the volume receiving prescribed dose and Total Reference Air Kerma (TRAK) values were higher (2.3% and 1.6% respectively) in the plans normalized to point A as defined by the ABS.

The results of the study demonstrated small but statistically significant differences in dosimetric parameters between the plans generated as per two definitions of point A when current commercially available Fletcher-Suit applicators were used. These differences appear to be small and unlikely to have clinical impact, however, this needs to be validated in different patient cohort and other applicator types.

O-21

A SIMPLE NOVEL TECHNIQUE FOR RING APPLICATOR CATHETER RECONSTRUCTION ON CT AND MRI 3D IMAGE BASED BRACHYTHERAPY PLANNING FOR CERVICAL CANCER

Devaraju Sampathirao, S. V. Jamema, Yogesh G. Ghadi, Umesh Mahantshetty, Deepak Deshpande

Department of Radiation Oncology and Medical Physics, Tata Memorial Hospital, Parel, Mumbai, Maharashtra, India. E-mail: devaraju.sr@gmail.com

Background and Objective: Catheter reconstruction is a vital step in the BT planning process. This has been further challenged by successful implementation of CT/MR Image based BT in cervical cancer. MR compatible applicators catheter reconstruction is complex and based on water dummies. The annulation and orientation of the ring applicator poses a major challenge for reconstruction. With an aim to make the reconstruction simpler, yet accurate, we undertook this study and form the basis of this abstract.

Materials and Methods: CT/MR compatible ring applicator (Make: Nucletron, Model: 101.036, Ring Tube) of 26 mm diameter used. After defining the origin along the axis of the tandem and surface of the ring, central tandem reconstruction was done by selecting index number 3 (TPS: Oncentra, v4.3). Loading of the active dwell positions in central tandem was done and in the transverse orientation (view) the isodose line passing through the dummy at the level of the ring was utilized to perform the manual ring catheter reconstruction. The reconstruction performed by this method was verified using the auto radiograph and compared with the dwell positions obtained during applicator commissioning.

Results and Discussion: It was observed that the planned and delivered active dwell positions within the tolerance of +1 mm. The novel technique described above was faster and less error prone. This is a time efficient method as compared to manual reconstruction; however the limitation of this method is that the source path in the ring may not be perfectly circular as the isodose lines. Commissioning of the applicators is mandatory before the clinical use.

Conclusion: A simple novel and time efficient technique for accurate reconstruction of the ring applicator catheter seems feasible and should be the preferred method in busy BT workload environment.

O-22

CURRENT STATUS AND TECHNICAL CHALLENGES OF SECONDARY CALIBRATION SYSTEM FOR RAKR OF ^{192}IR HDR BRACHYTHERAPY SOURCE IN JAPAN

S. Kawamura, T. Yamada[1], T. Mikamoto[2], J. Itami[3]

Faculty of Fukuoka Medical Technology, Teikyo University, [2]Japan Radioisotope Association, [3]Department of Radiation Oncology, National Cancer Center Hospital, Tokyo, [1]Kindai University Atomic Energy Research Institute, Osaka, Japan. E-mail: kawamura@fmt.teikyo-u.ac.jp

Introduction: The national standard of ^{192}Ir brachytherapy source in terms of reference air kerma rate (RAKR) had been prepared by National Metrology Institute of Japan (NMIJ) in 2015.[1] Following this, the secondary calibration service system of ^{192}Ir for limited medical users had been started by Japan Radioisotope Association that is secondary calibration laboratory in Japan. We experimentally carried out the calibration of well-type dosimeter using primary standard source provided by NMIJ.

Objectives: The purpose of this study is to appear the problems and challenges of this calibration system. We make it a goal to complete the calibration system for all medical users by 2018.

Materials and Methods: 35 well-type dosimeters which have collected for calibration from medical user were calibrated in terms of RAKR. Indicated air kerma rate of each dosimeter had compared with RAKR obtained by secondary standard dosimeter, which was calibrated by primary standard source I_{user} is current obtain by well-type dosimeter of user, k_{tp} is air temperature and pressure correction factor. $k_{ion,user}$ is ion recombination correction factor of user dosimeter. $S_{k,JRIA}$ is air kerma rate measured by secondary standard dosimeter of JRIA. kT is correction factor of reduced radioactivity.

Results: The average and standard deviation of the calibration coefficient of each dosimeter Nsk, JRIA ($Gyh^{-1}A^{-1}$) were evaluated. We have successfully carried out calibration of well-type dosimeters.

Conclusion: We evaluated the calibration coefficient of well-type dosimeter of medical user which used MicroSelectron. We will plan to expand other equipment user by 2018.

Reference

1. Kessler C, Kurosawa T, Mikamoto T. Comparison BIPM.RI(I)-K8 of high dose-rate Ir-192 brachytherapy standards for reference air kerma rate of the NMIJ and the BIPM. Metrologia 2016;53 Suppl 6001:10.

O-23

ANALYSIS OF DOSES TO ORGANS AT RISK WHILE DEFINING THE POINT A FROM THE MANCHESTER SYSTEM AND THE ICRU 89 RECOMMENDATIONS

X. Sidonia Valas, S. Purnima, T. Godwin Paul Das, K. Thayalan, G. Bharanidharan[1]
Medical Physics Division, Dr. Kamakshi Memorial Hospital, [1]Department of Medical Physics, Anna University, Chennai, Tamil Nadu, India.
E-mail: sidoniavalasx@gmail.com

Introduction: Point A is the major critical surrogate for dose specification of Intracavitary Brachytherapy. The original definition of Point A, define by Tod and Meredith (1938) intended to indicate the point where uterine artery crosses the ureter and is defined from the surface of the ovoids, which were not feasible to locate using the imaging modalities at that time. The Modified Manchester System by them changed the location of point A to be derived from the bottom of the tandem sources or the stopper of the tandem at the os level. The recent ICRU 89 recommendations, guides to locate the Point A from the surface of the ovoids which could be easily adopted by today's imaging modalities.
Aim: This study attempts to investigate the dosimetric impact of Point A on the OAR doses of bladder, rectum and sigmoid defined by the Manchester System and the ICRU 89 recommendation.
Materials and Methods: Fifty High Dose Rate (HDR) plans of patients treated for carcinoma cervix by Intracavitory Brachytherapy post external beam radiotherapy at our centre were chosen retrospectively for this study.
The patients were implanted with the standard Fletcher Tandem-Ovoid applicator under general anesthesia and the CT images were obtained for planning. Two sets of plans were created by specifying dose to Point A s; one derived from the Manchester System i.e., from the os level/stopper of the tandem and the other one by the ICRU 89 recommendations i.e., from the surface of the ovoids or by drawing a central intersection line at the centre of ovoid sources and including the radium of the ovoid used. The volume of pear shape of the prescription dose and 0.1 cc and 2 cc of bladder, rectum and sigmoid were compared.
Results and Discussion: The point A is defined from the two systems get located in two different dose gradient regions. The volume of the pear shape is higher for ICRU 89 point A. This gives a consequent increase of the dose received by all the OARs and maximum of 14% increase of dose is found in 2 cc of bladder volume. It is also noted that the patients with early diseases have a better anatomy and thus a comparatively a good application of brachytherapy. In such cases, there is no much difference in the location of Point A s derived from the two methods.

O-24

3-DIMENSIONAL VERIFICATION OF PEAR-SHAPED DOSE DISTRIBUTIONS OF HDR INTRACAVITARY BRACHYTHERAPY DELIVERIES USING NORMOXIC POLYMER GEL DOSIMETRY: A COMPARISON BETWEEN GEL DOSIMETRY AND TPS RESULTS

Devi Nand Singh
Department of Radiation Oncology, Command Hospital, Kolkata, West Bengal, India.
E-mail: dnsinghnrl@rediffmail.com

Introduction: The gel dosimeters are tissue equivalent materials used for relative dose measurement of modern radiotherapy deliveries such as IMRT, VMAT, SRS, SRT and HDR Brachytherapy. MRI and X-ray computed tomography based HDR brachytherapy treatment planning and volumetric dose calculations are being used at many radiotherapy clinics. A variety of dosimeters are commercially available for volumetric dose verification of EBRT deliveries but there is a lack of such dosimetry tool for HDR brachytherapy.
Objective: The purpose of this study was to verify the pear-shaped dose distributions of HDR intracavitary brachytherapy deliveries using normoxic polymer gel dosimeter and compared the results with that of TPS calculations.
Materials and Methods: N-isopropyl acrylamide (NIPAM) based normoxic polymer gel dosimeter was prepared inhouse on the bench-top of radiotherapy department following methods described elsewhere.[1] For dose-response linearity study, 30 mL gel-filled vials were irradiated from 1-15 Gy dose. 50 patients diagnosed with carcinoma cervix with FIGO staging (IIA, IIB, IIIB) were included in this study. These patients were subjected to weekly HDR Intracavitary Brachytherapy followed by external beam radiation therapy (EBRT) to pelvis. Brachytherapy planning was performed on a treatment planning software to deliver the prescribed dose to different anatomical reference positions. Similar plans were executed onto a self-designed gel phantom filled with NIPAM gel loaded with applicator and ovoids. The imaging of the irradiated gel phantom was performed using X-ray CT modality of PET-CT scanner. The DICOM images were analysed using modified MATLAB software. The pear-shaped dose distributions derived with 1 mm resolution were compared with TPS calculations. Statistical analysis was performed with help of Epi Info (TM) 3.5.3 which is a trademark of the Centers for Disease Control and Prevention.
Results and Discussion: The dose response was linear from 1 to 15 Gy ($p < 0.001$) with dose sensitivity of 0.46 ± 0.05 HU/Gy. The results of this study showed that there was good agreement between the gel dosimetry measurements and TPS calculations. Brachytherapy gel dosimetry provides dose distributions in all 3 dimensions, which enables us to define the dose distributions in any plane with high resolution (~1mm). It has been reported in many studies that 2D point dosimetry based on ICRU 38 may either over or under estimating the actual dose to the anterior rectal wall.[2,3] To meet out these challenges, ABS and GEC-ESTRO has recommended for 3D imaged based brachytherapy practices.[4,5] The results of this study will be helpful for pre-treatment verification of three-

dimensional dose distributions of typical HDR brachytherapy deliveries.

References

1. Senden RJ, De Jean P, McAuley KB, Schreiner LJ. Polymer gel dosimeters with reduced toxicity: A preliminary investigation of the NMR and optical dose-response using different monomers. Phys Med Biol 2006;51:3301-14.
2. Ling CC, Schell MC, Working KR, Jentzsch K, Harisiadis L, Carabell S, *et al*. CT-assisted assessment of bladder and rectum dose in gynecological implants. Int J Radiat Oncol Biol Phys 1987;13:1577-82.
3. Schoeppel SL, LaVigne ML, Martel MK, McShan DL, Fraass BA, Roberts JA, *et al.* Three-dimensional treatment planning of intracavitary gynecologic implants: Analysis of ten cases and implications for dose specification. Int J Radiat Oncol Biol Phys 1994;28:277-83.
4. Viswanathan AN, Thomadsen B, American Brachytherapy Society Cervical Cancer Recommendations Committee, American Brachytherapy Society. American brachytherapy society consensus guidelines for locally advanced carcinoma of the cervix. Part I: General principles. Brachytherapy 2012;11:33-46.
5. Viswanathan AN, Beriwal S, De Los Santos JF, Demanes DJ, Gaffney D, Hansen J, *et al.* American brachytherapy society consensus guidelines for locally advanced carcinoma of the cervix. Part II: High-dose-rate brachytherapy. Brachytherapy 2012;11:47-52.

O-25

MONTE CARLO STUDY OF WATER-EQUIVALENCE OF VARIOUS SOLID PHANTOM MATERIALS FOR ^{131}CS, ^{125}I AND ^{103}PD LOW ENERGY BRACHYTHERAPY SOURCES

Subhalaxmi Mishra, T. Palani Selvam

Radiological Physics and Advisory Division, Bhabha Atomic Research Centre, Mumbai, Maharashtra, India.
E-mail: b.subwu@gmail.com

Introduction: Experimental brachytherapy dosimetry is a challenge in terms of positional accuracy due to steep gradients in dose and dose rate, low photon energies, and spectral changes with distance from the source. Solid phantom materials can be easily machined to accommodate the source and detector in a precise position, facilitating an accurate measurement and reproducibility in source-detector geometry. Several solid phantom materials are being used for the dosimetric measurements of brachytherapy sources. However, for low energy brachytherapy sources (less than 50 keV), the dose distributions are highly sensitive to phantom compositions due to the predominance of photoelectric effect.
Objective: The aim of this work is to study the water-equivalence of various solid phantom materials for low energy brachytherapy sources such as ^{131}Cs, ^{125}I and ^{103}Pd using Monte Carlo-based EGSnrc code system.
Materials and Methods: The brachytherapy sources included in this study are ^{125}I (model Selectseed), ^{103}Pd (model IRA1) and ^{131}Cs (Isoray model Cs-1). The solid phantom materials investigated are PMMA, polystyrene, solid water, virtual water, RW1, RW3, A150 and WE210. The detectors investigated in this study are diamond, $Li_2B_4O_7$ and LiF.
Phantom scatter correction at distance (r) along the transverse axis of the source, $k_{phan}(r)$, can be calculated at a brachytherapy beam quality Q for solid-state detector by using the following relation:
$k_{phan}(r) = [D_{det,Q}(r)/D_{det,phan,Q}(r)]$
Where, $D_{det,Q}(r)$ and $D_{det,phan,Q}(r)$ are the absorbed dose to a given detector material in liquid water and in the solid phantom at a distance r along the transverse axis of the photon emitting brachytherapy source of beam quality Q, respectively. Note that, $k_{phan}(r) = 1$ means the phantom material is water-equivalent.
In the Monte Carlo calculation of absorbed dose to detectors in water and in solid phantom materials were based on the FLURZnrc user-code of EGSnrc code system. The source is positioned at the centre of a 40 cm diameter and 40 cm height cylindrical phantoms (liquid water and solid phantoms). The photon fluence spectrum is scored in 0.5 mm thick and 0.5 mm high detector materials at different positions varying from 0.5 cm to 10 cm along the transverse axis of the source. The fluence spectrum is converted to collision kerma to water and collision kerma to detector materials by using the mass-energy absorption coefficients of water and detector, respectively. Up to 10^9 photon histories are simulated. The statistical uncertainties on the calculated values of $k_{phan}(r)$ is less than 0.5%.
Results and Discussion: The study shows that for a given detector $k_{phan}(r)$ depends on r for the investigated phantom materials, but the degree of deviation from unity depends on the type of solid phantom and the brachytherapy source. For all the detectors, $k_{phan}(r)$ decreases with *r* for polystyrene, PMMA, RW1 and RW3 phantom materials and increases with *r* for the remaining phantom materials. k_{phan}(r) values are calculated for diamond, $Li_2B_4O_7$ and LiF detectors for ^{125}I, ^{103}Pd and ^{131}Cs brachytherapy sources, respectively.
Phantoms such as solid water, virtual water and WE210 are water-equivalent at short distances (less than 3 cm) for all the investigated detectors and brachytherapy sources. However, as the distances increases these phantom materials tend towards non water-equivalence (at 10 cm, $k_{phan}(r)$ value is about 20 % larger than unity). Remaining phantoms such as PMMA, RW1, RW3 and PMMA showed significant $k_{phan}(r)$ values (about 80 % lesser than unity at 10 cm distance). The solid phantom materials such as solid water, virtual water and WE210 can be treated as water-equivalent phantoms at short distances (less than 3 cm) for the dosimetric measurements of low energy brachytherapy sources.

O-26

VALIDATION OF HETEROGENEOUS ALGORITHM USING EBT2 STACK FILM WITH METAL AND SHIELDED APPLICATOR IN HDR BRACHYTHERAPY

Mourougan Sinnatamby, Vivekanandan Nagarajan[1], Sathyanarayana Reddy K[2], Gunaseelan Karunanidhi

Department of Radiotherapy, Regional Cancer Centre, JIPMER, Puducherry, [2]Regional Cancer Centre, JIPMER and Head, Oncology, Mahatma Gandhi Medical College and Research Institute, Puducherry, [1]Department of Medical Physics, Cancer Institute, Chennai, Tamil Nadu, India. E-mail: mourougans@gmail.com

Introduction: Worldwide the importance of prior independent verification of treatment plan has been recognized in HDR brachytherapy. The measurement of planned dose distributions poses a challenging task due to large dose ranges, high dose gradients, and small spatial scales. A number of experimental and Monte Carlo (MC) studies have been reported in literature representing the influence of inhomogeneity in brachytherapy treatments and the shielding effect created by the applicators. It is essential that QA needs to be in line with progress as recommended in TG-186 for HDR brachytherapy treatment planning and delivery to ensure an appropriate level of dosimetric accuracy and quality.

Objectives: To validate the model based dose calculation algorithm using EBT2 stack film with metal and shielded applicator in HDR brachytherapy.

Materials and Methods: Three different experimental setup with the applicators used in Varian Medical System, GammamediX plus viz., interstitial metal catheters, ring applicator with ring cap and rectal retractor, vaginal mould partially shielded applicator used in conjunction with multiple EBT2 Gafchromic film to study the planar fluence pattern calculated using Varian Medical System, AcurosTM BV (Grid Based Boltzmann solver) heterogeneity algorithm. EBT2 Gafchromic stack film can be read with Epson Expression 10000XL flatbed scanner to validate AcurosTM BV in HDR brachytherapy. Film QA Pro 2015 software used to validate the different criteria set for gamma analysis. The IBM SPSS version 21 software used for the data analysis and paired t-test tool showed a comparison of the mean difference between paired data.

Results and Discussion: The point doses calculated with AcurosTM BV using a virtual phantom created in the TPS, which agreed with MC based calculation mostly within 2%. Based on the recommendations given in IAEA TRS 430 report, the commissioning of brachytherapy TPS, a 5% dose /2 mm distance criterion for gamma function was studied and the results showed 95% passing rate. Whereas in this study the gamma pass percentage was higher than the conventional TG-43 based calculation. To verify this dose with heterogeneity algorithm with gamma pass criteria of 5% and 1 mm, a gamma pass rate of 96% shown. In reviewing the literature, the common standard set for gamma criteria in brachytherapy was 5% and 2 mm. The EBT2 film stacked one after another without air gap to enable to verify the fluence at a different plane, however, this method was a modified method of a study conducted by Palmer et al, where in validation done by placing the film at regular interval. In the Interstitial Metal Catheters setup, analysis of plane by plane showed maximum gamma difference as 1.45%, DD -0.817%, DTA 1.38% and all showed no statistically significant difference. In titanium ring applicator with the acetal ring cap and rectal retractor setup. The sagittal fluence and frontal fluence were generated in single exposure simultaneously and analyzed. On comparing one plane with another plane maximum gamma difference noted in frontal and sagittal as 4.0% and 3.82%, DD showed 2.72% and 2.25% difference, DTA showed 3.72% and 2.71% difference in the frontal and sagittal plane. In the vaginal mould partially shielded setup, stack film was placed both in the shielded as well as in the unshielded area. The shielded area showed no dose to compare which was confirmed with TPS calculation. The unshielded portion of the applicator where films are stacked showed dose and was analyzed plane by plane, the maximum difference in Gamma showed -5.28%, DD with 2.95% and DTA with 3.71%. Thus methods used provide a comprehensive verification for validation of the heterogeneity algorithm and stack film dosimetry can be a useful 3D tool for QA program in HDR brachytherapy.

O-27

RADIATION SHIELDING EVALUATION OF MODEL LAYOUT PLAN FOR REMOTE AFTERLOADING IRIDIUM/COBALT SOURCE BRACHYTHERAPY TREATMENT ROOM: THEORETICAL CALCULATION

Mahendra More, S. P. Srivastav
Kiran Multi Super Speciality Hospital and Research Center, Surat, Gujarat, India.
E-mail: mahendra_more@yahoo.com

Introduction: Radiotherapy continues to be the main stay of cancer management globally and more than 60% patients receives radiotherapy for the treatment of cancer, and of these 5–15% patients are treated by brachytherapy as a single or combined modality. Brachytherapy continues to be the most conformal treatment modality with very high dose delivery to the core of target volume and excellent dose fall off, to spare the organs at risk (OARs) with least integral dose. It continues to have radiobiological superiority and it has the ability to boost the target volume with judicious choice of target volume to achieve better outcome.

Objectives: The aim of this study is to evaluate the model layout plan for remote afterloading Iridium (Ir-192) and Cobalt (Co-60) source brachytherapy treatment room design and the factors affecting these designs and to optimize protection of patient, staff and public.

Materials and Methods: Use of Iridium-192 and Cobalt-60 source in High Dose Rate (HDR) brachytherapy unit has come for discussion in recent publications. For these units treatment room or vault must be designed and constructed with due considerations in shielding design, equipment type, workload, use factor, shielding material, available space, ALARA principle, Regulatory constraints etc.

Model layout room plan for Ir-192 HDR room with 10 Ci Source and Co-60 HDR room with 2.0 Ci source were studied. The workload was calculated on basis of 4.0 hours of machine ON time per week.

WORK LOAD (W) = Activity of source X Max. weekly ON Time of the machine for treatment of patients X Specific Gamma Ray Constant = cGy/wk at 1 metre.

W (Ir-192) = 20 cGy/wk at 1 metre

W (Co-60) = 10 cGy/wk at 1 metre

We further calculated the dose rate at a certain distance from the source due to primary, scattered and leakage radiation and from it one could derive how many TVL's we need to bring the radiation levels to the dose constraints OR annual dose limits to occupational workers or public specified in safety reports.

This institute has constructed room for Cobalt-60 unit and will install remote after loading brachytherapy unit. The existing room is to conform to radiological safety requirements of Cobalt-60 brachytherapy unit. This study presents theoretical approach and complete details about design of HDR brachytherapy treatment room and evaluation of model plans in view of radiation safety around the installation.

Results and Discussion: The calculated wall thicknesses are appropriate for annual exposure dose limits for public area as well as for occupational worker. The thickness of primary wall 0.45 m is adequate as there is no occupancy towards these walls and the thickness of wall towards CT simulator room is increased to 0.50 m so as to reduce the exposure.

Design dose limits should also be considered while planning treatment room for radiation facility as specified in radiation safety code.

O-28

PROBABILISTIC SAFETY ASSESSMENT OF REMOTE AFTERLOADING HIGH DOSE RATE BRACHYTHERAPY FACILITY

Rajib Lochan Sha, D. B. Nagrale[1], Alok Pandey, Pankaj Tandon, A. U. Sonawane

Radilogical Safety Division, Atomic Energy Regulatory Board, [1]Nuclear Safety Analysis Division, Atomic Energy Regulatory Board, Mumbai, Maharashtra, India. E-mail: rajibsha@aerb.gov.in

Introduction: All kinds of medical radiation facility may lead to potential exposure of patients. However, there may be more probability for serious accidents in radiotherapy than in other medical practices, because of the high doses and high activity sources used. In this study, the safety evaluation for radiotherapy RAL HDR Brachytherapy facility is carried out considering the fatality due to radiation overexposure.
Objective: Probabilistic safety assessment (PSA) is essentially used for safety evaluation of radiation facilities to reduce the radiological risk from the possible potential exposures to the patients, occupational workers and the member of public.
Materials and Methods: The approaches and methodologies to assess the safety are very much matured in case of nuclear facilities with comparison to non-nuclear facility. The present PSA study is undertaken for RAL HDR Brachytherapy equipment "GammaMed Plus iX" utilise Ir-192 gamma irradiation source for the purpose of delivering treatment of cancer patient. In this treatment a pre-determined dose is delivered to specific portion of patient, such that the intended therapeutic result is obtained. Considering the serious deterministic effect and fatality due to radiation over exposure as a risk measure, the application of PSA to safety evaluation of GammaMed Plus iX RAL HDR Brachytherapy facility is presented in this paper. The safety assessment is carried out taking all possible failures in the design and safety system/interlock of the facility. Two models such as event tree and fault tree are used to present the logical structures in a manner suited for quantitative analysis.
Results and Discussion: The frequency (per year) of getting inadvertent high dose to patient is found as 6.09E-7 from the probabilistic safety assessment of GammaMed Plus iX RAL HDR Brachytherapy facility. The results indicate that frequency of fatal exposure is below the acceptance criteria. The overall risk to the overexposure can be reduced by providing the adequate training to the operator and improving the good safety culture in the medical institution, without major modification in the design and safety system/interlock of existing GammaMed Plus iX RAL HDR Brachytherapy facility. However, additional safety locking mechanism for the source should be provided to ensure the immobilisation of the source while not used. The source locking will be used manually to lock the source after the use of the HDR brachytherapy unit. Due to presence of the source locking wire the source will not be able to come out of the safe parking position.
Conclusion: The probabilistic safety assessment of GammaMed Plus iX RAL HDR Brachytherapy facility indicates that the frequency of inadvertent high dose (for a patient) of RAL HDR Brachytherapy facility is less than 1E-6 per year. The international guidelines for risk from food irradiation facility is mentioned as 1E-6 per year as per ICRP-76.
Acknowledgment: We are thankful to the technical staff of M/s. Varian Medical System, International India Pvt. Ltd, Supplier of GammaMed Plus iX RAL HDR Brachytherapy facility for providing the necessary informations in detail of GammaMed Plus iX for our PSA study.

O-29

PRE-TREATMENT VERIFICATION OF ADVANCED RADIOTHERAPY USING ELEKTA LINAC PARAMETERS TRACKED IN REAL-TIME

Nur Shaheera Midi, Hafiz Mohd Zin

Oncology and Radiological Sciences Cluster, Advanced Medical and Dental Institute, Universiti Sains Malaysia, Penang, Malaysia. E-mail: hafiz.zin@usm.my

Pre-treatment verification of IMRT ensures accurate delivery of the treatment planned. The current practice is to use a dosimetry system to verify the dose delivered by the linac. Any errors undetected during treatment delivery may jeopardise the cancer cure and increase the severity of radiation side effects. However, dose measurement may take time to perform and is prone to error if the detector is not calibrated correctly. The approach may be inconvenient for a busy radiotherapy treatment facility due to high patient load and low staff ratio. Varian linac records treatment delivery parameters as log files that is accessible to the end users. However, Elekta linac does not provide such log file but has a function to log the delivery parameters in real-time using the service graphing function available from the linac control computer. The study has developed an algorithm to analyse the real-time data using Matlab (MathWorks, Natick, MA). The algorithm measures any errors in the treatment parameters and reconstructs the parameters into dose given to cancer patient during radiotherapy. The technique simplifies the conventional processes using a detector, but at the same time efficiently ensure that the radiation delivered to cancer patient is accurate. The algorithm has been tested to verify the accuracy of radiotherapy treatment for head and neck cancer patients in Advanced Medical and Dental Institute, Universiti Sains Malaysia. The results agree well with the standard measurements using radiation detector but significantly reduce the time required to perform the check. Additionally, the algorithm can also be used to analyse detailed performance of radiotherapy treatment parameters such as MLC positions and other treatment delivery parameters such as gantry and collimator angle. Acknowledgement: This work is funded by Fundamental Research Grant Scheme, Ministry of Education Malaysia, 203/CIPPT/6771383.

O-30

DOSIMETRIC COMPARISION OF COPLANAR AND NON-COPLANAR INTENSITY MODULATED RADIATION THERAPY PLANNING FOR ESOPHAGEAL CARCINOMA

Vinay Desai, B. Shwetha, M. Ravikumar, K. M. Ganesh, S. Sathiyan, C. Varatharaj

Department of Radiation Physics, Kidwai Memorial Institute of Oncology, Bengaluru, Karnataka, India. E-mail: vinaydesaimsc@gmail.com

Introduction: The curative potential advantage of radiation therapy in the management of esophagus cancer is greatly enhanced by the use of IMRT. The success of IMRT requires the high radiation dose delivery to the tumor, while sparing the surrounding normal tissues. The aim of this study is to compare the feasibility of coplanar and non-coplanar Intensity Modulated Radiotherapy (IMRT) plans to improve the treatment.
Objective: To compare the dosimetric impact of coplanar and non-coplanar IMRT plans for esophageal carcinoma and to optimize the treatment approach for the esophageal cancer.
Materials and Methods: In this study CT images of 20 esophageal carcinoma patients, who had undergone the IMRT treatment, were considered. Six of them had cervical and upper thoracic tumors and were grouped together as 'Group 1', and the remaining fourteen patients had middle and lower thoracic section tumors and they were grouped separately as 'Group 2' and 'Group 3' (seven patients each). The contouring and treatment planning was performed in the Eclipse treatment planning system (TPS). The dose to 95% tumor volume, dose received by heart, lung and spinal cord were calculated using the DVH from Eclipse TPS. The dose distribution of PTV was assessed by evaluating the maximum dose (Dmax), mean dose (Dmax) and minimum dose (Dmin). To evaluate the plan quality with respect to the dose delivered to the tumor, the Conformity number (CN) conformity index (CI) and heterogeneity index (HI) were computed.
Results: For Group-1, Group-2 and Group-3 patients mean dose of coplanar plan were much better than those in non-coplanar plan, but the mean dose gradient in non coplanar plan didn't show much significant difference. For group-2 patients the non coplanar IMRT plan could reduce the dose to the lung tissue, thus reducing the probability of radiation pneumonia to esophageal cancer patients. The drawback of non-coplanar IMRT is that, it resulted in higher dose to the heart and spinal cord compared to the coplanar plan.
Discussion: In this study, for all groups of patients it was found that coplanar IMRT plan produced higher mean dose to PTV than non-coplanar IMRT plan. Maximum dose to the PTV is found to increase in the non-coplanar plans when compared to coplanar plans. Although HI of both the plans was almost equal to one, coplanar IMRT plans showed better HI values. Mean lung dose (MLD) is found to be reduced in non-coplanar IMRT plans when compared to coplanar plans as lung can be spared due to non-coplanar entry of the beam through the body. Radiation pneumonitis is the main factor to limit clinical therapeutic effect and the goal was to reduce the irradiation to the lung. Hence in this study it was found that the non-coplanar IMRT plans could have been the effective tool to reduce the irradiation of lung. However as shown for non-coplanar plans, reduction in the irradiation of lung may also reduce the conformality of the plan. It was also found from this study that non-coplanar IMRT plans increased the dose to the heart while reducing dose to the lung. For Group-2 and Group-3 patients the dose to the heart was considered as the constraint and it was found that there was a significant increase in the mean dose of heart and spinal cord in non-coplanar IMRT plan. The drawback of non-coplanar IMRT is that, although within tolerance limits, it delivers a higher dose to the heart and spinal cord compared to the coplanar plan.

O-31

LUNG AND BREAST CANCER RISK ESTIMATES FOLLOWING INVOLVED-SITE RADIATION THERAPY FOR SUPRADIAPHRAGMATIC HODGKIN'S DISEASE IN FEMALE PATIENTS

M. Mazonakis, E. Lyraraki[1], J. Damilakis

Department of Medical Physics, Faculty of Medicine, University of Crete, [1]Department of Radiotherapy and Oncology, University Hospital of Iraklion, Heraklion, Greece. E-mail: mmazonakis@med.uoc.gr

Introduction: The Hodgkin's disease (HD) is a highly curable malignant disease which often affects young adults. Radiation therapy plays a major role in the management of this malignancy. However, the therapeutic irradiation with both extended and involved fields may be associated with an increased second cancer risk. A new concept, known as involved-site radiotherapy (ISRT), was recently introduced to restrict the treatment volumes. Limited information has been published about the probability for the appearance of secondary malignancies following ISRT for HD.
Objectives: The purpose of the current study was to estimate the lung and breast cancer risks in female patients undergoing ISRT for supradiaphragmatic HD.
Materials and Methods: The study population consisted of thirteen consecutive female patients who had been previously irradiated for HD in our department. All patients had mediastinal disease with or without involvement of the cervical nodes. An experienced radiation oncologist defined the planning target volume corresponding to the ISRT technique on the CT scans of each patient. The lungs and breasts, which are characterized by a high susceptibility for radiation carcinogenesis, were manually delineated on a slice-by-slice basis. Three-dimensional plans were generated with 6 MV X-ray beams giving 30 Gy to the tumor site in 15 fractions. Differential dose-volume histograms (DVHs) of the breasts and lungs were calculated by the radiotherapy plans. The dose calculation interval was equal to 0.01 Gy in all histograms. The DVHs were used to determine the organ equivalent dose (OED) of the lungs and breasts and the relevant patient- and organ-specific lifetime attributable risk (LAR) for cancer development with the aid of a non-linear mechanistic model. The above risk model accounted for the effects of the tumor dose fractionation in radiotherapy and the repopulation ability of each tissue between two dose fractions. The estimated LARs were compared with the respective organ-dependent lifetime intrinsic risk (LIR) values of cancer induction for unexposed people as provided by the most recent SEER Cancer Statistics Review.
Results: The OED of lungs due to ISRT for HD varied from 1.7 to 2.8 Gy whereas the respective variation for breasts was 0.3-1.3 Gy. The LAR for lung cancer development in irradiated females was 1.4-2.8 % depending upon the organ exposure and the patient's age. The corresponding radiotherapy-induced lifetime risk range for the appearance of breast malignancies was 0.2-2.6 %. The individualized LARs for lung cancer induction after ISRT were 2.2-4.3 times low in comparison with the LIRs. The probabilities for the development of radiation-induced breast malignancies were more than 4.7 times smaller than the respective LIRs.

Conclusions: The LARs for lung and breast cancer induction following ISRT for supradiagramatic HD in female patients are lower than the nominal cancer incidence rates but they should not be considered as insignificant. The presented probabilities for second cancer development may be useful for the follow-up of the HL survivors.

O-32

COMPARISON OF VOLUMETRIC MODULATED ARC THERAPY AND HELICAL TOMOTHERAPY PLANS FOR HIGH RISK PROSTATE CANCERS USING DOSIMETRIC AND RADIOBIOLOGICAL INDICES

Sneha S. Nair, M. K. Ashitha, P. S. Renil Mon, C. O. Clinto, E. Sreedevi, Raghavendra Holla, Bhaskaran K. Pillai

Department of Medical Physics and Radiation Safety, Amrita Institute of Medical Science and Research Center, Kochi, Kerala, India. E-mail: n.sneha85@gmail.com

Introduction: Very few studies have compared various techniques of IMRT (Intensity Modulated Radiation Therapy) based on radiobiological indices in high risk prostate cancer till date. In high risk prostate cancer, the target volume includes pelvic lymph nodes in addition to the prostate and seminal vesicles. This makes target volume irregular and complex. Also, a lot of normal tissues will come into contact with target volume. Simultaneous Integrated Boost approach is used in high risk prostate cancer in which a higher dose is delivered to prostate and seminal vesicles compared to pelvic lymph nodes. This will make the treatment planning process in high risk prostate cancer more challenging compared to low and intermediate risk prostate cancer. In this study, we compare plan quality based on dosimetric and radiobiological parameters of ten prostate cancer patients using VMAT (Volumetric Modulated Arc Therapy and HT (Helical Tomotherapy) techniques.

Objectives: Aim of this study is to verify the efficacy of newly installed HT (Helical Tomotherapy) in comparison with the existing VMAT (Volumetric Modulated Arc Therapy) technique.

Materials and Methods: Ten patients treated with VMAT by Simultaneous Integrated Boost (SIB) approach were selected from our database. For each patient, two clinical target volumes were defined. Planning Target Volume 70 Gy (PTV_{70Gy}) included gross tumor and entire prostate with 8 mm margin on all sides except posteriorly where a 5 mm margin was given. Clinical Target Volume 50.40 Gy ($CTV_{50.4Gy}$) includes pelvic lymph node stations. A $PTV_{50.4Gy}$ was created with 3-mm auto margin to $CTV_{50.4\ Gy}$. Organs At Risk (OAR) rectum, bladder and femoral heads were also contoured. Each patient's data were exported to TomoTherapy planning station and new plans were created and compared with the existing VMAT plan. VMAT plans were done using Monaco5.1 for Elekta synergy 6MV accelerator. Dosimetric indices such as Conformity Index (CI), Conformity Number (CN), Homogeneity Index (HI), Dose Volume Histogram (DVH) and Radiobiological indices, Equivalent uniform Dose (EUD), Tumour Control probability (TCP) and Normal Tissue Complication Probability (NTCP) were compared. Other treatment parameters like beam on time and Monitor Unit (MU) were also analysed. Statistical significance of the comparison was reported using paired Student's t-test.

Results and Discussion: Both HT and VMAT are able to produce clinically acceptable plans with adequate target coverage. Differences in the high dose region of PTV_{70Gy} DVH infer that both plans are not in congruence in case of homogeneity of dose distribution and hotspot inside the target volume. The homogeneity indices quantified as 0.03 (0.01) for HT and 0.06 (0.01) for VMAT plan. $D_{2\%}$ of HT was 70.63Gy (0.29) and that of VMAT was 72.36Gy (0.61) The CI and CN values of PTV_{70Gy} shows that VMAT plans are more conformal than HT plans. In case of OAR sparing, VMAT is more efficient in high dose sparing while HT give more low dose sparing. Analysis of plan quality based on Radiobiological indices showed only a marginal difference and which are not statistically significant. Treatment delivery time was about 60% higher in HT, MU also increased tremendously.

O-33

EFFICACY OF SHORT SPINAL ARC LENGTH IN VOLUMETRIC MODULATED ARC THERAPY BASED CRANIOSPINAL IRRADIATION

Upendra K. Giri, Biplab Sarkar, Kanan Jassal, Anusheel Munshi, Sandeep Singh, Salih Osman, V. Karthik, Tharmar Ganesh, Bidhu K. Mohanti

Department of Radiation Oncology, Fortis Memorial Research Institute, Gurgaon, Haryana, India. E-mail: upendragiribhu@gmail.com

Introduction: Medulloblastoma and primitive neuroectodermal tumours (PNET) are common paediatric tumours treated by CSI along with the systemic chemotherapy or (and) hormone therapy and surgery. Radiotherapy techniques for CSI include simulator based 2D technique, CT based three dimensional conformal radiotherapy (3DCRT), intensity modulated radiotherapy (IMRT) and volumetric modulated arc therapy (VMAT). The advantage of VMAT technique is that it does not require any junction shift since it employs overlapped fluence pattern between brain-spine and spine-spine fields to take care of dose matching in the junctions.

Objective: Objective of the study was to establish the dosimetric superiority of short arc lengths over large arc lengths, for craniospinal irradiation (CSI), using volumetric modulated arc therapy (VMAT).

Materials and Methods: For a cohort of ten patients, two VMAT CSI plans were created for each patient, one using the conventional full 360° arc (VMAT_FA) for the spine and the other using 100° posterior arc (VMAT_PA) for 23.4 Gy and 35 Gy prescriptions. In both the plans 360° arc fields were employed for treating cranial volume. Non-tumour integral dose (NTID), which is the dose to body excluding planning target volume, was compared with VMAT_FA and VMAT_PA plans. In addition to these VMAT plans, a 3DCRT plan was also created for all these patients to compare the NTID and target volume related dose constraints.

Results: Mean V95% difference between the two VMAT plans did not exceed 1.3% for cranial and spinal targets for both prescription levels. Conformity index, averaged over both prescription doses, were similar for VMAT_FA and VMAT_PA plans at 0.84 ± 0.04 and 0.82 ± 0.05 respectively. V95%,

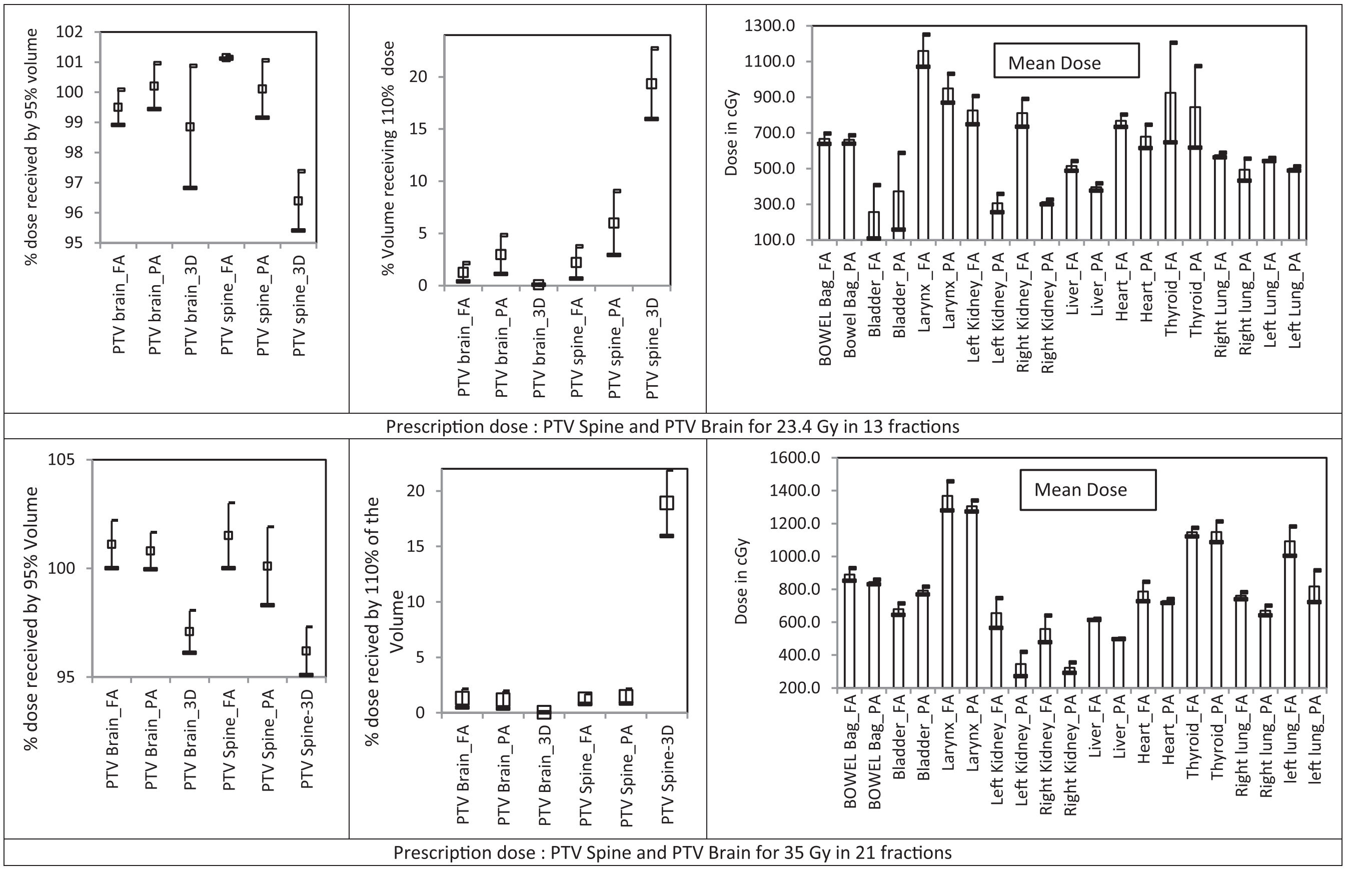

Figure 1: Comparison of PTV coverage (V95%) hot spot (V110%) and mean OAR doses between VMAT spine full arc, spine partial arc and 3DCRT

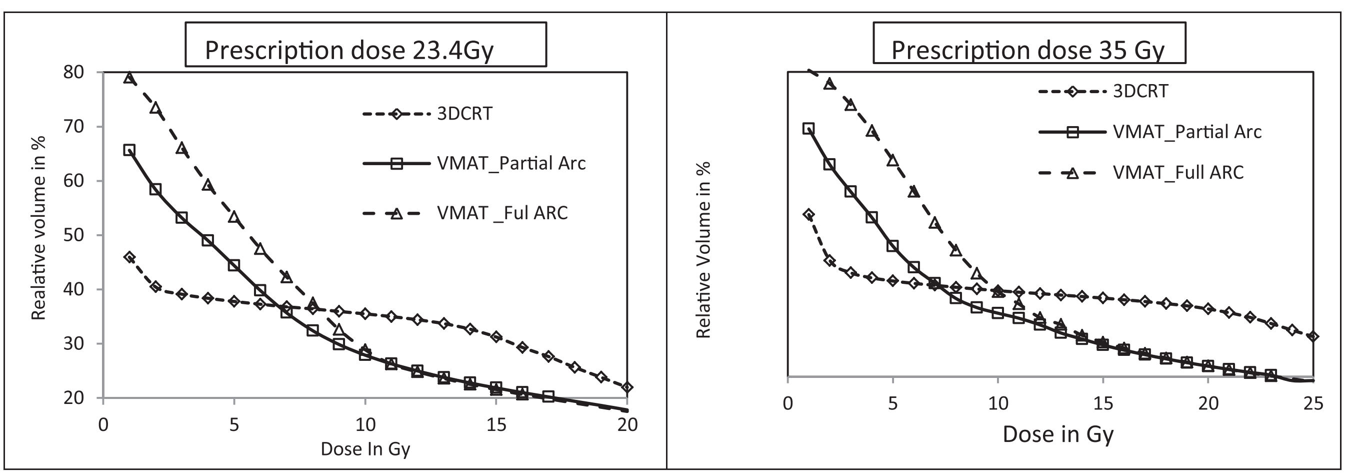

Figure 2: Spillage dose to Body-PTV (NTID: non-tumour integral dose) for 3DCRT, partial arc VMAT and full arc VMAT for prescription dose of 23.4 Gy in left panel and for 35Gy dose in right panel respectively

V110% and conformity index did not exhibit a statistically significant difference between partial- and full-arc VMAT plans. However, the VMAT_PA plan exhibited a lower NTID compared to VMAT_FA plans ($0.007 \leq p < 0.05$) in the 1-5 Gy range. Partial arc plans yields a statistically insignificant dose reduction for delineated organs, compared to full arc plans, except heart. PTV coverage as well as spillage dose to body-PTV is shown in Figure 1 and 2 respectively.

Discussion: VMAT radiation treatment techniques are gaining popularity due to their simplicity and faster treatment delivery. In our study, we observed that use of partial arcs could substantially reduce the dose to kidneys, lung, larynx and body, although dose reduction in organs like liver, thyroid, heart, and bowel were not significant. For left kidney, a dose reduction to the magnitude of 5.2 Gy and 3.2 Gy were observed for VMAT_PA plans against VMAT_FA plans for prescription doses of 23.4 and 35 Gy. Dose to larynx was reduced by 2 Gy in VMAT_PA plans when the prescription dose was 23.4 Gy. Similarly, for lungs, partial arc plans resulted in a dose reduction of 1-2 Gy for both prescription levels; however, they were not statistically

Supplementary Table 1: Reviewed papers for volumetric modulated arc therapy based craniospinal irradiation (first/corresponding author and publication year)

Investigator	*Centre*	*Upper spine isocentre (start angle/end angle)*	*Lower spine isocentre (start angle/end angle)*	*Prescription dose (Gy)*	*Number of fractions*	*Mean dose (Gy)*										
						Heart	*Thyroid*	*Esophagus*	*Left lung*	*Right lung*	*Combined lung*	*Liver*	*Right kidney*	*Left kidney*	*Combined kidney*	*Larynx*
Antonella Fogliata (2011)	Centre a	181°/179°=358°	181°/179°=358°	36	20	7.1	14.9	19.2			11	9.7			8.5	18.8
Antonella Fogliata (2011)	Centre b	181°/179°=358°	181°/179°=358°	36	17	9	13.6	15.7			5.4	6.2			4.4	13.6
Matthew T. Studenski (2013)		200°	-	36	20	5	11	13			9.8	5.5	13.2	10		
Qilin Li (2015)		(180°–240°) + (300°–60°) + (120°– 180°)=240°	-	36	20	6.3	12.9	15.1			6.2	5.3			4.8	
Antonella Fogliata (2011)	Centre e	180°/180°=360°	179°/180°=360°	23.4	13	5.3	9.9	13.7			8.2	6			7.4	13.6
Lee YK (2012)		179°/181°=358°	-	23.4	13	4	15	14			4	6	9	9.5		
Pamela A. Myers (2014)		360°	-	23.4	13	13.7	19		4.1	5.8		5.6	5.3	4.2		
Antonella Fogliata (2011)	Centre c	(180°/310°) + (50°/179°)=260°	(180°/310°) + (50°/179°)=260°	30.6	8						Different prescription					
Antonella Fogliata (2011)	Centre d	180°/180°=360°	(180°/215°) + (276°/84°) + (142°/180°)=237°	12	13						Different prescription					
Andrej Strojnik (2016)		(180°/310°) + (50°/179°)=260°	-	30.6	17						Not presented					
Anders T. Hansen (2015)		182°/179°=357°	-	36	20						Not presented					
Pamela Myers (2013)		360°	-	23.4	13						Not presented					

Data shows a comparison between arc angles for different spinal isocentres, prescription dose and organ at risk doses different. The only statistically different OAR doses were observed for bilateral kidneys in 23.4 Gy dose level.

Supplementary Table 1 presents OAR doses reported by different investigators in the past. It is apparent that the ranges of reported OAR doses are wide and inconsistent. Kidney (combined and individual) doses were reported to be in the range of 4.4-13.2 ± 12 Gy for 36 Gy prescriptions in different reports. In our study, for a prescription dose of 35 Gy, dose to kidney(s) were 3.2-3.4 Gy for VMAT_PA plans and 5.5-6.5 Gy for VMAT_FA, pointing to better plan quality observed for VMAT_PA plans.

O-34

A HYBRID CONFORMAL PLANNING TECHNIQUE WITH SOLITARY DYNAMIC PORTAL FOR POST-MASTECTOMY RADIOTHERAPY WITH REGIONAL NODES

K. Mohamathu Rafic, Timothy Peace Balasingh, Ebenezer Suman Babu, I. Rabi Raja Singh

Department of Radiotherapy, Christian Medical College, Vellore, Tamil Nadu, India. E-mail: raficmphy@gmail.com

Introduction: Computing an optimum treatment plan for post-mastectomy radiotherapy (PMRT) with regional nodes (supraclavicular and axillary nodes) is one of the challenging tasks in radiotherapy. At present, field-in-field (FinF) technique is a widely accepted for breast radiotherapy. However, very few reports on PMRT with regional nodes have been reported in the literature. Further, there is no published data that deals with fluence verification of dynamic FinF portals.

Purpose: The primary objective of this study focuses on incorporation of a solitary dynamic portal (SDP) in conformal planning for PMRT with regional nodes with an intention to overcome the treatment planning limitations imposed by conventional techniques. Secondary objective is to demonstrate in-air fluence verification of SDPs using amorphous silicon electronic portal imaging device (EPID).

Materials and Methods: 24 patients who underwent surgical mastectomy followed by PMRT were included in this study. The planning CT images patients from the level of “C2” to “start of adrenals” were acquired using Biograph True Point HD CT (Siemens Medical Systems, Germany). Initially, a treatment plan comprising of tangential beams fitted to beam’s-eye-view (BEV) of chest-wall and a direct anterior field fitted to BEV of nodal regions, both sharing a single isocenter was generated using Eclipse treatment planning system (Varian Medical Systems, Palo Alto, CA). FinFs (10 to 15 fields) were added only in the medial tangent that were re-fitted to BEV of entire target volume and shared about 30-50% beam weight of medial tangent thereby increasing the tumor dose across the nodal regions while reducing the dose above and below the direct anterior portal. These multiple lower weight (3-5% relative weight per field) irregular FinFs were then converted into a dynamic field referred to as “solitary dynamic portal”. Dosimetric analysis of treatment plans were performed and compared with summed doses of chest-wall and regional nodes treatment plans computed with typical tangential conformal beams with dynamic wedges and tilted direct anterior field respectively. Furthermore, fluence verification for the dynamic portals was performed using EPID and portal dosimetry software.

Results and Discussion: Conformal plans with SDP showed excellent dose coverage ($V_{95\%}$ >95%, $V_{105\%}$ <6.5% and $V_{107\%}$ <0.5%), higher degree of dose conformity (≤1.25) and homogeneity (≤0.12) without compromising the OAR sparing for PMRT with nodal-region. Treatment plans with SDP considerably reduced the lower isodose spread to the ipsilateral lung, heart and healthy tissue without affecting the dose homogeneity. Since, majority of dose contributions are from static tangents, the dose to lung (ipsilateral and contralateral) and contralateral breast were comparable to the typical conformal plans. Furthermore, we have recorded considerable reduction in heart dose ($V_{25\,Gy}$ ≤ 10.1 ± 1.4%). SDP fluence map generated in our study is less complex than IMRT portals, having lower MU in the order of 45 - 60. Furthermore, gamma evaluation showed more than 96% pixel pass-rate for standard 3%/3 mm dose-difference and distance-to-agreement criteria. Hybrid conformal plans with SDP offers less probability of “geometrical-miss” at the highly irregular chest-wall with regional nodal radiotherapy.

Conclusion: From our results we conclude that the hybrid conformal plans with SDP would facilitate improved dose distribution and reduced uncertainty in delivery and promises to be a suitable treatment option for complex post-mastectomy chest-wall with regional nodal irradiation. The future scope of this study is to adapt deep inspiration breath-hold technique while delivering the dynamic portal to avoid displacement of dose gradients and thereby enabling higher degree of dose homogeneity across the moving target.

O-35

SIMULTANEOUS INTEGRATED BOOST FOR CARCINOMA LEFT SIDED BREAST: PLAN QUALITY COMPARISON OF HELICAL TOMOTHERAPY WITH VOLUMETRIC MODULATED ARC THERAPY

B. Subbulakshmi, T. K. Bijina, A. Pichandi, C. A. Muthuselvi

Department of Radiotherapy, Healthcare Global Enterprises, Bengaluru, Karnataka, India. E-mail:subbu.phy@gmail.com

Introduction: Breast cancer is the leading cancer diagnosis among women in developed countries, and it is one of the most common cause of cancer death globally. It is well known that breast conservation with lumpectomy and adjuvant radiation treatment has shown to improve both local control and overall survival in early stage breast cancer patients. Simultaneous Integrated Boost (SIB) in breast conserving radiotherapy is known for its advantage in reducing dose to normal tissues with relatively lesser skin toxicity and reduced number of fractions.

Objective: To quantify the dosimetric results of Helical Tomotherapy (HT) and Volumetric Modulated Arc Therapy (VMAT) plans using the SIB technique for carcinoma left breast.

Materials and Methods: Nine left sided female breast patients were selected for this retrospective study. The patients were immobilized using thermoplastic cast with the abduction of hands above head. CT scan images of slice thickness 2.5 mm were acquired on GE PET CT scanner in supine position as per the institution protocol. The acquired images were transferred to Eclipse Treatment Planning System (TPS) and Planning Target Volume (PTV_{Breast}), PTV_{Boost} volume and OAR’s such as heart, contralateral breast, ipsilateral lung and contralateral lung were delineated by radiation oncologist. Both PTV's were cropped 5 mm from skin. The prescription dose was 60.2 Gy to boost volume and the entire breast volume received 50.4 Gy in 28 fractions. The VMAT plans were generated using two partial arcs in the Monaco5.1 TPS. Monte Carlo dose calculation algorithm was used to calculate VMAT plans. The HT plans were done in VoLO TPS and the plan parameters comprised of 2.5-cm field width, pitch value 0.287 and Modulation factor 2-3. Beam entry was restricted by directionally blocking from contralateral side. Collapsed cone convolution dose calculation algorithm was used to calculate HT plans. The optimization prescription was defined to deliver prescribed dose to 95% of the target volumes and to minimize the volume receiving ≥107% of the boost dose. The quality of plans were evaluated by calculating Homogeneity Index (HI), Conformity Index (CI),mean dose to OAR's such as ipsilateral and contralateral lung, heart, contralateral breast, volume dose to ipsilateral lung and heart.

Results and Discussion: The mean volume of PTV_{Boost} and PTV_{Breast} were 102.62 cm^3 and 877.39 cm^3 for nine patients respectively. The target coverage (D_{95}) was similar for PTV_{Breast} in both plans, whereas in VMAT plans, the PTV_{Boost} received nearly one Gy more than the prescription dose. The mean and minimum dose to PTV_{Boost} were 62.08 ± 0.47 Gy and 57.57 ± 0.69 Gy for HT plans and for VMAT plans it was 62.51 ± 0.29 Gy and 57.50 ± 0.86 Gy. Minimum dose to PTV_{Breast} was 37.52 ± 3.26 Gy and 35.84 ± 2.96 Gy. The maximum dose to PTV_{Boost} was lower by 2% in HT plans than VMAT plans The plan quality parameter $D_{2\%}$ for PTV_{Boost} was lesser in HT plans compared to VMAT plans (63.78 ± 0.61 Gy vs 64.34 ± 0.41 Gy).The conformity (1.15 vs 1.21) and homogeneity (1.06 vs 1.07) index were better in HT plans compared to VMAT plans. The average beam on time was 7.57 min and 1.9 min for HT and VMAT plans. The mean dose to the heart, ipsilateral lung, contralateral lung and breast were similar in both plans. HT plan resulted in lower volume for heart dose, measuring 10, 30 and 40 Gy compared with VMAT (6.5% vs. 7.1%, 0.35% vs. 1.07%, and 1.97 vs 3.48%, respectively). The low dose volume (V_5) for heart in HT plan were 19.6% higher, whereas volume receiving 5 Gy for ipsilateral lung was 17% lesser in HT plans compared to VMAT plans.

Conclusion: HT plans produced plans of higher quality and conformal dose distributions, at the cost of longer planning and treatment times compared to VMAT plans.

O-36

BIOLOGICAL AND DOSIMETRIC EVALUTION OF FLATTENING FILTER FREE BEAM PLANS OVER FLATTENED BEAM BEAM PLANS IN HEAD AND NECK CANCER

K. K. D. Ramesh, Vyankatesh Shejal[1], Ch. Chandrasekhar Reddy, Rama Krishna

Department of Radiotherapy, Manipal Super Specialty Hospital, Vijayawada, Andhra Pradesh, [1]Department of Radiotherapy, Manipal Hospital, Bangalaru, Karnataka. India. E-mail: kkdramesh@gmail.com

Purpose: To quantitatively evaluate the Biological and Dosimetric differences in VMAT plans with Flattening Filter Free (FFF) and Flattened photon Beam (FB) in H and N cancers.

Materials and Methods: Treatment plans with volumetric modulated arc therapy were generated for 10 Head and Neck patients for both flattened and unflattened photon beams on Elekta Infinity linear accelerator with Agility MLC system using Philips Pinnacle® treatment planning system (V9.8). Beam energy of 6 MV was chosen for all cases and identical dose constraints, Arc angles and number of Arcs were used for both flattened and unflattened photon beams. The Gross Target volume (GTV) and planning target volume (PTVP) were contoured for the individual treatment plans. Total prescription was 60 Gy (54 Gy for PTVp and 60 Gy for GTV). In order to analyze the biological effectiveness of treatment plans, dose volume histograms (DVH) were utilized. Flattened and FFF beam plans are quantitatively compared.

Results: The FFF beam plans provided improved dose sparing compared to the flattened beam plans. Overall, the FFF beam provides lower mean and maximum dose and NTCP values to OARs.

Conclusions: In general, the treatment plans utilizing FFF beam can provide similar target coverage as that of flattened beam with improved dose sparing to OARs. Significant dose sparing effect is obtained for the cases involving relatively large field sizes due to lower dose to the out-of-field region compared to flattened beam.

O-37

USE OF PORTAL DOSIMETRY TO MONITOR TREATMENT CONSISTENCY FOR HEAD AND NECK CANCER THROUGHOUT THE COURSE OF TREATMENT

Sudesh Deshpande, Suresh Naidu, Vikram Mittal, R. Bajpai, V. Anand, V. Kannan

P.D. Hinduja National Hospital and MRC, Mumbai, Maharashtra, India. E-mail: sudeshpande72@gmail.com

Purpose: Use of portal dosimetry software to check treatment delivery consistency and to monitor changes in patient anatomy during course of treatment.

Materials and Methods: Varian portal dosimetry software and Electronic Portal Imaging Device (EPID) aS1200 were used to study consistency of treatment. Patients undergoing VMAT treatment for head and neck cancer were enrolled in this study. Patient plan was delivered after correcting set up error and transmitted images were acquired by the EPID aS1200 during the treatment. The transmitted dose images were acquired by EPID after the beam passes through patient. Images were acquired in continuous mode at source to imager distance SID = 150 cm on the 1, 2, 3, 5, 10, 15, 20, 25 fraction number. Before measuring transmitted dose images cone beam CT was performed to eliminate any set up error. Day one transmitted dose images were defined as base line images. On an average 8 images were acquired during treatment for each patient. These images were compared with base line image. Gamma index evaluation was performed with 1 mm and 1% parameter using Varian portal dosimetry software.

Result: For the first five images i.e. up to tenth fraction we got average gamma index passing 98.3% which is within action level threshold of 97%. We observed gamma passing percentage varies during fag end of treatment. For 18% of patient gamma passing variation was more than threshold level at fraction number 20.

Conclusion: Dosimetric measurement during treatment is good tool to investigate error during the treatment. Portal vision is mostly used for patient set up and pre treatment QA of patient. We found that portal dosimetry is useful tool for checking consistency of treatment delivery and monitoring changes in patient contours.

O-38

IDENTIFICATION OF EQUIVALENT LUNG VOLUME FROM 4DCT DATA FOR TREATMENT PLANNING AND DELIVERY IN SBRT OF LUNG CANCER

N. V. N. Madhusudhana Sresty, A. Mallikarjuna, T. Anil Kumar, A. Krishnam Raju

Basavatarakam Indo American Cancer Hospital and Research Institute, Hyderabad, Telangana, India.
E-mail: srestybarc@rediffmail.com

Introduction and Objectives: Motion correlated CT (4DCT) is frequently used for lung cancer cases and it is a most important requirement in SBRT of lung. Usage of conventional CT for lung tumor leads to several types of artifacts due to different respiratory phases and limited field of view. Most of the studies clearly demonstrated that, the lung tumor motion is very complex and hysteric in nature. Hence, patient specific motion correlated CT is highly essential for hypo fractionated SBRT planning to identify the internal target volume. But, there is a considerable lung volume variation with different phases of 4DCT. Again, these volumes are different from the ungated CT lung volume. This is an important factor for the cases which are suitable for Gating. Hence, the objective of this study was to determine the suitable lung volume for treatment planning purpose from the 4DCT data.
Materials and Methods: 10 patients of stage I non small cell lung cancer (NSCLC) were analyzed in this study. All cases were treated by hypo fractionated SBRT. 3D and 4DCT scans were taken using brilliance big bore CT unit (Philips Medical Systems, The Netherlands). 4D CT scans were done using Real time position management system (Varian Medical systems, Palo Alto, USA) and 4D imaging software available with our CT. In this procedure, a marker block was placed on the patient's thorax. The markers were tracked by infrared camera. The respiratory signals were recorded based on these reflecting markers during breathing. Coached breathing helped us for better scans. The 4D data sets were sorted out for ten phase bins (0% to 90% phases). We evaluated maximum intensity projection (MIP), average intensity projections (Avg. IP) and minimum intensity projections (Min I P) with all generated phases using brilliance software. All the CT data sets were then transferred to Eclipse treatment planning system (Varian Medical systems, Palo Alto, USA). Lung volumes were identified in all the data sets.
Results and Discussions: We found that the CT data of average intensity projections (Avg I P) is closely matching with 3D CT data, with a maximum difference of 3.2% of the total lung volume. Also, 20% phase and 80% phases looked similar to average intensity projection volumes with maximum variations of 1.8% and 2.7% respectively. The lung volume in MW was clearly less in all the cases with the maximum difference of 9.1%. This is due to the fact that, the ITV in MIP is created with the union of GTVs of all the phases.
Conclusions: The lung volume derived from either Avg. IP or mid inhalation phase or mid exhalation phase should be used in the treatment planning for lung cancer. Though, MIP is useful in the identification of ITV, this phase underestimates the lung volume. This method can be utilized for non gating treatment. But, proper data set selection is very important in the treatment planning if the patient is identified for gating based treatment delivery.

O-39

NOVEL METHOD OF ERROR REDUCTION IN QUANTIFYING THE SHIFT IN ISOCENTER USING LINE SPREAD FUNCTION APPROACH

C. Vineeth, Manoj S. Kumar, C. V. Midhun, M. M. Musthafa

Centre for Radiation Physics, University of Calicut, Calicut University, Malappuram, Kerala, India.
E-mail:cvineeth94@gmail.com

Purpose: Application of Line Spread Function in minimising the experimental errors associated with the QA test for verifying the accuracy of position of radiation isocentre in Radiotherapy. Conventionally 2 mm is accepted as the tolerance in fixing the isocentre.
Materials and Methods: Two sets of EBT3 Gafchromic films were irradiated in the conventional angles, one under the gantry star pattern configuration and the other in arc mode exposure using a needle, of 1 mm dia, placed at the isocentre along the gantry axis as shown in Figure 1. The error estimation for first film is done using conventional metre scale measurement and digitalised image processing method. The second set of film is analysed using LSF method using image processing. LSF is generated by the line shadow of the steel needle created in the film, which is fixed on EPID positioned at 105. The process is performed both in stationary mode and single full arc mode under identical condtion. The arc mode exposure is expected to produce broadening in the LSF, if there is any shift in central axis.

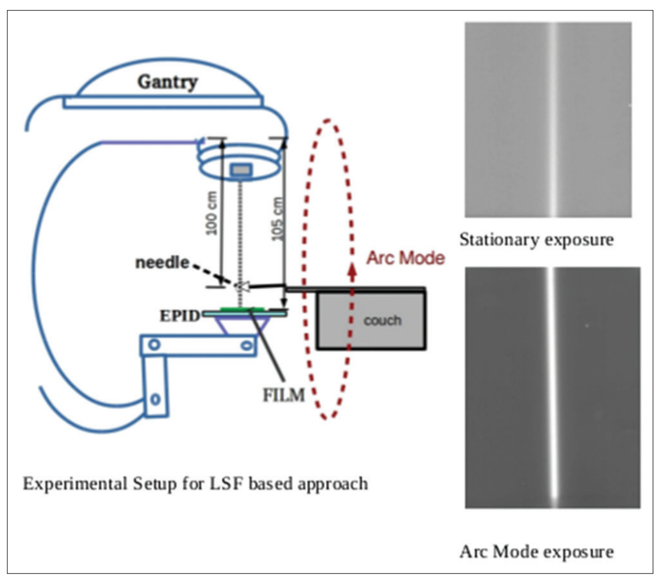

Figure 1: Schematic diagram of experimental setup and projections of needle in the stationary and arc mode exposures

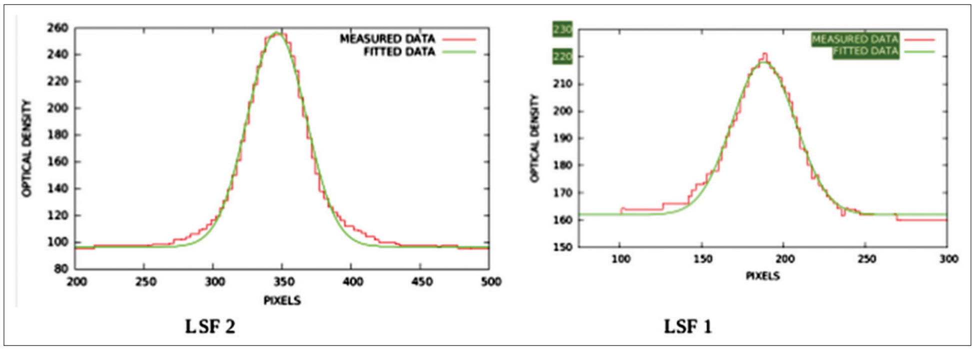

Figure 2: Gaussian fitted and measured line spread functions in the LSF based exposures

In the first conventional setup, width of the center darkness is measured with common metre scale having least count 1 mm for an image of size 2 mm leading to an estimation of 50% error. In the second method the above pattern is subjected to digitilization using a digital scanner having 300 dpi under normal mode. The image was processed using ImageJ™ software, based on the optical density profile of the region of interest. This results in a Gaussian distribution. This information is converted in ASCII format (8 bit) and reduced chi-square fit is performed. The pixels were converted into mm with 0.1 mm/pixel. The FWHM is evaluated as 1.6 mm with a relative error of 6.25% leading to an absolute error of 0.104 mm at the peak postion. This is significanly lesser in comparison with the error found in the conventional approach. In the third method, the second set of films are exposed under arc mode and stationary mode, the films are scanned and processed using ImageJ™ software and the crossline profile is generated for both cases and Gaussian fit is performed.The image is magnified to correspond 0.01 mm/ pixel. The FWHM of the LSF generated in stationary and arc mode are analysed as shown in Figure 2. The difference in width of LSF in each case is taken as the shift in isocentre. Present measurement gives a shift of 1.23 mm with an error of 0.141 mm and having percentage error of 7.1% leading to an absolute error of 0.01 mm.

Result: The error assosiated with the conventional star pattern tests are verified and shows a very higher relative error of 50% with absolute error of 1 mm. When it modifies with the digital verification through the chi-square minimized gaussian fits, the error then reduces into 6.25% with absolute error of 0.1 mm. With an approach of Line Spread Function (LSF), the absolute error reduces to 0.01mm. This leads to absolute errors in each case to 1 mm, 0.1 mm and 0.01 mm respectively. Using this approach, we can define the new limits for QA programme which is meaningful in present situations like SRS that demands sub-mm precesion.

Conclusion: The random error associated with conventional star pattern test is evaluated with chi-square minimized Gaussion fit on the digitalized cross line profile of the film increase the accuracy by one order. The LSF approach improves the accuracy by further one order leading to higher order accuracy in advanced radiotherapy procedure.

O-40

DEVELOPEMENT OF A CMOS-BASED OPTICAL COMPUTED TOMOGRAPHY SYSTEM FOR 3D RADIOTHERAPY DOSIMETRY

Nurul Farah Rosli, Hafiz Mohd Zin, Ahmad Taufek Abdul Rahman[1,2]

Oncology and Radiological Sciences Cluster, Advanced Medical and Dental Institute, Universiti Sains Malaysia, Penang, [1]School of Physics and Material Studies, Faculty of Applied Sciences, [2]Faculty of Applied Sciences, Universiti Teknologi MARA, Selangor, Malaysia.
E-mail: ahmadtaufek@salam.uitm.edu.my

Optical Computed Tomography (CT) is a bench top 3D imaging system for radiochromic PRESAGE dosimeters. The imaging system reconstructs dose distributions delivered to PRESAGE that changes its colour when irradiated. Alternatively, magnetic resonance imaging (MRI) may be used for imaging the dosimeter but MRI is not widely accessible. Current optical CT systems in the market are based on CCD image sensor and have slow imaging speed. The study characterises components in a CMOS-based optical CT imaging system developed in-house and investigates the feasibility of the system for imaging 3D radiochromic dosimeters. The study exploited recent advances in CMOS image sensor (CIS) technology to improve the imaging speed of the optical CT system. A rotary stage was constructed using a stepper motor to hold and rotate the dosimeter between the CIS and a large area LED. The components of the imaging system were integrated and controlled using LabVIEW (National Instrument, Austin, TX). A graphical user interface (GUI) was also developed to acquire projection images of the dosimeter. The measured field of view (FOV) of the CIS is 125 mm by 90 mm that can cover the whole PRESAGE dosimeter. A projection image can be captured at every 1.8 degree rotation of the dosimeter at every second that would amount to 200 projection images for a 360 degree rotation. Current limitation of the imaging speed is the rotation speed of the motor of 1.8 degree per second which can be improved with upgrading the stepper motor. At an imaging speed only limited by the maximum sensor frame rate of 28.5 fps, the scanning time will be reduced to 7 second compared to 200 second. A green dye solution of various concentration was used to mimic variation in PRESAGE colour from its response to radiation dose. The solution was filled in a plastic cylinder to study the linearity and uniformity of the system. The results show that the system is capable of capturing the projection images of a 3D translucent object with good linearity and uniformity. Further experiments will be carried out to optimise the development of the system to reconstruct dose distributions in 3D from a PRESAGE dosimeter.

O-41

MEASUREMENT AND COMPARISON OF SURFACE DOSE OF UNFLATTENED AND FLATTENED PHOTON BEAMS FOR DIFFERENT FIELD SIZES

P. Suresh Babu, Sebeerali, Daicy George, V. Ramya, S. Sowmya Narayanan

Department of Radiation Physics,
Vydehi Institute of Medical Science and
Research Centre, Bengaluru, Karnataka, India.
E-mail: sureshbabu_medphy@yahoo.com

Purpose: Flattening Filter Free (FFF) x-rays can provide more efficient use of photons and a significant increase of dose rate compared with conventional flattened x-rays, features that are especially beneficial for Stereotactic Radio Surgery (SRS) and Stereotactic Body Radiotherapy (SBRT). FFF x-rays are thought to offer dosimetric advantages such as reduced peripheral doses, out of field scatter doses and head scatter. The FFF beams contain more low energy components and have softer energy spectra than the corresponding flattened beams which can lead to increased dose in the build-up region. Meanwhile the FFF beams undergo less head scatter because the flattening filter is absent from gantry head of the linear accelerator, which may decrease the dose in the build-up region. Thus the two competing factors determine the build-up dosimetric characteristics of the FFF photon beams. The purpose of this study was to investigate the surface dose of FFF photons in the build up region and to compare it with that of conventional flattened photons.

Materials and Methods: Versa HD linear accelerator (Elekta Medical Systems, UK) has been in full clinical operation with 6MV, 10MV, 6FFF and 10FFF photons. Surface dose was measured using Markus parallel plate chamber (PTW Freiburg) with electrometer (PTW UNIDOSE) in solid water phantom. All four beams delivered for different field sizes ranging from 5 x 5 cm^2 to 30 x 30 cm^2. A solid water phantom (perspex slabs) was set up with SCD of 90 cm. The build-up depths for 6MV flattened and FFF beams were 0, 1, 2, 3, 4, 5, 16 mm and for 10MV flattened and 10 FFF beams were 0, 1, 2, 3, 4, 5 and 22 mm. We maintained 10 cm backscatter material. In this study surface dose is defined as the dose at a depth of 0.5 mm with respect to the dose at dmax.

Results: Surface dose increased linearly with field sizes for both FFF and flattened photons as shown in Figure 1. The FFF beams had marginally higher surface dose than flattened beams for smaller field sizes, but had lower surface doses for larger field sizes. The surface dose of 22.7% at 5 x 5 cm^2, 28.94% at 10 x 10 cm^2, 38.55% at 20 x 20 cm^2, 46.39% at 30 x 30 cm^2 for 6 MV flattened beam compare to 25.38% at 5 x 5 cm^2, 30.29% at 10 x 10 cm^2, 36.23% at 20 x 20 cm^2, 39.64% at 30 x 30 cm^2 for 6 FFF beams. Also, 16.58% at 5 x 5 cm^2, 23.83% at 10 x 10 cm^2, 35.56% at 20 x 20 cm^2, 43.51% at 30 x 30 cm^2 for 10 MV flattened beam and 21.15% at 5 x 5 cm^2, 26.15% at 10 x 10 cm^2, 31.86% at 20 x 20 cm^2, 34.65% at 30 x 30 cm^2 for 10 FFF beams as shown in Figure 2.

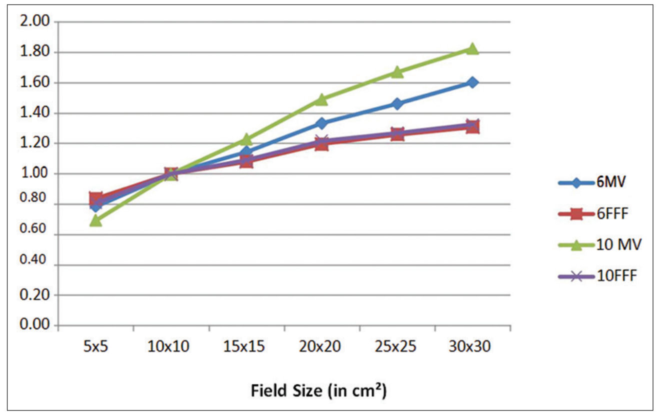

Figure 1: Relative Surface Dose normalized to the 10 x 10cm^2 reference field size

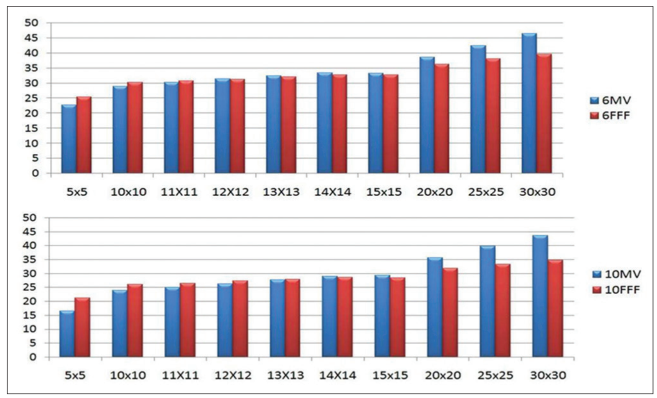

Figure 2: Variation of Surface doses with field size for flattened and FFF beams for jaw settings of 5 x 5 cm^2 to 30 x 30 cm^2

Conclusion: The FFF photons have a higher surface dose than that of the corresponding flattened photons for field sizes smaller than 10 x 10 cm^2 and lower surface dose for larger field sizes. It indicates that softer energy is more present in FFF beams whose contributions are proportionally more in smaller field sizes. For larger field sizes, in flattened beams the filter contribution itself is very larger results in higher scattered electrons. Though FFF tends to give higher surface dose as compared to FF beams for smaller field sizes, the overall surface dose values are well within the prescribed limit. Hence higher surface dose levels in FFF beams may not yield clinical significance.

O-42

DETERMINATION OF STEREOTACTIC SMALL FIELD OUTPUT FACTORS WITH DIFFERENT DETECTORS

Seby George, Henry Finlay Godson, A. Sathish Kumar, Y. Retna John, B. Paul Ravindran

Department of Radiotherapy, Christian Medical College, Vellore, Tamil Nadu, India. E-mail: sebageo7@gmail.com

Introduction: Accurate dosimetry of small photon fields in modern radiotherapy is challenging due to lateral electronic disequilibrium, partial occlusion of source, steep dose gradients, and size of the sensitive volume of the detector as well as itscomposition. These challenging effects instigated an investigation on the acquisition of output factor with different type of detectors.

Objectives: To determine the output factor for small radiation fields defined by micro multi-leaf collimator and circular

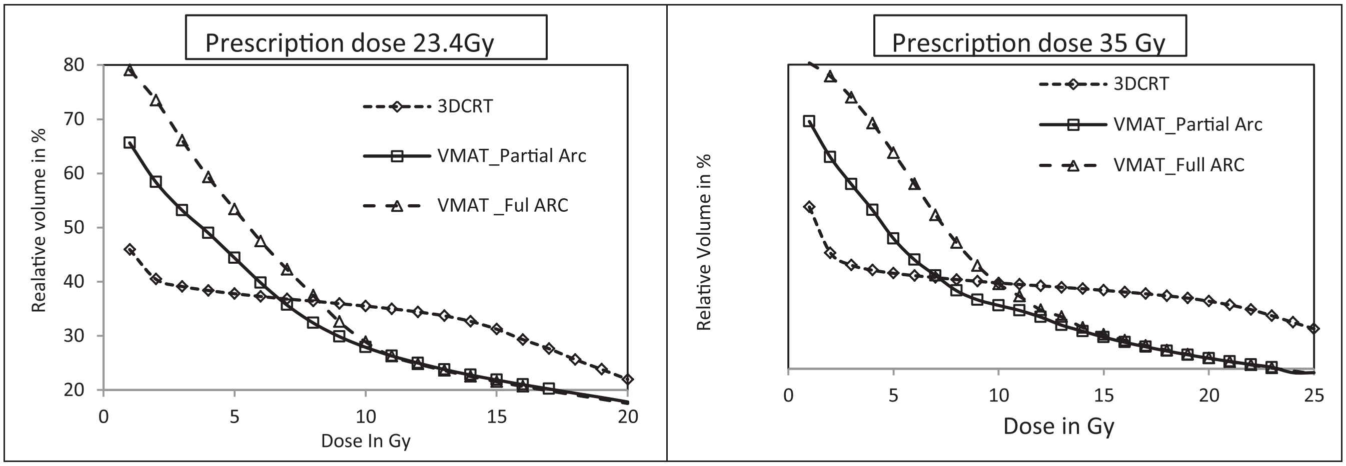

Figure 1: Comparison of output factors for the fields shaped by BrainLab circular cones with different detectors

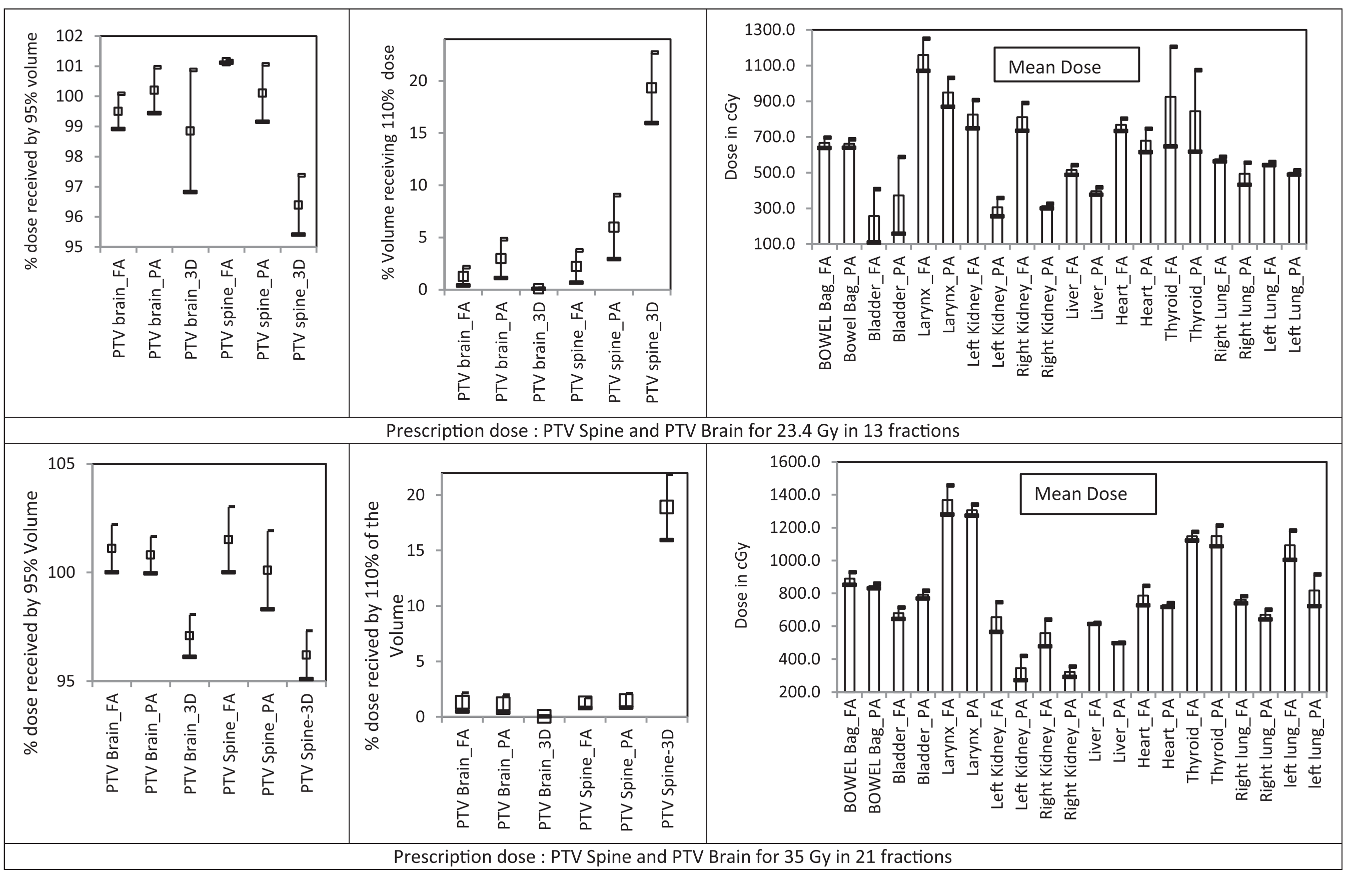

Figure 2: Comparison of output factors for the fields shaped by BrainLab mMLC with different detectors

cones with different types of detectors and decide on the appropriate detector for small field dosimetry.

Materials and Methods: Small field output factor measurements were carried out using 6 MV photon beams in Primus linear accelerator with BrainLab mMLC and circular cones as add-ontertiary collimators. PTW microDiamond, PTW SRS diode and PTW pinpoint ion chamber were used toacquire output factors of square fields (0.6 x 0.6 cm^2 to 10 x 10 cm^2) and circular fields (1 cm to 4 cm diameter) defined by BrainLabmMLC and circular cones respectively. Output factors were measured with a source-to-surface distance of 100 cm at a depth of 10 cm in PTW MP3 RFA for all measurements.

Results: The data obtained with different detectors show differences in output factor for all collimating systems. Good agreement in output factors of BrainLab mMLC and circular cones were observed in field sizes greater than ~ 2 x 2 cm^2 for all detectors and all tertiary collimators. The spread in output factors of different detectors with PTW microdiamond reference values for the stereotactic fields shaped by BrainLab circular cones is depicted in Figure 1. For the smallest cone (1 cm diameter), pinpoint ion chamber underestimate the output by 4.8% whereas SRS diode overestimate the output factor by 1.7% when compared to PTW microdiamond detector. The influence in output factors for small fields due to the presence of BrainLab mMLC as add-on accessory to the Primus linear accelerator is depicted in Figure 2. For the smallest field (6 x 6 mm^2) defined by BrainLab mMLC, an underestimation of 23.9% and an overestimation of 1.9% were noticed with pinpoint ion chamber and SRS diode respectively.

Daisy chaining method has been adopted to correct the over response of SRS diode detector in the determination of output factors of circular fields and square fields. The output factors obtained with SRS diode were compared with the reference value (PTW microdiamond detector) and the percentage deviation has been reduced to 0.7% and 0.2% for 1.0 cm and 1.5 cm diameter cone respectively.

Discussion: The microDiamond detector has shown to be a promising detector for the measurements of output factors in small fields. The sensitive volume of the microDiamond detector is relatively large and exhibits volume averaging effect. But this effect is partially compensated by the over-response of the detector due to the presence of high density material. The volume averaging across the beam due to the relatively large sensitive volume is the main cause for the lower values measured with pinpoint ion chamber. The over-response noticed with diode detector in small fields is due to the presence of a high density silicon chip and the non-water equivalency of the dosimeter.

Conclusion: The output factor values were observed to be highly dependent on the configuration of secondary and tertiary collimator and the position of detector as well. Monte Carlo simulation with appropriate codes would improve the accurate determination of output factors while eliminating the experimental uncertainties.

O-43

QUALITY ASSURANCE PROGRAM AT DURHAM REGIONAL CANCER CENTER, ONTARIO CANADA

D. Patel[1], M. D. Jensen[1,2], D. Mason[1]

[1]Radiation Oncology Medical Physicist, R. S. McLaughlin Durham Regional Cancer Centre, Lakeridge Health, Oshawa, [2]Department of Radiation Oncology, University of Toronto, Ontario Canada. E-mail: dpatel@lakeridgehealth.on.ca

A comprehensive quality assurance (QA) program is an essential component of safe and effective radiation oncology practice. The objective of this presentation is to provide an overview of the QA program of the Durham Regional Cancer Centre (DRCC), a clinic that delivers approximately 2700 courses of radiation therapy per year in Ontario Canada.

The DRCC radiation oncology program is subject to regulatory requirements from the national nuclear energy regulator, and provincial health and labour authorities, who stipulate a set of safety requirements for the QA program to meet. However, the larger quality assurance program is based on guidance documents created by an alliance of the radiation treatment professional societies (physicians, physicists, therapists) in Canada, known as the Canadian Partnership for Quality Radiotherapy (CPQR). The Technical Quality Control Guidelines published by CPQR, available free of charge, provide the technical basis from which the quality control (QC) procedures for the radiotherapy equipment at DRCC are based. The technical QC results are monitored and reported to the local Radiation Treatment Quality Assurance Committee, as recommended by CPQR. The committee oversees all quality within the radiation program, including monitoring of quality indicators, incident reporting, and staff's maintenance of certification.

A set of software forms the core of the QA program documentation. Sharepoint manages the lifecycle of the policies, procedures and forms of the QA program, as well as the assignment and tracking of recurring (monthly or less frequently) QA tasks to physicists and physics associates. QATrack+ is a free, open source, QA database platform used to collect the results of QC procedures, including daily morning tests performed by the therapists. QATrack+ includes simple reporting and plotting, and is built on a modern database allowing for 3rd party reporting software if necessary. Email notifications are generated when QC tests fall outside of tolerance limits, alerting the physics team to potential issues. Finally, physicist activity (projects and machine QC) are logged in a weblog, powered by the free and open-source software package elog. This provides a central, searchable and widely accessible platform for documenting physics activities. Service engineer activity is currently logged in hard-copy log books, but online logging is being investigated. Results of technical QC performed on the equipment are reviewed weekly and monthly by a physicist. Each treatment unit is assigned to a primary physicist, who has responsibility for ensuring QC activities and resulting actions are completed. Annual QC testing is also the responsibility of the primary physicists. Independent review of the annual QC is completed by a different physicist in the group. External review and comparison occurs through several activities, such as output and IMRT planning tests with IROC, and planning and delivery comparisons against other centres in Ontario.

The quality assurance program at DRCC is constantly evolving to meet the requirements of the clinic and nation and provincial regulations and guidelines. For example, the program is shifting many tests to Doselab EPID-based collection, which eliminates the need for special devices and allows faster collection and analysis of VMAT-related QA measurements. Further refinements are continually being made based on the data analyzed from the software databases. Continuing improvement of the QA program is a vital part of providing safe and effective radiation treatment.

O-44

STUDY ON THE MEASUREMENT OF SURFACE AND BUILDUP DOSES USING DIFFERENT IONIZATION CHAMBERS

E. Sreedevi, C. O. Clinto, P. S. Renilmon, S. Sneha, Raghavendra Holla, Bhaskaran K. Pillai

Department of Medical Physics and Radiation Safety, Amrita Institute of Medical Sciences, Kochi, Kerala, India. E-mail: krishnansreedevi@yahoo.com

Introduction: In the measurement of surface and buildup doses, active volume and the electric field inside the chamber play an important role. According to the difference in chamber design (parallel plate or cylindrical), arrangement of field lines inside the chamber varies. The role of volume becomes vital if the region of measurement is a steep gradient one. Any detector will average the dose over its volume. If the dose varies over the volume of the detector, this average effect can give a different signal compared to the signal obtained by a point detector. Both the above factors can cause considerable differences in their responses in a gradient region.

Objective: The goal of this work was to study the effect of different ion chambers on the measurement of surface and buildup region doses.

Materials and Methods: A 30 x 30 x 30 Water phantom with a fine micrometer alignment tool was positioned on the treatment couch of Elekta Synergy® Linear accelerator with field size 10 x 10 in SSD 100 cm. For analyzing the volume effect, cylindrical chambers 0.01 cm^3 (SCANDITRONIX WELLHOFER CC01), 0.125 cm^3 (TN31010, PTW-Freiburg) and 0.6 cm^3 (TN30013, PTW-Freiburg) were used. The parallel plate chamber 0.4 cm^3 (IBA PPC 40) was also used to compare the field gradient effect. Cylindrical chambers 0.6 cm^3, 0.125 cm^3 and 0.01 cm^3 were centrally aligned with their effective point of measurement (0.6 rcavfor photons and 0.5 rcav for electrons as per recommendation). Phantom was exposed with 6MV, 4MV photons and 6MeV, 8MeV electrons. The same alignment can be done for the buildup region also. Meter readings were noted and the doses were calculated for both the positions by correcting for temperature, pressure, polarity and saturation. The above measurements were done with a parallel plate chamber of volume 0.4 cm^3 (PPC 40) where the effective point at the front surface of the cavity. Most detectors will show a slight dose rate dependence. It should be considered before performing the measurement.

Results and Discussion: As the volume of the chamber increases, the dose averaging effect also increases. Larger volume underestimates the point dose in gradient regions like surface or buildup region. The gradient effect of electric field is more for cylindrical chamber because of its design. And these effects were observed much significant at the surface. As per the recommendation, for parallel plate chambers the effective point of measurement is at the inner face of the front plate and for cylindrical one, it is displaced 0.6 rcav for photons and 0.5 rcav for electrons from the center. Even with this recommended shift, observed a difference in doses at both surface and buildup region. With a guard electrode, parallel plate chambers are having a uniform field strength throughout the volume. In cylindrical geometry, electric field is not constant (E= -grad V). This can cause a difference in their responses.

O-45

IMPACT ON GAMMA INDEX ON MEASUREMENT WITH TWO DIFFERENT ARRAY DETECTORS

S. Praveenkumar, M. Muthukumaran, Mariyappan

[1]Department of Radiation Oncology, Apollo Speciality Hospital, Chennai, Tamil Nadu, India.
E-mail: praveenmedicalphysicist@gmail.com

Objective: The Feasibility of estimating Patient – Specific Quality Assurance is the predominant solution for VMAT Quality Assurance. The main objective of the study is to analyze the Gamma Index prediction Accuracy for small field VMAT patients with two different Detectors.

Materials and Methods: Thirty patients of 6MV of FF Beam with Field Size of less than 10 × 10 cm^2 who underwent VMAT in our Facility were retrospectively selected. VMAT plans were created using Eclipse Treatment Planning System and were transferred to a Varian True beam STx which has HD 120 MLC configuration. The Measurements have been taken with an Octavius 4D Phantom which motorized and cylindrical which has diameter of 320 mm and length 343 mm. The density of the phantom is 1.05 g/cm^3.

The detector of Octavius 729 detector which has large field coverage and better detection of hot spots is selected and Octavius Detector 1000 SRS which has liquid filled ionization chambers with presized detector spacing is selected.

The measurements have been analyzed with the PTW Verisoft software. Hence, using all these we study the Impact of Gamma Index on both the Detectors. The Gamma Index pass Rates were evaluated under 3% 3 mm and 2% 2 mm criteria with a Threshold of 10%. 2D Gamma, 3D Gamma and 3D volume Gamma for both Local and Global is verified.

Results and Discussion: The Gamma Index pass rates in the planes of Coronal, Sagittal and Transversal is analyzed. We compare the results of both the detectors. As the result, the Gamma Index passing rates is higher due to the High Spatial Resolution and High Accurate Dose measurements of very small regular and irregular fields and regions with steep dose gradient in 1000 SRS is slightly greater than that of Octavius Detector 729. In SRS 1000 Detector the passing rates for both local Gamma and Global Gamma is very much higher in all planes.

Conclusion: Based on our study and Results obtained with two different detectors, we can infer that the Octavius 1000 SRS predicts the better Gamma passing percentage for the small field VMAT Patient- Specific Quality Assurance.

O-46

VOLUMETRIC MODULATED ARC THERAPY DOSIMETRY QA USING LIQUID IONISATION CHAMBER

Nitin R. Kakade, Rajesh Kumar, S. D. Sharma, Sudesh Deshpande[1], D. Datta

[1]Radiological Physics and Advisory Division, Bhabha Atomic Research Centre, [2]P.D. Hinduja Hospital and Medical Research Centre, Mumbai, Maharashtra, India.
E-mail: ni3kakade@gmail.com

Introduction: Volumetric Modulated Arc Therapy (VMAT) is an advanced radiotherapy technique capable of producing complex dose distribution in single or dual arc rotation. It improves the conformity as well as delivers homogeneous dose to target volume. Because of the presence of steep dose gradient between target volume, organ at risks and normal structures as well as the contribution of manifold intensity modulated small fields approaching from different directions, it becomes essential to perform pre-treatment dose verification using a suitable detector. Pre-treatment dose verification of VMAT using liquid ion chamber can enhance the confidence for precise and accurate dose delivery from the complex techniques.

Objective: To explore practicability of a liquid ionization (LIC) chamber (PTW microLion) for dosimetry QA in an advanced radiotherapy techniques such as VMAT.

Materials and Methods: The PTW microLion liquid ionization chamber having sensitive volume of 0.0017 cm^3, filled with isooctane liquid was used for this study. The stand-alone high voltage supply and calibrated UNIDOS webline electrometer was used for charge measurement. The LIC was polarized at 800 V. All the measurements were performed with Varian TrueBeam linear accelerator for 6 MV filtered photon beam. The dosimetric characteristics which include repeatability, sensitivity, dose response, monitor unit linearity, dose rate dependence and output factor were studied. The repeatability and sensitivity of 0.13 cc air ion chamber (AIC) was also studied and sensitivity of both detectors was compared. Dose rate dependence of LIC was studied with dose rates of 60, 100, 200, 300, 400, 500 and 600 MU/min. The LIC was cross calibrated against the 0.13 cc ion chamber in two different orientations: the LIC was positioned such that the beam was parallel to the detector axis (axial orientation) and perpendicular to the axis (perpendicular orientation) with the sensitive volume centred at 0.975 mm from the entrance window. The perpendicular orientation calibration factor was applied for pre-treatment dose verification. All the measurements were performed in 1D Scanner water phantom at 5 cm depth with a source to surface distance of 100 cm for field size of 10 x 10 cm^2. For pre-treatment dose verification, a dedicated insert was fabricated to incorporate LIC at proper location in the IMRT thorax phantom. The insert was able to replace with insert which can incorporate 0.13 cc ionization chamber. This heterogeneous thorax phantom consists of different materials, representing tissues inside the thorax: lungs, spinal cord and soft tissue. The computed tomography scans of phantom were send to treatment planning system (TPS) and planned dose were recalculated. The five treatment plans of different sites were chosen for this purpose and absolute point dose measurement were performed using LIC and AIC respectively. The TPS calculated and measured dose were compared.

Result: The sensitivity of LIC and AIC in perpendicular orientation was found to be 10.14 and 3.47 nC/Gy respectively. The response of the LIC was 2.92 fold more than the AIC. The repeatability and output factor of LIC was found to be within 0.02% and 0.76% respectively. The percentage difference between the TPS calculated and measured dose ranges from -0.84 to +1.46 and -2.29 to +2.05 for LIC and AIC respectively.

Discussion: The liquid ionisation chamber results appear closer to TPS calculated dose in comparison to air ionisation chamber. It may be attributed to small sensitive volume of LIC. The study also confirms that the liquid filled ionization chamber may also be a suitable detector for pre-treatment dose verification of VMAT.

O-47

DOSIMETRIC CHARACTERISTICS OF DIGITAL MEGAVOLT IMAGER FOR FLATTENING FILTER FREE BEAMS

S. Vendhan[1,2], R. Murali[2], N. Arunai Nambiraj[3], M. Muthukumaran[1], S. Saraswathi Chitra[1], V. Murali[1]

[1]Department of Radiation Oncology, Apollo Cancer Institute, Chennai, [2]Department of Physics, School of Advanced Sciences, VIT University, [3]Centre for Biomaterials, Cellular and Molecular Theranostics, VIT University, Vellore, Tamil Nadu, India. E-mail: subramanivendhan@yahoo.co.in

Introduction: New amorphous silicon based electronic portal imaging device (aS-EPID) called Digital Megavolt Imager (DMI) (aS1200) has higher pixel resolution (0.34 mm) and increased active area (40 x 40 cm^2) than its predecessor aS1000 (0.39 mm and 40 x 30 cm^2). The new aS1200 detector panel is also capable to acquire dosimetric (integrated over all frames) images of Flattening Filter Free (FFF) beams at higher dose rates.

Objective: To evaluate the dosimetric characteristics of aS1200 megavolt (MV) detector for flattening filter free (FFF) beams.

Materials and Methods: Recently commissioned Varian Truebeam SVC linear accelerator at our clinic is equipped with aS1200 MV detector panel. The dosimetric response of the detector for 6X-FFF beam was tested and evaluated for its signal saturation, linearity with dose, dose-rate dependence, change in Source-Detector Distance (SDD), signal lag (ghosting), and back scatter contribution from imager Exact-arm (E-arm).

To evaluate the linearity, detector was positioned at 100 cm SDD, irradiated with 6X-FFF beams at the maximum available dose rate (1400 MU/min) and dosimetric images were acquired for 3 different square fields (3 x 3 cm^2, 10 x 10 cm^2 and 40 x 40 cm^2) irradiated with 5, 10, 15, 20, 25, 50, 75, 100, 150, 200, 250, 300, 400, 500, 750 and 1000 monitor units (MU). 100 MU were delivered at various dose-rates 400, 600, 800, 1000, 1200 and 1400 MU/min for field sizes 3 x 3 cm^2, 10 x 10 cm^2 and 40 x 40 cm^2 and acquired images were analyzed for dose-rate dependency. Change in detector response with SDD were studied by acquiring images for 100 MU at various SDD ranging from 100 cm to 150 cm for 3 different field sizes (3 x 3 cm^2, 10 x 10 cm^2 cm to and 25 x 25 cm^2) at 1400 MU/min dose-rate. The effect of signal lag was evaluated at both minimum (400 MU/min) and maximum (1400 MU/min) dose-rates by acquiring 3 images of 100 MU each: a 30 x 30 cm^2 (reference image), next after five minutes with a 15 x 15 cm^2, followed immediately by irradiating second 30 x 30 cm^2 (ghost image) and measuring residual signal left in it. The MUs were increased to 250 and 500 for 15 x 15 cm^2 field and the intensity of ghosting effect was studied. Dosimetric

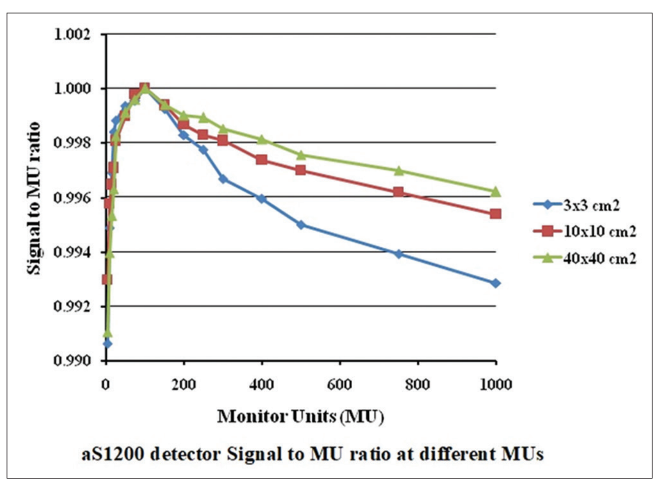

Figure 1: aS1200 detector Signal to MU ratio at different MUs

images were acquired for 100 MU at different field sizes >8 x 8 cm^2 and the ratio of detector signals at ±3 cm from the center pixel along the Gun-Target direction was calculated to evaluate back scatter contributions from imager support arm. Recommended setting of 2 mm x 2 mm Region of Interest (ROI) was used throughout the study to sample the dose in the detector.

Results and Discussions: The detector signal to MU ratio drops drastically at lower MUs below 25 MU. For irradiations between 50 to 1000 MU, the signal to MU ratio varies within 0.7% and reaches maximum at 100 MU for all field sizes as shown in Figure 1. The detector linearity with dose is within 1% and no evidence of signal saturation as such. The aS1200 response variation across various dose rates and SDD for all field sizes is <0.4% and <0.2% respectively. The effect of ghosting increased distinctly at higher dose rate but however it is negligible (0.1%). The impact of back scatter at all field sizes is <0.3% because of additional shielding provided at the back of the detector.

Conclusion: Our initial study results on dosimetric characteristic of DMI detector at high dose rate FFF beams has shown its potential ability as a pretreatment verification tool for FFF beams.

O-48

STUDY ON RADIOLOGICAL PROPERTIES OF WOODEN DUST AS A SUBSTITUTE OF LUNG FOR THE DOSIMETRIC PURPOSE

Priyusha Bagdare, Swati Dubey, Om Prakash Gurjar[1]
School of Studies in Physics, Vikram University, Ujjain, [1]Roentgen-SAIMS Radiation Oncology Centre, Sri Aurobindo Institute of Medical Sciences, Indore, Madhya Pradesh, India. E-mail: priyushabagdare@gmail.com

Introduction: The thoracic cavity poses complexity in accurate dosimetry due to its curved topology and heterogeneity coupled with inner organ motions. The heterogeneity in thoracic region arises mainly due to the combination of chest wall, lung and soft tissue behind the lung. In order to quantify the dose delivered to a tissue of interest, the measurement is done on the phantom. As ~ 65% of human body consists of water, thus the phantoms suggested for dosimetry are homogenous and water equivalent whereas human body comprises of varied densities which make it complex heterogeneous medium.

To develop such a heterogeneous phantom there is a need of material which can mimic the heterogintiеs inside the thoracic cavity. Present study focuses on determination of radiological properties of wooden dust which can represent the lung part of thoracic cavity and can be use for designing thoracic phantom in future.

Objective: To study the radiological properties of wooden dust using 6 mega voltage (MV) photon energy.

Materials and Methods: Density of wooden dust of pine and thoracic region of patient were calculated by Hounsfield units (HU) measured from computed tomography (CT) images of each medium. The depths of isodose curves of 100%, 95%, 90%, 85%, 80%, 75%, 65%, 60%, 55% and 50% were measured in CT images of both the mediums on TPS for 10 × 10 field size. Photon beam of 6 MV energy with field size 5 × 5, 7.5 × 7.5, 10 × 10, 12.5 × 12.5, 15 × 15 and 17.5 × 17.5 cm^2 was incident on CT images of chest wall and on combination of slab wooden dust slab (SWS) perpendicular to the surface as shown in Figure 1. Dose at depth 4 cm and 10 cm with field size 5 × 5, 7.5 × 7.5, 10 × 10, 12.5 × 12.5, 15 × 15 and 17.5 × 17.5 cm^2 were measured on CT images of patient and in the combination of SWS using anisotropic analytical algorithm (AAA) on treatment planning system (TPS). Same measurements were taken on linear accelerator (LA) for the SWS combination with the help of ionization chamber.

Results and Discussions: The mean density of wooden dust, slabs, soft tissue, chest wall and lung was found to be 0.271, 0.994, 0.980, 0.947 and 0.287 gm/cc respectively. The isodose depth (of 100%, 95%, 90%, 85%, 80%, 75%, 65%, 60%, 55% and 50%) for patient (1.53, 2.97, 4.23, 5.57, 7.39, 9.52, 11.28, 12.82, 14.42, 15.95 and 17.66 cm) and for SWS (1.47, 2.92, 4.14, 5.43, 7.05, 9.03, 11.19, 13.75, 16.83, 20.15 and 23.85 cm) are approximately same. The mean percentage variation between planned dose on CT images and combination of SWS at depth 4 cm and 10 cm for field size 5 × 5, 7.5 × 7.5, 10 × 10, 12.5 × 12.5, 15 × 15 and 17.5 × 17.5 cm^2 were found to be -0.3079 and -0.4599 respectively. The mean percentage variation between planned and measured dose for combination of SWS at depth 4 cm and 10 cm for field size 5 × 5, 7.5 × 7.5, 10 × 10, 12.5 × 12.5, 15 × 15 and 17.5 × 17.5 cm^2 were found to be -0.0453 and 0.0236 respectively.

Conclusion: The radiological properties of wooden dust are found to be equivalent to that of lung, thus it can be use as a lung substitute for designing chest phantom in future.

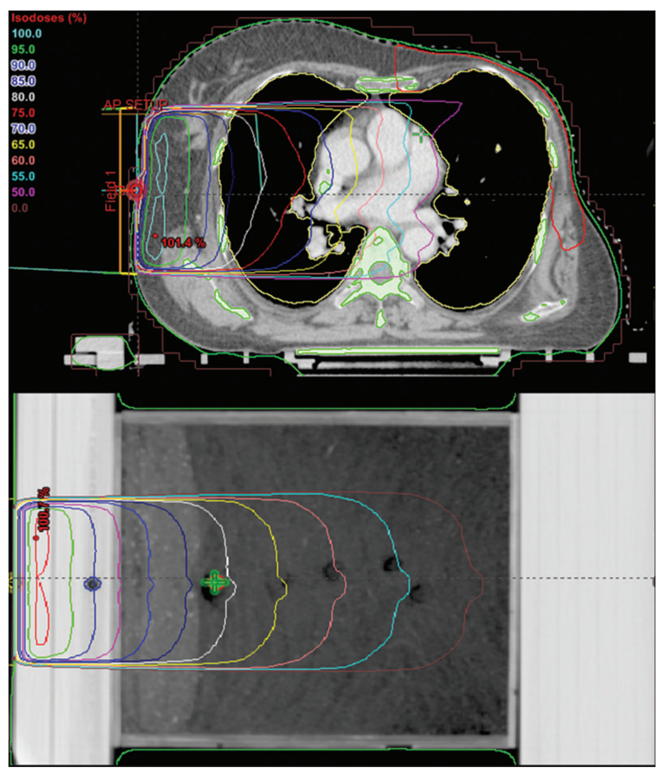

Figure 1: Isodose curves in CT slice of actual patient and in combination of slab-wooden dust-slab

O-49

EVALUATION OF SETUP UNCERTAINTIES AND CLINICAL TARGET VOLUME TO PLANNING TARGET VOLUME MARGIN FOR VARIOUS TUMOR SITES WITH VMAT TREATMENTS USING CBCT

Dilip Kumar Ray, Srimanta Pramanik[1], Poonam Ray[2], Arko Choudhury[1], S. K. Asik Iqbal[1], Amithabh Roy[1], Sayan Kundu[1], Sandip Sarkar[1]

Department of Medical Physics, Chittaranjan National Cancer Institute, [1]Department of Medical Physics, Ruby General Hospital Ltd., [2]BC-185, Sudha Apt. Samarpally, Krishnapur, Kolkata, West Bengal, India.

E-mail: dkray.cnci@gmail.com

Objective: The aim of this study was to determine the patient setup errors for different tumor sites based on clinical data for the treatment of volumetric arc therapy (VMAT) using pre-treatment verification with KV-CBCT and also we found out the institutional based CTV to PTV margin for various sites based on an analysis of systematic and random errors.

Materials and Methods: In this study the tumor sites were divided in three categories 1) Head and Neck (37 number of patients), 2) Thorax (18 number of patients) and 3) prostate (17 number of patients). All the patients underwent pretreatment verification by KV-CBCT imaging for the determination of overall distributions of setup corrections in the directions of anteroposterior (Z), mediolateral (X) and craniocaudal (Y) with 3D vector length and also CTV to PTV margins were analyzed from ICRU 62, Stroom's and Van Herk's formulas.

Results and Discussions: The displacements were within ±3 mm in 14.28% case in anteroposterior direction (AP), in 15.58% case in mediolateral direction (ML), and in 11.03% cases in craniocaudal direction (CC) for H and N tumor. For thorax lesion the displacements within ±3 mm in 16.32% case in (AP) direction, in 17.14% case in (ML) direction, and in 18.77% cases in (CC) direction. The displacements were within ±3 mm in 14.07% case in (AP) direction, in 21.97% case in (ML) direction, and in 15.06% cases in (CC) direction for prostate tumor as presented in Figure 1. The cumulative frequencies of 3D vector length of ≥5 mm were rare for Head and Neck (H and N) but more common for thorax and prostate case at 9.79% and 12.83% respectively. The largest magnitude of systematic error for H and N, thorax and prostate lesions were 0.129 cm in vertical (Z) direction, 0.148 cm in longitudinal (Y) direction and 0.144 cm in lateral (X) direction respectively. The largest magnitude of random error for H and N, thorax and prostate lesions were 0.167 cm in lateral (X) direction, 0.290 cm in longitudinal (Y) direction

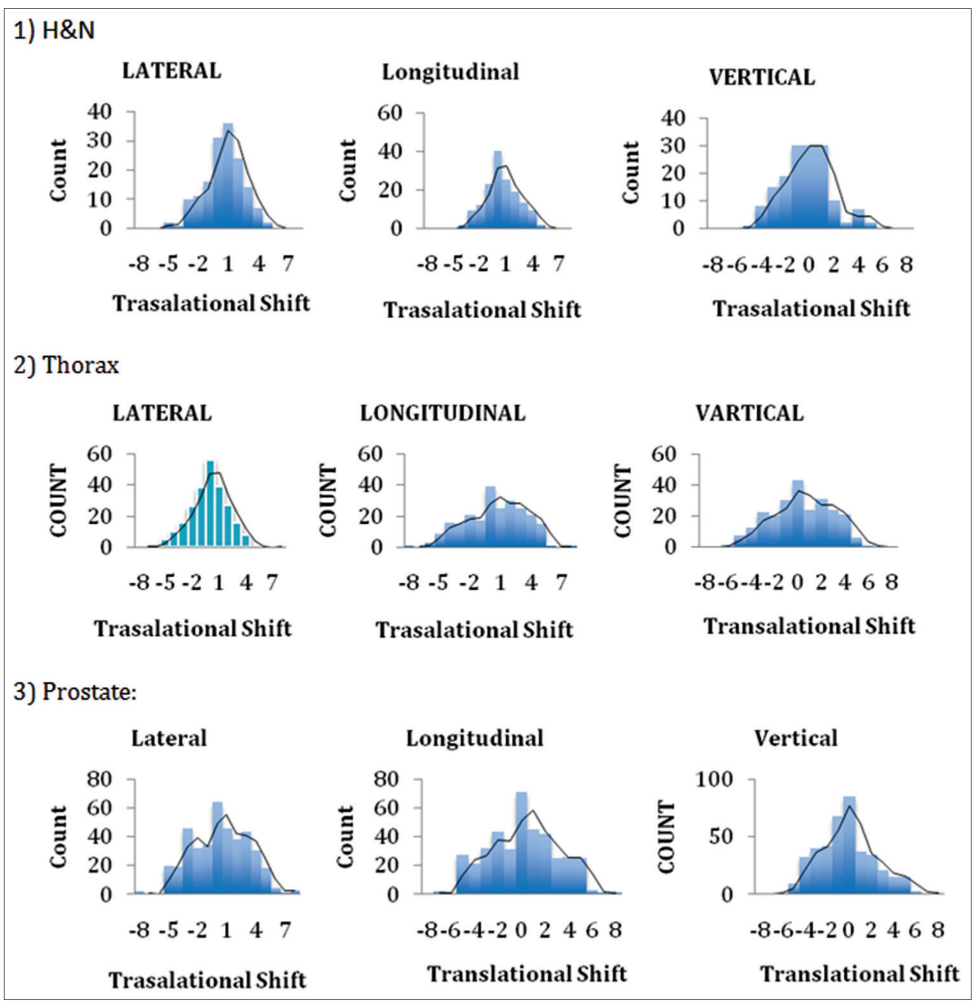

Figure 1: systematic error for H and N, thorax and prostate lesions in vertical (Z) direction, longitudinal (Y) direction and lateral (X) direction. (1) H and N, (2) Thorax, (3) Prostate

and 0.303 cm in longitudinal (Y) direction respectively. The CTV to PTV margins for H and N calculated by ICRU formula were 2.34 mm, 2.32 mm and 2.39 mm; by stroom's formula they were 3.50 mm, 3.51 mm and 3.68 cm; by van Herk's formula they were 4.1 mm, 4.10 mm and 4.33 mm (X, Y, Z directions). The CTV to PTV margins for thorax calculated by ICRU formula were 2.44 mm, 3.51 mm and 2.81 mm; by stroom's formula they were 3.43 mm, 4.98 mm and 3.93 cm; by van Herk's formula they were 3.93 mm, 5.72 mm and 4.50 mm (X, Y, Z directions). The CTV to PTV margins for prostate calculated by ICRU formula were 3.33 mm, 3.49 mm and 2.76 mm; by stroom's formula they were 4.76 mm, 4.86 mm and 3.91 cm; by van Herk's formula they were 4.76 mm, 4.86 mm and 3.91 mm (X, Y, Z directions).

Conclusion: For the better target coverage and dose distribution, van Herk calculated CTV to PTV margin is adequate for most of the tumor site except SRS and SRT for brain tumor. The establishment of institutional based PTV margins and reducing of setup uncertainties frequently CBCT is essential because setup errors vary according to each immobilization systems, patients and daily setup.

O-50

RADIOTHERAPY WITH TELE-COBALT MACHINE: EFFICACY AND NEED FOR TISSUE COMPENSATION IN HEAD AND NECK TREATMENTS

Ramamoorthy Ravichandran

Cachar Cancer Hospital and Research Centre, Silchar, Assam, India. E-mail: ravichandranrama@rediffmail.com

External Beam Radiotherapy (EBRT) remains the mainstay for radical treatments, in malignancies in head and neck regions. Head and Neck malignancies form around 50% of radiotherapy patients in the north eastern parts of the Indian subcontinent. Because of less inter-field separations, the penetration requirements of the treatment plans makes the telecobalt beam sufficient for executing radiotherapy, with proper immobilization and use of wedges if required. Inter-field thickness variations and irregular contour affect uniformity in delivered doses, and adverse reactions are encountered because of skewed isodose curves seriously affecting the volume dose variations in treatment planning. Normal tissue reactions, affect effectiveness of the treatment and therefore deter the Quality Of Life (QOL).

EBRT with a telecobalt machine (Theratron 780C) started in 2006 and completed a decade at our centre. About 15 patients per day receive radiotherapy for head and neck treatments. To overcome skin reactions and excess dose due to small contour of neck, a need was felt to introduce tissue compensation. Ellis type tissue compensation using 1 cm thick Aluminum metal is introduced. The tissue deficiency is measured by an L shaped gridded type Lucite frame work. For individual patients the custom type compensator tray is prepared on a Lucite plate, mountable in the shadow tray of the cobalt machine. The attenuation coefficient of metal rods $\mu = 0.1462$ cm^{-1} (1cm Al = 2.57 cm water). A simple type of POP immobilization is prepared in place of thermoplastic immobilization shell. The Lucite mounting tray has attenuation about 4%.

Lateral opposing fields with compensation reduced resultant isodoses 180% and 170% in neck and chin levels to 150% with uniform tumor volume homogeneous dose of 160%. Portal radiographs with and without compensator showed uniform tissue irradiation, also a method to verify field positions. This method is applied to all the head and neck radiotherapy patients receiving lateral field treatments. So far about 40 patients completed full course of radical radiotherapy with least skin morbidity, and overdose effects significantly brought down. This makes telecobalt treatments more effective, good patients compliance and this plan could be feasible in all centres. In the era of high technology radio-therapy, these type of innovations at hospital level promotes cost-effective radical treatments to cancer patients, because cancer care all over the globe becomes unaffordable.

O-51

EVALUATION OF CBCT AND 4DCT BASED PLANNING TARGET VOLUMES IN NON-SMALL CELL LUNG CARCINOMA AND ITS EFFECT ON CRITICAL STRUCTURE DOSES

K. Sebeerali, Vyankatesh Shejal, N. Vinod Kumar, R. Ramu, B. M. Vadiraja

Department of Radiotherapy, Manipal Hospital, Bengaluru, Karnataka, India. E-mail: sebeerali.k@gmail.com

Introduction: Large tumor motion often leads to larger treatment volumes, especially for the lung tumor located in lower lobe and adhered to chest wall or diaphragm. Variety of geometrical uncertainties such as respiratory motion, baseline variation and set-up errors, limits the precision of radiation therapy (RT) for lung cancer. According to ICRU report 62, internal target margin (ITV) and set-up margin (SM) should be included in the PTV to compensate geometrical uncertainties including tumor centroid movement, tumor boundary and set-up displacement. However, the tumor boundary displacement merely discussed about margin calculation previously. It would be assessed in present study.

Objective: Present study would evaluate changes in tumour motion magnitude and set-up error by 4DCT at planning and CBCT at treatment, and calculate the variation in planning target volume (PTV) margins devised from both imaging techniques to compensate for these changes.

Materials and Methods: Ten patients with the lung tumour located in lower lobe and adhered to chest wall or diaphragm that underwent VMAT were considered for the current study. Four-dimensional computed tomography scans (4DCT) were acquired at simulation to evaluate the tumor intra-fractional centroid and boundary changes, and Cone-beam Computed Tomography (CBCT) were acquired during each treatment to evaluate the tumor inter-fractional set-up displacement. Brilliance CT Big bore from Philips medical system along with Pinnacle 3 treatment planning system and XVI imaging from Elekta was utilized for current study. The margin to compensate for tumor variations uncertainties was calculated by using Van Herk et al margin calculation recipe published in the exiting literatures and PTV volumes were evaluated for its accuracy.

Results and Discussion: Current Study revealed that CBCT based margins overestimated the planning target volume in comparison with 4DCT based treatment planning volumes.

This inaccuracy could be due to the fact that theoretical formula for margin calculation would fall inadequate as it does not incorporate the tumour motion seen in various respiratory phases of 4DCT scan. Hence it is recommended for the patients receiving external radiation for NSCLC; an ITV based approach shall be adopted for the estimation of PTV margins for accurate patient dosimetry.

O-52

DESIGN AND DEVELOPMENT OF MINIATURE PRIMARY STANDARD FOR AIR-KERMA MEASUREMENT OF LOW ENERGY SYNCHROTRON RADIATION

Sudhir Kumar, S. D. Sharma, D. Datta
Radiological Physics and Advisory Division, Bhabha Atomic Research Centre, Mumbai, Maharashtra, India.
E-mail: sktomar1@yahoo.co.in

Introduction: The limitation of the clinical imaging methods arise mostly due to insufficient spatial resolution, contrast and quantitative scaling. The advent of synchrotron radiation (SR) has the potential to override these limitations because of very high intensity beam and broad energy spectra.[1] Further, monoenergetic photons extracted from synchrotron radiation offer the unique opportunity to study the energy response of radiation detectors. The SR source is available from INDUS-II high energy accelerator at Raja Ramanna Centre for Advanced Technology (RRCAT), Indore. The SR beam is generated at the bending magnet of the 2.5 GeV electron storage ring of INDUS-II accelerator. The SRs are essentially high intensity and predominantly low energy (critical energy 6 keV) photon beams used for various scientific studies. A dedicated beamline [Beamline-4 (BL-4)] has been provided at INDUS-II offering facilities for both the conventional as well as advanced x-ray imaging experiments. However, outputs of these beams (8 to 25 keV) have not yet been standardised due to non-availability of a suitable radiological standard.
For low energy region, the photoelectric effect is a dominant interaction process and the photoelectric cross section has a strong dependence on the atomic number of material. Hence, radiation detectors generally show strong energy response dependent characteristic in the low energy region. For the low and medium energy x-ray beams, the free-air ionization chamber (FAIC) is considered to be a primary standard for the determination of air kerma.[2] The FAIC is an energy independent instrument as it relies on the principle that the walls of the chamber do not influence the measurement of charge. To fulfill this requirement, it was decided to design and develop a miniature FAIC to measure the air kerma rate from the low energy SR beams. This paper describes the constructional details as well as output measurement methods of SR beams using the locally designed parallel-plate type FAIC.
Materials and Methods: Ionization chamber: The miniature parallel-plate FAIC was designed and fabricated for SR beam up to 25 keV energy. The *continuous slowing-down range,* R_{csda} for 25 keV is ≈1. 20 cm in air. The gap between the high voltage electrode and the collecting electrode to achieve the charge particle equilibrium (CPE) should be 2.4 cm. However, inter-electrode spacing was taken as 3 cm to avoid the loss of charged particles (i.e. electrons) created by interaction of synchrotron radiation in the defined collecting air volume. The seven guard rings made of copper of thickness 2 mm, electrically isolated from each other, were inserted at a regular interval of 2 mm in order to align and produce the uniform electric field over the interaction volume. These rings were connected in series to a chain of resistors (100 kilo-ohm each). Additionally, an enclosure with adequate shielding thickness (1 mm SS + 5 mm Pb + 1 mm SS) was provided around the chamber to keep the contribution of scattered and transmitted radiation as minimum as possible (within 0.01% of primary radiation). The salient features of the miniature FAIC is given in Table 1 below. Output measurement of synchrotron radiation: The output of various monochromatic SR beams of BL-4 at Indus-II, RRCAT was carried out using this FAIC. For this purpose, the miniature FAIC was aligned perpendicular to the central beam axis of the SR beam for the field size mentioned in Table 2 and was located at 30-meter distance from the tangent point of storage ring. The parallelism of the entry and exit apertures of the chamber with the SR beam line was verified using Gafchromic EBT3 film. In order to verify the inter-electrode spacing, the charge saturation at 25 keV was investigated experimentally. The charge (q) was measured as a function of applied voltage (V). The inverse of q was plotted against $1/V^2$ and extrapolated to $1/V^2$ equal to zero from which the value of saturation charge (qs) was derived. The charge collection efficiency (f) at 25 keV for a derived value of saturated charge (6.543 × 10^{-9}C) corresponding to 1800 V was estimated theoretically by using Mie's formula.[2]
The chamber was irradiated by 8, 10, 15, 20 and 25 keV energies of SR beams. The average meter readings (charge) corresponding to each setting was corrected for variations in environmental conditions and other corrections factors mentioned later. The ion recombination correction was computed for each beam using two voltage method used for pulsed beam.[2] The air kerma rate was determined using:

$$\dot{K}_{\text{air}} = \frac{q}{\rho_{\text{air}} V_{\text{air}}} \left(\frac{\overline{w}}{e}\right)_{\text{air}} \left(\frac{1}{1-\overline{g}}\right) \prod k_i \quad (1)$$

where q is the measured charge collected for one minute; ρ_{air} = 1.205 kg/m³, density of dry air (20°C and 1013.2 mbar); Vair is the detector sensitive air volume; $(\overline{w}/e)$=33.97 J/C; g is the average fraction of the initial electron energy lost by bremsstrahlung production in air and Πk_i are the product of correction factors (recombination factor, k_s, air attenuation factor, k_a, polarization factor, $k$pol, photon scattered factor, k_{sc}, electron loss factor, k_e and transmission factor via front face/diaphragm, k_t).
Results: At an operating voltage of 1800 V for the SR beam of 25 keV energy, the f (which is defined as the ratio of q by q_s) was found equal to be 0.9989 at 1.36 Gy/min. The f estimated using Mie's formula[2] was found equal to 0.9991. These two values of f are in excellent agreement to each other within 0.02% which indicates that additional margin of 0.6 cm in addition to 2.4 cm to keep the plate separation equal to 3 cm is sufficient to prevent any ion loss from the sensitive volume of the chamber. The air kerma measured using miniature FAIC at BL-4 at RRCAT, Indore for SR beam energies of 8, 10, 15, 20 and 25 keV is listed in Table 2.
It is observed from the Table 2 that the output of the beam is maximum at 15 keV which is expected as per the shape of SR spectra. The expanded uncertainty in the measurement of air kerma rate is 1.2% (k = 2).

Table 1: Physical data of the free-air ionization chamber

Chamber geometry	*Parallel plate*
Collection efficiency	99.9%
Mass of the sensitive air volume	1.789×10^{-7} Kg
Plate separation	3 cm
Length of collecting electrode	2 cm
Length of guard electrodes	1 cm
Gap between collecting and guard electrode	0.1 cm
Applied potential	*Variable based on beam energy*
Aperture diameter of beam entry	0.3 cm

Table 2: The measured air kerma rate of various monochromatic synchrotron radiation beams using locally designed miniature free air ionization chamber at 30 meter from the tangent point of 2.5 GeV electron storage ring

SR energy (keV)	*SR beam size (FWHM) (mm)*	*Storage ring current (mA)*	*Air K (/Gyhat30m)*
8	80×7.40	112.1	1.455×10^{2}
10	80×6.75	114.4	5.628×10^{2}
15	80×5.65	125.9	5.840×10^{2}
20	80×4.99	121.4	1.673×10^{2}
25	80×4.53	118.8	8.170×10^{2}

SR: Synchrotron radiation, FWHM: Full width at half-maximum

Conclusions: The performance of this chamber was found satisfactory as per design and expectation and qualify to be a primary standard for measurement of air kerma rate of low energy synchrotron radiation beams of energy up to 25 keV. This chamber can be used for various dosimetry measurements with synchrotron radiation including calibration of another dosimeters.

Acknowledgement: The authors express their sincere thanks to Shri P. K. Sahani, IOAPDD, RRCAT; Dr. G. Haridas, HPD, BARC; Shri Amit Jain, RSSD, BARC and Dr. Ashish Kumar Agarwal, TPD, BARC for their help in this work.

References

1. Suortti P, Thomlinson W. Medical applications of synchrotron radiation. Phys Med Biol 2003;48:R1-35.
2. Attix FH. Introduction to Radiological Physics and Radiation Dosimetry. New York: Wiley; 1986.

O-53

CHARACTERISATION AND PERFORMANCE STUDY OF NEWLY DEVELOPED N-TYPE SKIN DIODE DOSIMETER FOR HIGH PHOTON ENERGY (6 AND 18 MV) SKIN DOSIMETRY

Zakiya S. Al-Rahbi[1,2], Dean L. Cutajar[1,3], Ziyad A. Alrowaili[1], Anna Ralston[1,3], Peter Metcalfe[1], Anatoly B. Rosenfeld[1]

[1]Centre for Medical Radiation Physics, University of Wollongong, Wollongong, [3]St George Cancer Care Centre, St George Hospital, New South Wales, Australia, [2]Department of Radiotherapy, National Oncology Center, The Royal Hospital, Muscat, Oman.
E-mail: z.alra7bi@gmail.com

Purpose: To investigate the feasibility of using the newly developed n- type Skin Diode for *in-vivo* skin dosimetry through characterisation on the surface of a phantom simulating the condition for *in-vivo* skin dosimetry for megavoltage photon beams.

Materials and Methods: The response of the Skin Diode was investigated for different field sizes and radiation incident angles using both 6MV and 18MV photon beams. The percentage depth dose (PDD), dose rate dependence, dose linearity, output factor (OF), and exit doses were measured. All Skin Diode measurements were compared with the MO*Skin*™ and Attix ionisation chamber measurements.

Results: The Skin Diode showed a good linearity ($R^2 = 0.9928$) for a dose range of 50 cGy to 500 cGy for both the 6MV and 18MV photon beams. For field size dependence, the Skin Diode measurements were within experimental agreement with the MO*Skin*™ dosimeter (3.66% for 6MV) and Attix chamber (3.93% and 3.38% for both 6MV and 18 MV photon beams respectively). For the 6MV photon fields (10 cm x 10 cm), the mean surface dose measurement of the MOSkin™, Attix and Skin Diode were 18.3 ± 1.7%, 16.2 ± 0.1% and 25.5 ± 2.0%, respectively, with all measurements relative to the Dmax of each individual detector. The average PDD difference, beyond Dmax, between the MO*Skin*™ and Attix chamber was 1.9%, and between the Skin Diode and Attix chamber was 2.3%, for 10 cm x 10 cm 6 MV photon fields. There was no significant dose rate dependence observed for the Skin Diode for 6 and 18 MV photon fields (within experimental error). The agreement in the exit dose measurements between the Skin Diode and Attix chamber was within ±2.4%.

Conclusions: *In-vivo* dosimetry is important during radiotherapy to ensure the accuracy of the dose delivered to the treatment volume. A dosimeter should be characterised based on its application before it is used for *in-vivo* dosimetry. The newly developed n-type Skin Diode responses were investigated on the phantom surface to determine its applicability to be used for *in-vivo* skin dosimetry. The Silicon Diode showed a feasible response to different field sizes, radiation incident angles, PDD, output, entrance and exit dose measurements. The entrance doses, as measured by the Skin Diode, were higher than desired, which will be corrected through a re-engineering of the top encapsulating layer through subsequent updates of the design. The Skin Diode may provide a good possibility for real time *in-vivo* skin dosimetry during external beam X-ray radiotherapy.

O-54

NANO KCL:SM^{3+} AS A NEW OPTICALLY STIMULATED LUMINESCENT PHOSPHOR

Pratik Kumar, Mini Agarwal, K. Asokan[1]

Medical Physics Unit, IRCH, AIIMS, [1]Inter-University Accelerator Centre, New Delhi, India.
E-mail: drpratikkumar@gmail.com

Radiation is widely used in various applications like medical, industry, agriculture, research and military purposes. All these applications have their unique features and requirements. Some of them require small doses of radiations (μGys) like medical imaging and specific use of radiopharmaceuticals. Efforts are always made to reduce these doses further by inventing better technique and technologies. On the other hand a few applications such as industrial, food and military related need very high doses (in kGys) and some of them may be trying to escalate even further to test the forward limit. Obviously all such radiation applications entail hazard and warrant precise measurement of doses. Passive dosimeters like Thermo-luminescent Dosimeter (TLD) and relatively recent addition Optically Stimulated Luminescent (OSL) dosimeter are widely used for these purposes. However, there is only two commercial OSL phosphors namely Al_2O_3:C and BeO. The former form M/S Landauer is well known while the later is yet to be marketed aggressively. OSL has many advantages over TL as the former is excited by light which is controlled better unlike the later which is excited by heat. OSL is known to be able to measure smaller doses, has better reproducibility, has less cumbersome procedures, may be made portable and may measure the dose repeatedly for the same exposure. We attempted to prepare a new OSL phosphor KCl:Sm^{3+} (nano-crystalline) which may measure high radiation doses. Sm-doped nanocrystalline KCl was synthesised by solid state reaction at a high temperature of 200°C for 3 hours with high-quality precursors of KCl (M/S Merck, AR grade, 99.95 % pure) and $SmCl_2.6H_2O$ (M/S Alfa Aesar, 99.5% pure). The sample was prepared by adopting the following reaction (chemical):

KCl + $2SmCl_3.6H_2O$ Heating at 363 K for 3 hours KCl: Sm + 6HCl + $9H_2O$

During synthesis, precursor KCl was mixed with various concentrations of dopant precursor Sm (such as 0.15mol%, 0.25mol%, 0.45mol% and 0.50 mol%) to investigate the role of concentration of the dopant Sm in OSL signal. The resultant product was grounded to prepare homogenous powder and was further subjected to thermal treatment at 80°-90°C for 3 hours to obtain fine nano phosphor. This nano powder was annealed (thermally) in Muffle furnace at various temperatures for 2 hours (from 650°-740°C) with a heating rate of 15°C per minute. *In-situ* cooling of the mixture up to temperature 300°C was achieved by keeping it in the furnace for about 20 minutes after switching the furnace off. The powder was taken out from the furnace when the temperature of the furnace falls to 300°C and was kept on the metal block at the room temperature for further cooling. The powder and pellet form of the same mixture was used for various studies. KCl:Sm^{3+} was made with varied concentration of Sm and the optimised concentration was found to be with 0.45% of Sm which gave the maximum OSL signal. We confirmed the structural and morphological characteristics of our phosphor with XRD which revealed its poly-crystalline nature with grain size 20-60 nm. This observation was also supported by the Selected Area Diffraction (SAD) pattern of Transmission Electron Microscopy (TEM). The presence of Sm in the KCl matrix was confined by Energy-Dispersive X-ray Spectroscopy (EDS) analysis while existence of trivalent Sm^{3+} was corroborated by X-ray Photoelectron Spectroscopy (XPS) analysis. The OSL response was linear from 100 mGy to 750 Gy. Our KCl:Sm^{3+} showed fading of 20% in 50 days and 7-8% in 12 days. It showed variation of 6-7% in signal for exposure-reading-annealing cycles. The overall sensitivity of KCl:Sm^{3+} was found to be about 80% of that of Al_2O_3:C and BeO. During course of preparation we did attempt to prepare KCl:Sm and KCl: Sm^{2+} as well but they showed much higher fading making them impractical for dosimetry. KCl:Sm^{3+} was found with least fading and highest sensitivity since trivalent Sm^{3+} created permanent and stable defects in the KCl lattice. Al_2O_3:C and BeO phosphor being propriety items are costly and therefore, indigenous search for other efficient OSL phosphor is the need of the hour. KCl:Sm^{3+} nano phosphor is an efficient doismetric material due to its storing efficiency and reusability which is highly desirable in radiation therapy and imaging in medical diagnostics. Because of its long linear dose response KCl:Sm nanophosphor is the efficient candidate for the space, military, food irradiation and other dosimetric applications and even futuristic real-time online dosimetery.

O-55

DEVELOPMENT OF CRYOSTAT INTEGRATED TL/OSL READER FOR ITS APPLICATION IN RADIATION DOSIMETRY

Anuj Soni, D. R. Mishra, P. Kadam, D. Datta

Radiological Physics and Advisory Division, Bhabha Atomic Research Centre, Mumbai, Maharashtra, India.

E-mail: anujsoni.phy@gmail.com

Introduction: Thermoluminescence (TL) studies provide vital clues in connection with the mechanism of trap formation, concentration and nature of the traps. For a radiation phosphor generally, dose readout is carried out at the temperatures that are much higher than normal room temperature where shallow traps are ineffective and as such cannot contribute to the TL response. In OSL based dosimetry, however, the measurement is usually carried out at room temperature, where these shallow traps can significantly affect the OSL response. The TL measurement at low temperatures gives the useful information about such shallow traps which may be having metastable life-time of the order of a few ms at room temperature. It has been observed that these traps exercise a decisive influence over the OSL response of samples as they lead to a delayed optically stimulated luminescence (DOSL) in which charges released from dosimetric traps, upon optical stimulation get re-trapped at shallow traps. At lower temperatures (below room temperature), these traps may contribute to the total OSL signal and at the same time the contribution of higher temp TL traps will decrease due to the temperature dependence of photoionization cross-section. Thus, they can seriously affect the overall calibration factor for any dosimeter with the change in the readout temperature. This can have implication in optical fibre based online OSL dosimetry which can find application in medical dosimetry. This lead us to develop the low temperature TL/OSL reader to study the TL/OSL of Al_2O_3:C OSL phosphor to be used in optical fibre based OSL dosimetry.

Objective: Design and development of a programmable cryostat integrated TL/OSL reader to study the temperature dependence of OSL. These studies will give useful information on the effect of readout temperature on OSL signal and thus the overall calibration particularly in optical fibre based online OSL dosimetry having application in medical dosimetry.

Materials and Methods: A K-type thermocouple based PID circuit was used to control the temperature in the reader system. The reader comprises of a bialkali Photomultiplier tube as a detector having response in the range 300-700 nm, for detecting the luminescence. The reader is connected to the PC through an RS-232 serial interface. The commercially available α-Al_2O_3:C (TLD-500K) crystal from Laundauer Inc., was subjected to irradiation by UV light on the heater planchet held at various low temperatures. The sample was subjected to OSL measurement at various low temperatures.

Results and Discussion: A programmable cryostat integrated TL/OSL reader has been designed and developed to study the effect of readout temperature on the OSL intensity. The reader system measures the temperature of the planchet with ±0.5 °C precision. We report the results of OSL experiments on α-Al_2O_3:C, and of generalized numerical simulations of potential OSL behaviour with temperature. The photoionization cross-section of shallow as well as dosimetric traps has been evaluated numerically as well as experimentally. At lower temperatures, the photoionization cross-section of main dosimetric traps becomes very low (~10^{-20} cm^2 at 250K) and they act like deeper traps and very less OSL is observed from them. The main TL glow peak due to this dosimetric trap is not found to be completely bleachable with blue light stimulation at low temperatures. Further, the TL peak (8°C at 0.33K/s) due to shallow trap becomes active at low temperatures and contributes in OSL more than the main dosimetric trap. It is concluded that the stimulation and irradiation/calibration temperatures need to be maintained fixed throughout the experiment i.e. the dose estimation process.

O-56

ENERGY DEPENDENCE OF NANODOT OSL DOSIMETERS TO LOW ENERGY X-RAYS USING MONTE CARLO SIMULATION CODE EGS5

V. L. E. Cruz[1], S. Goto[2], T. Okazaki[1], H. Hayashi[2], E. Tomita[2], Y. Mihara[2], T. Asahara[2], T. Hashizume[1,3], W. H. Cheng[1], I. Kobayashi[1]

[1]Nagase Landauer, Ltd., Tsukuba, [2]Tokushima University, Tokushima, [3]SOKENDAI, Hayama, Japan.
E-mail: vergilcruz09@gmail.com

Low energy X-rays have been increasingly used in medical diagnostic procedures. Procedures such as Computed Tomography, Interventional radiology, etc. uses low energy X-rays and results in the exposure of patient and in some cases, of the medical staff. Managing and measuring the radiation dose received by patients and medical staff should be done and a suitable radiation dosimeter must be used. A small type optically stimulated luminescence (OSL) dosimeter called "nanoDot" was designed and is expected to be used in measuring and estimating the radiation dose received from medical procedures using X-rays. nanoDots uses OSL technology which offers advantages over other types of passive dosimeters such as its ability to be read repeatedly since it uses visible light instead of heat to read the stored dose. However, in low energy X-rays, the response of the OSL dosimeter to incident photons is not constant and varies depending on the energy used for each situation. This is a concern when using nanoDots in radiation dosimetry for low energy X-rays. The main objective of this study is to evaluate the energy dependence of the OSL dosimeter to low energy X-rays, in particular; ISO narrow beam series X-rays, mono energetic X-rays and polychromatic X-rays used in medical diagnosis. This study also aims to evaluate the response of the nanoDot OSL dosimeter using different X-rays radiation qualities. The Monte Carlo simulation code EGS5 was used and experiments were carried out to determine the energy dependence of the nanoDot OSL dosimeter to ISO narrow beam series X-rays, polychromatic X-rays and mono energetic X-rays. The results from simulations and experiments were compared and the accuracy of the EGS5 simulation was evaluated. The experiments using ISO narrow beam series X-rays were carried out in the National Institute of Advanced Industrial Science and Technology (AIST) which is a primary standard in Japan. Furthermore, the experiments using polychromatic X-rays were also performed. The experimental data of ISO narrow beam X-rays were in good agreement with its simulation, and they were also consistent with the simulated data for mono-energetic X-rays. In addition, experimental data of polychromatic X-rays is also in good agreement with its corresponding simulation. These facts indicate that the use of EGS5 is a reliable way in determining the energy dependence of an OSL dosimeter. The energy dependence curve for polychromatic X-rays calculated by EGS5 simulation is different from the ISO narrow beam X-rays and mono-energetic X-rays, nevertheless the energy dependence curve of mono-energetic X-rays and ISO narrow beam series X-rays are the same. One reason of this difference is that the energy spectrum used in polychromatic X-rays is different with the ISO narrow beam series X-rays or mono energetic X-rays. This result shows that the energy dependence curve of the nanoDot also depends on the overall energy spectrum of the radiation source. Proper evaluation of the energy dependence is necessary for low energy X-rays since there are differences in the response depending on the energy spectrum of the radiation source. In Conclusion, Evaluation of the energy dependence of the nanoDot OSL dosimeter for different X-ray qualities is essential. This will allow the nanoDot to be a very reliable and suitable dosimeter in any situation for radiation dosimetry of patients and medical staff.

O-57

SYNTHESIS AND CHARACTERIZATION OF HO^{3+} DOPED HAFNIUM OXIDE TLD FOR RADIATION DOSIMETER

Nandakumar Sekar, Bharanidharan Ganesan, Hajee Reyaz Ali Sahib, Prakasarao Aruna, P. Thamilkumar[1], R. R. Rai[1], Singaravelu Ganesan

Department of Medical physics, Anna University, [1]Department of Radiotherapy, Dr. Rai Memorial Medical Cancer Centre, Chennai, Tamil Nadu, India. E-mail: nandasekar58@gmail.com

Introduction: Cancer is a dreaded disease which is treated by Radiotherapy, Chemotherapy and Surgery. Radiotherapy plays a vital role in treatment of cancer and recently measurements of invivo radiation dosimeteric in patient is of great interest due to high dose gradients in advanced technology like IMRT, IGRT etc. Hence, for the last few decades, a great degree of interest has been shown for the hafnium oxide for radiation dosimeteric applications, due to its high dielectric constant, wide band gap and better interface properties such as chemical stability, conduction band offset and thermodynamic stability. In the present study, Synthesis and characterization of $H0^{3+}$ doped Hafnium oxide were carried out and its applications towards radiation dosimeter were investigated.

Materials and Methods: Pure and Extrinsic HfO_2 NPs with different Ho content (2.5-10% in weight) was prepared by precipitation method and they were investigated by X-ray diffraction, FESEM-EDAX, UV-Visible Spectrophotometer, Fluorescence spectrophotometer, FTIR, Raman Spectroscopy, True Beam-Varian, Long stand and TLD glow curve determined by using Thermoluminescence Reader (Nucleonix TL 1009I).

Results and Discussion: Intrinsic and Ho^{3+} doped HfO_2 powder were obtained by the precipitation route and calcined at 800°C for 2 hrs in air. The crystal structures, size of the resultant materials were investigated by powder X-ray diffraction (XRD) measurements. The obtained XRD-spectrum is in good match with the standard JPCDS. The composition and morphology of the synthesized NPs have been examined using FESEM-EDAX. The optical absorption spectra of Pure and Ho^{3+} doped HfO2 dispersed in water were recorded using a UV–Vis spectrophotometer. The band gap of the NPs was calculated from the UV absorbance spectra. The emission properties for various Holmium concentrations have been studied by means of Photoluminescence. The presence of the water related bonds in the samples were confirmed by using FTIR. Raman measurements show that the crystalline phase of monoclinic to cubic phase transformation and Evidence to the XRD. A typical TL glow curve of pure and dopant HfO_2 pellets exposed to 10 MV X-ray photon beam were taken in order to in order to study the dose response of HfO_2 for its application in Radiation Dosimetry and also its Reproducibility and Fading characteristic were carried out to study the trap parameters, including geometric factor (μg), activation energy (E) and frequency factor (s) associated with HfO_2:Ho.

Conclusion: Pure and Ho^{3+} doped HfO_2 NPs powder were synthesized and characterized to determine the Kinetic parameters and dosimetric characteristics. These favorable TL characteristics of prepared NPs may contribute towards the development of HfO_2: Ho radiation dosimeters which can be effectively used for in vivo dosimeter in future.

O-58

PATIENT SPECIFIC QA ON CYBERKNIFE M6 ROBOTIC RADIOSURGERY SYSTEM USING IN-HOUSE FIDUCIAL BASED POLYSTYRENE PHANTOM

R. Holla, B. Pillai, D. Khanna[1]

Department of Medical Physics and Radiation Safety, Amrita Institute of Medical Science and Research Center, Kochi, Kerala, [1]Department of Physics, Karunya University, Coimbatore, Tamil Nadu, India. E-mail: raghavendra.holla@gmail.com

Purpose: Placing the Phantom and measurement chamber as per the ‘Align Centre’ chosen during the treatment planning is very challenging for Cyberknife Radiosurgery Plans involving small fields. This step plays a major role in the patient specific QA as targeting multiple beams to the chamber is based on the align center. Hence the purpose is to design a polystyrene phantom for patient specific QA on Cyberknife M6 system which uses fixed tracking method.

Methods: Three pieces of polystyrene blocks of the dimensions 20 cm x 20 cm x 5 cm thickness are used for designing the phantom. A chamber holder for 0.01CC pinpoint chamber (IBA, Germany) is drilled to this block such that the chamber center is at 2.5 cm depth. Four numbers of stainless steel fiducials of 0.7 mm diameter are implanted to this block. Two more 5 cm polystyrene phantom blocks are implanted with one fiducial each making the total number of fiducials to 6. The chamber holder is sandwiched between these two blocks making the total thickness of the phantom to 15 cm. 4 aligning corner screws will hold the phantom blocks together without sliding. The position of all the fiducials are such that they do not overlap in 45 and 315 degree X ray images. All fiducials are fixed in the drilled position by pouring hot wax. CT Scan of the phantom is acquired and imported to Multiplan (ACCURAY, USA). A clinical treatment plan is overlaid on this phantom and the dose is calculated. This plan is delivered to the phantom on the treatment unit using fiducial tracking method.

Results: The phantom with the chamber is accurately placed using fiducial based tracking method. The measured dose in the phantom is in agreement to the planned dose within 3%.

Conclusion: A polystyrene fiducial phantom has been designed for patient specific QA on Cyberknife M6 system.

O-59

NANODOTS, ALANINE, AND TLD100H DOSIMETERS INVESTIGATIONS AND ITS TREATMENT FOR STEREOTACTIC ABLATIVE RADIOTHERAPY PRE-TREATMENT VERIFICATION

N. U. Esen[1,2], R. Prabhakar[1,2], M. Geso[2]

[1]Peter MacCallum Cancer Centre, [2]Medical Radiations Science, RMIT University, Melbourne, Victoria, Australia. E-mail: nsikanjesus@yahoo.com

Purpose: Stereotactic Ablative Radiotherapy (SABR) is a standout amongst the chosen radiation therapy practices for early stage bronchogenic carcinomas. Procedures stretched to other treatment locales like Spine, Scapula and Sternum, and so on. Pre-treatment verification confirms the patient got the planning dose. Distinctive class of dosimeters or dose-measuring devices have been employed for pre-treatment check that incorporates ionization chamber, diode, TLD, 2D Array etc. SABR employed small fields which order the utilization of scale down detectors for pre-treatment confirmation. Alanine and nanoDots are new class of dosimeters that should be typified for pre-treatment verification. It was the aim of the present study to investigate the influence quality (e.g. energy, dose rate, directional dependency, etc.) of alanine, nanoDots dosimeters and compare with TLD100H and explore the feasibility of using these dosimeters for pre-treatment verification of the dose delivered to patients undertaking stereotactic ablative radiotherapy.

Methods: Bruker EleXsys E500 EPR spectrometer of

9.5 MHz was used to read the Alanine pellet dosimeters signals and the Harshaw QS 5500 automatic TLD reader was used for reading the TLDs. Also, Microstar Reader from Landauer Inc. was used to study the signal of the irradiated nanoDots OSL dosimeters. All the irradiation was done on ClinaxTH 21ix at 6MV x-ray beam. Three Dimensional (3-D) phantoms were design for each detector and were place separately inside in-house Rod phantom made of Perspex to perform SABR pre- treatment patient verification.

Results: The relationship between dose measured using Alanine, TLD100H and nanoDots dosimeters followed a linear curve ($R2 = 0.998$, $R2 = 0.999$, $R2 = 0.989$) and no meaning distinction with dose rate, and energy was observed for the detectors. The contrasts between the measured and the TPS computed dose were fewer than 2% and 3% with Alanine, nanoDots and TLD respectively. Specifically, the rate increment of nanoDots and alanine dosimeters to TLD is half.

Conclusion: From the results obtained, this study indicates that the SH EPR-Alanine pellets and nanoDots dosimeters are predictable and agree well between the measured and the figuring measurement. It likewise affirmed that both alanine and nanoDots dosimeters are profitable dosimeters for SABR pre-treatment verification.

O-60

INVESTIGATING POLARITY AND ION RECOMBINATION EFFECTS OF SIX IONIZATION CHAMBERS FOR SMALL RADIATION BEAM APERTURES

K. J. Maria Das, Arpita Agarwal[1], Nikhil Rastogi[1], S. A. Yoganathan, D. Udayakumar, Shaleen Kumar

Department of Medical Physics, Sanjay Gandhi Postgraduate Institute of Medical Sciences, Lucknow, [1]Department of Physics, School of Science, IFTM University, Moradabad, Uttar Pradesh, India. E-mail: kjmariadas@hotmail.com

Objectives: Micro ionization chambers are the favorable dosimeter for small field measurements. However, because of their reduced sensitive volume, they are more susceptible to chamber specific effects such as polarity, ion recombination and leakage effects. The purpose of this study was to evaluate the polarity and ion recombination effects of small volume ionization chambers.

Materials and Methods: The polarity and recombination effect of six commercially available ionization chambers (Exradin A16 (0.007 cc), Exradin A18 (0.125 cc), IBA CC01 (0.01 cc), IBA CC13 (0.13 cc), PTW markus (0.055 cc) and IBA PPC 40 (0.40 cc)) were investigated for two photon beam energies; 6 MV and 15 MV. Each chamber was placed (perpendicular to the central beam axis) at a depth of 10 cm inside a radiation field analyzer (RFA, BP2, IBA dosimetry, Schwarzenbruck, Germany) and source to surface distance (SSD) was set to 100 cm. All the ionization chambers were connected to an electrometer (Unidos E, PTW, Germany) via a cable to collect the charge. The voltage was set to +300 V for all the ionization chambers and the meter readings were taken for the jaw collimated field sizes 0.5 x 0.5, 0.8 x 0.8, 1.0 x 1.0, 2.0 x 2.0, 3.0 x 3.0, 5.0 x 5.0 and 10.0 x 10.0 cm^2 at dose rate 400 MU/min. The polarity of the applied voltage was reversed and same procedure was repeated to account the effect of polarity. In order to measure the ion recombination effect, the applied voltage was reduced to +100 V and again all the measurements were performed. The polarity correction factor (K_{pol}) and ion-recombination correction factor were calculated as per TRS 398 protocol. Same experiment was repeated for other depths i.e. d_{max} and 5 cm.

Results: Polarity effect was observed to be more at smaller field sizes i.e. <2 x 2 cm^2; whereas for larger field sizes (>2 x 2 cm^2) the K_{pol} was within the specified range (0.996 – 1.004). A16 ion chamber was the exceptional one which maintained K_{pol} value within the specified range even for small field sizes. The polarity effect was observed to be depending slightly on the measurement depth and it was higher at shallower depths compared to deeper depths. At d_{max}, the maximum deviation in K_{pol} values of ion chambers was in the order of ±3%; whereas the same was reduced to nearly ±2% and ±1% at 5 cm and 10 cm depths respectively. When comparing the polarity effect between 6 MV and 15 MV photon beam energies, it was found to be slightly larger for 6 MV. On contrary, the recombination correction factor was observed to be less than 0.5% for all measurements.

Conclusions: All the investigated chambers showed anomalous polarity effect at smaller field apertures except A16; whereas the recombination effect was found to be negligible (<0.5%) for all. The polarity effect was relatively larger for smaller field sizes below 2.0 x 2.0 cm^2; it was highest for plane parallel chambers followed by A18 and CC13 ion chambers, while it was least for CC01 and A16 chambers.

O-61

SMALL FIELD DOSIMETRY MEASUREMENTS

Ganesan Ramanathan[1,2]

[1]Ex-Senior Radiation Scientist, ARPANSA, Australia, [2]Department of Medical Physics, Bharathiar University, Coimbatore, Tamil Nadu, India. E-mail: ganesan.ramanathan@gmail.com

Introduction: Modern radiotherapy treatment modalities such as Intensity Modulated Radiotherapy (IMRT), Volumetric Arc Therapy (VMAT) and Streotactic Radio Surgery (SRS) make use of small fields. Improper dosimetry in small field has led to few incidents harming the patients. There is no primary standard for absolute dosimetry. IAEA has proposed an ad hoc formalism to extend the reference dosimetry measurements done using IAEA TRS-398 and AAPM TG-51 protocols which implies the use of adequate correction factors. AAPM TG-155 and IAEA TRS-483 protocols for bringing uniformity in small field measurements are yet to be implemented. Experimental measurements done at ARPANSA by the author to issue advice on appropriateness of certain detectors for small field measurements and any other issues of small field measurements are presented in this talk.

Objectives: (1) Select the best detector for small field measurements for fields down to 5 mm diameter conical fields. (2) Determine the best geometry and reproducibility in measurements. (3) Achieve concurrence in output factors among the detectors. (4) Evaluate the correct sensitive volumes of solid state detectors which will improve the agreement between experimental and Monte Carlo calculated correction factors.

Materials and Methods: Beam profile measurements and output factor measurements were done using IBA blue phantom and Omnipro software. Measurements were done at 6 MV photon beam from Elekta Synergy accelerator. Field sizes used were MLC fields from 10 x 10 cm^2 to 1 x 1 cm^2 and Elekta SRS cones with diameters from 50 mm to 5 mm. The detectors studied were PTW 60017 electron diode, PTW 60019 micro-diamond, PTW Pinpoint chamber 31014 and IBA CC13 compact ionization chamber. Output factor measurements were done using PTW Unidos electrometer and the integrated charges for 100 MU were measured. A number of five readings were taken each time and standard deviation and estimated standard deviation of the mean were calculated. All measurements were done at 100 cm SSD, 10 cm depth in water. From the measurements of in-line and cross-line profiles the 80% - 20% penumbra widths and FWHM values were calculated using MATLAB script. For the evaluation of the sensitive volumes of solid-state detectors measurements were done at 100 cm SSD, 10 cm depth in water and square field of 10 cm x 10 cm with NE 2571 Farmer chamber calibrated against the primary standard graphite calorimeter and the solid-state detectors in the same geometry. The centering of the detectors were done by recording the profiles and tweaking the position of the detector so that the center of the profile lies on the central axis.

Results and Discussion: Reproducibility of profile scans with repeated MLC settings was <1% (0.8% for 1 x 1 cm^2). Reproducibility of profile scans with SRS cones was <1% for cones of diameters 7.5 mm to 50 mm. Reproducibility with 5 mm cone was 1.25%. The output factors for the solid state detectors corrected using published correction factors lie within 1%. Uncertainty in measurements is estimated to be ~1.6% at 1 sigma level. The sensitive volumes for soild-state detectors along with the manufacturer's values are given. These values will reduce the disagreement between the experimental and Monte Carlo calculated values.

O-62

PLANNING CONSIDERATIONS FOR UNFLAT BEAMS

S. Sowmya Narayanan, P. Suresh Babu, V. Ramya, Daicy George, S. Geeta Narayanan[1]

Departments of Radiation Physics and [1]Radiation Oncology, Vydehi Institute of Medical Sciences and Research Centre, Bengaluru, Karnataka, India.
E-mail: dearnarayanan@gmail.com

Introduction: The advent of advanced beam therapy techniques, such as Stereotactic Radio Surgery/Radio Therapy (SRS/SRT) where inhomogeneous dose distributions are applied using intensity modulated radiotherapy (IMRT) or Volumetric Modulated Arc Therapy (VMAT) in which varying fluence pattern across the field are delivered have stimulated the increasing interest in operating standard Linear Accelerator (LINAC) in a Flattening Filter Free (FFF) mode. FFF beams show the potential for a higher dose rate and lower peripheral dose. Definite clinical benefits can be anticipated in the motion management using FFF beams since the beam ON time is less compared to FF. A National Task Group on acceptance criteria for flattening filter-free photon beam published by Atomic Energy Regulatory Board (AERB) was reviewed for this study.

Materials and Methods: A medical linear accelerator (Versa HD, Elekta Medical Systems, UK) having FFF photon beams have been installed in our centre recently. Commissioning of this LINAC was performed using standard protocols as prescribed by AERB. Baseline value for routine QA was established from Treatment Planning System (TPS) commissioned data. Parameters such as penumbra, degree of unflatness, surface dose were given prime significance for periodic performance evaluation of FFF beams. Treatment planning for dose delivery in this Linear Accelerator was carried out using TPS (Monaco v 5.11.01, Elekta Medical Systems) having various sophisticated algorithms. Planning was carried out for various treatment sites in Brain, Head and Neck, Thorax, Abdomen and Pelvis for different treatment techniques comparing FF and FFF beams. The planning considerations, dose fractionation regimes and dose constraints for Stereotactic techniques using FFF beams were also reviewed.

Results and Discussions: Dosimetric evaluation reveal that Plan quality of FFF beams used in 3D-CRT was inferior than beams. For IMRT and VMAT, plan qualities were comparable. FFF beams require more MU to deliver a particular dose as compared to FF beams, which does not pose any dosimetric disadvantage, owing to higher dose rate mode in FFF beams. Surface doses of FFF were comparable to FF beams. Planning considerations for Stereotactic techniques involves hypofractionated dose regimes with < 80% marginal dose coverage for PTV. Dose constraints need to be selected for the chosen dose fractionation regime. Report by Emami on Tolerance of Normal Tissue to Therapeutic Radiation was chosen in our institution. Planning aspects related to Monaco treatment planning system includes a minimal conformality constraint, whereas strict Normal Tissue Objectives (NTO) are used to achieve conformal distribution in Eclipse treatment planning system (Eclipse v 11.1, Varian Medical Systems, Palo, Alto). Motion errors for stereotactic techniques were corrected using 6D couch available with linear accelerator. Studies related to treatment planning and dose delivery of various clinical cases using FFF beams in modulated treatments demonstrate their clinical suitability and superiority over FF photon beams.

O-63

EVALUATION OF SYSTEM ACCURACY AND PTV MARGINS FOR SBRT IN LUNG AND LIVER USING NOVALIS TX™ ADAPTIVE GATING AND EXACTRAC® 6D SYSTEM

Himank Kalra, Anil K. Bansal, R. K. Munjal, Kartikeshwar Patro, H. Malhotra Singh, Naveen Kumawat

Department of Radiation Oncology, Max Super Speciality Hospital, New Delhi, India. E-mail: mscgju@gmail.com

Target volume is of main concern for irradiation of tumors affected by the respiratory motion such as in lung and liver. With reduction of the target volume decreased complication rates of organs at risk is expected. Stereotactic body radiation therapy (SBRT) is popular choice with ultrahigh doses per fraction (6 to 30 Gy), in a hypo fractionated regimen of five or fewer fractions. To deliver such high doses per fraction respiratory motion need to be account during the course of radiotherapy. We used Novalis Tx™ ExacTrac® Adaptive Gating technique for increasing accuracy in dose delivery and to reduce the target volume. System consists of a linear accelerator, two stereoscopic X-ray tubes, Infrared markers, camera and a 6D couch. The study was done using a phantom (ExacTrac® Gating Phantom) which contains a Dose Cube with dedicated slot for film placement below it and vertical moving platform with passive infrared markers to simulate patient's breathing pattern and is software controlled. Phantom is embedded with a 5 mm diameter steel ball and a 2 cm long helical marker similar to the gold marker used to insert into the patient's body using CT guidance. To Evaluate system errors Gated Winston lutz test was performed in gating condition with collimator opening of 10 mm by targeting the steel ball embedded in the Dose Cube with a EBT3 film just below the phantom. With the use of ExacTrac® Gating phantom Beam profile of 3 X 3 cm^2 field size using EBT3 Gafchromic film by irradiating it with different beam on window (10%, 20%) under gating and non gating conditions are obtained. The cube phantom with a volume of 125 cc and equivalent sphere radius 6.2 cm is manually contoured using Eclipse™ contouring station for 10 times on 10 different scan to find the volume of the contour and equivalent sphere radius to calculate contouring system error. For setup errors the intrafraction shifts of total 7 patients has been analyzed out of which 4 patients were of liver and 3 were of lung cases. Intrafraction shifts were applied 107 times during the treatment of these patients.

Result and Discussion: The Gated Winston lutz test showed a special accuracy of 1 mm. Beam penumbra increased by 1-2 mm as we go from no gating and gating with 10% beam on window to 20% beam on window. Average deviation in contouring volume in terms of equivalent radii was less than 1 mm. Maximum deviation between IR marker and KV-Xray setup are 1.44 $\pm$ 1.33 lateral, 4.78 $\pm$ 3.51 mm Longitudinal and 2.29 $\pm$ 0.91 mm Vertical with a standard deviation of 2.04 mm. Calculated PTV margin with account of beam penumbra shows 5 mm PTV margin is adequate for SBRT using ExacTrac® Adaptive Gating. Target volume with ITV+PTV and with PTV margins were analyzed for the same set of patients with average volume reduction of 50.8% ranges from 37-58%.

O-64

EXPERIENCE IN IMPLEMENTING AND CONDUCTING THE AUSTRALASIAN COLLEGE OF PHYSICAL SCIENTISTS AND ENGINEERS IN MEDICINE (ACPSEM) RADIATION ONCOLOGY MEDICAL PHYSICS TRAINING EDUCATION AND ASSESSMENT PROGRAM (ROMP-TEAP) IN A REGIONAL AUSTRALIAN RADIOTHERAPY CENTRE

A. K. Mishra, D. Banjade, G. B. Warr, S. Tan, G. Dillon, G. Stevens, K. Thuraisingam, R. Hammond, M. Fuller, S. McDonell

Department of Radiation Oncology, Central West Cancer Care Centre, Orange Hospital, New South Wales, Australia. E-mail: ajeet.mishra@health.nsw.gov.au

Introduction: The shortage of clinically qualified medical physics specialist (QMPS) has been an acute problem in regional radiotherapy (RT) centres in Australia. The ACPSEM ROMP-TEAP has ameliorated this to some extent however it is still a challenge for some remote centres. Orange Health Service provides radiation oncology to the Far and Central West NSW region. The centre has experienced challenges in recruiting and retaining qualified Medical Physicists since it was established in 2010. However, despite this being an ongoing issue, a core team of QMPS has been established, which has enabled implementation of ACPSEM ROMP-TEAP at the centre.

Objectives: The objective of implementing this program at the centre is to address this workforce issue.

Materials and Methods: The centre used the methodology outlined in the ACPSEM Clinical Training Guide (CTG) for ROMP-TEAP. The program is supported by radiation oncologist, radiation therapist and professionals of radiology department. Brachytherapy training was performed at other specialised training centres.

Results: The centre has been running the program since February 2015 and has progressed from provisional to full accreditation as a training centre over a period of two years. A ROMP registrar was recruited to the program in 2015. The registrar has successfully achieved all the level two clinical learning outcomes of the program's CTG and passed the written exam component of the program. The registrar is on course to complete the clinical component of the program within the recommended 3-year timeframe and thereby complete all components of the program.

Discussion: Registrar has gone from being a trainee under close supervision to contributing to the clinical workload of the department under minimum supervision. Enabled review of department practices and implementation of kV therapy using AAPM TG 61 protocol. He has taken a leading role in the implementation of VMAT techniques in the department. The registrar also automated the light field vs X-ray QA checks with Matlab code.

Being a regional centre, there are less options to familiarise with more advanced RT techniques such as stereotactic radiosurgery, adaptive RT and Tomo therapy, however, core competencies were achieved by organizing visits to other centre as required.

Acknowledgements: Adrian Bailey and all staff of the CWCCC. The TEAP program is supported by the Commonwealth Government of Australia.

O-65

ESTIMATION OF EYE LENS EXPOSURE FROM WORKLOADS DURING INTERVENTIONAL PROCEDURES IN SOUTH AFRICA, TAKING MODIFYING FACTORS INTO ACCOUNT

M. A. Sweetlove, A. Rose[1], W. I. D. Rae[2]

Medical Physicist, Bloemfontein, South Africa, Departments of [1]Community Health and [2]Medical Physics, University of the Free State, Bloemfontein, South Africa. E-mail: ann@aberan.co.za

Introduction: Eye lenses are radio sensitive organs, and cateractogenesis is the consequence of high levels of ionising radiation exposure. Use of Personal Protective Equipment (PPE) during interventional procedures significantly decreases the exposure to the eyes. In order to relate eye effects to exposure levels, some categorisation of dose levels is required. Operator dose estimation is a challenge if not measured directly, because of the many factors affecting dose and especially scattered dose. An estimate of the amount of exposure and how it is modified by eye PPE utilisation may be useful in scaling risk and grouping interventionists into eye exposure level categories. The objective of this study was to estimate the relative eye lens exposure from workloads of Interventionalists in the South African (SA) context taking modifying factors into account.

Materials and Methods: Workload was calculated from self-administered questionnaires completed by interventionalists (total 95) who indicated type of procedure, the number of procedures per week and the number of years worked with fluoroscopy guided interventional procedures. These data were obtained from 21 radiologists, 41 adult cardiologists and 33 paediatric cardiologists. Average Dose Area Product (DAP) values per procedure were obtained from previous work done in SA. As DAP reflects not only the dose within the radiation field, but also the area of tissue irradiated it is a better indication of scattered radiation which is the source of radiation to the eye. Three categories of modifiers were considered: (1) a reducing modifier accounting for attenuation afforded by the use of ceiling suspended screens and the frequency of use of these screens; (2) a similar modifier for the use of lead glasses and the frequency of use of these glasses; and (3) an escalating modifier for radial (as opposed to femoral) approach and its frequency of use. The maximum modifying factors were taken from published data.

Results: The average number of years worked with fluoroscopy was 12, median 10. The longest was a cardiologist who worked 40 years. The study showed a wide range of estimated eye lens workload exposures ($Gy.cm^2$). Average 354255 ± 675851, median 77418, maximum was a cardiologist 4 320 504, Median for cardiologists 291 346, radiologists 105 680 and paediatricians 35 972. The estimated eye lens workload exposures were not compared to published values, as they are simply a way of assessing which interventionalists receive the greatest exposures to their eyes according to the individual's workload, PPE utilisation and approach. PPE utilisation, specifically ceiling suspended screens, have a large effect on eye exposure, especially for cardiologists, average decrease of 36%. Median before modifiers for cardiologists, radiologist and paediatricians respectively 706 560, 128 579 and 43 245 and after modifiers 291 346, 105 680 and 35 972. Estimated eye workload exposures indicate at least three groups of exposures.

Discussion: There are many factors that influence the scattered exposure to the eyes. This study serves as an indication of the eye exposure received by Interventionalists in SA which could cause cateractogenesis. Another study will compare this data to the cataract findings obtained during lens screening of these same interventionists.

O-66

CATARACT FINDINGS AMONG SOUTH AFRICAN INTERVENTIONALISTS

A. Rose, W. I. D. Rae[1]

Departments of Community Health and [1]Medial Physics, University of the Free State, Bloemfontein, South Africa.
E-mail: roseas@ufs.ac.za

Introduction: Ionising radiation is indispensable as a diagnostic, prognostic and therapeutic modality in modern western medicine. Ionising radiation is an established occupational health hazard in the catheterisation laboratory. Exposure may result in health effects such as skin changes, carcinomas, chromosomal aberrations and cataracts. The lenses of the eyes are higher radiosensitive and cataracts in radiation health workers commonly occurs in the posterior capsular (PC) region of the lens. The left eye is often affect up to three times more commonly than the right eye. The dose per procedure varies from 10 to more than 1 000 micro Sievert and depends on the type and duration of the procedure, the skill of the operator and the dose reduction strategies employed (such as personal protective equipment (PPE) used and policies and guidelines followed).

Objectives: The aim of this study was to describe the prevalence of occupational related radiation induced cataracts in South African interventionalists.

Materials and Methods: This study was a cross sectional observational study. The participants were from several different cities in South Africa and were recruited at various conferences. The participants included exposed doctors (interventional radiologists, cardiologists and paediatric cardiologists) and a comparative group of unexposed doctors. All participants completed a survey which collected data on their risk for cataracts, their occupational history, their utilisation of PPE and their training in radiation safety. They had their eyes dilated and had a slit-lamp examination. The data were analysed using STATA 12®. Descriptive and analytical analysis was done. The study received ethical approval from the University of the Free State (UFS44/2014).

Results: There were 351 participants (144 exposed) and 267 (119 exposed) had their eyes screened. The median age was 46.1 (exposed) and 45.5 years (unexposed). There were 89 (72.4%) men and 34 (27.6%) women (exposed). The median years worked was 10 (exposed) and 14 (unexposed). The median years doing fluoroscopic procedures was 9.5 years. The risk factors for cataract included diabetes 5 (4.1%) in exposed and 12 (5.9%) in the unexposed ($p=0.473$); BMI 25.5 ± 3.5 (exposed), 26.2 ± 4.7 (unexposed); there were two participants that used steroids (unexposed). There were 53 radiologists, 54 adult cardiologists and 37 paediatric cardiologists. In the left eye, there were 34 cataracts (16 in exposed group). In the right eye, there were 25 cataracts (exposed). In the left nucleus, there were 16 opacities (5 in the exposed) and in the right nucleus there were 15 opacities (4 in the exposed). In the left cortex, there were 31 opacities (15 in the exposed). In the right cortex, there were 25 opacities (10 in the exposed group). In the left posterior capsule, there were 11 cataracts, 6 (5.0%) in exposed and 5 (3.4%) in unexposed ($p=0.195$). In the right posterior capsule, there were 5 cataracts 2 (1.7%) in exposed and 3 (2.0%) in the unexposed ($p=0.831$). Nuclear and cortical cataracts were the most common which is expected. Cataracts were more common on the left in the exposed.

Discussion: Interventionalists are at increased risk to develop radiation related cataracts. Cortical and nuclear cataract was more common which may be associated with age related changes. The increased prevalence in left side in exposed participants' cataracts suggest an occupational cause. There was a significant difference between exposed and unexposed participants in the posterior capsular category. In conclusion, there should be increased vigilance in radiation protection measures to protect interventionalists from developing cataracts due to ionising radiation exposure.

O-67

A PROSPECTIVE APPROACH OF QA IN RADIATION ONCOLOGY AND IMPLEMENTATION OF AAPM TG 100

D. Banjade, A. Mishra, G. Warr, S. Tan, M. Fuller, R. Hammond, K. Thuraisingam, G. Stevens

Department of Radiation Oncology, Central West Cancer Care Centre, Orange Hospital, New South Wales, Australia. E-mail: dilli.banjade@health.nsw.gov.au

Implementation of quality management (QM) system in Radiation Oncology (RO) will improve work efficiency in radiotherapy (RT) and prevent the prospective risk associated in the process. Traditionally, QM in RT has focused on device centric approaches, however, many of the safety and quality issues in RT have been identified as human factors. Therefore, assurance of quality and safety of the department is not only the quality assurance (QA) of the equipment and instruments but also requires implementation of QA programs covering personnel and procedures as a whole.

Founding an interdisciplinary team with full cooperation in the department to focus on mitigating the process-related errors can establish a risk based QM program. Various activities, procedures and work performance can be strengthened by formulating QM systems in RT, emphasizing a proactive response to near misses rather than responding to unacceptable events.

Identifying the likelihood of occurrences, likelihood of failure being undetected and outcome severity of events on the paths of a fault tree analysis (FTA) process can prevent harm to the patient during the RT process. The implementation of total QM approach with procedures, rules and regulations can detect each failure mode on each process and pave the way to deliver safe and quality treatment.

This presentation will review the insights of the AAPM TG-100 QM formalism applied to local processes including error propagation and risk assessment at CWCCC Orange NSW, a regional RT centre in Australia. The QM tool of failure mode and effect analysis (FMEA) and FTA will also be discussed with examples. In addition, the presentation will explore the prospective approach of TG 100 as an integrated QM measure in Radiation Oncology.

O-68

PERFORMING TG-142 QUALITY ASSURANCE PROCEDURES ON LINEAR ACCELERATORS USING PIPSPRO SOFTWARE

K. R. Muralidhar, P. Srinivas, K. Jayaram, M. Rambabu, M. Prabhakar, Krishna Komanduri

Department of Radiation Physics, American Oncology Institute, Hyderabad, Telangana, India. E-mail: muralidharkr@americanoncology.com

Introduction: In Radiation Oncology, increase intechnology and treatment techniques made it possible and desirable to perform quality assurance (QA) with increased accuracy. For this Task group-142 (TG-142) from American Association of Physicists in Medicine (AAPM) was developed and published a comprehensive guideline. Recommendations of TG-142 tests are technically challenging both to perform as well to analyze to a high degree of accuracy that the recommendations call for. The objective of this work is to perform and report TG-142 in Linear accelearators using PIPSpro software and phantoms using Electronic Portal Imaging Device (EPID) and KV imager.

Materials and Methods: TG-142 was performed on True beam STx linear accelerator. Imaging is performed using the on board imaging (OBI) and EPID. All monthly and annual TG-142 quality assurance tests were performed and analyzed. Pipspro was designed to be used with portal images. The portal images and KV images in DICOM format were transferred to PIPSpro software for analysis. The tests that were performed were, Imager QA, Radiation light field QA, Star shot image analysis QA with collimator, gantry and table rotation, MLC QA (MLC transmission, MLC position, MLC Multiport test), Stereotactic Test and Image Guided Radiotherapy test.

QC-3 Phantom, supplied by manufacturer was used in Imager QA, for analyzing QA on EPID and OBI images. This test will be useful to observe the changes in performance of EPID and OBI image quality in the long run. For the radiation light field QA, FC-2 phantom was used. Star shot test was performed and Images were obtained from EPID using an equidistant 30 degree angles while rotating collimator, gantry and couch respectively. MLC QA (MLC leaf position, leaf width, and multi-port and leaf transmission) was performed using the MLC phantom on the treatment couch at isocenter by positioning EPID imager at 105 cm SSD. The Stereotactic Module allows the user to perform the Winston-Lutz test. They are 2D and 3D tests that that determines planar radiation-mechanical isocenter offsets and “Optimal Isocenter Shift”. The IGRT module was used to perform QA on positioning/repositioning and imaging and treatment coordinate coincidence on a daily basis with the help of IGRT QA phantom.

Results: All tests gave accurate and reliable resultsand presented in both numerical and graph. In imager QA report, modulation versus Frequency graph obtained and special resolution (line pairs/mm) of F50, F40, F30, Uniformity values that obtained were 0.487, 0.621, 0.755, and 98.305% respectively. In radiation light field displacement, the maximum displacement shown was 0.6 mm and the jaw displacement shown was 0.42 mm respectively. MLC multiporttests have shown that the deviation of leaves in left bank and right bank at various positions (70 mm, 40 mm, 10 mm, -20 mm, -50 mm) were within the tolerance limits (1 mm). Image based MLC QA shown all MLC positions are within 1 mm deviation. MLC Interleaf leakage and interbank leakage were found to be 0.557% and 30.436% respectively. Start shot analysis has shown that the isocenter shift from gantry and collimator was a sphere with 0.29 mm radius. Stereotacticreport had shown a deviation of 0.2, 0.5 and 0.8 mm in x, y and z directions respectively. Positioning and repositioning variations on daily basis were presented in IGRT report.

Conclusion: We performed TG-142 several times repeatedly and at various intervals on True Beam STx and found the performace of the machine is well within tolerance limits protocols. The results are consistent and well within the specifications. We found using PIPSpro istime saving, economical, easy and accurate to perform TG-142 in a busy department.

O-69

THE APPLICATION OF TEXTURE ANALYSIS FOR DISCRIMINATION FATTY LIVER BY ULTRASOUND IMAGES

Akbar Gharbali, Milad Zeinali Kermani

Department of Medical Physics, Urmia University of Medical Sciences, Urmia Iran.
E-mail: gharbali@yahoo.com

Introduction: Fatty lever or Hepatic steatosis is an abnormality in excessive accumulation of lipids mainly triglyceride in liver that can cause far reaching metabolic consequences. Early detection and reliable diagnosis of fatty liver increase the cure rate and provide optimal treatment. Ultra-Sonography is a non-invasive and more common and convenient medical imaging to interpret fatty liver. Biopsy has accepted for confirming the ultrasound imaging results. So, it is not possible to demonstrate any significant increase in diagnostic accuracy with conventional way – just visual texture analysis and interpretation of the radiological image.

Objective: To evaluate diagnostic potential of computer aided texture analysis methods in differentiation of fatty liver from normal liver by ultrasound (US) imaging to improve radiologist confidence in identification mild fatty liver with no need for other examination and pathological testing.

Materials and Methods: Database consists of ultrasound images of 35 mild fatty liver and 36 normal liver. By loading ultrasound images in the MaZda software, regions of interests (ROIs) were defined within the fatty liver and normal liver. Gray levels intensity within a ROI normalized according to three normalization schemes:N_1: default or original gray level, N_2: μ+/- 3 σ (μ= mean and σ= variance), N_3: present intensity 1%-99%. Then per ROI per normalization schemes, up to 270 multi scale texture features parameters were computed as descriptors of ROI texture pattern. Then texture features parameters eliminated to the 10 best and most effective features based on applied two algorithms: maximum Fisher Coefficient and or minimum probability of error and average correlation coefficients (POE+ACC). Each ROI within fatty and normal liver US images discriminated by this features data under two standard schemes with three texture analysis methods: PCA (principal Component analysis), LDA (Linear Discriminant analysis) under first nearest neighbor (1-NN) classifier and NDA (Non Linear Discriminant analysis) under artificial neural network (ANN) classifier. The confusion matrix and Receiver Operating Characteristic cure (ROC) analysis were used for examining the discrimination performance of the texture analysis methods under applied options.

Results: The best result for discriminating fatty liver from healthy liver was related to NDA texture analysis method with sensitivity, specificity and area under the EOC cure of %99, %98 and 0.98 respectively.

Discussions: Our result indicate that automated texture analysis is a reliable and powerful method for discriminating fatty liver from normal liver tissue in ultrasound images. So, it has the potential to boost the radiologist's accuracy and therefore confidence for effective use in differentiation of fatty liver on liver US image.

Poster

P-1

INTENSITY MODULATED RADIOTHERAPY PLAN VERIFICATION FOR DIFFERENT DOSE RATES AND DIFFERENT GRID SIZES USING FLUENCE MEASUREMENT

Rahil Anjum, C. Varatharaj, M. Ravikumar, K. M. Ganesh, S. Sathiyan, B. Shwetha

Department of Radiation Physics, Kidwai Memorial Institute of Oncology, Bengaluru, Karnataka, India. E-mail: rahilanjum1995@gmail.com

Introduction: The principle of Intensity Modulated radiotherapy (IMRT) is to deliver a high dose to the target volume and an acceptably low dose to the surrounding normal structures. Thus choosing an optimum grid size plays a vital role for planning in radiotherapy cases especially while treating with IMRT. A minimal change of even 1 mm of grid size can result in large variation in the treatment planning. The aim of this study is to find the optimal IMRT plan by comparing the IMRT pre-treatment Quality Assurance (QA) verification plan for different dose rates (300, 400, 500 and 600 MU/min) and for different grid sizes (2.5 and 5 mm) using fluence measurement in a 2D array (I'MatriXX).

Materials and Methods: 20 patients (10 Brain and 10 Head and Neck cases) are planned for the IMRT and the verification plans are created for different dose rates and for different grid sizes in the Treatment Planning System (TPS) for each patient. The totals of 160 verification plans are created, Clinac 2100-DHX linear accelerator and I'MatriXX are used for the execution of the verification plans. All the 160 verification plans were executed and the obtained data for all the plans is saved in the PC for the later analysis. The obtained data is analysed between the TPS obtained dose plane and the measured dose plane using the OmniPro I'mRT software.

Results and Discussion: In our study, the correlation coefficients were calculated for TPS v/s I'MatriXX and the values lie between 0 and 1. The quantitative analysis between the calculated and measured dose distribution was evaluated using Distance to Agreement (DTA) and Gamma-index. The tolerance of 3% dose difference and 3 mm DTA and Gamma tolerance ≤ 1 was set for the analyses. In our results there is no significant change in mean coefficient of variation between the measured fluences v/s TPS calculated data in all brain and H and N cases. The variation in percentage of pixels passing gamma also found that there is no significant changes with respect to grid size of 2.5 mm and 5 mm of different dose rates in both brain and head and neck cases. We observed lower passing rate of DTA in head and neck cases and which is similar in grid size variation and also with respect to dose rates. Similar work published by other researchers using portal dosimetry was found that, there was a significant change in passing rate due to dose rate change, but in our case we found that, which is insignificant. This could be because of finite size of the ionization chamber and the spacing between the chambers in I'MatriXX device where as the resolution in portal imaging device is better and having finite pixel size in the portal imaging devices.

Conclusion: The qualitative analysis using comparison of profile and isodose lines were found to be insignificant change between the calculated and measured fluences. The quantitative analysis was done using gamma evaluation method and finding the correlation coefficient. Based on the our obtained data analysis we could not found much difference between the measured and calculated fluences both in terms of qualitative and quantitatively for change in dose rate and grid sizes. Hence, we conclude that, this could be due to the volume average effect of finite size of the detectors in the I'MatriXX and the finite spacing between the detectors.

P-2

REDUCTION METHOD OF THE SKIN SURFACE DOSE IN MEGAVOLTAGE PHOTON RADIOTHERAPY

Masahiko Okumura, Mikoto Tamura[1], Hajime Monzen[1,2], Kenji Matsumoto, Masakazu Otsuka[1], Kohei Hanaoka, Kohei Shimomura[3], Yasumasa Nishimura[3]

Department of Central Radiology, Kindai University Hospital, [1]Department of Medical Physics, Graduate School of Medical Science, Kindai University, [2]Department of Radiation Oncology, Faculty of Medicine, Kindai University, Osaka, [3]Department of Radiological Technology, Faculty of Medical Science, Kyoto College of Medical Science, Nantan, Japan. E-mail: 1615060015@edu.med.kindai.ac.jp

Introduction: Many kinds of carbon couches are commonly used in megavoltage radiotherapy to provide patient support. However, the carbon couch causes the increase of surface dose due to shifting the depth dose profile to the patient surface, which is associated with skin toxicity.

Objectives: A novel rigid couch (HM board) constructed from polycarbonate foam core sandwiched by two thin layers of glass fiber has been developed. In this study, we evaluated the increase or decrease of surface dose with various tools on the carbon couch and verified whether the HM board was able to reduce the surface dose compared to the carbon couch in megavoltage photon radiotherapy.

Materials and Methods: We measured the absorbed surface doses with comfort tools (cloth mat and 5 cm Styrofoam board) and immobilization device (vacuum-fixed cushion) on a carbon couch (iBeam Couchtop STANDARD; BrainLab) and H-M board alone for 6 and 10 MV photon beams by a plane-parallel ionization chamber. The prescribed dose at 5.0 cm depth in solid water phantom (SCD = 100 cm) was 2.0 Gy with a field size of 10×10 cm^2. We also measured the depth dose profiles for 6 and 10 MV photon beams with various thickness of the Styrofoam board on the carbon couch and the H-M board alone.

Results and Discussion: The absorbed surface doses were 2.209, 2.200, 2.169, 2.079, and 2.027 Gy for the carbon couch alone, with cloth mat, vacuum-fixed cushion, and 5 cm Styrofoam board on the carbon couch, and the H-M board alone, respectively, with 6 MV photon beams. With 10 MV photon beams, the absorbed surface doses were 1.980, 1.998, 1.958, 1.823, and 1.741 Gy, respectively. The Styrofoam board on the carbon couch had no impact on the depth dose profile, while the H-M board shifted approximately 0.4 cm to the depth direction compared with the carbon couch alone. The 5 cm Styrofoam board reduced the surface dose by 5–7%. The H-M board, with a tissue equivalent thickness 0.4 cm less than carbon couch, reduced the surface dose approximately 3–4% compared with 5 cm Styrofoam board on the carbon couch. The H-M board could be more useful in clinical situations instead of carbon couch since it provided the sufficient space compared to a couch plus the Styrofoam board in megavoltage photon radiotherapy.

P-3

VERIFICATION OF INTENSITY MODULATED RADIATION THERAPY TREATMENT USING FLUENCE MAP RECONSTRUCTED FROM VARIAN LINAC LOG FILES

Nur Shaheera Midi, Hafiz Mohd Zin

Oncology and Radiological Sciences Cluster, Advanced Medical and Dental Institute, Universiti Sains Malaysia, Bertam, Penang, Malaysia. E-mail: hafiz.zin@usm.my

Intensity Modulated Radiation Therapy (IMRT) delivers highly conformal dose to the tumour using dynamic multileaf collimator (dMLC). The dMLC moves continuously at variable speed during treatment and is prone to delivery errors. Pre-treatment verification of IMRT ensures accurate delivery of the treatment planned. The study develops computer algorithm to analyse treatment log files from a Clinac iX linac with 120 MLC leaves (Varian Medical Systems, Palo Alto, CA). Varian log file records the prescribed and delivered MLC leaves position and other linac parameters at 20 Hz. The algorithm reconstructs the IMRT dose delivered and calculate errors between the planned and the actual IMRT treatment. Dose reconstruction and analysis were performed using Matlab (MathWorks, Natick, MA). Five clinical IMRT cases were evaluated in this study. The MLC speed ranged from 1.6 cm per second to 4.0 cm per second. Using gamma index at 3% dose difference and 3 mm distance to agreement (DTA) to compare between the planned dose map and delivered dose map, all cases obtained 100% pass rate. Application of the log file in verification of dMLC based radiotherapy delivery is useful and can be used as supplementary data in dosimetry based IMRT pre-treatment check. **Acknowledgement:** This work is funded by Fundamental Research Grant Scheme, Ministry of Education Malaysia, 203/CIPPT/6771383. The authors would like to acknowledge LF Chin for his preliminary work for this study and LC Lim for providing log files in this work.

P-4

INVESTIGATION ON THE FEASIBILITY OF USING CBCT (CONE BEAM COMPUTED TOMOGRAPHY) AS A READOUT TOOL FOR NIPAM POLYMER GEL DOSIMETRY

Winfred Michael Raj, S. Ebenezer Suman Babu, K. Mohamathu Rafic

Department of Radiotherapy, Christian Medical College, Vellore, Tamil Nadu, India.
E-mail: winfredmichaelraj@gmail.com

Introduction: The post readout of polymer gel is often performed by various imaging modalities such as MRI, and X-Ray CT. Since, these imaging modalities are not easily available due to patient load and also involves significant time for imaging, in this study, we have investigated the feasibility of using a CBCT scanner that makes use of a cone beam of X-ray to read out the NIPAM (N-Isopropylacrylamide) polymer gel dosimeter.

Aim and Objectives: To assess the feasibility of using CBCT scanner as a readout tool for analyzing the NIPAM polymer gel. (1) To investigate the dose readout capability of an On-Board Imaging Cone Beam Computed tomography (CBCT) setup to read and quantify the change in Hounsfield Units due to polymerization in a NIPAM gel dosimeter. (2) To remove noise in the recorded dose information. (3) To develop a MATLAB code that quantifies the Hounsfield for different region of interests in a CBCT image. (4) To quantify the amount of polymerization by measuring the change in Hounsfield Units with respect to the dose in a NIPAM gel dosimeter.

Materials and Methods: The polymer gel dosimeters in this study are co-solvent free and the recipe is as proposed by chain et al with increased sensitivity and resolution for X-Ray CT dose response. The NIPAM gel dosimeter was prepared by soaking and dissolving gelatin, by stirring for about 1 hour. Once the gelatin is completely dissolved and the solution becomes clear, the gelatin solution is cooled down and NIPAM and the cross linker (Bis) after which, the oxygen scavenger (THPC) is added (5 mM) and it is stirred for about 30 seconds.

Initially the dose signal build-up time was analyzed in the irradiated gel and the time taken for the polymerization process to complete is found, following which the gel dosimeters irradiated for different known doses are read out using a CBCT, and the change in density is quantified by analyzing the Hounsfield units across the irradiated region for which a separate Matlab code was developed.

A separate MATLAB code was developed to average the images slice by slice, to reduce noise and to increase the signal to noise ratio in the irradiated gel.

Results and Discussions: The exclusive study on the buildup shows that complete dose signal development is achieved after 10 hours of irradiation and the gel dosimeter can be readout any time after that.

In our study, the effect of image averaging was found to be close to what was proposed by Hilts et al. Image averaging filter used in our study was found to be effective in gel dosimeters with and without dose. A very high increase in the SNR could be seen as a result of averaging.

The NCT values that are calculated from the Average HU values that are measured in four different Regions of Interest (10 x 10 mm^2, 8 x 8 mm^2, 6 x 6 mm^2, and 4 x 4 mm^2) are found to be linear as proposed by Johnston et al.

P-5

GENERATION OF MAGNETIC RESONANCE IMAGE WITH TEETH RESTORATIONS FROM COMPUTED TOMOGRAPHY SEGMENTATION

Min-Young Lee, Kyu-Ho Song, Bo-Young Choe, Tae-Suk Suh

Department of Biomedical Engineering, College of Medicine, The Catholic University of Korea, Seoul, Korea. E-mail: suhsanta@catholic.ac.kr

Introduction: The purpose of this study was (a) to develop a CT/MR oral phantom and design containers with insertable dental implants; (b) to optimize the parameters for metal artifact reduction by a multi modal system; and (c) to register CT/MR to generate non-artifact MR images with dental restorations.

Materials and Methods: The phantom comprises sphere which shaped to simulate the anatomical structures of a human head with real teeth and dental implants. All measurements were done using a human 3T MRI with spin echo (SE) and gradient echo (GRE) sequences image scan together with CT high resolution image. Firstly, the metal regions and normal teeth parts are extracted with a suitable threshold from an initial image reconstructed without metal artifacts reduction from the CT images. Secondly, corrected metal projection regions of MR images and finally, CT images are applied into artifact-reduced MR images.

Results: The dedicated CT/MR phantom was performed to assess the magnitude and spatial dependence of MR image geometrical distortion and CT artifact accuracy in various sequences. After CT/MR registration, spin echo sequence presented 12.0 mm and 24.0 mm differences in X and Y axes and gradient echo sequence showed 18.0 mm and 36.6 mm differences in X and Y axes.

Discussion: The dedicated phantom provides a unique and useful tool in head and neck research in offering references of metal artifact reduction and registration methods for multi-modality medical images. Therefore, the contrast-enhanced dental MR image offers a means of visualizing the different anatomical structures in diagnostic system.

P-6

THE EVALUATION OF GAMMA INDEX FOR EPID BASED PORTAL DOSIMETRY WITH PROCESS CAPABILITY ANALYSIS IN PATIENT-SPECIFIC VOLUMETRIC MODULATED ARC THERAPY QUALITY ASSURANCE

Samju Cho, Rena Lee, Chunhee Lee, Minsoo Chun, Sohyun Ahn[1], Suk Lee[2], Kyubo Kim

Department of Radiation Oncology, Ewha Womans University Medical Center, [1]Department of Radiation Oncology, College of Medicine, Yonsei University, [2]Department of Radiation Oncology, College of Medicine, Korea University, Seoul, Korea.
E-mail: chosamjugmail.com

Introduction: Electronic portal image device (EPID) based portal dosimetry is wildly used for Patient-specific volumetric modulated arc therapy (VMAT) Quality Assurances (QA). The Gamma pass index and rate to ensure the VMAT are 3 mm/3% and 95% at our institution. However, errors could be made if the gamma indexes are based on 3 mm/3% due to the large error tolerance during the complex radiation therapy process.

Objectives: The purpose of this study is to establish appropriate patient-specific QA gamma index with process capability analysis using a method of statistical process control (SPC) for the VMAT portal dosimetry.

Materials and Methods: The recent 43 data patient-specific QA cases using the portal dosimetry (PD) were selected in this study. The patient-specific QA, sorted from gamma criteria respectively, were analysed retrospectively using a method of statistical process control (SPC). The values of gamma indexes were 3 mm/2%, 2 mm/3%, 2 mm/2%, 2 mm/1.5%, 1.5%/2 mm, 2 mm/1% and 1 mm/2% in comparison to our institution's standard value of 3 mm/3%. The first 20 cases were selected in order to set up accurate control limits for SPC analysis, and were analysed with the control limits. We compared each process capability index (PCI) using the process capability analysis of the GPR with the gamma index.

Results: The analysed PCI values with respect to gamma indexes were calculated to be 0.89 for 3 mm/3%, 1.07 for 3 m/2%, 0.91 for 2 mm/3%, 1.11 for 2 mm/2%, 1.16 for 2 mm/1.5%, 1.12 for 1.5 mm/2%, 1.2 for 2 mm/1% and 1.15 for 1 mm/2%. The mean gamma pass rate were 98.9% for 3 mm/3%, 97.1% for 3 m/2%, 97.6% for 2 mm/3%, 95.1% for 2 mm/2%, 92.6% for 2 mm/1.5%, 92.8% for 1.5 mm/2%, 89.2% for 2 mm/1% and 88.5% for 1 mm/2%.

Conclusions: The PCI at a gamma index of 3 mm/3%, which is currently used at our institution, appeared to be the lowest and the process capability index was the highest at gamma index of 2 mm/1%. The gamma index of 3 mm/3% for patient-specific QA could be considered to have an unstable process factor as process capability indices over 1.0 are considered to be relatively stable. The PCI values tend to increase as the values of gamma index decline according to the results. The GPR value of 1.2 applied with gamma index of 2 mm/1% was the highest among the results and is considered to be a relatively stable process for our institution with EPID based portal dosimetry.

Acknowledgement: This research was supported by Basic Science Research Program through the National Research Foundation of Korea (NRF) funded by the Ministry of Education (No. 2015R1D1A1A01060463) and the Radiation Safety Research Programs (1305033) through the Nuclear Safety and Security Commission.

P-7

EVALUATION OF EBT3 FILM DOSIMETY USING DUAL-CHANNEL MERGED METHOD FOR STEREOTACTIC BODY RADIOTHERAPY QUALITY ASSURANCE

Sang-Won Kang, Jin-Beom Chung[1], Kyeong-Hyeon Kim, Keun-Yong Eom[1], Jeong-Woo Lee[2], Yong-Jin Kim, Tae Suk Suh

Research Institute of Biomedical Engineering, College of Medicine, The Catholic University of Korea, [2]Department of Radiation Oncology, Konkuk University Medical Center, Seoul, [1]Department of Radiation Oncology, Seoul National University Bundang Hospital, Seongnam, Korea.
E-mail: : kangsangw@gmail.com

Introduction: This study assessed the feasibility of a dual-channel (DC) merged method for film dosimetry. The red channel (RC) is usually used to ensure dosimetric quality using a conventional fraction dose because the RC is more accurate at low doses within 3 Gy than the green channel (GC). However, the RC is prone to rapid degradation of sensitivity at high doses, while degradation of the GC is slow. Thus, in this study, we designed the dual-channel (DC) merged method which was merged RC and GC dose measurement according to dose ranges.
Objectives: The purpose of this study is to verify the dual-channel (DC) merged method on EBT3 film dosimetry for stereotactic body radiotherapy (SBRT).
Materials and Methods: The film calibration was performed in doses ranging from 0 to 15 Gy with 6-MV photon beams at the 10 × 10 cm^2 field. The single channel net-optical density (net OD) was obtained with the measured film for each red and green channels (RC and GC). To acquire the merged net OD of DC, the net ODs of RC and GC were combined at 6, 8, and 10 Gy dose level. To compare the RC, GC and DC, the several SBRT treatment plan cases were applied and measured by EBT3 film. The calculated and measured dose distributions were evaluated with root-mean-squares-error (RMSE) and gamma analysis.
Results and Discussion: For RMSE value of each channels, the RC is more accurate than GC for low doses when comparing the calculated dose distribution, while the RC is more accurate in higher doses than 8 Gy. The accuracy of DC was increased than the RC regardless of low and high doses. For the gamma passing rate with acceptance criteria of 3%/3 mm and 2%/2 mm, all plans for each channel met agreement more than 94% and 84%, respectively. Within the 3%/3 mm gamma criteria, the mean passing rate (97.48%) of DC method was the highest when comparing with single channel method such as the RC (97.42%) and GC (96.92%).
The DC method devised in this study will be more suitable in clinical radiation therapy, especially the dosimetric QA (DQA) for SBRT using high doses. In general, the result of DQA for SBRT is evaluated using the RC with the pretreatment QA plan downgraded for prescription dose. However, this downgraded evaluation has difficulty in reflect real clinical practice due to affect in variation of dose distribution and dose rate in pretreatment QA plan by dose degradation. Our DC method does not necessary need a dose downgrade for pretreatment QA plan. DQA is practical in the real clinical application. Therefore, we recommend the use of DC method in DQA using film dosimetry, especially in high dose treatments, such as SBRT and SRS.
This study found that the DC method has the advantage of reducing single-channel analysis errors in high doses for film dosimetry. Therefore, we recommend that the use of DC method is more appropriate as the dosimetric QA for SBRT using EBT3 film.

P-8

PHATOM DEVELOPMENT FOR DOSE AUDIT OF CARBON ION RAIDOTHERAPY CENTERS IN JAPAN

H. Mizuno, A. Fukumura, S. Fukuda, N. Kanematsu, S. Yonai, M. Fukahori, T. Shirai
Department of Charged Particle Therapy Research, National Institute of Radiological Sciences, QST, Chiba, Japan. E-mail: mizuno.hideyuki@qst.go.jp

Introduction: In a multi-center clinical trial, it is important to implement a quality assurance program ensure that all centers provide the same dose to patient and achieve high quality trial results. Japan Carbon-ion Radiation Oncology Study Group (J-CROS) was founded in 2014. The purpose of this group is to obtain clinical evidence through multi-center clinical trials among participated facilities to demonstrate the efficiency of carbon ion radiation therapy. In order to implement the quality assurance program from the view point of dose audit it is necessary to prepare auditing tools, especially new phantom.
Objectives: The aim is to develop a phantom suitable for dose auditing. There are many restrictions on the on-site dose measurement. Since it is usually done after patient treatment, the auditing time is limited at the hospital. Quick alignment is required. Furthermore, in order to avoid breakage, it is necessary to attach the chamber easily and safely to the phantom. Of course, the phantom should be easily carried around.
Materials and Methods: Produced phantom was a simple PMMA water tank with ionization chamber holders. The inner side wall of the tank has a groove structure for inserting the ionization chamber holder at every 5 mm depth in a direction towards the horizontal beam axis. Several types of holders were made to support several ionization chamber types such as farmer type, parallel plane type and pinpoint type. We also made an alignment holder with iron ball inside. By using this, we can run end to end tests.
Results and Discussion: The phantom was successfully produced and applied to the dose audit for the J-CROS facilities. Setup time was very short, making the measurement very efficient. Even in the two ionization chamber measurements, one is from the auditor and the other is from hospital, the time loss during ionization chamber exchange was carried out within 2 minutes and setup position was precise. The phantom was also used for the annual dose monitoring as a credentialing for another international multi-center clinical trial.

P-9

COMPARING DOSIMETRIC PARAMETERS OF INTENSITY MODULATED RADIATION THERAPY AND VOLUMETRIC MODULATED ARC RADIATION THERAPY FOR STOMACH CANCER

Sruthy P. Kumar, C. Paranthaman, S. Prabakar, P. Loganathan, Lalitha Kameshwari, David K. Simson, Parveen Alhawat, Harpreet Singh
Department of Radiation Oncology, Action Cancer Hospital, New Delhi, India.
E-mail:sruthyprasannakumar23@gmail.com

Introduction: Radiotherapy as an adjuvant treatment plays an important role in the multidisciplinary treatment of gastric cancer. Earlier, with the availability of older radiotherapy techniques the doses delivered to operative bed were high resulting in higher doses to normal surrounding tissues, thus higher toxicities. In modern era of precision radiotherapy, especially with the advent of intensity modulated radiotherapy

(IMRT) it has been possible to improve target coverage, at the same time better sparing of organs at risk (OARs). Various modifications have evolved in since the inception of IMRT technique with regard to dynamics of multileaf collimators, such as step and shoot IMRT, dynamic IMRT, and arc-based therapy (VMAT). So far there has been sparse literature on comparison between these techniques. The aim of our research is do a dosimetric comparison between Dynamic IMRT and arc-based therapy (VMAT) techniques.

Materials and Methods: Twenty eight consecutive patients with gastric cancer who underwent adjuvant radiotherapy were enrolled in this study. Two plans were created for each patient, IMRT (7F-IMRT), and VMAT (Double Arc) techniques with Total Prescribed Dose of 45Gy in 25 fractions. The two plans were compared with regard to PTV coverage, doses received by OARs, Homogeneity Index (HI), Conformation Number (CN) and Monitor Units (MUs).

Results and Discussion: There was no statistically significant difference in PTV coverage ($D_{98\%}$, $D_{95\%}$, $D_{50\%}$, $D_{2\%}$, $V_{110\%}$, and $V_{93\%}$) however, CN was significantly better with VMAT (0.871 v/s 0.790; $p = 0.050$). There was no statistically significant difference in OARs doses (Kidney D_{mean}, Kidney V_{18Gy}, Small bowel D_{mean} and Dmax and V_{15Gy} and V_{45Gy}, Spinal cord PRV D_{max}, and Pancreas D_{mean} and D_{max}) except liver; liver D_{mean} and V_{30Gy} being significantly lesser with VMAT (D_{mean} 18.04 v/s 21.49 Gy; $p=0.028$ and V_{30Gy} 55.84 v/s 74.82Gy; $p=0.036$). There was no significant difference in HI between the two plans ($p=0.674$). There was significantly lesser MUs delivered with VMAT (446.5 v/s 1451.6; $p=0.012$). The low dose tissue bath (i.e. larger volume of tissues receiving lesser dose) was significantly lesser with VMAT than with IMRT, V_{10Gy} (6379.8 v/s 6778.8cc; sp=0.025), V_{15Gy} (4894.4 v/s 54456.5cc; $p=0.012$), V_{20Gy} (3724.4 v/s 4102cc; $p=0.017$), V_{25Gy} (2723.1 v/s 3145.2cc; $p=0.017$), V_{30Gy} (2040.4 v/s 2427.8cc; $p= 0.05$).

Thus, from the findings of this research we conclude that VMAT has certain dosimetric advantages over IMRT with regard to liver sparing, CN, MUs delivery and low dose tissue bath. There is no impact of technique used on target coverage, remaining OARs and HI. What implications these dosimetric advantages of VMAT over IMRT have on clinical outcomes and toxicities is yet to be studied. What is certain with our study and few previous studies is that VMAT has advanstages over IMRT in terms of shorter treatment delivery time, thus with a potential to decrease set up errors and patient discomfort. Another advantage of VMAT is the lesser MUs delivered, thus a potential decrease in the incidence of second malignancy by virtue of lesser integral dose, however this is still a hypothesis generating and yet to be verified in clinical studies.

P-10

STEREOTACTIC RADIOTHERAPY FOR PITUTARY ADENOMA: CYBERKNIFE VS RAPIDARC PLAN COMPARISON

T. K. Bijina[1,2], K. M. Ganesh[3], B. Subbulakshmi[1], A. Pichandi[1]

[1]Department of Radiotherapy, Healthcare Global Enterprises, [3]Department of Radiation physics, Kidwai Memorial Institute of Oncology, Bengaluru, Karnataka, [2]Research and Development Centre, Bharathiar University, Coimbatore, Tamil Nadu, India.
E-mail: tkbijina@gmail.com

Introduction: Pituitary adenomas are slow growing tumors that arise from pituitary gland and it represents nearly 10% to 15% of intracranial tumors in adults. Radiation therapy is an integral part of postoperative treatment for pituitary adenomas. Stereotactic Radiotherapy (SRT) is a high precision radiotherapy technique which delivers accurate dose to tumor and reduces toxicity to surrounding normal tissues. The objective of the study is to analyze and compare the plan results of Robotic Cyberknife (CK) and Rapidarc (RA) based SRT treatment for pituitary adenomas.

Materials and Methods: Ten patients with pituitary adenoma treated with SRT using CK facility with a dose of 25Gy in 5 fractions planned usingMultiplan4.6treatment planning system (TPS) were taken for the study. CK plans were generated with stepwise multi criteria based sequential optimization using Ray tracing algorithm. Fixed collimators were chosen depending on the target volume. Computed tomography (CT) data sets (slice thickness-1.25 mm) from Multiplan TPS were imported to Eclipse TPS for calculating RA plans. All patients were replanned with RA using Eclipse13.7 for comparison study.

TrueBeam accelerator with 120 multileaf collimator (Varian Medical System, PaloAlto, CA) having 6MV photon energy were used for planning. RA plans were done using noncoplanar arcs (clockwise rotation 181°– 179°; 180.1°–330° with couch 45° and counterclockwise rotation 179.9–30° with couch 315°). RA optimization was performed using Photon Optimizer (PO_13.7.16) and dose were calculated using analytical anisotropic algorithm (AAA_13.7.16) with a grid size of 1.25 mm. Prescription isodose line was chosen such that 95% of the target volume received prescription dose for CK plans whereas dose was normalized in RA plans to achieve same coverage and typical beam arrangements shown in Figure 1. The dosimetric parameters evaluated for plan comparison wereD_2, D_{98}, D_{max}, Naukarma Conformity Index (nCI), Homogeneity index (HI), Dose Spillage Index (DSI_{75}, DSI_{50} , DSI_{25}) and maximum dose to organ at risk such as brainstem, optic chiasm, optic nerve and eyes.

Results and Discussion: The median target volume of ten patients was15.15cc (range 2.17cc to 29.09cc). In three cases, the optic nerve dose was restricted to prescription dose since optic nerve was overlapping with target volume. Beam intersection was not allowed through both lens in CK plans whereas avoidance sector were used to limit the dose in RA plans. The dosimetric parameters such as D_2, D_{98} of PTV for CK and RA planswere 28.06 ± 1.00Gy, 27.30 ± 0.58Gy and 24.70 ± 0.2Gy, 24.58±0.32Gy respectively. The maximum dose to

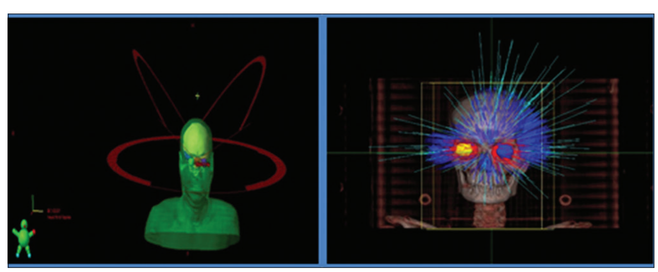

Figure 1: Rapidarc (with avoidance sector) and Cyberknife (with blocked beams) beam arrangement

PTV in CK plans is higher by 2.5% than RA plans. RA plans showed better conformity 1.38±0.07 as compared to1.31 ± 0.18 in CK. Also, RA plansshowed more homogenous dose distribution than CK plans (10.86 vs13.9). The maximum doses to the brainstem and opticchaism were 20.1 ± 5.30Gy, 22.35 ± 4.73Gy and 20.51 ± 4.26Gy, 22.63 ± 4.71Gyfor CK and RA respectively. The integral dose to the whole brain was3.41 ± 1.61Gy-L for CK plans compared to 3.01 ± 1.10Gy-L for RA plans. Mean MU per fraction was found to be 5332 for CK plans and 1264 for RA plans. Volume receiving 5Gy in body (V_{5Gy}) for CK and RA plans are 365.75cc and 291.01cc respectively. Least difference was observed in Dose Spillage Index (DSI_{75}, DSI_{50}, DSI_{25}) among the compared plans.

Conclusion: The dosimetric differences between the two techniques wereminimal, hence the choice of techniquehad to focus on the delivery accuracy.

P-11

DOSIMETRIC COMPARISON OF DOSE TO WATER AND DOSE TO MEDIUM PRESCRIPTION IN MONTE CARLO ALGORITHM FOR LUNG, PELVIS AND HEAD AND NECK CASES

V. Ramya, Daicy George, P. Suresh Babu, S. Sowmya Narayanan

Department of Radiation Physics, Vydehi Institute of Medical Sciences and Research Centre, Bengaluru, Karnataka, India. E-mail: kvramya86@yahoo.co.in

Introduction: Conventional Algorithms for photon beam dose calculations report absorbed dose to water (D_w) which is energy absorbed in small cavity of water divided by the mass of that cavity. Instead of treating human body as water of various densities, Monte Carlo (MC) dose calculation engine calculates dose to medium (D_m). D_m is energy absorbed in small cavity of tissue divided by the mass of the tissue element. There are arguments to support both the D_w and Dm. Doses reported in clinical trials are based on D_w and hence therapeutic ratio and Normal Tissue Tolerance are based on D_w. Hence D_w to be followed. To support D_m, it is said that, it is the quantity inherently computed by MC algorithm.

Objectives: When the calculation method changes, the absorbed dose of the given tissue changes and any difference between D_w and D_m leads to change of dose prescription. Hence in planning one has to decide whether to prescribe D_w or D_m. So far comparative study for D_w and D_m using commercially available MC is not conducted for various sites. There are methods available to convert D_w and D_m. If the dosimetric difference between D_w and D_m is known, the significance of conversion can be found. This study compares the Dosimetric quantities such as Planning Target Volume (PTV) maximum dose (D_{max}), PTV minimum dose (D_{min}), coverage (D_{95}), Organ At Risk Maximum doses (OAR_{max}) between the prescription methods of D_w and D_m for Head and Neck (HN), lung and pelvic cases using MC algorithm for photon beam calculation.

Materials and Methods: The study includes 5 HN, 5 cervix and 5 lung cases. Monaco (v 5.11.01) Treatment Planning System which is capable of doing biological optimization using X-ray Voxel Monte Carlo (XVMC) was used for planning. Calculation voxel size used was 3 mm. Lung cases were

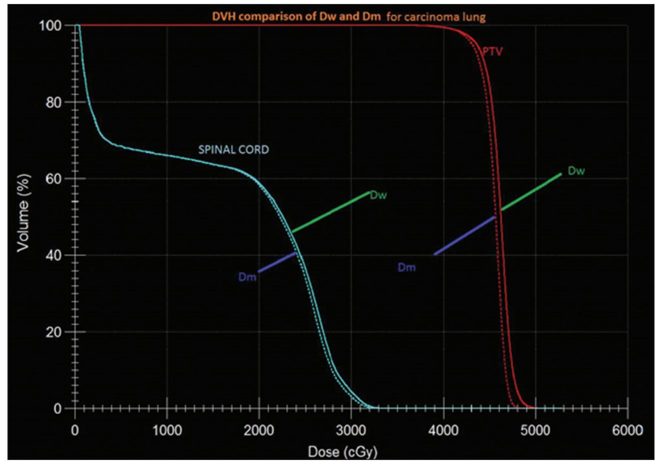

Figure 1: DVH comparison of D_w and D_m for carcinoma lung

planned for Intensity Modulated Radiation Therapy (IMRT). Cervix and HN cases were planned using Volume Modulated Arc Therapy (VMAT). The initial plan was done using dose to medium (D_m) prescription. Keeping the optimization and other calculation properties same, the prescription changed to dose to water (D_w) and the plan was recalculated.

Results and Discussion: The difference between D_w and D_m was calculated using $D_w - D_m \times 100$. We found that for the entire lung, cervix and Head and Neck cases D_w estimates more dose than D_m for D_{max} of PTV and OAR_{max} doses. For Lung cases the D_{max} of PTV differs by 2.3 ± 1.4%, for carcinoma cervix cases 2.8 ± 1.9% and for HN cases 3.6 ± 1.3%. Spinal Cord in Lung cases differs by 2.8 ± 1.4% and Spinal Cord in HN cases differs by 2.2 ± 0.6%. The PTV mean, D_{95}, OAR mean doses differs by less than a percentage in all the cases. And in carcinoma cervix the Maximum dose of head of femur differs by 4.0 ± 1.1%. Spinal Cord receives more dose in D_w prescription due to the fact that higher density bone causes higher fluence of secondary electrons when cells are infiltrated in bony tissue. It was found that for the bony structures and Spinal Cord, D_{max} was more in D_w prescription and it was also found that PTV_{max} dose was higher in D_w prescription. Mean dose of PTV and OAR differences were negligible. OAR differences were negligible asshown in Figure 1. While using sophisticated algorithm such as MC, it is desired to evaluate the plans using D_m parameter, as D_m yields better dose volume predictor than D_w.

P-12

DESIGN AND DEVELOPMENT OF IN-HOUSE MULTICHANNEL APPLICATOR FOR HDR VAGINAL BRACHYTHERAPY AND DOSIMETRIC COMPARISION WITH SINGLE CHANNEL APPLICATOR

G. Kesavan, S. Senthilkumar[1]

Department of Radiotherapy, Vadamalayan Hospitals Pvt. Ltd., [1]Department of Radiotherapy, Madurai Medical College, Govt. Rajaji Hospital, Madurai, Tamil Nadu, India. E-mail: kesavanmp@gmail.com

Introduction: Endometrial cancer is one of the most common gynecologic malignancy. Vaginal cuff brachytherapy is a standard treatment option for postoperative endometrial and selective postoperative cervical cancer cases for women at high risk for vaginal recurrence. Single-channel vaginal cylinders are frequently used to treat the vaginal cuff, but they are limited in their ability to sculpt dose away from organs at risk (OARs). Multichannel applicators, through modulation of dwell times in various positions along the channels, improve the ability to optimize target coverage and to minimize dose to OARs. Despite evidence showing that the multichannel applicators significantly reduce dose to OARs compared with single-channel applicators. The ideal configuration of the multichannel applicator (shape, location and number of channels) is unknown. There are various multichannel applicator designs currently used in clinical practice.

Objectives: The main objective of this study was to design and development of a in-house multichannel applicator for HDR vaginal brachytherapy and dosimetric compression with the single channel applicator.

Materials and Methods: The multichannel applicator with a 3 cm diameter solid cylinder made up of PMMA. One channel in the centre of the applicator and eight are in the peripheral, which is 0.5 cm from the surface. The peripheral source channels of the multichannel cylinder are placed close to the treatment volume, which means that the dose gradient in the radial direction is steep. Therefore the dose is enhanced close to the cylinder surface and lowered at larger distances as compared to the central channel cylinder. We randomly selected 5 patients with endometrial carcinoma were CT-scanned twice with a vaginal cylinder single and multichannel applicator. CT-based 3D dose-planning was done for both applicator. The dose calculation algorithm is based on the TG-43 formalism, as recommended by the American Association of Physicists in Medicine (AAPM). Dose–volume histograms were compared for both target and organs at risk.

Results and Discussion: The Multichannel applicator design improves the dosimetry over single channel applicators. Results showed that a uniform dose around the dome of a cylinder as compared to single channel. In addition a more uniform dose distribution can be attained. Vaginal HDR brachytherapy using a multichannel vaginal applicator and inverse planning provides dosimetric advantages over single channel cylinder, by reducing the dose to organs at risk without compromising the target volume coverage, but at the expense of an increased vaginal mucosa dose.

P-13

STUDY THE EFFECT OF PELVIC HETEROGENEITIES ON RECTUM DOSE MEASUREMENTS INSIDE AN INDIGENOUSLY MAKE FEMALE PELVIC PHANTOM AND RANDO FEMALE PELVIC PHANTOM USING MOSFET DOSIMETERS

Deepak shrotriya, R. S. Yadav[1]

Department of Radiation Oncology, J.K. Cancer Institute, G.S.V.M. Medical College, [1]Department of Physics, DAVPG College, Kanpur, Uttar Pradesh, India. E-mail: shrotriya2007@gmail.com

Introduction: Human body consists of variety of heterogeneous tissues and pelvis is the most heterogeneous regions. Pelvis has various tissues and materials like bones, soft tissues, fat, air cavities, faecal matter, urine, sometimes artificial prosthesis etc. For the successful radiotherapy treatment of female pelvic cancers, there is a need to study the effect of tissue heterogeneities on dose distribution inside the tumor and adjacent normal tissues.

Objective: The direct use of, in water dosimetric data, in the treatment planning of female pelvic cancer patients gives erroneous results. The aim of this study is to direct measure the planned doses at different rectum points inside an indigenously make female pelvic phantom and Rando female pelvic phantom using in-vivo dosimeters.

Materials and Methods: TN502RD mobile MOSFETs (Best Medical Canada) of standard sensitivity along with the reader module TNRD70W dose verification system is used for direct dose measurements at different rectal points inside both female pelvic phantoms, assuming that rectum is empty. Both phantoms are scanned using SOMATOM Emotion 16-Slice CT-Simulator (Siemens make) in 5 mm thick slices and CT-slices are transferred to Oncentra 3D-TPS in DICOMRT format. Doses are calculated by the TPS and the results are compared to in-vivo dose values measured with MOSFET dosimetric system at same rectal points.

Results and Discussion: Dose calculation algorithm in the TPS is designed such that the rectum is filled with water equivalent material but this assumption is not correct. The rectum is a hollow pipe filled with air and faecal matter and surrounded with other heterogeneous tissues, having different electron densities than water. In case of empty rectum, it is assumed that only air is filled in the rectum and results indicate that the dose measured in the both female pelvic phantoms by the MOSFETs' dosimetric system are in the range of 18-21% lower than the dose calculated by the TPS.

Conclusion: The treatment planning system has overestimated the rectum dose because it has not considered the pelvic tissue heterogeneities. Therefore, the direct dose measurements in female pelvic phantoms are useful for designing the HDR treatment plans before actual dose delivery.

P-14

HDR BRACHYTHERAPY SOURCE CALIBRATION BY USING SOLID PHANTOM

M. Athiyaman, Hemalatha, Arun Chougule[1], David, H. S. Kumar[2]

Departments of Radiological Physics and [2]Radiotherapy, S.P. Medical College, AG Hospitals, Bikaner, [1]Department of Radiological Physics, S.M.S Medical College, Jaipur, Rajasthan, India. E-mail: athi.roja87@gmail.com

Introduction: The description "source calibration" refers to the estimation of the source strength expressed in one of the internationally recommended quantities either reference air kerma rate or air kerma strength. The modern Treatment planning systems dose calculation is performed by taking the Air kerma strength as the input. In routine practice the Air Kerma strength is measured in the Well type Ion chambers. However there are other methods such as In Air calibration method and calibration using solid phantoms. The use of In Air calibration method is limited to very few centers worldwide due to the involvement of complex parameters. In present scenario the source strength calibration is performed in solid phantoms along with well type Ion chambers.

Objective: Estimation of Airkerma strength by using solid phantoms and exploring the associated influencing parameters

Materials and Methods: The measurements were performed for miniature Co-60 source in HDR Brachytherapy machine (Make: Eckert and Ziegler GmbH Bebig, Model: Multisource, Sr. No: 542) for miniature Co-60 source. The cylindrical solid phantom made by PMMA material was used. In water calibrated Farmer type ionization chamber, 0.60 cm^3 (PTW Freiburg, S. No: 007023) was used for ion collection. The clinically used Esophagus guide tube was used for positioning the source. The ion chamber is kept at the fixed distance of 8 cm from the guide tube inside the phantom. The maximum response position was found and the meter reading was obtained.

The air kerma strength is estimated as below mentioned

Sk = Nk M ku kτ kρ kt k p k ion kv kwall k appl k ph (A)

Sk – air kerma strength in cGy h^{-1} cm^2, Nk - air kerma calibration factor of the chamber for the γ -energy of the radionuclide considered, usually expressed in Gy/C, M-measured charged collected during time interval, Along with routine influence factors such as temperature and pressure, ion recombination and polarity correction factors additional factors were considered namely gα, kph, kwall, μen/ρ (air to water) where, gα – energy fraction of the electrons liberated by photons in air, that is lost to radiative processes, kph – correction factor to account for the existence of the phantom material and hence, some absorption and scattering effects, when the material is compared to air, kwall – correction factor accounting for attenuation and scattering effects of the chamber wall, μen/ρ (air to water) - ratio of mass energy absorption coefficient of air to that of water.

Results: The Airkerma strength was estimated as per above mentioned formula A. The measured strength was compared with the TPS Airkerma strength. The deviation is 2% from the measured value and within the tolerance.

Discussion: The estimation of source strength through solid water phantom is simple procedure and it can be extended for many clinical Brachytherapy units. The values of influence parameters have to be added carefully to obtain accurate result.

P-15

DOSIMETRIC EFFECTS OF STEP SIZE OF COBALT-60 HDR SOURCE IN INTRA LUMINAL BRACHYTHERAPY

Pawan K. Jangid, Arvind Shukla, Narendra Rathore, Abhay Jain, Vikram S. Rajpurohit, Vaihav Gagrani

Department of Radiotherapy, RNT Medical College and Associated Hospitals, Udaipur, Rajasthan, India.

E-mail: pawanjangid2013@gmail.com

Introduction: The step size plays major role in optimization process where optimization is maximum acheiveable. The challenge is to select the optimal step size for the unique clinical situation of patient is to spare normal tissues and to best implementation of optimization technique. Most of brachytherapy systems use standard step size as 2.5 mm for treatment. The step size is the distance between two dwell positions. In the present work we have studied the role of step size in brachytherapy treatment planning as it is a very important parameter and to evaluate the optimum source step size for better treatment of cancer patients using a Co-60 source.

Table 1: Variation of standard deviation with step size in esophagus cancer

Step size (mm)	*SD at depth 0 mm*	*SD at depth 2.5 mm*	*SD at depth 5 mm*	*SD at depth 10 mm*
1	1.13	0.53	0.34	0.17
2	1.05	0.50	0.31	0.16
3	0.98	0.46	0.29	0.15
4	0.89	0.43	0.27	0.14
5	0.85	0.39	0.25	0.13
6	0.81	0.36	0.23	0.12
7	0.98	0.47	0.29	0.15
8	0.87	0.43	0.27	0.14
9	0.90	0.47	0.30	0.16
10	0.77	0.29	0.17	0.09
Average	0.92	0.43	0.27	0.14

SD: Standard deviation

Objective: The objective of the present study is to analyze the effects of Step Size of cobalt-60 HDR source in esophagus cancer.

Materials and Methods: A Bebig Multisource® HDR Brachytherapy unit with cobalt-60 HDR miniature source (Eckert and Ziegler, Bebig, Germany) was used for study. The Co-60 source has an active core 0.5 mm diameter and 3.5 mm active core length. HDR 2.5 plus (Eckert and Ziegler, Bebig, Germany) Treatment planning system was used for the study. 10 patients of carcinoma esophagus were taken for the study of dose distribution around the single intraluminal catheter of 8 cm length. The effect of step size around the catheter was studied for depth doses were calculated at 0, 2.5, 5 mm and 10 mm from the applicator surface. Dose point based optimization and normalization were used to calculate the 4.0 Gy prescription dose at 5 mm depth. Dose distribution and homogeneity for the various source step sizes were evaluated by performing dose computations per step size and calculating the average dose and standard deviation at each depth.

Results and Discussion: The study shows that standard deviation between the doses reduces as depth increases. The average standard deviation was 0.92, 0.43, 0.27 and 0.14 for depth 0 mm, 2.5 mm, 5 mm and 10 mm respectively [Table 1]. Study in carcinoma Esophagus concludes that homogeneity increases as the step size reduces.

P-16

A REFERENCE STUDY OF DETECTOR MATERIALS FOR BNCT-SPECT IMAGING: A SIMULATION STUDY

Moo-Sub Kim, Joo-Young Jung, Han-Back Shin, Sunmi Kim, HyeJeong Yang, Kazuki Kubo[1], Kohei Shimomura[1], Hajime Monzen[1], Do-Kun Yoon, Tae Suk Suh

Department of Biomedical Engineering, Research Institute of Biomedical Engineering, College of Medicine, Catholic University of Korea, Seoul, Korea, [1]Department of Medical Physics, Graduate School of Medical Science, Kindai University, Osaka, Japan.

E-mail: dbsehrns@naver.com, suhsanta@catholic.ac.kr

Purpose: To investigate the optimal detector material for prompt gamma ray imaging during boron neutron capture therapy (BNCT) with a Monte Carlo simulation.

Materials and Methods: Sixteen detector materials used for radiation detection were estimated to assess their advantages and drawbacks. The estimations used previous experimental data to build the simulation codes. The energy resolution and detection efficiency of each material was investigated.

Results: Prompt gamma ray images during BNCT simulation were acquired using only the detectors that showed good performance in our preliminary data. From the simulation, we could evaluate the majority of detector materials in BNCT as shown in Figure 1. We also could acquire a prompt gamma ray image using the six high ranked-detector materials and lutetium yttrium oxyorthosilicate as listed in Table 1.

Conclusions: We provide a strategy to select a detector material for the prompt gamma ray imaging during BNCT.

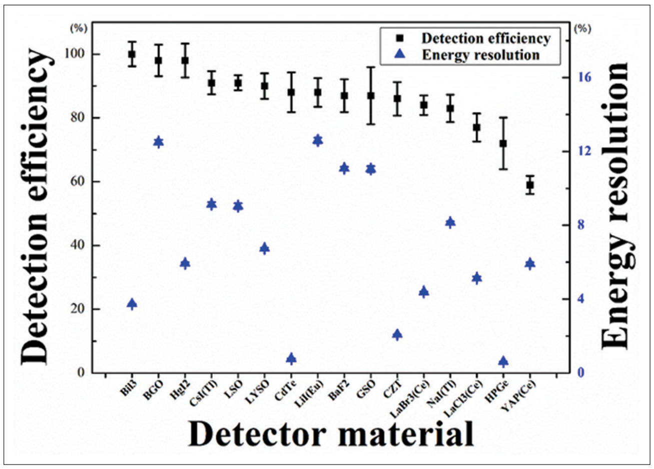

Figure 1: Trend of detection efficiency (left label, black square) and energy resolution (right label, blue triangle) according to the detector material. The best detector efficiency was observed when BiI_3 was used as the detector material. Each detection efficiency value was normalized by using the detection efficiency of BiI_3 as reference. Each energy resolution value at 478 keV prompt gamma ray peak was calculated from the energy spectrum of each detector material

Table 1: Units for list of the sixteen detector materials for prompt gamma ray imaging during boron neutron capture therapy

Detector material	*Density (g/cm3)*	*Energy resolution at 511 keV (%)*	*Energy resolution at 662 keV (%)*	*GEB-A*	*GEB-B*
BGO	7.13	14.20	12.50	−0.0050	0.1084
HPGe	5.32	0.70	0.27	0.0164	−0.0180
CZT	5.60	2.00	1.00	0.0360	−0.0360
$LaCl_3$ (Ce)	3.64	5.10	3.30	0.0556	−0.0413
NaI (Tl)	3.67	8.60	6.50	0.0486	−0.0065
CsI (Tl)	4.51	9.50	7.70	0.0286	0.0279
CdTe	6.20	1.20	2.00	−0.0459	0.0728
LYSO	7.30	8.00	8.90	−0.0923	0.1864
GSO	6.70	12.00	8.90	0.0760	−0.0205
LSO	7.40	10.00	8.40	0.0159	0.0492
BaF_2	4.90	11.40	8.00	0.0941	−0.0502
YAP (Ce)	5.40	6.70	5.70	0.0072	0.0378
LiI (Eu)	4.08	12.90	7.50	0.1814	−0.1615
BiI_3	5.80	3.80	2.90	0.0201	−0.0010
HgI_2	6.40	6.50	5.96	−0.0137	0.0657
$LaBr_3$ (Ce)	5.29	4.30	2.80	0.0460	−0.0336

For each detector material, two GEB numbers were acquired by using energy resolution values at 511 keV and 662 keV. Specifications including density values, atomic components and GEB numbers were applied to the simulation code. GEB: Gaussian energy broadening, BGO: Bismuth germanate oxide, HPGe: High purity germanium, CZT: Cadmium zinc telluride, $LaCl_3$ (Ce): Lanthanum chloride (cerium), NaI (TI): Sodium iodide (thallium), CsI (TI): Cesium iodide (thallium), CdTe: Cadmium telluride, LYSO: Lutetium yttrium oxyorthosilicate, GSO: Gadolinium oxyorthosilicate, LSO: Lutetium oxyorthosilicate, BaF_2: Barium fluoride, YAP (Ce): Yttrium aluminum perovskite (cerium), LiI (Eu): Lithium iodide (eurodium), BiI_3: Bismuth tri-iodide, HgI_2: Mercuric iodide, $LaBr_3$: Lanthanum bromide (cerium)

P-17

DATA DRIVEN MOTION CORRECTION OF SPECT USING DEVELOPED ALGORITHM WITH PARTIAL RECONSTRUCTION

Md. Nahid Hossain, Kamila Afroj Quadir[1], Adnan Kiber[2], Roger Fulton[3]

National Institute of Nuclear Medicine and Allied Sciences, [1]Bio-Science Division, Bangladesh Atomic Energy Commission, [2]Department of Electrical and Electronic Engineering, University of Dhaka, Dhaka, Bangladesh, [3]Department of Medical Physics, Westmead Hospital, Westmead, Australia.

E-mail: nahidhssnyahoo.com

Introduction: In a Single Photon Emission Computed Tomography (SPECT) study, the data acquisition is performed over a relatively long time, typically in the range of 5-30 minutes. Patient movement frequently occurs for longer time of data acquisition in clinical procedure. This movement causes misalignment of the projection frames, which degrades the image quality. These motion artifacts may significantly affect the diagnostic accuracy. When motion occurs between discrete acquired projections, consistency is lost and errors are generated in the reconstructed estimate. Motion correction is the task of obtaining consistent projection data from the acquisition. Therefore, the motion correction of patients in tomography images is very much essential for accurate diagnosis and hence achieves the quality of the images.

Objectives: In this work, we corrected a SPECT study for a single movement during acquisition. Data driven motion correction was applied in the SPECT data using developed algorithm with partial reconstruction.

Materials and Methods: Different data without motion were acquired by using a Dual head SPECT camera and a Hoffman 3D brain phantom. The SPECT camera has two opposing heads, and acquires 64 views over 360 degrees. For that the camera makes 32 steps. We worked with 64 x 64 x 64 voxel reconstructions. We reconstructed the data with ordered subsets expectation maximization (OSEM) algorithm. This required to define the number of projections per subset. The natural choice of subsets for OSEM is therefore 1 subset = 1 pair of opposing views. First we created some simulated data. We created an arbitrary using algorithm transformation. We applied 6 degree of freedom parameters like (0, 0, 0) for translations and (15, 8, 0) for rotations to the data and created another data. There are two SPECT scans (simulated) with the phantom in two orientations. We could combine projections from both to create a simulated SPECT scan with a movement at the mid-scan point. We performed motion corrected reconstruction of the simulated SPECT scan in which 16 projections were acquired prior to the motion, and 16 were acquired after the motion. The motion was treated as instantaneously occurring between projections 16 and 17. Any other timing of the motion could be simulated in the same way. The next step was to perform motion correction. First we reconstructed from the first 16 pairs, to obtain a partial reconstruction. Then we reconstructed simulated data from the second 16 pairs. When we applied the invert transformation with the data, we achieved the final motion corrected data. The all algorithms were developed with Interactive Data Language (IDL) program.

Results: The six degree of freedom (dof) motion parameters were converted to a transformation matrix using the developed algorithm. A 4x4 transformation matrix was produced. This transformation was applied to the reconstructed data. After correcting motion the reconstructed image was shown with motion free. But when we compared the corrected final data with the motion free data, we observed that corrected final was more blurred. This was due to interpolation effects when applying the transformations.

Discussion: Motion detection techniques are classified into two categories, external based or internal based. The data driven method was included in internal based technique. The field of motion detection and correction in SPECT is very open to future novel ideas especially software based improvement of motion estimation, characterization and compensation. The simulated data is very essential for examining the algorithm base methods.

P-18

PRACTICAL ASPECT OF DESIGN OF OPTICAL STIMULATION ASSEMBLY FOR MULTISAMPLE TL-OSL READER SYSTEM

L. Paliwal[1], M. Uke[1], M. S. Kulkarni[2], D. Dutta[1]

[1]Radiological Physics Advisory Division, Bhabha Atomic Research Centre, [2]Radiation Safety System Division, Bhabha Atomic Research Centre, Mumbai, Maharashtra, India. E-mail: lovelypaliwal21@gmail.com

Introduction: The thermoluminescence (TL) and optically stimulated luminescence (OSL) reader systems are in great demand in all the research institutes and universities for their manifold applications in radiation dosimetry and luminescence dating. The advance integrated TL-OSL reader systems commercially available are not only expensive but the maintenance of such systems is also difficult and expensive. Therefore, indigenous development of TL-OSL reader system has a great scope for further expansion in India for environmental monitoring, medical and retrospective radiation dosimetry. The development of a multiple sample TL-OSL reader system as shown in Figure 1 was undertaken by us which is low cost but equally competent having facility for readout of eight samples in sequence in a programmed way. This paper reports the practical aspect of design of a new Multisample TL-OSL Reader System which works either in TL, OSL or simultaneous TL-OSL modes of operation.

Materials and Methods: The optical stimulation (photo excitation) of the samples is carried out by power LED clusters (Blue LXHL-NB98 and IR HSDL 4230). High power Blue LEDs that yields an output of 1.0 W at $\lambda_p \approx 470$ nm and $\Delta\lambda \approx 20$ nm. A long pass filter (GG-435) is incorporated in front of each blue LED cluster to minimise the amount of directly scattered blue light reaching the detector system. Optical stimulation assembly consists of two blue LEDs placed in two channels facing each other at an angle of 30° with the vertical axis with 20 IR LED arranged in circular fashion as shown in Figure 1. The user can select the blue or IR light stimulation depending on the OSL samples under study and the current is passed through the selected LEDs only. During the stimulation cold nitrogen gas is flushed continuously on it at a flow rate of ≈ 3 LPM to ensure that the junction temperature remains well within the tolerance limit. In principle, If the sample is heated or illuminated on a metal support, the maximum light signal is then reduced to about 50% (to 2πr geometry). To reduce sample-to-PM tube distance sample is lifted through slots in indexing disc into the measurement position by a lift, which also functions as heating element. In the measurement position the sample can be stimulated thermally and/or optically. The emitted luminescence is measured by the light detection system.

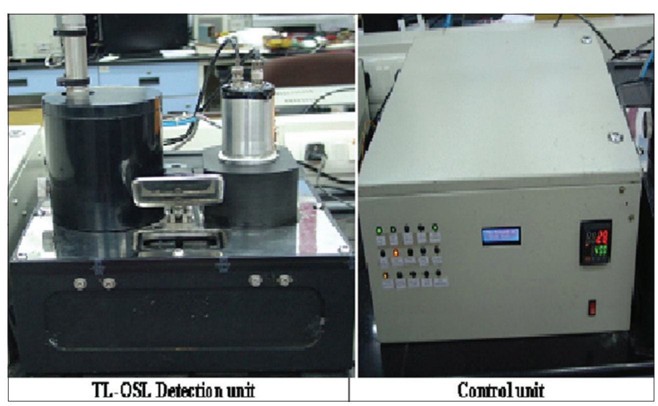

Figure 1: Multisample TL-OSL Reader System

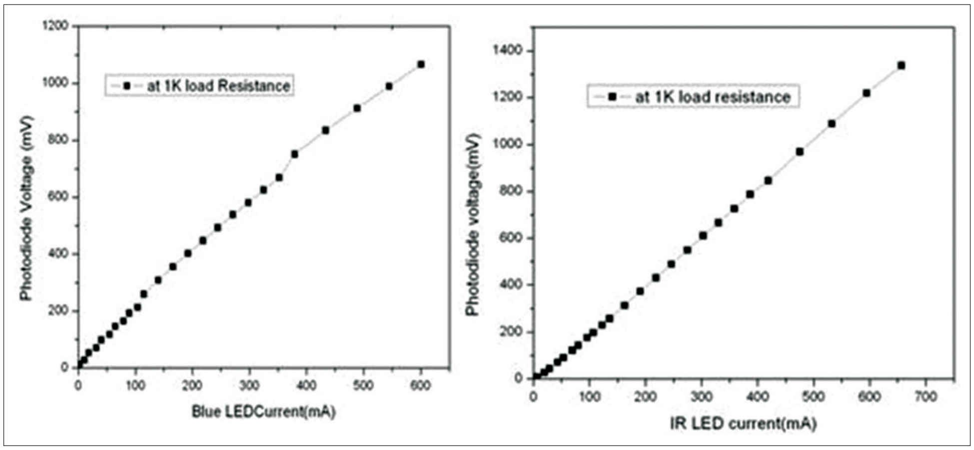

Figure 2: Blue LED response with photodiode and IR LED response with photodiode

DC motor has been used to lift the sample mounted on indexing disc for measurement and also for heating. As the stimulating light beam is focused on the sample in the lifted condition, design care has been taken to achieve repeatability within ± 0.01 mm at the lifted extreme end. Another DC motor has been used to move the photodiode plate to measure the stimulating light on sample. Four Proximity sensors (Flush type) have been provided to get the feedback on extreme positions.

Results and Discussion: In reader S1133-14 photodiode has been used to determine the stimulation light intensity at the sample position for the given wavelength. Photosensitivity of photodiode is .22 A/W for Blue LED (435 nm) and .37 A/W for IR LED (875 nm). The light intensity at the sample position varied in the range of 0.02 mW/cm^2 to 100 mW/cm^2 (percentage standard deviation of ±5%) by controlling the DC current through the LED cluster as shown in Figure 2. The light intensity is measured to be 100 mW/cm^2 through the blue LED cluster and 67 mw/cm^2 for 600 mA through IR LEDs.

P-19

DEVELOPMENT OF IN-LINE HOLOGRAPHIC PHASE-CONTRAST IMAGING SYSTEM USING INDUSTRIAL X-RAY SYSTEM

Daisuke Shimao, Erika Nakajima[1], Hitoshi Sato[1]
Department of Radiological Technology, Faculty of Health Sciences, Hokkaido University of Science, Sapporo, [1]Department of Radiological Sciences, Ibaraki Prefectural University of Health Sciences, Inashiki, Japan.
E-mail: shimao-d@hus.ac.jp

Introduction: X-ray imaging has been widespread diagnostic tool in medicine which is based on X-ray absorption. Its image contrast is sufficient for boundaries between tissues with greatly different absorption coefficient, but little or no image contrast appears with almost the same absorption coefficient. Over the past 20 years, alternative imaging techniques based on X-ray refraction (phase shift) have been intensively explored and developed to overcome weak image contrast in soft tissue imaging by existing method based on X-ray absorption. Such alternative imaging techniques include in-line holographic phase-contrast imaging, angle-analyzer-based imaging, and crystal interferometry. All of these techniques can produce fine images of soft tissues when using synchrotron X-rays which provide both monochromatic X-ray with sufficient intensity and high directivity. Necessity of synchrotron faculty for these alternative imaging techniques, however, is an obstacle for these techniques to be used in medicine.

Objectives: To develop in-line holographic phase-contrast imaging system needing no synchrotron X-rays, but based on the industrial X-ray tube.

Materials and Methods: We utilized X-ray generator with fixed anode X-ray tube (ISOVOLT Titan E; GE Measurement & Control Solutions) that has a generating capacity of 3 kilowatts. The target material was molybdenum and the focus size was 1 mm by 5 mm. Characteristic X-rays of molybdenum (17.4 keV and 19.6 keV) were extracted by a monochromator made by perfect silicon crystal. The monochromator produced vertically long X-ray beam of 17.4 keV and 19.6 keV at Bragg reflection condition, which appeared side by side with each other at the distance of around 1 m from the monochromator. Because of vertically long X-ray beams, we performed line scan technique to acquire two dimensional images of objects. We utilized imaging plate or X-ray CCD camera as image detector and adopted X-ray chart or breast cancer specimen as the imaging objects. The distance between objects and image detector was set at approximately 1 m.

Results and Discussion: Clear edge enhancement could be acquired on both X-ray chart and breast cancer specimen. The edge enhancement appeared only in the horizontal direction. This is because plane of incidence for the monochromator was horizontal plane and then divergence angle of reflecting X-ray beam from monochromator was collimated only horizontal direction. On the other hand, reflecting X-ray beam from monochromator in vertical direction diverged naturally and then X-ray images were enlarged in the vertical direction. Although exposure times were considerably prolonged due to weak X-ray intensity compared to synchrotron radiation, we could acquire phase-contrast images in in-line holographic method using industrial X-ray system.

P-20

FOUR-DIMENSIONAL DIGITAL TOMOSYNTHESIS BASED ON VISUAL RESPIRATORY GUIDANCE

Dong-Su Kim[1], Seungwan Lee[2], Siyong Kim[3], Tae-Ho Kim[1], Seong-Hee Kang[1,4], Kyeong-Hyeon Kim[1], Dong-Seok Shin[1], Hye Jeong Yang[1], Tae Suk Suh[1]

[1]Department of Biomedical Engineering, Research Institute of Biomedical Engineering, College of Medicine, The Catholic University of Korea, [4]Department of Radiation Oncology, Seoul National University Hospital, Seoul, [2]Department of Radiological Science, College of Medical Science, Konyang University, Daejeon, Korea, [3]Department of Radiation Oncology, Virginia Commonwealth University, VA, USA.
E-mail: suhsanta@catholic.ac.kr

Introduction: Patient breathing-related sorting method of projections in 4D digital tomosythesis (DTS) can be suffered from severe artifacts due to non-uniform angle distribution of projectionsand noncoplanar reconstructed images for each phase. In this study, we propose a method for optimally acquiring projection images in 4D DTS.

Materials and Methods: In this method every pair of projections at x-ray tube's gantry angles symmetrical with respect to the center of the range of gantry rotation is obtained at the same respiration amplitude. This process is challenging but becomes feasible with visual-biofeedback using a patient specific respiration guide wave which is in sinusoidal shape (i.e., smooth and symmetrical enough). Depending on scan parameters such as the number of acquisition points per cycle, total scan angle and projections per acquisition amplitude, acquisition sequence is pre-determined. A simulation study for feasibility test was performed. To mimic actual situation closely, a group of volunteers were recruited and breathing data were acquired both with/without biofeedback. Then, x-ray projections for a humanoid phantom were virtually performed following (1) the breathing data from volunteers without guide, (2) the breathing data with guide and (3) the planned breathing data (i.e., ideal situation). Images from all of 3 scenarios were compared.

Results: Scenario #2 showed significant artifact reduction compared to #1 while did minimal increase from the ideal situation (i.e., scenario #3). Also, the scan angle dependence-related differences in the DTS images could reduce between using the proposed method and the established patient breathing-related sorting method.

Conclusion: Through the proposed 4D DTS method, it is possible to improve the accuracy of image guidance between intra/inter fractions with relatively low imaging dose.

P-21

AN *IN-VITRO* STUDY TO DIAGNOSE AND DISTINGUISH BREAST AND LUNG CANCERS USING THE PCB TECHNOLOGY BASED NANODOSIMETER

P. Venkatraman, C. S. Sureka

Department of Medical Physics, Bharathiar University, Coimbatore, Tamil Nadu, India.
E-mail: surekasekaran@buc.edu.in

Introduction: In the modern field of nanodosimetry, the Printed Circuit Board (PCB) technology based positive ion detector has been identified as a device to detect cancers in lungs and breast region. In the nano environment, these cancer cells have been diagnosed by the exhalation of specific volatile organic compounds (VOCs) which serves as eminent source biomarkers for cancer diagnosis. Earlier studies reported that lungs emit various VOCs include Benzene, Ethylbenzene, Cyclohexane, methanol, ethanol, dodecane and tridecane, and the Ca. breast emit alkanes, alkenes, ketones, halogenated hydrocarbons, aldehydes, alcohols, esters, unsaturated hydrocarbons, terpenes, siloxanes, and aromates. By employing VOCs exhalation, the field of nanodosimetry aids as a direct evidence that the diagnosis of critical organs like lungs and breast cancer cells without harming the patients is possible.

Objective: The objective of the present work is to diagnose lung and breast cancers and distinguish them using the PCB technology based Nanodosimeter.

Materials and Methods: The normal lung and breast tissues were placed separately inside the chamber and it was evacuated in order to remove all other molecules present in the chamber. Then, it is allowed to exhale molecules at various pressures in order to measure the amplitude, rise time, fall time, and number of pulses of the signal. Later, these normal tissues were replaced by cancerous tissues of stage 4 in the evacuated medium and the same was allowed to exhale Volatile Organic Compounds (VOCs) to capture signal at various pressures ranging from 1 to 10 Torr. This procedure was repeated for 3 sets of both normal and cancerous tissues of breast and lung at stage 4 to assure reliability.

Results and Discussion: It is observed that the signal amplitude, rise time, fall time and number of pulses of normal lung and breast tissues was found to be 72.9±0.02 Volts, 2.4±0.005 ms, 480±0.0 μs, 781±72 and 74.1±0.08 Volts, 2.4±0.005 ms, 480±0.0 μs, 581±40.5 respectively. Similarly, the signal amplitude, rise time, fall time and number of pulses at stage 4 of lung cancer tissues was found to be 86.3±0.06 Volts, 1.3±0.01 ms, 430 ±0.012 μs and 3008±231.125 and for breast tissues: 91.5±0.03 Volts, 470±0.2 μs, 480±0.0 μs, and 4077±210.12. From this data, it is found that the signal amplitude, rise rime, fall time and number of pulses are higher for breast cancer tissues than lung tissues. This is due to the higher rate of emission of VOCs from breast cancer tissues than the lung cancer tissues. Based on these, it is concluded that the PCB technology based 3D positive ion detector can be developed to diagnose and distinguish breast and lung cancers.

P-22

INDIGENOUS PREPARATION AND STUDY OF RADIOCHROMIC FILM AS RADIATION DOSIMETER FOR MEDICAL APPLICATIONS: A PRELIMINARY WORK

Apoorva Mittal, Rahul Sharma[1], ParveenSaini[1], R. K. Kotnala[1], Pratik Kumar

Medical Physics Unit, Dr. B.R.A. IRCH, All India Institute of Medical Science, [2]Environmental Sciences and Biomedical Metrology Division, CSIR-National Physical Laboratory, New Delhi, India.
E-mail: drpratikkumar@gmail.com

Introduction: In medical field, radiation dosimetry is concerned with quantifying the energy deposited in terms of absorbed radiation dose. Ionizing radiations are widely used in medical procedures such as computed tomography, fluoroscopy, x-ray radiography, mammography etc. which help the doctors in better diagnosis and treatment. However, radiation exposure in any amount entails potential risk which increases with the radiation dose. It is extremely important to accurately determine and optimize the amount of radiation dose to which a patient is exposed during any radiological procedure. Radiochromic films are used for the measurement of radiation dose. These films change color directly upon exposure to radiations. They have high spatial resolution. However, commercially available radiochromic films, for which there is currently a sole manufacturer, are very expensive which limits their regular use in radiation dosimetry. Also, they have major limitations like post-irradiation instability, temperature dependence and ambient light sensitivity. The sensitive layer of presently available films has a preferred direction for irradiation and literature reports that scanning in different direction produces anomalous results. It is extremely important to minimize the effect of various factors like temperature, humidity, pressure etc. on the stability of these films. All these limitations restrain their ease of handling and stability. This creates the necessity for indigenous development of radiochromic films having distinguished advantages in terms of performance, cost and availability.

Objectives: Development of low cost radiochromic films with improved characteristics in terms of sensitivity and handleability.

Materials and Methods: Herein, we have prepared monomeric ingredients based polymeric radiochromic films by simple and cost effective solvent casting method. These monomeric species in the films undergo radiation induced polymerization involving cross-linking of polymers which is eventually responsible for change in optical properties particularly the color and its intensity.

Results: The prepared films are bubble-free, flexible and sturdy. The optical characterization of these films showed a change in optical density before and after the exposure.

Discussion: This work offers a cost-effective way of fabricating indigenous radiochromic films via a facile route which may be easily scaled up for commercial development of radiochromic films. These films may also be used as radiation dosimeter in the food industry, agricultural and other strategic sectors. The self-indicating nature of radiochromic films can also be used as immediate responders in case of any nuclear accident or for early detection of radiation leakage from other sources.

P-23

DOSIMETRIC EFFECTS OF BRASS MESH BOLUS ON SKIN DOSE AND DOSE AT DEPTH FOR POSTMASTECTOMY CHEST WALL IRRADIATION

Zakiya S. Al-Rahbi[1,2], Dean L. Cutajar[1,3], Peter Metcalfe[1], Anatoly B. Rosenfeld[1]

[1]Centre for Medical Radiation Physics, University of Wollongong, Wollongong, [3]St. George Cancer Care Centre, St. George Hospital, Kogarah, Australia,
[2]Department of Radiotherapy, National Oncology Center, The Royal Hospital, Muscat, Oman.
E-mail: z.alra7bi@gmail.com

Purpose: To investigate the feasibility of using the Brass Mesh Bolus as an alternative to tissue-equivalent Bolus for post mastectomy chest wall cancer by characterizing the dosimetric effects of the 2-mm fine Brass Bolus on both the skin dose and the dose at depth.

Materials and Methods: Surface dose and percent depth dose data were acquired for a 6 MV photon beam in a solid water phantom using MO*Skin*™ dosimeter, Gafchromic EBT3 film and an Advanced Markus ionization chamber. Data were acquired for the case of: no bolus, Face-up Brass Bolus, Face-down Brass Bolus, Double Brass Bolus, 0.5 cm and 1.0 cm of Superflab TE bolus. The exit doses were also measured via MO*Skin*™ dosimeter and Markus ionization chamber.

A tangent chest wall field was delivered to the curved phantom with no bolus, brass mesh bolus, and Superflab bolus, and Gafchromic EBT3 film was used to measure surface dose over the irradiated area.

Results: The surface dose measured under the Bolus by Markus ionization chamber increased from 17.1% without bolus to 55.5%, 54.2% 72.9%, 90.1% and 102.2% (± 0 SD) with Face-up Brass Bolus, Face-down Brass Bolus, Double Brass Bolus, 0.5 cm and 1.0 cm TE-Bolus, respectively, whereas, the surface dose measured under the Bolus via MO*Skin*™ dosimeter increased from 19.2 ± 1.0% without bolus to 63.0 ± 2.1% and 61.5 ± 0.5% for Face-up Brass Bolus and Face-down Brass Bolus, respectively. The surface dose measured by Gafchromic EBT3 film showed that the surface dose increased from 24.0 ± 1.0% to 58.6 ± 1.1% with only one layer of Brass Bolus and 71.0 ± 1.0% with double layer of Brass Bolus.

The measured exit doses increased from 53.8% without Bolus to 78.8%, 79.4%, 86.3%, 63.5% and 64.3% for the cases of Face-up Brass Bolus, Face-down Brass Bolus, Double Brass Bolus, 0.5 cm and 1.0 cm Superflab TE-bolus measured by Markus ionization chamber, where the exit doses measured by MO*Skin*™ increased from 47.9 ± 0.5% without Bolus to 74.1 ± 0.4% for Face-up Brass Bolus and 77.5 ± 0.1% for Face-down Brass Bolus.

The Markus ionization chamber measurements show that the doses at depth 100 mm is nearly the same for brass mesh bolus versus no brass bolus, where the percent difference is less than 0.5% with Brass Bolus versus without Brass Bolus, whereas the doses decrease by approximately 1.0% for TE-bolus.

For the tangent field measured in the curved phantom with Gafchromic EBT3 film, the surface dose ranged from 23.5% - 59.9% of the delivered dose in case of no Brass Bolus. The surface dose is increased to 62.0% - 89.9%, 63.5 – 92.2%, and 75.4 – 94.3% of prescription dose for the Face-up Brass Bolus, Face-down Brass Bolus and Double Brass Bolus, respectively. The TE Bolus increase the surface dose more than the Brass bolus. The surface dose increased to 94.9% and 107.5% of prescription dose for the 0.5 cm TE Bolus and 1.0 cm Superflab TE Bolus respectively.

Conclusions: Brass Mesh Bolus does not significantly change dose at depth (less than 0.5%), and the surface dose is increased similar to TE bolus. Considering this, brass mesh may be used as a substitute for TE bolus to increase superficial dose for chest wall tangent plans.

P-24

PERIPHERAL PHOTONEUTRON DOSE MEASUREMENT IN MEDICAL LINEAR ACCELERATOR USING BD-PND BUBBLE DETECTOR

K. Hajee Reyaz Ali Sahib[1,2], Bharanidharan[1], Nandakumar[1], Ben Johnson[3], D. K. Mohapatra[2], Prakasarao Aruna[1], Thilagam[2], Kathiresan[3], Muthuvel Murgan[3], Singaravelu Ganesan[1]

[1]Department of Medical Physics, Anna University, [2]Nuclear Safety Analysis Section, Safety Research Institute, Atomic Energy Regulatory Board, Kalpakkam, Chennai, Tamil Nadu, [3]Department of Radiation Oncology, VPS Lakeshore Hospital, Kochi, Kerala, India. E-mail: ganesanbharani@annauniv.edu

Introduction: Cancer is the one of the greatest threat and leading death worldwide. Megavoltage photon beams operating above threshold energy of 10 MV produce photoneutron contamination by (γ, n) reaction. These photoneutron gives additional dose to patients and increase the integral dose. Hence, determination of photoneutron dose in a LINAC is current research interest.

Objective: The present study analyze and estimates the effective peripheral photo-neutron dose along the patient plane produced in linear accelerator (Elekta Versa HD) for 10 MV (FF and FFF) and 15 MV photon beams using BD-PND bubble detector.

Materials and Methods: The BD-PND bubble detector has flat dose response for range 200 KeV to 15 MeV. The BD-PND bubble detector used in our study has sensitivity 1.1 bubble/μSv. In air out-of-field neutron dose were measured by placing the BD-PND bubble detectors on horizontal plane at source to detector distance (SSD) of 100 cm. For the measurement the gantry angle and collimator angle were fixed at 0^o and the dose of 200 MU was delivered at a dose rate of 550 MU/Min for 10 MV (FF), 2180MU/Min for 10 MV (FFF) and 635 MU/Min for15 MV (FF). Photoneutron doses equivalent (μSv/MU) were measured by placing BD-PND detectors along axis on the patient plane i.e. (Longitudinal In and Out, Lateral Left and Right) at 10 cm, 20 cm and 30 cm away from standard reference field size of 10x10 cm^2.

Results and Discussion: From the analysis; outside the primary beam no photoneutron dose was observed for6 MV (FF & FFF) photon beam along the patient plane. Where as a photoneutron dose was observed in 10 MV (FF & FFF) and 15 MV photon energies. For equivalent distance from the primary beam on each side, it has been observed that there is a negligible variation of photoneutron dose. It has also been observed that the dose is inversely proportional to the distance. Comparing 10 MV (FF) with 10 MV (FFF), latter accounts less photoneutron dose due to absence of Flattening Filter, whereas 15 MV (FF) exhibits higher photoneutron dose compared with 10 MV (FF) by a factor of 2.5 to 2.8 in all peripheral distances.

Conclusion: From our study, we can conclude that for clinical usage of photon energies above 6 MV the contamination of scattered photoneutron field increases. The maximum allowed neutron leakage percentage in patient plane is much less than permissible limits govern by regulatory board requirements. It is also concluded that BD-PND bubble detector is reliable, accurate, high sensitivity in neutron dosimetry for photoneutron dose measurement in accelerator because of it is unique attractive features such as instant dose calculation, Isotropic nature, less weight, compactable size, no moderator and flat dose response for wide neutron energy. However the BD-PND bubble detectors have limited life time, the recovery time of 3 hours between two consecutive readings, the sensitivity in dose prediction varies (±10%) for the same point in the same conditions on frequent usage, improper storage and ageing factors affect the temperature compensation resulting in the increase of the sensitivity at elevated temperatures, the detector also becomes sensitive to gamma radiation.

P-25

INVESTIGATION OF RECONSTRUCTED FILTERS OF OPTICAL COMPUTED TOMOGRAPHY FOR POLYMER GEL DOSIMETER

H. Kawamura, T. Takanashi[1], Y. Sato, Y. Shimada, S. Abe

Department of Radiological Sciences, Ibaraki Prefectural University of Health Sciences, Inashiki, [1]Innovation Center, 3D Gel Dosimeter Research Laboratory, RIKEN, Wako, Japan. E-mail: kawamura@ipu.ac.jp

Polymer gel dosimetry, which utilizes chain polymerization that is proportional to radiation dose, is a new three-dimensional dosimetric tool for quality assurance. It could potentially be used to measure 3D doses in clinical radiotherapy. Dose evaluation method for polymer gels was selected R2 method using MRI for dose linearity and image quality.

In this study, we construct optical computed tomography (OCT) system for evaluation of polymer gel dosimeter. Some advantages of the dose evaluation using OCT are low cost, bench top, capability of reading dose distribution with high spatial resolution and low noise. The original OCT was composed of He-Ne laser for light source, photodiode for detector, rotation and linear motion stage, controller for stage operation. Projection data per angle were acquired from turned gel samples using mechanical stages for moving and turning. Acquired transmission data per angles was reconstructed with Filtered Back-Projection (FBP) method. Irradiated PAGAT polymer gel samples were prepared. The gel samples were irradiated to 2, 4, 6, 8 Gy respectively, with X-ray beams. The non-irradiated and irradiated samples were scanned using the OCT. The mean optical density from reconstructed images using OCT data was measured. The dose-response curves of the ROI measurements from different pre-reconstructed image filters, Hann filter, Butterworth filter, Ramp filter were compared.

The results of the optical density from irradiated gel samples were tends to raise with increasing dose. The dose responses using three filters were not linear. The dose response curve from reconstructed images using Hann filter could be adapted polynomial curve (correlation coefficients: r^2=0.994). The dose response curve using Hann filter was shown excellent result from correlation coefficients.

P-26

EVALUATION OF DISPLACEMENTS FOR SET UP REPRODUCIBILITY IN LEFT SIDED BREAST CANCERS WITH PORTAL IMAGING AND DIGITALLY RECONSTRUCTED RADIOGRAPHS

Deboleena Mukherjee, Sachin Taneja, Kirti Tyagi, Arti Sarin[1]

Radiation Oncology Centre, INHS Asvini, [1]Nuclear Medicine Department, INHS Asvini, Mumbai, Maharashtra, India. E-mail: deboleena.rso@gmail.com

Introduction: Breast cancer is the most frequently diagnosed cancer among women in 140 of 184 countries worldwide. Studies of setup reproducibility in radiotherapy (RT) for breast cancer have largely focused on breast tangential treatments alone. Inaccuracies in treatment set up reproducibility may increase toxicities to organs at risks (OARs) (heart and lung) especially in left sided breast cancers. Studies have shown that the central lung distance (CLD) measured by an electronic portal images (EPIs) are due to displacements in three directions namely, anterior-posterior (AP), superior-inferior (SI), and medial-lateral (ML) for the three dimensional (3D) treatment plan with treatment planning system (TPS). In this paper we will discuss the evaluation of displacements in these three directions with EPIs and digitally reconstructed radiographs (DRRs) of left sided breast patients.

Materials and Methods: This study was carried out on approximately 50 patients (left sided), breast conserving surgery (3/50) and mastectomy (47/50) between ages 25-75 yrs (median age 50 yrs) treated with external beam radiation therapy (EBRT) during a period of 24 months at INHS Asvini. Patients were clinically marked for breast/chest wall field borders with fiducial radio opaque markers and then immobilized on a commercially available inclined Breast board in treatment position for whole breast scan (virtual simulation) by 16 slice CT scanner (Siemens). Three markers were placed at the central axis of the treatment field. Two straight lines meeting the SI and ML field borders and joining the central marker was drawn and four reference markers were placed, one each at the midline of this SI and ML field borders and distances from upper, lower and lateral borders with this central marker were noted. These DICOM CT images were imported to TPS Oncentra™ (Elekta) for contouring OARs and Planning Target Volume (PTV) on each CT slice for all these patients. A 3D treatment plan with 6MV photons (Linear Accelerator, Siemens) for a prescribed dose of 50 Gy in 25 fractions at isocentre with two coplanar conventional tangential fields at two gantry angles as per International guidelines was generated. Mean doses to OARs and linear measurements for set up SSD (distance of the perpendicular drawn from isocentre to the upper skin border (AP) distance) and CLD on isocentric slice was calculated for each case on the 3D reference approved plan and was exported to Primeview workstation (Siemens) for EPIs for both tangential fields. Reference DRR and EPIs obtained on first day and weekly thereafter was superimposed to verify deviations in all the three directions for all patients.

Results: In the analysis of magnitude and directions of all displacements of the EPIs compared with the DRRs (n=141) for the supraclavicular nodal Anterior field of 47 chest wall irradiation patients, 75% were ≤5 mm, 11% were >5 mm and ≤7 mm, 9% were >7 mm and <10 mm, and 5% were ≥10 mm in the all three directions, and for tangential breast/chest wall fields of all 300 EPIs with DRRs of all 50 patients, 87% were ≤5 mm, 3% were >5 mm and ≤7 mm, 7% were >7 mm and <10 mm, and 3% were ≥10 mm in the AP direction, the corresponding values in ML direction were 92%, 6%, 1%, and 1% and in the SI direction, the corresponding values were 90%, 5%, 3% and 2%, respectively. The shifts observed in CLD was more for obese patients with set up SSD > than 4.5 cm due to difficulty in maintaining the arm position on breast board and motion of heart due to respiration.

Conclusion: Using portal imaging and DRRs, the treatment set up reproducibility of patient position is improved significantly in left sided breast cancer.

P-27

EFFECT OF CONTRAST AGENTS ON SPATIAL DOSE DISTRIBUTION USING DIFFERENT CALCULATION ALGORITHMS

M. Kang[1,2], B. Park[2], Y. Bae[2,3], J. Lee[2,3]

[1]Department of Medical Physics, Korea University, [2]Department of Radiation Oncology, Konkuk University Medical Center, [3]Department of Convergent Medical Physics, Konkuk University, Seoul, Korea. E-mail: polirain@naver.com

Introduction: Intravenous (IV) contrast agents have been used widely in planning CT since contrast agents can improve the visualization of normal organs and malignant tissue in CT scans. However, there is concern that high atomic number of a contrast agent (CA) may cause errors in the dose calculation in radiation planning process. Dose discrepancy due to CA could affect monitor unit (MU) calculation as well as spatial dose distribution. It could be more critical issues in intensity-modulated radiation therapy (IMRT) using non-uniform small beamlet than in conventional uniform beam treatment. Therefore, it is necessary to investigate the effect of CA on spatial dose distribution and dose calculation in IMRT. In this study, we investigate and quantify the effect of CA on dose distribution using home-made phantom. In addition, the dependency of dose calculation algorithms on the effect of CA was also evaluated with IMRT plans.

Materials and Methods: The phantom was designed with the square size of 40×40 cm^2 plastic material with 20×20 cm^2 central hole filled with paraffin. The cylindrical CA container (diameter of 3 cm, thickness of 5 cm) was placed in the center of the phantom to simulate an enhanced tissue with CA. The CA was mixed with sodium chloride saline and diluted to be approximately 500 Hounsfield Unit (HU). We made two volumetric modulated arc therapy (VMAT) plans with/without CA to evaluate the effect of CA on spatial dose distribution. Once a treatment plan was generated based on anisotropic analytical algorithm (AAA) in the treatment planning system (Eclipse, v.13.6, Varian, Palo Alto, USA), it was recalculated using the Acuros® XB (AXB) to compare the dependency of dose calculation algorithms. The volumetric dose data was analyzed with the $V_{n\%}$ (defined by volume receiving n% dose). The dose was segmented with a contoured structure to determine the dose-volume. To quantitatively analyze spatial dose distribution, we used gamma index in commercial dose analysis software (OmniPro IMRT v.1.7, IBA, Germany).

Results: The maximum differences in volumetric dose were 19% and 13% for AXB and AAA respectively as shown in Figure 1. The average differences in the high dose (≥95%

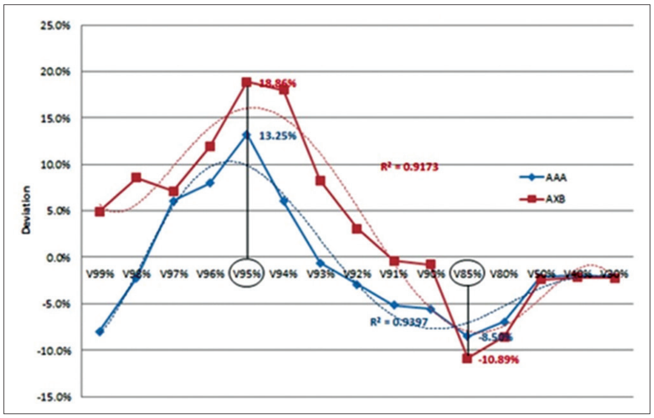

Figure 1: Volumetric dose deviation in phantoms

of prescribed dose) area were 8% for AXB and 6% for AAA, while those in the low dose (≤50% of prescribed dose) area were around 2% for both AXB and AAA. The results showed that the variation of dose distribution with/without CA did not meet more than 90% criterion for gamma index of 2%/2 mm. The passing rate was 86.5% and 81.0% for AXB and AAA in the gamma index histogram. It was shown that there was a significant difference in the high dose area. The dose uniformity in the high dose was within 1%, while there was a large difference in the spatial analysis of the dose distribution.

Discussion and Conclusion: The discrepancy of spatial dose distribution could be critical problem to choose the optimal treatment based on highly modulated VMAT plans. In conclusion, the effects of CA in the VMAT plan should be evaluated appropriately in the clinic, especially in where the beam passes through the contrast-sensitive organs such as liver, spleen, or kidneys with increased HU values due to CA.

Acknowledgement: This research was supported by a grant of the Korea Health technology R and D Project through the Korea Health Industry Development Institute (KHIDI), funded by the Ministry of Health and Welfare, Republic of Korea (Grant Number: HI15C0638).

P-28

DOSIMETRIC ANALYSIS OF PLAN QUALITY OF INTENSITY-MODULATED RADIATION THERAPY VERSUS RAPID ARC WITH BONE MARROW SPARING FOR CERVICAL CANCER

Vuppu Srinivas, Gangarapu Sri Krishna

MNJ Institute of Oncology and Regional Cancer Centre, Hyderabad, Telangana, India. E-mail: srinivasvuppu@gmail.com

Objective: The aim of the present study was to compare intensity-modulated radiation therapy (IMRT) vs. Rapid Arc for treatment of cervical cancer with bone marrow sparing.

Materials and Methods: Fifteen cases of cervical cancer cases were selected for retrospective analysis. All the cases were previously treated using IMRT technique with bone marrow sparing (BMS-IMRT) as extra constraint. For this study, plans using Rapid Arc with bone Marrow sparing (BMS- RA) were created again for all patients following Radiation Therapy Oncology Group (RTOG) guidelines. The plan having coverage of 95% of PTV receiving 95% of prescribed dose is accepted. The plans were compared on the basis of planning target volume (PTV) coverage (dose to 2%, 98% of target), Constraints of OAR (Organs at Risk) were volume of 40% < 40 Gy for normal bladder and rectum, (volume receiving dose 5Gy) V5<95%, V10<80%, V20<60%, V30<50% and V40<35% respectively for Bone marrow were given for planning criteria. Apart from this, homogeneity index (HI), conformity index (CI) and Dose spillage index (R50%) was also calculated with respect to PTV coverage. The prescribed dose (PD) of 50Gy in 25 fractions was given.

Results and Discussion: Better PTV coverage with less OAR doses for bladder and rectum in case of Rapid Arc compared to IMRT. Bone marrow doses are comparable in both the techniques.

Conclusion: Using Rapid Arc technique better PTV coverage is possible with similar OAR doses compared to IMRT.

P-29

SPATIOTEMPORAL DOSE EVALUATION IN VMAT PLANS FOR PROSTATE CANCER: SIMULTANEOUSLY INTEGRATED BOOST WITH HYPOFRACTIONATED SCHEMES

Byung-Moon Park[1], Yong-Ki Bae[1,2], Min-Young Kang[1,3], and Jeong-Woo Lee[1,2]

[1]Department of Radiation Oncology, Konkuk University Medical Center, [2]Department of Convergent Medical Physics, Graduate School of Engineering, Konkuk University, [3]Department of Medical Physics, Graduate School of Biomedical Engineering, Korea University, Seoul, Korea. E-mail: polirain@kuh.ac.kr

Introduction and Aim: As a prostate cancer is increasingly regarded to have a lower alpha/beta ratio (<1.5 Gy) with confidential intervals, contemporary randomized clinical studies have been suggested encouraging tumor control in hypofractionated dose schemes without significant late toxicity. To evaluate spatial and temporal effect of treatment schedule and dose optimization with simultaneously integrated boost (SIB) in volumetric modulate arc therapy (VMAT), dose distributions and effectiveness were compared with conventional 2-Gy based sequential VMAT.

Materials and Methods: Ten patients with prostate cancer were divided into two groups according to their prostate resection: intact prostate (Pint) and post-prostatectomy (Ptomy). The VMAT plans with sequential boost (VMAT-SEB) for the Ptomy were optimized to deliver dose of 46 Gy in 23 fractions to planning target volume including prostate bed and regional lymph nodes (PTV46). The boosting dose of 20 Gy was sequentially delivered more to prostate bed only (PTV66) in 10 fractions. While the VMAT plans with SIB (VMAT-SIB) were optimized to concurrently deliver dose of 46 Gy and 66 Gy to PTV46 and PTV66, respectively, in 23 fractions. The same dose scheme was remained for the PTV46 of the Pint, however, PTV including intact prostate cancer and seminal vesicles (PTV66) and high-risk PTV only (PTV76) were additionally defined. Total dose of 66 Gy in 10 fractions and 76 Gy in 5 fractions were delivered to each PTV sequentially in VMAT-SEB, whereas VMAT-SIB completed all dose delivery in 23 fractions. The spatial and temporal effect by non-uniform dose distributions and treatment schedule was evaluated with generalized equivalent uniform dose (gEUD), EUD-based equivalent dose in 2-Gy fractions (EEQD2), EUD-based tumor-control probability (TCP) and normal tissue complication probability (NTCP), and therapeutic efficiency for each organs of interest as well as physical evaluation.

Results: The VMAT-SIB achieved more conformal or competitive dose distributions with sparing irradiated volume of both bladder and rectum up to 3% at high and intermediate doses.

The rectal volumes received more than 60 Gy was effectively spared more than average 7%, especially for Pint. In addition, the hypofractionated scheme and dose optimization in the VMAT-SIB brought out promising improvement of biological effectiveness to both patient groups. The spatiotemporal effectiveness for the PTV showed increased EEQD2 more significantly with higher prescribed dose: 20 Gy for PTV66 of both groups and 30 Gy for PTV76 of Pint. Accordingly, EUD-based TCP was improved more than 20%, while the VMAT-SIB achieved comparable dose sparing of critical organs for Ptomy or slight increase EEQD2 and NTCP less than 3 Gy and 1.5%, respectively, for Pint. It led to increase therapeutic efficiency more than 20%.

Conclusion: In this study, the VMAT-SIB could provide optimized dose distribution to deliver differential prescribed doses to PTVs in hypofractionated schedule. The achieved spatiotemporal effectiveness of VMAT-SIB may allow treatment efficiency to potentially increase by significantly increasing EEQD2 of PTV and effectively sparing critical organs in prostate treatment.

Acknowledgement: This research was supported by a grant of the Korea Health Technology R and D Project through the Korea Health Industry Development Institute (KHIDI), funded by the Ministry of Health and Welfare, Republic of Korea. (Grant Number: HI15C0638).

P-30

COMPARISON OF RAPID ARC, HELICAL TOMOTHERAPY, SLIDING WINDOW IMRT AND CONFORMAL RT FOR CARCINOMA PROSTATE TREATMENT PLANNING.

Amol Pawar, Kalpana Thakur[1], Rajesh Kinhikar[2], Sanjay Dhole[3]

Department of Radiation Oncology, Sir H N Reliance Foundation Hospital and Research Centre, [1]Department of Radiation Oncology, Holy Spirit Hospital, [2]Department of Medical Physics, Tata Memorial Hospital, Mumbai, [3]Department of Physics, University of Pune, Maharashtra, India. E-mail: amolpawar1010@gmail.com

Helical Tomotherapy (HT), a complex treatment strategy for intensity modulated radiation therapy, may increase treatment efficiency and has recently been established clinically. This analysis compares Helical Tomotherapy against established RapidArc, IMRT and 3Dimensional conformal radiation therapy (3DCRT) delivery techniques.

Introduction: Objective: The potential benefits and limitations of the new RapidArc treatment concept compared to Helical Tomotherapy, fixed gantry intensity modulation techniques and conformal radiation treatment have been assessed at treatment planning level on ten patients presenting with prostate sites tumours.

Materials and Methods: CT datasets of ten patients were included in the study. Plans were optimised with the aim to assess organs at risk and healthy tissue sparing while enforcing highly conformal target coverage. Here we use simultaneous integrated boost technique. Planning objectives for PTV were: maximum significant dose lower than 64.2 Gy and minimum significant dose higher than 57 Gy and same for CTV were: significant dose lower than 70.88 Gy and minimum significant dose higher than 62.93 Gy. For organs at risk, the mean and median doses were constrained to be lower than 42-45Gy (rectum), 45-48Gy (bladder); additional objectives were set on various volume thresholds. Plans were evaluated on parameters derived from dose volume histograms. We were used Eclipse planning system to contouring the structure and generate rapidarc, IMRT & 3DCRT plans. For helical tomotherapy plans, we were used HI-Art Tomotherapy planning system. Plan quality was assessed by calculating homogeneity and conformity index (HI and CI), dose to normal tissue (non-target) and D98% and D2% (dose encompassing 98% and 2% of the target volume respectively). The MU and delivery time were scored to measure expected treatment efficiency.

Results: Both helical tomotherapy and rapidarc resulted in better target coverage but helical tomotherapy had an improved homogeneity and conformity index as depicted in Figure 1. For RA/HT/IMRT/3D-CRT, mean CI was 1.0/1.0/1.0/1.0 &1.0/0.99/0.97/0.98 and HI was 0.03/0.05/0.03/0.03 & 0.11/0.16/0.12/0.06 for CTV & PTV respectively. For a prescribed dose of 66.25 Gy and 60 Gy to CTV and PTV respectively, mean doses to organs-at-risk (OAR) were 23.68Gy/24.55Gy/19.82Gy/23.56Gy for the bladder and 36.85Gy/33.18Gy/33.18Gy/38.67Gy for the rectum. D98% was 65.68Gy/66.23Gy/64.27Gy/61.56 for CTV and 59.54Gy/58.27Gy/57.95Gy/57.83Gy for PTV. D2% was 67.46Gy/69.72Gy/66.29Gy/59.53 for CTV and 66.13Gy/67.74Gy/64.99Gy/61.45Gy for PTV. Mean treatment time was 1.45 min/3.64 min /2.36 min /1.48 min.

Conclusion: All approaches yield treatment plans of improved quality when compared to 3D conformal treatments, with helical tomotherapy providing best OAR sparing by using directional block method in planning and RapidArc being the

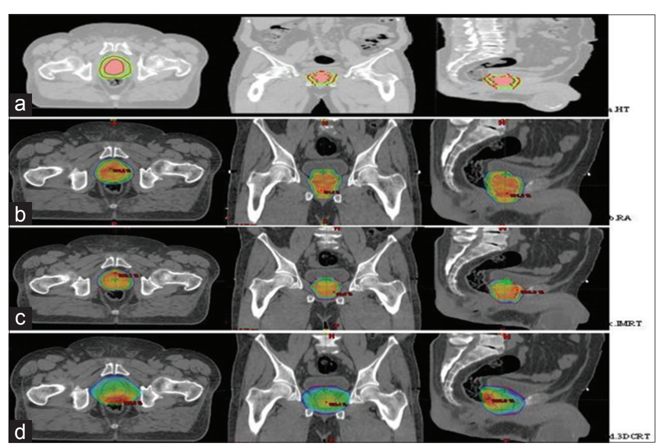

Figure 1: Isodose distribution of 95 % of prescribed doses to PTV and CTV-P for (a) Helical tomotherapy (b) RapidArc (c) Sliding window intensity modulated radiation therapy (d) 3DCRT techniques

most efficient treatment option in our comparison.
RapidArc was investigated for prostate sites cancer showing significant improvements in organs at risk and healthy tissue sparing with uncompromised target coverage leading to better conformal avoidance of treatments w.r.t. IMRT and 3DCRT. This, in combination with the confirmed short delivery time, can lead to clinically significant advances in the management of this highly aggressive cancer type. Clinical protocols are now advised to evaluate prospectively the potential benefit observed at the planning level. Plans which were calculated with 3DCRT provided good target coverage but resulted in higher dose to the rectum and bladder.

P-31

DOSIMETRIC COMPARISON FOR ACTIVE BREATHING COORDINATOR REDUCES RADIATION DOSE TO THE HEART AND LUNGS IN PATIENTS WITH LEFT BREAST CANCER USING VMAT TECHNIQUES.

C. Prabagaran, S. S. Mokha, Piyush Jain, Gaurav Kumar, Chhamta Dutt, D. Manigandan[1]
Department of Radiotherapy, City Hospital and Research Centre, Jabalpur, Madhya Pradesh, [1]Department of Radiotherapy, Medanta-The Medicity, Gurugram, Haryana, India. E-mail: cprabagaran@gmail.com

Introduction: For women with left-sided breast cancer, there is risk of potential cardiotoxicity from the radiation therapy. Different breath-hold methods have been utilized. The two dominant methods are the spirometry-based active breathing coordinator (ABC R3.0) system (Elekta Ltd, Crawley, UK) and the video-based real-time position management (RPM) system (Varian Medical Systems, Palo Alto, USA). The ABC device was developed at the Manipal Hospital Vijayawada, AP. The device is essentially a mouth piece attached to a spirometer and the patient's nose is pegged to ensure they are breathing only through the device. As the spirometer is connected to a computer, the Radiation Teams are able to visualize the patient's level of inspiration. Once the patient has reached the required threshold, pinch valves in the spirometer remotely close, preventing the patient from exhaling or inhaling outside the required threshold. A wide array of planning techniques has been reported in the DIBH literature, but one planning study compared VMAT-Deep Inspiration Breath-Hold (DIBH) Technique and VMAT-Free-Breathing (FB) Technique. DIBH allows this potentially superior planning technique to be used while minimizing cardiac dose.
Materials and Methods: The Pinnacle treatment planning system, v.9.8 (Philips Radiation Oncology Systems, Fitchburg, WI) employs a collapsed cone convolution (CCC) algorithm method is currently regarded as one of the better practical options for dose calculation. Philips Pinnacle v9.8 TPS is used to generate VMAT plans, for a Elekta Infinity machine with a Agility 160 MLC (Elekta Ltd, Crawley, UK). Our VMAT planning protocol uses a single isocenter with two partial composite arcs, each consisting of two complementary arcs of identical gantry rotations. Again Plan is used to generate Free-Breathing (FB plans, for Infinity with a Pinnacle TPS. The plan quality was evaluated by dose conformity, homogeneity, dose fall-off and leakages. Efficiency is measured in treatment planning and delivery time. In order to investigate the dosimetric impact of the ABC, two sets of CT images were acquired.

Table 1: 6 MV photon average dose for both volumetric modulated arc therapy (deep inspiration breath-hold) and volumetric modulated arc therapy (free-breathing) plans for all 10 patients

Organs	*VMAT (DIBH) technique*	*VMAT (FB) technique*
CI	1.08	1.12
HI	1.13	1.18
Heart-mean dose (cGy)	727	1450
Left lung-mean dose (cGy)	1360	1741
Right lung-mean dose (cGy)	313	658
Opposite breast (cGy)	218	490
Spine maximum dose (cGy)	180	296
MUs	535	561

VMAT: Volumetric modulated arc therapy, DIBH: Deep inspiration breath-hold, FB: Free-breathing, HI: Homogeneity index, CI: Conformity index, MUs: Monitor units

Results and Discussion: Ten left-sided breast cancer cases are studied. The PTV volumes plan range from 534 to 620 cc. Plans were evaluated by target coverage, minimum and maximum dose to target, Quality of Coverage (QI), Homogeneity Index (HI) and conformity index (CI) as shown in Table 1. Dosimetric parameters for analysis included RTOG protocol in Heart, Left Lung, Right Lung, Greater Vessels, Opposite Breast, Liver, Spine max dose including Monitor Units (MU). Patient selection is long breath-hold 20-30 sec is desirable.
All plans were optimized using six megavolts (6 MV) X-ray, and the objective dose-volume parameters were identical at the beginning of optimization for the different plans, Planning study compared VMAT-Deep Inspiration Breath-Hold (DIBH) Technique and VMAT-Free-Breathing (FB) Technique. DIBH allows this potentially superior planning technique to be used while minimizing cardiac dose, Lungs dose etc. ABC is viable options to reducing margin for respiratory motion and main advantage was automated beam on and off during treatment of the patients without man interrupts the machine beam.

P-32

HIGHER HOMOGENEITY INDEX IN CLOSE PROXIMITY TARGETS WITH DIFFERENT DOSE PRESCRIPTION WITH VMAT COMPARE TO IMRT

Jayapalan Krishnan[1,2], Jayarama Shetty[2], Suresh Rao[1], Sanath Hegde[1]
[1]Department of Radiation Oncology, Mangalore Institute of Oncology, [2]Department of Radiation Oncology, K.S. Hegde Medical Academy, Mangalore, Karnataka, India. E-mail: nkjayapalceg37@gmail.com

Introduction: Many advanced treatment delivery technologies like IMRT, VMAT, tomotherapy have been used widely in Radiotherapy. In the different delivery techniques, the relative merits of dosimetric advantage and the feasible treatment parameters play an important role in the decision making at the time of plan approval for clinical treatment. In the context of a plan with different levels of dose prescriptions for two or more targets, higher dose spillages are presented in the targets with lower dose prescription. This can be resulted an heterogeneous dose distribution. Therefore, the plan evaluation has to be carried out to identify the amount of homogeneous dose distribution in the targets with a lower dose prescription.

Objectives: Aim of this study was to analyse the homogeneity index with different levels of dose prescription to the close proximity targets using VMAT at different treatment sites and comparison of the same with IMRT.

Materials and Methods: 120 patients, includes 60 head and neck, 15 prostate, 20 cervix with Para aortic node, and 25 lower third oesophagus cancer patients. Two levels of dose was prescribed to the all patients in the all cases. The higher dose was to GTV target and lower dose was to CTV target. Dual arc VMAT and 7-9 field IMRT plans were generated for all the patients and optimized using similar planning objectives in Eclipse treatment planning system (10.0.39) for 6MV photons. Both plans were calculated using AAA at 2.5 mm grid size. Both the techniques VMAT and IMRT plans were evaluated based on the dosimetric score such as the Conformation Number (CN), Homogeneity Index (HI), Dose Gradient Index (DGI), and OARs sparing. Student 't' test was used to find out the significant difference between the techniques.

Results and Discussion: Results showed that conformity index, conformation number, and UDI of the higher dose prescribed target was significantly better with VMAT than IMRT plan ($p<0.001$) in all the sites. The average HI, coverage index of higher dose prescribed target of all sites did not differ significantly between VMAT and IMRT. However, the HI index of close proximity lower dose prescribed target was significantly better with VMAT plans than IMRT in all the sites ($p < 0.001$) without compromising target coverage. These results, implies that the dose fall-off with VMAT was more and resulted in sharp dose gradient to achieve homogeneity in close proximity target as well. This improved homogeneity effect in all the targets achieved with VMAT technique can avoid the risk of higher dose irradiation of serial organ with in the target as well as the clinical outcome can be assessed effectively.

P-33

WEIGHTAGE OPTIMIZATION FOR THE HYBRID VMAT FOR CA. OROPHARYNX CANCERS

J. Antony Paull[1], G. Madhan Kumar[1], C. Krishnappan[1,2], C. Anu Radha[2]

[1]Apollo CBCC Cancer Care, Gandhinagar, Gujarat,
[2]School of Advanced Sciences, VIT University, Vellore, Tamil Nadu, India. E-mail: j.antonypaull@gmail.com

Introduction: In India the head and neck cancer is over 40% of all cancers. In the western region the head and neck cancer is over 55% due to higher tobacco use. Treating such cancers by simple bilateral and anterior beams may restrict to deliver required dose due to the spinal cord. If a higher end technique like Intensity Modulated Radiation Therapy or Volumetric Modulated Arc Therapy is used then the dose to the uninvolved respiratory related structures like Larynx, Constrictor muscle, cervical esophagus, trachea and thyroid gland need to be compromised. So h-VMAT is the emerging technique to achieve the both objectives. But with h-VMAT the dose to lungs is comprised. So the vital role is plays by weightage optimization.

Table 1: The dose-volume histogram variation for all structure for three type of plans

	VMAT	*h-VMAT*	
		80:20	*40:60*
PTV I	58.2±0.4	58.4±0.7	59.3±0.4
PTV II	52.4±0.5	52.9±0.5	52.9±0.4
Spinalcord	34.8±6.1	36.1±1.0	33.2±1.5
Parotid left	26.6±0.5	26.9±0.3	27.8±0.4
Parotid right	31.2±6.9	32.4±9.7	33.7±11.0
Larynx	48.9±4.2	35.6±7.3	35.6±9.2
IPCM	49.0±5.0	33.3±6.0	33.3±6.0
MPCM	61.7±1.3	62.4±0.8	63.3±1.2
SGL	59.3±2.5	54.0±5.4	55.3±6.6
Lung left	12.6±7.8	10.8±2.1	12.4±3.8
Lung right	13.1±7.9	12.7±1.3	14.8±3.9
Thyroid	31.3±8.9	29.6±0.7	30.3±1.2
Trachea	29.6±0.7	21.4±3.1	20.5±5.8
GL	42.8±3.5	23.2±7.0	22.5±7.1
Cer. oeso	37.0±1.0	25.6±1.6	25.2±3.4

h-VMAT: Hybrid volumetric modulated arc therapy, PTV: Planning treatment volume

Objective: To optimize the weightage h-VMAT plans for Oropharynx cancers especially at the respiratory structures and lungs.

Materials and Methods: The 30 patients which have been treated earlier by VMAT technique are taken for the study. Delineation of PTVs and OARs and other respiration related structures were created by oncologist as per RTOG guidelines for Carcinoma of Oropharynx. Upper neck PTV was prescribed 60Gy in 30 fractions and lower neck PTV was prescribed 54Gy in 30#. Two h-VMAT plans are created for all the patients with the weightage of 80:20 and 40:60. h-VMAT plans were created at Eclipse treatment planning system with two mono isocentric plans in two steps. Dose calculations were performed by AAA (v11.01) algorithm with grid size of 2.5 mm. The isocentre was placed at the level of Larynx. as the first step, 80% of the prescribed dose the lower neck PTV was planned with static AP/PA fields with half-beam block technique and mid-line blocked by MLC to reduce the dose to the respiratory structures and to the spinal cord. as second step, a VMAT plan with two co-planar arcs for both upper and lower neck PTVs was created to deliver 100% dose to upper neck PTV and remaining 20% dose to Lower neck PTV by taking the AP/PA plan as a base dose plan during the optimization. The same procedure has repeated with the weightage changing of 40% at AP/PA fields and 60% at VMAT plans. As a prerequisite of the clinical acceptable plan, further DVH of respiratory structures and lungs are analyzed.

Results and Discussion: No significant variation at PTV, spinal cord and Parotids of all three types of plans. Significant variation is found at respiratory structures like larynx, PC Muscles, cervical esophagus, thyroid gland and trachea at hybrid plans in compared to VMAT plans. If further look at weightage variation the 80:20 plans has the edge over 40:60 in respiratory structures and lung dose. The DVH variation for all structure is shown in the Table 1. Our results show that h-VMAT doses are optimally reducing the dose to uninvolved structures like Larynx, PC Muscles, Cervical Esophagus, Thyroid gland and trachea in the treatment of Ca. Oropharynx over the VMAT. The weightage shared between the static field plan and VMAT in h-VMAT plan plays a vital role, care must be taken while deciding the dose prescribed in static field plan.

P-34

COMPARITIVE STUDY OF IMRT AND VMAT FOR CANCER OF MIDDLE THIRD OESOPHAGUS

C. Shambhavi, N. Jyothi1, Sarath Nair[1], Shree Kripa Rao, B. Ramya[1], G. C. Srinidhi[1], Krishna Sharan[1]

[1]Department of Radiotherapy and Oncology, SOAHS, Kasturba Medical College, Manipal University,
[2]Department of Radiotherapy and Oncology, Kasturba Medical College, Manipal University, Manipal, Karnataka, India

Introduction: Radiotherapy plays a major role in the treatment of esophageal carcinoma. 3-Dimensional Conformal Radiotherapy (3DCRT) planning is the method of choice since many years. Innovative technologies in radiation delivery such as Intensity Modulated Radiotherapy (IMRT) offer potential for better tumor coverage reducing doses to normal tissues. The Volumetric Modulated Arc Therapy (VMAT), a novel form of IMRT allows intensity modulated radiation delivery during gantry rotation with dynamic multi leaf collimator (MLC) motion and dose rate alteration simultaneously.
Objective: The aim of this study is to determine the clinical impact of VMAT in middle third esophageal cancer and evaluate its various dosimetric indices by comparing with the IMRT.
Materials and Methods: Six patients with esophageal cancer were selected for this retrospective study. Planning CT scans were acquired with 5 mm slice thickness. The target, organs at risk (OARs) were then delineated. All plans were done in Monaco (version 5.1) planning system for Elekta Versa HD Linac with 80 pairs MLC for 6MV photon. A dose of 59.4Gy was prescribed to the planning target volume PTV59.4Gy and 45Gy to PTV45Gy in 33 fractions. 7-field IMRT, and single and double-arc VMAT plans were generated with the aim to spare OARs and healthy tissue while delivering highly conformal target dose. All plans aimed to achieve target coverage of 95% and hotspot within 107% of the prescribed dose. The objectives for OARs were as follows: spinal cord Dmax <45 Gy; and lung V20Gy<30%. And mean dose of Total lung <20 Gy; heart V45Gy <67%. Data analysis of plans were performed by means of DVH Statistics summary. For PTV59.4Gy and PTV45Gy, the values of D98% and D2%, minimum and maximum doses were reported. The Homogeneity Index (HI) in PTV59.4Gy was expressed in terms of (D2% - D98%)/D50%.
The degree of conformity of the plans measured with the Conformity Index (CI95%) expressed in terms of (TV95%/TV) was reported. Total MU (monitor unit) and treatment time in QA (quality assurance) mode also accounted. Maximum dose to spinal cord; Lung V5Gy, V20Gy; mean dose of Total lung; Heart V45Gy were reported. The analyzed dosimetric indices between groups were compared using student't' test and p value < 0.05 was considered significant.
Result: All the 6 patients for which IMRT and both VMAT plans showed good tumor coverage of 95% prescribed dose with better homogeneity and negligible hotspot. Coverage of PTV45Gy was significantly better with dual arc VMAT (p =0.045) than IMRT and single arc VMAT without compromising conformity and homogeneity. In all the plans the dose to the OARs were within the limit. Both single arc and dual arc VMAT resulted in considerable reduction in maximum dose to spine compared to IMRT (p-0.024, p-0.027 respectively) and also showed significant and closer to significant reduction in MU (p-0.012, p-0.09 respectively) and treatment time.
Discussion: In the treatment of mid third Esophagus, all group plans achieved better tumor coverage with OARs sparing. However, Spine dose was reduced by single and double arc was similar and significantly better than IMRT. The reduced treatment time and MU can help in patient convenience and throughput performance of LINAC.

P-35

DOSIMETRIC ADVANTAGES AND DISADVANTAGES OF JUNCTION FREE VMAT BASED CRANIOSPINAL IRRADIATION TECHNIQUE OVER THE 3DCRT TECHNIQUE

Saneg Krishnankutty, Biplab Sarkar

[1]Department of Radiation Oncology, Fortis Memorial Research Institute, Gurugram, Haryana, India.
E-mail: saneg_krishna@yahoo.co.in

Purpose: This article evaluates the dosimetric advantages and disadvantages of the junction free craniospinal irradiation over the 3DCRT technique. Further we compare the junctional characteristic of between two techniques.
Materials and Methods: CT datasets of 10 patients who have already received a VMAT based CSI treatment has been planned using a 3DCRT technique in this dosimetric study. Serial plans were generated with 3D conformal radiotherapy (3DCRT) as well as volumetric modulated arc therapy (VMAT) for a prescription dose of 35Gy in 21 fractions. To verify the junctional characteristic of the 3DCRT and VMAT plans Isocentre positions were manipulated both superiorly and inferiorly by ±1, ±2, ±3, ±5 mm to generate an overlap or gap at the field junction. 3DCRT based CSI contains two cranial ports along with the one or two spinal beams depending on the length of the spinal target volume. Junctions were matched using collimator, couch and gantry rotation. 3DCRT based CSI requires a junction shift to feather out the cold or hot spots at the junction. Junction shift requires three sets of planning segregated as the 1/3[rd] of the total prescription. For a three iso-centric plans the number of treatment and imaging beams is counted as 12 and 27 respectively. It's always challenging for a therapist to handle large number of beams in the Record and Verify (R and V) system. VMAT based CSI uses a full arc (360°) cranial beam with 100° posterior arc (either one or two depending on the PTV length) for spinal target. Optimization was carried out for all isocentre in a synchronized setting. An unrestricted jaw movement was used to generate a low gradient junction over a length of more than 10 cm.

Results: Both with inferior and superior isocentric shifts, 3DCRT showed higher dose variation at the junction when compared with VMAT. With a 5 mm superior shift (creating gap between fields) there was average junctional underdose of 13.9 ±2.1 Gy and 4.8 ± 1.4 Gy for 3-D CRT and VMAT respectively. With a 5 mm overlap, 3D CRT and VMAT plans showed an overdosing of 10.3±2.5 Gy and 6.0±1.5 Gy respectively. For D1%_Spine statistically significant dose difference was obtained at -3 mm and -5 mm level. 1% dose to brain was not statistically different between 3DCRT and VMAT plans ($0.4 \leq p \leq 0.9$). Highest dose point between 3DCRT and VMAT shows a significant dose variation ($0.03 \leq p \leq 0.001$). Total 22 OAR's were evaluated dosimetrically between two plans. Midline structures like heart, esophagus and thyroid shows a higher dose in case of 3DCRT where the peripheral structure like kidney, liver shows an elevated dose for VMAT plans. However difference in dose to OAR attributed to different techniques are not statistically significant except thyroid. 3DCRT shows a lesser dose to (body-PTV) in <7Gy range, however above 10Gy 3DCRT spillage dose was higher than VMAT. VMAT require 2.2 times higher MU than 3DCRT required MU.

Conclusion: The low dose gradient junction based VMAT techniques do not have a specific junction hence insensitive to patient longitudinal setup error (1-3 mm). Unlike deliberate shifting of junction every 7th fraction with 3DCRT the low gradient technique does not require junction shifting during entire CSI course. VMAT shows a higher spillage dose than 3DCRT in the low dose range. VMAT require only 4 treatment and nine setup beams compared to 12 and 27 beams respectively for 3DCRT. 3DCRT demands an exact spatial position of the patient for reproducibility of the junction where the proposed junction free VMAT technique is insensitive to the accurate patient positioning; hence number of portal images or CBCT/isocentre/day can be reduced. OAR doses yields a mixed result with favoring VMAT technique.

P-36

INFLUENCE OF STATISTICAL UNCERTAINTY ON MONTE CARLO DOSE CALCULATION IN VOLUMETRIC MODULATED ARC THERAPY FOR GLIOBLASTOMA BRAIN TUMOR

P. Mohandass[1,2], D. Khanna[2], D. Manigandan[1], Midhun Kumar[1], Narendra Bhalla[1], Abhishek Puri[1], Pawan Kumar[1]

[1]Department of Radiation Oncology, Fortis Cancer Institute, Fortis Hospital, Mohali, Punjab, [2]Department of Physics, School of Science and Humanities, Karunya University, Coimbatore, Tamil Nadu, India.
E-mail: kpmds03@gmail.com

Introduction: Volumetric modulated arc therapy (VMAT) is an advanced modality of radiotherapy treatment delivery by varying gantry speed and dose rate with reduced treatment time. Dose calculation accuracy in radiotherapy is an important and crucial factor to prevent mistreatment of radiation treatment delivery. Ideally, the dose calculation algorithm should be accurate and able to generate quality plan with less calculation time. Although Monte Carlo (MC) dose calculation algorithms are recognized as the most accurate dose computation algorithms among the commercially available algorithms for treatment planning, its inherent statistical uncertainty (SU), determines the accuracy of the dose calculation and calculation time. During VMAT treatment, the Monaco™ treatment planning system (TPS) has an option to choose different SU (%) up to 5% for MC dose calculations. So it is necessary to evaluate optimal acceptance level of SU (%) for different treatment each clinical sites.

Objectives: To study the dosimetric impact of statistical uncertainty per plan on Monte Carlo calculation in Monaco™ TPS during VMAT for glioblastoma brain tumor.

Materials and Methods: Five glioblastoma (GBM) brain tumor patients treated with 60Gy/30 fractions were chosen for the study. VMAT plans were generated with Monaco™ treatment planning system (TPS-V5.11) for Elekta Synergy™ linear accelerator with 1 cm leaf width. Plans were generated using dual partial arcs with 2% statistical uncertainty per plan. By keeping all other parameters constant, plans were recalculated only by varying the SU, 0.5, 1, 3, 4, and 5%. For plan evaluation, conformity index (CI), Homogeneity index (HI) to planning target volume (PTV), dose coverage to PTV (D98%) was analyzed. The mean and max dose to organ at risk (OAR) was analyzed for brain stem, optical structures, and PTV–brain. The normal tissue volume receiving dose >5Gy and >10Gy and normal tissue integral dose (NTID) (patient volume-PTV), calculation time (mins), point dose measurement and gamma pass rate (<1.00) (3%/3 mm) were compared.

Results and Discussion: The CI and HI improve as the SU increases 0.5 to 5% ($p>0.05$). No significant dose difference was observed in Dmean, D98% to PTV, mean dose to brain stem, optical structures and PTV–brain ($p>0.05$). The Dmax to PTV, optic structures and brain stem were increases with increase of SU ($p<0.05$). Similarly, normal tissue volume receiving dose >5Gy and >10Gy and NTID showed no significant dose difference ($p>0.05$). Decrease in dose calculation time was observed with increase of SU ($p<0.05$). Gamma pass rates were observed >98% and <3% variations in point dose measurement in all VMAT plans. No significant dose variation was seen in calculation reproducibility ($p>0.05$).

The SU can be accepted up to 3% per plan with reduced calculation time without compromising target coverage, OAR doses and plan delivery for GBM VMAT plans. Only by accepting variations in point dose and inhomogeneous dose within target. There is no significant dose variation in calculation reproducibility.

P-37

PLANNING COMPARISON BETWEEN DYNAMIC IMRT, SINGLE AND DUAL ARC VOLUMETRIC MODULATED ARC RADIOTHERAPY FOR HEAD AND NECK CARCINOMA USING A SIMULTANEOUS INTEGRATED BOOST TECHNIQUE

C. Prabagaran[1], S. S. Mokha[1], Piyush Jain[1], Gaurav Kumar[1], Chhamta Dutt[1], D. Manigandan[2]

[1]Department of Radiotherapy, City Hospital and Research Centre, Jabalpur, Madhya Pradesh, [2]Department of Radiotherapy, Medanta-The Medicity, Gurugram, Haryana, India. E-mail: cprabagaran@gmail.com

Introduction: Compared to dynamic beam Intensity-Modulated Radiation Therapy (IMRT), the main advantage of Volumetric Modulated Arc Therapy (VMAT) is a shortened delivery time, which leads to improved patient comfort and possibly smaller intra-fraction movements. This study aims at a treatment planner-independent comparison of radiotherapy treatment planning of IMRT and VMAT for head-and-neck cancer performed based on the same CT- and contouring data. Radiotherapy for head and neck cancer can be challenging due to the complex anatomy of the head and neck region with these tumours often located within close proximity to critical structures which can limit radiation dose. Furthermore the ability of dynamic IMRT to produce inhomogeneous dose distributions can be exploited to simultaneously treat the primary and elective target volumes to different dose per fractions without increasing overall treatment time. This SIB technique allows both volumes to be treated within one treatment plan without the need for matching fields therefore reducing the potential risk of reduced dose coverage in the areas of matching beams.

Materials and Methods: The Monaco Treatment Planning System, v.5.1 (Elekta Ltd, Crawley, UK) employs a Monte-Carlo algorithm method is currently regarded as one of the better practical options for dose calculation. Elekta Monaco v5.1 TPS is used to generate VMAT plans, for a Elekta Synergy Platform Linear Accelerator Machine with a Agility Head 160 MLC (Elekta Ltd, Crawley, UK). 20 patients with loco regionally advanced the oropharynx, hypopharynx and larynx carcinoma were selected. The prescription dose was 70, 63 and 56 Gy to the high-dose, intermediate-dose and low-dose planning target volume (PTV), respectively, and planning parameters were according to Radiation Therapy Oncology Group IMRT protocols. VMAT and IMRT plans were calculated, and dose-volume histograms were created for plan evaluation and comparison. The VMAT delivered the dose rapidly with lesser Monitor Unit without compromising in target dose coverage, conformity and higher sparing of OARs than IMRT.

Results and Discussion: We compared single and double arc VMAT with 7-field fixed dynamic IMRT (SW) in 20 patients with advanced tumours of the oropharynx, hypopharynx and larynx and data presented in Table 1. The PTV coverage was similar between IMRT and VMAT with improved homogeneity when using two arcs with VMAT. Similarly there were no significant differences in the doses to the OARs, a slightly lower mean dose to the parotid glands with the double arc VMAT plans compared with the single arc and IMRT plans. Which compared single and double arc VMAT with 7 field fixed field dynamic IMRT (SW) in 20 patients with tumours of the oropharynx, hypopharynx and larynx. PTV coverage and conformity were similar in the two groups with better homogeneity in the double arc VMAT plans. In this study, the mean doses to the OARs were lower in the VMAT plans with double arc plans achieving significantly lower doses compared with single arc plans. For the spinal cord, the max dose was 33 Gy in the double arc VMAT plans and 35 Gy in the dynamic IMRT plans. For the brainstem max dose was 36.4 Gy for double arc VMAT and 39.1 Gy for dynamic IMRT. For the right side parotid glands, the mean dose was 22.3 Gy for double arc VMAT and 25.1 Gy for dynamic IMRT, while for the left side parotid glands the mean dose was 21.2 Gy and 23.6 Gy for the double arc VMAT and dynamic IMRT plans, respectively. Additional OARs, including cochlea, vocal apparatus and eyes constrictors, were also defined and evaluated in this study. Again there was greater sparing of these OARs with the VMAT plans achieving lower mean doses to these structures. Integral doses to the body were also lower in the VMAT plans by compared with the fixed field dynamic IMRT plans. Simultaneous integrated boost VMAT achieved comparable plans to dynamic IMRT in complex head and neck cases and used two-thirds less monitor units.

Table 1 : 6 MV photon average dose volume statistics comparing dynamic intensity-modulated radiation therapy, single arc volumetric modulated arc therapy and dual arc volumetric modulated arc therapy plans for all 20 patients

Serial number	*Structures*	*Statistic criteria*	*Dynamic (IMRT in Gy)*	*VMAT in Gy*	
				Single arc	*Dual arc*
1	PTV70	Maximum	74.50	74.30	74.10
		Minimum	64.60	66.10	67.40
		Mean	70.90	70.74	71.10
2	Spinal cord	Maximum	35.00	34.20	33.00
		Minimum	2.00	1.70	1.50
		Mean	24.80	23.00	22.30
3	Brainstem	Maximum	39.10	38.30	36.40
		Minimum	2.50	2.20	2.10
		Mean	15.30	14.20	12.00
4	Right parotid	Maximum	68.50	66.00	64.00
		Minimum	4.20	3.50	3.10
		Mean	25.10	23.40	22.30
5	Left parotid	Maximum	67.20	65.30	63.40
		Minimum	5.00	3.80	3.40
		Mean	23.60	22.50	21.20

PTV: Planning target volume, IMRT: Intensity-modulated radiation therapy, VMAT: Volumetric modulated arc therapy

P-38

INVESTIGATION OF EFFECT OF COLLIMATOR ANGLES ON DOSIMETRIC PARAMETERS IN DOUBLE-ARC VOLUMETRIC MODULATED ARC THERAPY OF HEAD AND NECK CANCER

Shefali Pahwa[1], Avtar Singh[1], Amit Saini[1], Tapas Kumar Dora[1], D. D. Deshpande[2]

[1]Department of Radiotherapy, Homi Bhabha Cancer Hospital, Sangrur, Punjab, [2]Department of Medical Physics, Tata Memorial Hospital, Parel, Mumbai, India.
E-mail: shefalipahwa.sp@gmail.com

Introduction: Volumetric Modulated Arc Therapy (VMAT) has become a technique of choice these days for almost all the treatment sites. Arc therapy technique which was originally developed for prostate, subsequently extended to all the sites like Head and Neck, Brain, abdomen, thorax and cervix. VMAT technology coordinates gantry rotation speed, multileaf collimator (MLC) motion, and dose rate modulation simultaneously. The advantage of VMAT technique is that highly conformal treatment is possible with optimal sparing of critical structures and with lesser overall treatment time, lesser monitor units (MU's) and more efficiency as compared to static gantry angle Intensity Modulated Radiotherapy (IMRT).

Aim and Objective: The aim of this study is to investigate the effect of different collimator angles on dosimetric parameters in double arc volumetric arc therapy of Head and Neck cancers. The collimator angle has the largest impact and is worth considering, so, its awareness is essential for a planner to produce an optimal VMAT plan in a reasonable time frame.

Materials and Methods: Fifteen patients undergoing VMAT for Head and Neck cancers are included in this study. Double-arc VMAT plans are created using Monaco® treatment planning system (version 5.11) with two full arcs i.e. one is clockwise arc and other is anticlockwise arc with collimator angle 0–0°. The plans are reoptimized with different collimator angles like 15–345°, 30–330°, 45–315°, 60–300°, 75–285°, 90–270°, 0–90°, 5–85°, 10-80°, 15– 75°, 30–60° and 45–45° using same optimization parameters. The conformity index (CI), homogeneity index (HI), gradient index (GI), machine monitor units (MUs), dose-volume histogram and mean and maximum dose of the PTV are calculated and analyzed. On the other hand, the dose-volume histogram and mean and maximum doses of the OARs such as the parotids, PRV spinal cord, brainstem and oral cavity for different collimator angles are determined from the plans.

Result and Discussion: Preliminary results show that dose coverage of target and OAR's doses depend significantly on the collimator angles due to the geometry of target and OAR's. These dosimetric results provide support and guidance to allow the clinical radiation physicists to make careful decisions in implementing suitable collimator angles to improve the PTV coverage and OARs sparing in Head and Neck VMAT.

Study is going on. Detailed results will be presented in full paper.

P-39

DOSIMETRIC EVALUATION OF DOSE REPORTING MODES IN MONACO TPS: DOSE TO MEDIUM VS DOSE TO WATER

Mamta Mahur[1,2], P. S. Negi[1], R. K. Grover[1], M. Sasindran[1], V. Gedam[1], R. Sharma[1], A. Singh[1], D. Kumar[1], M. Semwal[3], Munendra Singh[2]

[1]Delhi State Cancer Institutes, [3]Army Hospital (RR), New Delhi, [2]School of Basic Sciences and Research, Sharda University, Greater Noida,Uttar Pradesh, India.
E-mail: mamtamahur@gmail.com

Introduction: In radiation therapy treatment planning accuracy of dose calculation is crucial to achieve the clinical goal of radiotherapy i.e. to maximize tumour control probability and to minimise normal tissue complication probability. In radiotherapy treatment planning systems (TPS), photon dose calculations are performed including both simple correction based algorithm and model based algorithm and typically report the dose to water. With recent advancement in technology and computing power, improved Monte Carlo codes have been developed and employed in modern radiotherapy TPS for clinical practices.

Monte Carlo based dose calculations are considered as gold standard due to its accuracy in computing. Monte Carlo algorithm also has the ability to calculate energy deposition in different media accurately and reports dose to medium directly instead of dose to water as what conventional dose calculation algorithm does.

Objective: Monte Carlo dose calculation algorithm is available for external beam photon dose calculations in MONACO treatment planning system (TPS) v 5.11.01 which can report the absorbed dose in two modes: dose-to-water (D_w) and dose-to-medium (D_m). The main purpose of this study is to compare the dosimetric results of two dose reporting modes of Monte Carlo algorithm in MONACO TPS and clinical evaluation in real patient treatment plans of Ca Esophagus case.

Materials and Methods: Step and Shoot IMRT treatment plans were created in Monaco TPS using Monte Carlo algorithm for ten cases of Ca Esophagus for a dose of 5400cGy in 30 fractions using 6MV photon beam for ONCOR Expression linear accelerator. Treatment plans were computed using Dose to medium and Dose to water for identical beam arrangements, grid size and dosimetric constraints. Dosimetric evaluation of plans were done by comparing various dosimetric parameters in the plans for both the dose reporting modes.

Results and Conclusion: The preliminary comparative analysis of dosimetric results in our clinical study shows that selection of either Dw or Dm in Monte Carlo calculations in IMRT plans in MONACO TPS does not introduce significant dosimetric difference in target coverage and OAR DVH's. However doses reported in Dw were relatively higher in comparision to doses reported in Dm plans.

P-40

EVALUATION OF FFF BEAM IN HEAD AND NECK CANCER FOR RAPID ARC DELIVERY

Sandip Patil, Vaibhav Mhatre, Shaju Pilakkal, Rajkumar Chauhan, M. Vadivel, Kaustav Talpatra, Pranav Chadha

Department of Radiation Oncology, Kokilaben Dhirubhai Ambani Hospital and Research Centre, Mumbai, Maharashtra, India.
E-mail: vaibhav.mhatre@relianceada.com

Objective: Aim of this study was to investigate the applicability of flattening filter free (FFF) beams to fractionated radiotherapy of head and neck cancer.

Materials and Methods: Five head and neck cancer patients previously treated were selected for this study. All patients were treated on Edge linear accelerator which was recently installed at our Institute. Each plan was optimized for Rapid Arc therapy (RAT) using 2 full arcs on Eclipse Planning System v13.6. Prescription doses are 60 Gy to the primary and 54 Gy to the nodal target in 30 fractions. For each patient two plans were created by varying the photon beam energy (6X vs 6X FFF) for maximum dose rate 600 MU/min for 6X and 1400 MU/min for 6X FFF. For each patient the prescription dose and OAR dose limits remained unchanged. Furthermore, the number of optimization iterations remained the same for each plan without user interference. The plans were compared using dose volume histograms, conformity and homogeneity indices.

For the PTV, the homogeneity index (HI) and conformity index

(CI) were used as comparison metrics between FFF-RAT, FF-RAT plans. HI was defined as (Dmax)/Dp, where Dmax is the maximum dose received, Dp is the prescribed dose. CI was calculated as Vpi/PTV, where Vpi, and PTV represent the volume receiving a dose equal to or greater than the prescribed dose and PTV volume, respectively.

In the evaluation of the OAR dose, the maximum point doses to the spinal cord and brain stem were determined, and the mean doses to the parotid gland, larynx, and body were recorded. Finally, the number of MUs and the beam-on time (BOT) were evaluated for comparisons of the delivery efficiency.

Results: All plans met the clinical objectives. The RAT plan quality for 6X FFF (1.27) is similar to 6X (1.28). The mean doses for both the paratoids were almost similar. The FFF beams produce slightly better sparing for OARs such as brainstem and larynx. Total MUs are slightly higher in 6X-FFF compared with 6X. The mean body dose was lower in FFF.

Conclusion: For Head and Neck Cancers with conventional fractionation, FFF beam have little impact on Rapid Arc in terms of delivery, plan quality and OAR doses when compared with Flattened beam.

P-41

COMPARISION OF RADIATION TREATMENT PLANS FOR BREAST CANCER BETWEEN VMAT AND IMRT

N. Jyothi, C. Shambhavi, B. Ramya, G. C. Srinidhi, S. Sarath Nair, Shree Kripa Rao, Krishna Sharan

Department of Radiotherapy and Oncology, Kasturba Medical College, Manipal University, Manipal, Karnataka, India. E-mail: jyothi.nagesh@manipal.edu

Introduction: Breast cancer most common cancer in women. Radiotherapy following breast-conserving surgery (BCS) is currently the standard treatment for patients with early breast cancer. The main purpose is to improve local control in treated breast with minimum toxicity. With the advent of advanced sophisticated treatment planning software, Intensity Modulated Radiation Therapy and Volumetric Modulated Arc Therapy is becoming increasingly popular.

Objective: The aim of this study is to compare and analyzing the dosimetric aspects of Intensity Modulated Radiation Therapy (IMRT) and Volumetric Modulated Arc Therapy (VMAT) for Cancer of breast cases.

Materials and Methods: A total of Ten (10) patients who have under gone breast conservative surgery for breast cancer were considered for this study. CT images of the required region was acquired with slice thickness of 5 mm with sixteen slice Computed Tomography (CT) available at our center. After CT scan was done the DICOM images were transferred to treatment planning system. Clinical Target Volume (CTV), Planning Target Volume (PTV) and Organ at Risk (OAR) volumes were generated by Radiation Oncologist according to ICRU83 guidelines. PTV was excluded 3 mm from skin. All plans were generated in Monaco planning system version 5.1 using 6 MV X-RAY beam For Elekta HD versa linear accelerator integrated with 80 pairs of Multi Leaf Collimator (MLC). The dose prescribed was 50Gy in 25# to the PTV. Both VMAT (dual arc) and IMRT (7 fields) plans the dose calculation is done by using Monte Carlo Photon algorithm. Tissue heterogeneity correction was considered in the TPS optimization process. All plans were done to achieve a minimum of 95% of the prescribed dose to 95% Target volume. Plans were compared using Dose Volume Histogram (c-DVH) for maximum dose, Homogeneity Index (HI) and Conformity Index (CI) of the PTV as well as dose to OARs. The target dose uniformity and conformity are calculated and evaluated based on ICRU 83. The conformity index (CI) as defined in ICRU is CI = Volume of PTV covered by the reference isodose/Volume of PTV. CI = 1.0 is ideal value. The Homogeneity Index (HI) as defined in ICRU is HI = (D 2% - D 98%) / D 50%. HI = 0 (Zero) is ideal value.

Results: All the plans achieved minimum target coverage of 95% of the prescribed dose to 95% of the target volume. The dose to OARS are very low in VMAT than the IMRT plans. V10, V20, V5, Maximum dose, Mean dose for Ipsilataral lung are low in VAMT. Contralateral Lung, Total lungs, contralateral breast, Mean doses are low in VMAT compared to IMRT. Heart V10, V20, V25 are also low in VMAT plans. There is no significant difference interms of Tumor coverage, HI, CI in both the techniques. Maximum Dose to PTV and Monitor units are low in VMAT technique.

Conclusions: By comparing both the techniques though the CI, HI are similar, but the Dose to normal tissues are better spared in VAMT than the IMRT Treatment planning technique. Lesser monitor units in VMAT planning reduced the treatment time.

P-42

DOSIMETRIC IMPACT OF STATISTICAL UNCERTAINTY PER CONTROL POINT ON MONTE CARLO DOSE CALCULATION IN MONACO TPS VOLUMETRIC MODULATED ARC THERAPY FOR LUNG CANCER

P. Mohandass[1,2], D. Khanna[2], D. Manigandan[1], Midhun Kumar[1], Narendra Bhalla[1], Abhishek Puri[1], Pawan Kumar[1]

[1]Department of Radiation Oncology, Fortis Cancer Institute, Fortis Hospital, Mohali, Punjab, [2]Department of Physics, School of Science and Humanities, Karunya University, Coimbatore, Tamil Nadu, India.
E-mail: kpmds03@gmail.com

Introduction: The Monte Carlo calculations (MC) are potentially more accurate than the best currently available commercial algorithms. However, Monte Carlo calculations inherently contain random errors, or statistical uncertainty (SU), the level of which decreases inversely with the square root of computation time. The Monaco treatment planning system (TPS) uses MC calculation algorithm for the patient dose calculation in external beam radiotherapy beams. It has an option to choose different SU (%) per control point up to 10% during dose calculations. Therefore, to generate clinically acceptable plans with lesser time, the compromise between SU and dose calculation time must be understood and studied properly for various treatment sites.

Objectives: To study the dosimetric impact of statistical uncertainty per control point on Monte Carlo calculation in Monaco™ TPS during volumetric modulated arc therapy (VMAT) for lung cancer.

Materials and Methods: Five lung cancer patients treated with 60Gy/30 fractions were chosen for the study. VMAT plans were generated with Monaco™ treatment planning system (TPS-V5.11) for Elekta Synergy™ linear accelerator with 1 cm leaf width. Plans were generated using dual partial arcs with 5% statistical uncertainty per control point. By keeping all other parameters constant, plans were recalculated only by varying the SU, 1, 2, 3, 4, 6, 7, 8, 9, and 10%. For plan evaluation, conformity index (CI), Homogeneity index (HI) to planning target volume (PTV), dose coverage to PTV (D98%) was analyzed. Mean and max dose to organ at risk (OAR) was analyzed for spinal cord, pericardium, both lungs-PTV, esophagus and liver. The normal tissue volume receiving dose >5Gy and >10Gy and normal tissue integral dose (NTID) (patient volume-PTV), calculation time (mins), point dose, gamma pass rate (<1.00)(3%/3 mm) were compared. In addition, calculation reproducibility was analyzed.

Results and Discussion: CI and HI improve as the SU increases 1 to 10% ($p>0.05$). No significant dose difference was observed in Dmean to PTV, both lungs-PTV dose, mean dose to pericardium, esophagus and liver ($p>0.05$). Similarly, normal tissue volume receiving dose >5Gy and >10Gy and NTID showed no significant dose difference ($p>0.05$). Decrease in dose calculation time was observed with increase of SU ($p<0.05$). The Dmax to PTV and spinal cord was increases with increase of SU ($p<0.05$). The gamma pass rates were observed >97% and <3% variations in point dose verification in all VMAT plans. No significant dose variation was seen in calculation reproducibility ($p>0.05$).

The SU can be accepted between 4-7% per control point with reduced calculation time without compromising target coverage, OAR doses and plan delivery for lung VMAT plans. Only by accepting variations in point dose and inhomogeneous dose within target. There was no significant dose difference in calculation reproducibility.

P 43 ABS0051

P-43

VERIFICATION OF MONITOR UNIT CALCULATIONS FOR ECLIPSE TREATMENT PLANNING SYSTEM BY IN-HOUSE DEVELOPED SPREADSHEET

M. Athiyaman, Hemalatha, Arun Chogule[1], H. S. Kumar[2]

Departments of Radiological Physics and [1]Radiotherapy S.P. Medical College and AG Hospitals, Bikaner, [2]Department of Radiological Physics, S.M.S Medical College, Jaipur, Rajasthan, India.
E-mail: athi.roja87@gmail.co

Introduction: Computerized treatment planning is a rapidly evolving modality depends efficiently on hardware and software. Despite various ICRU recommendations suggest 5% deviation in dose delivery the overall uncertainty shall be less than 3.5% as suggested by B.J. Minjnheer. J. To ensure accurate dose delivery to the patients independent or secondary verification of Monitor Units (MU) check is preferred. In house spread sheets are developed by the clinical medical physicist to cross verify the dose calculated by the TPS. The Task Group 40 and 114 recommends that the calculation results of any TPS should be independently verified.

Objective: To develop an in-house spreadsheet for the secondary monitor unit verification for our Linear Accelerator for 6MV X-ray beams.

Materials and Methods: The Monitor unit verification calculation (MUVC) verification was tested for pre-approved and executed treatment plans taken from our Treatment Planning System (TPS) database (Make: Varian Medical System, Model, Eclipse version 13.7). The treatment plans were made for Linear Accelerator (Make: Varian Medical Systems, Clinac 2100CD, Palo Alto, CA) with integrated 80 leaf Multileaf collimator for 6MV X-ray beams. In house developed spreadsheet based on MS Excel was used in this study. The necessary dose calculation parameters such as Output Factor (O.F), Percentage Depth Dose (PDD) and off axis ratio (OAR) data were taken from the TPS. The TPS calculated MU for square fields, wedged fields, Head and Neck, Esophagus and Cervix cases were cross verified with the spreadsheet.

Results: MU ratio for square fields for fixed SSD technique and isocentre beams were within acceptable range for the taken depths of 5 cm, 10 cm and 15 cm. The overall MU ratio lies in the range of 0.999 to 1.02 for square field geometries which showed that there was a deviation of 1% between the TPS calculated and the spread sheet calculated. The MU ratios were 0.995 for Head and Neck plans and 1.012 for Cervix plans with a standard deviation of 0.024 and 0.029 respectively.

However we observed the mean MU ratio for Esophagus plans were 1.026 with the standard deviation of 0.040.

Discussion: The independent spreadsheet was designed and tested for most of the routine treatment sites and geometries. The designed spreadsheet is having good agreement with the Eclipse TPS version 13.8 for homogenous treatment sites such as Head and Neck and Cervix and it can be used a secondary MU verification tool.

P-44

A DOSIMETRIC FEASIBILITY STUDY ON FLAT AND UNFLAT BEAMS IN VMAT DELIVERY OF NASOPHARYNX CANCERS

S. Maruthu Pandian, S. Karthikeyan, J. Mathangi, T. Surendra Reddy[1]

Department of Radiation Oncology, BGS Global Hospitals, Bengaluru, Karnataka, India.
E-mail: maruthu50@gmail.com

Purpose: To evaluate Rapid Arc - volumetric modulated arc radiotherapy (VMAT) using coplanar arcs for the treatment of nasopharynx (NPx) carcinomas to achieve conformal dose distribution, homogeneous coverage of the planned target volume (PTV) using flattened beams (FF) and flattening filter free (FFF) beams. The purpose of this work is to evaluate any potential improvement in Rapid Arc plans using Flattening Filter Beams. This work represents one of the initial attempts to assess the usefulness of evaluating normal tissue dose reduction in dynamic VMAT using FFF beams on the True beam STx platform.

Methods: We use the Eclipse (version 13.7) and Truebeam STx linear accelerator which allows during VMAT delivery for both FF and FFF beams. We considered 25 NPx patients who underwent FF VMAT delivery. We set the collimator between 15° and 30° and generate plans with and without flattening filter for comparison. Special attention is given to the low dose regions. Clinical radiation treatment plans were converted to plans with the FFF plans g. Each plan with FFF beams were planned to obtain target coverage within 1% of that in the original FF plan. The new plans were compared to the original plans in a Varian Eclipse treatment planning system (TPS). Reduction in normal tissue dose was evaluated in the new plan by using the parameters V5, V10, and V20 in the cumulative dose-volume histogram for the following structures: Brainstem, Chiasm, Brain, Spinal cord, Parotids. Cochlea, Oral Cavity, Larynx and Mandible. In order to validate the accuracy of our beam model, MLC transmission measurements were made and compared to those predicted by the TPS.

Results: The greatest change between the original plan and new plan occurred at lower dose levels. The reduction in V20 was never more than 1.2% and was typically less than 1% for all patients. The reduction in V10 was never more than 1.6% and was typically less than 0.8% for all patients. The reduction in V5 was 1.2% maximum and was typically less than 0.5% for all patients. The variation in normal tissue dose reduction was not predictable, and we found no clear parameters that indicated which patients would benefit most from FFF beams. As expected FFF beams has 27% higher Monitor Units (MU) as compared to FF beams. Our TPS model of MLC transmission agreed with measurements with absolute transmission differences of less than 0.1% and thus uncertainties in the model did not contribute significantly to the uncertainty in the dose determination.

Conclusion: The amount of dose reduction achieved was not significant in VMAT delivery of FFF beams appears to be similar and not more than 2%. Currently we are analysing more plans for other sites and with other geometries to improve the statistical significance of our conclusion.

P-45

IMPACT OF DIFFERENT COLLIMATOR ANGLES ON DOSIMETRIC OUTCOME OF RAPID-ARC PLANS

Hemant Umbrani, Sadique Kazi, Anand Gudur

Krishna Hospital and Medical Research Center, Karad, Maharashtra, India. E-mail: hemantumbrani@gmail.com

Introduction: Dual arc Rapid-Arc™ treatment plans were mainly planned by assigning two different collimator angles. Generally both collimator angles were complement to each other. Present dosimetry study compares dual arc Rapid-Arc™ plans using various collimator angles set for each arc. Plans were compared using Dose Homogeneity Index and Dose Spillage Index.

Objective: To compare and study impact of various collimator angle settings on Dose Homogeneity Index and Dose Spillage Index for Rapid-Arc™ treatment planning.

Materials and Methods: Five head and neck cancer patients were selected for this dosimetric study. Five different dual arc Rapid-Arc™ plans were generated for each patient. These plans were generated with collimator angles values 10°-350°, 25°-25°, 25°-325°, 35°-325°, 45°-315° respectively for each patients. While gantry start and stop angles, field size, dose rate and optimization parameters were kept same for each plan of particular patient. Dual arc Rapid-Arc™ plan optimization was performed using Progressive Resolution Optimiser algorithm (Varian Medical System, Palo Alto, USA). Dose calculations were performed using 6 MV photons and algorithm used was Anisotropical Analytical Algorithm (Varian Medical System, Palo Alto, USA) in Eclipse treatment planning system. Comparison were made using Dose Homogeneity Index and Dose Spillage Index. Dose Homogeneity Index (DHI) is defined as, DHI= (D5-D95)/prescription dose. D5 and D95 were minimum doses to 5% and 95% of PTV respectively. Dose Spillage Index (R50%) was defined as, R50%=50% isodose volume/PTV volume. Smaller the value of DHI more is the homogeneous distribution in PTV. Lower R50% ratio indicates greater dose fall-off and better dose conformity around the PTV.

Result: DHI were found 0.0851 ± 0.00331, 0.08451 ±0.00321, 0.07467 ± 0.00316, 0.08379 ± 0.00303, 0.08245 ± 0.00411 respectively. DHI found higher in 10°-350° collimator angles plan than 45°-315° or 35°-325° plans. R50% were found 2.4255 ± 0.02489, 2.7418 ± 0.05185, 2.6428 ± 0.08001, 2.8339 ± 0.16329, 2.0775 ± 0.03118 respectively. R50% found more in 10°-350° collimator angles plan than 45°-315° or 35°-325° plans.

Discussion: By performing this dosimetric study it was observed that both Dose Homogeneity Index and Dose Spillage Index can be improved with different collimator angles value. We get better results in 35°-325° and 45°-315° collimator angle combinations in terms of homogeneity and dose spillage.

P-46

A DOSIMETRIC COMPARATIVE ANALYSIS OF TOMO-DIRECT 3DCRT AND CONVENTIONAL 3DCRT IN CASE OF LEFT-SIDED BREAST CANCER

Priya Saini, Ritesh Mhatre, Shrikant Kale, D. D. Deshpande

Department of Medical Physics, Tata Memorial Hospital, Mumbai, Maharashtra, India.
E-mail: priyasaininkt@gmail.com

Objective: Comparing the Dosimetric parameters of TomoDirect (TD) 3DCRT with Tomotherapy and Conventional 3DCRT on Eclipse Treatment panning systems for carcinoma of left sided breast.

Methods: 10 patients with left-sided breast cancer were selected for this study who had received whole breast radiotherapy following breast-conserving surgery. 3DCRT treatment plans were generated with Linear Accelerator on Eclipse TPS and TD-3DCRT on Tomotherapy TPS. Planning target Volume (PTV) andorgan at risk (OAR) such as lung and heart were contoured. The Hypo fractionated treatment regimen was used to prescribe the dose to the planning target volume (PTV), i.e. 40 Gy in 15 fractions. The treatment Plans were compared using to dose-volume histogram analysis in term of PTV coverage, HomogeneityIndex (HI), Conformity Index (CI) and dose to OARs.

Results: TomoDirect-3DCRT showed PTV coverage better than Linear accelerator based 3D-CRT. There was no significant difference in the mean PTV dose between 3DCRT and TD-3DCRT. Conformity of PTV was better in 3DCRT than that in TD-3DCRT (Mean CI 1.2 ± 0.08 vs. 1.7 ± 0.34, p=0.0005). However, homogeneity of PTV was better in TD-3DCRT than in 3DCRT (Mean HI 0.06 ± 0.039 vs. 0.13 ± 0.044, p=0.005). For ipsilateral lung, values of V5Gy, V10Gy, V12Gy, V20Gy and V30Gy were significantly lower in 3DCRT than those in TD-3CDRT. For heart, mean value of V2.5Gyin 3DCRT was lower than that in TD-3CDRT (Mean10.8 ± 9.45 vs. 14.8 ± 4.19, p=0.0001) and V105% of PTV was also found to be lower in 3DCRT than in TD-3CDRT. It was also found that, with increasing of CLD (1 Cm to 2.5 Cm), percentage volume receiving V12Gyof ipsilateral Lung was also increasing for both modalities.

Conclusion: The study showed that doses to OARs were lower for 3DCRT technique and higher for TD-3CDRT. The PTV coverage in both the techniques was found to be optimal from clinical point of view, but slightly superiorin case of TD-3DCRT. Based on these results 3DCRT technique in left breast cancer provides slightly more advantage.

P-47

HYBRID VMAT TECHNIQUE FOR POST-MASTECTOMY CHEST WALL IRRADIATION: A DOSIMETRIC COMPARISON AMONG DIFFERENT HYBRID VMAT PLANS.

K. Balaji[1,2], S. BalajiSubramanian[1], T. Moorthi[1], K. Sathiya[1] C. AnuRadha[2], V. Ramasubramanian[2]

[1]Department of Radiation Oncology, Gleneagles Global Hospitals, Chennai, [2]School of Advanced Sciences, VIT University, Vellore, Tamil Nadu, India.
E-mail: karthik.balaji85@gmail.com

Introduction: Hybrid Volumetric Modulated Arc Therapy (H-VMAT) is an innovative technique which uses conventional 3-Dimensional Conformal Radiotherapy (3DCRT) and VMAT. Several researchers have been compared hybrid IMRT/VMAT techniques with conventional 3DCRT, IMRT and VMAT techniques and reported the benefit of hybrid plans over conventional plans. Studies using H-VMAT in post-mastectomy setting are sparse. Majority of the published article favored VMAT technique over IMRT for chest wall irradiation.

Objective: In the present study, we used three different designs of VMAT for breast cancer patients to determine the optimal H-VMAT plan.

Materials and Methods: CT scan data of 10 post-mastectomy breast cancer patients (median age of 55 years) who received adjuvant radiotherapy were used for this study. Planning target volume (PTV) include chest wall and supraclavicular nodes (CW+SCL). The prescription dose was 50 Gy in 25 fractions (2Gy/fraction). The dose proportion of 3DCRT and VMAT used for hybrid plan was 80/20 percentage of prescribed dose. The isocenter was placed at CW and SCL junction. The 3DCRT plan consisted of two open tangential with half beam blocked fields for CW and one anterior oblique half beam blocked field for SCL. Three different VMAT designs include single partial arc (1A), two partial arcs (2A) and two tangential arcs (TA) were created. During VMAT optimization, the 3DCRT plan was kept as the base dose plan. All Plans were compared using various PTV dosimetric variables and Organs at Risk (OAR's) dose statistics.

Results and Discussions: The mean and standard deviation (SD) values of PTV coverage ($D_{95\%}$), conformity and homogeneity showed significant differences among all compared plans with p values 0.0006, 0.002 and 0.0002 respectively. Published clinical studies have cautioned about the potential risk for lung and cardiac injury even at low doses. The lung and heart low dose (V_{5Gy}) results showed significant differences (Lung V_{5Gy}: 53.79+1.59 Vs. 49.83+3.59, p=0.005 and heart V_{5Gy}: 24.28+8.44 Vs. 28.06+3.14, p=0.034 for 2A Vs. TA H-VMAT plans respectively). All other OAR's mean doses were comparable. Significant difference in MU (p<0.0001) and treatment time (p<0.0001) were observed among all compared plans. The 2A H-VMAT achieved better PTV coverage, conformity, homogeneity and sparing of heart at V_{5Gy} and V_{40Gy}. The results of present study suggest that 2 Arcs H-VMAT plan is superior.

P-48

DOSIMETRIC EVALUATION OF VMAT WITH FF AND FFF PHOTON BEAM FOR LOCALISED CA PROSTATE

Sarath S. Nair, G. C. Srinidhi, B. Ramya, Jyothi Nagesh, C. Shambavi[1], Shreekripa[1], Krishna Sharan

Department of Radiotherapy and Oncology, KMC, Manipal University, [1]School of Allied Health Science, Manipal University, Manipal, Karnataka, India.
E-mail: sarathshyam007@gmail.com

Introduction: Prostate cancer is the most common cancer in men, accounting for over one-fifth of male cancer diagnoses, Various radiotherapy techniques are used for treating prostate cancer have been considered effective treatment options. Especially for elderly patients and those unfit for surgery, VMAT improved delivery time and thus produced a highly conformal and accurate dose delivery when compared to intensity-modulated radiotherapy (IMRT). Recently, a new linear accelerator (linac) called ELEKTA HD versa with flattening filter-free (FFF) beams was introduced into our clinical operation. The benefits of removing the flattening filter is fast delivery time because of the high dose rates, and reduction of the head scatter and leakage, which leads to reduced exposure of normal tissue outside the target field. This study is to evaluate and compare the plan quality and efficacy of flattened and flattening-filter-free (FFF) photon beams in external beam RT for high-risk prostate cancer patients. Hereby we try to elucidate the difference in plan quality and treatment delivery time compared to flattening filter beams.

Materials and Methods: Eight patients for ca prostate are selected and planned. Using CT and MRI images all contours are drawn. Planning was done in monoco by using two full arcs with 6MV, 10MV flattened, and FFF photon beams. The prescribed dose was 72 Gy in 40 fractions for the planning target volume (prostate PTV), All plans were optimized using the same objectives and constraints in MONACO 5.11 planning system. Plans were then evaluated for PTV coverage, OAR. The number of monitor units and the treatment delivery times were also compared. For all cases, the objective of the planning was to cover at least 95% of the PTV with 95% of the prescribed dose (V95%≥95%).

We compared the cumulative dose-volume histograms

(DVHs) and technical parameters for all cases. We also measured the mean, maximum, and minimum doses for the PTV. For the target coverage, V95% for PTV (i.e., the volume of PTV receiving more than 95% of the prescribed dose) several quality parameters were analyzed for the plans. The homogeneity index (HI) of the PTV was defined as (D5%)/D98%), where D2% is the maximum dose. The Set of segmentation parameters used in planning included 3 mm grid size, maximum control point of 180, 0.5 cm minimum segment width and Monte Carlo photon algorithm.

Results and Discussion: There was no significant difference in the PTV dose coverage using all energies compared. The conformity index for all plan are ≥0.78. Homogenity index is found ≤1.2, V95% is ≥98%. It is found that the treatment plan quality there is not much changes, Superior plans were obtained using 10 MV beams in terms of mean and minimum OAR doses, even though this difference was negligible. Mean of bladder and rectum is ≤43Gy and 51Gy. While the treatment delivery time of volumetric modulated arc therapy (VMAT) is considerably shorter using FFF beams, even though the beam MU is more. MU ranges from 490-1047. Sparing for the bladder and rectum was slightly better with the 10 MV FF and FFF plans than with the 6 MV FF and FFF plans, but the difference was negligible. Follow-up studies are needed to confirm the clinical outcome and toxicity of prostate using 6, 10 Mv FF and FFF beams in clinical use.

P-49

EVALUATION OF RAPID ARC PLAN WITH ANISOTROPIC ANALYTICAL ALGORITHM AND ACUROS XB DOSE CALCULATION ALGORITHM FOR HEAD AND NECK CANCERS: OUR EXPERIENCE

K. Janish, Reshma Bhaskaran, R. D. Praveen Kumar, B. Aswathi, Sandeep Madhavan, T. Ajaya Kumar

Department of Radiotherapy, Govt. Medical College, Kozhikode, Kerala, India. E-mail: janishrin@gmail.com

Introduction and Aim: IMRT and RapidArc (RA) are the most common treatment techniques used in Radiotherapy now-a- days. The selection of the technique is in general the discretion of the people involved in treatment. Photon dose calculation algorithms in treatment planning system could affect the accuracy of dose delivery when tissue heterogeneity is involved along the path of the beam. Analytical anisotropic algorithm (AAA) is one of the widely tested and validated dose calculation algorithms in external beam photon radiation therapy. Recently, Acuros XB (AXB) was made available for photon dose calculations, and several studies have demonstrated better dose prediction accuracy of the AXB over AAA. This work aims to evaluate the Rapid Arc treatment plans for Head and Neck cancers with AAA and ABX dose calculation algorithms using the various plan comparison tools.

Materials and Methods: The study was done using Varian Eclipse (Ver.11) treatment planning system. 10 patients were selected. RA plans were done with two full arcs with 6MV and a dose rate of 600cGy/min for AAA and AXB. 2.5 mm grid size was used for both the calculations. The plans were optimized to get a minimum of 98% and maximum not more than 107% of prescribed dose to PTV. Both the plans were evaluated with DVH using tools like D2Gy (Dose received by 2% of PTV volume), D98Gy (Dose received by 98% of PTV volume), D95 Gy (Dose received by 95% of PTV volume), Dmean Gy (Mean dose for PTV), CI (Volume of PTV receiving 98% of dose/ Volume of PTV), HI (D2-D98)/DPTV).

Results and Discussion: Comparing the plans we see that D98 Gy for AAA is 6497.9 ± 76.9 Gy and for ABX is 6394.7 ± 98.2 Gy. D2Gy for AAA is 6498.1 ± 60.8 Gy and for ABX is 6919.4 ± 81.3 Gy. Dmean Gy for AAA is 6769.3 ± 48.1 Gy and for ABX is 6723.8 ± 55.7 Gy. Conformity Index, CI for AAA is 0.92 ± 0.05 and for ABX is 0.86 ± 0.10. Homogeneity Index (HI) for AAA is 0.10 ± 0.02 and for ABX is 0.11 ± 0.02. One of the biggest advantages with regard to the plan calculation with AXB is that the dose calculation time is significantly reduced as compared to AAA. This is very helpful in departments like ours where the patient load is very high.

From the results we see that the plans generated using AAA calculation algorithms have better conformity index. The homogeneity index is same for both the calculation algorithms. Even though these factors are same the most important parameter in the radiotherapy treatment planning is the accuracy of the treatment delivery. Hence the doses were physically verified using an indigenously developed phantom. Since head and neck regions involve several inhomogeneity we found that the plans calculated using AXB were in better agreement with the physically verified doses.

P-50

DOSIMETRIC AND RADIOBIOLOGICAL ANALYSIS FOR PROSTATE CANCER ON GRID SIZE AND DOSE CALCULATION ALGORITHM

Kyeong-Hyeon Kim, Sang-Won Kang, Jin-Beom Chung[1], Keun-Yong Eom[1], Yong-Jin Kim, Tae Suk Suh

[1]Department of Biomedical Engineering, College of Medicine, Research Institute of Biomedical Engineering, The Catholic University of Korea, Seoul, [2]Department of Radiation Oncology, Seoul National University Bundang Hospital, Seongnam, Korea.
E-mail: chunje0131@gmail.com

In this study, we evaluated the dosimetric and biological impact on volumetric modulated arc therapy (VMAT) plan according to the dose calculation algorithm and the dose grid size in prostate cancer patients. The VMAT plans were exported in different dose grid and algorithm case, and dose calculation were implemented. By using Acuros XB (AXB), 1 mm, 2 mm, and 3 mm dose grid size were applied, and 1 mm, 3 mm 5 mm dose grid size were applied in AAA. Dosimetric parameter such as D2%, V95%, the homogeneity index (HI), conformity index (CI), and conformal number (CN) were calculated, and tumor control probability (TCP) and normal tissue complication probability (NTCP) of bladder, rectum, and femoral head were calculated for the radiobiological impact evaluation. In AAA algorithm case, the dosimetric parameter and TCP to planning target volume (PTV) were decreased with increasing dose grid size. As dose grid size was increased, the dosimetric parameter and

TCP of AXB case were increased in the contrary with AAA. Average HI, CI, and CN showed worst value in AAA and 5 mm grid size, and were 0.13, 0.93, and 0.89 respectively. NTCPs of bladder, femoral head in all case were under 0%. NTCPs of rectum were 11.76 – 1.51%, and showed relatively large value in large PTV volume. Similarly with TCP, NTCP of rectum were increased with increasing dose grid in AXB, and decreasing dose grid in AAA. Calculation time of AXB were generally longer than that of AAA, and time difference between two algorithm were increase as dose grid size were decreased. As dose grid size were increased, dosimetric and biological impact of AXB and AAA algorithm showed different tendency, and calculation time increase according to dose grid size were different.

P-51

ASSESSMENT OF VOLUMETRIC MODULATED ARC THERAPY OPTIMIZATION STRATEGY FOR HYPOPHARYNGEAL CARCINOMA

N. Singh, S. Ahamed[1]

Department of Radiotherapy, King George's Medical University, Lucknow, Uttar Pradesh, [1]Department of Radiotherapy, Basavatarakam Indo-American Cancer Hospital and Research Institute, Hyderabad, Telangana, India. E-mail: navinkgmu@gmail.com

Introduction: The progressive resolution optimizer (PRO) of RapidArc volumetric modulated arc therapy (VMAT) generates varying field apertures alongside dose rate and gantry speed variations to arrive at variable MU per degree. MU objective tool available in Eclipse plan optimization environment controls monitor units and thus influences PRO.
Objective: To quantify relative merit of MU deprived plans against freely optimized plans in terms of plan quality and report changes induced by progressive resolution optimizer algorithm (PRO3) to the dynamic parameters of RapidArc.
Materials and Methods: Ten cases of carcinoma Hypopharynx were retrospectively planned in three sequential phases offering complex to simple combinations of target-critical structures. Each of the three clinical plans (baseline plans) was generated without using MU objective tool. Three plan replicas of baseline plans for each phase were reoptimized using the same tool intending to reduce MUs by 20%, 35%, and 50%. Intermediate dose feature along with MU tool was utilized to proceed with the baseline optimization for retaining a similar dose distribution but with lesser MU. This strategy helped to understand the changes made to baseline plans without starting a new loop which might produce but a different solution. Plan merit was quantified as an overall quality index, determined from individual dosimetric indices obtained from DVH for target and OARs separately. In addition to whole body integral dose, dose volume spread was also assessed at various dose levels in the entire patient and in CT sections containing target structures. Significant differences from plan sum comparisons were reported. To analyze the changes induced by PRO3 while reducing MUs, mean values of leaf aperture, CP area, and absolute delta dose rate variation were derived in addition to MU per Gy and dose rate. All plans were appraised for changes induced in RapidArc dynamic parameters and pre-treatment quality assurance (QA).
Results and Discussion: With increasing MU reduction strength (MURS), MU/Gy values reduced, for all phases with an overall range of 8.6–34.7%; mean dose rate decreased among plans of each phase, phase3 plans recorded greater reductions. MURS20% showed good trade-off between MUs and plan quality, yielding equivalent and acceptable plans. Dose-volume spread below 5 Gy was higher for baseline plans while lower between 20 and 35 Gy owing to the dose sculpting ability over the MU deprived plans. Integral dose was lower for MURS0%, not exceeding 1.0%, compared against restrained plans. Mean leaf aperture and control point areas increased systematically, correlated negatively with increasing MURS, resulting in increased effective field size. Absolute delta dose rate variations were least for MURS0%. MU deprived plans exhibited GAI (>93%), better than MURS0% plans, due to reduced modulation complexity.
Conclusions: In this retrospective study, a methodical approach was established to make use of MU objective tool in conjunction with intermediate dose feature and its influence on VMAT dynamic parameters. MU objective tool has a marked influence on the PRO3 algorithm in reducing MUs irrespective of the complexity or size of the target volumes and proximity of OARs. Baseline plans are superior to MU restrained plans. However, MURS20% offers equivalent and acceptable plan quality with mileage of MUs, improved GAI for complex cases. MU tool may be adopted to tailor treatment plans using PRO3.

P-52

LEFT BREAST IRRADIATION WITH TOMOTHERAPY: TOMODIRECT OR TOMOHELICAL - A DOSIMETRIC ANALYSIS

Jerrin Amalraj, S. Rajesh, A. Pichandi, A. Dinesh

Department of Radiation Oncology, Central Physics Division, HCG Enterprises Ltd., Bengaluru, Karnataka, India. E-mail: jerryamal@gmail.com

Introduction: Adjuvant whole-breast external beam radiation therapy is an integral part of the current standard multimodality approach for early stage breast cancer. Radiotherapy planning for breast cancer patients is technicallychallenging because of varying size and shape of the breast as well as setup reproducibility and respiratory motion. Different techniques have been adopted for radiotherapy of left breast say 3D conformal tangential fields with wedge filters, field in field techniques, intensity modulated radiotherapy (IMRT), volumetric arc etc. Over the years, Tomotherapy system was able to deliver highly conformal IMRT plans within helical geometry under image guidance for left breast irradiation. A platform upgrade named TomoDirect® in Tomotherapy empowered users to plan and deliver radiation at user defined static gantry angleswith the couch moving at a constant rate past a fixed binary multileaf collimator. This study investigates how TomoDirect (TD) is equitable with TomoHelical (TH) delivery for the radiotherapy of left breast.
Objective: The aim of this study is to investigate TomoDirect (TD) plans in terms of dosimetric outcomes of target coverage and organ at risk (OAR) sparing and to compare with TomoHelical (TH) counterpart for left breast irradiation.
Materials and Methods: Study population consist of 10

patients presented with carcinoma left breast submitted to whole breast radiotherapy. Retrospective plans are constructed with both TD and TH approach to a prescription dose of 50 Gyto the breast PTV with session dose of 200cGy. Planning were done with Tomotherapy planning station with VoLo Optimization. Clinically acceptable plans were generated for both techniques and compared. Dosimetric parameters such as $D_{98\%}$, $V_{105\%}$, $V_{110\%}$ for target volume and volume of organs receiving specific doses; say V_{5Gy}, V_{10Gy}, V_{20Gy}, V_{30Gy} and their mean doses were compared.

Results and Discussion: Plan quality were quantified with respect to target volume coverage, target homogeneity, low doses to OARs. Mean Dose to 98% Target volume for TD and TH are 48.6Gy ± 86 and 48.8Gy ± 87 respectively. TH plans showed slightly better PTV coverage and homogeneity compared to TD. Mean low dose volume V_{5Gy} to ipsi-lateral lung, Heart, contra-lateral breast and unspecified tissues of body were 48% ± 8.7, 25.5% ± 0.9, 1.72% ± 1.4, 13% ± 4 and 74.2% ± 16, 38% ± 17, 35% ± 16, 24% ± 10 for TD and THrespectively. It is observed that low dose regions to lungs, heart and unspecified tissue of the body were significantly lesser with TD compared to TH. However, mean lung and heart dose (TD: 1287Gy ± 41.6 and 684Gy ± 29; TH:1249Gy ± 21.4 and 589Gy ± 20) were lesser with TH compared to TD. Scoring of TD over TH could be based on the central lung distance (CLD) and maximum heart distance (MHD). It is observed that for plans with average CLD, MHD less than 1.7 cm and 2.5 cm respectively, TD scores over TH for overall OARs sparing and vice versa.

Conclusion: The choice of technique whether TD or TH is solely patient specific based on planning target volume delineation and the proximity of lungs and heart irradiation volume. CLD and MHD are useful parameters to decide the choice the technique to be used for planning left breast radiotherapy.

P-53

DOSIMETRIC COMPARISON OF FOUR DIFFERENT INTENSITY MODULATED RADIOTHERAPY TECHNIQUES IN CARCINOMA OESOPHAGUS

Soumya N M, Ranjitha K H, Resmi K B, Silpa Ajay Kumar

Department of Radiation Oncology, Malabar Cancer Centre, Thalassery, Kerala, India .
E-mail: soumyamazhoor@gmail.com

Introduction: Radiation therapy is a clinical modality dealing with use of ionizing radiations in the treatment of patients. The aim of radiation therapy is to precisely deliver measured dose of radiation to a defined tumour volume with as minimal damage as possible to surrounding normal tissue. Linear accelerator can be used for the effective treatment delivery. Modern Linacs have different radiation treatment technique like Three Dimensional conformal radiation therapy 3DCRT, intensity modulated radiation therapy IMRT, volumetric modulated arc therapy VMAT (/RAPID ARC), Image guided radiation therapy IGRT, Stereotactic radiotherapy etc. Treatment planning in the system allows to achieve the goal of radiotherapy.

Aim: The aim of this study is to find out the best treatment technique in the case of oesophageal carcinoma.

Objective: In radiotherapy there are different types of treatment technique and beam orientations in treating oesophageal carcinoma. So it is very important to find out the best treatment technique in terms of target coverage and sparing of critical organs.

Materials and Methodology: 14 patients who were already treated for oesophageal carcinoma with a technique using a combination of volumetric modulated arc therapy (VMAT) and three dimensional conformal radiation therapy were considered for the study. All those cases were re-planned with VMAT, a 4 field intensity modulated radiation therapy (IMRT) technique and with a 9 field IMRT technique. The treatment plans were evaluated and compared to find out which plan is best among the four in terms of target dose coverage and sparing of organs at risk. Factors like dose received by 95% of the planning target volume, Homogeneity index, Volume of lung receiving dose of 20Gy (V20), V30, V10, V5, mean dose of lung, mean dose of heart and maximum dose to spinal cord were evaluated and compared. The treatment planning system Eclipse10.0 was used for creating plans.

Results and Discussion: All plans meet the target dose prescription requirements. The combined 3DCRT + VMAT technique provides good target coverage and homogeneity. The lung V20 is the least in this technique. The V30 of lung is less than 20%. The V10 and V5 values of lung are also least in this. Compared to other techniques, spinal cord dose is high. But still it can limit within the tolerance. In VMAT alone plans, the V20 values exceeds the limit of 30%. In 4 field IMRT and 9 field IMRT all OAR's can achieve with compromised target coverage. If we try to increase the coverage all the OAR's will exceed the tolerance doses.

P-54

DOSIMETRIC COMPARISON OF IMRT VERSUS 3DCRT FOR POST MASTECTOMY CHEST WALL IRRADIATION

Kartick Rastogi

Department of Radiation Oncology, Sawai Man Singh Medical College and Attached Group of Hospitals, Jaipur, Rajasthan, India. E-mail: kartickrastogi17@gmail.com

Introduction: Breast cancer is the most common cancer in females. In India, especially Rajasthan, most of the patients present with Locally Advanced Breast Cancer (LABC) so mastectomy is performed more often than Breast Conservative Surgery (BCS). Most of these patients require Post Mastectomy Radiotherapy (PMRT) to decrease locoregional recurrence. 3-dimensional conformal therapy (3DCRT) is widely employed radiation therapy technique, but there is still need to minimize the doses to organ at risk (OAR). A few clinical studies have discussed the role of intensity modulated radiation therapy (IMRT) to address this issue.

Objectives: To compare the dose distribution of 3DCRT and IMRT in post mastectomy left sided female breast cancer patients.

Materials and Methods: 110 post mastectomy left sided breast cancer patients were randomised for adjuvant chest wall irradiation in 3DCRT group (n=67) and IMRT group (n=43). All patients were treated on linear accelerator with 50Gy in 25 fractions. The mean doses of lung and heart, percentage volume of ipsilateral lung receiving 20Gy (V20) and heart receiving 25Gy (V25) were extracted from dose-volume histograms (DVHs) and compared between two groups.

Results: The target coverage was achieved with 90% prescription to the 95% volume of the PTV. On average, the V20Gy of ipsilateral lung was significantly higher in 3DCRT than in IMRT group (30.9% and 22.4% resp., $p< 0.05$) but V5 was significantly lower in 3DCRT than in IMRT group (51% vs. 64% resp., $p<0.05$). Similarly, the average V25Gy of heart was significantly higher in 3DCRT than in IMRT group (8.7% vs. 4.3% resp., $p<0.05$).

Discussion: IMRT for the chest wall irradiation of postmastectomy left sided breast cancer patients offers the potential to significantly reduce the high dose-volume of the ipsilateral lung and heart compared to 3D-CRT.

P-55

ANALYSIS OF PHOTON BEAM SKIN DOSE FOR PHYSICAL AND ENHANCED DYNAMIC WEDGES FOR DIFFERENT FIELD SIZES FOR 6 MV AND 15 MV PHOTONS

Titiksha Vasudeva[1,2], Baljeet Seniwal[1,2], Ranjit Singh[2], Arun S. Oinam[2]

[1]Centre for Medical Physics, Panjab University,
[2]Department of Radiotherapy and Oncology PGIMER, Chandigarh, India. E-mail: titiksha1701@gmail.com

The introduction of high energy linear accelerator in radiotherapy allows treatment of deep seated tumors with better dose homogeneity and conformity. The greater penetration of high energy mega-voltage X-rays results in reduction of doses to the skin surface. Apart from primary radiation, electron scattered from collimator head and patient's body contributes significantly to the skin dose. The patient scattered depends upon area of the irradiation and the contribution from collimator depend upon it's distance from the patient's surface. The commercially available treatment planning algorithm (Pencil beam algorithm (PBC), anisotropic analytical algorithm (AAA)) shows a significant variation at the surface interface and the dose gradient region.

Various beam modifying devices (e.g., wedges, shielding block, Multi leaf collimator (MLCs) etc.) are used in treatment planning system to adequately cover the target volume with the prescribed dose without exceeding the doses to the normal structures. The wedge filters are commonly used as a tissue compensator and it results in tilt of iso-dose curve toward thicker end. Physical and Enhanced dynamic wedges (EDW) are the two main class of wedge filters routinely used in radiotherapy. The skin dose drastically changes with the introduction of these two classes of wedge filters.

The aim of the present study is to evaluate skin doses for 6 MeV and 15 MeV photon beams at different field sizes (5×5, 10×10, 15×15, 20×20, and 40×40 cm^2) and for different wedge angle (15°, 30°, 45° and 60°). The experiment was performed on Clinac DHX dual energy linear Accelerator (Varian Oncology Systems, Palo Alto, CA). The solid water phantom RW3 (dimension 30×30 cm^2, 0.1-1 cm thickness range) (density 1.09 g/cc), parallel-plate ion chamber (PPC-40 (IBA (S/N-913) and supermax (Standard Imaging (S/N-P09133, +300 V polarizing potential) electrometer were used for the measurement. The source to surface distance (SSD) was 100 cm and all measurements were carried out upto a depth of 4 cm with backscattered thickness of 15 cm. The percentage depth dose data were measured for all wedge angles and field sizes. The meter readings (electrometer) were recorded and normalized with the meter reading obtained at the depth of maximum dose. The percentage depth dose at surface (PDD_0) increases with the increase in field size, both for enhanced dynamic (EDW) and physical wedged (PW). The surface doses are slightly higher for EDW as that for same angled physical wedge.

P-56

UTILITY OF MANUAL SELECTION OF JAW PLACEMENT AND COLLIMATOR ROTATION IN THE RAPID-ARC PLANNING FOR LARGE VOLUMES WITH HDMLC

R. C. Jaon bos, Gopinath Menon, Jayadevan Pattaloor, Jose Paul, Arunlal, Jino Joseph, Sreedev, Nizar

Department of Radiation Oncology, Aster Medcity, Kochi, Kerala, India. E-mail: jaon.bos@asterhospital.com

Introduction: Rapid Arc as it's known for, provides with increased degrees of freedom utilising entire span of Gantry and Multi-leaf Collimator movement and their speed along with dose rate modulation. While using High Definition MLC for extended target volumes, regions stretching beyond the limited width of HDMLC bank gets compromised in terms of degrees of freedom that Rapid-Arc provides resulting in in-homogeneous dose distribution and increased spillage of prescription and lower doses.

Objective: Utility of manual selection of jaw placement and collimator rotation in the Rapid-Arc planning with HDMLC for large volumes is studied. A technique of manual intervention in the planning process by limiting jaws and appropriately choosing collimator rotation to effectively increase the degrees of freedom that produces homogeneous and conformal distribution is presented.

Materials and Methods: High Definition MLC with 120 leaves by Varian Medical Systems on True-beam platform with Eclipse planning system were used for all Rapid-Arc planning. Maximum width of this HDMLC bank is 22 cm and region of targets extending beyond this limit suffers the aforementioned problem. Routinely 1 to 3 arcs with optimum collimator rotation of 30 and 330 suffices to achieve a clinically acceptable distribution.

Additional arc with feasible collimator rotation that make the leaves to travel along the maximum dimension of the

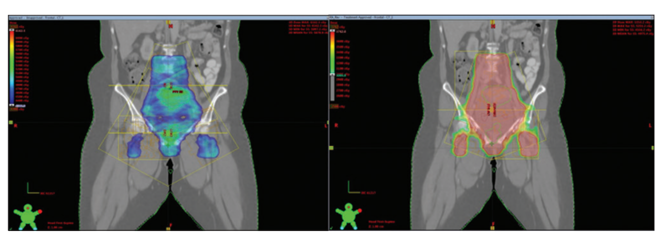

Figure 1: A two IC plan converted to single IC plan by splitting the additional arc into 2 arcs confined to superior and inferior aspect of PTV respectively with collimator rotation 90 and the resultant distribution obtained

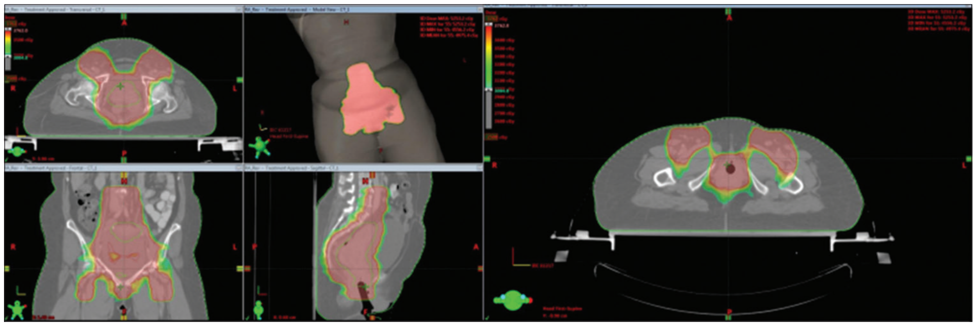

Figure 2: The single IC plan sparing normal tissue of 80% of prescription dose in split regions

target exploiting maximum over-travel distance of 15 cm works very well but has its own drawbacks when employed for large volumes as following. (1) Leaves have to traverse more distance and more number of them are pushed to travel at their maximum speed of 2.5 cm/s. Since leaf position uncertainty is found to be more with increase in their speed which in turn results in poor gamma in quality assurance. (2) Leaves modulating over the entire length of volume at a time diminishes the degrees of freedom of leaf positioning, i.e. constraints met at particular region of volume takes away freedom of achieving clinical goal in another region.

The methodology used for solution to this problem is to have the additional arc limited to modulate over the particular in-homogeneous region of target volume. This is achieved by limiting jaws to the particular region along with a collimator rotation that makes leaves travel along the longer dimension of target before proceeding to optimization. If needed, this additional arc can be split into two different arcs independently modulating over such different regions e.g. cranial and caudal extent of PTV with the collimator rotation 90 or lateral aspects of PTV with near zero collimator rotation one for left lateral and the other for right lateral.

With this method the connectedness existing among the DoF subsets of all arcs used for modulation is minimised and makes them mutually more exclusive.

Results and Discussion: "The jaw arrangement used for a pelvic volume with inguinal nodes, and the resulting distribution using this method is shown in Figure 1", and the resulting distribution using this method is shown in Figure 2. Distribution obtained with this method is superior in terms of conformity and spillage of lower doses as well.

Jaw arrangement used for a volume in the lungs extending cranially into neck region and resulting distribution is shown in Figure 2. The third arc used in this case produces better sparing of medial structures in its confined region.

Utilizing analogy of DoF with connectedness in topology could yield better solutions to optimization problem in near future.

P-57

SYSTEMATIC AND DOSIMETRIC EVALUATION OF STATIC AND DYNAMIC CONFORMAL RADIOTHERAPY PLANS USING DIFFERENT OPTIMIZATION PARAMETERS

Radhika Jain, Rose kamal[1], Pankaj Kumar, Sajal Kakkar, Varinder Singh Chabbra

Department of Radiation Oncology, Max Super Speciality Hospital, Mohali, Punjab, [1]Department of Radiation Oncology, Institute of Liver and Biliary Sciences, New Delhi, India. E-mail: radhikajain331@gmail.com

Introduction: The development of advanced techniques of Radiotherapy viz. IMRT, IGRT, SBRT, Gating techniques etc. has led to very precise delivery of dose to tumour, sparing surrounding normal tissues, increasing the efficacy of treatment. Accurate dose calculation in TPS is the key factor to achieve the aim. The grid size of dose calculation cube determines the resolution of dose calculation and hence accuracy at the boundaries of adjacent structures of tumours.

Aim and Objective: The aim of the study is to determine the site specific optimum grid size resolution and optimal parameters for dose calculation in TPS i.e. minimum segment widths, number of control points and to incorporate it in clinical protocols.

Materials and Methods: Monaco (5.11) treatment planning system is used to generate the plans for each site with different grid sizes. Plan evaluation is done on the basis of standard evaluation tools i.e. slice by slice and DVH comparison etc. A Medical Linear Accelerator Elekta Synergy Platform equipped with 80 MLC is used for dose delivery using VMAT and IMRT technique. IMATRIXX is used for verification of delivered dose using gamma evaluation method.15 patients of Head and neck, prostrate, Brain and cervix, and Breast evaluated and 3D Gamma analysis of each plan is done using IMRT phantom.

Results: There were no significant differences for dose volume histogram (DVH) values between grid sizes. The calculation time was significantly higher for grid size 1.0 - 2.5 mm. The Monitor units varied by 5-10%, for smaller grid size the MU was less. A 4-mm grid size changed the dose variation by up to 3–4% (50 cGy) for the heart and the spinal cord, while a 3-mm grid size produced a dose difference of <1% (12 cGy) in all tested OARs. The segment width showed comparative variation. As we change no of control points the number of MU is increased and quality by increasing number of control points but treatment delivery and calculation time increases. Gamma evaluation of calculated and measured dose distributions is within tolerance (3% and 3 mm).

Conclusion: Grid size of Dose calculation cube, segment width, and no of control points is an important factor for accurate dose calculation depending upon the site and corresponding surrounding structures adjacent of tumour for different sites. The optimal selection and combination of these three parameters effects the plan quality.

P-58

EFFECT OF MULTICRITERIAL OPTIMISATION OPTION IN MONACO V5.0 TPS ON SERIAL AND PARALLEL ORGANS

Rahul Phansekar, S. Divya, Vipul Patel[1], Hemendra Mod[1]

Departments of Medical Physics and [1]Radiation Oncology Aaruni Hospital Pvt. Ltd., Rajkot, Gujarat, India.
E-mail: rahulphansekar21@gmail.com

Introduction: The basic planning challenge of radiotherapy is to handle the trade-offs between achieving the required tumour dose meanwhile not overdos-ing the surrounding healthy organs. A multicri-terial optimisation (MCO) allows the treatment planners to explore and understand these trade-offs thus providing a means to select the best plan for each patient.
Objectives: This study is to investigate the effect of multic-riterial optimisation in MonacoV5.0 treatment planning system (TPS) on Serial and Parallel organs.
Materials and Methods: Our department is equipped with Elekta Com-pact 6MV Linac with 80 leaves MLC (MLCi2), Monaco V5.0 TPS. Fifteen IMRT cases were selected for this study. Five head and neck cas-es with bilateral neck nodes and 5 with unilater-al neck nodes; similarly 5 thoracic and abdo-minal cases with no GTV involved are selected. For each case we made 3 IMRT plans. First plan without applying MCO to any organ; second by applying MCO only to serial organs and in third plan applying MCO only to parallel organs. Dose calculations were performed by keeping same constraints for PTV and OARs in all cases. For all plans, dose was calculated with Monte Carlo algorithm with dose calculation grid of 3 mm. We analyzed the dose volume his-tograms of all three plans generated for each patient. The Parameters used for comparison of the plans are Total Volume of PTV (TV), Vo-lume of the PTV covered by 95% isodose line (VRI), which is our reference isodose line (RI), Maximum dose to the PTV (Dmax), Minimum dose to the PTV (Dmin), maximum dose to the Serial organs and mean dose to the parallel or-gans. From above obtained parameters Confor-mity Index (CI), Quality of coverage (Qcov) and Homogeneity index (HI) were calculated as proposed by Radiation Therapy Oncology Group (RTOG).
Conformity Index RTOG = VRI (95%)/TV (1)
Results and Discussion: It has been observed that there is no significant difference in conformity index, quality of cov-erage and homogeneity index for all three plans generated for each patient as depicted in Table 1-6.. We have no-ticed that the spinal cord doses are reduced significantly with MCO option selected. In head and neck cases with unilateral neck node PTV, the maximum reduction in spinal cord dose was (3925.9cGy to 3049.3cGy) and average reduc-tion was (4031.18cGy to 3514.58cGy). In head and neck cases with bilateral neck node PTV, the maximum reduction in spinal cord dose was (4329.7cGy to 3201.6cGy) (1128.1cGy) and

Table 1: Head and neck intensity modulated radiation therapy cases with unilateral planning target volume

Patient number	Spine dose without MCO (cGy)	Spine dose with MCO (cGy)	Reduction in spine dose (cGy)
1	3925.9	3049.3	875.7
2	4000.9	3555.6	444.3
3	4511.1	3958.7	552.3
4	3290.6	3020.5	270.1
5	4427.4	3988.8	438.6
Average	4031.18	3514.58	516.2
Patient number	*Contralateral parotid dose without MCO (cGy)*	*Contralateral parotid dose with MCO (cGy)*	*Reduction in contralateral parotid dose (cGy)*
1	1404.6	537.0	867.6
2	1020.3	647.1	373.2
3	949.8	786.8	163.0
4	1200.1	1030.8	169.4
5	1344.1	777.0	567.1
Average	1183.8	755.7	428.1

MCO: Multicri-terial optimization

Table 2: Head and neck intensity modulated radiation therapy cases with bilateral planning target volume

Patient number	Spine dose without MCO (cGy)	Spine dose with MCO (cGy)	Reduction in spine dose (cGy)
1	4457.0	3773.2	683.8
2	4695.6	4018.2	677.4
3	4330.4	3430.5	899.9
4	4329.7	3201.6	1128.1
5	4233.8	3522.1	711.7
Average	4409.3	3589.12	820.2
Patient number	*Left parotid dose without MCO (cGy)*	*Left parotid dose with MCO (cGy)*	*Reduction in left parotid dose (cGy)*
1	2477.0	2411.0	66.0
2	2259.1	2121.4	137.1
3	2493.8	2399.6	94.2
4	2579.9	1896.4	683.5
5	2575.0	2436.0	139.0
Average	2477.0	2252.9	224.0
Patient number	*Right parotid dose without MCO (cGy)*	*Right parotid dose with MCO (cGy)*	*Reduction in right parotid dose (cGy)*
1	2488.0	2474.0	14.0
2	2185.5	1895.1	290.4
3	2518.2	2349.8	168.4
4	2511.7	2021.4	490.3
5	2271.8	1653.8	618.0
Average	2395.0	2078.8	316.2

MCO: Multicri-terial optimization

Table 3: Abdominal and thorax intensity modulated radiation therapy cases

Patient number	*Spine dose without MCO (cGy)*	*Spine dose with MCO (cGy)*	*Reduction in spine dose (cGy)*
1	4518.0	3487.2	1030.8
2	3649.4	3649.4	2011.8
3	3362.4	3177.0	185.4
4	2957.0	2574.0	383.0
5	3994.2	3196.3	797.9
Average	3696.2	3216.78	881.8
Patient number	*Left lung dose without MCO (cGy)*	*Left lung dose with MCO (cGy)*	*Reduction in left lung dose (cGy)*
1	1391.8	1304.4	67.4
2	1094.3	910.7	183.6
3	1219.0	1016.0	203.0
4	924.5	812.4	112.1
5	1274.4	1201.7	72.7
Average	1180.8	1049.0	127.8
Patient number	*Right lung dose without MCO (cGy)*	*Right lung dose with MCO (cGy)*	*Reduction in right lung dose (cGy)*
1	1656.5	1635.0	21.2
2	827.7	726.2	101.5
3	1120.0	986.0	134.0
4	1283.5	1122.4	161.1
5	1470.2	1343.4	126.8
Average	1271.6	1162.6	108.9
Patient number	*Liver dose without MCO (cGy)*	*Liver dose with MCO (cGy)*	*Reduction in liver dose (cGy)*
1	1422.7	1018.3	404.4
2	1391.0	1354.2	36.8
3	1462.5	1291.9	170.6
4	154.7	86.9	67.8
5	1162.0	921.0	241.0
Average	1118.6	934.5	184.1

MCO: Multicri-terial optimization

average reduction was (4409.3cGy to 3589.12cGy) with MCO. In head and neck cases with unilateral neck node PTV the maxi-mum reduction in mean dose to contralateral parotid dose was reduced (1404.6cGy to 867.6cGy) and average reduction was (1183.8cGy to 755.7cGy) with MCO. In head and neck cases with bilateral neck node PTV the maximum reduction in mean dose to left and right parotid dose was (2579.9.cGy to 1896.4.cGy) and (2271.8.cGy to1653.8cGy) and average reduction was (2477.0cGy to 2252cGy) and 2395cGy to 2078.8cGy) respectively. In case of thorax and abdominal cases the maxi-mum reduction in spine dose was (3649.4 cGy to 1637.5cGy) and average reduction was (3696.2cGy to 2814.4cGy) with MCO. The maximum reduction in mean dose to left and right lungs dose was (1219.0cGy to 1016.0cGy) and (1283.5cGy to 1122.4cGy). Average mean dose reduction to both lungs was (1180.8cGy to 1049cGy) and (1271.6cGy to 1162.6cGy) with MCO. The maximum reduction in mean liver dose was (1422.7cGy to 1018.3cGy) and aver-age reduction was (1118.58cGy to 934.5cGy).

From above study we can say that mulilicriterial optimisation tool in Elekta Monaco TPS effec-tively helps to reduce the doses to critical or-gans in IMRT planning.

Table 4: Conformity index

Patient number	*Conformity index=(VRT [95%]/TV) without MCO*	*Conformity index=(VRT [95%]/TV) with MCO serial*
1	0.9797	0.9654
2	0.9840	0.9770
3	0.9949	0.9827
4	0.9873	0.9859
5	0.9828	0.9876
6	0.9814	0.9757
7	0.9577	0.9727
8	0.9737	0.9510
9	0.9921	0.9600
10	0.9885	0.9807
11	0.9806	0.9891
12	0.9853	0.9520
13	0.9922	0.9979
14	1.0000	1.0000
15	0.9944	0.9944
Average	0.9850	0.9781

AVE change in conformity index=−0.71%. MCO: Multicri-terial optimization, TV: Target volume, AVE: Average, VRT: Volume receiving the reference dose

Table 5: Quality of coverage

Patient number	*Quality of coverage=(D_{min}/RI [95%]) without MCO*	*Quality of coverage=(D_{min}/RI [95%]) with MCO serial*
1	0.9122	0.9123
2	0.9275	0.9262
3	0.9170	0.9498
4	0.9282	0.9000
5	0.9342	0.9245
6	0.9200	0.9263
7	0.9315	0.9315
8	0.9140	0.9295
9	0.9240	0.9324
10	0.9285	0.9118
11	0.9170	0.9089
12	0.9359	0.9384
13	0.9691	0.9644
14	0.9796	0.9915
15	0.9525	0.9380
Average	0.9327	0.9324

AVE change in quality of coverage=−0.31%. RI: Reference isodose line, D_{min}: Minimum dose to the PTV, PTV: Planning target volume, MCO: Multicri-terial optimization, AVE: Average

Table 6: Homoginity index

Patient number	Homoginity index=(D_{max}/RI [95%]) without MCO	Homoginity index=(D_{max}/RI [95%]) with MCO
1	1.1247	1.1336
2	1.1269	1.1278
3	1.1230	1.1189
4	1.1212	1.1168
5	1.1246	1.1310
6	1.1053	1.1140
7	1.1261	1.1240
8	1.1229	1.1221
9	1.1284	1.1277
10	1.0540	1.1111
11	1.1370	1.1371
12	1.0994	1.1263
13	1.1111	1.1209
14	1.1286	1.1279
15	1.1205	1.1197
Average	1.1169	1.1239

AVE change in homoginity index=0.62%. MCO: Multicri-terial optimization, D_{max}: Maximum dose to the PTV, PTV: Planning target volume, RI: Reference isodose line, AVE: Average

P-59

3DCRT BREAST IRRADIATION – ORGAN AT RISK DOSES FROM REDUCED TARGET VOLUME MARGINS

D. Basaula[1,2], N. P. Freeman[1], A. Quinn[3], A. Walker[2,4,5], V. Batumalai[2,4,6], S. Kumar[2,4,6], G. P. Delaney[2,3,6], L. Holloway[2,3,5,6,7]

[1]Department of Medical Physics and Radiation Engineering, The Canberra Hospital, Garran, [5]Centre for Medical Radiation Physics, University of Wollongong, Wollongong, [2]Ingham Institute of Applied Medical Research, [3]Northern Sydney Cancer Therapy Centre, Royal North Shore Hospital, [4]Liverpool and Macarthur Cancer Therapy Centres, [6]University of New South Wales, [7]Institute of Medical Physics, University of Sydney, Sydney, Australia.
E-mail: deepak.basaula@act.gov.au

Introduction: Three dimensional conformal breast radiotherapy (3DCBRT) results in radiation dose to organs at risk (OARs) such as heart, lung and contralateral breast. Radiation dose received to OARs during the course of breast radiotherapy has shown to be associated with increased risk of radiation induced health issues. Potentially, by reducing breast planning target volume (PTV) margin, OARs dose can be reduced.
Objective: This study investigates the effect of planning target volume (PTV) margin reduction for 3DCBRT in relation to dose received by organs at risk (OARs).
Materials and Methods Using ten retrospective patients computed tomography (CT) datasets, delineation of target volumes and OAR structure were made. For each patient, three different PTV were created by adding different margins (0 mm, 5 mm and 10 mm) to clinical target volume (CTV). Treatment plans were created for each PTV with a 3DCBRT field-in-field technique using the XiO version 4.64 treatment planning system (TPS). The compliance with the Radiation Therapy Oncology Group (RTOG) 1005 protocol requirements was followed. A prescription dose of 50 Gy in 25 fractions to the PTV was used to generate treatment plans. Each patient's dose volume histogram (DVH) data were extracted from treatment plans and used to evaluate the doses to OARs. Measurement of relative dose for comparison with treatment planning system calculated dose was performed in CIRS IMRT Thorax phantom.
Results and Discussion: By changing PTV margins from 10 mm to 0 mm, mean dose reduction of 31% (heart), 28% (lung) and 23% (contralateral breast) was obtained. Such reduction in dose would reduce the radiation induced health issues to OARs. However, careful consideration must be given to clinical implication of reduced PTV margins. Significant reduction in margin may cause inferior treatment outcomes.

P-60

TRACEABILITY OF DOSE BETWEEN TREATMENT PLANNING SYSTEM AND LINEAR ACCELARATOR FOR VARIOUS TREATMENT MODALITIES

Dince Francis, C. A. Shahan Shad, Daicy George, V. Ramya, P. Suresh Babu, S. Sowmya Narayanan

Vydehi Institute of Medical Sciences and Research Centre, Bengaluru, Karnataka, India.
E-mail: dincemedphy@gmail.com

Objectives: The goal of radiotherapy is to cure or locally control the disease while minimizing complications in normal tissues. The International Commission on Radiation Units and Measurements recommends that radiation dose has to be delivered within ±5% of the prescribed dose. Computerized Radiotherapy Treatment Planning Systems (RTPS) are used to get in-patient dose calculation using machine data. Precise dose delivery, both geometrically and dosimetrically is crucial for the successful outcome of the treatment. Thus, there is a need for rigorous dosimetry and quality controls in order to ensure precision and accuracy of dose estimation in treatment planning software. In this study, the traceability and reproducibility of planned dose between RTPS and Linear Accelerator for various treatment modalities is verified.
Materials and Methods: The equipments used for this study were Treatment Planning System (Eclipse, Version11.1, Varian Medical Systems & Monacco, Version5.1, Elekta Medical Systems), Medical Linear Accelerator (Clinac 2300C/D, Varian) able to deliver IMRT and VMAT with multi-leaf collimators and 4D CT Scanner (GE Medical Systems). The Dose calculation and delivery accuracy check was performed in homogeneous and non-homogeneous mediums for conformal static fields (3DCRT) as well as dynamic field techniques (IMRT, VMAT). The Mini water phantom was used for dose measurement in homogeneous medium whereas Lung phantom and CIRS phantom were used for the same in heterogeneous medium. The Pencil Beam Convolution (PBC), Anisotripic Analytical Algorithm (AAA) and Collapsed Cone Convolution (CCC) algorithms were used for dose calculation for 3DCRT plans whereas AAA was used for the same in IMRT and VMAT plans. The doses were calculated at different positions in the medium, i.e., at different densities within the phantom. The choice of detector (FC65G or CC13) for dose measurement was made according to the provision provided in the

phantom. The plan delivery was performed with the aid of IGRT capabilities to account for any geometrical shift of the target. The TPS calculated dose and the measured dose were compared and deviation is noted. The QA on homogeneous phantom was performed on monthly basis and checked for its consistency. In addition, accuracy check of dose delivery is supplemented using the TLD capsule irradiation for 2 Gy at 10 cm depth for 10 x 10 cm^2 field size for 100 cm SSD, for 6 and 15 MV energies.

Results and Discussion: The accuracy of dose delivery is within ±2% for simple field in homogeneous medium. For symmetric field technique, the accuracy of dose delivery lies within ±3% and for 3DCRT, IMRT and VMAT, the agreement was within ±5% for both algorithms in heterogeneous medium. The TLD response shows a difference of -0.5% and -1.3% for 6 and 15 MV respectively. The study over one year period ensures the acceptable quality of the RTPS, which is capable of delivering dose to the patient within an accuracy of ±5%. The dose delivery over the study period is found to be consistent.

Conclusion: The reproducibility and traceability of planned dose from TPS to the treatment unit was accurate. The quality and the functionality of the TPS is found to be within the accepted tolerances, which are mandatory to obtain the requisite clinical outcome with an optimal treatment delivery. This study enhances the level of confidence in the efficient treatment delivery.

P-61

CRANIO SPINAL IRRADIATION TECHNIQUES: A DOSIMETRIC COMPARISION OF HELICAL TOMOTHERAPY WITH VOLUMETRIC MODULATED ARC THERAPY

M. Sathiya Seelan[1,2], R. Murali[2], K. Tamilselvan[1], G. Padma[1], M. K. Revathy[1], N. Arunai Nambi Raj[2]

[1]Department of Oncology, Apollo Cancer Hospital, Hyderabad, Telangana, [2]School of Advanced Sciences, VIT University, Vellore, Tamil Nadu, India. E-mail: sakthiraji84@gmail.com

Objective: Cranio Spinal Irradiation (CSI) is a challenging procedure of treating various central nervous system malignancies. Large PTV size (includes whole Brain and Spinal Cord and overlying meninges) requires field matching due to technical limitations of conventional linear accelerators (LA), which cannot irradiate such volumes as a single isocentre treatment. Helical Tomotherapy (HT) could help to avoid these limitations as irradiation of long fields is possible without field matching. This study aims to assess the dosimetric comparision of treatment plans between HT and Volumetric Modulated Arc therapy (VMAT) of CSI.

Materials and Methods: CT datasets of Four (n=4) previously treated patients with medulloblastoma were used to generate VMAT plans in Eclipse V13.6 and HT plans in VoLO planning system V5.1.0.4. In both plans a total dose of 36Gy in 20 fractions with 2Gy per fraction was prescribed such that at least 98% of the volume of PTV received at least 95% of the prescription dose. Plans were compared using PTVs conformation number (CN), homogeneity index (HI), normal tissue mean dose statistics, body mean dose and treatment time.

Results and Discussion: HT plans showed better homogeneous dose distribution to PTV with a mean (SD) HI of 0.06 (0.006) vs. 0.10 (0.019) for VMAT plans. In terms of conformity VMAT plans showed marginally better CN with mean value of 0.83 vs. 0.76 for HT plans. Normal tissue mean dose statistics included the structures total lungs, total kidneys, heart, oesophagus, liver, thyroid, parotids, oral cavity showed 1.1-1.39 (mean, 1.25) times higher in VMAT plans compared to HT plans. Both the plans showed average body doses were same. HT plans showed mean beam on time 11 mins vs. 6.25 mins for VMAT plans. However, beam –on time is not necessarily representative of the total time the patient will spend in the treatment room, factors such as patient setup and imaging, shifting patients to different isocentres, gantry rotations must be considered to estimate the overall treatment time. Considering all such factors, in our institute the patient who underwent CSI treatment patient spent average of 30 mins and 25 mins for HT and VMAT respectively from setup to treatment delivery. In conclusion, radiation treatment planning and delivery of CSI with a homogeneous dose distribution remains one of the most challenging processes. HT for CSI is favourable in terms of PTV coverage, homogeneous dose distribution, conformity, OAR sparing. Overall HT is technically easier without any junction matching and dosimetrically superior than VMAT.

P-62

DOSIMETRY VERIFICATION OF STEREOTACTIC BODY RADIATION THERAPY FOR HEPATOCELLULAR CARCINOMA TREATMENT

R. P. Srivastava, B. Katarzyna, S. Junius, K. Thevissen

Centre Hospitalier Mouscron, Mouscron, Belgium.
E-mail: rajupsrivasstava@gmail.com

Purpose: A new radiotherapy technique, stereotactic body radiation therapy (SBRT) allows safe delivery of higher dose external beam radiotherapy to liver tumours and the focus of the treatment has shifted from palliative purposes to cure-oriented therapy. A dosimetric study was performed to evaluate the performance of stereotactic body radiation therapy with Rapid Arc on hepatocellular carcinoma.

Materials and Methods: Ten patients with unresectable HCC were enrolled in this study. The patients were calculated using the Eclipse planning system (version 11.0) with the 120-leaf multi-leaf collimator (MLC) (Varian Medical Systems). Dose prescription varied from 45 to 62.5 Gy to the Planning Target Volume of 80% prescribed dose in 3 to 10 fractions. A verification plan was created for portal dosimetry (PD) and PTW Octavius 4D phantom (Detector 1000 SRS). All plans were analysed using gamma-index with 3% dose tolerance and 3 mm (PD) and distance to agreement and 2%, 2 mm for Octavius 4D in relation to the treatment planning system.

Results: PD 95% and Octavius 4D phantom100 % confirmed a good agreement between the two distributions with high dose and conformed dose to the target and low dose to the organ at risk. All measurements passed with at least 95% of the measurements within gamma-criteria. SBRT allowed to achieve required target coverage as well as to keep within

normal tissue dose/volume constraints. The presentation will include some practical and pitfalls.

P-63

TUMOR AND CRITICAL ORGAN'S DOSE ARISING FROM DIFFERENT RADIOTHERAPY TECHNIQUES APPLIED TO PAROTID GLAND: A COMPARISON BETWEEN CALCULATED AND MEASURED DOSE

Mohammad Taghi Bahreyni Toossi, Hamid Gholamhosseinian, Atefeh Vejdani, Noghreiyan[1]

[1]Medical Physics Research Center, Faculty of Medicine, Mashhad University of Medical Sciences, Mashhad, Iran. E-mail: vejdania931@mums.ac.ir

Introduction: Parotid gland tumors account for 3% of head and neck tumors. Adjuvant radiotherapy is suggested for reducing the risk of high grade parotid tumors.
Objectives: the aim of the present study was to compare patient's dose arising from different techniques applied to treat parotid gland tumors and suggest useful modification, to optimize organ's dose.
Materials and Methods: The dose of target volume and OARs of three usual parotid gland radiotherapy techniques were measured on Rando phantom by TLDs. Tech1: mixed beam of 6 MV photons and 10 MeV electrons technique (weighting=1:2). Tech2: Paired wedged 6 Photon beams, Tech3: Paired wedged 6 Photon beams using MLC. Then, measured doses were compared with corresponding values obtained from treatment planning calculations. Finally, the best technique was suggested with respect to tumor dose sufficiency and homogeneity, and organ at risks protection. Results and discussion: Tech2 and tech3, significantly improved the dose homogeneity in PTV (ΔD95% - 5% =2.31, 2.28, respectively). Tech3 was the most effective factor in dose reduction to tissues beyond the target volume. Tech1 kept the lowest dose to oral cavity (1.9 Gy). PTV received at least 95% of the prescribed dose in all techniques. Based on the TRS-430 protocol, 95% of the measured dose by TLD inner and outer of the field was in good agreement with the treatment planning system calculations, for three techniques. In the studied techniques, tech1 can be considered for protecting oral cavity and preventing xerostomia. Regarding target dose homogeneity, tech2 and tech3 were considered as the optimal techniques; moreover, in reduction dose to structures sticking to target volume, tech3 was selected. It is suggested that, whether during the treatment, three techniques are used instead of single technique, the critical structures surrounding are spared more efficiently, and the tumor volume receives sufficient and homogeneity dose.

P-64

A TREATMENT PLANNING STUDY: STATISTICAL EVALUATION OF DYNAMIC AND STATIC IMRT TECHNIQUES

Kaur Amandeep, Sharma Ramita, Sachdeva Kanchan

Department of Radiotherapy, Sri Guru Ram Das Institute of Medical Sciences and Research, Amritsar, Punjab, India. E-mail: aman_07mar@yahoo.in

Introduction: Ra diotherapy is one of the most common modalities used for the treatment of cancer in addition to surgery, chemotherapy and hormonal therapy. External beam radiotherapy directs high energy rays from outside the body to the tumor. Intensity modulated radiotherapy (IMRT) is a mode of delivering high precision conformal radiotherapy with computer- controlled Linear Accelerator having multi-leaf collimation (MLC) system. IMRT is usually delivered via two techniques viz. the static or step and shoot (SS) mode and the dynamic or sliding window (SW) mode of delivery. In the static mode IMRT the radiation beam is ON only when the MLCs are set to the discrete aperture shapes and are stationary at each sub-field. While in the dynamic IMRT delivery mode the beam remains ON as the leaves move to take shape for the next sub-field.
Objective: The purpose of our study was to evaluate the statistical differences between the treatment plans generated for head and neck and pelvis cases at our centre with both the static and sliding window technique.
Materials and Methods: In this study, five cases each for head & neck and pelvis were planned with 6MV on Elekta Monaco 5.0 Inverse Treatment Planning Software for IMRT utilizing Monte- Carlo algorithm. The cases were planned with both step and shoot and dynamic IMRT techniques keeping the optimization constraints same. Gamma analysis was applied to the plans with the Compass software version 3.1 to meet the 95% pass criterion at 3%/3 mm. The plans for each individual case with both techniques were evaluated in terms of Dose Volume Histogram parameters viz. *Dmax*, *Dmean*, $D_{95\%}$, $D_{1\%}$ Uniformity index, Homogeneity index, Conformity index (at 95% isodose) and number of Monitor Units.
Results: On evaluation of plans, it was observed that there was comparable coverage for PTVs in both techniques for pelvis cases but for head and neck cases PTV receiving 95% dose was 96.14 ± 0.99% and 94.26 ± 1.07% for dynamic and SS techniques respectively. The maximum dose received by PTV for pelvis cases was 106.86 ± 0.25% and 106.65 ± 0.27% for SW and SS techniques respectively and the maximum dose received by PTV for head and neck cases was 107.71 ± 0.38% and 107.99 ± 0.29% for SW and SS techniques respectively. For the two sites studied, there was no significant change in Uniformity Index and Homogeneity Index values for both dynamic and SS techniques. However, there was significant difference observed in Conformity Index for pelvis as well as head and neck cases in both methods. The number of Monitor Units were also less in the step and shoot technique in comparison to the dynamic delivery for both the sites.
Discussion: The study indicates that the difference in PTV coverage was not significant in pelvis cases for both the techniques but it doesn't follow the same trend for head and neck cases. The doses to OARs were lower in the SS technique for pelvis cases but no significant difference was found in head and neck cases.

P-65

SET-UP ACCURACY IN DOSE DISTRIBUTION: COMPARISON BETWEEN CT-AND CBCT-BASED PLANS FOR OROPHARYNGEAL CANCER

Masakazu Otsuka[1], Hajime Monzen[1,2], Kazuki Ishikawa[2,3], Kenji Matsumoto[1],

Mikoto Tamura[1], Tamaki Nishi[1] Masahiko Okumura[2], Yasumasa Nishimura[3]

[1]Department of Medical Physics, Graduate School of Medical Science, Kindai University, [2]Department of Radiology, Kindai University Hospital, [3]Department of Radiation Oncology, Kindai University Faculty of Medicine, Higashiosaka, Japan.
E-mail: m-otsuka@med.kindai.ac.jp

Introduction: Oropharyngeal cancer patients are treated with the two-step intensity modulated radiotherapy (IMRT) in our institution. Deformable image registration (DIR) is a critical technic in adaptive radiotherapy (ART) for propagating contours between planning computerized tomography (CT) images and treatment CT/cone-beam CT (CBCT) images to account for organ deformation for treatment re-planning.
Objection: The aim of this study was to investigate an influence factor for the oropharyngeal cancer ART using weekly CBCT.
Materials and Methods: We employed the Exactrac and Varian's On-Board Imager (OBI) for image matching. Ten patients with oropharyngeal cancer were enrolled. The CBCT were used to estimate the dose distributions during the treatment. Planning Target Volume (PTV), spinal canal, brain stem and parotid gland (R, L) were propagated from pre- to mid-treatment images using DIR. The dose between pre-treatment plans and CBCT plans were evaluated by body weight, body surface contour and set-up errors.
Result and Discussion: The differences of mean dose for PTV, spinal canal, brain stem, and parotid gland (R, L) in the maximum weight loss of 8.9 kg were 1.5%, 0.3%, -0.1%, 1.7%, and 8.3% respectively, while in the maximum set-up error of rotating 3.5° at mandible bone, the differences were -1.3%, 1.2%, 5.3%, 2.6%, and 12.5%, respectively. The maximum change in body surface contour was observed the same patient of maximum weight loss. The high set-up accuracy (less than rotating 1° at mandible bone) was found that the differences were less than 2% in PTV, spinal canal and brain stem. Set-up accuracy was higher influence to dose distributions than body weight and body surface contour.
Two-step IMRT is used for dose escalation of parotid gland occurs due to body weight and body contour loss. However, set-up accuracy of patients had the most influence on dose distribution in this study. The most important factor was set-up accuracy of patients in ART, namely strategies for set-up are necessary at CT-simulation and treatment. Set-up accuracy of a patient should be performed ART according to loss of body weight and body contour.

P-66

DOSIMETRIC EVALUATION OF TITANIUM IN 16-BIT DEPTH AND 12-BIT DEPTH: MONTE CARLO STUDY

J. Jayapramila, A. A. Mohd Zahri

Oncology & Radiological Sciences Cluster, Advanced Medical and Dental Institute, Universiti Sains Malaysia, Penang, Malaysia. E-mail: jpramila_87@yahoo.com

Introduction: Accuracy of currently available algorithm for treatment planning system is limited and require full mode algorithm to know the true dose distribution. Monte Carlo (MC) algorithm in radiotherapy is the most accurate approach to perform radiation dosimetry calculation.
Objectives: This study compare dosimetric analysis of titanium rod in 12-bit depth and 16-bit depth DICOM image using MC code of linear accelerator (LINAC) Elekta Synergy.
Materials and Methods: Titanium rod was scanned in two computed tomography (CT) scanners (SIEMENS Somatom (12-bit depth); TOSHIBA Aquilion (16-bit depth)) at 120 kV using in-house built phantom. CT images transferred to MONACO treatment planning system (v.5). Anterior oriented beam plan consisted of 10 x 10 cm^3 generated. Collapsed cone (CC) algorithm was applied to deliver 200 MU EGSnrc MC simulation was validated first by comparing percentage depth dose and beam profile on water phantom. BEAMnrc/DOSXYZnrc MC codes with 5 x 10^8 particle histories traversing titanium rod in 10 x 10 cm^3 anteriorly. Point dose evaluation was carried for 12-bit depth and 16-bit depth DICOM images.
Result and Discussion: CT number for titanium rod in 12-bit image saturated at 3071 Hounsfield Unit (HU), whereas for 16-bit depth, mean CT number was 9996 HU. MC simulation is well matched with measured data (PDD and beam profile) with percentage difference of less than 2%. Treatment planning system comparison was compared with MC simulation with presence of titanium rod.
Conclusion: MC code for Elekta Synergy will be a benchmark for this institute. This code give confidence to the physicist to plan and deliver the treatment to patient accurately. 16-bit depth provide accurate dosimetric output than 12-bit depth.

P-67

RADIATION SHIELDING APPLICATION OF LEAD GLASS

R. Nathuram

Ex-Radiation Safety Systems Division, Bhabha Atomic Research Centre, Mumbai, Maharashtra, India.
E-mail: dr.nrohila@rediffmail.com

Nuclear medicine and radiotherapy centers equipped with high intensity X-ray or teletherapy sources use lead glasses as viewing windows to protect personal from radiation exposure. Lead is the main component of glass which is responsible for shielding against photons. It is therefore essential to check the shielding efficiency before they are put in use. This can be done by studying photon transmission through the lead glasses. The study of photon transmission in shielding materials has been an important subject in medical physics and is potential useful in the development of radiation shielding materials. In order to make use of the photon attenuation by HP Germanium gamma spectrometer. The counting setup used in the present measurements consists of a narrow beam collimator coupled to a HP Germanium gamma spectrometer. The experiment consists of measuring the ratio of photon beam intensity I, transmitted through an absorber of known thickness t, expressed in units of g.cm^{-2} to the photon beam intensity I_0 incident on it. Then the value of attenuation coefficient μ is obtained from the relation:-
$I / I_0 = e^{-\mu t}$
Each radioactive sources of Cs-137 and Co-60 were selected for the present study as they are used as teletherapy sources in radiotherapy department. Each chosen source of about

Table 1: Photon attenuation coefficients for lead glasses

Sample number	Weight fraction of lead (%)	Attenuation coefficients for photons μ/ρ (cm^2/g)		
		662.0 keV	1171.0 keV	1332.0 keV
1	41.30	0.0891	0.0604	0.0556
2	47.96	0.0931	0.0605	0.0558
3	53.73	0.0973	0.0600	0.0560
4	58.78	0.0979	0.0609	0.0564
5	63.24	0.0982	0.0611	0.0562
6	67.21	0.0991	0.0613	0.0563

These measured values of attenuation coefficients of glass samples can be utilised in compilation of shielding factors of lead viewing glass of known thickness

200 kBq in solid disc form was in turn placed in front of a lead collimator of 2 mm diameter. The photon beam leaving this collimator passed through the absorber and another identical collimator before being detected by a HP Germanium detector. The photon spectrum of transmitted and incident beam with and without absorbers were recorded on a 8K MCA. From the ratio of transmitted to incident photon beam I/I_0 and thickness 't' of the absorber, the value of attenuation coefficients were obtained. In Table 1, the experimental value of attenuation coefficients obtained against photon energy of each source used in the present investigation are presented compilation of shielding factors of lead viewing glass of known thickness.

P-68

SBRT OF KIDNEY: OUR INITIAL EXPERIENCE

R. Phurailatpam, S. Balara, S. V. Jamema, S. N. Paul, K. Joshi, D. D. Deshpande[1]

Department of Radiation Oncology, ACTREC, [1]Department of Medical Physics, TMH, Tata Memorial Centre, Mumbai, Maharashtra, India. E-mail: rphurailatpam@actrec.gov.in

Aim: To report our Initial Experience on Volumetric-Modulated Arc Therapy (VMAT) of SBRT Kidney.

Materials and Methods: Stereotactic body radiation therapy (SBRT) represents a novel treatment approach in the setting of renal cell carcinoma (RCC). Three patients of RCC already treated with VMAT, True Beam (Varian) were taken for this study. Three VMAT plans for gantry rotation angles of 360° and 180° viz 2 full-arc with flattening filter less 10 MV photon (2FA_10FFF), 2 half-arc with flattening filter less 10 MV photon (2HA_10FFF), 2 full-arc with flattening filter less 6 MV photon (2FA_6FFF) were created for each patient with the Eclipse treatment planning system (version 13.5). Dose prescription was 45Gy/3 fractions. Full-arc and half-arc VMAT plans were compared with regard homogeneity index (HI), coverage index (CI), Conformation Number (CN), dose to OARs (Spine, Duodenum, Stomach), total monitor units (MU), effective dose rates, delivery times, and gamma passing rate for delivery QA for each plan. Delivery QA for each plan is carried out using Arc check dosimetry (Sun Nuclear™).

Result: The HA plans achieved comparable HI, CI and CN to the FA plans. 2HA_10FFF resulted in 30% less MU and 50% shorter delivery time than 2FA_10FFF. Low dose volumes for normal tissues (V_5 and V_{10}) are upto 200cc more in 2FA_10FFF than in 2HA_10FFF. Maximum Dose to Spine, Duodenum, Stomach, are also 12%, 35% and 30% lesser in 2HA_10FFF plans than 2FA_10FFF. However for 2FA_10FFF and 2FA_6FFF plans, there is not much difference in dose to OARS and in treatment delivery time between the two plans as shown in Table 1. Delivery QA of all the plans were passing with 99% in 2% and 2 mm criteria.

Table 1: Plan parameters

Plans	MU	Effective dose rate (MU/min)	Treatment time (min)	DQA gamma (%)	CI	HI	CN
10FA_2	4075	1500	2.61	98	0.99	0.06	0.865
10_HA_2	2837	2139	1.32	99	0.99	0.07	0.852
6FA_2	3104	1104	2.87	99	1	0.08	0.843

CI: Coverage index, HI: Homogeneity index, CN: Conformation number, MU: Monitor units, DQA: Delivery quality assurance, HA: Half-arc, FA: Full-arc

Conclusion: 2HA_10FFF is more efficient than 2FA_10FFF in terms of treatment delivery and OAR sparing. However, there is no difference between 2FA_10FFF than 2FA_6FFF.

P-69

COMPARISON BETWEEN SINGLE AND DOUBLE VOLUMETRIC ARC THERAPY TECHNIQUE IN THE TREATMENT OF CERVIX AND BOT CANCER

Amit Saini[1], Avtar Singh[1], Shefali Pahwa[1], Ashok Kumar[1], D. D. Deshpande[2], Tapas Dora[1]

[1]Department of Radiotherapy, Homi Bhabha Cancer Hospital, Sangrur, Punjab, [2]Department of Medical Physics, Tata Memorial Hospital, Parel, Mumbai, India. E-mail: amitsaini6565@gmail.com

Introduction: Volumetric modulated arc therapy (VMAT) is a novel radiation technique, which can achieve highly conformal dose distribution with improved target volume coverage and sparing of normal tissues compared with conventional radiotherapy techniques. VMAT is a new form of IMRT, which allows irradiation with the simultaneously changing gantry position, dose rate and multileaf-collimator (MLC) position. VMAT also has the potential to offer additional advantages, such as reduced treatment delivery time compared with IMRT.

Aims and Objectives: The aim of this study was to investigate volumetric-modulated arc therapy (VMAT) with single arc (1 ARC) and dual arc (2 ARC), and to evaluate the quality. The quality of these plans was evaluated by calculating the quality index (QI) homogeneity index (HI), conformity index (CI), dose to PTV and dose to OAR. For the delivery efficiency of these plans, the numbers of monitor units (MUs) were evaluated.

Materials and Methods: A total of 15 patients (7 with cervix and 8 with base of tongue (BOT) were taken for this study. Patient's plans were created with single and dual arc on Monaco 5.1 Treatment Planning System. For comparison same VMAT planning constraints were utilized in all the single and dual arc plans for each patient and typical dose distribution is shown in Figure 1. All the plans had been calculated with constant dose calculation grid size of 3 mm using monte-carlo algorithm. After which dose volume histogram data used to calculate quality index (QI) homogeneity index (HI), conformity index (CI), dose to PTV and dose to OAR.

Results: As form the tables it was clearly shown that, in

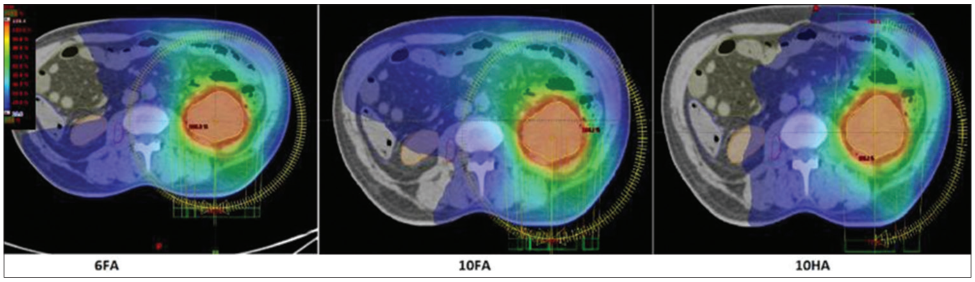

Figure 1: Dose wash (lowest isodose line is 10%)

cervix as well in BOT cases we evaluated that quality index (QI) homogeneity index (HI), conformity index (CI) were much better in dual arc as compared to single arc. Whereas, MU delivered and Coverage to PTV in dual arc were also more. There were not such big difference in the doses of Organ at Risk (OAR).

Conclusion: In comparison to the VMAT plan with one arc, the VMAT plan with multiple arcs has more control points that give higher degree of freedom for possible MLC positions. This could result in higher degree of modulation and better plan quality, especially for a complex-shaped target volume. However, a higher degree of modulation generally increases the planning time due to longer plan optimization and dose calculation processes.

P-70

DOSIMETRIC VERIFICATION OF TOTAL SKIN ELECTRON THERAPY BY USING CASO$_4$:DY THERMOLUMINESCENCE POWDER IN INDIGENOUS WAX PHANTOM

T. Natarajan, A. Chougule[1], T. Senthil Kumar
S. Venugopal, Umra Fatima, Jeev Raj Bhati,
K. Ratheesh, Rajkamal

Department of Radiation Oncology, Bhagwan Mahaveer Cancer Hospital and Research Centre, [1]Department of Radiological Physics, SMS Medical College and Hospital, Jaipur, Rajasthan, India.
E-mail: thirunatrajan@gmail.com

Indroduction: The aim of the study is to verify the six dual field Total Skin Electron Therapy radiation technique by using $CaSO_4$:Dy thermoluminescence powder in indigenously prepared wax phantom. This radiation technique is used for the treatment of mycosis fungoides.

Materials and Methods: The study involves the characteristics of the electron beam such as energy, dose rate, flatness at 100 SSD and Extended SSD at 400 cm. The electron beam with gantry angle 270±18.5 for 6MeV with HDTSe$^-$ mode which produces dose rate of 888 MU/Min is used for all the measurments. Parallel Plate Chamber is used for dose rate measurement in indigenously prepared wax phantom [Figure 1] which mimic the patient and vertical movement stand [Figure 2] uesd for vertical profile. TLD Reader is used to estimate the dose deposited in $CaSO_4$:Dy powder and 6 mm PMMA acrylic sheet [Figure 2] is used as a energy degrader.

Results: The horizontal and vertical profile was measured and the flatness is found within ±10% as shown in Graphs 1 & 2. The dose rate for six dual field was measured by determining factor A (=0.97061) and factor B (=3.1363) to find the required MU to deliver the prescribed dose.

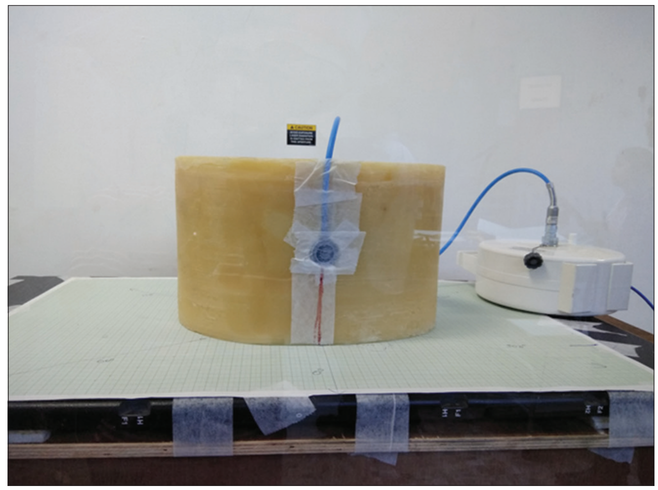

Figure 1: Position of Parallel Plate Chamber in waxphantom

Figure 2: 6 mm PMMA and phantom stand for vertical profile movement

Discussion: It was found that the required MU to deliver 200cGy at 400 cm SSD for each beam of 6MeV electron with HDTSe$^-$ mode is 504 MU. The areas in which the TLDs received less prescription dose is treated as a underdose area and those areas of the patient skin is treated with normal electron mode with 100 cm SSD.

Conclusion: Six dual field dosimetry was performed using $CaSO_4$:Dy thermoluminescence powder in indigenously prepared wax phantom and it is satisfactory method for verification of Total Skin Electron Therapy.

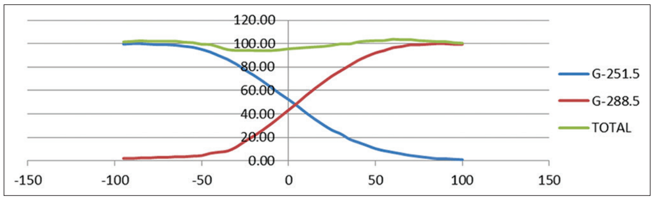

Graph 1: Vertical profile

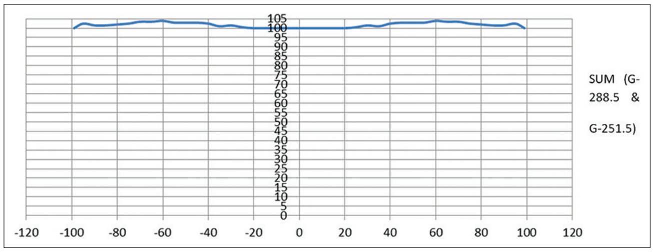

Graph 2: Horizontal profile

Acknowledgement: The author wish to acknowledge Department of Radiological Physics, SMS Medical College and Hospital, Jaipur for their valuable suppot.

P-71

DOSIMETRIC COMPARISON OF EPID AND OCTAVIUS ARRAY FOR VOLUMETRIC MODULATED ARC THERAPY AND QA OF VMAT

Felix M. S. Vijayan

Department of medical Physics, Anna University, College of Engineering, Chennai, Tamil Nadu, India.
E-mail: vidhya5795@gmail.com

Aim: The main aim of this study was to assess the reliability of VMAT delivery and compare the dosimetric technique of the portal dosimetry system and Octavius 4D phantom dosimetry for patient specific QA.

Materials and Methods: Dosimetric study has been performed by using the clinac iX, which is operated in the range of 6 MV. For the Patient specific QA, we have selected 7 patients and planned in TPS. These plans recalculated on EPID and Octavius 4D. Thimble chamber 0.65CC was used for measuring high-energy photon and electron radiation in air/in phantom material and also PTW 2D-Array were used. To assess the reliability of VMAT delivery, the accuracy of parameters such as variable dose rate, variable gantry speed, and dynamic MLC during gantry rotation were assessed using EPID.

Result and Discussion: For the comparison of these two dosimetric equipment's used the gamma analysis for the portal dosimetry system, and we found on an average value 98.4% of the pixels passed the criteria of 3%, 3 mm gamma with a standard deviation of 0.82 and with the 4D Octavius system, on an average value 99.37% of the pixels passed the criteria of 3%, 3 mm gamma with a standard deviation of 0.62 for rapid arc and the result shows that, both the systems can be used for patient specific QA measurements for rapid arc. The current study shows that the patient specific QA for VMAT, no significant differences were observed in the rapid arc gamma results of portal dosimetry as well as in the Octavius array system.

Conclusion: We conclude that the QA can also be carried out by EPID and 2D array for the routine patient specific QA in VMAT Radiotherapy.

P-72

MEASUREMENT OF SMALL IRRADIATION RELATIVE DOSE WITH VARIOUS DETECTORS FOR 6 MV PHOTON FROM CLINICAL LINAC

Santunu Purohit, S. M. Enamul Kabir[1], Md. Shakilur Rahman[2], Md. Kawchar Ahmed Patwary[3], A. K. M. Moinul Haque Meaze, Debasish Paul[2]

Department of Physics, University of Chittagong, Chittagong, [1]Department of Radiotherapy, North East Medical College Hospital, Sylhet, [2]Secondary Standard Dosimetry Laboratory, Bangladesh Atomic Energy Commission, Dhaka, [3]Department of Physics, Comilla University, Comilla, Bangladesh.
E-mail: shakilurssdl@baec.gov.bd

Now a days, modern radiotherapy techniques such as IMRT, IGRT, SRT/SRS etc where proper commissioning of Clinac is challenging due to absence of protocol in dosimetry of small field (where Bragg gray cavity theory actually does not exist). Relative dose of small fields were measured using Cross Calibration Factor (CCF) method and Daisy Chaining Output Factor (DCOF) method using different IBA Chambers. The absolute dose at 10 cm × 10 cm was measured with CC13 (ionization) chamber by IAEA protocol TRS-398. Afterward CC13 chamber was cross calibrated with CC01 (Ionization) and Razor (diode) chamber respectively for the measurement of dose in small fields. According Daisy Chaining factor method, CC13 (ionization) to Razor (diode) dose was also measured. The reference dose of small field was measured using CC13 (ionization) chamber applying newly proposed formalism (R. Alfonso *et al*. 2008). By introducing cross calibration and Daisy Chaining factor method, it was experimentally found that dose measured with Daisy Chaining factor method technically more suitable and closer result with small field reference dose. During cross calibration factor technique, the dose variation was measured in between CC01 (ionization) and Razor (diode) chambers which found to be close to 4% at field size close to 1 cm × 1 cm, 100 cm SSD and 10 cm depth. The correction factors of Razor chamber for small fields (less than reference size) were measured using CC13 (ionization) chamber. Uncertainties arises in this work both Type-A and Type-B were considered. Finally, combined standard uncertainty was measured 1.51% (1σ). Experimentally it was found that Diode dosimetry is suitable for small field dosimetry for measuring escalated low energy dose in penumbra region. Dosimetry of small field due to source occlusion effect, dose at the centre of field is falling down. In our recent work, it was experimentally found that special attention is needed when field size is close to 1 cm × 1 cm field. Because in 1 cm × 1 cm field, proper positioning of small volume ionization chamber is a challenging task. Most of uncertainties were introducing in dosimetry actually from calibration certificate and beam quality correction factor.

P-73

DOSIMETRIC STUDIES OF MIXED ENERGY (6 AND 10MV) OF FF AND FFF PHOTON BEAM ON RAPID ARC RADIOTHERAPY PLANNING OF CARCINOMA OF CERVIX

U. G. Ramanjaneyulu, G. Sri Krishna
MNJ Institute of Oncology and Regional Cancer Centre, Hyderabad, Telangana, India.
E-mail: ugraman9 @gmail.com

The objective of this study was to compare the dosimetric influence of filtered and flattening filter free beam of mixing 6MV and 10MV energy photon beam on the quality of Rapid Arc radiotherapy (RA) plans for patients with Cervical cancer. For this study, plans were created for all patients following Radiation Therapy Oncology Group (RTOG) guidelines. The prescribed dose (PD) of 50Gy in 25 fractions was given. The plan having coverage of 95% of PTV receiving 95% of prescribed dose was accepted. The plans were compared on the basis of planning target volume (PTV) coverage (dose to 2%, 98% of target), Constraints of OAR (Organs at Risk) were volume of 40% <40 Gy for normal bladder and rectum. Apart from this, homogeneity indexes (HI), conformity index (CI), total number of monitor units (MUs) and integral dose to normal tissue (NTID) were calculated to analyze plan quality. The present study reveals that the quality of plan is better for FF beam over the FFF beam in case of Cervical Cancer. Only treatment time decreases in case of FFF beam because of high dose rate.

P-74

RADIOTHERAPY FOR CARCINOMA OF BILATERAL BREAST

Kirti Tyagi, Sachin Taneja, Deboleena Mukherjee, Arti Sarin[1]
Radiation Oncology Centre, INHS Asvini, [1]Nuclear medicine Department, INHS Asvini, Mumbai, Maharashtra, India. E-mail: callkirti@yahoo.com

Objective: Breast cancer is the most common malignancy amongst females in the world, including Indian females. Cancer in both breasts is an uncommon presentation. Incidence of bilateral breast cancer (BBC) has been reported in the range of 1.4–11.8% with the majority being metachronous cancer. In this study we are discussing the effect of post operative radiotherapy in a patient presented at our centre with synchronous bilateral breast cancer.
Materials and Methods: Treatment in patients with BBC is similar to that in patients with unilateral breast cancer wherein adjuvant radiotherapy (RT) forms an integral part of the breast conservation algorithm. Adjuvant RT for breast cancer typically includes whole breast irradiation after lumpectomy or chest wall irradiation after mastectomy with or without regional nodal irradiation. This is accomplished using conventional bi -tangential portals that include part of the anterior chest wall adjacent to the RT target [4-6]. RT delivery in cases of SBBC is even more complex owing to multiple field junctions, which results in heterogeneous dose distributions as well as significantly higher irradiation volume of organs at risk (OARs) such as the lungs and heart. A 63 yrs female with carcinoma breast (right and left) was evaluated for receiving external beam therapy. She had been managed with 2 cycles of neoadjuvant chemotherapy followed by bilateral modified radical mastectomy. Histopathology confirmed infiltrating lobular carcinoma ypT2N1 on left side and ypT3N2 on right. After completion of another 2 cycles of planned adjuvant chemotherapy, she was planned for sandwich radiotherapy in view of large volume disease with close posterior margins. The radiotherapy was planned with medial and lateral tangential fields and supraclavicular field with the help of CT markers applied manually. A dose of 50Gy/25# (in 2Gy daily fractions) using 6 MV linear accelerator was prescribed as post mastectomy. During the course of radiation treatment the patient was taken up for clinical evaluation, verification of patient position on treatment couch and port film checks of the treatment field.
Conventional Planning: Conventional plans were made for each side respecting principles of conventional bi-tangential treatment planning consisting of two opposed tangential beams of 6-MV energies for unilateral breast RT with at least 0.7 to 1.0-cm gap between medial tangential portals of both sides. All plans were made on the treatment planning system ONCENTRA™ (M/s Elekta) for treatment on a Siemens Primus Hi Linear accelerator. The heart was spared by using multi leaf collimators (MLCs) whenever possible without compromising target volume coverage. Bolus was not used for any chest wall planning. The plan of each side was summated and the sum plans were evaluated respecting the International Committee on Radiation Units and Measurements (ICRU) criteria and disregarding contours.
Results and Discussion: The radiotherapy planning in this case was highly demanding due to huge target volumes and bilateral involvement of lungs and heart. In the study for our patient an arm support was used and no breast immobilisation system was used. The combined lung volume receiving 20 Gy was 3.28%. A dose of 2.87 Gy was in total delivered to 33% of the heart. Radiotherapy treatment was completed in time. Apart from mild acute skin reactions, no significant acute radiotherapy side effects were observed.
Conclusion: More numbers of patients with long term follow up is required to give a conclusion about radiotherapy treatment in post operative radiotherapy patients of bilateral breast carcinoma.

P-75

VOLUMETRIC INTENSITY-MODULATED ARC THERAPY VS. CONVENTIONAL INTENSITY-MODULATED RADIATION THERAPY IN LUNG CANCER: A DOSIMETRIC STUDY

Gangarapu Sri Krishna[1,2], Vuppu Srinivas[1], Palreddy Yadagiri Reddy[2]
[1]MNJ Institute of Oncology and Regional Cancer Centre, [2]Department of Physics, Osmania University, Hyderabad, Telangana, India. E-mail: gsrikrishna7@gmail.com

Dosimetric comparisons between Rapid Arc (RA) and conventional Intensity-Modulated Radiation Therapy (IMRT) techniques for left sided lung cancer were performed to address differences in dose coverage of the target, sparing of organs-at-risk (OARs), delivery of monitor units (MUs) and time, to assess whether the RA technique was more beneficial for treatment of lung cancer. 15 lung cases were taken for the study. Originally all plans were created using AAA algorithm (AAA) and the patients were treated using Intensity Modulated Radiotherapy (IMRT). Again all 15 cases were re-planned using RA technique. The evaluated plan parameters were PTV coverage at dose at 95% volume (TV95) of PTV (D95), the dose at 5% of PTV (D5), dose maximum (Dmax), the mean dose (Dmean), the percent volume receiving 5Gy (V5), 20Gy (V20), 30Gy (V30) of normal lung at risk (Left Lung-GTV), the dose at 33% volume (D33), at 67% volume (D67) and the mean dose (Gy) of Heart, the dose maximum (Dmax) of spinal cord. Also, Homogeneity index (HI), Conformity index (CI) and integral dose to normal tissue (NTID) were evaluated to check the quality of the plans. The advantages and disadvantages of RA over IMRT were presented in this paper.

P-76

COMPARATIVE STUDY OF DOSE DISTRIBUTION IN 3D CONFORMAL AND SIMULATED 2D PLAN OF LUNG CARCINOMA

Adhikari Matrika Prasad, M. Thapa[1], P.P. Chaurasia, C. S. Shrestha

B.P. Koirala Memorial Cancer Hospital, [1]Birendra Multiple College, Bharatpur, Nepal.

E-mail: adhikarimp10@gmail.com

Background: In this modern era, Radiation therapy is adopting newer and newer technology. In our center we have started 3DCRT in 2007. Undoubtably 3DCRT would be better choice of treatment than 2D system. We have tried to find the dose variation in 2D and 3DCRT plans and evaluate the plans with conformity index and heterogeneity index.

Objective: To compare the 3DCRT and simulated 2D plan and evaluate them by studying the dose conformity and dose heterogeneity between these plans.

Materials and Methods: This is a hospital based retrospective study.25 patients with lungs carcinoma were taken for this study. Eclipse treatment planning system is used to create both 3D and 2D plans. Both plans were prepared on the same patient body. The acceptable plans were optimized and compared for dose distribution. The conformity index and homogeneity index were calculated using the following relations from ICRU guidelines.

Results and Conclusion: The Conformity Index (CI) for 3D plan varies from 0.90 to 0.99 which indicates the less variation and hence better coverage of PTV while for 2D plan it varies from 0.56 to 0.99 indicates the poor coverage in many cases. The Heterogeneity Index (HI) value for 3D plans varies from 0.095 to 0.26 indicating less heterogeneity and hence less hot and cold spot, while in 2D plans it varies from 0.080 to 0.46, with indication of poor coverage and more hot and cold spots.

P-77

SIMPLE METHOD TO CORRECT FOR PITCH IN A NON 6D COUCH FOR A FRAMELESS STEREOTACTIC TREATMENTS

V. K. Sathiya Narayanan, Amit A. Nirhali, Pooja V. Moundekar, Mithun Sajeev, Surendra Pawar

Department of Radiation Oncology, Ruby Hall Clinic, Pune, Maharashtra, India.

E-mail: vsathiya7@rediffmail.com

Introduction: Stereotactic treatments has been in vogue for more than 3 decades and efforts were always made to reduce the errors in delivery by introducing a good number of quality assurance methods. The introduction of volumetric imaging before treatment delivery facilitated frameless stereotactic treatments. But, correcting for rotational errors required 6D couch. However, there are publications which show that 6D couch is an expensive technology and it is one among the many factors that contribute to the accuracy and its absence is not a major factor. In our setup, we have been performing stereotactic treatments with couches which has only translational movements. After introducing volumetric imaging and performing frameless stereotactic treatments, we found that rotational errors also need to be addressed. Out of the three rotational errors such as pitch, yaw and roll, we found that pitch is a rotational correction which is a dominant systemic error, has a significant role and it is addressed in our work.

Aim: The aim of this communication is to describe a simple method to address pitch rotation in non 6D couch and hence make the frameless stereotactic treatments of very high accuracy.

Materials and Methods: Siemens Oncor impression Plus machine which has the unflat beam and a Moduleaf tertiary mMLC is used for delivering stereotactic treatments. However, once, the tertiary mMLC leaf which has the leaf width of 2.5 mm is mounted, the size of the volumetric imaging becomes limited to a diameter of 10 cm with a length of 10 cm, which is not sufficient. Hence, we proposed a method of not mounting the Moduleaf, performing Carbon target based MV volumetric imaging, marking the laser centres then rotating the couch using column rotation and then mounting the Moduleaf for treatment delivery. The different sagging properties of CT couch and treatment couch introduces a systematic error of pitch. To quantify the tilt, we use a digital inclinometer which has a resolution of 0.1°. We use Somatom 6, which is a 6 slice CT for acquiring planning CT images. When the patient is with the localiser box on CTcouch, we find the inclination and it is usually between 0.4° to 0.5°, depending on the patient's weight. After the plan, when the patient is positioned for treatment, before the volumetric imaging is acquired, the pitch (tilt) is introduced. The Siemens couch Tx550 is used and the couch mount for stereotactic treatments, has the provision to control the pitch which is done using the tilt knob. We introduce the same tilt (0.4° or 0.5°) by using the digital inclinometer. By this method the pitch rotation is completely eliminated.

Resuts: We have so far implemented the idea of measuring the sag in CT couch with the digital inclinometer and introducing the same sag on the treatment table. The couch mount has this facility for introducing the tilt and the simple digital inclinometer with the resolution of 0.1° helps in introducing the same tilt just before imaging and this helps in eliminating the pitch.

Discussion: By preparing the double layered masks, it is easier to reduce the roll and yaw to the minimum. However, the systemic component of the pitch is due to the different couch sagging levels and pertains to the two couches that are involved in this situation. By using 3 linear and one rotational or angular correction, the delivery accuracy of the treatment can be brought to very high levels. The pitch can also occur due to the improper reproducibility of the patient inside the mask. However, this can be eliminated by taking special care while preparing the double layer mask.

P-78

ESTIMATION OF CUMULATIVE SURFACE DOSE WITH FFF BEAMS FROM LINEAR ACCELERATOR & TOMOTHERAPY FOR SBRT OF CA_PROSTATE: A PHANTOM STUDY

Lilawati Meena, R. A. Kinhikar, Priyadarshini Sahoo, C. M. Tambe, D. D. Deshpande

Department of Medical Physics, Tata Memorial Hospital, Mumbai, Maharashtra, India.
E-mail: meena.lk91@gmail.com

Introduction: Flattening filter free (FFF) beams are widely used for the treatment of lung, liver and prostate sites i.e. in Stereotactic Body Radiotherapy (SBRT) techniques. These treatments may be delivered either with linear accelerator or tomotherapy or other modalities like Cyberknife. High dose per fraction (≥7Gy) is delivered to the isocentre of PTV. So, it is important to know the dose received at the surface of patient using Rapidarc technique in Truebeam and rotational IMRT in Tomotherapy.
Objectives: To estimate the cumulative surface dose variation between 6X FFF energies of two different modalities i.e. Varian Truebeam and Accuray Hi-Art Tomotherapy. Also, variation between two energies i.e. 6X FFF and 10X FFF of Varian Truebeam using Rapidarc technique.
Materials and Methods: TLD-100 (LiF:Mg, Ti) was used for the measurements with Varian Truebeam linear accelerator and Accuray Hi-Art Tomotherapy. Five patients who have been already treated with Ca_prostate were selected for this study. Body phantom of dimension 30X90X20 cm^3 was assembled using different slabs of different dimensions. Phantom verification plans were created from the final approved plans. Then, those plans were made to run on the phantom created by various slabs. The total dose of 7Gy was delivered at the isocentre. In 10X FFF plans, two arcs were used one running in clockwise and the other one running in anti-clockwise direction from 179^0-181^0 and collimator angles used were 30^0, 330^0 . The tomo plans were made using field width of 2.5 cm, modulation factor of 2.5 or 2 and pitch of 0.3. TLD's were read with Rexon reader after 24 hours of exposure and readings at different distances were recorded. Calibration of TLD was also done using Elite-80 cobalt machine. TLD's were placed at isocentre and laterally on both sides at 7.5 cm distance from isocentre, and at depth of 5 cm and 10 cm on left and right side.
Results: Mean surface dose delivered with 6X FFF energy from Truebeam was 11.33% ± 3.43 of the prescribed dose of 7 Gy in single fraction whereas the surface dose delivered by Tomotherapy was 10.89% ± 1.3 of the prescribed dose. Mean surface dose delivered with 10X FFF energy of Truebeam was 9.48% ± 2.88.
Conclusion: Among two advance technologies delivering rotational IMRT with 6X FFF, there was no significant difference. Surface dose delivered by 6X FFF energy linear accelerator was slightly higher compared to Tomotherapy. Among two different beam energies of 6X FFF and 10X FFF, 10X FFF energy certainly showed reduction in surface dose by 2% compared to 6X FFF. But the deviation observed in the surface dose delivered by tomotherapy was less compared to Truebeam.

P-79

STEREOTACTIC BODY RADIOTHERAPY (SBRT) FOR METASTATIC SPINE TUMOURS USING HIGH INTENSITY FLATTENING FILTER FREE (FFF) PHOTON BEAMS - A PLANNING COMPARISON WITH FLATTENED PHOTON BEAM

T. Moorthi[1,2], K. Balaji[1], S. Balajisubramanian[1], P. Sumana[1], K. Sathiya[1], D. Khanna[2]

[1]Department of Radiation Oncology, Gleneagles Global Hospitals, Chennai, [2]Department of Physics, Karunya University, Coimbatore, Tamil Nadu, India.
E-mail: moorthiuts@yahoo.co.in

Introduction: V ertebral metastases are a common and progressive disease can result in pain, neurological disability and reduced quality of life. A recent development is the application of high precision stereotactic body radiotherapy (SBRT) for spinal metastases. Several reports indicate that durable improvement in pain control are possible with long-term local control by giving radiotherapy.
Objectives: To compare SBRT treatment for metastatic spine tumour using high intensity unflattened and flattened photon beams.
Materials and Methods: VMAT based SBRT treatment plans were generated for 10 metastatic lumbar spine patients using 6X-FFF, 10X-FFF and 6X-FF photons of TrueBeamSTx linear accelerator (Varian medical systems, USA), modeled in Eclipse Treatment Planning System (Version13.7). 8Gy in single fraction was delivered to the target volume using 1 full arc for 6X-FFF and 10X-FFF and 3 full arc for 6X-FF. Dose calculation was performed with Anisotropic Analytical Algorithm (AAA). All plans were normalized to 100% in target mean.
Comparison of plans generated has been established in terms of various dosimetric variables such as Quality Coverage for PTV (D95% in %), Conformality number (CN), Homogeneity Index (HI), Gradient Index (GI). Organs at Risk (OAR's) like kidneys, liver and small bowel mean doses were evaluated. Technical parameters of delivery such as total number of monitor units (MU) and Beam On time (BOT) were compared. ANOVA test was performed for statistical significance analysis.
Results and Discussion: The Mean ±SD value of Quality of Coverage D95% for 6X-FF, 6X-FFF and 10X-FFF were 94.60 ± 1.30, 93.52 ± 0.68 and 94.16 ± 0.99 % respectively ($p=0.07$). CN values for 6X-FF, 6X- FFF and 10X-FFF were 0.79 ± 0.04, 0.76 ± 0.03 and 0.80 ± 0.02 respectively ($p=0.005$). HI values for 6X-FF, 6X-FFF and 10X-FFF were 0.11 ± 0.02, 0.14 ± 0.02 and 0.12 ± 0.03 respectively ($p=0.02$). GI value for 6X-FF, 6X-FFF and 10X-FFF were 5.33 ± 0.64, 5.43 ± 0.45 and

4.97 ± 0.56 respectively (p=0.163). The Mean ± SD value of spinal cord (D2) for 6X-FF, 6X-FFF and 10X-FFF were 7.7 ± 0.16, 7.75 ± 0.04 and 7.71 ± 0.16 Gy respectively (p=0.783). The mean dose of small bowel for 6X-FF, 6X-FFF and 10X-FFF were 1.83 ± 0.67, 1.69 ± 0.59, 1.67 ± 0.56 Gy respectively (p=0.823). The mean dose of kidneys for 6X-FF, 6X-FFF and 10X-FFF were 1.51 ± 0.65, 1.49 ± 0.65, 1.26 ± 0.53 Gy respectively (p=0.600). The mean dose of liver for 6X-FF, 6X-FFF and 10X-FFF were 0.49 ± 0.52, 0.47 ± 0.50, 0.45 ± 0.50 Gy respectively (p=0.984). All normal organs shows comparable dose values in all plans. This study showed reduced MUs and BOT with improved treatment delivery for SBRT plan using 10X-FFF compared to 6X-FFF and 6X-FF. MU values (Mean ± SD) for 6X-FF, 6X-FFF and 10X-FFF were 1841.60 ± 178.77, 1881.90 ± 131.54 and 1768.00 ± 70.28 MU respectively (p=0.772). BOT values (Mean ± SD) for 6X-FF, 6X-FFF and 10X-FFF were 3.75 ± 0.0, 1.32 ± 0.05 and 1.25 ± 0.0 min respectively (p=0.00001).

The investigation of dosimetric performance and treatment delivery efficiency suggests that 10X-FFF Planning is promised for SBRT in the treatment of metastatic spinal column. Total beam on time is substantially reduced, because of reduced MUs and single arc with increased dose rate delivery with respect to 6X-FF and 6X-FFF. This gain in BOT with 10X-FFF mode adds patient's convenience.

P-80

NATIONAL UNIVERSITY HOSPITAL OF SINGAPORE EXPERIENCE: INTENSITY MODULATED RADIOTHERAPY COMMISSIONING BASED ON TASK GROUP 119, A REPORT FROM AAPM

Y. F. Leong, S. P. Bargarley

Radiation Therapy Centre, National University Cancer Institute, Singapore. E-mail: yuh_fun_leong@nuhs.edusg

Introduction: 3D conformal was the standard of care for radiotherapy before intensity modulated radiotherapy (IMRT) started in the late 1990s. Since then, usage of IMRT has been growing rapidly. IMRT involves an inverse planning approach with complex MLC movement and multiple gantry angles. In 2008, the Radiological Physics Center (RPC) irradiated 250 head and neck phantoms and found that 28% failed to meet either 7% dose accuracy in low gradient region or 4 mm DTA in high gradient, or both. This experience suggested that many clinics did not commission their IMRT system adequately. In 2009, Task Group 119 (TG-119) of AAPM produced a set of quantitative confidence limits as baseline expectation values for IMRT commissioning. These confidence limits (CL) were based on collective data from 9 facilities that had passed the RPC credentialing tests for IMRT. Any facility that wants to use these benchmarks should perform the planning, measurement and analysis as suggested by TG-119.

Objective: NUH evaluated its overall IMRT system performance based on the TG-119 guidelines and compared the results to the TG-119 benchmarks.

Materials and Methods: Scans were conducted on 20 cm solid water phantoms with 0.125 cm^3 Semiflex^{TM} ionization chamber inserted in the middle. 6 planning cases (multi-target, mock prostate, mock head, mock neck, C-shape easy and C-shape hard) were created using the recommended plan goals and beam arrangements to ensure that the beam modulation produced is similar to the benchmark plans. 2 preliminary tests (AP:PA 10 x 10 open fields and AP:PA five bands 3 cm wide) were planned, delivered and measured to demonstrate the reliability of the assessment system of non-IMRT dose delivery. Chamber measurements were done using 0.125 cm^3 Semiflex^{TM} ionization chamber and the agreement between planned and measured doses was determined at high and low dose region. Per-field measurements were measured with ArcCHECK (AC) cylindrical diode array phantom and measured fields were analysed using SNC Patient™ software.

Results: The benchmark confidence limits for chamber measurement at high and low dose region averaged over 9 institutions were 0.045 and 0.047 respectively. NUH achieved confidence limit of 0.040 for high dose and 0.024 for low dose. Benchmark confidence limit for per-field measurements was 7.0 and NUH achieved a confidence limit of 6.8.

Discussion: TG-119 commented that the confidence limits obtained by any facilities performing similar tests should be equal to or less than the confidence limits reported by TG-119. NUH met the benchmarks recommended by TG-119. Performing the TG-119 IMRT commissioning test and being able to meet the benchmarks gives NUH confidence in our IMRT delivery system. Institutions that are going to start new services in IMRT treatment or institutions that wish to evaluate their current IMRT system performance are recommended to perform this specific set of tests.

P-81

DESIGNING A NOVEL PHANTOM FOR DAILY QA OF CYBERKNIFE M6 ROBOTIC RADIOSURGERY SYSTEM

R. Holla, B. Pillai, D. Khanna[1]

Department of Medical Physics and Radiation Safety, Amrita Institute of Medical Science and Research Center, Kochi, Kerala, [1]Department of Physics, Karunya University, Coimbatore, Tamil Nadu, India.
E-mail: raghavendra.holla@gmail.com

Purpose: Performing daily QA on Cyberknife system includes routine linac output constancy and constancy check for energy. Placing the ionization chamber at 80 cm SAD as specified by the equipment supplier for Cyberknife system is difficult since the system is non isocentric. However, birdcage assembly, an assembly and detector mount for holding the ionization chamber at a fixed distance of 80 CM from the the radiation source can be used to monitor the output. But the measurement chamber is placed in air which is not suitable for 6MV photon beams. Hence a new phantom has been designed which can be fixed to birdcage assembly to monitor output and energy constancy in the medium (Polystyrene)

Methods: A polystyrene block of 5 cm thickness is designed to fit in the distal end of the birdcage and this block is drilled to accommodate 0.13cc (PTW, Germany) ion chamber at the dmax depth of 1.5 cm. The source to the chamber distance (SCD) is exactly 80 cm when the phantom is placed in the birdcage assembly. Two more polystyrene phantom blocks of 3.5 cm and 5 cm thickness are cut to fit inside the birdcage assembly. These 3 blocks gives us the measurements at depths of 1.5 cm, 5 cm and 10 cm. Primary calibration has been done in water. Standard readings in the polystyrene phantom are obtained by comparison with water measurements. Measurement at 1.5 cm depth corrected for temperature and pressure represents the output constancy of the Linac. The ratios of the readings 5 cm and 10 cm depths to 1.5 cm depth represent the constancy of beam quality.

Results: Daily measurements are performed with this phantom developed in-house.

Conclusion: Since the phantom is designed to fit inside the birdcage assembly, reproducibility of the setup is found to be very good therefore the readings will truly reflect the performance of the machine.

P-82

COMPARISON OF INHOMOGENEITY EFFECT FOR SMALL FIELD DOSIMETRY BETWEEN 6 MV FF AND FFF PHOTON BEAMS USING THE EGSNRC MONTE CARLO CODE

S. Sangeetha, C. S. Sureka[1]

Departments of Physics and [1]Medical Physics, Bharathiar University, Coimbatore, Tamil Nadu, India. E-mail: surekasekaran@buc.edu.in

Introduction: In recent years, a great deal of attempt has been carried out by the researchers on inhomogeneity effect in human body in the field of radiation therapy. Among these studies, accurate dose calculations of inhomogeneous organs such as lung; particularly for small field size has been considered to be the more challenging task in the field of radiation therapy.

Objectives: The objective of the present study is to analyze the inhomogeneity effect of lung region inside the inhomogeneous phantom for small field sizes of FF (Flattening Filter) and FFF (Flattening-Filter-Free) 6 MV photon beams using EGSnrc Monte Carlo user codes.

Materials and Methods: A 6 MV FF and FFF photon beams of a Varian Clinac 600C/D medical linear accelerator for small field dosimetry (0.5 x 0.5 cm^2 to 4 x 4 cm^2) were performed for homogeneous and inhomogeneous water phantom containing lung using EGSnrc Monte Carlo user codes (BEAMnrc and DOSXYZnrc) in order to calculate the dosimetric beam characteristics. The dimension of the water phantom was $30 \times 30 \times 30$ cm^3 with the voxels dimension of 0.5 x 0.5 x 0.5 cm^3 and the phase space source position was incident on the water surface at Z=0, so that the distance from the electron beam to the surface of the water phantom (SSD) is 100 cm. In all simulations, the charged particle and photon cut off energies were set as default to be 0.7 MeV and 0.01 MeV respectively and the water used with the density of 1g/cm^3 and 0.25 g/cm^3 is considered to resemble the material of soft-tissue and lung material in this present work.

Results and Discussion: The results were analysed in determining the inhomogeneity effect of lung region inside the inhomogeneous phantom for small field sizes of FF and FFF 6 MV photon beams using dosimetric beam parameters. The results obtained showed that the edges between inhomogeneity for all field sizes were evidently visible that the absorbed dose gets dramatically reduced in the lung region for FF beams while it gets minimally reduced for FFF beams with small discrepancies. It has been observed that the dose fall-off occurs in the edge between solid water and lung region and further, the dose gets increased in the edge of lung region and solid water for all field sizes. the dose reduction for FF beams inside the lung was found to be 50%, 44%, 23%, 15% and 10% for FF beams whereas for FFF beams, the dose reduction was 13%, 9%, 7%, 5% and 3% respectively for the smaller field sizes of 0.5 x 0.5 cm^2, 1 x 1 cm^2, 2 x 2 cm^2, 3 x 3 cm^2, and 4 x 4 cm^2. These dose fluctuations occur due to the variation in the density of the materials and due to the yield of secondary electrons. This study depicts that the FFF beams depicted minimal dose reduction in the lung dose region irrespective to the lung dose region in the FF beams for small field dosimetry and thus FFF beams are well suitable in delivering accurate dose calculations for inhomogeneity effect in small field sizes.

P-83

DOES HIGH DENSITY ARTIFACTS IMPACT STEREOTACTIC RADIOSURGERY OF POST ENDOVASCULAR EMBOLIZATION AVM? A DOSIMETRIC ANALYSIS

A. Jerrin[1,2], V. Ramasubramanian[2], A. Karuppusamy[3], A. Pichandi[1], A. Dinesh[1], P. S. Sridhar[1], N. Madhusudan[1], K. Roopesh[1]

[1]Cyberknife Center, HCG Enterprises Ltd., Bengaluru, Karnataka, [2]School of Advanced Sciences, VIT University, Vellore, Tamil Nadu, [3]Department of Radiation Oncology, Apex HCG Oncology Hospitals LLP, Mumbai, Maharashtra, India.
E-mail: jerryamal@gmail.com

Introduction: Cereberal Arteriovenous Malformation (AVM) is a tangle of abnormal and poorly formed blood vessel. This condition causes bleeding to surrounding brain and injure the surrounding brain which leads to headache, seizure, stroke or even death. Treatment of AVM relies on multimodality approach predominantly by surgery, stereotactic radiosurgery (SRS) and/or endovascular embolization depending on various condition like location, size, grade etc. Embolization can be used as curative procedure for smaller AVMs, however it is also used as adjuvant for surgery or Radiosurgery. Endovascular approach uses embolization agents such as n-butyl cyanoacrylate (n-BCA) called glue, Ethylene-vinyl alcohol copolymer (Onyx) etc. However post embolized AVMs possess challenges if treated further with radiosurgery due to high density of embolizing agents cause artifacts in CT images which affects the delineation of tumor. Also for small radiosurgical beam these artifacts affects plan quality due to missing tissue information. This study aims at analyzing the dosimetric inaccuracy caused by embolization agent for post embolization AVM radiosurgery treatment.

Objective: To analyze dosimetric impact of missing tissue information from CTdue to the presence of high density embolizing agents in the treatment of post embolization recurrent AVMs.

Materials and Methods: Two patients were presented with recurrent AVM post embolization. The planning CT images were taken with Siemens Biograph CT equipment. At 140 kVp, Hounsfield Unit (HU) of embolization agent oynx is found to be approx. 3059HU. Target and organ at risk delineation were carried out with assistance of MRI secondary images to overcome missing tissue information from CT images. Treatment planning was done with goal of achieving 16Gy to at least 95% Planning Target Volume in single session. In order to access the dose uncertainties caused by missing tissue information from CT, the plans made in original raw CT (RCT) were superimposed on HU enforced CT (HUeCT) imageswith enforced 40 HU to regions of of HU less than -60. Retrospectively, similar SRS plans with Dynamic Conformal Arc therapy (DCAT) and Volumatric Arc Therapy (VMAT) were made with Monaco® planning station for ElektaVersaHD with Apex Micro MLC unit. Treatment plans generated in CTs with and without HU corrections were compared and analyzed. Plan class verification measurements were also done for plans in CTs with and without HU corrections.

Results and Discussion: Dose distribution in two sets of CT images (RCT and HUeCT) were compared. Plan quality were quantified with respect to target coverage, maximum, minimum point dose and gradient scores. Out of three techniques used in this study, CK and VMAT plans on both CT sets varies by approx. 0.5% and DCAT plans varies by 2%. Radiosurgical plan quality evaluated with Gradient Index showed there werelittle changes in dose distribution isotropicallyfor all plan techniques, with VMAT plans having larger gradient up to 4 mm. Maximum dose to Organ at risks (OAR) closer to targetswere underestimatedin RCT and inversely for peripheral OARs.

Conclusion: Overall, all plans in both CT sets satisfy planning goals and there was no clinical significance found. Planning with high density artifact CT does not affect plan quality however care should be taken for OARs in close proximity with target. We suggest planners to set objectives with tight constraints much lower than allowed tolerances for OARs close to PTV.

P-84

ACCURACY OF POSITIONING ERRORS FOR PATIENT SET-UP ON SRS OR SBRT

Jinsook Ha[1,2], Taewon Kim[1], Mijin Jeon[1], Kwangwoo Park[2], Bo Young Choe[3], Tae Suk suh[3], Hong-Suk Jang[3]

[1]Department of Radiation Oncology, Gangnam Severance Hospital, [2]Department of Radiation oncology, College of Medicine, Yonsei University, [3]Department of Biomedical Engineering and Research Institute of Biomedical Engineering, The Catholic University of Korea, Seoul, Korea. E-mail: hjshjs83@gmail.com

Purpose: For stereotactic body radiation therapy (SBRT) or stereotactic radiosurgery (SRS), positional accuracy is crucial. We focused on isocentric positional error based on the several angles of gantry and treatment couch. The main purpose is to improve the accuracy of delivered dose for SBRT/SRS by applying offset corrections which are determined by Winston-Lutz test for each angles of gantry and couch.

Materials and Methods: Isocentric offset values are determined by rotating gantry angles (every 15 degree) for each couch angle (335, 15 degree). From the winston-Lutz test, offset values are obtained. As a preliminary study, we performed patient specific quality assurance (PQA) with and without isocentric corrections. For PQA, we measured point dose in high dose region and film image to analize gamma index. The phantom, StereoPhan (sun-nuclear) with A1SL ionization chamber (Exradin) is used. Gamma index analysis was performed using DoseLab Pro (sun-nuclear) with 3 mm/3% criteria.

Results: Based on the preliminary measurement, the accuracy of point dose was improved from -3.34% to -1.8%. Practical target volume is approximately 0.6cc which need a small field size where ionization chamber, A1SL usually measures underdose by volume averaging effect. Therefore, -1.8% is very accurate result. Gamma analysis showed also improvement after applying isocentric corrections. Gamma pass rates are 91% and 94% without and with corrections applied respectively.

Conclusion: We suggested the method which can be applied to actual treatment without work overloading. Isocentric corrections are determined before treatment using Winston-Lutz test, and applied to actual treatment. The result showed the improving accuracy of delivered dose.

P-85

DETECTOR ACCURACY COMPARISON FOR POINT DOSE MEASUREMENTS IN SMALL FIELDS

Silpa Ajay Kumar, Vipin M, Resmi K, Soumya N M

Department of Radiation Oncology, Malabar Cancer Centre, Thalassery, Kerala, India.
E-mail: shilpa.ajith@gmail.com

Introduction: The present aim in radiation therapy is to ensure that the uncertainty in the dose received by a patient does not exceed 5%. Considering all sources of uncertainty, this means that the dose at the calibration point of a Linear Accelerator has to be known to be within 2%. Commonly, a field size of less than 4×4 cm^2 is considered other than the conventional treatment field size that needs special attention both in dose measurements and in dose calculations. Small field dosimetry plays an important role in modem radiotherapy for many reasons. For fields this small, the physics of how the radiation is delivered is different from that of large fields and some traditional forms of dosimetry begin to fail. As such, it is imperative that accurate treatment planning and QA can be performed to ensure that these very small fields are being used safely and effectively.

Aim: To find out the suitable detector for point dose measurements in small fields.

Objective: The definition of a small field in radiation dosimetry is currently very subjective. A “small field” is generally defined as a field with dimensions smaller than the lateral range of the electrons that contribute to dose. Small fields are increasingly used in modern radiotherapy especially in volumetric modulated arc therapy and stereotactic radiosurgery treatments. In this study suitability of detector for small field dosimetry is checked.

Materials and Methods: Small field size plans were created in the water phantom in Eclipse treatment planning system version 10.0 at a specified depth (10 cm), These plans were delivered in a water phantom and point doses were measured with different detectors. Measured point doses were compared with point doses obtained from the treatment planning system. Then the detector efficiency is validated using IMRT plans.

All measurements were performed in a Varian Clinac iX linear accelerator equipped with a millennium 120 leaf collimator (Varian oncology systems, Palo Alto, CA) and the results will be cross compared with Eclipse treatment planning system version 10.0.

Results and Discussion: comparison of point dose calculated from the Eclipse Treatment planning system version 10.0 and measured point dose from the four commercial detectors available in our center using Radiation Field Analyzer (RFA) semi flex ionization chamber shows a variation of 6% while for pinpoint ionization chamber and diode detector an average percentage of variation of 2% and 1.5% respectively. A minimum variation of 1% observed with measurement using diamond detector.

Conclusion: Verification of the small field intensity modulated radiation therapy plans for exploring the efficiency of the different types of detectors available in our center concludes, microdiamond detector and diode detector are the excellent choice for small field dosimetry. Microdiamond detector and diode detector shows average percentage of variation less than 1% and 1.5% respectively.

P-86

POSITIONAL ERRORS IN LINEAR ACCELERATOR BASED FRAMELESS CRANIAL STEREOTAXY: A NOTE OF CAUTION

A. Manikandan[1,2], C. S. Sureka[1], S. Biplab[3]

[1]Department of Medical Physics, Bharathiar University, Coimbatore, Tamil Nadu, [2]Department of Radiation Oncology, Nagarjuna Hospital, Vijayawada, Andhra Pradesh, [3]Department of Radiation Oncology, Fortis Hospital, New Delhi, India.

E-mail:amanikandan720@yahoo.com

Introduction: Frameless stereotaxy (SRS/SRT) for cranial tumors has achieved considerable popularity because of its convenience over the invasive frame. BrainLab (BrainLab AG, Feldkirchen, Germany) is a major stereotactic solution provider worldwide which is compatible with both Varian (Varian medical system, Palo Alto, CA) and Elekta (Elekta AB, Stockholm, Sweden) linear accelerators. Frameless stereotactic therapy delivery uses a head and neck extension as a base plate. This base plate is an extension to main couch and attached at the cranial end using two clips as shown in Figure 1. With this arrangement, much of the patient's body lies on the main table while the head (with head rest) lies on the extended attachment. Main table and head neck extension are loosely attached to each other and act as a lever of class 1, hence exhibit a depression in the cranial end. This effect is observable in both Varian and Elekta make couches. When the patient lies on the couch, the cranial end of the couch tends to go down due to gravity. This introduces an unacceptably high rotational error about the X (lateral) axis (pitch) and translational error along Z (vertical) axis depending on the position of the tumor.

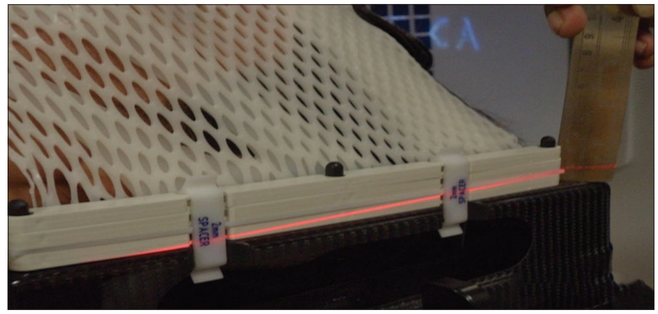

Figure 1: The laser shift due to cranial sagging attributed to the fulcrum effect in brainlab steriotactic baseplate. The laser shift noted in this particular case was 8 mm for frameless steriotactic cases

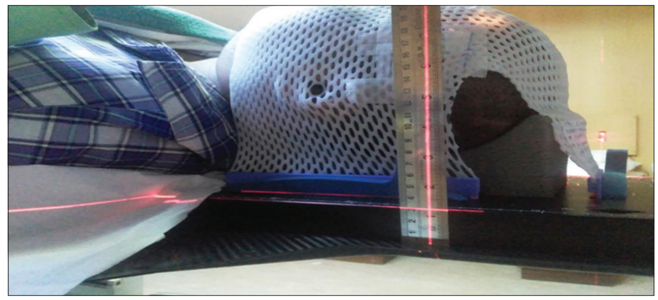

Figure 2: No cranial sagging when normal base plate was used

Objective: Objective of this work is to find out the need of 6D couch in stereotactic treatment delivery unlike the conventional couches, having only translational movements.

Materials and Methods: In this study we have included the regular brain tumor patients who were treated with all-in-one (AIO) base plate firmly adhered to the main table as shown in Figure 2. We assessed the cranial end sagging for regular cases and stereotactic cases for 90 patients by calculating the positional shifts in the three translational directions and the rotational shifts about the three axes.

Results and Discussion: We found that the mean± standard deviations (SD) for the vertical shifts (Delta Z) were - 0.11 ± 0.18 cm and 0.0 ± 0.48 cm for regular and SRS cases respectively and the mean± SD for the rotational shifts around x-axis (pitch) were 0.33 ± 0.77° and 0.41 ± 1.63° for the regular and SRS cases respectively. However, the SDs for the other translational and rotational axes were comparable between regular and SRS cases. For example, roll mean± SD for lateral (Delta X) shift for regular and SRS cases were -0.01 ± 0.19 cm and 0.08 ± 0.1 cm, respectively; mean± SD for craniocaudal (DeltaY) shift for regular and SRS cases were 0.16 ± 0.21 cm and 0.05 ± 0.17 cm, respectively; mean ± SD of rotational shifts about Y-axis (roll) for regular and SRS cases were - 0.32 ± 1.32° and 0.39 ± 1.05°, whereas that about Z axis (yaw) for regular and SRS cases were - 0.16 ± 1.34° and -0.17 ± 1.17°, respectively. Therefore, we conclude that SRS/SRT patients exhibit a higher positional error in terms of SD in vertical direction and in rotational pitch than that of regular cranial cases due to the use of cranial extension. Higher SD yields a higher setup margin. In the absence of a robotic couch that can account for rotational shifts in addition to the translational shifts, the residual rotational errors can result in unacceptably high error in spatial dose delivery.

P-87

MEASUREMENT OF DOSE IN 6MV AND 10MV FF AND FFF PHOTON BEAMS FOR SMALLER FIELD SIZE

M. A. Elan, L. Bharanidharan, Prakasarao Aruna, J. Velmurugan, P. Thamilkumar[1], R. R. Rai[1], Singaravelu Ganesan

[1]Department of Medical Physics, Anna University, [2]Department of Radiotherapy, Dr. Rai Memorial Cancer Institute, Chennai, Tamil Nadu, India.
E-mail: jeevanadhi007@gmail.com

Introduction: Small field dosimetry is a difficult task and no consistent data is available for modern radiotherapy techniques. Lateral electronic disequilibrium is an important factor and due to steep dose gradient, there is a high complication of radiation dosimetry for smaller field size. Modern technology in radiotherapy poses high level of uncertainties in small field dosimetry. The size of the detectors plays a vital role for the measurement of small field dosimetry.
Objective: The current study estimates the dose using various detectors like ionization chamber, diode and MOSFET detector as a function of field size.
The parameters like percentage depth dose, beam flatness, symmetry and penumbral width are evaluated for three detectors. Various small field sizes like 1 cm × 1 cm, 2 cm × 2 cm, 3 cm × 3 cm, 4 cm × 4 cm, 5 cm × 5 cm are evaluated for various detectors. The goal of our study is to evaluate the response of three active detectors exposed to 6MV X-ray beams.
Materials and Methods: The Linear Accelerator True Beam with long stand which was calibrated to deliver a dose of 1cGy per MU at 10 cm depth of water, a reference field size of 10 cm × 10 cm and a source to surface distance 100 cm for 6 MV and 10 MV respectively and the detectors used for the measurement were ionization chamber, diode and MOSFET. The phantom used for the study is 30 cm × 30 cm PMMA phantom.
Results and Discussion: Doses were measured using Ionization chamber, Diode detector and MOSFET detector for 6 and 10 MV photon beam with both FF and FFF as a function of field size viz, 1 cm×1 cm, 2 cm × 2 cm, 3 cm × 3 cm, 4 cm × 4 cm, 5 cm × 5 cm are evaluated and measured reading shows that the dose absorbed for 6 and 10 MV photon beam with FF is higher than FFF which may due to higher scatter dose caused due to the flattening filter. The response of the ionization chamber and diode detector is linear. MOSFET over estimates the dose and there was no significant difference.
Conclusion: Our study shows that the dose absorbed in ionization chamber and diode detector were consistent than MOSFET and also from our study it is concluded for FF beams the dose measured were higher than FFF due to high scatter.

P-88

A COMPARISON OF TWO DIFFERENT TREATMENT PLANNING SYSTEMS IN THE PLANNING OF STEREOTACTIC RADIOSURGERY OF SCHWANNOMAS USING UNFLAT BEAMS

S. Karthikeyan, Harikrishna Etti[1], S. Maruthu Pandian

Department of Radiation Oncology, BGS Global Hospitals, Bengaluru, Karnataka, [1]Department of Medical Physics, Bharathiyar University, Coimbatore, Tamil Nadu, India. E-mail: karthikeyanskk@yahoo.co.in

Objective: Currently the use of flattening filter-free (FFF) beams or unflat beams operating at higher dose rates which are available on an increasing number of commercial linear accelerators can lead to increased efficiency of treatment delivery especially for the treatment of stereotactic radiosurgery (SRS). There is a need for an assessment of the available treatment planning systems (TPS) in a single institution. This study compares the dose distributions of complex Intensity Modulated Radio Surgery (IMRS) plans produced by two TPSs: Varian Eclipse and Brainlab Iplan.
Materials and Methods: The Study was performed on Varian Eclipse (version 13.7) and Brain lab Iplan (version 4.5.3) which allows planning for 6 MV FFF beams for delivery on Truebeam STx linear accelerator. The two systems were commissioned with the same beam data and, as best as possible, matched configuration settings. IMRS treatment plans for twenty four schwannomas patients were produced on each system with pencil beam convolution (PBC) algorithm in Brain lab Iplan and Anisotropic Analytical Algorithm (AAA) in Varian Eclipse TPSs. All 48 plans were subjected to identical dose constraints, both for the target coverage and organ at risk (OAR) sparing, with a consistent order of priority. All plans were generated with non-coplanar beam geometry in both TPS.
Results and Discussion: Few statistically significant differences were found between the target coverage and OAR sparing of each system, with all optimizers managing to produce plans within clinical tolerances (D2 < 107% of prescribed dose, D5 < 105%, D95 > 95%, D99 > 90%, and OAR maximum doses) despite strict constraints and overlapping structures.
Conclusion: The study compared the plans produced by two TPSs — Eclipse and Brainlab Iplan — for the treatment of schwannomas with non-coplanar beam arrangement using unflat beams. Few statistically significant differences were found, but AAA Eclipse TPS generally gave lower OAR doses, with an integral dose outside the target 26% lower than PBC Brainlab Iplan TPS on average across all patients.

P-89

COMMISSIONING OF RAYSTATION TREATMENT PLANNING SYSTEM

B. Surendra

Department of Radiation Oncology, B P Koirala Memorial Cancer Hospital Yagyapuri, Bharatpur-7, Chitwan, Nepal.
E-mail: surendrachanda@yahoo.com

Introduction: The aim of this work is commissioning a collapsed cone (CC) convolution dose calculation algorithm for photons beam for clinical practice by modeling in RaySta-tion (RaySearch Laboratories) treatment planning system.
Materials and Methods: PDDs, profiles, output factors and beam calibration, for beam modeling were measured in a water tank. Pinpoint and semiflex ionization chambers were used for beam scanning and output factor measurement for field size 64 cm x 4 cm and >5 cm x 5 cm, respectively.

Farmer IC was used for reference dosimetry. The collected beam data were modeled in RayPhysics TPS module. The agreement of measured and computed beam were evaluated by using RMS difference and flat gamma analysis. Dose calculation algorithm validation has been performed in two steps: firstly, point dose measurements have been compared with calculated ones under reference and non-reference condition. Secondly, a fluence map comparison has been performed. Simple RT plans in water, and phantom as well as seven clinical VMAT plans for prostate, oesophagus, lungs, glioma and oropharynx were computed and measured by means of a PTW Octavius 729 ionization chambers matrix. VeriSoft software was used for gamma analysis. As additional valida-tion, CC dose calculation algorithm has been compared with Eclipse AAA. The DVH and gamma of dosemaps for both algorithms were also evaluated.

Results: Computed PDDs and profiles were found in good agreement with measured ones. The max RMS difference was (10.0 0.4) % in build up region and (7.0 2.5) % in penum-bra region. For FS 6 4 cmx4 cm but both were in tolerance. The gamma analysis of all PDDs and profiles was acceptable. In point dose verification, the measured and calculated point dose differences were found within 1%. In clinical RT plans, the gamma pass rate was above 92%. The gamma, 3%G/3 mm, of VMAT of prostate, and glioma were found 100% and decreased with more complex VMATs like oesophagus (95.7%) and orophar-ynx (92.4%). PTVs and OARs DHVs comparison results of two algorithms were found satisfactory. Maximum dose difference is less than 3%.

Conclusions: The results of validation test for beam model and collapsed cone convolu-tion dose calculation algorithm allowed to conclude that the commissioned CCC can be use for clinical practice.

P-90

ANALYSIS OF BEAM PROFILES, PERCENT DEPTH DOSE AND VOLUME EFFECT IN SMALL FIELDS USING DIFFERENT TYPE OF IN HOUSE AVAILABLE IONIZATION CHAMBERS

Ramandeep Singh, Pardeep Sharma, Shakhar Dwivedi, M. K. Mahajan

Department of Radiotherapy, Advance Cancer Institute, BFUHS, Faridkot, Punjab, India.
E-mail: mahi_dr@icloud.com

Introduction: With the advancement in technology in modern radiotherapy, small field dosimetry of photon beam has become the topic of interest. Specialized radiation treatments such as beamlet-based intensity-modulated radiation therapy (IMRT), image-guided radiation Therapy (IGRT), tomo-therapy, stereotactic radiosurgery (SRS) with high-resolution multileaf collimator, Gamma-Knife, and CyberKnife rely on small field sizes of order of a few millimeters to treat tumors and simultaneously spare normal structures. Compared to the conventional radiotherapy with fields ≥4 x 4 cm^2, small fields exhibit significant uncertainty in determination of dosimetric parameters. Small field dosimetry of photon beam is challenging task due to lack of lateral electronic equilibrium, source occlusion, high dose gradients, and detector volume averaging. It is recommended that detectors that are tissue equivalent and have small volume are best suited for small field dosimetry. This study includes analysis of dosimetric parameters such as beam profiles and percentage depth dose (PDD) using in-house available ion chambers of different volumes.

Aim and Objective: The aim of the study is to analyze Percentage Depth Dose and Beam Profiles for small field ≤5 x 5 cm^2 by using the different type of ionization chamber and their volume averaging effect in small field dosimetry of photon beam of energies 6 MV, 10 MV and 15 MV.

Materials and Methods: The study is being performed on Varian True beam medical linear accelerator using radiation field analyzer (RFA), a water phantom with dimensions 673 mm height, 875 mm width, 676 mm diameter of ring with integrated software (SNC dosimetery) version 3.2 from Sun Nuclear corporation and ionization chambers i.e. PTW Farmer chamber, SNC125c chamber, Markus chamber and PTW Pinpoint chamber. Different field sizes are opened from 1 x 1 cm^2 to 5 X 5 cm^2 with jaws and multileaf collimator along with standard field size 10 x 10 cm^2. For each field size beam data acquired using RFA. PDD and Beam profile data has been acquired with all the chambers. Other parameters including relative surface dose (Ds), depth of maximum dose (Dmax), PDD at 10 cm, beam flatness, penumbra are also analyzed to study the volume averaging effect.

Result and Discussion: Preliminary analysis shows good results for smallest volume ion chamber that is Pin-Point chamber. The analysis with other chambers is in progress using all available photon energies.

The detailed results will be presented in full paper.

P-91

TREATMENT TIME REDUCTION WITH THE USE OF A THREE DIMENSIONAL PRINTED ELECTRON BEAM MODIFIER FOR TOTAL SKIN ELECTRON TREATMENTS

S. Diamantopoulos, I. Kagkiouzis, G. Patatoukas, M. Dilvoi, E. Kipraiou, V. Kouloulias, E. Efstathopoulos, K. Platoni

Department of Radiology, Radiotherapy Unit, ATTIKON Hospital, University of Athens, Athens, Greece.
E-mail: info@theotokistravel.gr

Introduction: T otal Skin Electron Beam (TSEB) irradiation, is an effective treatment for skin malignancies. It is performed at an extended SSD, usually using two angled electron beams which create a large and homogenous field at treatment distance. Patients take successively six different positions to cover the entire skin. This procedure could be rather exhausting for the patients as it can last up to 30 min.

Objectives: The main objective of this work was to reduce treatment time and deliver the prescribed dose in a more comfortable way. Therefore, we tried to develop a variant of the already established six-dual field technique by creating a clinically acceptable single TSEB field.

Materials and Methods: To produce the single TSEB field various beam modifiers of different materials (aluminum and plastic) and shapes were tested. Utilizing 3D printing technology and the TSEB immobilization device of our department, thermoplastic modifiers were designed and constructed following a trial and error procedure. Electron beam characteristics were measured and calculated both at SSD=100 cm and at treatment level.

Results: The 3D printed modifier shaped the electron beam resulting to a clinically acceptable 6 MeV field of 176 cm x 70 cm field with 10% inhomogeneity in vertical and 3% in the lateral dimension with adequate skin coverage at SSD=400 cm. Underdosed areas do appear near the edge of the field, but in regions located far from the torso of the patient. Contaminating x-ray radiation is within clinically accepted levels (<5%).

Discussion: In general, aluminum scatterers of the same thickness, cause different modification according to the area of blocking. Smaller modifiers, cause proportionally smaller profile enlargement, in respect to the larger ones. With aluminum modifiers central dose deposition was reduced significantly and therefore MUs (and treatment time) should be increased in undesirable levels. On the other hand, plastic modifiers offer a good combination of field dimensions and treatment time. Furthermore, with 3D printing technology, they can be designed to produce the desired beam intensity at treatment plane.

The proposed modification of the original TSEB technique of our hospital could probably benefit mostly feeble patients who could not tolerate a thirty-minutes standing position without compromising the quality of their treatment.

P-92

EVALUATION OF EFFECT ON OUTPUT FACTOR IN CUSTOMIZED ELECTRON FIELDS COLLIMATION IN RADIOTHERAPY FOR VARIOUS ENERGIES

Mandvi Dixit, Anoop Kumar Srivastava, S. P. Mishra, S. Farzana, Soniya Pal, Madhup Rastogi, Rohini Khurana, Rahat Hadi, Kamal Sahni, Ajeet Gandhi, Shantanu Sapru

Department of Radiation Oncology, Dr. Ram Manohar Lohia Institute of Medical Sciences, Lucknow, Uttar Pradesh, India.
E-mail: anoopsrivastava78@gmail.com

Introduction: Electrons are widely used in combination with photon beams or as standalone modality for radiotherapy with energy ranging from 4MeV-15MeV. The electron beams are applied using varies sizes of applicator with cutouts to match the tumor topology and conform to the clinical requirements. However, in routine clinical practices customized electron cutouts of cerrobend are prepared which may be circular, rectangular or of any other geometry to meet the need of the target volume. The electron cutouts in combination with applicators affect the output, PDD and other dosimetric parameters. It has been reported that the changes in beam characteristic of high energy and small cutouts are more profound due to lack of lateral scattering contribution. In this study it was propose to evaluate the dosimetric parameters of cutout and compare it with electron beam characteristics obtain from the various algorithm of the treatment planning system (TPS). The measured data and the TPS generated values have been compared to obtain the perturbation that may be induced in clinical practice. This study attempts to demonstrate that small cutout dosimetry in electron is critical when used as standard alone modality or in combination with photon beam abutment.

Objective: The objective of this study is to evaluate the correlation between the beams profiles obtains through direct measurement for cutouts with TPS generated values using various algorithms.

Materials and Methods: PTW dosimetry (PTW Freiburg, Germany) with Markus chamber was utilized for measurement. The circular applicators of dia 2 cm, 3 cm, 4 cm, 5 cm and rectangular and square cutouts of dimension 4×4, 6×4, 8×5.5, 10×6, 14×8, 14×12 were evaluate. The cutouts factor and other beam characteristics were measured using solid water phantom for the energy range of 4MeV, 6MeV, 10MeV, 12MeV on Elekta infinity Linac system. The parallel plate chamber model no-TM 23343-004309 having sensitive volume of 0.055cc was used and IAEA TRS-398 protocol was followed in this study. The dosimetry was performed at 100 cm SSD by using 10 × 10 cm^2 applicator field size for standardization. The dosimetric patterns for circular, rectangular and other geometries were obtained and were normalized with respect to values for 10×10 cm^2 applicator. The data obtained is detailed in Table 1a and 1b.

Results and Discussion: It has been found that for applicator size 6 × 6 the TPS calculated values are higher at all energies than the measured values. However when large applicator of 14 × 14, 20 × 20, 25 × 25 were used the measured

Table 1: Electron applicator output factors for 4 MeV, 6 MeV, 10 MeV, 12 MeV electron energies

Collimated fields	*4 MeV*	*TPS*	*6 MeV*	*TPS*	*10 MeV*	*TPS*	*12 MeV*	*TPS*
(a) Comparison between measured data and TPS generated data								
Applicator 10×10	1.0	1.0	1.0	1.0	1.0	1.0	1.0	1.0
Applicator 6×6	0.9298	1.09	0.9259	1.08	0.9797	1.035	0.9856	1.015
Applicator 14×14	1.0390	0.96	1.0037	0.995	0.9861	1.03	0.9821	1.025
Applicator 20×20	1.0393	0.96	1.015	0.985	0.9714	1.035	0.9672	1.035
Applicator 25×25	1.0454	0.96	1.0272	0.975	0.9818	1.02	0.9816	1.02

Applicators	*4 MeV*	*6 MeV*	*10 MeV*	*12 MeV*
(b) Percent variation between measured and TPS generated data				
6×6	−17.22	−16.64	−5.6	−2.9
14×14	7.66	0.86	−4.4	−4.3
20×20	7.6	2.9	−6.54	−7.0
25×25	8.1	5.08	−3.8	−3.9

TPS: Treatment planning system

values for 4MeV, 6MeV are less than the calculated values. The observed variations have been found to be 4% to 17% for the cutout geometries evaluated. However for the larger applicators the calculated value from TPS for energy range of 10MeV, 12MeV are larger than the measured values. It is observe that for higher energies the calculated values by TPS always exceeds by the measured values. It can thus be concluded that pencil beam algorithm at higher energies for all sizes of applicator provided deviation than the measured values. The possible reason attributable to this aberration may be lack of lateral contribution of scattering. This study thus provides significant information that cutout factors for all fields which are customized to match the tumor topology should be independently measured and beam library thus accordingly prepared to obtain the dose profile in target volume. The resultant significant error may influence the clinical outcome if the TPS calculated values are utilized for routine dose calculation. It is essential to be careful in using the small cutout of the dia 2 cm to 4 cm where the deviation may be large enough to influence the dose homogeneity and clinical outcome. This aspect will be presented and discussed in detail.

P-93

FIRST APPLICATION OF HEMI-BODY ELECTRON BEAM IRRADIATION IN GREECE: SET UP, MEASUREMENTS AND DOSIMETRY

Platoni Kalliopi, Dilvoi Maria, Delinikolas Panagiotis, Patatoukas George, Kypraiou Eyfrosini, Kougioumtzopoulou Andromachi, Trogkanis Nikolaos, Gazouli Maria[1], Efstathopoulos Efstathios, Kouloulias Vassilis

Department of Radiology, University General Hospital "ATTIKON", School of Medicine, National and Kapodistrian University of Athens, [1]Department of Basic Medical Science, Laboratory of Biology, School of Medicine, University of Athens, Athens, Greece.
E-mail: info@theotokistravel.gr

Introduction: Half body (Hemi body) electron irradiation (HBIe$^-$) aims to deal with cases of superficial skin tumors with more symptomatic density on upper or lower body. Resembling Total Skin Electron Beam Technique (TSEB), the spectrum of using HBIe$^-$ includes various deceases such as Kaposi's sarcoma and T-Cell Lymphoma plus its product diseases. An attempt for the first application of this external radiation therapy technique in Greece took place at the Radiation Therapy Unit of 2nd Department of Radiology of University of Athens at University General Hospital "ATTIKON".

Objective: The purpose of this work is to present and to comment on the results of the first application of HBI electron beam irradiation in Greece. The procedure included amongst others, finding the proper beam angle for the lower torso, the deployment of a custom made shielding device for the upper torso, the appropriate positioning and immobilization of the patient's body and finally the dosimetric verification of this technique using thermo-luminescence dosimetry (TLDs), placed on the patient's skin.

Materials and Methods: The first patient, who treated with HBIe$^-$ technique, was male, 64 years old and had Kaposi's sarcoma, the disease was extended to the lower torso. HBIe$^-$ modality was developed on a linear accelerator VARIAN Clinac 2100C. To produce 6 MeV electron beams of field size 36 x 36 cm^2, delivered at the high dose rate of 2500MU/min at isocenter, a single beam with its central axis pointing vertically to treatment plane (Gantry angle at 279.5 degrees for Lower HBIe$^-$) at SSD 388 cm. The custom made chamber of our department, used for TSEB treatment was also utilized for HBIe$^-$, providing appropriate conditions for skin irradiation (energy degradation of nominal 6MeV electron beams, field size widening through scattering and patient positioning). Irradiation procedure demands a standing patient that takes, in total, six treatment positions. For the Lower HBIe$^-$ case, a custom made universal shielding was attached to the treatment chamber. Any additional shielding for sensitive areas and/or organs at risk (eyes, nails, genitalia etc.) should be designed for each patient individually. Finally dose uniform delivery was monitoredusing thermo-luminescence dosimetry (TLDs).

Results: The treatment was dosimetrically monitored during his first two sessions. Patient dosimetry showed a very good agreement with the expected mean dose of 2Gy as mean patient dose was (1.7Gy). Furthermore, minimum and maximum values were at the level of 2.6Gy and 1.1Gy respectively. Spatial variations of the dose distribution can provide essential insights on the patient irradiation conditions and can assist vitally in the dosimetric optimization of the applied clinical protocol.

Discussion: Beam quality indexes and dosimetry aspects were defined with precision in order to provide an effective treatment. Every physical parameter was in agreement with suggested values of the international guidelines. In conclusion, hemi body electron irradiation can be implemented efficiently and with safety at the Radiation Therapy Unit of Athens University's General Hospital 'ATTIKON'.

P-94

QUANTITATIVE ANALYSIS OF PROMPT GAMMA RAY IMAGING DURING PROTON BORON FUSION THERAPY ACCORDING TO BORON CONCENTRATION

Han-Back Shin, Moo-Sub Kim, Sunmi Kim, Kyu Bom Kim[1], Do-Kun Yoon, Hye Jeong Yang, Tae Suk Suh

Department of Biomedical Engineering, Research Institute of Biomedical Engineering, College of Medicine, The Catholic University of Korea, [1]Department of Electronic Engineering, Sogang University, Seoul, Korea.
E-mail: hbshin07@gmail.com

Introduction: proton boron fusion therapy (PBFT) has been suggested as a novel radiation therapy technique and tumor monitoring technique for use during treatment. The PBFT method is a treatment technique based on the proton-boron fusion reaction. We confirmed the generation of a 719 keV prompt gamma ray after the proton-boron reaction. Thus, it was possible to develop a tumor-monitoring technique using a prompt gamma ray during PBFT. The main benefit of this prompt gamma ray imaging technique is a tumor monitoring method that does not require an extra dose during treatment, unlike computed tomography (CT) and X-ray. In our previous studies, a prompt gamma ray image was acquired with a specific boron concentration that was much higher than the clinically appropriate boron concentration range, so those studies were more conceptual in nature.

Objectives: The purpose of this study is to evaluate prompt gamma ray images during PBFT with Monte Carlo simulations using the boron concentrations allowable in clinical application. This study shows the effectiveness of the prompt gamma ray imaging technique during PBFT. It can be reflected to actual imaging techniques using boron compounds in clinical applications.

Materials and Methods: To acquire a prompt gamma ray image from 32 projections, we simulated four head single photon emission computed tomography and a proton beam nozzle using a Monte Carlo simulation. In addition, we used a modified ordered subset expectation maximization reconstruction algorithm with a graphic processing unit for fast image acquisition. The therapeutic conditions of PBFT included a low-energy proton beam and boron concentrations from 20 to 100 μg at intervals of 20 μg. For quantitative analysis of the prompt gamma ray image, we acquired an image profile drawn through two boron uptake regions (BURs) and calculated the contrast value, signal-to-noise ratio (SNR), and difference between the physical target volume and volume of the prompt gamma ray image.

Results and Discussion: The relative counts of prompt gamma rays were noticeably increased with increasing boron concentration. Although the intensities on the image profiles showed a similar tendency according to the boron concentration, the SNR and contrast value improved with increasing boron concentration. In addition, the difference between the physical target volume and prompt gamma ray image volume in each BUR decreased as the boron concentration increased.

Conclusion: We confirmed that the prompt gamma ray images depending on the boron concentration were successfully deducted during PBFT. This study suggests that a tumor monitoring technique using prompt gamma ray detection can be clinically applicable even if the boron concentration is relatively low.

P-95

DEVELOPMENT OF WATER EQUIVALENT MULTI-LAYER IONIZATION CHAMBER WITH LIQUID CRYSTAL POLYMER

Shigekazu Fukuda[1], Hiroyuki Kobayashi[1,2], Soma Iwata[3]

[1]National Institute of Radiological Sciences, National Institutes for Quantum and Radiological Science and Technology, [2]Graduate School of Science, Chiba University, [3]Accelerator Engineering Corporation (AEC) Chiba, Japan. E-mail: fukuda.shigekazu@qst.go.jp

The dose distribution of the therapeutic carbon beams, especially, the depth dose distribution (DDD) is important, because the physical DDD of SOBP that can be converted to the homogeneous DDD biologically and clinically is not homogeneous but become decreasing according to the depth from the surface. So we have developed the water equivalent multi-layer ionization chamber (W.E.MLIC) that enable us to measure the physical DDD at one time with the equivalent results obtained by scanning an ion chamber in the water phantom which it takes much longer time.

In the study we developed new prototype of W.E.MLIC with Liquid crystal polymer (LCP). In the last study we evaluated stability of W.E.MLIC which consisted of PMMA and cupper plates and we found the short-term and long-term instability of the output from MLIC. Furthermore, there were proved two possible causes of these instability problem. The first cause was the irradiation of the carbon beams to the readout patterns which conducted collected charge. The second cause was that signal substrate made from PMMA, which has hygroscopicity, could be shrunken in a different manner of the cupper plates in a dry environment and resulted in the sensitive volume decreasing.

On the base of these results, we improved the readout pattern whose width was narrower (from 0.5 mm to 0.1 mm). In addition, we adopted substrate made from LCP which has lower hygroscopicity instead PMMA and cupper plates. By using carbon beams of 400 Mev/n accelerated by HIMAC, we measured the water equivalent thickness of LCP and examined the water equivalence and stability of the new prototype of W.E.MLIC. We obtained the results that the water equivalence was good like previous studies and the stability of the output from the new W.E.MLIC with LCP was better than previous one.

P-96

TEMPORAL CHANGES OF TARGET VOLUMES AND OAR VOLUMES DURING HIGH PRECISION RADIOTHERAPY: A PROSPECTIVE STUDY

Debojyoti Dhar, Saibal Mukherjee, Arundhuti Chakraborty, Liton Naha Biswas, Suman Mallik[1], Jyotirup Goswami[1], Akhter Jawade, Tanweer Shahid, Jibak Bhattacharya, Poopathi Venkataraman, Bipasha Pal[1], P. Nagendran, Subhra Biswal, Pramod Yadav, SaubhikGhosh

Department of Oncology Radiation, Apollo Gleneagles Hospital, [1]Department of Radiation Oncology, Narayana Superspeciality Hospital, Kolkata, West Bengal, India. E-mail: dhar.debojoyti@gmail.com

Introduction: Tumor shrinkage in response to radiotherapy, change in OAR (organ at risk) volume and weight loss may impact on the dose-distribution in both target and organ at risk (OAR) and hence the therapeutic outcome in patients with Head and Neck cancer. In this study, we investigated temporal changes of the target volumes and OAR volume during radiotherapy to adopt a strategy for adaptive radiotherapy.

Materials and Methods: Twenty-six patients who underwent radical chemo-radiotherapy (CTRT) for head and neck squamous cell carcinoma between April’12-April’13 were prospectively analyzed. After immobilization, Computed Tomography (CT) scans were taken from base of the skull to sternal angle using 3 mm slices by Siemens Somatom Emotion 16 slice CT scanner. Targets and OAR were contoured using Focal Sim. Treatment Planning was done on the XiO Treatment Planning System (ELEKTA AB, Sweden).

All patients underwent 3D-CRT/IMRT. The prescription dose was 59.4 Gy-70Gy @ 1.8 -2Gy/fraction. All patients underwent a CT scan after 20 fractions. Targets and organs at risk were similarly outlined on these scans as above. The cranio-caudal dimensions of the planning target volume (PTV) were kept the same. Only the part of PTV going out of body contour (due to weight loss) was changed. Volume changes of targets and OARs were analyzed using SPSS 16.

Results: Comparison between both CT-scan (planning CT and CT at 20th fraction.) showed changes in GTV (mean 24.56cc Vs 19.86cc p<0.001, 95% CI 2.86-6.54), PTV (mean 280.44cc Vs 255.1cc p=0.48, 95% CI -3.36-6.93), right Parotid (mean 27.43cc Vs 22.25cc p<0.001, 95% CI 3.44-6.90) and left Parotid (mean 25.38cc Vs 20.97cc p<0.001, 95% CI 2.81-5.99) volumes as depicted in Table 1.

Discussion: Anatomical changes can occur during radiation therapy of head and neck cancer patients. This can lead to difference between planned and delivered dose. After 4-5 weeks of adjuvant chemo-radiotherapy, it is commonly found that there is reduction in body weight due to oral mucositis. As a result, there is a change in the patient's contour and the relative positions of the GTV/PTV and OARs may change. In the present study, we have found significant changes in GTV volume (p<0.001), and also change in OAR volume, which in this case is the parotid glands (p<0.001 for both left and right parotids). On the other hand, the total PTV volume has not been found to change significantly (p=0.48), since the PTV volume is over the entire neck-nodal region. However, for some patients we have found the PTV volume to extrude outside the body contour. Though the PTV volume does not change appreciably, our findings point to the need for re-planning after repeat CT scan, since some of the OAR's migrate near or away from the GTV due to change in both GTV as well as OAR volumes, and due to PTV extending beyond body. It is essential to re-plan to identify dosimetric changes and to ensure adequate doses to target volumes and safe doses to normal tissues.

Conclusion: Volumetric changes in the target volume and OARs were observed could have potential dosimetric impact when highly conformal treatment techniques are used. It Suggest that adaptive strategies, where patients are re-imaged and possibly replanned during treatment, are worth evaluating.

Table 1: Variation in volume of GTV, PTV and Parotid

Scores	*Mean (cc)*	*95% CI*	*P*
GTV volume in cc-CT1	24.56	2.86–6.54	<0.001
GTV volume in cc-CT2	19.86		
PTV volume in cc-CT1	280.44	–3.36-6.93	0.48
PTV volume in cc-CT2	255.1		
Right parotid volume in cc-CT1	27.43	3.44–6.90	<0.001
Right parotid volume in cc-CT2	22.25		
Left parotid volume in cc-CT1	25.38	2.81–5.99	<0.001
Left parotid volume in cc-CT2	20.97		

GTV: Gross tumor volume, PYV: Planning target volume, CT: Computed tomography, CI: Confidence interval

P-97

DOSIMETRIC EVALUATION OF INDIGENOUSLY DEVELOPED NON METALLIC ARTIFACT FREE CT FIDUCIAL MARKER

G. Kesavan, S. Senthilkumar[1]

Department of Radiotherapy, Vadamalayan Hospitals Pvt. Ltd., [1]Department of Radiotherapy, Madurai Medical College, Govt. Rajaji Hospital, Madurai, Tamil Nadu, India. E-mail: kesavanmp@gmail.com

Introduction: Fiducial markers are used in a wide range of medical imaging applications. Fiducial markers are commonly used above the patient surface in target region and serve as a reference. Ideally, the fiducial markers should be easily identified and clearly visible on simulation. Difficulty arises when marker creating artifacts in the CT image, and these artifacts affect the clarity of the anatomical region of interest. There is significant error in CT number due to bright and dark streaks. Thin bright and dark streaks originating from the metal based fiducial markers.

Objectives: Aim of this study was to discuss the dosimetric evaluation of the indigenously developed non-metallic artifact free CT fiducial and compare with the metallic CT fiducial during CT based planning.

Materials and Methods: We have used the newly developed non-metallic CT fiducial for our RT planning CT simulation for Ca. patients in different sites such as Brain, Head and Neck, Thorax, Abdomen and Pelvis and also with phantom. Previously we have used metallic based fiducial for our routine RT planning and used to found the streak artifacts. These type of artifacts seriously degrade the quality of CT images and sometimes to the point of making them diagnostically unusable and also create problem during auto-contouring. Thin bright and dark streaks originating from the metal based fiducial markers. Difficulty arises when marker creating artifacts in the CT image and these artifacts affect the clarity of the anatomical region of interest. There is significant error in CT number due to bright and dark streaks. We have used the metallic fiducial on the right side and non-metallic on left side of the patient during CT simulation based on the laser reference. The same method was adapted for other sites as well as phantom.

Results and Discussion: We have found that the metallic fiducial produce isodose shift below to the fiducial on the particular slice and no shift in the non-metallic fiducial. Both metallic and non-metallic markers appeared similar visibility on the CT image and non-metallic not produce any artifact when compared with the metallic fiducial. Non-metallic has the electron density of 2000 but commercially available marker has more than 9000. So, non-metallic fiducial can be used for regular CT simulation in all clinical situation for better treatment without isodose shift. We conclude that the newly fabricated CT fiducial gives better clinical outcome compared with metallic fiducial.

P-98

VARIATIONS IN INTERNAL TARGET VOLUME OF A MOVING LUNG TUMOUR: ANALYSIS OF A MOVING PHANTOM USING FOUR-DIMENSIONAL COMPUTED TOMOGRAPHY

Arun Balakrishnan, S. Sriram Prasath, Raj Kumar Shrimali, Indranil Mallick, Sanjoy Chatterjee, Chandran Nallathambi, N. Arunai Nambiraj[2], K. Senthilnathan[1], P. Ramesh Babu[1]

Department of Radiation Oncology, Tata Medical Center, Kolkata, West Bengal, [1]Department of Physics, School of Advanced Sciences, VIT University, [2]Centre for Biomaterials, Cellular and Molecular Theranostics, VIT University, Vellore, Tamil Nadu, India.
E-mail: arun.medphy@gmail.com

Background: A typical Four-dimensional Computed Tomography (4DCT) for lung stereotactic body radiation therapy (SBRT) contains images captured through the whole breathing cycle divided into ten phase-bins. However, in practice, inconsistencies in the breathing pattern and duration prevails and could potentially result in phase errors.
Objective: To evaluate the probable variation in internal target volume (ITV) of a moving lung tumour during stereotactic body radiation therapy due to inconsistency in free breathing rate using a programmable Quasar Phantom and Four-Dimensional Computed Tomography (4DCT) and also to analyse the phase error after binning in the moving phantom.
Materials and Methods: A programmable motion Quasar phantom with 6 mm longitudinal displacement of a lung equivalent cedar cylinder insert containing off-set placed 2.5 cm diameter tumour density sphere as tumour and sine wave rotational mode with 1 cm amplitude platform with a 6-dot marker was used. Seconds per breath was set at four seconds. In CT machine, 1/10th of the breathing period read from the Real-time Position Management (RPM) console was fed as the cine time between images. Cine duration was set with one second added breathing period and inter-scan time was set as one second. The images were sorted into ten phases based on the temporal correlation between surface motion and data acquisition with Advantage Workstation. The results of GE Advantage 4D, binned ten phase images, maximum intensity projection (MIP) and average intensity projection (AIP) were imported into Varian Eclipse version 10.0. The percentage of phase error with respect to 4 s is shown in Table 1. From the MIP set, ITV (tumour sphere created elliptical volume) structure was created under -400 HU window width to estimate the volume (cc). The same procedure was repeated with a known error value of ±0.5 seconds in cine time between images and the whole procedure was repeated five times for consistency.
Results: The observed ITV variation was ≤-1.9% error and <2% maximum phase error than the actual 4DCT breathing period setting in the 10-bins 4DCT image protocol.
Conclusion: There is no significant error due to small averaging variations of breath period entered cine time between images during 4DCT imaging.

P-99

EVALUATION OF PLANNING TARGET VOLUME MARGIN FOR TWO IMAGING PROTOCOLS

G. Muthu Krishnan, S. A. Yoganathan[1], K. J. Maria Das[1], D. Udayakumar[1], C. S. Sureka, Shaleen Kumar[1]

Department of Medical Physics, Bharathiar University, Coimbatore, Tamil Nadu, [1]Department of Radiotherapy, Sanjay Gandhi Postgraduate Institute of Medical Sciences, Lucknow, Uttar Pradesh, India.
E-mail: mkrish190@gmail.com

Purpose: Usually, two imaging protocols such as daily and weekly portal imaging are used to study the setup error. The purpose of this work was to evaluate the setup error and derive the PTV margin for the above two imaging protocols in brain and prostate cancer patients.
Methods: Ten patients of each brain and prostate cancer (implanted with gold seeds) were retrospectively included in this study. All the brain patients had a pair of orthogonal 2D MV portal images and bony matching was used to analyze the setup accuracy; where as the prostate patients had 2D kV images and the marker matching method was used to analyze the setup accuracy. Two type of setup errors were calculated; one using daily portal imaging and other using weekly (first three fractions and then weekly once) portal imaging. The planning target volume (PTV) margins were calculated (excluding rotational error) for the observed setup error based on Marcel Van Herk recipe.
Results: The PTV margins for brain cases based on daily imaging were 2.6 mm, 4.0 mm and 2.7 mm in medio-lateral, cranio-caudal and anterior-posterior direction respectively; where as the same for weekly imaging were 2.9 mm, 4.7 mm

Table 1: Percentage of phase error with respect to 4 s (actual setting of SPB in phantom)

Cine time	*Cine time + add on time*	*Phase 0*	*Phase 10*	*Phase 20*	*Phase 30*	*Phase 40*	*Phase 50*	*Phase 60*	*Phase 70*	*Phase 80*	*Phase 90*	*ITV_MIP (volume)*
0.25	3.5	17	15	16	16	16	12	15	14	17	14	17.39
0.3	4	4	8	11	6	4	12	11	4	4	12	17.23
0.35	4.5	4	4	3	4	4	4	4	3	4	4	17.18
0.4	5	4	5	5	5	5	4	5	5	5	5	17.37
0.45	5.5	4	4	5	5	5	5	5	5	5	5	17.04
0.5	6	6	6	5	5	5	6	6	5	5	5	17.11
0.55	6.5	7	6	6	5	5	5	5	5	6	6	17.24
0.6	7	6	4	4	7	5	3	6	7	3	7	17.1
Static 0.4	5	6	6	4	4	4	4	5	5	5	5	13.99

ITV: Internal target volume, MIP: Maximum intensity projection, SPB: Seconds per breath and 2.5 mm respectively. Similarly, PTV margins for prostate cases based on daily imaging were 11.1 mm, 16.5 mm and 11.7 mm in medio-lateral, cranio-caudal and anterior-posterior direction respectively; where as the same for weekly imaging were 10.5 mm, 15.4 mm and 11.4 mm respectively.

Conclusions: Daily and weekly imaging protocols did not show any considerable variation (less Than 1 mm) for deriving PTV margins. Therefore the weekly imaging protocol is adequate for determining the PTV margin; which would also result in relatively lesser imaging dose to the patient.

P-100

ASSESSMENT OF SURFACE DOSE USING RADIOCHROMIC FILM (EBT3) IN CHEST WALL RADIOTHERAPY WITH SUPERFLAB™ GEL BOLUS

Challapalli Srinivas, Dilson Lobo, P. Suman Kumar, Sourjya Banerjee, P. U. Saxena, Dinesh Pai

Department of Radiotherapy and Oncology, Kasturba Medical College and Hospital (An Associated Teaching Hospital of Manipal University), Mangalore, Karnataka, India. E-mail: challapallisnvas@yahoo.co.in

Introduction: R adiotherapy is offered to the chest wall in post mastectomy patients to reduce the risk of loco regional recurrence. Tissue-equivalent materials are used as a bolus to provide dose build-up along the skin and superficial chest wall in order to adequately treat any residual disease out to the skin to the full prescription dose. Accurate skin dose assessment is essential to assure that it is sufficient, below the tolerance level.

Objectives: The aim of this study is to measure the surface doses using radiochromic film (EBT3) a) in a locally fabricated semi breast phantom and b) in post mastectomy patients (6Nos) undergoing three dimensional conformal radiotherapy (3DCRT) to the chest wall, with 5.0 mm Superflab ™ gel bolus.

Materials and Methods: A locally fabricated semi breast phantom having lung equivalent insert made with cork material (density 0.28 gm/cc), simulating the actual treatment of post-mastectomy chest wall radiotherapy is taken. Surface dose measurements were taken using EBT3 film with 5.0 mm gel bolus in predefined fiducial regions and were to compare the planned ones in treatment planning system (TPS). Post-mastectomy patients (6Nos) undergoing 3DCRT planned for chest wall to a total prescription dose of 50 Gray in 25 fractions were undertaken for surface dose measurements. Treatments were given with 5.0 mm gel bolus during first 15 fractions followed by without bolus to the rest of 10 fractions as per institution protocol. Two sets (with and without placing the 5.0 mm gel bolus sheet on to the chest wall) of simulated computed tomography (CT) scans in treatment position were obtained, keeping fiducial markers (with a thin copper wire) at five different locations (median, central, lateral, superior and inferior) around the scar region of chest wall. Treatment plans were generated in Xio TPS to the first set of CT scans (having gel bolus) to a dose of 30 Gray in 15 fractions to the clinical target volume (chest wall) with tangential beams of 6MV photon beam. Field in field technique, and / or motorized wedge filter was used to homogenize the dose distribution in all plans. Radiochromic EBT3 film pieces (of dimension 2 cm x 2 cm) were placed at predefined fiducial marker locations of chest wall and surface doses were measured three times during the course treatment of bolus plan which were compared with the calculated ones in TPS. Skin toxicity was assessed in all patients as per National Cancer Institute Common Toxicity Criteria (NCI CTC).

Results: Twelve patients with mean age of 52.4 years were treated with 5 mm bolus on to the chest wall during first fifteen fractions of prescribed dose. The mean percentage of planned dose (standard deviation) for median, central lateral, superior and inferior from EBT3 films were 101.1% (4.6%), 105.1% (6.3%), 97.1% (5.6%), 103.6% (6.3%), and 105.3% (4.6%) respectively. Three out of six patients experienced a maximum acute NCI CTC skin toxicity score of 2. There were no grade 3 and 4 toxicities.

Discussion: Chest wall radiotherapy with Superflab™ gel bolus of thickness 5.0 mm is a feasible regimen during first fifteen fractions of total prescribed dose with acceptable dose build-up and skin toxicity in post-mastectomy patients.

P-101

MEDICAL PROTON/CARBON DOSIMETRY USING OPTICALLY STIMULATED LUMINESCENCE FROM EASILY PREPARED KCL: SM^{3+} NANOPHOSPHOR

Mini Agarwal, K Asokan[1], Pratik Kumar

Medical Physics Unit, AIIMS, IRCH, [1]Inter-University Accelerator Centre, New Delhi, India.
E-mail: minia85@gmail.com

Optically Stimulated Luminescence (OSL) radiation dosimetry is widely used nowadays for the measurement of radiation dose in various field including industry, agriculture, research, space and medicine. All present OSL phosphors suffer one or other lacuna prompting us to synthesizes KCl:Sm nano phosphor which promises to be a cheap, easy to manufacture and have the capability to measure small and large radiation dose simultaneously with extraordinary efficiency. All the present OSL phosphors tend to saturate at higher doses ($\approx$ 5-10 Gy) if they are able to measure small doses ($\approx$ 1μGy). However, KCl:Sm nano phosphor defies this and can measure doses from 100 mGy to 1000 Gy with a linear response due to the incorporation of trivalent Sm^{3+} as stable defects. We prepared KCl:Sm by high-temperature solid-state synthesis method and optimized the concentration of Sm of 0.45%. We further investigated its promising use for medical carbon and proton dosimetry. We investigated optically stimulated luminescence (OSL) from KCl:Sm (0.45%) phosphor, potentially can be used for heavy ion radiotherapy (carbon ion heavier than protons). The OSL and TL just after OSL were recorded with irradiation of 500 keV proton and carbon ion beam with different fluences from 1 x 10^{13} to 6.25 x 10^{15}. The OSL decay response of low-LET protons was found to very significant at a fluence of 2.5 x 10^{14} ions/cm^2 than that observed for a high LET carbon ion beam. At at a fluence of 2.5 x 10^{14} ions/cm^2, the luminescence efficiency of high LET was decreased about 65%. While for higher fluence 6.25 x 10^{15} ions/cm^2, we observed a significant decrease in the luminescence efficiency with low LET protons about 70% than that was observed for high LET carbon ion beam. The ease of its preparation is striking and likely to be quite cheaper OSL phosphor than the later.

Application No: IS0018

P-102

EXTENDED CONE BEAM CT LOCALIZATION FOR ADAPTIVE RADIOTHERAPY AND DOSIMETRIC EVALUATION OF KILOVOLTAGE IMAGING

K. Mohamathu Rafic, Ebenezer Suman Babu, Timothy Peace Balasingh, B. Paul Ravindran

Department of Radiotherapy, Christian Medical College, Vellore, Tamil Nadu, India. E-mail: raficmphy@gmail.com

Introduction: Several authors have reported the practicability of computing dose calculation on CBCT images while addressing HU inaccuracies with appropriate scatter rejection and HU correction strategies. The off-centred detector panel arrangement in half-fan (HF) acquisition geometry of the OBI system limits the longitudinal coverage to a mere 16 cm with a maximum reconstruction diameter of 45 cm. However, in most clinical scenarios, the craniocaudal scanning length of CBCT is found to be inadequate for localizing the planning target volumes (PTV) with extended nodal coverage.
Objective: To develop extended tomographic localization and adaptive dose calculation strategies using *HU* corrected CBCT with an intention to overcome the limitation encountered in adaptive radiotherapy (ART) and explore dosimetric evaluation of kilovoltage (kV) imaging.
Materials and Methods: Planning CT (pCT) images of the Rando phantom (T12-to-midthigh) were acquired with pelvic-protocol using Biograph CT-scanner. Similarly, half-fan (HF) CBCT were acquired with fixed parameters using Clinac2100C/D linear accelerator integrated with on-board imager with 2-longitudinal positions of the table. For extended localization and dose calculation, two stitching strategies viz., one with "penumbral-overlap"(S_1) and the other with "no-overlap"(S_2) and a local *HU*-correction technique were performed using custom-developed Matlab scripts. Fluence modulated treatment plans computed on pCT were mapped with stitched CBCT and the dosimetric analyses such as dose-profile comparison, 3D-gamma (γ) evaluation and dose-volume histogram (DVH) comparisons were performed. Daily imaging dose from pre-treatment CBCT procedure has traditionally been ignored. Hence, planar dosimetry for kV CBCT imaging and the penumbral dose overlaps resulting from proposed S_1 and S_2 strategies was performed using Octavius 1500 ionization chamber array.
Results and Discussion: The scanning length of CBCT was extended by up to 16 cm in S_2 when the couch shift 'Δ' was equal to '*l*' of single HF-CBCT acquisition geometry. On the other hand, S_1 protocol resulted in an extended scan length of 15 cm with an overlap (n = 1 cm). The structures mapped from pCT to stitched CBCT (sCBCT) resulted in minor variations in the volumes of all the five structures. The treatment plans computed on the pCT when mapped onto the registered sCBCT resulted in small disparity in beam centre co-ordinates. The possible causes of this variation could be due to minor mismatch in registration, small differences in reconstruction diameter and the position of the center of mass of target volume. Both the strategies showed good match in the entire range of dose profile with respect to pCT, especially in the regions where the penumbral overlap and stitching were performed. Furthermore, the 3D γ-evaluation technique used in the present study would serve as effective quality assurance tool for comparing the pCT and sCBCT based treatment plans with high spatial resolution dose distributions generated in the Eclipse TPS. We observed that the 3D γ-evaluation results showed superior pass rate with more than 97.5% dose pixels passing both the γ-criteria. In addition, HF-CBCT imaging resulted in 6 - 7.5 cGy peripheral dose contribution overall. Absolute dose measured using Octavius 1500 array at the regions of penumbral overlap of S_2 was found to be relatively less compared to S_1 strategy due to 1 cm overlap which can be reduced by selecting optimum 'n' value. Due to the lateral scattering of kV beam, S_2 protocol also showed non-uniform dose at the penumbral region.
Conclusion: CBCT image stitching and HU-correction strategies were developed in our study to facilitate extended localization of target and normal tissues and accurate dose calculation. This enables routine adaptive replanning and reoptimization of treatment plans based on setup verification CBCT while circumventing the need for repeated planning CT that is a requisite for conventional adaptive radiotherapy.

P-103

THE MATHEMATICAL METHODS OF PROTON BEAMS MODELING IN THE TREATMENT PLANNING SYSTEM

Kunihiko Tateoka, Yuya Azuma, Yasuhiro Hasegawa, Keiji Nakazato, Ayaka Kikuchi, Hyuga Nireki, Masaru Takagi, Masato Hareyama

Proton Treatment Center, Sapporo Teishinkai Hospital, Sapporo, Japan. E-mail: tateoka@sapmed.ac.jp

Proton therapy system in Sapporo Teishinkai Hospital (Hokkaido, Japan) consists of a cyclotron (P235, Sumitomo Heavy Industries, Ltd.), an in-room CT (SOMATOM Definition AS), Oncology Information System (Mosaiq, Elekta) and Treatment Planning System (TPS) (Eclipse Protons ver.13.7, Varian Medical Systems, Inc).
Our facility has a multi-purpose nozzle which can irradiate both wobbler beam and scanning beam.
The commissioning for proton therapy with wobbler beam started from the summer of 2016.
In our TPS, a depth dose curve of a range-modulated proton beam with Ridge Filter is reproduced by weighting depth dose curves of mono-energetic beams with several ranges, and users must determine these weights for mono-energetic beam by hand. In order to determine these weights efficiently, two mathematical methods are used; one is the least squares method, and the other is the generalized reduced gradient method (it is built in Windows Excel solver tool).
γ-value (2% 2 mm) between TPS calculation and measurement data is required to pass in all depth region with reference conditions for modeling of a range-modulated proton beam. TPS calculations with different beam parameters (various energies, snout positions and field sizes) are compared to the beam data with the same parameters. In most cases, TPS calculations are consistent to the beam data with acceptable error but measurement data tends to be higher than TPS calculation in the plateau region of depth dose curve for the case that the field size is relatively small (40 mm × 40 mm at the isocenter).
In this presentation, performance of the two mathematical methods and the results of modeling for depth dose curves of range-modulated beams in our facility are reported.

Furthermore, the difference of the depth dose curve for small field case is also discussed.

P-104

ON THE DOSIMETRIC BEHAVIOR OF VMAT PLANS WITH RESPECT TO VARIOUS PHOTONS BEAM (FF) ENERGY USING MONTE CARLO DOSE CALCULATION FOR CARCINOMA CERVIX

N. Munirathinam, Pawaskar, S. H. Pawar, C. D. Lokahande

Department of Medical Physics, Centre for Interdisciplinary Research, D. Y. Patil University, Kolhapur, Maharashtra, India.
E-mail: munimedphy@gmail.com

This study was designed to evaluate the Plan quality (TCP and NTCP), Conformity index (CI), Heterogeneity index (HI), treatment planning time, total MU and estimated treatment delivery time with respect to different Photon energy (6, 10 and 15 MV) VMAT plans are created for cervix tumor and the ultimate goal is provide an efficient photon energy for VMAT planning for Carcinoma Cervix.

Methods: A total of 10 Cervix case used for the study. All the plans are made with full single- arc for different Photon energy namely 6, 10 and 15 MV with default 180 control points using Monaco™ (Elekta Medical Systems, Crawley, UK) treatment planning system. The photon dose calculation is done by using a Monte Carlo algorithm. The dosimetrics such as PTV coverage, organ-at-risk sparing, Conformity index (CI), Heterogeneity index (HI), integral dose, treatment planning time, MU and minimum/maximum/mean doses are evaluated. The VMAT plans were delivered using an Elekta Versa HD linear accelerator with 160 MLC; the treatment delivery parameters such as the total MUs and delivery time from different increment size plans are compared.

Results: Our results show a comparable coverage of planning target volume (PTV) and OARs sparing CI and HI for all three energies; The numbers of MUs were 14.2 ± 1.6% and 19.2 ± 1.8% higher and IDs. Based on this study, 6 MV photon beam is a good choice for VMAT planning in case of cervix carcinoma, as it does not deliver additional exposure to patients caused by photo neutrons produced in high energy beams.

Conclusions: We compared different Photon beam energy VMAT plans and we found that 6 MV beam is dosimetrically better in comparison to 10 and 15 MV for Carcinoma Cervix as it produces a highly conformal, homogeneous plan with superior target coverage and better OAR sparing.

P-105

OUT OFF FIELD PHOTONEUTRON SPECTRUM DETERMINATION ON THE PATIENT BODY SURFACE DURING RADIOTHERAPY WITH HIGH ENERGY X RAYS USING CR 39 FILMS

K. R. Rajesh, R. Ganapathi Raman[1], Naiby Joseph[2], M. V Dheepthi[2], Biju P. Thomas, N. M. Salim Sha

Department of Radiation Oncology, Caritas Hospital, Kottayam, [2]Department of Physics, University of Calicut, Malappuram, Kerala, [1]Department of Physics, Noorul Islam University, Kanyakumari, Tamil Nadu, India.
E-mail: rajeshkaliyan77@gmail.com

Introduction: The photoneutron spectrum at different locations of the patient body surface during radiotherapy is determined by using CR 39 film. CR 39 films are placed at different locations of the patient body surface and individual field neutron fluence is determined by placing separate CR 39 films for each field. The films are then etched with 6N NaOH at 70˚C for 6 hrs. Then the films are imaged with a microscope with recording ability. The tracks in the films are then counted and the parameters required for the recoil proton energy calculation are determined by using a programme TRIAC II written in MathLab. Then the neutron energy is calculated from this recoil proton energy by applying the required calibration factors. Then the spectrum is determined and plotted using GNU plot. The main reaction channels responsible for the photoneutron production are identified.

Photoneutron production during radiotherapy treatment is a major concern when considering its high LET nature. Photoneutrons are mainly produced from machine head, air and from the patient itself by the (gamma, neutron) reaction. The scattering of photoneutron causes dose deposition to the critical organs far away from the treatment site. This may cause secondary cancer induction in the future. The present treatment calculation algorithms are not taking care about this photoneutron dose. The present study is focusing on the photoneutron production from the patient body only.

Materials and Methods: 15 MV X rays from Siemens Primus Plus linear accelerator is used for this study. CR 39 films with size 1 x 1 cm^2 is used as the detector. The patients are classified based on the treatment site as pelvic, abdomen and thoracic cases. During the treatment delivery CR 39 films are placed at different locations of the patient body surface with respect to the isocenter in order to get the scattering dose to other normal areas. Each field is delivered separately and films are replaced field by field in order to get information from each field. The films are then tagged properly and taken for chemical etching. The chemical etching with 6N NaOH solution at 70˚C for 6 hrs is done and the tracks are visualised with a microscope with a recording capability.

The images are then subject to automatic counting using the TRIAC II, a Math Lab programme. The output in the excel format gives information about major axis, minor axis and angle of recoil. From this data and using a calibration graph the recoil proton energy is calculated. Then the photoneutron energy is calculated by using the equation $En = Ep/\cos^2 \theta$. Then the energy is corrected for crossection (using EXFOR ENDF) and efficiency, and is binned in to separate intervals. Then the spectrum is generated using GnuPlot. By knowing the Q value for each reaction separate reaction channels can be identified.

Results and Discussion: The out off field photoneutron spectrum on the patient surface is determined for different treatment sites. The result shows significant amount of photoneutron fluence that are produced by the interaction of photons with various body elements (isotopes of C, H, N, O etc). Later this fluence can be given as an input to one of the simulation programme like Geant4 and hence the dose can be calculated. The result shows significant amount of photoneutron dose which has to give prime importance while considering the biological effects and secondary cancer induction.

P-106

IMPACT OF CT NUMBER CALIBRATION ERROR IN RADIOTHERAPY TREATMENT PLANNING SYSTEM

M. Nakao[1], S. Ozawa[1,2], K. Yamada[1], K. Yogo[1], F. Hosono[1], M. Hayata[1], K. Miki[2], T. Nakashima[3], Y. Ochi[3], D. Kawahara[3], Y. Morimoto[4], T. Yoshizaki[5], H. Nozaki[6], K. Habara[6], Y. Nagata[1,2]

[1]Hiroshima High-Precision Radiotherapy Cancer Center, [2]Department of Radiation Oncology, Institute of Biomedical and Health Science, Hiroshima University, [3]Department of Clinical Support, Hiroshima University Hospital, [4]Department of Radiology, Hiroshima Prefectural Hospital, [5]Department of Radiation Therapy, Hiroshima City Hiroshima Citizens Hospital, [6]Division of Radiology, Hiroshima Red Cross Hospital and Atomic-bomb Survivors Hospital, Hiroshima, Japan.
E-mail: nakao@hiprac.jp

Introduction: The accuracy of computed tomography (CT) number calibration is a key component for dose calculations in an inhomogeneous medium. There are two types of CT calibrations in radiotherapy treatment planning systems (RTPSs) for external photon beam radiotherapy; one is CT to relative electron density (CT-ED) calibration and another is CT to mass density (CT-MD) calibration. In a previous work, tolerance levels of only CT-ED calibration were reported, and it was shown that the tolerance levels of CT-ED calibration became stricter with an increase in tissue thickness and decrease in the effective energy of a photon beam. For the last decade, a low effective energy photon beam (e.g. flattening-filter-free (FFF)) has been used in clinical sites. However, its tolerance levels for CT-ED and CT-MD calibrations have not been established yet.
Objectives: The purpose of this study was to establish tolerance levels of CT-ED and CT-MD calibration for each tissue type with an FFF beam used in treatment planning.
Materials and Methods: The tolerance levels were calculated using the tissue maximum ratio (TMR) and each corresponding maximum tissue thickness. To determine tolerance levels of CT-ED calibration, TMR data from a Varian accelerator and the adult reference computational phantom data in the International Commission on Radiological Protection publication 110 (ICRP-110 phantom) were used in this study. The 52 tissue components of the ICRP-110 phantom were classified by mass density as 5 tissues groups including lung, adipose/muscle, cartilage/spongy- bone, cortical bone, and tooth tissue. The CT-ED calibration tolerance level of each tissue group was calculated when the relative dose error to local dose reached 2%. In addition, averaged electron density and averaged mass density were calculated for 5 tissues groups with ICRP-110 phantom, and 5 proportionality factors were calculated for each tissues group. The tolerance levels of CT-MD calibration was converted from the tolerance levels of CT-ED calibration with above proportionality factors.
Results and Discussion: The CT-ED calibration tolerance levels of a 6 MVFFF beam for lung, adipose/muscle, and cartilage/spongy-bone were ±0.044, ±0.022, and ±0.044, respectively. The thicknesses of the cortical bone and tooth groups were too small to define the tolerance levels. The CT-MD calibration tolerance levels of a 6 MVFFF beam for lung, adipose/muscle, and cartilage/spongy-bone were ±0.045, ±0.022, and ±0.045, respectively. Because the tolerance levels are stricter with a decrease in the effective energy of the photon beam, the tolerance levels are determined by the lowest effective energy in useable beams for radiotherapy treatment planning systems.

P-107

DOSIMETRIC EVALUATION OF HEART DOSE USING INDIGENOUSLY FABRICATED BEE-WAX PHANTOM IN THE TREATMENT OF OESOPHAGEAL CANCER

T. Suresh

Department of Radiation Oncology, Bharath Hospital and Institute of Oncology, Mysore, Karnataka, India. E-mail: thasuresh@gmail.com

Radiotherapy affects both tumor cells and normal cells. The estimation of absorbed dose to the nearby Organs-at-Risk (OAR) in the IMRT treatment is essential. In-vitro dosimetric verification prior to patient treatment has a key role in accurate and precision radiotherapy treatment delivery. The aim of this study is to determine the absorbed dose to the heart in the treatment of Carcinoma Oesophagus based on the TPS calculation and direct measurements on the wax phantom. Ten Oesophagus cases were planned using Eclipse TPS. All the measurements were carried out on Siemens Primus Plus Linac with indigenously fabricated 'Bee-wax' Thoracic phantom. The dose is measured using 0.6cc ionisation chamber with PTW UNIDOS E electrometer. Ion chamber is fixed in the cavity at center of the phantom with its longitudinal axis perpendicular to the direction of the beam. 1.25 mm thickness CT slices of phantom were imported on TPS Eclipse version 13.6. The various plans already done for actual patients were imported on phantom and dose was calculated using anisotropic analytical algorithm version 13.07.16 with 2.5 mm grid size. Verification plan was created for each patient plan on to the wax phantom. The dose was calculated at the position of the heart, at a depth of 7 cm from the surface of wax phantom. The IMRT verification plans were delivered by Linac with dynamic dose delivery technique and doses were measured and compared with doses planned on TPS. The variation between planned and measured dose were calculated and is found to be within the tolerance limit (less than ±3%) as prescribed by ICRU 83. The percentage of variation measured in the wax phantom is slightly high for certain cases which might be due to high gradient dose distribution nature of IMRT and lack of lateral electronic equilibrium for small field. The electron density of water and bee wax are almost similar, and using the mentioned bees wax phantom was a good choice for primary study.

P-108

RELATION BETWEEN COMPOSITE AND INDIVIDUAL BEAM IMRT QA

Pooja Moundekar, V. K. Sathiyanarayanan, Amit Nirhali, S. Mithun, Basu Sumit, Bhooshan Zade

Department of Radiation Oncology,

Ruby Hall Clinic, Pune, Maharashtra, India.
E-mail: pooja27790@gmail.com

Aim: The purpose of the study is to find the relation between the composite and individual beam fluence gamma passing rate in a patient specific IMRT QA.

Background: IMRT has been implemented in most of the centers across the country. The proximity of the critical structure to the tumor leads to a very complex dose distribution with steep dose gradient justifying IMRT QA. The 3% dose and 3 mm distance to agreement is the most widely used criteria for accepting the IMRT QA. But not always this passing criteria is full filled and some plans fail with a very bad %gamma and it usually leads to repeating the QA. In this study gamma analysis for each beam is done separately and tried to find whether or not the gamma passing of individual beam plays some role in composite gamma passing rate.

Methods: The patient specific IMRT QA was performed using Siemens Oncor Impression LINAC with 82 leaf OPTIFOCUS MLC with 1 cm leaf width. The IMRT plan was executed on Iba's IMatrix with actual gantry and couch angles. 15 IMRT plans were selected for whom the IMRT QA gamma passing rate defined by 3%/3 mm criteria for composite plan were below 90%. For these plans individual beam analysis was performed. Comparison was done between the average of individual beam and the composite fluence gamma passing rate.

Results and Discussion: The comparison showed a large variation in the percentage difference between the average of the individual beam and the composite fluence gamma passing rate varying from as low as 0.65% to 61%.

It was observed that for the plans for which the composite fluence gamma passing rate was very low had one or more beam with very low gamma passing rate and for majority of such cases these beams being dead lateral i.e. gantry 90° or/and 270° or for beam angles very close to lateral angles. This could be consequence of combination of several things like effect of gravity at gantry angles closer to 90°/270°, positional inaccuracy of MLC's, angular dependency of response of IMatrix etc; which we assumed to get diluted due to averaging effect from all gantry angles. Also further study needs to be carried out using film dosimetry to include the effect of spatial resolution of the detectors.

It was also observed that for some IMRT plans, the individual beam gamma passing rate for every beam was above 90% and still the composite gamma passing rate was below 90%. From this, we can infer that the direct averaging of the individual beam gamma passing rate and the composite beam gamma passing rate are not related linearly and needs to be studied further.

Conclusion: For majority of the IMRT plans for which the composite gamma passing rate was very low either had lateral beam angles or angles very close to them indicating the gravity effect acting on the MLC's at such angles, which may be machine specific in addition to the angular dependency of the IMatrix response and thus justifying the low gamma passing rate.

The composite gamma passing rate and the individual beam gamma passing rate were compared and it was found that average of the individual beam gamma passing rate is not linearly related to the composite gamma passing rate and this relation needs to be studied further.

P-109

EFFICACY OF EPIQA IN QUALITY ASSURANCE OF RAPIDARC –OUR INSTITUTIONAL EXPERIENCE

S. Vendhan[1,2], R. Murali[2], N. Arunai Nambiraj[3], S. Dhivya[1], K. Ganapathy[1], S. Saraswathi Chitra[1], V. Murali[1]

[1]Department of Radiation Oncology, Apollo Cancer Institute, Chennai, [2]Department of Physics, School of Advanced Sciences, VIT University, [3]Centre for Biomaterials, Cellular and Molecular Theranostics, VIT University, Vellore, Tamil Nadu, India. E-mail: subramanivendhan@yahoo.co.in

Introduction: EPIQA™ (EPIdos, Slovak Republic) is a QA software that allows to convert a dosimetric image acquired by an Electronic Portal Imaging Device (EPID) into a dose map in water using Generalized Linear Algorithm for amorphous silicon (GLAaS) and to compare the dose map with a reference dose distribution from TPS. The GLAaS derives calibration factors for EPID's pixels using empirically measured dataset.

Objective: To evaluate the effectiveness of EPIQA in quality assurance (QA) of Rapidarc treatment plans.

Materials and Methods: For the purpose of EPIQA commissioning, set of dosimetric EPID images for open and transmitted fields of different field sizes are acquired for energies 6X and 10X. The acquired images along with output factor table using ionization chamber in a water phantom are fed into EPIQA to configure GLAaS algorithm parameter data file. This parameter data file is specific to individual linac and EPID for each energy.

Dosimetric images are acquired at isocenter plane with aS1000 EPID for twenty Rapidarc QA treatment plans delivered at Truebeam STx linac equipped with HD120 MLC. The acquired dosimetric images were used independently in EPIQA and Portal Dosimetry™ (Varian Medical Systems, Palo Alto) workspace for QA analysis as shown in Figure 1. For rapidarc plans, portal dosimetry QA using Portal Dose Image Prediction (PDIP) algorithm is the established standard practice at our institute. The actual treatment plan, reference dose distribution calculated at recommended geometry and EPID acquired dosimetric images exported from Eclipse TPS

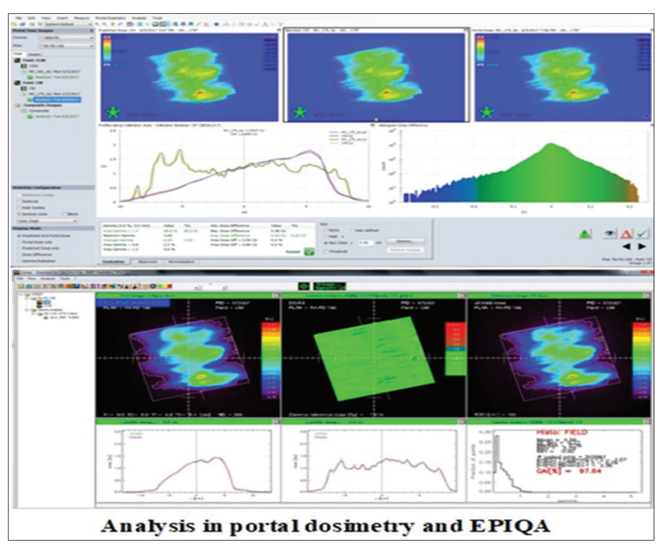

Figure 1: Ananlysis in portal dosimetry and EPIQA

to EPIQA for analysis. The 2D dose map generated by GLAaS from acquired image is compared with AAA calculated reference dose map where as in portal dosimetry, the acquired image is compared directly with predicted image by PDIP.

For both EPIQA and portal dosimetry standard 3 mm/3% (DTA/DD) gamma tools were used with area gamma ($\gamma<1$) as pass acceptance criteria for ≥95% analysed points.

Results and Discussion: Acquired portal image for all QA plans were individually analysed in EPIQA software and portal dosimetry workspace. Gamma analysis of all QA plans in EPIQA results in a minimum and mean area gamma<1 value of 95.2% and 98.1±1.5% respectively. A minimum and mean area gamma<1 value of 96.7% and 98.5±0.8% resulted in portal dosimetry.

Portal dosimetry verification is an integral part of patient database and an easy tool to execute and verify. The similar results of EPIQA software being an external third party verification tool gave more confidence on our existing QA verification system. In addition, EPIQA provides separate modules for machine QA and TPS QA which offers a valuable support in a busy radiation therapy department.

P-110

EFFECT OF LEAD FOIL ON ELECTRON CONTAMIATION TO PHOTON BEAM QUALITY INDEX: EXPERIMENTAL AND MONTE CARLO STUDY

A. S. Jagtap, Nitin R. Kakade[1], B. J. Patil[2], S. D. Sharma[1], S. D. Dhole

Department of Physics, Savitribai Phule Pune University, [2]Department of Physics,, Abasaheb Garware College, Pune, [1]Radiological Physics and Advisory Division, Bhabha Atomic Research Centre, Mumbai, Maharashtra, India. E-mail: amol_jagtapm@yahoo.com

Introduction: The photon beam quality index must be specified in order to determine the correct value of the beam quality conversion factor, k_Q. For the calibration of photon and electron beams, AAPM TG-51 and IAEA TRS-398 protocols are commonly used by radiotherapy centres globally. These dosimetry protocols are based on absorbed dose to water calibration of the recommended ionization chambers. Tissue Phantom Ratio ($TPR_{20/10}$) and percentage Depth Dose at 10 cm depth in water ($\%dd\,(10)_x$) due to photons excluding electron contamination are the recommended beam quality index in TRS-398 and TG-51 respectively. TG-51 protocol recommends to specify the photon beam quality for beams with energy 10 MV or above by measuring the value of $\%dd\,(10)_{Pb}$ with a 1 mm lead foil positioned in the path of the beam to reduce the effects of the electron contamination from the accelerator to a negligible level. The quantification of electron contribution due to presence of lead foil will enhance the confidence for safe delivery of radiation dose to patient.

Objectives: To estimate the effect of lead foil on the contribution of electron contamination for 15 MV photon beam using TG-51 protocol, both experimentally and by Monte Carlo (MC) simulation. Also, to estimate beam quality index using TRS-398 and TG-51 protocol with Monte Carlo method.

Materials and Methods: The Varian Clinac iX medical linear accelerator equipped with 6 and 15 MV photon beams was used in this study. The PDD was measured for field size 10×10 cm^2 using 0.13 cc cylindrical ionization chamber in 48×48×45 cm^3 water phantom for 6 and 15 MV x-rays. In case of 15 MV photon beam, the lead foil of thickness 1 mm was used to measure beam quality according to TG-51 protocol. Moreover, the accelerator was modelled using the EGSnrc based BEAMnrc user code. The percentage depth dose (PDD) was estimated for 6 and 15 MV photon beams at source to surface distance of 100 cm. For the case of 15 MV PD D was also estimated by keeping 1 mm thick lead in the path of beam. The particle histories of 2×10^8 were simulated to achieve required statistical accuracy less than ±1%.

Results and Discussion: The measured and MC simulated PDD values for 10×10 cm^2 field of 6 and 15 MV photon beams are well within ±1%. The comparison of beam quality index using TRS-398 and MC simulation are found to be 0.89% and 1.7% for 6 and 15 MV photon beams respectively. The percentage depth dose at 10 cm depth estimated by MC simulation for 15 MV photon beam with lead and without lead foil is within ±0.1% with the measurement. It has been observed that the contribution of electron contamination in 15 MV photon beam is reduced in the build-up region due to insertion of 1 mm lead foil. The calculated PDD of 15 MV photon beam for 10×10 cm^2 field size at SSD 100 cm with and without 1 mm lead foil shows that the contribution of electron contamination is nearly negligible after 4 cm depth. It is concluded that the Monte Carlo simulation gives the accurate estimation of effect of lead foil used by TG-51 protocol. Moreover, the beam quality index measured by TRS-398 and TG-51 is matching well with Monte Carlo simulation.

P-111

NOVEL PRECISE MEASUREMENT METHOD OF GAMMA KNIFE PERFECTION IRRADIATION TIME

Takashi Aizawa, Koji Sasaki[1], Emiko Fujii[2], Kenji Taguchi, Noriyuki Kasai[3], Naoto Yanagisawa[3]

Aizawa Health Checkup Center, Matsumoto, [1]Department of Radiation Therapy Education and Research, Gunma Prefectural College of Health Sciences, Graduate School of Radiological Technology, Maebashi, [2]Department of Pediatrics, Takamatsu Red Cross Hospital, Takamatsu, [3]Aizawa Hospital, Matsumoto, Japan.
E-mail: lupin_japan@yahoo.co.jp

Introduction: Gamma knife quality assurance guideline was issued by the Japanese Leksell Gamma Knife Society in Japan, but there is no description concerning the measurement of the irradiation time, and is not measured even by the manufacturer's inspection.

Objective: To devise a new highly accurate irradiation time measurement method and to examine its measurement accuracy.

Materials and Methods: The spherical phantom which attached to the gamma knife was installed in the movable couch and the dosimeter (PTW Freiburg TN 31010) was inserted into the spherical phantom. Then we measured irradiation time using the electrometer (TomoElectrometer; Standard Imaging) which could measure it over time. The irradiation time was calculated from the FWHM of the rising part and the falling part at a curved line of the measurement data, and the difference from the set irradiation time was measured as an error.

Results and Discussion: By using an electrometer that can measure at a sampling interval of approximately 200 ms, it becomes possible to precisely measure the irradiation time of the gamma knife. The irradiation time tended for each collimator, and it was found that there was an error of about -200 ms at 4 mm, about -40 ms at 8 mm, and about 90 ms at 16 mm. Even if the irradiation time was changed, the error was similar. Since each sector is synchronized, the difference between one sector measurement and all sector measurements is small. We have devised a new precise measurement method of gamma knife perfection irradiation time and confirmed that the irradiation time error is reproducible. By staying in control of the inherent error value for each collimator diameter, quality control by the user can be easily performed.

P-112

COMPARISON OF BEAM CHARACTERISTICS FOR FIXED AND IRIS COLLIMATORS OF M6 FI+ CYBERKNIFE® SYSTEM

M. Kannan, J. Ninan, P. Chandrasenan, H. Kaur, K. Verma, S. Goel, S. C. Pande

Department of Radiation Oncology, Artemis Hospital, Gurgaon, Haryana, India.
E-mail: mageshraja.k@gmail.com

Introduction: The CYBERKNIFE® M6 FI+ unit has two collimator systems in which the IRIS™ Variable Aperture Collimator is a computer-controlled collimator whereas the aperture of fixed collimators is static. The beam characteristics of CYBERKNIFE® vary with the configuration of the collimator.

Objective: We compared the beam characteristics of these two different collimators in M6 FI+ CYBERKNIFE® SYSTEM.

Materials and Methods: The PTW Diode E, PTW PinPoint 0.015 cm^3, GAFchromic™ film (EBT3), PTW SCANLIFT MP3 RFA, IRIS QA software were used to procure data for beam characteristics of different aperture sizes. Statistical analysis was conducted to evaluate the difference between fixed collimator and IRIS™ collimator.

Result and Discussion: The maximum relative error in aperture size was -6.8% for 5-mm collimator while the minimum relative error was -1.54% for 60-mm collimator. Output factor for fixed and IRIS™ were compared with the Composite Data, the maximum relative error was 2% and 7.3% for 5-mm collimator using PTW Diode E. Same measurements were repeated using PTW PinPoint and the maximum relative error was -23.8% and -20.57% for 5-mm collimator. In PDD measurement, the Dmax increased with increase in aperture size up to 2.5 cm for both the collimators and beyond that, there was no difference in Dmax. Surface dose was less in IRIS™ as compared to fixed collimator where the maximum relative error was -6.48% for 10 mm-collimator while the minimum relative error was -0.01% for 60-mm collimator. For both collimators, the penumbra increased with increase in aperture size. The maximum relative error was 28.7% and 32.8% for 60-mm collimator. Flatness and beam symmetry decreased with increase in aperture size for both the collimators.

P-113

EVALUATION OF HALF VALUE LAYER AND TOTAL FILTRATION IN VARIAN TRUEBEAM KV-CBCT

C. Senthamil Selvan, C. S. Sureka, M. Vadivel[1], A. Pichandi[1]

Department of Medical Physics, Bharathiar University, Coimbatore, Tamil Nadu, [1]Department of Radiation Oncology, Bangalore Institute of Oncology, Bengaluru, Karnataka, India. E-mail: surekasekaran@buc.edu.in

Introduction: The intensity of X-ray beam is an important property in kilovoltage cone beam computed tomography (kV-CBCT) for safety measures. In kilovoltage energy region, the half-value layer (HVL) is often used to describe the X-ray beam quality and characterize the effective energy by converting the HVL to the linear attenuation coefficient or mass attenuation coefficient. The HVL of a beam is the thickness of material required to reduce the intensity of an X-ray beam to one-half of its initial value. The total filtration (TF) of the beam includes the inherent and added filtration.

Objectives: To measure the half value layer and total filtration values of low kVp to high kVp in kilovoltage (kV) cone beam computed tomography (CBCT) using Nomex multimeter.

Materials and Methods: The Varian TrueBeam On-Board Imager (Varian Medical Systems, USA) and PTW-NOMEX multimeter (PTW-FREIBURG, Germany) were used to measure the output of the X-ray machines. Aluminium attenuators of 10 × 10 cm with thicknesses of 1 mm were used. The square shaped additional Al filter of more than 99.8% purity has been designed. The multimeter was positioned at 100 cm perpendicular to the X-ray tube. The first measurement was done without the aluminium attenuator. Next, the measurement was repeated with a 1 mm Al attenuator in place between the X-ray tube and the multimeter. The exposure was repeated with increasing the thickness of the aluminium in the order of 1 mm until the value approached the expected HVL value. The operating parameters were subsequently repeated for X-ray tube voltage in the range of 40 kVp to 140 kVp in 20 kVp intervals for the tube current of 100 mA and exposure time of 100 msec. In addition, a final exposure without an aluminium attenuator was repeated for every voltage to confirm the output stability.

Results and Discussion: From this study, it is measured that the averaged HVL value is 1.52 mm Al at 40 kVp and 5.83 mm Al at 140 kVp without any attenuator. With 1, 2 and 3 mm of Al, the HVL value is 1.68, 1.91 and 2.04 mm Al respectively at the lower tube voltage of 40 kVp. Similarly, at the higher X-ray tube voltage of 140 kVp, the HVL values are 6.45, 6.87, 7.28, 7.59, 7.86, 8.12 and 8.35 mm Al respectively. The measured total filtration value is 3.1 mm Al at 40 kVp, 2.7 mm Al at 80 kVp, 2.8 mm Al at 100 kVp, 120 kVp and 140 kVp without added attenuator. The measured total filtration value is 3.8 mm Al at 40 kVp, 3.3 mm Al at 80 kVp, 3.5 mm Al at 100 kVp, 3.6 mm Al at 120 kVp and 3.8 mm Al at 140 kVp with 1 mm Al. The measured total filtration value is 8 mm Al at 140 kVp with 7 mm Al etc. It is also found that these HVL and TF values are in good agreement with the International Electrotechnical Commission (IEC 2008) report, Food and Drug Administration (FDA) report, the American Association of Physicists in Medicine (AAPM) Report 08 and Atomic Energy Regulatory Board (AERB) report.

P-114

EFFECT OF PLASTIC TRAY ON THE PHOTONEUTRON DOSE EQUIVALENT AT THE ISOCENTER AND THE MAZE ENTRANCE OF MEDICAL LINACS: A MONTE CARLO SIMULATION

S. M. Hashemi Dizaji
Radiation Application Research School, Nuclear Science and Technology Research Institute (NSTRI), Tehran, Iran.
E-mail: mehdihashemmi@yahoo.com

One of the important problems of using high energy linacs is the production of photoneutrons. Besides the clinically useful beam, high energy photon beam, medical linacs produce secondary neutrons. These phtoneutrons increase dose equivalent at the isocenter of medical linac. This causes the increase of the neutron shield thickness of the treatment room maze door. In this study, the effect of plastic tray on reduction of photoneutron dose equivalent produced by a high energy medical linac at patient plane and near the maze door is investigated by Monte Carlo simulation. To determine the photoneutron dose equivalent received by the isocenter and the maze door a simplified linac head simulated. A 1 cm thick tray defined near aperture of simplified linac head. The bunker defined as a typical treatment room with the walls made of standard concrete. Neutron detectors defined as 20 cm diameter spheres at isocenter and near the maze door. Four different situations were considered, one without tray and three others with tray. Simulation carried out by running the computer to produce 1 billion particles for each case. The results show that by inserting the plastic tray in the path of the X ray beam, the photoneutron dose equivalent at the isocenter was decreased obviously compared to open field. But there is not any change in photoneutron dose equivalent near the maze door. It may be concluded that using plastic tray, decreasing photoneutron dose equivalent at the isocenter, does not reduce the photoneutron dose equivalent at the vicinity of the maze door.

P-115

AN INVESTIGATION OF COLLIMATOR HEAD SCATTER WITH COLUMNAR MINIPHANTOM

S. Palit, B. Pal, S. Das, P. Sarkar
Department of Radiotherapy, Narayana Superspeciality Hospital, Kolkata, West Bengal, India.
E-mail: bipashapal@gmail.com

Introduction: T he initial reason for introducing output factor in air is for the determination of phantom scatter factor (*Sp*). The most common method involves the measurement of the total scatter factor, *Scp*, in a phantom and the head-scatter factor output factor, *Sc*. The phantom scatter, *Sp*, is then calculated as $Sp = Scp/Sc$. AAPM Task Group 74 report recommends that build up caps with sufficient lateral and longitudinal thicknesses to eliminate electron contamination and maintain transient electron equilibrium, be used for the measurement of *Sc*. These are generally called as columnar miniphantoms.
Objectives: Our objective has been to measure head scatter factors for 6MV beam of Elekta Versa HD using high atomic number build up caps provided by the TPS vendor, and compare this with the same measurements using a water equivalent miniphantom fabricated in-house, made as per recommendation of AAPM Task Group 74. We have also included measurements of head scatter factors of unflattened (FFF) beams available in Versa HD for comparison with the same measurements for flattened (FF) beams.
Materials and Methods: The Versa HD Linac has Agility multileaf collimator with 160 leaves of projected width 0.5 cm at the isocenter**.** There are no backup collimators. Two different types of build up caps viz, made of brass and of PMMA were used to measure *Sc*. The brass build up caps were cylindrical, of wall thickness equivalent to dmax, the depth of maximum dose for a given energy. The density was 8.7 g/cc. The miniphantom had a density of1.16 g/cc and a radiological depth of 10 g/cm. The effect on *Sc* of varying SSD from 80 cm to 120 cm, for both types of build up caps was studied. The effect of wedges on *Sc* was investigated. The *Sc* was measured for the rectangular fields to check the collimator exchange effect. PTW 0.6cc chamber and Unidos electrometer were used for the measurements.
Results: A variation of *Sc* values of 2.2% was observed over the entire range of 4 x 4 cm^2 to 40 x 40 cm^2 field sizes for 6 MV-FFF. The SSD had no influence on head scatter for both flattened and unflattened beams. The *Sc* values with and without the wedge is compared in PMMA, and increases up to 5.2% in larger fields compared to without wedge. The collimator exchange effect reveals that the opening of upper jaw (MLC) increases the value of *Sc* and it is less significant in FFF beams. Sc is slightly higher (0.7%) with brass build-up cap than with PMMA mini phantom measured values, irrespective of 6MV-FB, 6MV-FFF. The Sc for 6MV-FB is lesser than the 6MV-FFF 5 x 5 cm^2 field sizes, and a maximum deviation of Sc values is 3.8%. The Sc for 6MV-FB was higher than the 6MV-FFF in 40 x 40 cm^2 field sizes, and a maximum deviation of Sc value was 1.6%. With the effect of collimator exchange, Sc values varied from 0.98% to 0.26% (6MV-FB), 0.27% to 0.18% (6MV-FFF), for field sizes from 4 x 40 cm^2 to 40 x 30 cm^2.
Discussions: The measurement of *Sc* with brass build-up cap was found to be slightly higher than PMMA mini phantom, suggesting the electron contamination at dmax depth. This emphasizes the need of *Sc* measurement at 10 cm with columnar mini phantom. *Sc* values of FFF photon beams were lesser than the FF photons beams. Our results confirm the removal of flattening filter causes a decrease in the head scatter factor. The effect of SSD is studied and has no influence on *Sc*. The presence of wedge influences the *Sc* value. The results also reveal that the *Sc* is higher, whenever X- jaw (which is actually MLC leaf bank) is set for higher field size. This may be due to the back scatter from the dose monitor chambers. The measured *Sc* values are in good agreement with the published data.

P-116

CALIBRATION OF IONIZATION CHAMBERS AND INTERCOMPARISON OF RADIOTHERAPY DOSIMETRY IN BANGLADESH

Shakilur Rahman, Shamsuzzaman, Tanjim Siddiqua, Debasish Paul, Meher Nigar Sharmin[1], Imrose Jahan[2], M. A. Mamun[2], S. M. Enamul Kabir[3]
Secondary Standard Dosimetry Laboratory, Health

Physics and Radioactive Waste Management Unit, Atomic Energy Research Establishment, Savar, [2]Department of Physics, Jahangirnagar University, Dhaka, [1]Cancer Center, Khwaja Yunus Ali Medical College and Hospital, Enayetpur, Sirajgonj, [3]Department of Radiotherapy. North East Medical College and Hospital, Sylhet, Bangladesh.
E-mail: shakilurssdl@baec.gov.bd

Introduction: Radiotherapy is the leading mechanism for the treatment of cancer patients in all over the world. External beam radiotherapy includes mainly high energy photon and electron beam from linear accelerator, tele-cobalt therapy. The outcome of the radiotherapy is highly dependent on how precisely the dose is delivered to the tumor which should not exceed ±5% of the prescribed dose including all types of uncertainties involved in the treatment procedure such as dosimetry, treatment planning and dose stability of the treatment unit etc. Current international protocols TRS-398 (IAEA), TG-51 (AAPM), and DIN-6800-2 (German) for absorbed dose to water determination are based on the calibration factor of the ionization chamber in-terms of absorbed dose to water with ^{60}Co quality. To maintain the precisional dosimetry of radiotherapy beam the Secondary Standard Dosimetry Laboratory (SSDL) of BAEC acts as a link between the field oncology centers in Bangladesh and International Atomic Energy Agency (IAEA). The ionization chambers are used at the oncology centers in Bangladesh which are calibrated from SSDL, Bangladesh against reference standard. On the other hand, the best available process of quality assurance of dosimetry of field oncology centers are to participate intercomparison by postal dose quality audit. The details of calibration of ionization chamber and intercomparison program for radiotherapy dosimetry are discussed.
Objectives: The main objectives of this research program is to ensure dose delivering to the patients and traceability of radiotherapy dosimetry and QA performed by the radiotherapy centers in Bangladesh.
Materials and Methods: A total number of 23 thimble (0.1 cc to 0.6 cc) and 3 parallel plate ionization chambers of different oncology centers of Bangladesh have been calibrated in terms of absorbed dose to water at ^{60}Co quality with standard procedure set-forth by SSDL. These chambers are regularly used for the dosimetry and Quality Control (QC) check of the respective radiotherapy centers. A participation of IAEA/WHO TLD intercomparison program has been initiated for cobalt and linac beams for oncology centers in Bangladesh by Thermoluminescence Dosimeter (TLD) postal dose quality audit program. A total number of 35 linac photon (4, 6, 10, 15 MV) and 5 cobalt beams of radiotherapy centers were participated in the intercomparison program under QA program. The TLDs (LiF powder) were irradiated with a dose of 2 Gy at reference depth 10 cm and field size 10 cm × 10 cm using standard water phantom. The irradiated TLDs were measured with PCL3 automatic reader (Fimel, France). Several correction factors such as holder, non-linearity and fading correction were applied for the absorbed dose to water measurement.
Results and Discussion: The maximum variation of calibration factors of the chambers between the manufacturer values and SSDL values have been observed within ±2.2% with an uncertainty of ±1.98% *(k=2)* for the determination of calibration coefficients at approximately 95% confidence level. The deviation of stated dose to measured dose of photon beams lies between 0.1-4.5% for linac photon and 0.6-4.0% for cobalt with an uncertainty of ±1.8% (*k=1*) . The discrepancies of one 15 MV photon beam was found 7.6%, that might be due the calibration factor of the ionization chamber. Three other photon beams were found in a large deviation which were detected due to dose calculation method. The reason of discrepancies was determined and correction is made by onsite visit by SSDL personnel.
Conclusion: The result shows an excellent agreement of calibration coefficient of ionization chamber provided by SSDL with previous values given by manufacturers. The Quality Assurance of dosimetry by hospitals meet good in agreement with international standard.

P-117

QUALITY ASSURANCE TESTS OF KV AND MV IMAGING CONDUCTED ON NOVALIS TX LINEAR ACCELERATOR

V. Poopathi, Purnendu Adak, P. Nagendran, Saibal Mukherjee
Department of Radiation Oncology, Apollo Gleneagles Hospital Ltd., Kolkata, West Bengal, India.
E-mail: vpoopathi@yahoo.com

Introduction: Commercial CT based Image Guided Radiotherapy systems allow widespread management of geometric variation in patient setup and internal organ motion. The physicist emphasis on reducing the volume of radiation therapy fields while maintaining or improving the precision radiotherapy. Reducing radiation related normal tissue toxicity, treatment position verification and correction before delivering radiotherapy had gained major importance. The LINAC manufacturers and third party vendors have developed integrated imaging systems to improve and facilitate internal patient anatomy visualization, enabling efficient positioning of the anatomical structures relative to the treatment room parameters.
Objectives: This work is to ensure the proper functioning of the integrated imaging systems in LINAC. To measure the dose contributed by the integrated imaging system and thereby ensuring the patient safety by kV and MV imaging procedures. It is also necessary to obtain proper quality of the images for the IGRT applications. Performance tests also ensure that the incorporated imaging systems will have the normal functions.
Materials and Methods: The use of imaging devices for verification and correction of patient position and target localization prior to treatment has spread widely. Novalis Tx linear accelerator include following three imaging system. i) Varian OBI system: OBI consists of two mounted arms – one for kV X-ray source (kVS) (generates photon spectra with kVp max to 150 kV/ 320 mA, collimates X-ray beam 2 X 2 cm^2 to 50 X 50 cm^2 at 100 cm from the focal spot) and other is flat panel Si detector (kVD) with size 40 X 30 cm^2. ii) Electronic Portal Imaging Devices: EPID consists of flat panel detector with sensitive area 40 X 30 cm^2 (features a matrix of 1024 X 768 pixel). EPID can be used for 2D radiographic acquisition or cine image acquisition. iii) Brainlab ExacTrac: Which includes dual diagnostic kV inclined (45^0) X-ray tubes

and a-Si flat panel detectors with a robotic couch, infrared video detectors and set of infra-red markers. The detectors have pixel size 0.4 mm and maximum sensitive area is 20.5 X 20.5 cm^2 with fatures a matrix 512 X 512 Pixel. The positioning accuracy of ExacTrac (±1 mm translational displacement and ± 1° rotational errors) can be a valuable tool in implementing frameless extra-cranial stereotactic radiotherapy.

Result and Discussion: The functionality of OBI and ExacTrac imaging system depends on various parameters such as kV and mA mechanical integrity tests and stability of X-ray tubes. We also evaluated the EPID for the safety and performance. The Winston-Lutz test was carried out for the isocenter verification. The isocenter measured was ≤1 mm. The measurement of LINAC isocenter and ExacTrac imaging isocenter was found to be within 1.1 ± 0.30 mm. The isocenter test for both kV and MV imaging was within 1.2 mm accuracy. The total filtration are measured as 3.15 mm Al for ExacTrac and for OBI 2.69 mm Al. The consistency of radiation output (CoV) are 0.005 for Exactracc and for OBI is 0.002. Accuracy of operation potential for both OBI and ExacTrac are with in ±1kV i.e. also within the tolerance limit ±5 kV. For kV imager mA linearity in terms of coefficient of linearity are within 0.02. In image quality test, visible hole is 2 mm for kv and for MV 5 mm and can resolve 1.5l p/mm. On position leakage at collimator level is 0.011 mGy in one hour for ExacTrac and that for OBI is 0.004 mGy in one hour.

We have reviewed the measured parameters and found, well within the tolerance limit. Our results also assure that the performance of the inbuilt imaging devices are suitable for radiotherapy applications.

P-118

EVALUATION OF DOSIMETRIC CHARACTERISTICS OF 2D ION CHAMBER ARRAY OCTAVIUS 729 FOR CFF AND FFF BEAMS

Bhagat Chand, Amrinder Singh Chhabra

Department of Radiotherapy, MM Institute of Medical Sciences and Research, Mullana, Ambala, Haryana, India. E-mail: bhagatbhardwaj@gmail.com

Introduction: With advances in the radiotherapy techniques like IMRT and VMAT, more robust, fast, accurate and reliable device is required for pre treatment dose verification. There are several commercially available devices for this purpose. In order to attain sufficient confidence in treatment accuracy, it is customary for medical physicists, to perform all essential dosimetric checks of such devices before clinical use.

Objectives: This study was aimed to evaluate the dosimetric response and directional dependence of the two dimensional ionisation chamber array Octavius 729 in cFF and FFF beams and to validate the performance of this device for clinical use.

Materials and Methods: The detector Octavius 729 ion chamber array (PTW Dosimetry Germany) was used in this work. It has 729 vented ionization chambers, each of 0.125 cm^3 volume, uniformly arranged over 27 x 27 cm^2 area. The array was used with solid water phantom slabs and an octagon shaped phantom (Octavius Phantom). All measurements were performed on VersaHD medical linear accelerator (Elekta Medical Systems UK). PTW Pin-point ion chamber (0.015 cc), semiflex chamber (0.125 cc) and farmer chamber (0.6 cc) were used for comprehensive differentiation of parameters.

The device was analyzed for dose linearity, SSD, dose rate dependence and output factor for all available photon beam energies. The directional dependence as a function of beam angle was measured for 6MV and 6MV FFF beam energies. The methodology for direction dependent correction factors suggested by Boggula et. al. excludes the effects of mechanical factors and that of octavius phantom was used, according to which

$$CF = \frac{R_{MATangle} / R_{MATzero}}{R_{ICangle} / R_{ICzero}}$$

where $R_{MATangle}$ and $R_{ICangle}$ are the dose measured at angles other than zero degree, and $R_{MATzero}$ and R_{ICzero} are the dose measured at zero degree with array (MAT) and semiflex chamber (IC).

Results and Discussion: All the parameters measured in chamber array were compared with the ionisation chamber response.

Linearity: The coefficient of linearity (CoL) for dose higher than 20cGy was within tolerance value of 1% for all energies. For low dose range of 2cGy-10cGy the CoL was more than 1% for all energies and maximum value of 3.86% was found for 10MV FFF. The maximum variation in linearity was 1.889% for 6MV FFF.

Dose Rate Dependence: Dose rate dependence was evaluated energy wise from 50 MU/min to 2400 MU/min. The array was found almost dose rate independent. The maximum variation in response was found within 0.1% over the range of dose rates.

SSD Dependence: The detector array shows SSD dependence similar to the farmer chamber over SSD ranges from 85 cm to 115 cm. The highest deviation in response was at lowest and highest SSDs. The variation is + 1.0%.

Output Factors: The output factors were measured for 3 x 3 cm^2 to 25 x 25 cm^2 fields. The variation found in small fields was due to overestimation in response of matrix array. The deviation in output factor measurement was higher for FFF beams.

Directional Response: Directional response as function of beam angle in increments of 5 degree was measured for 6MV CFF and 6 MV FFF beams. The array shows directional dependence and, and maximum in the angles ranges from 88 degree-110 degree and 250 degree-272 degree. Maximum value of CF is 1.043 and 1.050 for 6MV and 6MV FFF respectively.

Many investigations have been done using this device in cFF beams but not much data is available for FFF beams. Necessary action levels should be established and proper calibration must be performed with profound accuracy before use in clinical practices and in plans involving small dosimetric fields.

P-119

PERFORMANCE EVALUATION OF ONLINE IMAGING SYSTEMS ATTACHED TO MEDICAL LINEAR ACCELERATOR

C. A. Shahan Shad, Dince Francis, Daicy George, V. Ramya, P. Suresh Babu, S. Sowmya Narayanan

Vydehi Institute of Medical Sciences and Research Centre, Bengaluru, Karnataka, India.
E-mail: shahanshad23@gmail.com

Objectives: During fractionated radiotherapy, it is essential to account for inter and intra fraction movements. Quantification of such variations are done using sophisticated linacs equipped with online imaging during Radiotherapy. This technology necessitates a comprehensive Quality Assurance (QA) program to maintain and monitor the system performance characteristics, which was established at the time of commissioning. The objective of this study is to perform periodic QA on imaging systems as per various protocols and to verify the functionality, accuracy, stability and image quality of the radiographic and CBCT mode.
Materials and Methods: We tested the real time imaging systems attached to two linear accelerators, viz Varian On-Board Imaging system (OBI) and Elekta XVI. The QA tests were divided into four parts: safety and functionality, geometric accuracy, image quality and generator checks.
Geometry QA verifies the geometric accuracy and stability of the system hardware/software such as imager isocenter accuracy, 2D-2D/3D-3D matches, couch shift accuracy, magnification accuracy, field size accuracy, scaling accuracy and central beam alignment. Image quality QA checks spatial resolution and contrast sensitivity of the radiographic and CBCT images. In addition to that HU linearity and uniformity, spatial linearity, and scans slice geometry were evaluated for CBCT images. Generator check ensured that the technical parameters (KVp and mA) applied onto the system were reproduced on the X-ray tube.
A cube phantom was used to study the agreement with treatment isocenter for both kV-images and CBCT images. A marker seed phantom was used to evaluate the applications in 2D/2D and 3D/3D image registration. Printed circuit board (PCB) was used for all other geometric QA. Leeds phantom was used for verification of image quality accuracy for 2D image sets whereas Catphan® phantom was used for CBCT images. A KVp meter was used to verify the generator performance and estimating dose for a given tube rating.
Results and Discussion: The isocentric accuracy of both imaging systems was found to be stable and within 0.5 mm relative to treatment isocenter over a period of one year.
The consistency in 2D-2D and 3D-3D match was found to be within tolerance. A maximum of disagreement from expected shift is observed as 0.5 mm and 0.4 mm for OBI and XVI respectively. All other geometric verifications were found to be within tolerances and consistent over the study period.
The radiographic image of Leeds phantom showed good spatial resolution (visibility of 11th and 15th line group for OBI and XVI respectively) and contrast resolution (18th disc for both system) for 2D images. CBCT images were verified with Catphan phantom and it shows appreciable spatial resolution (7-8 disc for both system) and contrast resolution (OBI-10th line group, XVI-14th line group). The HU measurements show that the CBCT imaging system is relatively stable over time. HU uniformity were found to be 0.6% and 0.15% for OBI and XVI respectively.
Conclusion: The online imaging system is one of the most attractive features of modern radiotherapy. The proper implementation of the unit results in acquisition of better desired clinical outcome. This study shows that the OBI and XVI are precise and stable in their performance. Geometric precision of the same are within 2 mm and it is maintained through periodic verifications. Precise performance of such online imaging system reduces the setup uncertainties and thereby enhances the confidence level in delivering highly conformal radiation therapy such as SBRT, SRT, SRS, IMRT and VMAT.

P-120

MERIT OF 4D OCTAVIUS AS A PRETREATMENT QUALITY ASSURANCE TOOL IN LARGE VOLUME TARGET IRRADIATION

M. R. Mariyappan, S. Saraswathi Chitra, A. Donna, M. MuthuKumaran, V. Murali, Bhargavi Sanjay Chanderasker, B. Rajendran
Department of Radiation Oncology, Apollo Specialty Cancer Hospital, Chennai, Tamil Nadu, India.
E-mail: mari_ceg@yahoo.co.in

Introduction and Objective: Volumetric Modulated Arc Therapy (VMAT) delivery technique has proven its capability in sparing critical and normal tissues when administering large volume target plans. In general practice of VMAT treatment technique, patient plan specific Quality Assurance (QA) has been done using stationary 2D detectors with or without phantoms. Availability of limited QA equipment and the equipment's own limitations demand the end user to ensure and verify the accuracy in delivering the complex highly conformal VMAT plans.
Materials and Methods: Patients with larger target volumes like Wilm's Tumor, whole Lung and whole abdominal RT, Mesothelioma tumors with concave shaped target, Lung Sarcomas etc., with volumes ranging from 1000 cc to 2250 cc are taken for the study. Treatment plans are generated in Varian Eclipse v13 using AAA dose calculation algorithm, with a single isocentric multiple arc VMAT technique.
Achieving coverage for large target volumes with optimal normal tissue sparing required multiple arcs, making the plans more complex and warranted for verification on multiple planes. The 4D Octavius with 729 detector array, a real 3D measurement tool combined with the dose reconstruction method presented a better option for multiple planar analysis with its special function called 4D volume analysis. The 4D Octavius phantom with inclinometer rotates synchronously with gantry acquires time and gantry angle – resolved dose measurements.
Verification plans are created on the 4D Octavius phantom and delivered using TrueBeam SVC Linear Accelerator (LINAC). Gamma Analysis with 4D was performed in PTW Veri Soft IMRT QA software, keeping Treatment Planning System (TPS) dose as reference dose against the acquired dose.
Results: For the ten plans taken up for this study, pass percentage ranged from 96.4%-100% points using analysis criteria of 3%-3 mm for 3D Gamma Evaluation. When 4D calculation methods is used multiple plane such as Axial, Coronal and Sagittal comparison is possible in Array Measured data against TPS dose matrix and the gamma pass percentage ranging from 96.6-99.1%. The evaluation of sample cases is shown in Figures 1-4.
Discussion: Patient oriented pre treatment checks in addition to the 2D planar verification with 4D Octavius demonstrated the actual level of dosimetric reliability in other planes, has given confidence in executing complex irradiation methods employing VMAT for large target volumes.

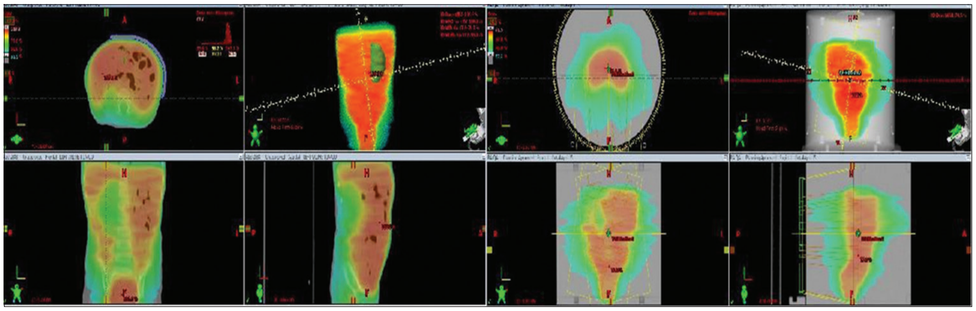

Figure 1: Patient plan and Verification plan for Wilms tumor whole abdomen RT shows the organ sparing for the large volume target

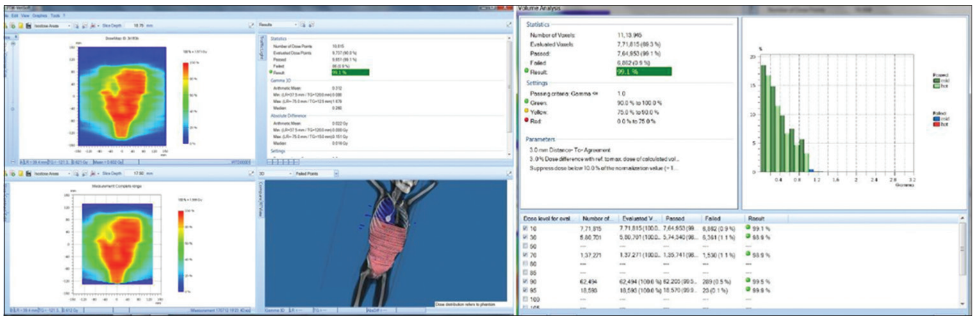

Figure 2: Octavius measurement is evaluated and shows the gamma passing results are seen in OAR (Kidney and Liver) level. Second image depicts the volume analysis using 4 Dimensional calculation method

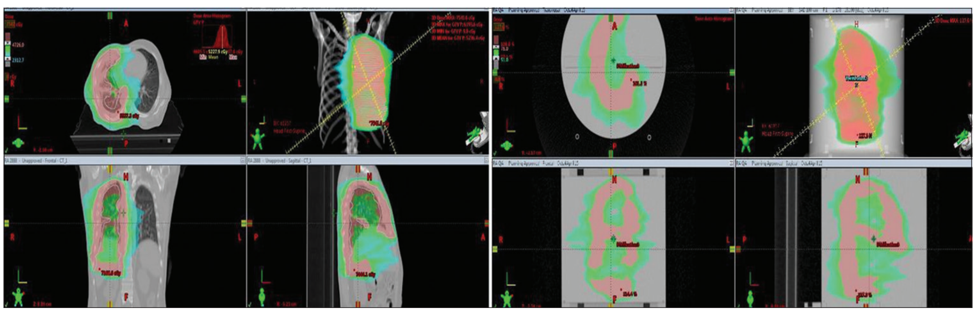

Figure 3: Patient plan and Verification plan for Mesothelioma tumors explains the complex shape of the tumor with organ sparing

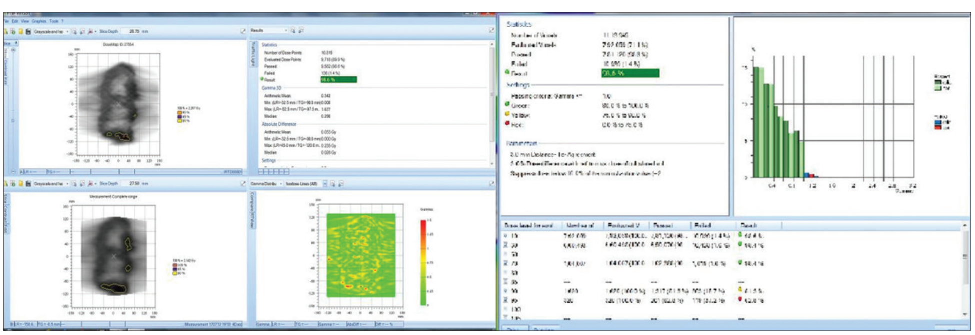

Figure 4: Octavius measurement is evaluated and shows the gamma passing results are seen in OAR (Lung) level. Second image depicts the volume analysis using 4 Dimensional calculation method

P-121

VALIDATION OF THE OCTAVIUS 4D SYSTEM WITH PORTAL DOSIMETRY FOR VMAT PATIENT-SPECIFIC QA

L. Jose Solomon Raj, S. Timothy Peace, Henry Finlay Godson, I. Rabi Raja Singh, B. Paul Ravindran

Department of Radiotherapy, Christian Medical College, Vellore, Tamil Nadu, India. E-mail: josesarc@gmail.com

Aim: To validate the Octavius 4D system with Portal Dosimetry using EPID for VMAT patient-specific QA.

Objectives: (1) To perform Patient specific QA using Octavius 4D and EPID. (2) To analyse the difference in gamma pass rate between EPID and Octavius 4D system.

Materials and Methods: The Octavius-4D system and EPID-based Portal Dosimetry were used to verify dose-maps for VMAT plans of 20 patients. Each plan consisted of two rotational arcs with a maximum dose rate setting of 600 MU/min. The recently acquired Octavius-1500 array detector consists of 1405 vented ionization chambers (0.44 x 0.44 x 0.3 cm^3). The Octavius-4D detector measured dose-maps in synchrony with gantry rotation with detector orientation perpendicular to the central axis of the beam. The aS1000 EPID detector panel with active matrix of 1024 x 768 and detector resolution 0.39 mm was used to acquire the dose-maps at SDD of 105 cm and synchronous rotation with gantry. The Octavius-measured dose-maps were compared with calculated dose-maps using Verisoft Software while the EPID dose-maps were compared using Portal Dosimetry software by gamma evaluation method.

Results and Discussion: On evaluation of the VMAT plans using EPID and Octavius 4D, the global gamma evaluation (3 mm distance-to-agreement/3% dose-difference) was found to agree well with an average pass rate of 97.83% and 99.87% pixels respectively. The slightly lower pass-rate of the high-resolution EPID could be due higher detection probability of detecting errors to and the inability of the portal prediction to model MLC leakage. The Octavius 4D showed higher gamma pass rate while providing additional 3D reconstructed dose for the treatment volume.

Conclusion: Thus Octavius 4D system was validated with EPID and was found to provide accurate dose-maps when compared with the predicted dose maps. It is concluded that the Octavius 4D with its advantage of evaluating the 3D dose information empowers the authentication of delivered dose to the entire treatment volume and proves to be an ideal tool for VMAT patient-specific QA.

P-122

STUDY OF RADIOLOGICAL CHARACTERISTIC OF SOLID PHANTOM

P. Kaliyappan, Vidya Shree

Govt. Stanley Medical College, Department of Medical Physics, Anna University, Chennai, Tamil Nadu, India.
E-mail: drkaliyappan@gmail.com

Introduction: The several solid water phantoms have been developed as being enough to natural water that they can be used for radiation dosimetry purpose. We evaluate the water equivalency of water equivalent solid phantom materials in terms of the depth dose measurement. Acrylic solid water equivalent phantoms are used extensively for the dosimetry of photon and electron beam. There are situations where a solid slab phantom is required. Many radiation detectors are not waterproof in which case a solid slab phantom must be used. Solid slab phantoms are also more useful for routine measurements since they tend to be more robust and easier, convenient to setup for any radiation measurement than water phantoms.

Objective: To evaluate the radiological characteristic of Acrylic solid phantom for radiation dosimetry and to compare the measured percentage depth dose data with published depth dose date of BJR – report number-25.

Materials and Methods: Acrylic phantom material is a clear plastic with the chemical formula $(C_5H_8O_2)_n$, polymethylmethacrylate (PMMA). It is a water equivalent with polystyrene, material composition of polystyrene with an admixture of Tio2 (2.1% ± 0.2%). It has a mass density of 1.045 g/cm^3, (Z/A)r value: 0.536, Electron density (e/g): 3.386 $x10^{23}$, Electron concentration (e/cm^3): 3.539 $x10^{23}$. The acrylic study phantom consists of 25 numbers slab; among these there are 3 slabs with 2 cm thickness, 1 slab with provision of chamber insert and the other 21 slabs with thickness of 1 cm and 1 slab with thickness of 0.5 cm. The outer dimension of all the slab is 40×40 cm. To create adequate backscatter 5 cm of slab thickness placed below the ionization chamber which is used to measure depth dose beam data.

The measurements of Percentage Depth Dose of Acrylic solid phantom was carried out using Theratron Phoenix Cobalt-60 unit, 0.65cc ionization chamber along with CD-SSD-92 electrometer. PDD was measured at the treating distance of 80 cm SSD for various field sizes 6×6 cm^2, 8×8 cm^2, 10×10 cm^2, 15×15 cm^2, 20×20 cm^2, 25×25 cm^2, 30×30 cm^2 and at depths ranging from 0.5 cm to 17 cm.

Result and Discussion: The PDD was calculated using measured depth dose data for various field size and depths. The measured PDD was compared with BJR-25 for all field size which indicates that the transmission through slab phantom are as similar to that of water, the range of deviation was found to be 0 to -0.01%, which reveals that the characteristic of slab phantom is in close agreement with water phantom. The accuracy of the slab thickness was checked and rescaled. According to the IAEA International Code of Practice TRS-398, solid phantoms in slab form such as polystyrene, PMMA, and certain epoxy resin "solid water" (water substitute) phantom materials such as solid water, can be used as solid phantom for dosimetry purpose.

Conclusion: The result of PDD conforms that the characteristics of acrylic phantom is similar to that of water. Therefore conclude that the radiation beam characteristics of the acrylic solid slab phantom are equivalent to water phantoms. This acrylic solid phantom can be used for clinical dosimetry and quality assurance purpose.

P-123

DOSIMETRIC COMPARISON BETWEEN THE IMRT PLANS WITH THREE DIFFERENT BEAM NUMBER TECHNIQUES IN PATIENTS WITH CARCINOMA OF SUPRAGLOTTIC LARYNX AND INVESTIGATE THE IMPACT OF INCREASING BEAM NUMBERS ON PTVS AS WELL AS OARS

Shayori Bhattacharjee, Pranjal Goswami, Moirangthem Nara Singh, Shashi B. Sharma, Sachindra Goswami, Mithu Borthakur

Department of Medical Physics, Dr. B Borooah Cancer Institute, Guwahati, Assam, India.
E-mail: shayori.888@gmail.com

Introduction: Radiation efficiency and treatment-plan quality are closely tied to beam angle arrangements and the number of beams used in IMRT. Based on which a retrospective study has been carried out to account the effects of increasing beam numbers.

Objective: The main objective of the study is to compare dosimetrically between the IMRT plans with three different beam number techniques in patients with Carcinoma of

Supraglottic Larynx and investigate impact of increasing beam numbers on PTVs as well as OARs.

Materials and Methods: For our study, we included 10 patients which were planned on CMS XiO (4.80) TPS for seven-beam, nine-beam and eleven-beam techniques by step and shoot IMRT. All patients were simulated with contrast-enhanced CT imaging for better visualization of nodes and contouring were done in 3 mm slice thickness. The dose prescription for primary tumor (PTV1) is 66 Gy and for the nodal irradiation (PTV2) is 60 Gy, delivered in 30 fractions with the Simultaneous integrated Boost technique. Analyses were performed on comparing the Dose volume histograms (DVHs) values. Target coverage and plan quality were evaluated for parameters V95% and V107% of PTV, Dmax, CI and HI. In term of Dmax, the OARs being evaluated in this study were the Eyes, Optic Nerves, Optic Chiasm, Brainstem, Spinal Cord and in case of parotids and parotids-PTV both Dmax and Dmean values were analyzed. To determine statistical significant result, both Wilcoxon Signed-Rank sum test and Dunnet Multiplication Comparison test were performed for all the parameters.

Results: IMRT plan with Eleven-beam technique has shown better result w.r.t the parameters V95% and CI with p value 0.0084 and 0.0248 respectively for PTV2 and data presented in Table 1. In case of OARs, the DVHs analysis for both Left Optic Nerve and Spinal Cord shown that Eleven-beam was considerably best in reducing the Dmax dose with p= 0.0028 and P= 0.001 respectively as shown in Table 2. But in contrary to above two parameters, Nine-beam technique for Right Parotid and Seven-beam technique for Left Parotid with p= 0.0454and p= 0.0162 respectively shown better Dmax dose reduction compared to rest of the techniques. In addition to this, when the dosimetric data for OARs were analyzed by using Wilcoxon Signed Rank Test, statistically significant results were found in Left Optic Nerve, spinal cord, Right Parotid-PTV and Right Parotid. Eleven-beam technique was considerably

Table 1: Statistical data for comparison of dosimetric parameters of both planning target volumes

Structure	*Dosimetric parameters*	*7-beam technique*	*9-beam technique*	*11-beam technique*	*Wilcoxon signed rank test*		*Dunnet multiple comparison test*
					(7 vs. 9) beam	*(11 vs. 9) beam*	
	V95%	184.1±26.86	183.8±27.09	185.1±27.49	0.6953	0.16	0.4397
	V107%	3.548±1.462	3.832±2.109	3.570±2.089	0.4688	0.652	0.9802
PTV1	D_{max}	7226±67.57	7278±74.78	7272±75.27	0.1055	0.695	0.4054
	CI	0.9788±0.01046	0.9753±0.01073	0.9801±0.01026	0.6953	0.16	0.6653
	HI	0.1159±0.009475	0.1138±0.00960	0.1138±0.009609	0.995	0.846	0.6115*
PTV2	V95%	233.6±34.74	236.49±35.04	236.51±34.97	0.0371*	0.734	0.0084
	V107%	6.286±3.646	8.483±5.570	7.297±3.090	0.1934	0.995	0.6933
	D_{max}	6675±54.10	6680±52.39	6737±81.75	0.8457	0.77	0.4018
	CI	0.9807±0.02643	0.9929±0.02778	0.9937±0.02932	0.084	0.652	0.0248*
	HI	0.1347±0.009027	0.1291±0.006355	0.1301±0.005584	0.2274	0.55	0.5617

Symbol "*" indicate that the *P*-value is statistically significant. V95%: Volume receiving at least 95% of the prescription dose, V107%: Volume receiving at least 107% of the prescription dose, D_{max}: Maximum dose, CI: Conformity index, HI: Homogeneity index, PTV: Planning target volume

Table 2: Statistical data for comparison of dosimetric parameters of all the organ-at-risks

Structure	*Dosimetric parameters*	*7-beam technique*	*9-beam technique*	*11-beam technique*	*Wilcoxon signed rank test (P)*		*Dunnet multiple comparison test (P)*
					(7 vs. 9) beam	*(11 vs. 9) beam*	
Right eye	D_{max}	272.2±72.13	275.6±72.24	285.8±70.50	0.153	0.4142	0.3183
Left eye	D_{max}	266.5±54.79	265.0±57.20	313.1±77.82	0.5139	0.1641	0.2898
Right optic nerve	D_{max}	173.0±14.42	175.6±15.20	174.7±14.88	0.1132	0.9995	0.0596
Left optic nerve	D_{max}	164.4±11.31	171.2±11.97	163.7±12.09	0.0128*	0.0065*	0.0028*
Optic chiasm	D_{max}	164.3±11.94	165.7±11.46	163.8±11.68	0.26	0.5728	0.418
Brainstem	D_{max}	3608±205.2	3474±241.1	3361±246.0	0.1309	0.1602	0.0596
Spinal cord	D_{max}	3454±65.81	3284±93.76	3061±141.3	0.0407*	0.0137*	0.001*
Right parotid-PTV	D_{max}	5322±181.6	5400±176.5	5383±130.0	0.5566	0.8457	0.7273
Right parotid-PTV	D_{mean}	1845±97.34	1910±99.26	1870±115.6	0.0488*	0.3223	0.197
Left parotid-PTV	D_{max}	5453±286.5	5533±298.0	5553±316.5	0.1309	0.9219	0.3978
Left parotid-PTV	D_{mean}	1910±91.89	1873±83.37	1891±84.37	0.5566	0.6781	0.6201
Right parotid	D_{max}	6346±165.5	6336±156.2	6480±149.2	0.7695	0.0645	0.0454*
Right parotid	D_{mean}	2945±187.8	3015±210.9	2994±184.4	0.0488*	0.6953	0.1593
Left parotid	D_{max}	6558±145.5	6647±149.0	6733±139.0	0.1055	0.0664	0.0162*
Left parotid	D_{mean}	3016±173.7	3004±202.1	3020±180.4	0.984	0.625	0.8871

Symbol "*" indicate that the *P*-value is statistically significant. D_{max}: Maximum dose, D_{mean}: Mean dose, PTV: Planning target volume found better in reducing the Dmax dose with (p= 0.0128 & p= 0.0065) for Left Optic Nerve and (p=0.0407& p=0.0137) for Spinal Cord when compared first with Seven-beam technique and then with Nine-beam technique respectively. But in case of both Right Parotid-PTV and Right Parotid, Seven-beam technique had shown better reduction in Dmean dose with p=0.0488 compared to Nine-beam technique.

Discussion: IMRT plan with Eleven-beam technique, achieved better PTV coverage with parameter V95% and CI compared to other two techniques. However Seven-beam technique has shown better in reducing the dose for OARs such as Right Eye, Right Optic Nerve, R Parotid-PTV, L Parotid-PTV, Left Parotid. But if we exclude the OAR Parotid then Eleven-beam technique has found better in sparing the OARs like Left Optic Nerve, Optic Chiasm, Brainstem, Spinal Cord. This is because a larger number of beams provide more parameters to adjust and therefore a greater flexibility to achieve the desire dose coverage to target and spare the OARs before comes.

P-124

FEASIBILITY OF COMPUTED RADIOGRAPHY FOR PERFORMING QUALITY ASSURANCE TESTS OF TELETHERAPY MACHINES

K. C. Mahitha, Jayapalan Krishnan[1], Iqbal Ahmed

Department of Radiation Oncology, Victoria Hospital, Bangalore Medical College, Bengaluru, [1]Department of Radiation Oncology, Mangalore Institute of Oncology, Mangalore, Karnataka, India.

E-mail: mahitha.8@gmail.com

Introduction: Some of the routine quality assurance procedures performed in Radiotherapy requires usage of films or Electronic portal imaging devices (EPID). Extended Dose Rate (EDR2) and X-omatV films are widely used and require processing post exposure which requires an automatic film processor or dark room facilities, which are almost non-existent in most institutes as they have migrated to digital radiography. Gafchromic films on the other hand are self-developing but are more expensive. EPID is a good alternative to films but is a facility only available with advance linear accelerators. Many institutions in India still function with telecobalt units and/or linear accelerator with basic facilities. Though films are a gold standard in radiotherapy, there is a need to find an alternative that is simple and cost effective to perform some of the frequency based quality assurance tests like Light and radiation field congruence, Spokes test for collimator, couch and gantry isocentre and Parallelism of jaws as per the TG-142 and AERB protocols.

Objectives: This study aims at finding the feasibility to use Computed radiography (CR) for performing quality assurance tests like Light and Radiation field congruence, Collimator, couch and Gantry spokes test and Parallelism of jaws in Telecobalt and Linear accelerator units.

Materials and Methods: CR cassette was used for the tests on Linear accelerator and Telecobalt units. For all the above mentioned tests except the gantry isocentre, the CR cassette was placed perpendicular to the beam axis with the gantry in 0^{o} position. The cassette was placed and the sensitive plane of the cassette was matched at the isocentre with 1 to 2 cm build up in Telecobalt unit and no build up in Linear accelerator unit. Field size of 10x10, 15x15 and 20x20 cm^2 were irradiated to check for the light and radiation field congruence with the minimum MU/ beam ON time. Lead wires were placed at the field edges and at the centre of field to distinguish the field edges. For the Collimator and couch isocentre the X jaws were closed completely and the Y jaws were opened to 20x20 and the Collimator and couch were rotated at a 30 degree interval to obtain a star pattern. The gantry isocentre test was performed in a similar fashion but with the CR cassette placed vertically on the couch. These tests were only performed on the linear accelerator unit and not on the Telecobalt unit because of the machine limitations. To check for the parallelism of jaws the CR cassette was irradiated for a field of 10x10 anteriorly and a field of 20x20 posteriorly. Lead wires were placed at the field edges for ease of measurement. The garden fence test for quality assurance of multileaf collimators (MLC) was also performed to check whether CR can be an additional tool for the MLC static and dynamic positional quality assurance procedures.

Results and Discussions: The results were within the tolerance limits for the respective tests. CR cassettes provided images with good contrast and resolution with minimum exposures and are a good alternative to films as they mimic the film in most aspects (except dose rate) but are reusable, inexpensive and much easier to process unlike films. These can be a good alternative in place of films at institutes with no facilities for electronic portal imaging and/or where they cannot afford to use slow films for routine quality assurance procedures.

P-125

TO INVESTIGATE THE EFFECTIVENSS OF EDGE DETECTOR FOR DEPTH DOSE MEASUREMENT IN BUILDUP REGION OF 6 AND 10 MV FFF PHOTON BEAMS

A. S. Jagtap[1,2], C. V. Arundev[2]

[1]Department of Physics, Savitribai Phule Pune University, Pune, [2]Department of Radiotherapy, Alexis Multispeciality Hospital, Nagpur, Maharashtra, India.

E-mail: amol_jagtapm@yahoo.com

Objectives: To investigate the effectiveness of the edge detector over 0.125 cc cylindrical chamber and parallel plate chamber for the measurement of percentage depth dose curves in the buildup region of 6 and 10 MV FFF beam for the commissioning.

Introduction: Commissioning is one of the most important parts of the entire QA programme for both the treatment planning systems (TPS) and the planning process. Dosimetric parameters such as percentage depth dose, profiles and output factors are important for the commissioning of treatment planning systems in radiotherapy. Nowadays, along with nominal photon beams, flattening filter free (FFF) beams are being used for the treatments where high dose is required in single or few fractions. Since FFF beam uses very high dose in very short time, the accurate measurement of dosimetric data for FFF beam becomes very important. Thimble ionization chamber with volumes of the order of 0.1-0.2 cc is commonly used for these types of measurements. The disadvantage of 0.1-0.2 cc chamber is they are not suitable for the measurement of PDD in shallow depths due to the wrong estimation of surface doses. A buildup region is the most sensitive region of PDD curve, which if not measured accurately, would lead to wrong dose calculations by TPS.

Materials and Methods: For this work, all the measurements are done on Varian made TrueBeam machine. This machine is equipped with 6, 10, 15 MV nominal photon beams and 6, 10 MV FFF beams. We have used 6 & 10 MV FFF beam for PDD measurements, especially in the buildup region. PDD is measured for 5x5, 10x10, 15x15, 20x20 cm^2 field sizes at source to surface distance of 100 cm. Three chambers, including 0.125cc cylindrical chamber, edge detector and parallel plate chamber from Sun Nuclear Corporation have been used for the PDD measurement in a circular water phantom. All the measurements and setup are done according to the TRS-398 protocol.

Results and Discussion: For all field sizes and both FFF photon beams, in buildup region, parallel plate chamber is giving more PDD values as compared to the edge detector and 0.125 cc ion chambers. The surface dose of 6MV FFF beam at a depth of 0.5 mm measured for 5x5 cm^2 field size by edge detector, 0.125 cc ion chamber and parallel plate chamber are 60.15%, 61.90%, 74.21% and for 20x20 cm^2 field size it is 67.28%, 69.21%, 79.08%. However, The surface dose of 10 MV FFF beam at a depth of 0.5 mm measured for 5x5 cm^2 field size by edge detector, 0.125 cc ion chamber and parallel plate chamber are 43.55%, 44.44%, 55.51% respectively and 51.35%, 52.73%, 62.79% respectively are for 20x20 cm^2 field size. The value of Dmax for 6MV FFF using edge detector, 0.125 cc ion chamber and parallel plate chamber are 1.26 cm, 1.27, 1.139 cm respectively for 5x5 field size and 1.27 cm, 1.14 cm, 1.145 for 20 x 20 cm^2 field size respectively. Similarly the value of Dmax for 10 MV FFF beam using edge detector, 0.125 cc ion chamber and parallel plate chamber are 2.14 cm, 2.14 cm, 2.14 cm respectively for field size of 5x5 cm^2 and 2.03 cm, 2.01 cm, 1.89 cm respectively for 20 x 20 cm^2. It has been concluded that edge detector is good choice for the measurement of PDD in the buildup region during commissioning.

P-126

IS THE TPS NEED TO RECOMMISSONED AFTER THE REPLACING THE BEAM CENTER ALIGNMENT?

C. Krishnappan[1,2], C. Anu Radha[2], G. Madhan Kumar[1], J. Antony Paull[1]

[1]Department of Radiation Oncology, Apollo CBCC Hospitals, Gandhinagar, Gujarat, [2]School of Advanced Sciences, VIT University, Vellore, Tamil Nadu, India.
E-mail: c.krishnappan@gmail.com

Introduction: In developing countries like ours wherein the ratio of the number of linacs available per million population is very less, the patients need to travel miles to get the radiotherapy treatment. Naturally, it is expected to maintain as minimal downtimes as possible and finish the treatment at earliest. But Instances like the failure of ion chamber, waveguide or beam centerline requires an enormous amount of post replacement work from a medical physicist so as to ensure radiation safety to patients. The quality assurance (QA) work starts with few basic tests and measurements to check for the beam properties. The big challenge for the physics team is to take the call on beam data matching, the entire beam data have to compare and match with the previous data on which the TPS is being commissioned.

Objectives: Assurance of the beam matching after replacing the beam center alignment of the Varian Unique machine.

Materials and Methods: To check the feasibility to continue the same existing beam data of 6MV Xray in TPS, different types of plans which were earlier generated with old beam data in TPS were delivered at machine, measured in a phantom and the results are compared. Point dose measurements have made for three open fields, static MLC fields at different region as mentioned in TG 53 and its comparison with TPS calculated value. And For dynamic treatemnts TG 119 Test cases are compared at point dose with portal dosimetry levels. The generated plans for some test cases are shown in Figure 1. For patient specific assurance especially of the treatments like IMRT/Rapidarc, three patients each with different sites (Brain, H&N, Pelvis) which are planned earlier with old data. Patient specific QA of point doses at isocenter and off axis were measured and compared. Also IMRT/VMAT QA has been repeated and verified using EPID for the same patients. For evaluation the portal dosimetry the 3 mm/3% DTA/DD criteria is set.

Results and Discussion: For Maximum point dose vartiation at static (open & MLC) fields for the inner and outer region is 1.3% & 0.90% of the field size of 25x25 cm^2. For the same static fields the maximum variation of buildup and penumbra region is 2.4% and -11.70% of the field size of 25x25 cm^2 and 10x10 cm^2 respectively. In the case of dynamic fields TG 119 Test case plan QA results the confiedence limit is 0.022 and 0.033 for high and low dose region. The portal dosimetry results for the same test cases the average area gamma variation less than one are 98.4%. Patient specific point dose QA results for all IMRT/Rapidarc plans were found less than 1.6%. Analysis of portal dosimetry for the same patients plans average area gamma variation less than one are 97.6%. Our results show that after the replacement of beam center alignment, there is no significant variation at machine specific or at patient specific QA due to beam data. The 6MV photons before and after beam center line replacement are said to be matched and clinically patients can be taken with greater confidence

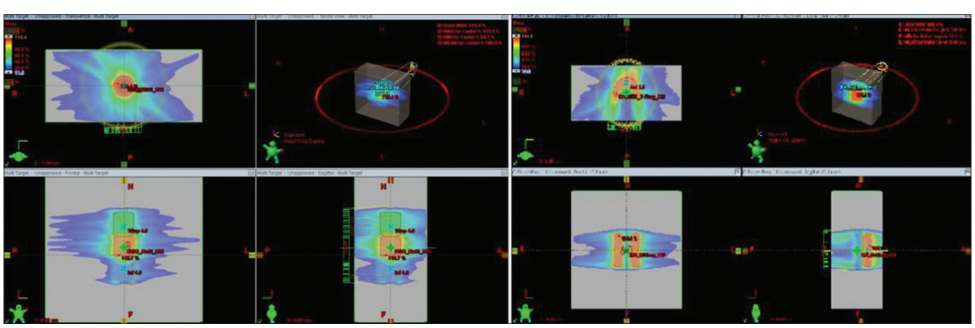

Figure 1: Plans generated for the TG119 test case suite

without any need for beam data modification in TPS. Since the beam center alignment is directly related to the beam data without a second thought, it is recommended to ensure the beam data matching before and after the replacement. If any notable difference is found at any stage it is better to recommissioned the beam data.

P-127

PATIENT SPECIFIC IMRT QA BY USING EBT GAFCHROMIC FILM QA PRO2016 SOFTWARE – INITIAL EXPERIENCES

V. R. Gedam, P. S. Negi, M. Sasindran, M. Mahur, R. Sharma, A. Singh, D. Kumar, R. K. Grover
Delhi State Cancer Institute, Delhi, India.
E-mail: varshadhargave@gmail.com

Introduction: Radiographic films have been regularly used in routine commissioning of treatment modalities and verification of treatment planning system. The radiation dosimetry based on radiochromic film has ability to give absolute two-dimensional dose distribution and prefer for the IMRT quality assurance. It is mandatory to do patient specific dose verification before irradiating the plan on patient. To ensure accurate radiation delivery before IMRT treatments, pretreatment verification prior to clinical implementation must be adequately tested in the form of delivery quality assurance to identify any potential errors in the treatment planning process and in machine deliverability. Various two-dimensional (2D) array quality assurance systems have been used for patient specific IMRT QA.
Objective: The purpose of this work is planar dose measurements were performed using Film QA Pro2016 software and compare result with ImatriXX 2-D array system of IBA. Percentage of pixels passed the 3%-3 mm gamma criterion (% dose difference and distance to agreement-DTA) was taken for the comparison. Point dose measurements were also performed and the percentage deviation of the calculated doses versus measured doses was compared.
Materials and Methods: Gafchromic EBT3 films were irradiated at different dose levels between 50cGy to 400 cGy with open fields 10 x 10 cm^2 at SSD setup and film at 5 cm depth on 6MV Oncor Expression linac. After 24 hours scanned all films on Epson Expression 11000-XL flatbed scanner and calibration curve drawn for each color blue, red, and green.
Patient specific QA was performed for 10 IMRT plans and analyzed measurements are presented here. We took 5 brain and 5 head and neck plans made on Monaco TPS 5.11.01 by using Monte Carlo algorithm. Made IMRT patient QA plans for each patient and irradiate on the solid phantom with film and on the imatrix on the linac and measured dose distribution. Now compared these dose distributions with TPS calculated dose distribution by using IMRT OmniPro software and Film QA pro2016 software. Calculate the gamma and DTA of the compared plan by using gamma index method. QA results are considered acceptable when the passing rate is greater than 95% using the gamma criteria a tolerance of dose difference (DD) of 3% and a tolerance for distance to agreement (DTA) of 3 mm
Result and Conclusion: The pretreatment verification of the IMRT for the two treatment sites was evaluated using two QA systems. The IMRT patient QA plans were verified using the gamma index method and found to be within acceptable criteria. Overall, this study confirmed that both the QA systems perform well in terms of delivery errors. However, excellent agreement (more than 90%) between the measured and calculated dose distributions for the both criteria was found for both the QA systems and treatment sites. Therefore, the results of this study suggest that the Film QA systems are also reliable verification systems for IMRT pretreatment as Imatrixx system.

P-128

ANALYSIS OF PHOTON BEAM SKIN DOSE FOR PHYSICAL AND ENHANCED DYNAMIC WEDGES FOR DIFFERENT FIELD SIZES FOR 6 MV AND 15 MV PHOTONS

Baljeet Seniwal[1,2], Ranjit Singh[2], Arun S. Oinam[2]
[1]Centre for Medical Physics, Panjab University,
[2]Department of Radiotherapy & Oncology PGIMER,
Chandigarh, India. E-mail: balysingh786@gmail.com

The introduction of high energy linear accelerator in radiotherapy allows treatment of deep seated tumors with better dose homogeneity and conformity. The greater penetration of high energy mega-voltage X-rays results in reduction of doses to the skin surface. Apart from primary radiation, electron scattered from collimator head and patient's body contributes significantly to the skin dose. The patient scattered depends upon area of the irradiation and the contribution from collimator depend upon it's distance from the patient's surface. The commercially available treatment planning algorithm (Pencil beam algorithm (PBC), anisotropic analytical algorithm (AAA)) shows a significant variation at the surface interface and the dose gradient region. Various beam modifying devices (e.g., wedges, shielding block, Multi leaf collimator (MLCs) etc.) are used in treatment planning system to adequately cover the target volume with the prescribed dose without exceeding the doses to the normal structures. The wedge filters are commonly used as a tissue compensator and it results in tilt of iso-dose curve toward thicker end. Physical and Enhanced dynamic wedges (EDW) are the two main class of wedge filters routinely used in radiotherapy. The skin dose drastically changes with the introduction of these two classes of wedge filters. The aim of the present study is to evaluate skin doses for 6 MeV and 15 MeV photon beams at different field sizes (5×5, 10×10, 15×15, 20×20, and 40×40 cm^2) and for different wedge angle (15°, 30°, 45° and 60°). The experiment was performed on Clinac DHX dual energy linear Accelerator (Varian Oncology Systems, Palo Alto, CA). The solid water phantom RW3 (dimension 30×30 cm2, 0.1-1 cm thickness range) (density 1.09 g/cc), parallel-plate ion chamber (PPC-40(IBA(S/N-913) and supermax (Standard Imaging (S/N-P09133, +300 V polarizing potential) electrometer were used for the measurement. The source to surface distance (SSD) was 100 cm and all measurements were carried out upto a depth of 4 cm with backscattered thickness of 15 cm. The percentage depth dose data were measured for all wedge angles and field sizes. The meter readings (electrometer) were recorded and normalized with the meter reading obtained at the depth of maximum dose.

The percentage depth dose at surface (PDD0) increases with the increase in field size, both for enhanced dynamic (EDW) and physical wedged (PW). The surface doses are slightly higher for EDW as that for same angled physical wedge.

P-129

DOSIMETRIC EVALUATION OF FLATTENING FILTER FREE AND FLAT BEAMS ON ELEKTA INFINITY LINEAR ACCELERATOR

Vyankatesh Shejal, K. K. D. Ramesh[1], N. Vinod Kumar, R. Ramu, Sebeerali

Department of Radiotherapy, Manipal Hospital, Bengaluru, [1]Department of Radiotherapy, Manipal Superspecialty Hospital, Vijayawada, Andhra Pradesh, India. E-mail: kkdramesh@gmail.com

Introduction: Elekta Infinity linear accelerator system with agility head introduces a number of novel components which could uniquely impact imaging and treatment workflows. Existing linear accelerator configuration has standard features such as dynamic leaf guide, no backup jaws and Standard dose rates. One hundred and sixty 5 mm (projected width at isocenter) multileaf collimators (MLCs) travel up to 3 cm/s over the full 40x40 cm^2 field-of-view. The MLC carriage can travel at 3.5 cm/s for a maximum MLC leaf speed of 6.5 cm/s. However since higher dose rate on the existing machine was not a licensed option; this study was intended towards the licensing/type approval testing of High dose rate modes on Infinity linear accelerator.

Objective: The purpose of this study was to qualitatively evaluate the dosimetric characteristics of flattening-filter-free (FFF) and flattened beams on Elekta Infinity Medical Linear accelerators after its upgrade with High dose rate mode.

Materials and Methods: Two Elekta Infinity Medical Linear accelerators (Sr. No. 153324 & Sr. No. 153237) were qualitatively evaluated in this study. During the acceptance testing and commissioning measurement of unflat mode, prior upgrade & post upgrade measurements were performed on Elekta Infinity linac equipped with 160 leaf multi-leaf collimators (MLCs), five photon (4 MV, 6 MV, 10 MV, 6 FFF and 10 FFF) and six electron energies. The beam data's were confirmed to be within the manufacturers and National Task Group recommendations for its clinical use. Primarily, mechanical and dosimetric data's were measured and evaluated to check the consistency of data. The analyzed data included the PDDs, profiles, penumbra measurements, surface doses, out-of-field doses, output factors & MLC transmission for flat and unflat beams on Elekta Infinity Linear accelerator.

Results and Discussions: The Measured TPR20, 10 Values in both 6 and 10 MV flat & unflat modes were found identical. In comparison to flattened beams, Dmax for FFF beams was deeper for all field sizes measured. The 6MVFFF and 10MVFFF beams had higher surface doses than the corresponding flattened beams for field sizes of up to 10X10 cm^2 but had lower surface doses for larger fields. The penumbras of FFF beams for smaller field sizes were found to be sharper than those of flattened beams due to the reduced head scatter however a wider penumbra was observed for larger field sizes. The FFF beams showed smaller variations in beam quality along the off-axis in comparison with flat beams. The head scatter factor on an average showed lesser variations for the 6MVFFF and 10MVFFF beams, respectively and the variations in the phantom scatter factor were also smaller. Both FFF beams had lower average MLC transmissions & the out-of-field doses than the flattened beams.

P-130

COMPARATIVE STUDY OF PERCENTAGE SURFACE DOSE MEASUREMENT FOR 6MV FLATTENED AND 6MV FLATTENING FILTER FREE PHOTON BEAMS USING PARALLEL PLATE CHAMBER INCLUDING AND EXCLUDING ITS OVER-RESPONSE CORRECTION.

Srimanta Pamanik, Dilip Kumar Ray[1], Arka Choudhury, Asik Iqbal, Amitabh Ray, Sayan Kundu, Sandip Sarkar

Department of Medical Physics, Chittaranjan National Cancer Institute, [1]Department of Medical Physics, Ruby General Hospital Ltd., Kolkata, West Bengal, India. E-mail: skpramanik20@gmail.com

Objectives: The purpose of this study was to investigate the surface dose of 6MV flattening filter free (FFF) photon beam in the build-up region and to compare it with 6MV flattened (FF) photon beam with the help of parallel plate chamber with and without its over-response correction. Correction factors are specific to each chamber as ion chamber has its own guard size, plate separation and volume.

Materials and Methods: A Varian Clinac iX with 6MV FFF mode linear accelerator has been in clinical operation with 6MV, 15MV, flattened and 6MV (FFF) unflattened photon beams. The entrance dose was measured for 6MV FF & 6MV FFF energies using a parallel plate chamber (Markus; product code-23343; PTW Freiburg) with a thin (0.025 mm) entrance window of water equivalent material in a solid water phantom with build-up region 0-20 mm depth for different field sizes 5x5, 7x7, 10x10, 15x15, 20x20, 25x25 and 30x30 cm^2. In SAD technique we measured the tissue maximum ratio (TMR) with temperature and pressure correction and was converted into PDD with over response correction (Mellenberg correction) for parallel plate chamber. From the above measurement we had found a depth-dose curve which was a sixth order polynomial equation for each field size. From the polynomial equation percentage surface dose had been calculated at 0.5 mm depth.

Results and discussion: The percentage surface dose was measured from sixth order polynomial equation ($Y = aX^6 + bX^5 + cX^4 + dX^3 + eX^2 + fX + g$), where Y and X were percentage dose and depth (in mm) respectively. The study shows the percentage surface dose was 5 to 7 percent higher for 6MV FFF photon beams than 6MV FF photon beams for all field sizes. The percentage linearly increased with field size for both energies. Applying over response correction for Markus type parallel plate chamber, the percentage surface dose reduced significantly up to 10 to 12 % for both energies from uncorrected over response values for all considered field sizes.

Conclusion: The estimation of surface dose in the build up region without over-response correction for parallel plate chamber shows over dose for both flattened and unflattened photon beam. For surface dose measurement in the build-up region one should consider the overresponse correction for the considered ionization chambers for all photon energies and field sizes.

P-131

MEASUREMENT OF PERCENTAGE DEPTH DOSE BASED ON POINT DOSIMETRY FOR TELECOBALT UNITS

A. Hemalatha, M. Athiyaman, Arun Chougule[1], Ganga, H. S. Kumar[2]
Departments of Radiological Physics and [2]Radiotherapy, S.P. Medical College and AG Hospitals, Bikaner, [1]Department of Radiological Physics, S.M.S Medical College, Jaipur, Rajasthan, India.
E-mail: athi.roja87@gmail.com

Introduction: Percentage depth dose is one of the essential parameters for dose calculation for teletherapy based treatment machines. The telecobalt units percentage depth dose of any cobalt machines are taken from the published data such as Br J Radiol 1978, and related appendix provided in various text books. The clinical physicist have to follow the published tables for dose calculation for SSD based treatments. Even though these tables provide accurate values of PDD there may be a need to verify these published values; In routine the PDD values can be measured only with the beam profiler and hence the hospitals that have single telecobalt units may lack of having the beam profiler. In this study we attempted to provide a solution to measure the PDD values based on point Dosimetry by clinically used secondary standard dosimeter. The measured PDD values by our suggested method was compared with the standard published tables and their percentage of deviation is estimated.
Objective: To estimate the PDD values of three telecobalt units available in our department based on point Dosimetry by using Farmer type Ion chamber.
Materials and Methods: The ionization measurements are carried out in the telecobalt units. Solid phantom with thickness of 1gm/cm^2 is used for this study. Measurements were performed at the depths of 1 cm, 5 cm, 10 cm, 15 cm, 20 cm & 25 cm for the square field sizes 5, 10, 15, 20, 25, 30 cm^2. Considering the necessity of getting the d_{max} ions at surface is measured by keeping SSD 79 cm and the ion chamber at 1 cm depth. The D_{max} is estimated by interpolating the values of 1 cm & Surface measured values. All the other values are normalized with respect to the 0.5 cm values. The in-between values are estimated by applying Linear interpolation method. The obtained values were compared with the standard published tables and their percentage of deviation was estimated.
Results: To gain initial confidence on this work the standard and routinely used values, PDD @ 5 cm & 10 cm depth for 10x10 cm^2 are noted in the calculated values. It is found that the calculated PDD values were 78.5% & 55.6% respectively for 5& 10 cm depths. The estimated average percentage of deviation is within -0.68% and maximum of 3.85%.
Discussion: The proposed method of measuring the PDD, interpolating from the fixed depth ionization values, can be used in telecobalt units for cross verifying the standard published values. This method is performed without the beam profiler. Also this can be extended to linear accelerator measurements.

P-132

COMPARING AND ESTIMATING THE BUILDUP DOSE FOR 6MV AND 10MV PHOTON BEAM WITH FF AND FFF USING VARIOUS DETECTORS

S. Surekha, G. Bharanidharan, Prakasarao Aruna, J. Velmurugan, P. Thamilkumar[1], R. R. Rai[1], S. Singaravelu Ganesan[1]
Department of Medical Physics, Anna University, [1]Department of Radiotherapy, Dr. Rai Memorial Cancer Institute, Chennai, Tamil Nadu, India.
E-mail: jeevanadhi007@gmail.com

Introduction: During the last years Radiotherapy has been practiced with flat beam profile. Recently, evolution of technology introduced a Flattening Filter Free photon beams which have stimulated medical physicist to carry out the research in radiotherapy. The removal of flattening filter alters the physics around flattening beam and the significant increase in dose rate causes softening of beam spectrum and reduction in scatter as well as decrease in neutron and photon leakage in the head.
Objective: The current study aims to compare the buildup region with FF and FFF beam for 6MV and 10 MV photon beam in a Varian True beam Medical Linear Accelerator.
Materials and Methods: The Linear Accelerator True Beam with longstand which was calibrated to deliver a dose of 1cGy per MU at 10 cm depth of water, a reference field size of 10 cm ×10 cm and a source to surface distance of 100 cm for 6MV and 10MV respectively. The detectors used were Ionization chamber, Diode detector, MOSFET (Thomson Neilson) and EDR3 Radiochromic film.
Results and Discussion: The buildup region was measured using Ionization chamber, Diode detector, MOSFET and Radiochromic film by placing the detectors at a distance of 98.5 cm and 97.5 cm at a SSD of 100 cm for 6 MV and 10 MV photon beams and 0.5 cm thickness slab were introduced one above the other to check the buildup dose for 6 MV and 10 MV photon beams. The dose response of the detectors shows that for both 6 MV and 10 MV photon beams with FFF the dose measured was higher than the FF which may be due to the scattered dose. Ionization chamber, Diode Detector and Radiochromic film shows a linear response whereas MOSFET shows linearity within slight deviation.
Conclusion: Determination of buildup dose were carried out using Ionization chamber, Diode Detector, MOSFET and Radiochromic film which clearly states that for both 6 MV and 10 MV photon beam with FFF shows a higher build up dose than beams with FF and no significant dose response was found between the detectors. Hence the study clearly concludes the buildup dose with FFF is higher than FF but the difference between the two is not significant.

P-133

FABRICATION OF QUALITY ASSURANCE TOOLS FOR QUICK QUALITY ASSURANCE TESTING OF LINEAR ACCELERATOR

S. D. Mishra
HCG-MNR Curie Cancer Centre, Ongole, Andhra Pradesh, India. E-mail: vipula_vageesha@hotmail.com

Introduction: The quality assurance tests are essential to ensure the proper functioning of the medical linear accelerator within the requisite tolerance. Various tools are required to carry out these tests. Considerable time has to be spent to carry out these tests.
Objectives: Some quality assurance tools are fabricated in the Radiotherapy Department of our centre with the following objectives.

1. Saving time by providing facility of carrying out many tests with one tool in one setting.
2. Providing an affordable alternative to costly imported tools with comparable quality.

Materials and Methods: Following tools are fabricated in the department.

1. One water phantom with a leveled platform is so fabricated that all required daily quality assurance tests can be carried out using this in one setting. This phantom can be utilised for quality index of the beam also.
2. One versatile tool to check the congruency of light field with the radiation field visually. This tool helps avoiding the inherent subjectivity in such test.
3. One accurate scanner mechanism which can be operated manually as well as electronically. This fits on the existing 30 cm X 30 cm X 30 cm water phantom. Beam profiles can be drawn on the graph paper with the help of this. Symmetry and flatness of the radiation beam can also be determined. This mechanism can be used to scan radiation beam in air. This can also be used to check the radiation field congruency with the light field.

Results and Discussion: These tools are easy to use. The setting time of these tools for the measurement is very less. These tools are cheap. The results of tests carried with these tools are comparable to the results obtained for the same tests with standard and expensive tools.
Conclusion: The quality assurance tools developed in the department are useful for a busy radiotherapy department. These tools are also affordable for the department with limited resources.

P-134

IMPACT OF PHOTON BEAM ATTENUATION AND MODELING OF TREATMENT COUCH: ANGLE AND ENERGY DEPENDENCE

M. Rafiqul Islam[1,2], P. Colleoni[2], C. Bianchi[2], M. Fortunato[2], S. Andreoli[2], M. Monjur Ahasan[1]
[1]Nuclear Medical Physics Institute, Bangladesh Atomic Energy Commission, Bangladesh, [2]Department of Medical Physics, ASST Papa Giovanni XXIII Hospital, Bergamo, Italy. E-mail: mripbaec@gmail.com

Introduction: Nowadays Carbon fiber is the material of choice for radiotherapy treatment couch. Attenuation of the photon beams is influenced not only by the thickness of the carbon fiber used in the construction of the couch surface but also by the internal materials used to sandwich the plies. The dosimetric impact from couch on dose calculation is a complex combination of increased skin dose, reduced deep dose and modified dose distribution.
Objectives: The objective of this study is to quantify the attenuation of megavoltage photon beams through carbon couch at various angles and energy and to find the correct modelling of the treatment couch parameters in the treatment planning system (TPS). A method for the evaluation of the most appropriate Hounsfield Unit (HU) sets is proposed.
Materials and Methods: The transmission of 6 MV and 15 MV photon beams from linear accelerators (Varian, USA) through IGRT carbon fiber couch was measured using the 10X10 cm^2 field size for various gantry angles. A cylindrical ionization chamber (semiflex 31010, PTW, Germany) with 0.125cc volume was inserted inside a 30x30 cm^2 slab phantom (1.045 g/cm^3) (RW3 Phantom PTW-Germany). The chamber was positioned at isocenter in the middle of a 10 cm high phantom. The attenuation was measured for two beam angles: oblique (45°-135°) and orthogonal (0°-180°), for three couch thickness (thin, middle and thick). In the TPS (Eclipse Varian – V10.0.34) the attenuation of the treatment couch model was evaluated for different sets of HU numbers. Measured and calculated attenuation was optimized to find the best modelling inside TPS.
Results: The most significant beam attenuation was observed with thick couch and oblique incidence, respectively 3.2% for 6 MV and 2.0% for 15 MV. The smallest attenuation was observed with 15 MV beam and thin couch (0.3%). Minimum aberration between the calculated and measured attenuation of the treatment couch was found for the HU values of -700 HU for the carbon couch surface, -960 HU for the inner part for 6MV and 15MV beams.
Discussion: The geometrical model of the couch in the TPS is reliable and no CT scan of the real couch seems to be necessary. A limited set of measurements for the three couch thicknesses provides reference values for attenuation at different gantry angles for low and high energy beams. This method of couch attenuation modelling into the treatment planning system is fast and easy and can result in more acceptable dose calculation accuracy.

P-135

ESTIMATION OF UNCERTAINTY BUDGET IN CROSS CALIBRATION OF SMALL VOLUME IONIZATION CHAMBERS IN CO^{60} BEAM – AN APPROACH TOWARDS QUALITY CONTROL IN DOSIMETRY

Narender Kumar, LibinScaria, Rajesh Kinhikar, C. M. Tambe, J. P. Agarwal[1], D. D. Deshpande
Departments of Medical Physics and [1]Radiation Oncology, Tata Memorial Hospital, Mumbai, Maharashtra, India. E-mail: narenderkumar816@yahoo.com

Introduction: The advance radiotherapy (RT) involves high precision treatments like SRT, SRS, IMRT and VMAT which includes small fields. The dosimetry with the benchmark small volume detectors is extremely desired. Ionization Chambers (IC), supposed to be the benchmark detectors for such dosimetry need to be monitored for its valid calibration coefficient provided by Primary Standard Dosimetry Laboratory (PSDL) or Secondary Standard Dosimetry Laboratory (SSDL) traceable to PSDL. Due to ageing or post-major repairs and possible damage, response of the IC and in turn the calibration coefficient may change. Due to the limitations and logistics, PSDL may have challenges to calibrate small volume chambers for the entire country. At busy institutes, it may be challenging to keep the track of the calibration validity of the detectors and this may raise a question or there may be an ambiguity to use these detectors for absolute dosimetry for high precision RT to maintain high quality control in dosimetry. This can be overcome by cross calibrating chambers against a reference chamber traceable to PSDL. The cross calibration alone is not sufficient, hence one need to estimate the uncertainty budget as well. At our institute we have multiple ICs (with different volumes), out of which more than 10 chambers were found with calibration date expired.

Objective: To cross calibrate small volume ionization chambers & to estimate Uncertainty (Type A & B) Budget.

Materials and Methods: Chambers to be cross calibrated are three IBA CC13 (0.13cc), two PTW Semiflex (0.125cc), two Tomotherapy chambers, Standard Imaging A1SL (0.053cc), one IBA PPC_05, one PTW Pinpoint Chamber (0.015cc). An IAEA protocol TRS 469 was used for this purpose. All the measurements were performed at 5 cm depth in water with Elite 80 telecobalt machine for reference field size of 10 cm x 10 cm at source to axis (SAD) distance of 80 cm. Substitution method was followed, and a recently calibrated chamber FC65G, (0.6cc) was used as Reference chamber. Reference chamber's central electrode was placed at 5 cm depth and irradiated for 2 minutes, multiple reading were collected at +300, -300 & +150 volts to estimate saturation & polarity correction factor, temperature & pressure reading were noted for estimating $K_{T,P}$ correction factor. Shutter timer error was also taken into account. Reference IC was replaced with Field chamber to be cross calibrated and whole set of measurement was repeated. Ratio of mean value of corrected meter reading of two chambers and value of calibration coefficient of Reference IC were used to calculate calibration coefficient for field IC. For uncertainty budget estimation Guide to Uncertainty Measurement (GUM) & IAEA Tecdoc-1585 were followed. For Type A uncertainty: positional uncertainty, uncertainty in meter reading collected (reproducibility), and uncertainty in temperature were estimated. For Type B uncertainty due to Resolution of electrometer, Thermometer, Barometer& uncertainty quoted in calibration certificate provided from PSDL for reference chamber were estimated. Finally total relative standard uncertainty was estimated.

Results and Discussion: Calibration coefficient for each detector were calculated and percentage deviation from the original calibration certificate (old $N_{D,W}$) were estimated. The mean deviation (percentage) for CC13 0.36% (0.27 to 0.63%), Semiflex 1.05% (0.33 to 1.78%), A1SL 1.58% (1.03 to 1.87%), PPC_05 0.34%, Pin_Point 3.68%. Uncertainty in $N_{D,W}$ @ 95% (or 2σ) confidence level is ±3%. It was observed that due to ageing Response of Pin point Chamber might changed, new calibration coefficient has been estimated and being used for small field dosimetry.

P-136

CHARACTERISTICS COMPARISON BETWEEN PHYSICAL WEDGE AND VIRTUAL WEDGE USING 6 MV PHOTON BEAM

N. Singh, A. Sinha[1], K. Purushothaman[1], R. N. L. Srivastava[1], N. K. Painuly, T. Verma, S. Srivastava

Department of Radiotherapy, King George's Medical University, Lucknow, [1]Medical Physics Section, J.K. Cancer Institute, Ganesh Shankar Vidyarthi Memorial Medical College, Kanpur, Uttar Pradesh, India.
E-mail: ashutosh22jan@yahoo.com

Introduction: In modern era most of the cancer centers are having Megavoltage Linear Accelerator machines. From the supplier of LIANC, wedge filters were supplied as accessories. Besides physical wedge, virtual wedge produces the same wedge intensity gradient by closing one jaw gradually while the beam is in on position. Wedge can be used to compensate for sloping surface as well to compensate for missing tissues. In our study we discuss about the charactertiricts of both types of wedge taking in to account various parameters. Further surface dose was also measured using both type of wedge.

Objective: This study aims to investigate the physical characteristics of the physical wedge and virtual wedge for clinical conditions.

Materials and Methods: Siemens Primus Linear Accelerator has been used for the study having dual photon energy and range of six electron energies from 4 to 15MeV. We have physical wedges of 15°, 30° and 45°. We investigated the characteristics of physical wedge and virtual wedge angles 15°, 30° and 45° using 6 MV photon beam. Wedge factors were measured in water using an ion chamber for various field sizes. In case of virtual wedge device as upper jaws (X-axis) moves during irradiation. Measurements were done using Farmer type ionization chamber (PTW, Germany) and Unidos E electrometer. Surface dose were measured using Markus chamber (volume 0.055 cc), and slabs of various thickness.

Results and Discussion: We have studied depth dependence and field size dependence of both type of wedge i.e. physical and virtual at various wedge angles. For various field sizes, virtual and physical wedge factors were changed by maximum 2.4% and 3.6%, respectively. For various depths, virtual and physical wedge factors were changed by maximum 1.7% and 2.6%, respectively. Apart from studying depth and field size dependence, surface dose were also measured. Surface dose with physical wedge was reduced by maximum 18 to 20% (x-ray beam: 6 MV, SSD; 100 Cm) relative to one with virtual wedge.

Conclusion: We compared the characteristics of virtual wedge and physical wedge considering different parameters such as depth and field size. Virtual wedge having smaller depth dependence then physical wedge. Field size dependence of virtual and physical wedge was also analyzed. Further it was interesting to note that for physical wedge, surface dose was found to be less in comparison to virtual wedge at all wedge angles taken in our study.

P-137

EVALUATION AND DOSIMETRIC COMPARISON OF OFF AXIS RATIO FOR 6MV PHOTON IN VARIOUS WEDGED ANGLE BEAMS AT DIFFERENT DEPTHS

Soniya Pal, Anoop Kr. Srivastava, S. Farzana, Mandvi Dixit, S. P. Mishra, Madhup Rastogi, Rohini Khurana, Rahat Hadi, Kamal Sahni, Ajeet Gandhi, Shantanu Sapru

Department of Radiation Oncology, Dr. Ram Manohar Lohia Institute of Medical Sciences, Lucknow, Uttar Pradesh, India.
E-mail: anoopsrivastava78@gmail.com

Introduction: Wedge beams are utilised in conformal radiotherapy plan in various sites to obtain the dose conformity and homogeneity in the desired target volume (TV). The beam data plan generated in treatment planning system (TPS) by various algorithm calculates the off axis ratio to produce the isodose profile for planning. TPS generated isodose pattern and actual measured values should conform to avoid undesirable consequences in plan outcome. 3DCRT often uses suitable wedge angulations (5^{O}, 10^{O}, 20^{O}, 30^{O}, 45^{O}, 60^{O}) or any other suitable wedge to provide both tissue compensation and beam shaping for homogeneity and conformity. In the present study comparative evaluation of off axis ratio (OAR) has been made between isodose generate by superposition algorithm in TPS for wedge angles 5^{O} - 60^{O} at practical depth of 5, 10, 15 cm. The dosimetry data has been directly measured for all wedges for 6 MV photons and at practical depth in the solid water phantom using TRS-398 protocol. The OAR measurements have been made at 5 cm, 10 cm and 15 cm depths. The isodose pattern generated by TPS by superposition algorithm in the Xio TPS version 5.0 has been utilized for comparison. The study has been designed to compare TPS data as well as measured beam library for standardised the reliability of the TPS algorithm at various depths. **Objective:** The objective of this study is to verify the accuracy of isodose pattern generated by superposition algorithm for wedges of 5^{O} - 60^{O} at depth of 5, 10, 15 cm for 6 MV photons and compare the same with dosimetric data generated with the PTW dosimetric system in solid water phantom.

Materials and Methods: For this study PTW (Freiburg, Germany) 0.6cc ion chamber was utilized and measurement were carried out in SAD setup (100 cm) in solid water phantom at reference depth of 10 cm and off axis value for 6MV photon for 10x10 cm^2 field size, both in negative and positive direction of central axis at 1 cm interval were obtained. The data were generated for open field as well as for 5^{O}, 10^{O}, 20^{O}, 30^{O}, 45^{O} and 60^{O} wedge angles which are most often used. Similarly, measurements were also carried out at 5 and 15 cm depth. A phantom of similar characteristic was generated in Xio version 5 for off axis values for the aforesaid wedge angles and depths using superposition algorithm was generated. A comparative chart was generated with measured and TPS generated OAR values which are detailed in Table 1.

Results and Discussion: Accuracy of dosimetry and selection of algorithm for conformal planning is essential for the success of radiotherapy. It is thus imperative to verify quantitatively TPS data with actual dosimetry. It is further important to evaluate OAR in heterogeneous medium where charge particle equilibrium is lost which influence the profile generated. This study thus aims to develop a standard practice to verify the wedge beam profile and compare with the actual dosimetric data at the central axis at depth of 5, 10, 15 cm, the variations found are significant and the deviation at the edge of the field are larger. For this study measurements were carried out in homogeneous phantom and this work will be further extended to heterogeneous phantom with various algorithm and energies. The significance of this study is to generate the beam library and carry out a comparative evaluation for acceptance of TPS data for clinical practices. A variation 10-40% at field edge may have significance influence to obtain better conformity index or desired matched peripheral dose of 95% - 98%. The measure data and the comparison with TPS value will be represented in detail for various energy and depths.

P-138

STATISTICAL ANALYSIS OF DOSIMETRIC PARAMETERS OF FF AND FFF PHOTON BEAM

Dwivedi Shekhar, V. K. Dangwal[1], S. K. Kansal[2], P. Sharma, R. Singh, M. K Mahajan

Department of Radiotherapy, Advanced Cancer Institute, [2]Department of Physics, MRSPTU, Bathinda, [1]Department of Radiotherapy, GMC, Patiala, Punjab, India. E-mail: shekharbhu1@gmail.com

Objective: The removal of the flattening Filter (FF) results in significant increase in dose rate and dose per pulse, softening of X-ray spectrum, reduction in the energy variation across the beam, decrease in head scattering, and hence reduces the leakage and out-of-field dose respectively. The purpose of this research work is to statistically analyse the dosimetric properties of a Linear accelerator with FF and without FF photon beams.

Materials and Methods: In this research paper, the radiation dosimetry and quality assurance of Varian TrueBeam Medical

Table 1: Percentage variation in off axis ratio value at 5, 10, 15 cm depth between TPS and measured data

Off axis distance (cm)	*TPS value at 5 cm*	*Measured value at 5 cm*	*Percentage variation at 5 cm*	*TPS value depth 10 cm*	*Measured value at 10 cm*	*Percentage variation*	*TPS value at 15 cm depth*	*Measured value at 15 cm depth*	*Percentage variation*
1	0.97	0.97	0	0.968	0.97	0.2	0.97	0.97	0
2	0.95	0.95	0.6	0.946	0.94	0.6	0.94	0.93	1.06
3	0.92	0.92	0	0.918	0.91	0.8	0.91	0.95	4.2
4	0.86	0.8	6.9	0.87	0.86	1.1	0.87	0.92	5.7
5	0.3	0.19	36	0.5	0.3	40	0.67	0.67	0
−1	1.02	1.03	0.9	1.01	1.02	0.9	1.01	1.03	1.9
−2	1.06	1.06	0	1.04	1.04	0	1.04	1.05	0.9
−3	1.09	1.09	0	1.06	1.07	0.9	1.05	1.07	1.8
−4	1.07	1.09	1.8	1.05	1.07	1.9	1.06	1.07	0.9
−5	0.38	0.3	21	0.6	0.68	13	0.8	0.7	12.5

TPS: Treatment planning system

Linear Accelerator has been performed with the help of the dosimetry system. The protocols used for radiation beam data collection and acceptance testing are as accordance with the recommendation of international practice and guidelines such as AAPM (American association of Physicist) TG (Task Group)-142 &106 reports, TRS (Technical report series) -398 and AERB (Atomic energy regulatory board, INDIA) guidelines. The ionization chambers, radiation field analyser and water phantom are used for beam data collection and dosimetric measurements. Beam data measurement was performed for standard photon energies 6 MV, 10 MV flattening filter beam and 6 MVFFF, 10 MVFFF flattening filter free beams.

Results and Discussion: The dosimetric parameters evaluated for FF and Flattening filter free (FFF) photon beams are Percentage depth dose (PDD), percentage surface dose, percentage symmetry and percentage output factor. The dependent paired t-test analysis showed that the significant value of paired t-test for PDD, percentage surface dose and percentage output factor was less than 0.05; it means the removal of flattening causes a significant difference between the their mean values measured for FF and FFF photon beams. While the significant value of paired t-test for percentage symmetry was greater than 0.05; it means the removal of flattening causes no significant difference between the mean of percentage symmetry measured for FF and FFF photon beams. The Removal flattening filter changes various dosimetric parameters such as PDD, percentage surface dose and percentage output factor and therefore, all of them need to be redefined for FFF beam other than FF beam.

P-139

ENTRANCE DOSE MEASUREMENT USING SILICON DIODES IN EXTERNAL RADIOTHERAPY

S. M. Pelagade, Laishram Suchitra

Department of Medical Physics, Gujarat Cancer and Research Institute, New Civil Hospital Campus, Ahmedabad, Gujarat, India.
E-mail: satishpelagade@gmail.com

Introduction: The aim of radiotherapy treatment is to deliver radiation dose to various malignant or non-malignant targets efficiently, accurately and safely. As the number of radiation incidences reported due to human errors, separate patient dose verification (in-vivo) is required during the actual treatment delivery in external beam radiotherapy (EBRT). In this paper, we will be discussing how we established in-vivo dosimetry (using p-type silicon diodes) technique by measuring various correction factors.

Materials and Methods: The measurements were performed on a Elekta Synergy linear accelerator, providing a 6 MV photon beam. Two identical diodes from IBA Dosimetry [EDP -10 /5143 and EDP -10 /5144 detectors (p-type silicon diodes)] with hemispherical build-up cap with DPD-12 (emX) electrometer were tested for entrance dose measurements. These diodes were calibrated against an ionization chamber (FC65) from Scanditronix Wellhofer in a 6 MV photon beam from a linear accelerator. In reference conditions, each diode was taped to a solid water phantom (dimensions: 30 cm x 40 cm x 40 cm) at a distance of 100 cm from the accelerator focus, in the center of an open treatment field measuring 10 cm x 10 cm and with gantry angle set to 0°. The ionization chamber was irradiated with the same treatment parameters at depth dose maximum, 1.5 cm below the phantom surface. Throughout the calibration and *in vivo* measurements, each diode was connected to a dedicated channel on a DPD-12 (emX) Scanditronix Wellhofer electrometer.

Results: In addition to the calibration factor, various correction factors accounting for non-reference conditions were determined.

Field Size Correction Factors: For 6-MV x rays, the field size correction factors for two identical diodes are very similar for the entire range of field sizes considered here. FFS for the EDP-10 / 5143 diode are 0.9108 for the field size of 3 x 3 cm^2 and 1.0854 for the field size 40 x 40 cm^2, while the FFS for the EDP-10 / 5144 diode are 0.9136 for the field size of 3 x 3 cm^2 and 1.0853 for the field size of 40 x 40 cm^2.

SSD Correction Factors: For 6-MV x rays, the FSSD for the EDP-10/5143 diode are 0.95013 at SSD of 80 cm and 1.04366 at SSD of 120 cm, while FSSD for the EDP-10/5144 diode are 0.95438 at SSD of 80 cm and 1.05125 at SSD of 120 cm. of 130 cm.

Angular Dependence Correction Factor: Angular dependence correction factor gives the dependence of diode for different angle between the central beam axis and the symmetry axis of the diode. Directional response of diode from -45° to +45° for both axial and tilt is less than 3 %.

Temperature Correction Factor, Ftemp: A linear increase of the diode signal with temperature is found. It is recommended that if Ftemp is smaller than 0.4% per °C, no temperature correction is needed for in vivo dosimetry. For each radiation field used in treatment a measured dose on the patient skin and calculated dose from treatment planning system were compared using a 5% tolerance. The maximum entrance dose deviation was observed to be 4.1 % for all the considered 10 cases.

Conclusion: In vivo entrance measurements have been proved to be a very useful as check for the dose delivered to a given patient. It can detect serious errors including an incorrect daily dose, treatment with the wrong beam energy, omission or use of the wrong wedge, and setup errors. A high precision can be obtained when the calibration and correction factors are carefully determined and applied to convert the diode signal in adsorbed dose.

P-140

OUT-OF-FIELD RADIATION ORGAN DOSE MEASUREMENTS AND ASSOCIATED SECONDARY CANCER RISK ESTIMATION IN PATIENTS TREATED WITH BREAST CANCER IN LEBANON

Ibrahim Duhaini, Saad Ayoubi, Mahmoud Korek[1]

Chief Medical Physicist & RSO, Rafik Hariri University Hospital, [1]Department of Physics, Beirut Arab University, Beirut, Lebanon. E-mail: duhaini@yahoo.com

Introduction: According to the National Cancer Registry in Lebanon for the years 2003 till 2007, more than 40 % of registered cancers in Females have Breast Cancer. According to the latest Report published by the NCR, Breast cancer remained the most relatively frequent cancer throughout the years (42-43%). The annual incidence rate for breast cancer has been increasing from 72/100,000 in 2005, to 87/100,000 in 2007. According to the World Health Organization 2003 Report, Breast cancer is the leading cause of cancer deaths worldwide in women under the age of 55 and more than one million women are diagnosed with breast cancer each year. Breast Cancer patients have different options of treatment depending on the age, type of cancer and other factors. These options include: Surgery, Chemotherapy, Hormonal Therapy, Radiation Therapy and other non-traditional therapies. In radiation therapy, our concern, the tumor in the Breast will be exposed to high-energy X-rays that destroy cancerous cells. It is often used as post-surgery therapy in an effort to kill any remaining undetectable cancer cells that may have invaded areas nearby the original site of the tumor.

Purpose: During radiation therapy of the breast, other organs in the body may receive a significant radiation dose that triggers a secondary cancer in these organs. In this study, the Out-of Field radiation doses will be measured in some organs and will be evaluated for the development of radiation induced cancer as recently defined by the International Commission on Radiological protection (ICRP).

Materials and Methods: An anthropomorphic phantom was used with Thermo- Luminescence Dosimeters (TLD) to physically measure organ doses when the breast is irradiated with a complete clinical dose prescription for cancer treatment.

Results: The measured organ dose values were done and found that the estimated risk factors on inducing cancer in these organs were very minimal compared to the standard values.

P-141

DEVELOPMENT OF REAL TIME ABDOMINAL COMPRESSION FORCE MONITORING AND VISUAL BIO FEEDBACK SYSTEM

Tae-Ho Kim, Siyong Kim[1], Dong-Su Kim, Seong-Hee Kang, Min-Seok Cho, Kyeong-Hyun Kim, Dong-Seok Shin, Hye Jeong Yang, Tae-Suk Suh

Department of Biomedical Engineering, the Catholic University of Korea, Seoul, Korea, [1]Department of Radiation Oncology, Virginia Commonwealth University, VA, USA. E-mail: rlaxogh0331@gmail.com

Introduction: Hard-plate based abdominal compression is known to be effective, but no explicit method exists to quantify abdominal compression force (ACF) and maintain the proper ACF through the whole procedure. In addition, even with compression, it is necessary to do 4D CT to manage residual motion but, 4D CT is often not possible due to reduced surrogating sensitivity. In this study, we developed and evaluated a system that both monitors ACF in real time and provides surrogating signal even under compression. The system can also provide visual-biofeedback.

Materials and Methods: The system developed consists of a compression plate, an ACF monitoring unit and a visual-biofeedback device. The ACF monitoring unit contains a thin air balloon in the size of compression plate and a gas pressure sensor. The unit is attached to the bottom of the plate thus, placed between the plate and the patient when compression is applied, and detects compression pressure. For reliability test, 3 volunteers were directed to take several different breathing patterns and the ACF variation was compared with the respiratory flow and external respiratory signal to assure that the system provides corresponding behavior. In addition, guiding waveform was generated based on free breathing, and then applied for evaluating the effectiveness of visual-biofeedback.

Results and Discussion: We could monitor ACF variation in real time and confirmed that the data was correlated with both respiratory flow data and external respiratory signal. Even under abdominal compression, in addition, it was possible to make the subjects successfully follow the guide patterns using the visual biofeedback system. The developed real time ACF monitoring system was found to be functional as intended and consistent. With the capability of both providing real time surrogating signal under compression and enabling visual-biofeedback, it is considered that the system would improve the quality of respiratory motion management in radiation therapy.

P-142

RESOLUTION PROPERTIES OF THREE GENERATIONS OF MEGAVOLTAGE IMAGERS IN RADIATION THERAPY

K. Loot, O. Waletzko[1], R. Rohn[1], B. Spaan, A. Block[2]

TU Dortmund University, [1]Clinic for Radiation Therapy at Klinikum Dortmund, [2]Institute for Medical Physics, Klinikum Dortmund GmbH, Dortmund, Germany. E-mail: katharina.loot@tu-dortmund.de

Mega Voltage (MV) imaging has evolved alongside radiation therapy, moving from film verification to electronic portal imaging devices (EPIDs) which nowadays offer support with patient positioning as well as dose verification. In this work, we will determine the spatial resolution properties of three EPIDs by measuring their modulation transfer function (MTF). The MTF maps the transfer of contrast (or modulation) as a function of spatial frequency. We measure the presampled MTF, which considers the entire detection process before the sampling of the signal. The phantom for MTF measurement consists of a tungsten plate with a polished edge, which is placed in front of the detector surface to create an input signal with step function characteristics. The measured edge spread function (ESF) is differentiated and Fourier transformed to yield the presampled MTF. We investigated the following three EPIDs:

- System A: TheraView by Cablon Medical, fluoroscopic-optical system with CCD camera, linac: GE Saturne 43
- System B: PortalVision aS500 by Varian, first generation flat panel imager, linac: Varian Clinac 2100
- System C: PortalVision aS1200 by Varian, latest generation flat panel imager, linac: Varian VitalBeam

All images were acquired using 6 MV photons, source-to-phantom and source-to-detector distance were kept constant for all accelerators. The MTF analysis software was written using Mathematica (Wolfram Research) and results are depicted in Figure 1. The range of spatial frequencies for which the MV imaging systems show significant transmittance is limited to about 1 mm^{-1}. The MTF of the camera-based system A exhibits lower values than that of the flat panel systems B and C for the entire spatial frequency range. The MTF drops to 50% at 0.16 mm^{-1} and reaches 20% at 0.35 mm^{-1}. The first-

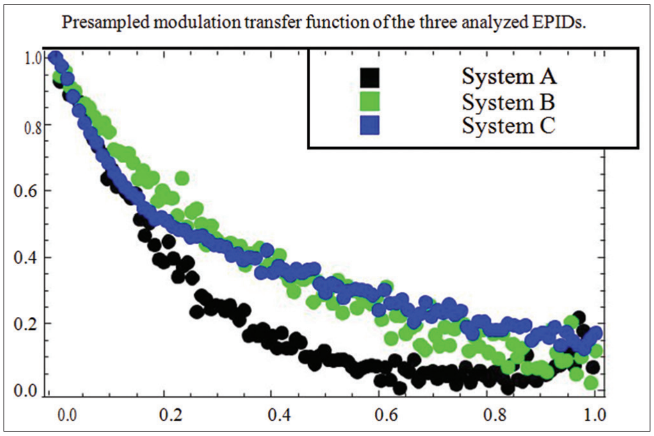

Figure 1: Presampled modulation transfer function of the three analyzed electronic portal imaging devices

generation flat panel imager B shows the highest values in the frequency range up to 0.4 mm^{-1}. The MTF reaches 50% at 0.26 mm and 20% at 0.62 mm^{-1}. The currently produced flat panel imager C shows the most balanced MTF, with moderate results for lower spatial frequencies but the highest values for spatial frequencies above 0.4 mm^{-1}. The MTF shows 50% at 0.20 mm^{-1} and 20% at 0.80 mm^{-1}. All three systems convert the high-energy photons into optical photons by means of a metal plate and a phosphor screen (scintillator). System A directs the optical photons to a CCD camera, whereas in the Systems B and C, the photons are detected by an amorphous silicon panel placed in direct contact with the phosphor screen. All three systems suffer from the spread of high-energy particles and optical quanta in the phosphor screen, leading to an overall low limiting resolution. The resolution of System A is deteriorated further by the spread of optical quanta in the camera lens. System C shows an optimized contrast transfer for higher spatial frequencies, caused by two alterations in the detector design: The thickness of the phosphor screen is reduced and the thinner scintillator allows less spreading of photons and improves the spatial resolution. System C also features an additional backscatter shielding to prevent irregular scatter from the support arm of the detector. Both modifications lead to the improved contrast transfer of 20% at 0.8 mm^{-1} spatial frequency. Our results document that there has been a steady improvement in the MTF with each successive imager generation. Further research will investigate the noise transfer properties of the system in a similar fashion. Our long-term goal is to correlate these physical quantities with the diagnostic image quality.

P-143

DEVELOPMENT OF NEW NON METALLIC ARTIFACT FREE CT MARKING WIRE FOR RADIOTHERAPY

S. Senthilkumar

Department of Radiotherapy, Madurai Medical College and Government Rajaji Hospital, Madurai, Tamil Nadu, India. E-mail: senthilgh@gmail.com

Introduction: In Radiotherapy computed tomography (CT) marker wires are frequently used to obtain accurate treatment field area for further processing. The placement of such markers is usually on the skin surface. CT marking wires should therefore exhibit the following features such as clear visibility, should not produce any artifacts and should be easy to use. Most commercially available CT marking wire are made of high-Z materials, which typically cause streaking artifacts, decreasing image quality of the subsequent reconstruction. In this work I have developed a new non metallic artifact free CT marking wire for External Beam Radio Therapy (EBRT).
Objective: The objective of this study was to fabricate indigenously non metallic artifact free CT marking wire which is alternative to lead wire.
Materials and Methods: A new type of non metallic CT marking wire were developed using various combination of low atomic number materials. The materials are in the powder form which can be modifiable to versatile shape and size according to the needs. Lead based CT marking wire and newly fabricated non metallic marker wire were used to evaluate the visibility of marker wire, CT number and artifact. Both the marker wire were placed in a 30x30x30 cm^3 sheets of solid phantom (PTW) and imaged on a Toshiba multi slice CT scanner for quality analysis. The phantom was scanned using the similar imaging parameters such as 2 to 3 mm slice thickness, as commonly used in the simulation. For the visibility test I have done the CT scan topographic as well as in axial section. The CT artifact of marker were analysed using a J-image software.
Results and Discussion: On analyzing the CT scan of both the marker wire on phantom, it has been found that the newly fabricated marker wire has the equal visibility and almost no CT artifact when compared with the commercially available marker wire. The metallic marker wire produced bright streak artifact on the CT image but non metallic marker wire were not producing any streak artifact. The newly fabricated marker wire density has nearly equal to human bone density so, it appears as bright spot on CT without streak artifact. To conclude that the newly fabricated CT marker wire will be an alternative to the existing commercially available marker wire with almost no artifact and also cost effective, which can be used for the clinical CT simulation for all the anatomical sites and breast scar marking without producing any metal streak artifact.

P-144

RESIDUAL ROTATIONAL SET-UP ERRORS AFTER DAILY CONE BEAM COMPUTED TOMOGRAPHY IMAGE GUIDED RADIOTHERAPY OF PROSTATE CANCER

Soumya Roy

Department of Radiation Oncology, AMRI Hospital Ltd., Kolkata, West Bengal, India.
E-mail: soumyaroy91@gmail.com

Introduction: Prostate/pelvis radiotherapy often requires a large field. An uncorrected rotational error could lead to a geometrical miss of the target volume for such extended field. This study was design to evaluate the residual rotational set up errors after using daily cone beam computed tomography (CBCT) based patient positional verification for prostate cases.
Materials and Methods: Total 608 sessions of CBCT for 22 patients receiving radiotherapy for locally advance prostatic and lymphnodal irradiation has been incorporated in this study.

Patients were placed in head in supine position with appropriate immobilization devices like knee rest and primary patient positing was done matching three LASER with the skin marking. Further a cone beam CT was acquired with scan parameters 120 kV & 650 mAs and further patients positional error was corrected An automatic rigid volumetric image registration was performed between the cone beam and planning CT scan. Matching was based on the soft tissue information available inside the volume of interest. Only translational degrees of freedom were allowed during online registration. The systematic and random errors (Σ & σ) attributed to the translational corrections were calculated as defined by Van Herk. Margins were calculated according to the equation 2.5 Σ+0.7 σ. The move was quantified in terms of the 3D vector composed of shift in the three translational directions: 3D vector = $\sqrt{(a^2+b^2+c^2)}$, where a, b and c represent the lateral, longitudinal, and vertical shifts performed in the clinic. Translational shifts obtained in the clinic were retrospectively analyzed prior to each treatment fraction as well as the residual rotational errors remaining after translational correction. Average, maximum, minimum, standard deviation of systematic and random errors along each translational direction.

Results: The image quality of the CBCT images varied within and between patients and depended in particular on artifacts attributed to the volume of air present in the bowel bag. Nevertheless the image quality was adequate for visualization of bony structure while soft tissues were most often partly visible. The CBCT – guided couch movement resulted in a mean translational 3D vector correction of 5.03 mm. Pitch was the most frequent source of residual rotational errors and resulted in shifts exceeding 6 mm in 50 fractions. The margins along vertical, lateral and longitudinal directions are found to be 7.3 mm, 6.8 mm, 5.6 mm respectively and the analysis shown in Table 1. Residual rotational error resulted in a target shifts exceeding 5 mm in 81 out of 608 sessions. Three patients out of total 22 patients alone accounted for 55 of these 608 treatment fractions. For 11 patients had shifts below 5 mm and 6 patients had 5 or less treatment fractions with such shifts i.e. 5 mm.

Conclusion: 18 of the 22 patients have none or few treatment fractions with target shifts larger than 5 mm due to residual error. In large treatment field even small rotational errors may result in substantial shifts at the edge of the treatment field. A setup margin (CTV to PTV margin) of 7 mm was sufficient to take into account residual set up errors in majority of the cases. In general, variation in pitch rotation was larger than yaw and roll rotation, which is in agreement with previous reports as well. Higher pitch rotation attribute to the fact that pitch positioning is difficult is using skin markers. However, three patients display a significant number of shifts suggesting a more systematic set up error.

Table 1: The translational corrections made in the clinic (mm)

Variable	Vertical	Lateral	Longitudinal	3D vector
Minimum	−11.70	−10.20	−8.80	1.00
Maximum	10.10	8.80	5.80	14.36
Mean	−0.40	−0.57	0.48	4.41
Σ	2.08	2.01	1.66	
σ	2.99	2.59	2.05	
Margin	7.29	6.83	5.58	

Σ is the calculated SD of the systematic error and σ is the SD of the random error. SD: Standard deviation, 3D: Three-dimensional

P-145

DETERMINATION AND EVALUATION OF INTRA FRACTIONAL AND SET-UP CHANGES DURING RADIOTHERAPY TO THE CERVICAL CARCINOMA USING CONE BEAM COMPUTED TOMOGRAPHY

Pankaj Pathak, Rajesh Kumar, Praveen Kumar Mishra[1], Narendra Birbiya, Manisha Singh[2], Pankaj Kumar Mishra[2]

Department of Radiation Oncology, BIMR Hospitals, [1]Department of Radiation Oncology, G.R. Medical College, [2]Department of Applied Physics, Amity University, Gwalior, Madhya Pradesh, India.
E-mail: pankaj2002@hotmail.com

Aim and Objective: To confirm the accuracy of the location of the Fudicial markings in relation to the actual isocentre of the irradiated volume due to Intra-fractional & Set-Up changes in Cancer Cervix with the help of Cone Beam computed Tomography (CBCT).

Materials and Methods: 15 patients of Cancer Cervix were treated by Intensity Modulated Radiotherapy (IMRT) in 25 fractions to a median dose of 50Gy @ of 2Gy/#. The CT scans acquired for verification were registered with simulation CT scans. The target volumes (GTV, CTV, and PTV) were contoured on all verification CT scans and compared to the initial GTV, CTV, and PTV in treatment planning system.

Results: We acquired Cone beam Computed Tomography (CBCT) for consecutive Three Days of 15 Patients of Cancer Cervix. The patients were treated with full bladder and empty rectum. We evaluated & tabulated the mean of all the shift acquired during CBCT of each patients in the form of Table 1(a), (b) and (c) and the mean of means of shifts in Right -Left (RL), anterior-Posterior (AP) and Superior – inferior (SI) directions for each patients were determined & evaluated and tabulated in the form of Table 2. We found the mean of means in (RL): 0.6378 mm, mean of means in (AP): -1.1489 mm & Superior –inferior (SI) directions: -3.4732 mm respectively.

Conclusions: Organ motion and patient setup variation are two major concerns during radiation delivery for Cervix cancer because they lead to shift of the target from its reference frame in the CT treatment-planning. Depending on the treatment margins, uncorrected target shifts may lead to under-dosage of the Cervix, thus decreasing local tumor control, or over-dosage the Bladder & rectum, thus increasing rectal complications. Understanding the inter fractional target shifts due to interfractional target motion and daily setup error and their management becomes a critical issue for Cervix cancer radiotherapy. Image-guided radiotherapy is used for correcting interfractional organ shifts before radiation delivery with image guidance. We observed that consecutive three days CBCT is sufficient for Final Isocenter marking but Daily CBCT is recommended for every Cervical Cancers to reduce the radiotherapy errors to give accurate and precise treatment.

Table 1: Shifts obtained from consecutive three days cone beam computed tomography for 15 patients in right-left, anterior-posterior and superior-inferior directions for each patients

Patient number	RL (cm)	SI (cm)	AP (cm)
(a) The mean of shifts obtained on day 1			
1	−0.21	−0.56	0.19
2	0.55	−1.31	−0.48
3	1.24	0.39	−0.49
4	−0.6	−0.44	−0.31
5	0.17	−0.2	−0.51
6	0.01	−2.04	−0.13
7	0.19	0.76	−0.38
8	0.16	−0.55	−0.52
9	0.29	−1.49	0.3
10	0.14	0	−0.1
11	−0.44	−1.89	−0.32
12	0.31	−1.08	0.25
13	0.53	−1.24	0.08
14	−0.25	0.03	0.03
Day 1	−0.02	−0.94	−0.47
Mean (cm)	0.138	−0.704	−0.19067
(b) The mean of shifts obtained on day 2			
1	−0.05	2.33	−0.44
2	0	0.2	−0.88
3	−0.36	0.96	−0.16
4	−0.03	1.38	−0.38
5	0	−0.5	−0.13
6	0.07	0.72	0.33
7	−0.07	0.61	0
8	−0.01	−0.55	−0.14
9	0.26	−1.49	0.11
10	−0.17	0	−0.27
11	0.3	−1.89	−0.44
12	0.1	−1.08	0.7
13	0.28	−1.24	−0.08
14	0.27	0.03	0.39
Day 2	−0.46	−0.94	0.3
Mean (cm)	0.008667	−0.09733	−0.07267
(c) The mean of shifts obtained on Day 3			
1	−0.65	−0.14	0.22
2	0.56	1.26	−0.67
3	0.14	−0.11	−0.37
4	0.3	1.46	−0.32
5	0.21	−0.99	−0.24
6	0.31	0.44	0.06
7	−0.07	−0.54	−0.27
8	−0.04	−1.01	0.16
9	−0.37	−0.79	0.19
10	0.05	−0.27	−0.24
11	−0.68	−0.82	−0.38
12	0.46	−1.07	−0.28
13	0.24	−0.05	−0.02
14	0.36	−0.53	0.46
Day 3	−0.15	−0.45	0.48
Mean (cm)	0.044667	−0.24067	−0.08133

RL: Right-left, SI: Superior-inferior, AP: Anterior-posterior

Table 2: The mean of means of shifts in right-left, anterior-posterior and superior-inferior directions for each patients

Days	RL (cm)	SI (cm)	AP (cm)
Day 1	0.138	−0.704	−0.19067
Day 2	0.008667	−0.09733	−0.07267
Day 3	0.044667	−0.24067	−0.08133
Mean of means	0.063778	−0.34733	−0.11489

RL: Right-left, SI: Superior-inferior, AP: Anterior-posterior

Acknowledgment: The Authors are thankful to the Department of Radiation Oncology, BIMR Hospitals, Gwalior, Madhya Pradesh, India and Clearmedi Healthcare Pvt. Ltd., Delhi, for the support.

P-146

EVALUATION OF SIX DIMENSIONAL CRANIAL TARGET LOCALIZATION ACCURACY IN TWO DIFFERENT IMMOBILIZATION SYSTEM USING EXACTRAC

K. Tamil Selvan[1,2], P. Ramesh Babu[2], N. Arunai Nambi Raj[3], K. Senthilnathan[2], M. Sathiya Seelan[1], G. Padma[1], M. K. Revathy[1]

[1]Department of Oncology, Apollo Cancer Hospital, Hyderabad, Telangana, [2]School of Advances Sciences, Vellore Institute of Technology University, [3]Centre for Biomaterials, Cellular and Molecular Theranostics, Vellore Institute of Technology University, Vellore, Tamil Nadu, India. E-mail: rk.tamilselvan@gmail.com

Introduction: The precision and accuracy of the intracranial sterotactic positioning systems used for sterotactically applied radiation is critical for the success and safety of the treatment. Reducing geometric uncertainties helps in increasing therapeutic ratio. The patient setup errors can be obtained by comparing the images acquired during the treatment delivery with that of the planned position. By imaging several patients of a specific patient group regularly, the typical size of the systemic and random deviations for that group can be determined and based on the obtained values C; inical Target Volume (CTV) to Planning Target Volume (PTV) margin can be estimated.

Objective: The aim of this study is to determine the impact of immobilization on patient positioning in cranial radiotherapy using ExacTrac system. The six dimensional target localization accuracy between the dedicated sterotactic mask and conventional head mask was compared with the Exactrac X-ray 6D system (interfraction setup data).

Materials and Methods: Ninety one patients with cranial lesions were included in this study (34 sSterotactic radiosurgery (SRS), 27 Sterotactic radiotherapy (SRT) & 30 non SRS/SRT). For SRS and SRT patients dedicated sterotactic mask was used and the initial positioning to isocenter was done by Exactrac system using infrared positioning array. For all the other patients conventional head mask was used and alignment to isocenter was manually done with the external fiducial markers and lasers. Exactrac image-guided positioning system is utilized to obtain daily translational and rotational patient positioning drift from intended (planned) position. The 6D setup data is analyzed to obtain population mean, systemic and random errors in all the three scenario. Obtained systemic and random errors were used to derive CTV to PTV margin.

Results and Discussion: In SRS the population mean setup errors were 0.48, 0.56 and 1.28 mm in the lateral, longitudinal and vertical translational dimensions and 0.26°, 0.60° and 0.08° in the roll, pitch and yaw rotational dimensions. The margin requirements in translational directions ranged from 1.6 to 3.5 mm based on Van Herks and Strooms margin recipes. The margin requirements in rotational dimensions ranged from 2.2 to 2.8°. In SRT the population mean setup errors were 0.14, 0.62 and 0.98 mm in the lateral, longitudinal and vertical translational dimensions and 0.12°, 0.43°and 0.02° in the roll, pitch and yaw rotational dimensions. . The margin requirements in translational directions ranged from 1.7 to 3.9 mm based on Van Herks and Strooms margin recipes. The margin requirements in rotational dimensions ranged from 2.1 to 2.9°. With 3clamp head mask the population mean setup errors were 0.63, 0.12 and 0.91 mm in the lateral, longitudinal and vertical translational dimensions and 0.50°, 0.17° and 0.04° in the roll, pitch and yaw rotational dimensions. The margin requirements in translational directions ranged from 4.4 to 6.2 mm based on Van Herks and Strooms margin recipes. The margin requirements in rotational dimensions ranged from 3.1 to 4.4°.

Conclusion: In this study, we have evaluated the setup deviations observed during treatment positioning with two different immobilization systems. Further, we could validate the PTV margin requirements. The results show that there is a significant reduction in the target positioning errors with the dedicated sterotactic mask as compared with conventional cranial mask. With daily exactrac image guidance one might expect similar outcomes for both the immobilization system but due to residual errors and system limitations, dedicated sterotactic mask provides better target localization accuracy.

P-147

ABSOLUTE DOSE VERIFICATION OF FFF BEAMS USING ION CHAMBER AND OPTICALLY STIMULATED LUMINESCENCE DOSIMETERS WITH CIRS ELECTRON DENSITY PHANTOM FOR ANISOTROPIC ANALYTICAL ALGORITHM AND ACUROS XB ALGORITHMS

Vaibhav Mhatre, Shaju Pilakal, Arjun Mengal, Sandip Patil

Department of Radiation Oncology, Kokilaben Dhirubhai Ambani Hospital and Research Centre, Andheri West, Mumbai, Maharashtra, India. E-mail: vaibhav.mhatre@relianceada.com

Introduction: Aim of this study was to measure the absolute dose for AAA and Acuros XB dose calculation algorithm using farmer chamber and optically stimulated luminescence dosimeters (OSLD) for 6X and 10X FFF beams with CIRS electron density phantom (EDP).

Materials and Methods: Recently we installed Edge linear accelerator at our Institute first of its kind in India. The 6X and 10X FFF photon beams was investigated in this study. The CIRS EDP with various tissue equivalent plugs (lung exhale, lung inhale, liver, breast, muscle, adipose, bone) was used in this study. The EDP has 17 holes to hold different types of tissu-equivalent inserts. Each cylinder-like (they are not exactly cylinders – the diameter on one side is slightly smaller than the other side) insert is about 3 cm in diameter and about 5 cm in length. Nine inserts are in the small inner ring section and the other 8 inserts are in the outer ring section as shown in Figure 1. Only the 8 inserts on the inner section were investigated in this work. The absolute dose was measured using farmer ionization (0.6 cc) chamber (PTW) and OSLD's. The In-Light nanoDots OSLD system from Landauer was used for this study. The Optically-Stimulated Luminescence (OSL) dosimeter with aluminum oxide doped with carbon has been extensively used to monitor personal occupational radiation dose and the use of OSL dosimeters for dose measurements at therapeutic level in the last few years. All plans were created in Varian Eclipse treatment planning system (TPS) v.13.6 with one single AP field and calculated using Anisotropic Analytical Algorithm (AAA) and Acuros XB (AXB) algorithm for 6X and 10X FFF beams with gantry and collimator 0° on Edge Linear Accelerator. A dose of 200 cGy was prescribed at a depth of 6 cm for all plans with a field size of 5x5 cm. To measure the actual dose delivered to the prescription point, the individual plans were delivered to treat the EDP as shown in Figure 1. The MU's delivered were defined by the related treatment plans and the dose was measured using farmer ion chamber and OSL dosimeters. All measured doses were compared with calculated doses from treatment plans.

Results: The absolute dose for 6X FFF and 10X FFF beams for AAA algorithm was ± 5 % as compared to Acuros XB was within ± 3% for both ion chamber and OSLD's. Figure 2 shows the variation of absolute dose for farmer chamber and OSLD's for both the energies.

Conclusion: This study demonstrated that the dose calculation with Acuros XB algorithm for FFF beams can reach an accuracy of ± 3% considering the uncertainty of ion chamber and electrometer. Furthermore, we found that

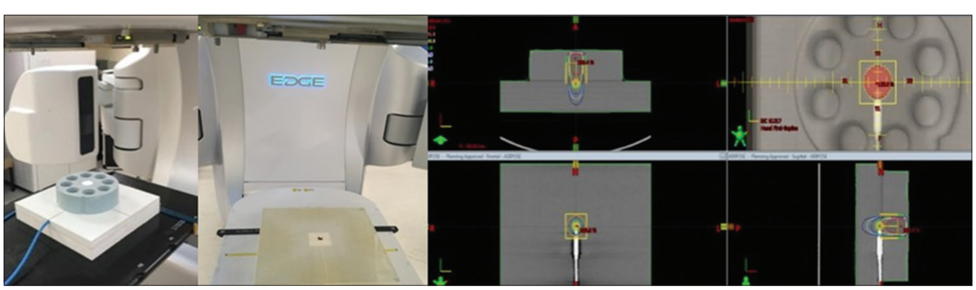

Figure 1: Absolute Dose measurement using Ion Chamber and optically stimulated luminescence dosimeters with CIRS Electron Density Phantom

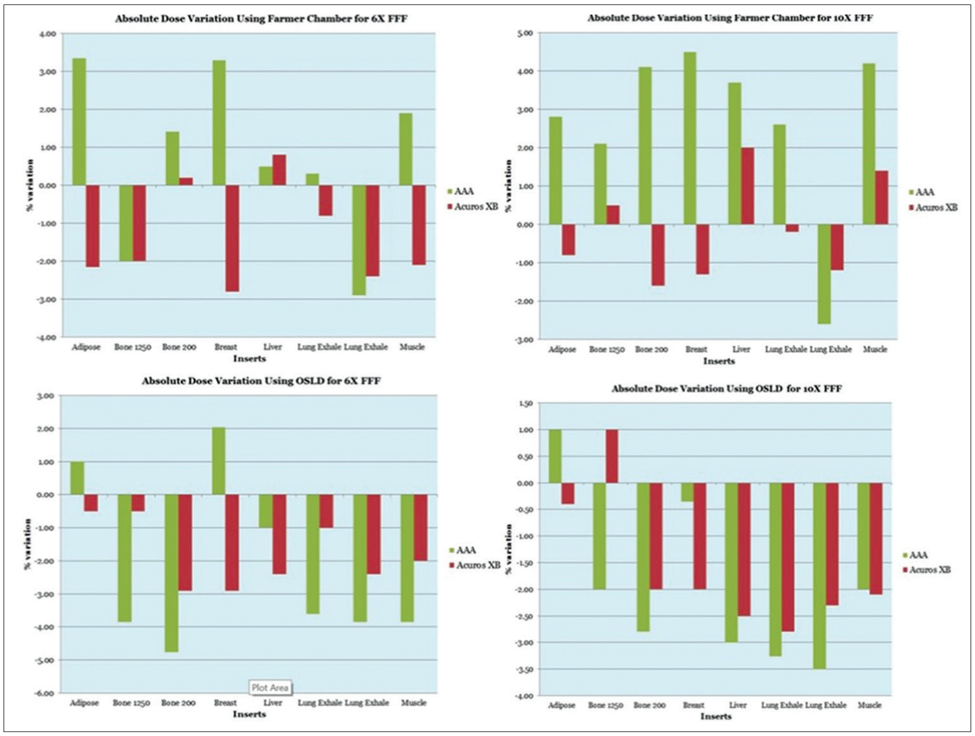

Figure 2: Histogram of percent variation for 6X FFF and 10X FFF beams using optically stimulated luminescence dosimeters and Ion chamber.

the Acuros XB was superior in Bone and lung inserts when compared against AAA algorithm.

P-148

RELATIONSHIP BETWEEN DOSE–VOLUME HISTOGRAM AND OVERLAP VOLUME HISTOGRAM OF RECTUM IN PROSTATE CANCER TREATMENT PLAN

Gipson Joe Anto, K. R. Sivaramakrishnan, Bojarajan Perumal, Kumar Raja Gattamaneni, Girish Kumar Chegu

Philips Innovation Campus, Bengaluru, Karnataka, India.
E-mail: gipson.anto@philips.com

Introduction: Recently, radiation treatment plan prediction is emerging as new area of interest for many researchers. Radiotherapy plans are predicted based on many parameters. One of them is Overlap Volume Histogram (OVH). The OVH describes the fractional volume of the structure of an OAR that is within a specified distance of a target.

Objective: Objective of this study is to find relationship between Overlap Volume Histogram of Rectum in Prostate cancer and corresponding DVH in treatment plans.

Materials and Methods: Study is performed in 5 Prostate cases prescribed with a dose of 78Gy. Released version of Pinnacle Radiation Treatment planning system is used for the study. Auto Planning feature of Pinnacle Treatment planning is used which would eliminate the subjectivity of Planning. Same treatment Technique is used in Treatment planning for all 5 cases. OVH of Rectum is calculated for five cases with the Target volumes. The calculation of the OVH can be thought of as two steps – Uniform expansion and contraction of the target: (1) Target expansion: We first uniformly expand the target with a distance of *a* mm in all directions. The overlap volume between the expanded target and OAR is then calculated. The expansion with *a* mm is repeated until the expanded target fully encompasses the OAR, in which situation the overlap volume is the volume of the OAR. Calculation of the overlap volume between the expanded target and OAR is also repeated after each expansion. (2) Target contraction: The target is uniformly contracted with a distance of *a* mm in all directions. Such contraction is repeated until there is no overlap between the contracted target and OAR. During each *a* mm contraction, the overlap volume between the contracted target and OAR is calculated. The curve resulting from the target expansion and contraction is the OVH that characterizes the relative spatial configuration of the two objects. DVH is obtained from the plan generated by Auto planning tool.

Results and Discussion: A trend analysis is performed on the OVH s and DVHs of five cases. It is observed that there is a definite relationship between OVH and dose to the OAR, Rectum in our case is reflected in the DVH. If the expansion distance required is higher to completely cover the rectum lower is the dose to OAR. In OVH at a definite expansion distances if the curve is steep it is difficult to spare the OAR and vice versa. This relationship between OVH which can be obtained without even placing a beam and Dose to OAR can be exploited for plan prediction and would enable the planner to squeeze the dose to OARs.

P-149

INDIGENOUSLY DEVELOPED MONITOR UNIT CALCULATION SOFTWARE "MUCAL" FOR VERIFICATION OF 2D AND 3D TREATMENT PLANS

R. Holla, Amal Jose, B. Pillai

Department of Medical Physics and Radiation Safety, Amrita Institute of Medical Science and Research Center, Kochi Amrita Vishwa Vidyapeetham, Amrita University, Kochi, Kerala, India. E-mail: raghavendra.holla@gmail.com

Introduction: The basic requirement of radiotherapy clinical software incorporates verification of the treatment plans. A software program, "MUCAL", has been developed to perform an independent monitor unit calculation and compare it to the monitor unit calculated from the XiO (Elekta Medical systems, India) treatment planning system. The software helps to import treatment plans from the XIO treatment planning system and uses basic algorithms for dose calculation and evaluates the monitor unit on a distinct platform.
Objectives: In radiation therapy it is mandatory to verify the Monitor Units calculated by the planning system by a secondary dose calculation algorithm. There are several commercial solutions for performing this activity. We created an independent software "MUCAL" using MATLAB software platform that calculates and compares the monitor units calculated by XiO treatment planning system.
Materials and Methods: The Graphical User Interface that extracts the Beam Entry Point, Dose Specification Point, MLC Leaf Positions, SSD, number of beams etc, from DICOM treatment plan and performs the dose calculation. Percentage Depth doses, Collimator and Phantom scatter factors for several field sizes of Linac for 4 MV, 6 MV, 15 MV Photons and, 6 MeV, 8 MeV, 10 MeV, 12 MeV and 15 MeV electron energies were initially fed in to the generated software MUCAL. The software has the capacity to import MLC files from TPS and any other DICOM systems for performing the 2D dose calculations accurately. It also has the feature to enter the beam input parameters directly and calculate the dose and MU as 2D treatment planning system. DICOM files of several patients have been imported for calculation and compared the variation with TPS Monitor Unit.
Results: The mean deviation in the Monitor unit calculated by the XiO Treatment Planning system to the MUCAL software is found to be less than 5%. The developed software automate the entire process of secondary dose calculation check which improves the efficiency of the department.

P-150

DEPENDENCE OF TISSUE INHOMOGENEITY CORRECTION FACTORS ON TISSUE PHANTOM RATIO ($TPR_{20,10}$)

M. Akhtaruzzaman, P. Kukolowicz[1]
Faculty of Physics, University of Warsaw, [1]Department of Medical Physics, Maria Skłodowska-Curie Memorial Cancer Centre and Institute of Oncology, Warsaw, Poland. E-mail: akh_zam@yahoo.com

Introduction: Commissioning of the treatment planning system includes the accuracy of dose calculation in the inhomogeneous absorber. Several results of measurements of inhomogeneity correction factors (CFs) have been published. However, a dependence of CFs on beam energy may preclude such results from being applied to the general user's beam. The aim of the study was to assess the dependence of CFs on the photon beam energy.
Materials and Methods: CFs were calculated with the Batho method for several slab geometries comprising lung of 0.25 g/cm^3 and water of 1.00 g/cm^3. The CFs were calculated for 6MV (TPR 20/10 = 0.67±0.001) and for 15 MV (TPR 20/10= 0.76±0.001), k = -3, - 2, -1, 0, 1, 2, 3. All calculations were performed in the region were charged particle equilibrium exists.
Results: Changes of CFs of less than 2% were observed across the considered energy ranges. With a change of the TPR20,10 of 0.01, both for 6 and 15 MV at a depth of 5 cm below the lung; and lung thickness of 3, 5 and 8 cm, for field size of 10x10 cm^2, the change in CF never exceeded 2.4%. The dependence of changes of CFs on TPR20,10 were 1.74% and 1.2% for field size of 5x5 cm^2 and 20x20 cm^2 respectively. Comparison of 42 6 and 15MV linear accelerators installed in Poland showed that the maximum differences of TPR20,10 for 6 MV and 15 MV were 4.2% and 2.2% respectively.
Conclusion: A linear dependence of CFs on energy were obtained. The smaller is the field size and deeper is the point of interest below lung the larger dependencies on energy were observed.

P-151

FLUENCE RECONSTRUCTION FOR RAPIDARC TREATMENT PLANS

Rose Kamal, Gaganpreet Singh, Arun S. Oinam[1], Vivek Kumar
Centre for Medical Physics, Panjab University, [1]Department of Radiation Therapy, Regional Cancer Centre, PGIMER, Chandigarh, India. E-mail: rose.kamal22@gmail.com

Introduction: EPID verification of dose, 3D reconstruction of dose, various verifications of treatment plan. etc demands for the fluence data. The primary beam fluence information is not directly available for rapid Arc treatment plans in Eclipse Treatment planning system in contrast to IMRT treatment plans.
Objective: The aim of the study is to reconstruct primary beam fluence for RapidArc treatment plans from its DICOM beam parameters and treatment delivery records i.e. dynalog files and to validate the reconstructed fluence.
Materials and Methods: Eclipse treatment Planning system (v 11.0.31) is used to generate the RapidArc plans. A Medical Linear Accelerator of Varian Medical Systems, Palo, Alto, CA equipped with 120 multi leaf collimators is used to deliver the treatment plan. The DICOM-RT files of the patient are exported and the information related to beam parameters is extracted using MATLAB® software version R2008b (The MathWorks, Natick, MA). The fluence is reconstructed from extracted data of beam parameters for each gantry angle. The other set of fluence is again reconstructed from recorded dynalog files and validated against the fluence reconstructed from beam parameters. Gamma analysis between the reconstructed fluences is done using indigeneously built software.
Results and Discussion: The reconstructed fluence from both DICOM-RT file and dynalog files as shown in Figure 1, also passes the gamma criterion of 1% dose difference and 1 mm distance to dose agreement tolerance limits for 95%

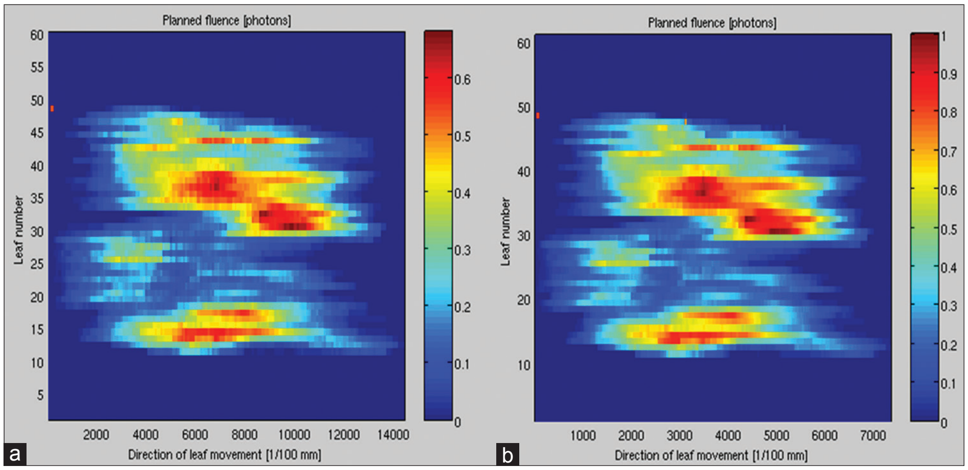

Figure 1: (a) Reconstructed fluence from beam parameters, (b) reconstructed fluence from treatment delivery records

bixel population. The fluence data reconstructed can further be used for 3D dose reconstruction to model an indigenous dose calculation algorithm and verification of delivered dose.

P-152

EFFECT OF CT TO ED IN RADIOTHERAPY TREATMENT PLANNING WITH ALGORITHMS AVAILABLE IN CMS XIO TREATMENT PLANNING SYSTEM TO VERIFY INHOMOGENEITY CORRECTION

Suman Kumar Putha, Challapalli Srinvias, B. M. Vadhiraja[1], Raghavendra Holla[2], Dilson Lobo, P. U. Saxena, Sourjya Banerjee, Dinesh Pai Kasturi

Department of Radiotherapy and Oncology, Kasturba Medical College Hospital (An Associated Teaching Hospital of Manipal University), Mangalore, Karnataka, [1]Department of Radiation Oncology, Manipal Hospital, Bengaluru, Karnataka, [2]Department of Medical Physics and Radiation Safety, Amrita Institute of Medical Sciences, Kochi, Kerala, India. E-mail: physicssuman@gmail.com

Purpose: The aim of this study to verify the effect of CT to ED in radiotherapy treatment planning using available algorithms in Elekta CMS XiO treatment planning system (TPS) for inhomogeneity corrections.

Materials and Methods: Gammex Computed tomography electron density phantom is used to generate the CT to ED curve with high speed GE CT scanner. Two sets of CT to ED files were generated with and without the presence of water medium. Dose calculations were performed with CMS XiO with three inhomogeneous phantoms (comprising combination of water, lung and bone equivalent slabs). Three inhomogeneous phantom combinations were considered to mimic the homogenous (water equivalent), lung equivalent and bone equivalent tissues. CMS XiO treatment planning system is used for dose calculations with different field sizes (5×5, 10×10, 15×15 and 20×20) using Convolution, Superposition and Fast superposition algorithms to account inhomogeneous corrections.

Results: The dose calculations were over estimated by Convolution algorithm with mean deviation of -5.8, -3.2 and 2.1 in Phantom A, Phantom B and Phantom C respectively compared to Superposition and Fast superposition algorithms. The percentage variation of 0.2, -0.5 and -0.2 was observed among the with A, B and C phantoms using the CT to ED conversion files with homogeneous (water) medium and without homogeneous medium.

Conclusion: Superposition and Fast superposition algorithm dose calculations were superior compared to Convolution algorithm in CMS XiO treatment planning system. The deviation observed in the case two CT to ED sets with and without homogeneous medium observed to be minimal.

P-153

DEVELOPMENT OF AN ANTHROPOMORPHIC DEFORMABLE LUNG PHANTOM

Dong-Seok Shin, Seong-Hee Kang[1], Kyeong-Hyeon Kim, Tae Ho Kim, Dong-Su Kim, Do-Kun Yoon, Tokihiro Yamamoto[2], Tae Suk Suh

Department of Biomedical Engineering, Research Institute of Biomedical Engineering, College of Medicine, The Catholic University of Korea, [1]Department of Radiation Oncology, Seoul National University Hospital, Seoul, Republic of Korea, [2]Department of Radiation Oncology, University of California Davis School of Medicine, Sacramento, USA.
E-mail: remember21@catholic.ac.kr

Several deformable lung phantoms have been proposed for investigation of 4D imaging and radiotherapy techniques. However, the complex anatomy of the lungs and airways is not typically modeled. The purpose of this study was to develop an anthropomorphic deformable lung phantom and evaluate its characteristics. The phantom consists of: (1) an iodine-infused flexible urethane foam to simulate the lung parenchyma, (2) a 3D-printed deformable airway model, and (3) an in-house programmable motion platform. A 3D-printed airway model (diameter range, 1–16 mm) was developed using diagnostic CT image of a canine through image segmentation, computer-aided design modeling, and 3D printing. The 3D-printed airway model was used as a mold to cast the flexible foam such that the airway was surrounded by the foam. Repeat CT scans

Table 1: Volume change and computed tomography numbers for the iodine-infused flexible urethane foam

Data set	*Volume change (%)*	*CT number (HU)*			
		End-inhalation		*End-exhalation*	
		Mean±SD	*Peak value*	*Mean±SD*	*Peak value*
1	24.3	−643.5±246.4	−804.0	−559.0±301.5	−710.0
2	24.5	−642.7±247.1	−797.0	−556.8±303.3	−708.0
3	24.4	−644.2±245.8	−797.0	−556.2±303.7	−708.0
4	24.3	−644.7±244.3	−799.0	−554.9±304.3	−717.0
5	24.5	−643.5±245.9	−794.0	−555.4±303.8	−710.0

CT: Computed tomography, SD: Standard deviation

Table 2: Length of deformation vector fields difference between reference data set and other data sets

Case	*Length of DV difference (mm), mean±SD*
Reference - data set 2	0.18±0.15
Reference - data set 3	0.22±0.20
Reference - data set 4	0.23±0.19
Reference - data set 5	0.24±0.22

Reference: Data set 1. DV: Deformation vector, SD: Standard deviation

were performed at end-inhalation and end-exhalation phases over the time frame of 2 hours to quantify the density, motion, and deformation of the lung parenchyma, and to evaluate their reproducibility. Deformation vector fields (DVFs) were acquired using deformable image registration. The diameter variation of the airway was calculated to evaluate the airway deformation. The peak CT numbers of the parenchyma model were -798.2±3.3 and -710.6±3.3 HU on average at end-inhalation and end-exhalation, respectively as shown in Table 1, which were comparable to the human lung density. Variations in the peak CT number were less than 7 HU. From visual inspection, the DVF was also similar to the human lung with greater displacements in lower regions than in upper regions. The length of deformation vector differences between the repeat scans was found to be less than 1 mm on average and data presented in Table 2. The mean difference of the airway diameter between two phases was 0.81±0.43 mm. The deformable lung phantom proposed in this study was found to mimic the human airways and lung parenchyma with reproducible density, motion, and deformation.

P-154

REVIEW OF DOSIMETRY FOR TOTAL SKIN ELECTRON THERAPY USING DIFFERENT DETECTORS

Shantanu Kumar Mishra, C. M. Tambe, S. N. Kale, D. D. Deshpande

Department of Medical Physics, Tata Memorial Hospital, Mumbai, Maharashtra, India. E-mail: shantanumishra92@gmail.com

Introduction: Total Skin Electron Therapy is a standard modality for the treatment of Mycosis Funcoides. It affects only a first few mm depth of skin over the entire body. This obviates the use of low energy electron beams, large field sizes of 80 cm width and 200 cm height at patient surface and large Focus to Skin Distances (FSD). In our institution, Modified Stanford technique is used to execute TSET.

Objective: The aim of this project is to review the dosimetry of TSET following AAPM TG-30 report and using TLDs and Radiochromic films.

Materials and Methods: A Varian Truebeam LINAC with 6 MeV HDTSe- mode for TSET having a dose rate of 2500 MU/min was used in the project. A wooden frame was designed with a slot for a Perspex scatterer/degrader of dimension of 110 cm × 195 cm × 2 mm. The calibration point is at a distance of 26 cm from the degrader. FSD is kept at 463 cm. Depth dose and profile measurements were done using PPC05 chamber and Solid water phantom (SP). Verification of PDD was done by sandwiching a Radiochromic film in SP. Profiles were verified using TLD with wax bolus for buildup. Angle of tilt was determined geometrically by superimposing 2 vertical profiles using FWHM and verified dosimetrically. PDD for 6 dual field was determined by placing film in a cylindrical wax phantom (WP). Absolute dose measurement was done at the calibration point (Umbilicus) using Roos chamber according to TG-30 and TRS-398 recommendations. MUs were delivered to get the prescribed dose for single dual field to the WP with TLDs attached in 3 positions 60° apart with 1.5 mm buildup. The same was verified in body phantom. Treatment skin dose was measured by exposing the WP to 6 dual fields with TLDs placed in all 6 positions and film wrapped around it with buildup.

Results and Discussion: Single TSET field has a mean energy of 4.2 MeV, most probable energy of 5 MeV at surface and X ray contamination of 1.5%. Uniformity for a single field in the central 60 cm × 160 cm region is 30% vertically and 5% horizontally which is below the recommended guidelines. To improve uniformity, the use of dual field becomes necessary. Angle of tilt calculated graphically, measured with TLD and determined dosimetrically are 15.5°, 16° and 17° respectively. However compared to other beam angles, at 17° tilt angle the best uniformity of 2% is obtained and considered appropriate [Figure 1]. The characteristics for both single and dual field are identical, both having dmax at 8 mm. Due to contribution of other beams the dmax for 6 dual field is 1.2 mm [Figure 2]. Measured absolute dose at Calibration point using dual field is 0.038cGy/MU. For a planned dose of 1.2 Gy for a dual field, the measured dose was 1.1 Gy. For prescribed skin dose of 3.6 Gy for 6 dual field, the measured dose was 2.92 Gy. This variation is due to uncertainty involved in the technique and needs to be explained to Physician in determining prescription dose. The ratio of Treatment Skin dose to Calibration point dose (B factor) was found to be 2.65 which is within the range specified

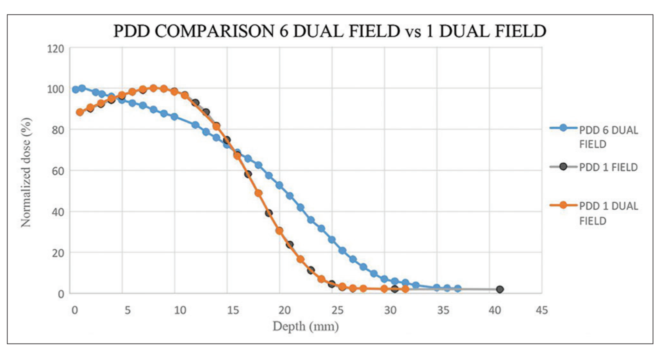

Figure 1: PDD curve of single field (black), 1 dual field (orange) and 6 dual field (blue). The dmax for 6 dual field is 1.2 mm compared to 8 mm of single or dual field.

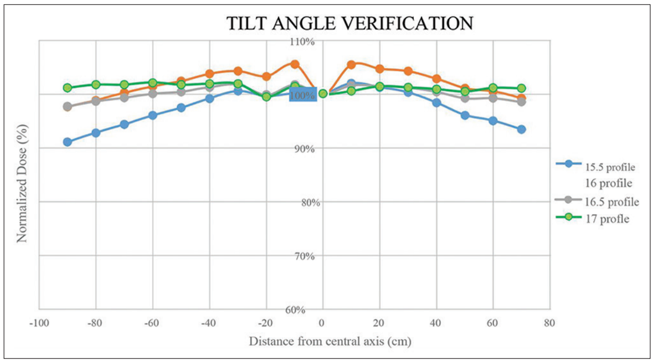

Figure 2: Tilt angle verification using profiles of 15.5˚ (blue), 16˚ (orange), 16.5˚ (grey) and 17˚ (green). A ±2% of uniformity is obtained for 17˚ tilt angle in solid phantom.

in TG. Film result shows ±10% variation in uniformity around the surface and Dmax show a periodicity every 60˚ when exposed with 6 dual fields.

Conclusion: Result shows a better uniformity of dose and hence can be used clinically.

P-155

RADIATION DOSE TO ADJACENT ORGANS-AT-RISK FROM INVOLVED-FIELD AND INVOLVED-SITE RADIOTHERAPY FOR LYMPHOMA

Mazonakis, E. Lyraraki[1], J. Damilakis

Department of Medical Physics, Faculty of Medicine, University of Crete, [1]Department of Radiotherapy and Oncology, University Hospital of Heraklion, Heraklion, Crete, Greece. E-mail: mmazonakis@med.uoc.gr

Introduction: The conventional involved-field radiotherapy (IFRT) or the modern involved-site radiotherapy (ISRT) can be used for the management of Hodgkin and non-Hodgkin lymphoma above the diaphragm. Both radiotherapy techniques unavoidably expose the surrounding healthy tissues to ionizing radiation and they might lead to long-term complications such as second cancers and/or cardiovascular disorders.

Objectives: The aim of this study was to compare the radiation dose received by adjacent organs-at-risk from IFRT and ISRT for lymphoma.

Materials and Methods: Ten male patients with lymphoma in the region of mediastinum were referred for three-dimensional conformal IFRT in our department. The patients underwent a treatment planning computed tomography (CT) on a 16-slice scanner. The lungs, thyroid gland, esophagus, heart and spinal cord were defined as the organs-at-risk and they were manually traced on the patients' CT images. For each study participant, a new three-dimensional plan was generated for the ISRT technique in accordance with the guidelines of the International Lymphoma Radiation Oncology Group. The IFRT and ISRT plans were designed using 6 MV photon beams. The prescription dose was 30 Gy for all plans. The dose volume histograms derived from the above treatment plans were used to find the average radiation dose (Dav) received by the lungs, thyroid, esophagus and heart. The maximum dose (Dm) to spinal cord was also recorded.

Results: The planning target volume in all treatment plans received at least 95 % of the prescribed dose. The Dav of each organ-at-risk and the Dm of the spinal cord as calculated by the ISRT plans were significantly lower than those from the IFRT ($p<0.05$). The mean value of the Dav of the lungs, thyroid gland, esophagus and heart associated with IFRT was 1205±122 cGy, 910±770 cGy, 2193±477 cGy and 1686±586 cGy, respectively. The corresponding mean values due to ISRT were equal to 626±117 cGy, 70±47 cGy, 1358±198 cGy and 512±442 cGy. The mean Dm of the spinal cord from IFRT and ISRT was 3127±201 cGy and 3034±135 cGy, respectively.

Conclusions: The use of ISRT for lymphoma may significantly reduce the radiation dose to the adjacent organs-at-risk compared with the organ doses attributable to IFRT. The above dose sparing should be taken into account by both radiation oncologists and medical physicists in the choice of the proper irradiation technique.

P-156

COMPARISON OF MEASURED DOSE VERSUS TPS CALCULATED DOSE IN THE INDIGENOUS PHANTOM CONSTRUCTED WITH STAINLESS STEEL (316L SS) IMPLANT

Bhudevi Soubhagya N. Kulkarni, Gowtham Raj, Ravikumar Manickam[1], M. Chandrasekhar[2], Alok Kumar[3], B. Naveen, Gururaj Deshpande, Vasant Harsur

VTSM Peripheral Cancer Institute, Branch of Kidwai Cancer Center, Kalaburagi, Karnataka, [1]Kidwai Cancer Center, Bengaluru, Karnataka, [2]Jawaharlal Nehru Technological University, Hyderabad, Telangana, [3]Netaji Subhas Chandra Bose Institute, Kolkata, West Bengal, India. E-mail: bhudevi10@yahoo.com

Introduction: The outcome of radiotherapy depends on multiple factors such as accurate organ delineation, including the tumor volume, optimization of beam angles and intensities, voxel-based dose calculation and accuracy of dose delivery within the patient. The accuracy and resolution of the CT image set used for treatment planning is crucial. And the lack of it can fail all of these processes. Patients undergoing radical treatment of tumors in pelvic region with a steel implant leads to the CT artifacts which results in errors for treatment planning process. To evaluate the adverse effects on dose due to the presence of steel implants.

Objectives: To measure the dose at the interface between a hip metallic implants and surrounding area with an indigenous phantom at peripheral cancer hospital.

Materials and Methods: Materials for the implant phantom (IM-p) were chosen with the same goals as with previously developed phantoms: to caricaturist physical properties, such as density and attenuation coefficients, with simple manufacturing techniques. The IM-p was manufactured with the acrylic solid cylinder with openable 3 cylindrical holes of different sizes. The three acrylic openable wholes can be replaced with any materials of different density. In this study we have designed to insert three different size cylindrical steel rods. The steel used for the construction of phantom was 316L SS type which is commonly used in the orthopedic bone implants. For the point measurement the phantom was provided with the chamber holder where we can measure the TPS planned dose. The IM-p was scanned with the 3 acrylic cylinders on Philips Big bore computed tomography (CT) for oncology. The same phantom was scanned with the three steel implants inserted for the study. The Axial cuts were taken with matrix size of 512 × 512. The image sets were reconstructed with 2 mm slice thickness. The Philips big bore CT is provided with orthopedic metallic artifacts reduction (O-MAR) algorithm. These were transferred to the radiation therapy treatment planning workstation through digital imaging and communication (DICOM) to Eclipse (Palo Alto, USA Version 13.7) treatment planning system (TPS). A total of three image sets were exported one with acrylic inserts and second one with the 316L type inserts and the third one with the O-MAR corrected image set. A plan was constructed on both the image sets.

Results and Discussion: The phantom is under construction and the results will be presented during the conference.

P-157

SURFACE DOSE VARIATIONS IN 6 AND 10 MV FLATTENED AND FLATTENING FILTER-FREE PHOTON BEAMS

Avtar Singh, Amit Saini, Shefali Pahwa, Ashok Kumar, D. D. Deshpande[1], Tapas Dora, Amrinder Chhabra, Varinder Chhabra

Department of Radiotherapy, Homi Bhabha Cancer Hospital, Sangrur, Punjab, [1]Department of Medical Physics, Tata Memorial Hospital, Parel, Mumbai, India. E-mail: avtar.medphy@gmail.com

Introduction: As the use of linear accelerators operating in flattening filter-free (FFF) modes becomes more widespread, it is important to have an understanding of the surface doses delivered to patients with these beams. Flattening filter removal alters the beam quality and relative contributions of low-energy X-rays and contamination electrons in the beam. Having dosimetric data to describe the surface dose and buildup regions under a range of conditions for FFF beams is important if clinical decisions are to be made.

Aims and Objectives: The purpose of this investigation was to evaluate and compare trends in surface dose for 6 and 10 MV flattened and FFF beams under conditions routinely experienced in radiotherapy treatments. These conditions were:

- o Variations in field size (square fields, sizes 3 × 3 to 40 × 40 cm^2)

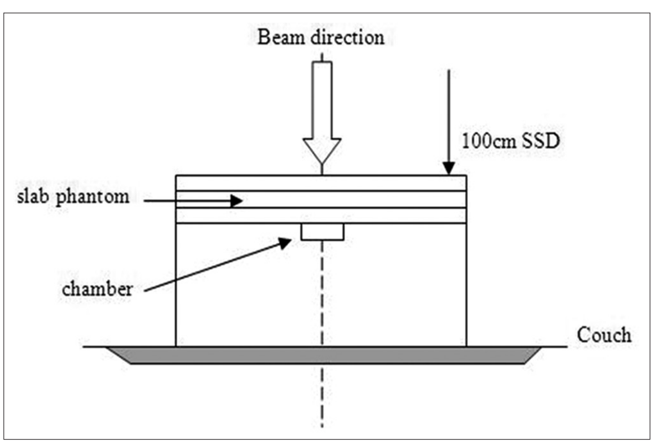

Figure 1: Experimental setup for surface dose and buildup

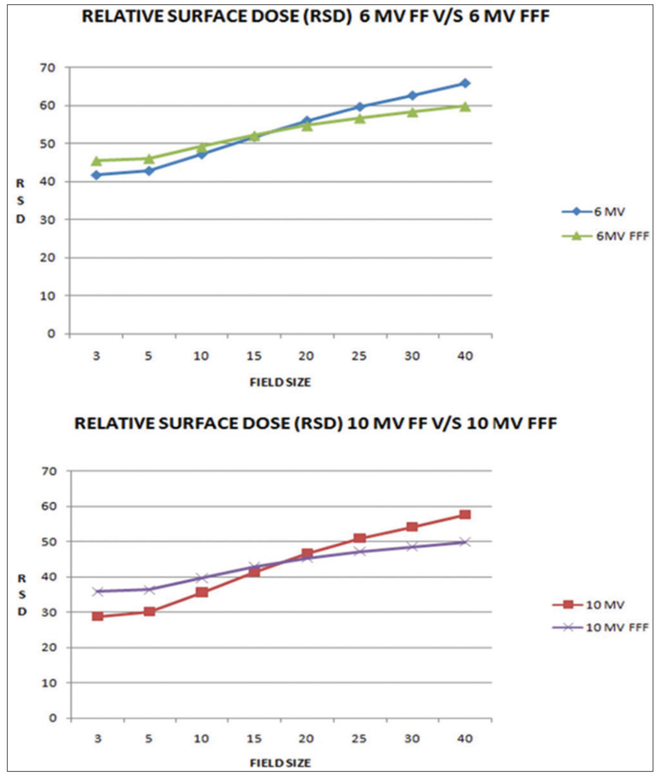

Figure 2: Variation of surface dose with field size for flattened and flattening filter-free beams for jaw settings of 3 × 3 to 40 × 40 cm^2: 6 MV and 10 MV

- o Variation in source-surface-distance (SSD) (70 to 110 cm)

Materials and Methods: An Elekta Versa H.D linear accelerator (Elekta) with a standard 160-leaf MLCi2 head has been used for measurements. The flattening filter is replaced with a 2 mm stainless steel plate that is used to shield out contamination electrons from the primary collimator. Measurements were taken in a slab phantom composed of 30 × 30 cm^2 Solid Water equivalent slabs of varying thickness as shown in Figure 1. A thin window parallel plate chamber SNC350p (Sun Nuclear Corporation). Surface dose readings are therefore reported as relative surface dose (RSD) where *RSD* = dsurface /dmax.

Results: Field Size Variation: Surface doses are seen to increase almost linearly with increasing field size, albeit at a shallower incline for FFF beams than for the conventional [Figure 2]. At 6 MV the unflattened beam shows a slight increase in RSD at smaller field sizes and decrease at larger with equivalency at 15 × 15 cm^2. At 10 MV there is again far less variation in the RSD with field size for the FFF beams, but the conventional beam generally exhibits lower surface doses [Figure 2]. The surface doses are of equivalent magnitude at a field size of 20 × 20 cm^2. For the 6 MV beam, there is a variation in RSD of 24.1% in changing field size from a 3 × 3 to 40 × 40 cm^2, compared to 14.4% for the FFF. At 10 MV these values are 28.75 % for 10 MV and 13.8 % for 10MVFFF.

SSD Variation: At 6 MV there is little difference between the FFF and conventional beams, except near the treatment head where the FFF beams show a reduction in surface dose of up to 4% for large filed size 20 x 20 cm^2 but for small filed size 5 x 5 cm^2 is increased by 2% [Figure 3]. The 10 MV FFF beam again shows the same behavior as that of 6 MV beam. RSD is very stable between 90 and 110 cm SSD.

Discussion and Conclusions: Removal of the flattening filter has been shown to have many potential benefits over

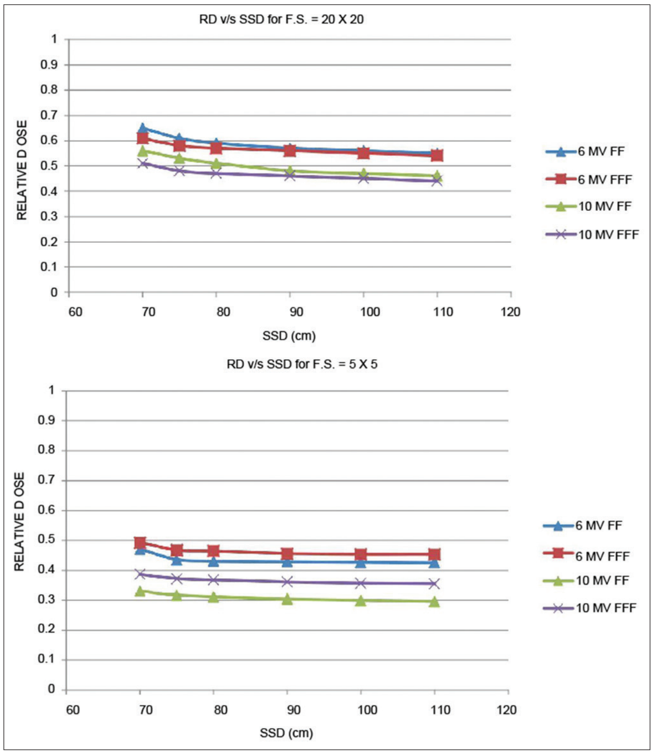

Figure 3: Variation of surface dose with source-surface distance for flattened and flattening filter-free beams for jaw settings of 20 × 20 and 5 × 5 cm^2: 6 MV and 10 MV

con-ventionally filtered beams for the delivery of treatments techniques such as SRT, SBRT, and IMRT. The present study indicates that the surface doses from these beams are very similar to those experienced for conventional flattened beams, and are therefore unlikely to cause concern in a clinical setting.

P-158

COMMISSIONING AND DOSIMETRY OF TOTAL BODY IRRADIATION

Sabari Kumar, S. Sathiyan, M. Ravikumar, K. M. Ganesh, B. Shwetha, C. Varatharaj

Department of Radiation Physics, Kidwai Cancer Institute, Bengaluru, Karnataka, India.
E-mail: sabari_kumar6@yahoo.ca

Introduction: Total Body Irradiation (TBI) is a treatment technique that involves the irradiation of the whole body. Several disorders where the entire body requires treatment have been proven to respond to TBI, including Lymphomas, Leukemias and Aplastic Anaemia. In situations where an allogeneic bone marrow transplant (BMT) or stem cell transplant is prescribed it is common for such patients to undergo TBI in combination with chemical therapy as part of a pre-transplant cytoreductive conditioning process. Total Body Irradiation (TBI) is frequently used to destroy the bone marrow and leukemic cells, to immune suppress the patient prior to receiving a bone marrow transplant (BMT) or both. TBI differs in many aspects from the standard irradiation procedures, because the whole body, including the skin is the target volume. There are many factors that work to limit dose homogeneity when the total body is the target of irradiation. Such as irregularity of the irradiation volume, thickness variation, skin sparing effect of high energy radiation beam, significant amount of scatter radiation and dose measurement limitations etc,. Therefore beam calibration, radiation field analyze, in-phantom measurements and treatment setup are important considerations in the whole chain of TBI success.

Materials and Methods: In TBI, whole body is the target volume; the treatment field to entire patient body can be achieved at the extended distance from source (Geometric Divergence of Radiation beam) 400 cm. The dosimetry data at this SSD is little complicated due to phantom dimension limitation. The dosimetry data such as PDD, Beam Profile and Beam Calibration was analyzed at this extended SSD setup by considering different parameters of side scatter, beam modifier and dose rate etc,. The dose was estimated on the surface of Rando Phantom using OSLD and wax buildup.

Results and Discussion: Basic inverse square measurements showed around 17% deviation from calculated value of Standard SSD. The effect of side scatter on beam output was found negligible around 0.6%. The dose rate effect on the beam output was shown the significant large deviation of 4.5% in 6MV photon beam and 3.5% in 18MV photon beam. The deviation between the measured and calculated (using Mayneord Factor) PDD was 4.5% with 6MV photon beam and 4% with 18MV photon beam at the extended SSD. The beam modifier (1 cm Prespex sheet) placed at a distance of 15 cm from phantom surface is increases the surface dose to 95%. The humanoid Rando phantom was used for the dose verification. The dose was estimated on the surface phantom (Umbilicus, Head, Neck and Chest level) using OSLD. The deviation between the measured and calculated dose was within 4.5%.

Conclusion: This study shows that the standard dosimetric data is not adequate for the TBI treatment planning. It is mandatory to perform the necessary dosimetric measurement at the treatment distance before the treatment delivery.

P-159

DOSIMETRIC CONSIDERATIONS FOR TOTAL SKIN ELECTRON THERAPY: OUR INITIAL EXPERIENCE

Daicy George, V. Remya, P. Suresh Babu, Geeta S Narayanan[1], S. Sowmya Narayanan

Departments of Radiation Physics and [1]Radiation Oncology, Vydehi Institute of Medical Science and Research Centre, Bengaluru, Karnataka, India.
E-mail: daicy.george91@gmail.com

Introduction: Total Skin Electron Therapy (TSET) is undoubtedly an effective method for the treatment of cutaneous T-cell lymphoma often referred as mycosis fungoids. Since there are many challenges in the choice of treatment technique, its dosimetry and execution, there is a necessity of special attention towards all of the aspects.

Objectives: The objective of this study is to develop a TSET program in our institution and to review the dosimetric considerations of the same.

Materials and Methods:

Choice of Treatment Technique: Although phantom studies suggest patient rotation using platform provides best uniformity over body surface, six- dual- field technique (modified Stanford techinique) widely used with isocentrically mounted linacs was chosen for the ease of treatment execution. Clinac 2300C/D (Varian Medical Systems, Palo Alto, CA) equipped with the special procedure HDTSe- (high dose rate total skin electron mode, E=6 MeV) was employed to perform TSET irradiation. To achieve wider angular spread of dose distribution at patient surface, acrylic scatterer of 1 cm was placed 20 cm in front of the patient. The planned treatment distance from isocentre was 3.5 meters.

Characterization of Beam at Treatment Plane: PDD measurements were carried out using perspex slabs arranged at 20 cm from the beam scatterer for 4 MeV and 6 MeV. Measurements were also done without beam scatterer for 4 MeV electrons. The most probable energy was calculated from the practical range. Beam profile measurement was done by raising the platform height for the chosen energy. Parallel Plate chamber (PPC 40) was used for all the dosimetric measurements.

Determination of Hinge Angle: Appropriate hinge angle for the dual field was calculated to obtain best dose uniformity along the vertical axis of treatment plane. Measurements were carried out at 270^0 and for different hinge angles varying from 15^0 to 20^0. Beam profile measurement was done for the selected hinge angle as well.

Patient Shielding: Eyes were shielded using lead equivalent spectacles 2 mm thickness. Toe nails and finger nails were shielded using combination of bolus and 5 mm Lead. Bolus was used to degrade the incident electron energy.

***In vivo* Dosimetry:** In vivo dose measurement was done using Optically Stimulated Luminescence Dosimeter (OSLDs) and Metal Oxide Semiconductor Field Effect Transistor (MOSFETs) at calibration point and different regions.

Local Boost: Soles were found to be underdosed from *in vivo* measurement, hence require boost. Output was measured for Gantry 180° for 4 MeV electrons in a basin filled with water which acts as electron absorber. Local boost for scalp can be given in Table 90° and Gantry 270° position if dose measured by *in vivo* measurement is inadequate.

Results and Discussion: 6 MeV electrons at accelerator plane with degrader which produces 4 MeV electrons at the treatment plane was chosen for the treatment based on requisite penetration depth for the patient. Hinge angle was determined to be 17°. Symmetry of profile measured at treatment plane was found to be 3%. Dose rate was measured using parallel plate chamber at the calibration point in the treatment plane. Output for local boost for soles was also measured. Dose measured by *in vivo* measurements were found to be close to the prescribed dose.

Conclusion: It is important to consider the dosimetric characteristics of TSET for each patient and for different treatment setups. Dosimetric considerations of TSET using six- dual- field technique using linear accelerator is challenging yet possible with available resources and is an effective treatment modality for mycosis fungoids.

P-160

THE RESPONSE OF WELL CHAMBER TO PRESSURE VARIATIONS AT HIGH ALTITUDES - A MONTE CARLO STUDY FOR ^{169}YB SOURCE

Sridhar Sahoo, T. Palani Selvam, Arghya Chattaraj, D. Datta

Radiological Physics and Advisory Division, Bhabha Atomic Research Centre, Mumbai, Maharashtra, India.
E-mail: barcsridhar@gmail.com

Introduction: Well-type ionization chambers traceable to national standards laboratory are routinely used to measure air-kerma strength of brachytherapy sources. During measurements, a temperature and pressure correction factor (K_{TP}) factor is applied to account for the change of air density in chamber volume. Pressure, P is directly proportional to air density at a constant temperature, T (^{0}C). P falls exponentially with height, h (m) and is given by the Barometric formula $P=P_0 \exp(-Mgh/R\,(T+273.15))$, where P_0 is standard pressure (1013.2 mbar) at h=0, M is molecular mass (29 g/mol), g is acceleration due to gravity (9.8 m/s^2), R is the universal gas constant (8.314 J/mol. ^{0}K). For example, air density at Shimla (h=2276 m) is 0.94 kg/m^3, which is about 78% of standard air density of 1.197 kg/m^3.

Objectives: The K_{TP} corrected normalized response ($K_{TP,\,NR}$) of a Standard Imaging HDR 1000 plus well chamber to air density variations at high altitudes for ^{169}Yb source is studied using EGSnrc and FLUKA Monte Carlo code. The ^{169}Yb 4140 source model developed for HDR application is considered in this study. In addition, response of hypothetic well chamber made of graphite, copper and C-552 is also investigated.

Materials and Methods: The HDR 1000 plus chamber is 10 cm-dia and 16 cm-height, made of an aluminum foil on the butyrate inner wall, an aluminum collecting electrode and outer wall. Well chamber with investigated source is modeled in the CAVRZnrc user-code of the EGSnrc and FLUKA code. Simulations are carried out for air densities ranging from 0.862 kg/m^3 (3048 m) to 1.197 kg/m^3. These air densities cover cities in the world at different altitudes including Indian cities mentioned in Table 1. The energy response is obtained by multiplying the dose deposited in the cavity with the air density and normalized with respect to standard density. Assuming $T=T_0=22\ ^0C$, $K_{TP} = P_0/P$. The $K_{TP,\,NR}$ is presented in Figure 1 for standard aluminum well chamber as well as for copper, C-552 and graphite materials for ^{169}Yb source.

Results and Discussion: Table 1 presents the $K_{TP,\,NR}$ for Standard Imaging HDR 1000 plus well chamber (made of aluminum) calculated for different cities at high altitudes for ^{169}Yb source. This response is about 1-3%, which is due to the range of electrons is higher than cavity dimension and few electrons will stop in the cavity. For air density 0.862 kg/m^3, which corresponds to 3000 m height, the $K_{TP,\,NR}$ is 9% and 4% higher than unity for copper and aluminum chamber, respectively [Figure 1]. The response is about to unity for C-552 chamber and 1-2% lower than unity for graphite chamber. The uncertainties in the Monte Carlo calculations are in the range of 0.6 - 0.8%. The $K_{TP,\,NR}$ is higher for aluminum, copper chamber than graphite, C-552 chamber. This is due to (a) production of more electrons in copper and aluminum

Table 1: Air densities of various cities having different altitudes and the variation in normalized response of aluminum chamber

City	*Height (m) above sea level*	*Air density (kg/m^3)*	*K_{TP}* normalized response for aluminum chamber for ^{169}Yb source*
Shimla	2276	0.937	1.032
Mexico city	2240	0.940	1.031
Darjeeling	2042	0.961	1.029
Srinagar	1585	1.009	1.024
Bengaluru	920	1.084	1.013
Pune	560	1.127	1.007

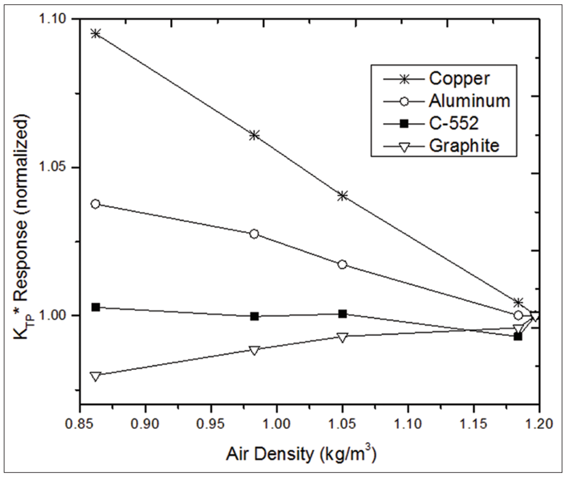

Figure 1: Graph represent the variation in the normalized response of chamber with air density for different chamber material.

chamber and (b) higher photon cross section in aluminum and copper than for C-552 and graphite.

P-161

DECOMMISSIONING OF HDR BRACHYTHERAPY UNIT AS PER REGULATORY REQUIREMENT G-3

Gayatri Sahu, Prakash Shinde, Sharmila Agarwal
Department of Radiation Oncology, Jaslok Hospital and Research Centre, Mumbai, Maharashtra, India. E-mail: gayatrisahu2008@gmail.com

Objective : Objective of this paper is to promote cost effective decommissioning of HDR brachy unit and safe disposal of decayed source as per AERB safety guideline AERB /RF/ SG/G-3 on consenting process for radiation facility through eLORA. Decommissioning is a process by which radiation unit is taken out of operation in a manner that provides adequate protection to health and safety of the workers, public and environment and ensure the safe radioactive waste management practice.
Materials and Methods: Micro Selectron HDR 080.0 classic remote after loading brachy therapy machine having serial no. -38023 that uses Ir-192 source was installed at Jaslok Hospital & Research Centre Mumbai in 2005 with maximum capacity of 10 Ci by Nucletron India Pvt Ltd (Now it is Elekta medical system Pvt Ltd.). Machine was operational till 2014 and unit was used for treatment of carcinoma of cervix and for breast implants. HDR model classic reached it's end of guaranteed support period, after which source production for classic HDR was stopped. Decommissioning work executed by M/s Elekta Medical System India Pvt. Ltd in 2016. Decayed radioactive source need to be removed in to an approved transport container and the unit has to be decommissioned. Decommissioning may include dismantling and reuse of machine components. The disused radioactive source and any contaminated material need to be disposed off separately. Decommissioning may be initiated after getting NOC from AERB. Consent for decommissioning of HDR unit and permission for export of radioactive source to its original supplier was obtained through eLORA. Ir-192 source having activity of 0.0001Ci was transferred into the approved container; subsequently container was sealed and labelled as radioactive package. Labelling of the package, transport index and category of package were calculated by maximum radiation level at 1 meter from external surface of the packages. HDR Unit was checked for contamination after transfer of the source into the container and found no contamination. Machine was dismantled and unit and parts like source storage unit, head unit, power supply, and control unit were handed over to BME of Jaslok Hospital for scraping.
Following information was labelled on the surface of package:

- Activity of source
- Address of the consignor and consignee
- Type of package
- United nation no
- Proper shipping address

Decayed source container was re-exported to original supplier with Transport Index, and container serial no. For radiation safety, TLD need to be worn during the source transfer and decommissioning process, radiation survey meter was also used to know the instant radiation level. Report on completion of decommissioning, safe disposal of source and personnel dose received during decommissioning operation was submitted to AERB.
Result: Decommissioning process was completed smoothly within the stipulated time period. The radiation protection survey conducted during the decommissioning process was found at background level. No contamination was found on head and source storage of the unit and at the end AERB was intimated about the decommissioning and safe disposal of source.

P-162

A BRACHYTHERAPY SIMULATOR

Thayal Singh Elias
Division of Radiation Physics, Regional Cancer entre, Thiruvananthapuram, Kerala, India.
E-mail: eliasjoy@gmail.com

In Radiation Oncology, keeping the radiation sources of different activity (strength) into the tumour volume or body cavities is called Brachytherapy. For a complete Radiation Oncology centre, Brachytherapy facility is mandatory. Cancer of the uterine cervix is one of the major diseases treated by a Brachytherapy equipment. In this mode of treatment, applicator positional accuracy is very critical as the radiation dose exposure gradient is very steep. For treatment dose calculations using treatment planning software, the position of the treatment applicator is reconstructed using isocentric orthogonal radiographs. In this procedure, it is important to retain the position of the applicators from the time of applicator imaging until the end of the radiation treatment. Normally in the absence of a dedicated Brachy Simulator, the patient will be physically shifted/ moved from the applicator insertion table to Simulator or X-ray machine, then to the treatment cot/couch. These three/four physical transfers greatly

affect the positional accuracy. To stop this error, this new system is designed. In this system, a C-Arm machine is integrated with the treatment applicator application table in such a way to take perfect orthogonal Radiograph and an automatic patient transfer mechanism to a trolley is provided. So in this system there is no need for any physical shifting of the patient. This provides an excellent treatment applicator positional accuracy for treatment planning and quick treatment execution leading to high patient comfort during treatment preparation and treatment execution. So it is expected to a good cancer growth control and cure.

P-163

DETERMINATION OF BLADDER AND RECTAL DOSE USING MOSFET AND RADIOCHROMIC FILM: A PHANTOM STUDY

A. Jeeva Bharathi, G. Bharanidharan, Prakasarao Aruna, J. Velmurugan, X. Sidonia Valas[1], S. Purnima[1], Thayalan Kuppusamy[1], Singaravelu Ganesan

Department of Medical Physics, Anna University, [1]Department of Radiation Oncology, Dr. Kamakshi Memorial Hospital, Chennai, Tamil Nadu, India.
E-mail: jeevanadhi007@gmail.com

Introduction: Dosimetry measurements are important for quality assurance in Brachytherapy sources with energy more than 100kev. Even 1.25MeV sources were used, hence the major challenge in brachytherapy is to verify the accuracy of dose distributions calculated by the treatment planning system. In vivo study of bladder and rectal dose in HDR is a tedious process and the patient safety is of higher concern. In this regard, measuring the bladder and the rectal dose is of prime concern with respect to intracavitary brachytherapy.
Objective: In the current study, it is aimed to determine the bladder and the rectal dose using MOSFET and radiochromic film in an indigenous phantom.
Materials and Methods: The measurements were carried out using 18 channels Microselectron - HDR. The doses were measured using Thomson Neilson MOSFET and EDT-3 radiochromic film. The calibrations of the radio chromic film were carried out for the Iridium source and the accuracy of the indigenous phantom was also determined using the HDR after loading system. The phantom has been designed which contains both the bladder and the rectum equivalent material and can accommodate the tandem and the ovoids assembly, which is normally used for brachytherapy.
Results and Discussion: Measurements were carried out by delivering the dose through the tandem and the ovoids in the phantom which contains the bladder and the rectum material. The detectors were placed over the bladder and the rectum material and the dose were delivered with respect to the reference points. The result shows that the dose received in the film is in good agreement with the planning system whereas for the MOSFET, it over estimates the dose.
Conclusion: The dose verification phantom for the rectum and the bladder was designed and their doses were estimated using MOSFET and radiochromic film, in which the radiochromic film and the MOSFET gives the dose which is in good agreement with the TPS.

P-164

SURFACE MOULD TECHNIQUE FOR MEIBOMIAN GLAND CARCINOMA – A CASE STUDY

G. Madhan Kumar[1], C. Krishnappan[1,2], C. Anu Radha[2], J. Antony Paull[1], Chirag Amin[1]

[1]Department of Radiation Oncology, Apollo CBCC Hospitals, Gandhinagar, Gujarat, [2]School of Advanced Sciences, VIT University, Vellore, Tamil Nadu, India.
E-mail: madhan@cbccusa.in

Introduction: Meibomian gland carcinoma is a very rare case, overall 1% or less of all cancers. It is about 3.2% among malignant tumors and 0.8% of all eyelid tumors. Meibomian gland carcinomas are typically found in women, most often in the seventh decade of life, and they usually are on the upper eyelid margin. The clinical appearance of Meibomian gland carcinoma is highly variable. They simulate such benign conditions as chalazion, blepharoconjunctivitis, keratitis, and other malignant or benign skin lesions. Many of the skin tumors have a predilection for the upper eyelid and have a yellowish appearance. Tumors at the eyelid margin commonly cause loss of eyelashes. Due to its surface irregularity it is a very challenging task for planning and delivery of radiotherapy. It is very difficult to choose the treatment technique for these types of tumors.
Objective: Aim of this study is to treat successfully of the Meibomian gland carcinoma which is located in the upper eyelid of the patient.
Materials and Methods: A male patient of age 42 years, is diagnosed with Meibomian gland carcinoma in his right upper eyelid has been taken for this study. According to the histopathological report, the size of the tumour was 2.5x1.5x1.1 cm with staging of pT3aN1. The tumour infiltrated to skeletal muscles also. In the CECT 2.2x1.0x1.5 cm sized mildly enhancing soft tissue density lesion is noted involving upper eyelid on the right side medially. And also the patient is having Metastatic carcinoma in right intraparotid lymphonode at the same side. Our team decided to treat this patient with surface mould brachy therapy. Surface mould is prepared with wax bolus and flexible implant catheters. The applicators were tagged with numbers to avoid the errors in treatment. A 5 mm thickness of the bolus is used to separate from the skin. We used four flexible implant catheters with spacing of 1 cm to cover the region and for better dose distribution. A CT scan is taken and from Vertex to the thorax. Planning and source optimization are done at Varian Brachy Vision 11.0 treatment planning system and the treatment was executed in Varian Gamma Medplus. Dose Prescribed for 50Gy in 25 fractions at every day one fraction. Metastatic carcinoma in right intraparotid lymphonode at same side treated with IMRT.
Results and Discussion: The patient has treated successfully. The progress of the treatment and the reactions were monitored on a weekly basis. The patient tolerated well and redness of the retina also minimal. The first three month follow-up shows the recovery of skin with hypopigmentation. Meibomian gland carcinoma is a malignant tumor and it tends to recur. Radiotherapy is quite effective in preventing local recurrences and controlling the long term control rates in these type of tumors. Treating with electron is another option for same patient. However to treat at the complex area of eyelid conventional surface mould brachy therapy has an edge over the electrons to save the vision of the patient and with minimal damage to the corneal. Taking call as brachy

therapy as a choice to treat the Meibomian gland carcinoma is a good substitute for external radiation. The Brachy therapy technique is labour intensive with compared to External radiation. Even though it is labor it worthwhile to go for brachy therapy for the cases like an eyelid.

P-165

ISOLATION ROOMS FOR RADIOACTIVE IODINE (I-131) THERAPY, INTRODUCTION OF GLASS WINDOW ON THE WALL FOR PATIENT COMFORT AND BETTER AMBIENCE

Marwa Al Aamri, Ramamoorthy Ravichandran[1], Naima Al Balushi

Department of Nuclear Medicine, Royal Hospital, Muscat, Oman, [1]Department of Radiotherapy, Medical Physics Unit, Cachar Cancer Hospital and Research Centre, Silchar, Assam, India.
E-mail: s44127@student.squ.edu.om

For administration of radioactive iodine for the treatment of differentiated cancer thyroid patients, activities ranging between 1.85GBq to 7.0GBq are used. Safety guidelines stipulate isolation of patients till their radioactive burden reduces to a level <10 μSv/h at 1 m. The construction of concrete rooms cleared by national regulatory authorities do not recommend presence of windows on the walls. Centralized air-conditioning with filters is incorporated in the design. Two isolation rooms originally designed for manual brachytherapy with Cs-137 and Ir-192, were being used for I-131 isolation work. Our experience over a decade showed many patients have phobia to stay in isolation rooms for more than 3 days, and hence many did not take the treatments. A necessity was felt to introduce glass window on the opposite side wall of entrance window, which had a service corridor with restricted entry, opening towards garden area. Commercially available lead glass used for x-ray CT scanner of size 1380 mm x 620 mm, of physical thickness 8.5 mm (2 mm Pb Equivalent) was fixed on the 0.35m thick concrete wall in both the rooms. The adequacy of protection offered by the lead glass was determined using a 600MBq I-131 capsule moved at a distance 50 cm away from the wall inside the room, and measuring transmission outside the room. An end window pancake type beta gamma survey meter with uncertainty ±15% was used for measurements. The measured values were normalized for 3.7GBq at 2m bed position in μSv/h. The obtained maximum exposure rate was 7.85 μSv/h, transmitted from the glass window, against 0.012μSv/h transmitted at full concrete wall level. As the patients provide shielding to the administrated activity, also the activity is progressively decreasing fast with an effective half life, the stray radiation levels will be decreasing outside, increasing the efficacy of protection. The patient's bed position is at lower level by 0.5m from the lower edge of the lead glass, so that during patient is in bed the stray radiation levels reduce further. The isolation rooms were handed over back after the present modification, with recommendations a) to have a cloth screen on the window inside the room for patient's privacy and b) to have a caution radioactive sign abstaining use of the service corridor by patients and relatives unless there is emergency. As there are no reports about such facility for isolation rooms, this report may be of value in health physics literature.

P-166

OCCUPATIONAL DOSES OF RADIATION WORKERS IN NUCLEAR MEDICINE DEPARTMENT, MINISTRY OF HEALTH, OMAN: A DOSE ANALYSIS

Sharifa Al-Kindy, Nadia Al-Isaee, L. S. Arun Kumar, Jamal Al-Shanfari

Department of Medical Physics and Radiation Protection Service, DGPEA, Ministry of Health, Muscat, Oman.
E-mail: shhh.alkindi@gmail.com

Use of ionizing radiation in the Sultanate of Oman is increasing with the proliferation of hospitals and clinics. The great benefits of increased and improved diagnostic services have improved the quality of life for those in Oman. The World Health Organisation in 2000 applauded the quality, efficiency and delivery of health care to the population and ranked the Oman's health care system eighth in the world.[1] The increased resources are clear from the statistics: in 1970 there were only 2 hospitals in Oman, in 2010 the number was 50 and with 172 health centres.[2] One of the balancing consequences of increased x-ray use in Oman is the increased radiation dose to the population. Medical radiation accounts for the majority of the manmade radiation dose to populations.[3] Use of radiation must always be according to the ALARP (as low as reasonably practical) philosophy so as to avoid unnecessary radiation doses and minimise the doses where required which in turn reduces the occupational exposure. During 2015, a total of 15,56,686 radiological procedures were performed in Ministry of Health (MOH) institutions. The corresponding number in 2000 was 799,452. This shows that there is about 95% increase in radiological examinations for the last 15 year period. This indicates that the population dose is on the rise as the radiological facilities are increasing in Oman which in turn increases the occupational dose of radiation workers. The occupational exposure of radiation workers of MOH hospitals were monitored by Thermo Luminescent Dosimeters (TLD's) which are dispatched to each location in MOH by post. We have developed an in-house dose management software - Centralised Dose Recording System (CDRS) for the management of dose records of Ministry of Health (MOH) radiation workers which manage TLD serial number allocation, issue to various hospitals/institutions, collection from respective hospitals/ institutions after wear period, dose assessment and monitoring, recording the doses and finally dispatching the dose reports to MOH hospitals/ health centres / institutions. Also, the same software will handle the individual dose (s) of each worker (s) and their dose history. Every month we are dispatching more than 1600 plus badges to 160 hospitals/ institutions of MOH throughout the Sultanate of Oman after tagging in CDRS. Thus we keep track of the TLD badges of each worker in every location of MOH on a monthly basis. Some of the above locations are very remote (few thousand kilometers away from the capital city- Muscat). In this study, we have analysed the dose pattern of radiation workers in the Nuclear Medicine Depts. of Ministry of Health for the ten year period 2006-2016. The range of whole body effective doses (Hp (10)) of the workers for the year 2016 is shown in Table 1.

The total number of workers wearing WB badges is 47 and the total number of workers wearing Ring badges is 35.

Similarly the extremity doses for both left finger and right finger badges were evaluated for the 35 workers.

The total number of workers wearing Left Ring badges is 8 and Right Ring badges are 27 and data of extremity doses of the workers is presented in Table 2.

Table 1: Whole body effective doses of radiation worker

Whole body effective dose range (mSv)	*Number of workers*	
	Wearing WB badges	*Wearing ring badges*
0.0-0.5	103	45
0.5-1.0	10	19
1.0-2.0	1	11
2.0-5.0	0	10
5.0-10	1	3
10-15	0	0
15-20	0	1
Above 20	0	0

WB: Whole body

Table 2: Extremity doses of radiation worker

Extremity dose range (mSv)	*Number of workers*	
	Wearing left ring TL badges	*Wearing right ring TL badges*
0.0–0.5	9	36
0.5–1.0	4	15
1.0–2.0	2	9
2.0–5.0	3	7
5.0–10	1	2
10–15	0	0
15–20	0	1
Above 20	0	0

TL: Thermo luminescent

It has been observed that workers in Nuclear Medicine receive relatively the same whole body effective doses compared to majority of the radiation workers of Ministry of Health and comparatively very low doses when compared to those in interventional radiology and cardiology depts. However, the extremity doses of the workers were found to be reasonably high as expected, particularly those who are involved with the hot lab and radiopharmacy operations. Further details will be discussed during presentation.

P-167

DOSE CALIBRATOR LINEARITY TEST USING I-131 AND ^{18}F-FLURO DE-OXY GLUCOSE.

Radha Muthuswamy, T. Suresh, S. Amutha
Department of Radiotherapy, HCG Bharath Hospital and Institute of Oncology, Mysuru, Karnataka, India.
E-mail: radham10@gmail.com

Dose Calibrators are devices used in radiotherapy to ensure that the dose delivered is what is intended. Dose calibrators are one of the most important and most frequently used instruments for the determination of activities in nuclear medicine. For guaranteeing a constant quality of the dose calibrators' measurements, constancy checks including the examination of the system linearity have to be performed regularly. Linearity test check confirms that, for an individual radionuclide, the same calibration setting can be used to indicate the correct activity over the range of use of that calibrator. We participated in 17th National Audit of I-131 Activity Measurements conducted by RSSD, Bhabha Atomic Research Centre.

Objective: The present study was aimed at performing the linearity test in dose calibrator at our Hospital using I-131 and ^{18}F-Fluro de-oxy Glucose. We are using dose calibrator manufactured by COMECER.

Introduction: Dose calibrator is a gas-filled cylinder with a well in the center of the ionization chamber into which the radioactivity is placed. An ionization chamber is an instrument constructed to measure the number of ions within a medium. It usually consists of a gas filled enclosure between two conducting electrodes (the anode and cathode). Typically, highly pressurized Argon [18-Ar] gas, compressed to around 20 atmospheres is used to fill the ionization chamber radiation detector. When gas between the electrodes is ionized by any means, such as by gamma rays or other radioactive emission, the ions and dissociated electrons move to the electrodes of the opposite polarity, thus creating an ionization current which may be measured. A voltage potential can be applied between the electrodes; depending on the application. Ionization chambers are widely used in the nuclear industry as they provide an output that is proportional to radiation dose.

Materials and Methods: The test was performed using Dose calibrator manufactured by COMECER. The schematic diagram of a Dose Calibrator is shown in Figure 1. Sources used for the test were I-131 and ^{18}F-Fluro de-oxy Glucose. The linearity test must be tested upon installation and at least quarterly thereafter as well as after repair. In this study we have used the Decay method.

Decay Method: This method involves a single radioactive source which is periodically measured over several days.

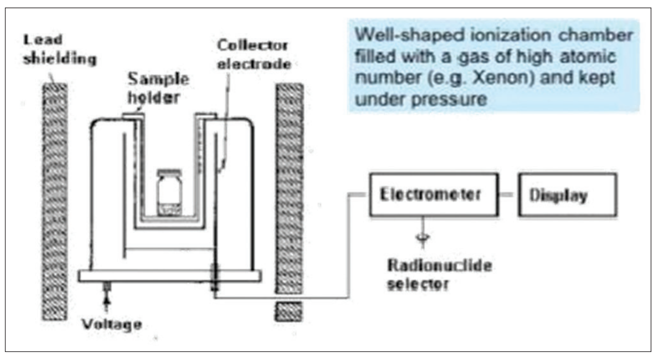

Figure 1: Schematic diagram of a dose calibrator

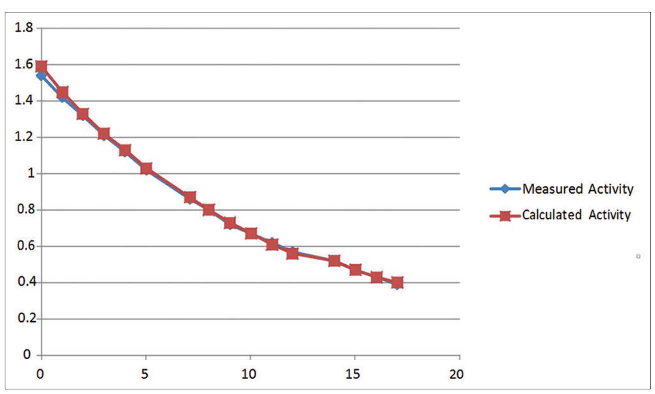

Figure 2: I-131 source activity decreases as a function of time

Table 1: Deviations between experimental and theoretical activities for I-131 at different times and measurement windows

Date of measurement	*Time of measurement*	*Measured activity (mCi)*	*Calculated activity (mCi)*	*Time elapsed since the first essay (days)*	*Percentage error*
February 27, 2017	12:19 pm	1.54	1.59	0	−3.14
February 28, 2017	12:33 pm	1.42	1.45	1.01	−2.06
March 01, 2017	12:04 pm	1.32	1.33	1.99	−0.75
March 02, 2017	12:22 pm	1.21	1.22	3.00	−0.82
March 03, 2017	12:14 pm	1.12	1.13	4.00	−0.88
March 04, 2017	12:49 pm	1.02	1.03	5.02	−0.97
March 06, 2017	02:54 pm	0.86	0.87	7.11	−1.15
March 07, 2017	12:57 pm	0.80	0.80	8.02	0
March 08, 2017	12:58 pm	0.72	0.73	9.03	−1.37
March 09, 2017	01:18 pm	0.67	0.67	10.04	0
March 10, 2017	01.13 pm	0.62	0.61	11.04	1.64
March 11, 2017	12.53 pm	0.57	0.56	12.02	1.78
March 13, 2017	12.55 pm	0.52	0.52	14.02	0
March 14, 2017	01.10 pm	0.47	0.47	15.03	0
March 15, 2017	01.11 pm	0.43	0.43	16.04	0
March 16, 2017	12.57 pm	0.39	0.40	17.03	−2.5

Half-life of I-131 is 8.0233 days

1. Assay the I-131 activity to be used in a syringe or vial in the dose calibrator, and subtract background to obtain the net activity in millicuries. Record the date, time to the nearest minute, and net activity.
2. Repeat the assay everyday about the same time.
3. Convert the time and date information you recorded to days elapsed since the first assay as shown in Table 1.
4. The measured activities and the calculated activities are then plotted versus time graphically [Figure 2]. Label the vertical axis in milli curies to represent the measured activity and label the horizontal axis as Time elapsed since the first essay in days. Calculate the percent error for each activity level/time interval.
   Use the formula:
   $$\%\text{error} = \frac{\text{expectedreading} - \text{actualreading}}{\text{expectedreading}} \times 100\%$$
5. Repeat the same procedure for ^{18}F-Fluro de-oxy Glucose. The results are shown in Table 2. The graph is as shown in Figure 3.

Measurements carried out for 17th National Audit of I-131 Activity Measurements:

Table 2: Deviations between experimental and theoretical activities for ^{18}F-fluorodeoxyglucose sources at different times and measurement windows

Date of measurement	*Time of measurement*	*Measured activity (mCi)*	*Calculated activity (mCi)*	*Time elapsed since the first essay (min)*	*Percentage error*
March 03, 2017	5:55 am	160	159.7	0	0.19
	6:55 am	109.3	109.3	60	0
	7:55 am	74.82	74.88	120	−0.08
	8:35 am	58.12	58.17	160	−0.09
	9:10 am	46.64	46.63	195	0.02
	10:00 am	34.01	34.00	245	0.03
	10:45 am	25.6	25.59	290	0.04
	11:20 am	20.49	20.52	325	−0.15
	11:50 am	17.02	16.98	355	0.23
	12:15 am	14.32	14.50	380	−1.24
	12:46 am	11.09	11.42	411	−−2.89
	01:15 pm	9.83	9.92	440	−0.91
	01:46 pm	8.01	8.16	471	−1.83
	02:14 pm	6.71	6.83	499	−1.76
	03:08 pm	4.76	4.86	553	−2.06
	04:36 pm	2.78	2.79	641	−0.36
	05:14 pm	2.18	2.19	679	−0.46
	06:15 pm	1.49	1.49	740	0
	06:55 pm	1.14	1.16	780	−1.72

Half-life of ^{18}F is 109.8 min

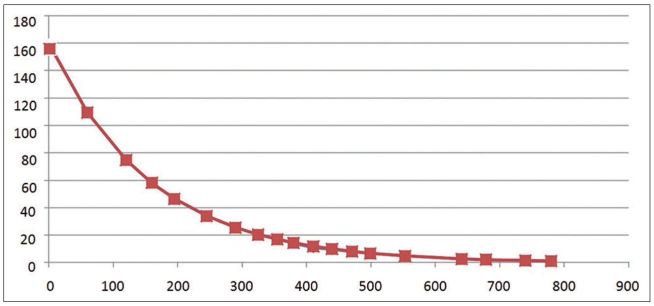

Figure 3: F-18 source activity decreases as a function of time

1. Ensure that radionuclide selected in the display is I-131.
2. Take 10 readings within 20 minutes, each time removing the source from the chamber and replacing it back into chamber for the next reading.
3. Calculate Mean and standard deviation.
4. Repeat the measurements on the next day at about the same time.

Discussion: The results of the study showed that the dose calibrator is working satisfactorily and has passed the linearity test. The graph plots for measured data perfectly fits the calculated data for both I-131 and ^{18}F sources. The discrepancy between measured data and calculated data were within +4%. If the deviation is more than +10% then an investigation has to be done on the dose calibrator. Our Hospital Dose Calibrator showed deviation of -3% relative to BARC activity.

P-168

ENHANCING RADIATION SAFETY AND PATIENT COMFORT BASED ON ANALYSIS OF RADIATION DATA AT THE TIME OF DISCHARGE OF RADIOIODINE THERAPY PATIENTS

K. S. Shekhawat, Prakash Yadav[1], Harshul Sharma[1], J. K. Bhagat[1], R. S. Lokhande

School of Life & Basic Sciences, Jaipur National University, [1]Department of Nuclear Medicine, Bhagwan Mahaveer Cancer Hospital and Research Centre, Jaipur, Rajasthan, India. E-mail: shekhawat.kan@gmail.com

Objective: To work out the radioiodine therapy plan by predicting hospital stay duration based on retrospective data of patient radiation level at discharge.

Materials and Methods: Radiation monitor readings of patient radiation level at discharge of 500 Cancer thyroid patients who have received radioiodine therapy at BMCHRC, Jaipur was analysed. The patient were categorized based on level of blood markers, residual tissue, nodal status, lung and bone involvement, 131-Radioiodine dose, duration of stay, etc. Statistical analysis was done using biostatics.

Discussion: The disease status and radioiodine dose amount play very crucial role for the planning and management radioiodine therapy patients. However, the level of radiation at the time of discharge can vary from patient to patient due to variation in absorption of oral radioiodine and biological half life of radioiodine in the patients. Averaging the values of Radiation monitor readings of patient radiation level at discharge can help in approximate prediction of duration of stay for various categories of patient. This can be helpful in scheduling the patients for radioiodine therapy.

Conclusion: The readings of patient radiation level at discharge can be helpful for better management.

P-169

PERFORMANCE CHARACTERISTICS OF POSITRON EMISSION TOMOGRAPHY SCANNERS

Hemant Kumar

Department of Radiodiagnosis, SMS Medical College, Jaipur, Rajasthan, India.
E-mail: chhimpajihemant0001@gmail.com

Medical imaging is the technique that uses the radiation as a tool to create visual representations of body interior for clinical analysis. Positron emission tomography (PET) is nuclear medicine functional imaging technique that introduced to observe metabolic processes in the body. PET provides the most specific and sensitive means for imaging molecular pathways and interactions in the tissues of man. In this technique small amounts of radioactive materials called radiotracers are introduced into body that emit positrons generate anti matter annihilation effect at 180 degree. Produced gamma rays can be detected by computer detector and produce functional image. The resulted image from PET shows bright spots on film reveals higher level of chemical activity and details about the function of tissue or organs. Significantly PET imaging shows physiological imaging, differentiate between malignant and benign tumor, tumor staging, pharmacokinetics of several novel antibiotics can be measured in human being etc. PET is also used to analysis in recurrent of various carcinomas. A major goal of the PET studies is to obtain a good quality and detailed radiological image of an object by the PET scanner. It depends on how well the scanner performs in image formation. There are several parameters associated with the scanner are critical to good quality image formation, which include spatial resolution, sensitivity, noise, scattered radiations, and contrast. These parameters are interdependent, and if one parameter is improved, one or more of the others are compromised.[1] In PET systems the clinical image is assumed to be linearly related to the activity uptake; because scatter adds a smoothly varying background to the image, it degrades the quantitative accuracy of the image and adds to the image noise, even when accurately estimated and subtracted.[2] There are many other performance characteristics that reflect a given aspect of a nuclear medicine PET imager. However, the Quantitative linearity and calibration is an important measurement for PET systems that aim to relate pixel values to activity concentrations.

References

1. Saha GB. Basics of PET Imaging – Physics, Chemistry & Regulations. Berlin: Springer; 2010.
2. Bailey DL, Humm JL, Pokropek AT, Aswegen AV. Nuclear Medicine Physics: A Handbook for Teachers & Students. Vienna: IAEA; 2014.

P-170

ESTIMATES OF ENTRANCE SKIN DOSE FOR PATIENTS UNDERGOING COMMON RADIOGRAPHIC EXAMINATIONS

S. C. Uniyal, S. D. Sharma[1], S. Raghuvanshi

Department of Radiology, Himalayan Institute of Medical Sciences, SRH University, Dehradun, Uttarakhand, [1]Radiological Physics and Advisory Division, Bhabha Atomic Research Centre, Mumbai, Maharashtra, India. E-mail: dr.suniyal@gmail.com

Introduction: Diagnostic X-ray imaging is the largest contributor to total population radiation exposure from man-made radiation sources. This is attributed to better technology and growing usage of diagnostic x-ray imaging methods. Patient dose involved in a diagnostic X-ray examination is a function of several parameters such as performance of X-ray machine, type of image receptor and selection of exposure parameters. The International Commission on Radiological Protection (ICRP) recommends that the patient doses should be measured on regular basis to optimize patient protection. So under realistic conditions of exposure, patient dose should to be estimated and verified against the established national diagnostic reference level (NDRL). DRLs for radiographic projections are often expressed in terms of the entrance skin dose (ESD), which is a measure of the amount of energy imparted per gram of tissue at the entrance surface.
Objectives: The present study was aimed to evaluate ESD for common types of radiographic examinations and to validate the results against established NDRLs.
Materials and Methods: The study was carried out on 1545 adult patients (age > 18 years) undergoing 10 commonly performed diagnostic X-ray examinations viz., chest posterior-anterior (PA), chest anterior-posterior (AP), cervical spine AP, cervical spine LAT, abdomen AP, lumbar spine AP, lumbar spine LAT, pelvis AP, thoracic spine AP and thoracic spine LAT performed in five X-ray rooms. ESD per X-ray projection was estimated by using an indirect method using following expression:
$ESD = \text{Tube output } (\mu Gy/mAs) \times mAs \times (100/FSD)^2 \times BSF$
Where FSD and BSF are focus-to-skin distance and backscatter factor respectively. Fixed focus-to-film distances (FFDs) of 180 cm and 100 cm were used for chest PA and rest of the X-ray projections respectively. FSD was calculated by subtracting patient thickness from the focus-to-film distance (FFD). Although values of BSF vary with X-ray beam qualities used for different radiographic projections, a single average value of 1.35 was used for the estimation of ESD in the present study. The output of each X-ray tube was measured by using a factory calibrated RaySafe Xi R/F detector from UnforsRaySafe AB, Billdal, Sweden.
Results and Discussion: Descriptive statistics of the obtained ESD data were presented in terms of mean, standard deviation, median and third quartile values. The lowest and highest average values of ESD were 0.29 mGy and 7.39 mGy for chest PA and lumbar spine LAT examinations respectively. For a given projection, the variation ESD was expressed in terms of the ratio of its maximum to minimum values. This ratio ranged from 5.05 for thoracic spine AP to 16.87 for chest PA X-ray examinations. The observed wide variation in the estimated ESDs for individual projections was attributed to the variation in patient thickness, operator specific selection of exposure factors and the radiographic technique used. The third quartile values of estimated ESDs were compared with respect to Indian NDRLs proposed in 2001 (Sasane et al.) and 2010 (Sonawane et al.). The majority of values were found smaller than the recommended NDRLs. The 3rd quartile values of the estimated ESDs were recommended as local/institutional DRLs.

P-171

OUR EXPERIENCE WITH THE ACCEPTANCE AND DOSIMETRIC VALIDATION OF SOMATOM FORCE DUAL HEAD MDCT IN THE ROYAL HOSPITAL, OMAN

Ruqaia Al-Harthi, Munira Al-Kalbani, L. S. ArunKumar, Jamal Al-Shanfari
Department of Medical Physics and Radiation Protection Service, DGPEA, Ministry of Health, Muscat, Sultanate of Oman. E-mail: ruqaiaalharthi@gmail.com

Introduction: Computed Tomography (CT) has revolutionized diagnostic imaging since its discovery in early 70’s. In Oman; 70,353 CT examinations were carried out in the year 2015. The increase in CT examinations will eventually result in the increase of population dose and the consequent risk of cancer in adults and particularly in children. Here, we discuss and share our experience with the acceptance and dosimetric validation of second Dual Head Somatom Force MDCT installed in the Royal Hospital, Oman using Ministry of Health’s radiation acceptance and quality assurance protocol, before handing over for routine patient care work.
Materials and Methods: The parameters measured included - scatter radiation, CTDI, Noise, CT numbers and Slice thickness. Scatter radiation levels were measured using perspexbody phantom and Victoreen NERO 8000 by connecting externally a 400 cc scatter chamber to it. CTDI was estimated using 100 mm pencil CT ion chamber along with NERO 8000, PMMA head and body phantoms. Weighted CTDI (CTDIw) and normalized weighted CTDI (nCTDIw) were estimated. nCTDIw was estimated for each tube separately and in the combined dual energy mode as well. Image noise, slice thickness and CT numbers were measured with AAPM CT performance phantom (Victoreen).
Results and Discussion: The scatter radiation was measured at different positions around the scanner. The results show that the radiation levels around the scanner are distributed based on the invers square law. The radiation levels at the rear side of the gantry are little more than the front side due to the attenuation of radiation through the gantry. The normalized weighted CTDI (nCTDIw) values for head and body phantoms were measured for various kVp’s and collimations for each tube separately and in dual energy mode as well. All results were analyzed, which were in good agreement with manufacturer’s values. The CT number insert in the AAPM performance phantom had Polyethylene, polystyrene, nylon, polycarbonate and acrylic with HU -68, -24, 92, 102 and 120 respectively. The CT number was measured for various kVp’s for each tube separately and in dual energy mode as well. The measured CT values were in good agreement with the quoted CT numbers. The image noise was analysed by measuring the mean CT number of the ROI and standard deviation. The image noise was analysed for various kVp’s for each tube separately and in dual energy mode as well. All measurements were within the limit. Different slice thicknesses were set and measured in the AAPM performance phantom at different kVp’s for both tubes. The measured slice thickness were in good agreement with the set values.
Conclusion: In this study we have tried to validate the standard QA protocol of Ministry of Health for CT scanners in this DE MDCT as well. Results showed that the measured parameters were in close agreement with the manufacturer’s specs. Surveys shown that CT scanners operating at correct

parameters deliver optimal radiation exposure to patients whereas dose to the patients will be significantly affected if not set properly. Thus a well performed QA programme in accepting and validating CT scanners will yield good quality scans which in turn delivers an optimal dose to the patients undergoing CT investigations.

P-172

ESTIMATION OF ENTRANCE SKIN DOSE DURING ABDOMINAL DIAGNOSTIC X-RAY EXAMINATIONS USING OPTICALLY STIMULATED LUMINESCENCE DOSIMETER

M. Kumaresan, Anuj Soni[1], R. Kumar[1], A. Chaubey, S. Kantharia

Department of Radiology, Medical Division, Bhabha Atomic Research Centre, [1]Radiological Physics and Advisory Division, Bhabha Atomic Research Centre, Mumbai, Maharashtra, India. E-mail: kumaresa@barc.gov.in

Aim: The aim of this study was to use the indigenously developed optically stimulated luminescence (OSL) dosimeter for estimation of entrance skin dose during abdominal diagnostic X-Ray examinations and evaluate the work practice on the basis of radiation safety point of view.

Materials and Methods: The α-Al_2O_3:C OSL dosimeter used in this study was developed in Bhabha Atomic Research Centre, Mumbai. The α-Al_2O_3:C OSL pallets used were having diameter of 0.7 cm and thickness of 0.014 cm and are prepared by mixing the α-Al_2O_3:C powder of grain size (75-100 μm) between and Teflon in 1:3. OSL disc were sealed in a black light-tight polythene pouch to make it light insensitive. This pouch was kept on the patient's body in the center of the field of the radiographic projection. After experimental irradiation, the OSL discs were read individually using RISO TL/OSL reading system TL/OSL-DA-15 which has a cluster of 42 blue light emitting diodes (α =470 ± 30 nm) for stimulation. A band pass UG1 filter which prevents the scattered blue light from reaching the photomultiplier tube was used. The OSL was recorded at a power of 40 mW-cm^2 for 60 s. The background data from control cards (dosimeters) were subtracted from the irradiated dosimeters to evaluate the net dose. The dosimeters were calibrated in RSS, RSSD BARC for the energy 80 kV. The Shimadzu Q-Rad 50 x-rays unit with Konica Minolta DR system was used in this study. The exposure parameters (kVp, mAs, focus to skin distance, field sizes) of the studied patients were recorded. The kV, mAs, ranges from 60 - 70 kVp, 80-160 mAs, respectively. Focus to imager distance and field size was set as 110 cm and 40 x 35 cm^2 respectively. All measurements were performed in bucky mode. ESD of 53 patients of different age and sex were measured.

Results: Measured average entrance skin doses during abdominal radiography were ranges from 5.15 mGy to 17.86 mGy for AP and 7.33 mGy to 30.74 for lateral radio graphical examination setup. The average values were 9.43 mGy and 14.21 mGy for AP and LAT radio graphical examination respectively. The variation in the measured dose may be attributed to different imaging parameters used for different patients.

Conclusion: BARC developed OSL Dosimeter are found suitable to measure the patient dose during abdominal radiography. Further the measured doses are in line with reported dose by other researcher.

P-173

QUALITY ASSURANCE ASSESSMENT OF CONVENTIONAL DIAGNOSTIC X-RAY INSTALLATIONS IN MIZORAM

Jonathan Lalrinmawia, Kham Suan Pau[1], Ramesh Chandra Tiwari

Department of Physics, Mizoram University, [1]Department of Oncology, Mizoram State Cancer Institute, Aizawl, Mizoram, India. E-mail: ramesh_mzu@rediffmail.com

Introduction: The main purpose of Quality Assurance (QA) is to have finest X-ray image with lowest dose delivered to the patient and to reduce the rejection of poor images. In Mizoram there were 195 X-ray facilities installed in 118 different institutions till June 2016. However, in the present study, we considered 135 conventional X-rays because 90.94% workload of all diagnostic procedure in the present study area comes under these equipment [Figure 1]. Among 135 equipment 24 were condemned and the average age of the 111 equipments was 7.95±7.51 years. To the best of authors' knowledge, no proper QA assessment had been done so far in the present study area.

Materials and Methods: To measure output radiation dose, a battery operated portable dosimeter RAD-CHECK^{TM}PLUS (FLUKE-USA), was used. The calibration measurements were traceable to National Institute of Standard and Technology. By an internal ionization chamber, X-ray was measured in Roentgens and it can measure from 0.001 R-1.999 R. The portable digital kVp meter (FLUKE-USA) was used to measure noninvasively the effective peak potential. Others safety parameter, frequency of QA, type of Patient entrance Door (PED), availability of Personnel Monitoring Service (PMS) etc. was studied. Data presented as mean ± standard deviation (SD) were analyzed in SPSS version 17.

Results and Discussion: Coefficient of Linearity (CL) of time ranged from 0.00 to 0.93 with mean 0.20±0.19SD, 59.18% units were having CL above 0.1 (n=98). CL of current varied from 0.00 to 0.97 with mean 0.25±0.18SD, 82.61% were having CL above 0.1 (n=69). Coefficient of Variation (CV) for tube output reproducibility ranged from 0.00 to 0.72 with mean 0.08±0.12SD. Among them 35.05% were having CV above 0.05 (n=97). Tube output (70kV, FDD=100 cm) ranged

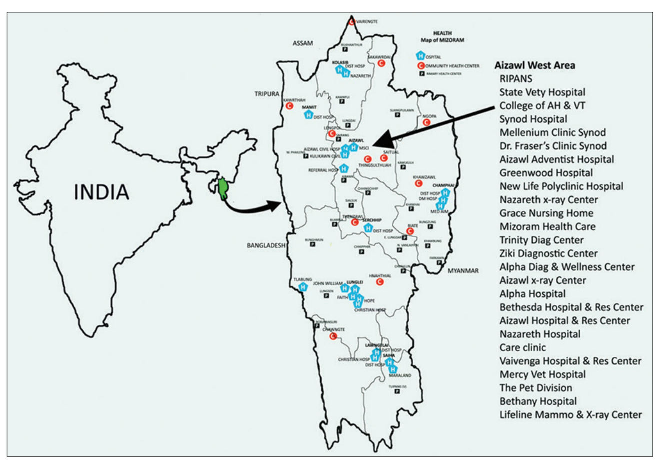

Figure 1: The locations of 135 conventional diagnostic X-rays installed in 82 institutions

from 1.57 to 236.82 μGy/mAs with mean 31.00±33.63SD. While, 7.22% were having table dose between 43-52 μGy/mAs, 25.77% were having 26-43 or 52-69 μGy/mAs and 67.01% were having dose <26 or >69 μGy/mAs (n=97). Voltage accuracy ranged between -0.32 to 0.88 with mean -0.16±0.20 SD. Among them 10.30% units come under ±5%, 10.30% units under ±10% and the rest 79.38% were above ±10%(n=97). It was found that more than half of the units were having problem in X-ray generators, voltage accuracy and table dose. Improper quality control, old equipments and lack of awareness among radiation workers may be the main reason. In other safety parameter, 39.8% X-ray rooms were not sufficient; 97.96% equipments were not facing QA test after installation; 6.12% installations were without PED and 82.65% were using non-lead-line PED; 33.67% installations were not having barrier however 25.51% were using barrier without lead-glass; 3.06% institutions were having waiting area inside the room and 20.41% near PED; chest stand of 10.20% were placed near window and 12.24% put near PED; 86.73% were not having warning light; only 8.16% used PMS; 93.88% repeated exposure occasionally due to patient movements/over/under exposed; 21.88% collimator bulbs were not working; 10.20% equipment were not having operator; 1.02% X-ray workers were not qualified (n=98) and all data presented in Table 1. It shows that most of the institutions were not following national and international recommendation [Table 1].

Table 1: Different important safety parameters

Parameters	n	Variables	Number of X-ray units	Percentage
X-ray room layout	98	Adequate and proper	59	60.20
	98	Adequate but not proper	21	21.43
	98	Not adequate	18	18.37
Frequency of QA	98	Regular	0	0
	98	Once	2	2.04
	98	Never	96	97.96
PED	98	Lead lining	11	11.22
	98	No lead lining	81	82.65
	98	No door	6	6.12
Protective barrier	98	With lead glass	40	40.82
	98	Without lead glass	25	25.51
	98	No barrier	33	33.67
Waiting area	98	Away from PED	75	76.53
	98	Near PED	20	20.41
	98	Inside	3	3.06
Chest stand	98	Away from PED and window	76	77.55
	98	Near PED	12	12.24
	98	Near window	10	10.20
Warning light	98	Available and working	11	11.22
	98	Available but not working	2	2.04
	98	Not available	85	86.73
PMS	98	Available and used	8	8.16
	98	Available but not used	8	8.16
	98	Not available	82	83.67
Lead apron	98	Available and used	63	64.26
	98	Available but not used	13	13.27
	98	Not available	22	22.45
Gonad shielding	98	Available and used	2	2.04
	98	Available but not used	0	0
	98	Not available	96	97.96
Dark room	98	CR	13	13.27
	98	Completely dark	77	78.57
	98	Partial dark	8	8.16
Repeated exposure	98	Mostly	2	2.04
	98	Sometimes	92	93.88
	98	Never	4	4.08
Repetition reason	98	Over/under exposed	43	43.88
	98	Film spoil	28	28.57
	98	Patient movement	67	68.37
Collimator bulb	96	Available and working	75	78.12
	96	Available but not working	11	11.46
	96	Not available	10	10.42
Field size knob	98	Available and working	87	88.78
	98	Available but not working	4	4.08
	98	Not available	7	7.14
Personnel	98	Qualified	87	88.78
	98	Not qualified	1	1.02
	98	Not available	10	10.20

*As already mentioned data can't accessed from all conventional units.
QA: Quality assurance, PED: Patient entrance door, PMS: Personnel monitoring service, CR: Computed radiography

P-174

3D IMAGING PERFORMANCE CHARACTERIZATION IN PROTOTYPE BREAST TOMOSYNTHESIS

Seungyeon Choi[1], Sunghoon Choi[2], Haenghwa Lee[2], Donghoon Lee[1], Dohyeon Kim[1], Young-Wook Choi[3], Hee-Joung Kim[1,2]
Departments of [1]Radiation Convergence Engineering and [2]Radiological Science, Yonsei University, Wonju, [3]Korea Electrotechnology Research Institute, Ansan, Korea.
E-mail: sychoi324@gmail.com

Introduction: In recent years, digital breast tomosynthesis (DBT) has been developed and investigated in clinical practice because it provides a three-dimensional (3D) information of internal structures with much lower dose compared to computed tomography (CT) using relatively simple hardware. Similar to CT, the reconstructed image quality from DBT depends on the variety of parameters during reconstruction process. To achieve the best clinical outcome, it is crucial to understand the fundamental imaging characteristics. The spatial resolution and noise are the standard image quality metrics for assessment in both 2D radiography and 3D tomographic images.

Objectives: The authors observed 3D imaging performance in a prototype DBT system using two different reconstruction algorithms: a filtered back-projection (FBP) and ordered subset expectation maximization (OSEM). The main focus of the current work is not to rate the superiority of two algorithms, but mainly focused on comparison of imaging characteristics which depend on imaging conditions.

Materials and Methods: In this study, we used the prototype DBT system developed by Korea Electrotechnology Research Institute for breast imaging research, which is currently under evaluation for clinical application. The system is based on a flat-panel-detector (2923MAM, Dexela Ltd., UK) with a pixel size of 0.075×0.075 mm^2. The system acquired a total of 11 projection images while moving over a total angular range of $\pm9°$ with angular spacing of 2.5°. The detector was stationary during tomosynthesis acquisition. The FBP and OSEM reconstruction algorithms were implemented using total 11 projection views. Iteration numbers for OSEM were varied with 8, 12 and 16 and the number of subsets was set to 3 during whole reconstructions. Spatial resolution and noise of the system were quantified based on in-plane modulation transfer function (MTF), in-plane noise power spectrum (NPS), and voxel variance. For MTF measurement, a slanted edge of a 0.8-mm thick stainless steel plate was placed on 2 cm above the center of the detector surface near the chest wall side. The ensemble averaged 1D edge spread function (ESF) over the same reconstructed in-planes of 20 repeated acquisitions was calculated. On the other hand, in-plane NPS was calculated as a quantum noise of a volume-of-interest in the scanned breast phantom, removing mean signals of 20 repeated tomosynthesis images from original image. In-plane NPS was calculated by taking Fourier transform of the ensemble averaged mean subtracted sub-images in a targeted in-plane.

Results and Discussion: The spatial frequencies at which the in-plane MTF reduced to 50% were 0.86, 0.93, 0.93, and 0.94 cycles/mm for FBP, and OSEM with iteration number of of 8, 12, and 16, respectively and data presented in Figure 1. The FBP provided inferior resolution than OSEM with iteration number of 8, 12 and 16. The in-plane NPS for FBP and OSEM showed exactly symmetrical patterns followed by the central slice theorem, however, FBP presented more anisotropic .shape compared to OSEM as shown in Figure 2. Voxel variance that was measured by integrating the whole 3D NPS was proportional to the number of iterations in the OSEM, giving 0.89×10^6, 1.67×10^6, and 2.54×10^6 for iteration number of 8, 12, and 16, respectively. The FBP data was 1.42×10^6, which was in the middle of the data from 8 and 12 iterations of the OSEM.

Conclusion: A comparative study between FBP and OSEM reconstruction schemes would provide the quantitative imaging characteristics in the DBT system.

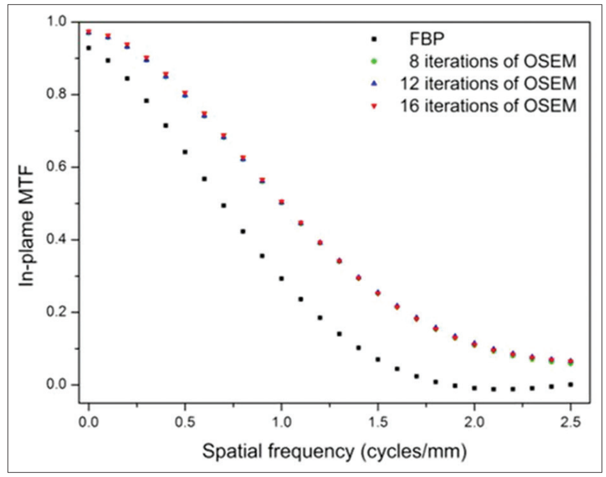

Figure 1: The in-plane modulation transfer function for filtered back-projection and ordered subset expectation maximization with iteration number of 8. The modulation transfer function data for ordered subset expectation maximization with iteration number of 12 and 16 were similar to that from 8 iteration

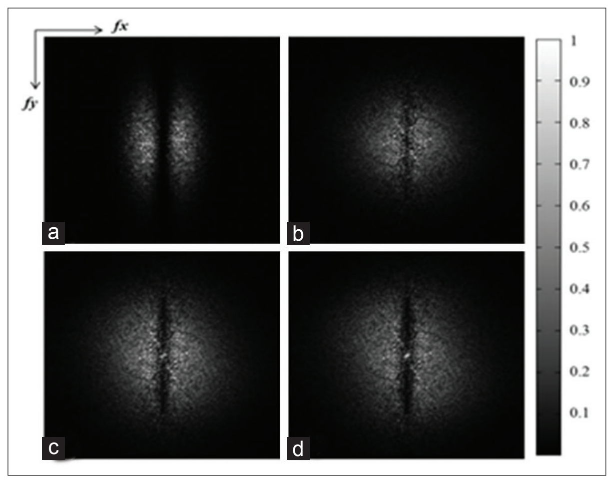

Figure 2: The normalized in-plane noise power spectrum for (a) filtered back-projection, (b) ordered subset expectation maximization with iteration number of 8, (c) 12, and (d) 16

P-175

COMPARATIVE PERFORMANCE ANALYSIS FOR LUNGMAN PHANTOM SIMULATED TUMORS DETECTABILITY ACCORDING TO COMPUTED TOMOGRAPHY RECONSTRUCTION ALGORITHM: FOCUSED ON ADVANCED MODELED INTERATIVE RECONSTRUCTION ALGORITHM

Jun-Bong Shin, Do-kun Yoon, Tae Suk Suh, Seong-Yong Pak[1], Yang-Ho Kwon[1]

Department of Biomedical Engineering, College of Medicine, The Catholic University of Korea, [1]Siemens Healthcare, Seoul, Republic of Korea.

E-mail: ossianbong@naver.com

Introduction: As a development of a computed tomography (CT) device progresses, reconstruction techniques of the CT have been advanced simultaneously. In addition, a requirement of new CT reconstructions has been improved for a clinical field. Thus, we analyzed the difference of the performance CT images depending on the type of CT reconstruction.

Objectives: We compared and analyzed the detectability performance regarding a LUNGMAN phantom including simulated tumors according to CT reconstruction algorithm.

Materials and Methods: In this study, three kinds of the reconstruction algorithm (filtered back projection; FBP, sinogran affirmed interative reconstruction; SAFIRE, advanced modeled interative reconstruction; ADMIRE) were used to deduce the detectability performance. In order to compare and analyze contrast to noise rate (CNR), coefficient of variation (COV) of the LUNGMAN phantom simulated tumors (15 variations 3 varietles of Hounsfield numbers: -800, -630, +100, 5 sizes for each time: diameter 3, 5, 8, 10, 12 mm), SOMATOM Definition Flash CT device were fixed at field of view (FOV) of 300 mm size, slice thickness of 3.0 mm/increment 3.0 mm, and reconstruction kernel I40f medium, and investigated for 10 repeated times with eight radiation energy conditions (120/100 kVp, 60/80/100/120 mAs).

Results and Discussion: Depending on three kinds of reconstruction algorithm (FBP, SAFIRE, ADMIRE), we will compare the images of the LUNGMAN phantom simulated tumors (15 variations 3 varietles of Hounsfield numbers: -800, -630, +100, 5 sizes for each time: diameter 3, 5, 8, 10, 12 mm). Then, you will find the mode of the algorithm suitable for the evaluation of the phantom images. Our study would suggest that the best CNR and the COV were high among three kinds of reconstruction algorithm.

P-176

CT NUMBER ACCURACY OF METAL ARTIFACT REDUCTION ALGORITHM AND ITS INFLUENCE ON RADIAOTHERAPY TREATMENT PLANNNG

Vishram Naik, R. Holla, B. Pillai

Department of Medical Physics and Radiation Safety, Amrita Institute of Medical Sciences, Amrita Vishwa Vidyapeetham, Amrita University, Kochi, Kerala, India.

E-mail: ???

Introduction: Artifacts can seriously degrade the quality of CT images which can make the images diagnostically unusable. To optimize image quality, it is necessary to understand why artifacts occur and how they can be suppressed. In following studies two metal artifact reduction algorithms SMAR (Smart Metal Artifacts Reduction) on GE optima 580W and OMAR (Orthopedic –Metal Artifact Reduction) on Philips ICT 256 are used.

Objectives: HU consistency is challenging when metal artifact reduction algorithm is used in radiotherapy treatment planning.

Materials and Methods: CT numbers were measured before and after applying the metal artifact reduction algorithm on both CT machine GE optima 580W and Philips ICT 256. We used Gammex 467 (Middleton, WI 53562, USA) tissue characterization having different tissue rods. The phantom was scanned with 80, 100.120, & 140 kV and FOV 50 cm. All reconstructed images were 12-bit depth images. The data was analyzed and HU error, diameter error of titanium and stainless steel and relative error was found.

Results and Discussion: Evaluation of CT number accuracy by two metal artifact reduction algorithms was studied. One is on GE optima 580W the algorithm is known as Smart Metal Artifacts Reduction (SMAR) and second is Philips ICT 256 the algorithm is known as Orthopedic –Metal Artifact Reduction (OMAR). Both showed good results in reducing metal artifact streaks and CT number accuracy at energy 140kV which error in HU was < 20 HU.

We studied metal detection technique an algorithm used to reduce metal artifacts on Siemens Somatom Evolution which is known as Extended CT Scale (ECTS) which extend the CT number -1024+3071 to -10240 +30710. We used titanium and stainless steel in study were we found that CT number increased from +3071 to +13650.65 HU at 80kV, +12250.55 HU at 100kV and +12076.34 HU at 130 kV for stainless steel and for titanium increased from +3071 to +9383.8 HU at 80kV, +7367.86 HU at 100kV and +6411.7 HU at 130 kV. It was observed that after applying ECTS as energy increases the HU number of metal was decreased. For rest all tissue equivalent plugs, HU were unchanged by applying ECTS technique. We also studied the metal diameter accuracy for a physical diameter of 13 mm for titanium and stainless steel. The metal diameters were measured on scan images from lower to higher energy. It was observed that diameter error was more for less energy. For 140kV diameter error after applying SMAR was 1.63 mm for titanium and 2.63 mm for stainless steel. For 140kV diameter error after applying OMAR was 1.65 mm for titanium and 2.97 mm for stainless steel.

P-177

EFFECTS OF SLICE THICKNESS FOR PROTOTYPE DIGITAL BREAST TOMOSYNTHESIS

Haenghwa Lee[1], Sunghoon Choi[1], Hyemi Kim[1], Donghoon Lee[2], Dohyeon Kim[2], Chao Zhen[2], Seungyeon Choi[2], and Hee-Joung Kim[1,2]

Departments of [1]Radiological Science and [2]Radiation Convergence Engineering, Research Institute of Health Science, Yonsei University, Wonju, Korea.

E-mail: tgcohost20@gmail.com

Digital breast tomosynthesis (DBT) is an emerging 3D imaging technology that can improve the detection of breast cancer by preventing tissue overlap. There are many parameters that must be decided to achieve maximum performance in DBT system, and one of these parameters is the slice thickness. The purpose of this study was to evaluate the effects of slice thickness on the detection of micro-calcification for prototype DBT system. A prototype DBT system (Korea Electrotechnology Research Institute) consisted of an X-ray tube (XM1016T, Industria Applicazioni Elettroniche, Italy) and a CsI (Tl) scintillator/CMOS flat panel digital detector (2923MAM, Dexela Ltd., UK) with a matrix size of 3072 x 3888. The CIRS phantom (Models 014 series, USA) was included micro-calcifications with nominal specks size of 0.20 mm, 0.23 mm, 0.27 mm, and 0.39 mm. When we acquired the 15 projection views with a 42 angular range, average glandular dose (AGD) was about 1.08 mGy. The projection views were reconstructed using filtered back-projection (FBP) method, and a total of six different average slice thickness were used. We evaluated the quality of reconstructed images with contrast-to-noise ratio (CNR), artifact spread function (ASF), and quality factor (QF). We found that detection performance of calcification size was influenced by slice thickness in DBT system. Although CNR values raised to a peak when slice thickness was similar in size to the calcification to be detected, ASF curves for all calcifications improved with decreasing slice thickness. QF factors were more affected by CNR than ASF curves. These results showed that thinner slice thickness could improve detection of small lesions. In conclusion, optimal slice thickness of different calcification size could provide more satisfactory image for the detection of lesions using DBT system. Although proper slice thickness could yielded superior image quality, further studied are needed to evaluate the effect of slice thickness considering reconstruction speed.

Acknowledgment: This research was financially supported by the Ministry of Trade, Industry and Energy (MOTIE), Korea Institute for Advancement of Technology (KIAT) and Gangwon Insititute for Regional Program Evaluation (GWIRPE) through the Economic and Regional Cooperation Industry.

P-178

NEW PROTOCOL TO REDUCE FETAL RADIATION DOSE DURING PROPHYLACTIC BALLOON INSERTION IN PREGNANT PATIENTS WITH ABNORMAL PLACENTAL ADHERENCE

H. Al-Naemi, N. Iqeillan, A. Aly, A. Omar[1], A. Barah[1], A. Abualruz[1], M. B. Gomaa[1], A. Almuzrakchi[1], V. Chavan[1], O. AlMokdad[1]

Departments of Occupational Health and Safety and [1]Clinical Imaging, Hamad Medical Corporation, Qatar.
E-mail: Halnaomi@hamad.qa

Background: Abnormal Placental Adhesion (APA) is a life-threatening condition which occurs in approximately one in 2,500 deliveries,[1] it is divided into three grades based on histopathology: placenta accreta, placenta increta, and placenta percreta.[2] More than 50% of APA patients recieved blood transfusion or admitted to an ICU and the mortality rate is greater than or equal to 7%.[3,4] Moreover, placenta accreta is the leading cause of peripartum hysterectomy,[5] Prophylactic Iliac Balloon Insertion (PIBI) is introduce as an adjuvant therapy in order to minimize blood loss during cesarean or in conduct with conservative management with the intent of avoiding hysterectomy in selective cases.[6]

Objective: The purpose of the present study is to evaluate a new protocol aimed to minimize the fetal radiation exposure during PIBI in patients with high risk of morbidity due to APA and to assess its effect on technical success during the angiography.

Methods:

- Retrospective study comparing 2 groups of pregnant patients with APA eligible for PIBI.
- Control group: 11 patients underwent standard protocol of radiation dose reduction.
- Study group: 11 patients underwent new protocol of radiation dose reduction.
- Peak Skin Dose (PSD) and Fetal Absorbed Dose (FAD) were calculated indirectly from the peak Entrance Skin Air Kerma (ESAK).
- Radiation parameters measurements of the two groups were collected, compared and further compared to international standards.
- At the end of each PIBI, the difficulty of the procedure using new protocol was estimated based on the quality of fluoroscopy images and arterial anatomy.
- Used standard dose reduction parameters.

Results: Because of wide range of FAD and PSD in group 1, Mann-Whitney test has been used for *p* value calculation. The mean value of FDA was 21.92 +/- 19.1 in control group and was 1.5 +/-1.27 in study group ($p = 0.0001$). The mean value of PSD was 93.54 +/- 80.8 in control group andwas 6.29 +/- 5.39 in study group ($p = 0.0001$) as shown in Table 1 and Figure 1. There was no significant difference in mean fluoroscopy time between the two groups (1.88 +/- 0.66 vs 2.51 +/- 1.30, $p = 0.167$).

Discussion: Particular attention must be paid to dose reduction techniques in order to minimize the radiation exposure to the fetus during X-ray-based procedures. In our study, the median FAD from PIBI was reduced from 22 to 4.7 mGy by implementing the new protocol which decreases the stochastic effect. Compared to standard practice of PIBI, the main parameters that decreases the FAD during PIBI was the use of low dose protocol and the retrieval of the grid before the procedure. Operator experience may also influence FAD on PIBI procedures. In fact, experienced operators perform the procedure with confidence that they can achieve an appropriate compromise between the lower image quality due to the new protocol whilst achieving technical success as shown in Figure 2.

Table 1: Peak skin dose, fetal absorbed dose, fluoroscopy time and *P* value for study

Parameter	Control group	Study group	P
FAD, mean±SD (minimum–maximum)	21.92±19.1 (7.8–69.7)	1.50±1.27 (0.5–4.8)	<0.0001
PSD	93.54±80.8 (33.1–294.4)	6.29±5.39 (2.2–20.3)	<0.0001
FT	2.51±1.30 (1.5–5.2)	1.88±0.66 (1.1–3.0)	0.167

SD: Standard deviation, FAD: Fetal absorbed dose, PSD: Peak skin dose, FT: Fluoroscopy time

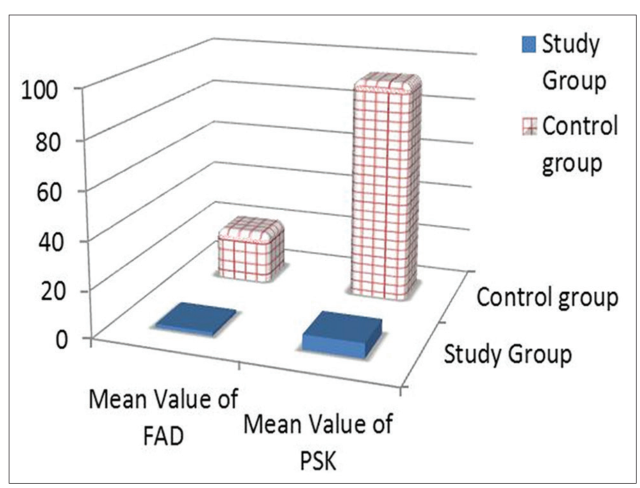

Figure 1: Mean values of fetal absorbed dose and peak skin dose for control group and study groups

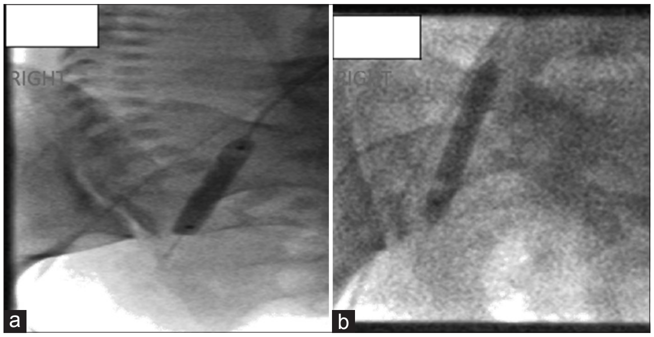

Figure 2: Fluoroscopy image showing the inflated balloon catheter in the right internal iliac artery using the standard protocol (a) and the new protocol (b), respectively

Conclusion: It has been demonstrated by the present study that the application of new protocol for radiation dose reduction significantly reduces the FAD and PSD during PIBI in pregnant patients with APA. This new protocol can easily be applied and does not affect the technical success of the angiography procedure.

P-179

IMPLEMENTATION OF THREE DIMENSIONAL MICRO CT IMAGE RECONSTRUCTION ON GRAPHICS PROCESSING UNIT

Kamirul, L. A. Fitri, F. Haryanto

Department of Physics, Faculty of Mathematics and Natural Sciences, Institut Teknologi Bandung, Bandung, Indonesia. E-mail: kamirul@s.itb.ac.id

A GPU-based (Graphics Processing Unit) program has been developed to perform reconstruction process on micro CT scanner projection images. The program was implemented using FDK (Feldkamp, Davis, and Kress) which is intended to reconstruct three dimensional volume from projection images acquired using conebeam X-ray with a planar detector configuration. Based on simulation performed on GTX 780 GPU (2304 cores), the program was able to accelerate filtered-backprojection process up to 89,90 times compared to Intel CoreTM i5-4330 CPU (Central Processing Unit) implementation on 2048^3 voxels phantom. By varying voxels number, it can be shown that acceleration values were influenced by the number of reconstructed voxels and available global memory size on GPU. Maximum total acceleration value was 27,93 obtained when 1024^3-voxel phantom was reconstructed on 2,05 GB GPU memory. Further result show that developed program was capable of producing acceleration values to 1.27 and 1.30 compared to NRecon software on medium (1120^3 voxels) and high (2240^3 voxels) resolution aquades phantom. While in low-resolution (560^3 voxels), the program yields a de-acceleration value of 0.85.

P-180

ESTIMATION OF RADIATION DOSES IN DIAGNOSTIC AND INTERVENTIONAL THERAPUTIC RADIOLOGICAL PROCEDURES

Bhupendra Singh Rana, Amitabh Sinha, Sanjeev Kumar[1], Naveen Kalra, N. Khandelwal

Department of Radiodiagnosis and Imaging, PGIMER, [1]Department of Physics, SD College, Chandigarh, India. E-mail: bhupendrasrana@gmail.com

Introduction: Interventional radiology (IR) is an important imaging modality for early detection and treatment of complex diseases, with advantages such as non-invasiveness, timeliness, reliability, and minimum pain to the patient.[1] However, these procedures result in significant radiation doses to the individuals undergoing imaging and therapeutic procedures as well as to the operators of the procedures. The high radiation doses delivered during IR procedures are associated with higher stochastic risk as well as higher chances of manifestation of deterministic injury to the patients, if a threshold dose to these deterministic effects is exceeded.[2] Skin tissue most likely to get maximum dose during IR procedures. There has been concern to minimize doses to some critical organs during interventional radiology. These concerns require modifications of work practices as well as optimization of procedures. However, the magnitude of dose delivered to the patients depends on many radiographic factors viz., use fluoroscopy on time, mA, tube voltage, radiosensitivity of the organ, complexity of the procedure, experience of the operator and patient specific parameters. Various authorities such as International Commission on Radiological Protection (ICRP)[3] and International Atomic Energy Agency (IAEA)[4] have expressed concern over patients' skin dose during interventional radiology procedures. In the present study, we measured the entrance surface dose (ESD) for various diagnostic and therapeutic interventional procedures.

Objectives: The aim of the work is to measure and analysis of skin entrance doses (SEDs) for various diagnostic and therapeutic interventional radiological procedures.

Materials and Methods: IR procedures were classified according to the type of examination outcome in two categories known as diagnostic IR and therapeutic IR. In present work we estimated the radiation exposures to the patients in six diagnostic (Cerebral angiography, abdomen angiography, IVC graphy, lower limb angiography/venography, upper limb angiography/venography and Spinal artery angiography) and six therapeutic (Abdominal procedures, angioplasty, AVM embolization, bronchial artery embolization, intra artery thrombolysis, renal artery embolization) interventional procedures from the registered dose area product (DAP). The measurements are part of quality assurance study comprised data recorded from all patients undergoing procedures in the interventional radiology section of PGIMER, Chandigarh. Data was gathered on 300 patients, patient age, sex, DAP reading, fluoroscopy time and type of procedure were recorded. All fluoroscopy and imaging were performed on Allura Xper FD 20/10 angiographic unit (M/s Phillips Medical systems, Germany). It is ensure that angiographic unit used in study met the quality assurance (QA) criterion for KVp, mAs, current, time, field size, filtration and radiation output as specified by Atomic Energy Regulatory Board (AERB), Mumbai. The initial evaluation independently verified the unit's entrance skin exposure calibration by measuring the beam output using 75 cc shadow free Ionization chamber and UnidosE dosimeter (PTW, Freiburg, Germany) and compared the measured output with the DAP readings shown on the units control console measured by inbuilt ionization chamber in the collimator of the machine.

Result and Discussion: It is clear from experimental results, in case of interventional radiological procedures patients undergone spinal artery angiography received maximum radiation exposure and minimum exposure in case upper limb angiography/venography procedure. On the other hand in case of therapeutic radiological procedures, patients received maximum exposure in abdominal and minimum exposure in intra artery thrombolysis. The present study shows that patients received doses that varied considerably during x-ray-based interventional imaging.

References

1. Hricak H, Brenner DJ, Adelstein SJ, Frush DP, Hall EJ, Howell RW, *et al.* Managing radiation use in medical imaging: A multifaceted challenge. Radiology 2011;258:889-905.
2. Klein LW, Miller DL, Balter S, Laskey W, Haines D, Norbash A, *et al.* Occupational health hazards in the interventional laboratory: Time for a safer environment. Catheter Cardiovasc Interv 2009;73:432-8.
3. Valentin J. Avoidance of radiation injuries from medical interventional procedures. Ann ICRP 2000;30:7-67.
4. International Atomic Energy Agency. IAEA-TECDOC-1641. IAEA; 2010.

P-181

GENERAL METHODS OF 2D, 3D AND DEFORMABLE IMAGE REGISTRATION

Bhumika Handa, Gaganpreet Singh, Rose Kamal, Arun S. Oinam[1], Vivek Kumar

Centre of Medical Physics, Panjab University, [1]Department of Radiation Therapy, Regional Cancer Centre, PGIMER, Chandigarh, India. E-mail: bhumika1051@gmail.com

Introduction: Image registration methods are of great interest these days due to the advancement in radiotherapy treatment techniques. Image registration includes various steps such as image segmentation, image fusion and post processing techniques. Many methods have been developed for 2d-2d, 3d-3d and deformable image registration techniques incorporating complex statistical and mathematical models.
Objective: Review of various image registration methods and development of image registration tool for various imaging modalities like CT, MRI to obtain complete information about the morphological changes inside the patient.
Materials and Methods: In this study Different image data sets of CT AND MRI are used. Indigenous image Registration tool is developed in MATLAB Software, which provides image registration of two or more data sets. 2-D image registration was performed using various methods like point Based Registration, Gradient Correlation and Principal Component Analysis. For 3-D image Registration various methods used are Principal Component Analysis, Iterative Closest point, Wavelet based, B spline based, and SVR (Special vector regression) based method. Extended version of these methods issued in deformable image registration.
Result and Discussion: To analyze the accuracy and uncertainty associated with the image registration techniques, various statistical parameters like mean Standard Deviation, Variance, Correlation, Entropy, Root Mean Square error and Chi Square test are used. Point based image registration is an error prone method because of the user inputsand intensity based method gives accurate result only in same modality images and difficult to use in different modalities. Various complex methods such as SVR, PCA, ICP have their advantages as well as limitations in different scenarios.
Conclusion: The 2d-2d and 3d-3d image registration methods include complex athematical formulism, which are still in growing stage. Although many methods have been developed, in present work it is found that every method has its own limitations. In this study various methods for planar and volumetric data has been used. This study can be further extended to built a generalized method for 2d, 3d and deformable registration.

P-182

STANDARD PROCEDURES FOR ESTIMATING THE UTERINE DOSE DURING FLUOROSCOPY EXAMINATION

K. Schröder, Kilian Seth, K. Loot, A. Block[1]

TU Dortmund University, [1]Institute for Medical Physics, Klinikum Dortmund GmbH, Dortmund, Germany.
E-mail: katharina3.schroeder@tu-dortmund.de

Introduction: The exposure of ionizing radiation on embryos during a medical indication can cause severe physical and mental disabilities. There are a couple concepts for theoretical determinations of the applied dose which can then be used to carry out a risk assessment of the radiation induced damage. Examples of these concepts are provided by the DGMP report No.7 of 2002. The Dose calculations in this report are based on a Three-Step-method. If the estimated dose of step one exceeds a threshold value, further calculations must be carried using concepts like the image receiver- or the source concept. In this work, the image receiver concept is used to compare reference-dose values from 15 years ago with recently measured ones to find out if they can be reduced.
For this, theoretical dose calculations as well as continuous and pulsed phantom measurements are carried out on three C-arms of various technical generations.
Objectives: The reference-dose values assumed at the time of the report are conservative. In order to estimate how conservative they are, theoretical calculations of the dosage were carried out with the Image receiver concept. That uses the formula:

$$D_u = K_E \, g \left(\frac{dE}{dE + x_U} \right)^2 g \frac{tw}{a} g T_a (x_u, F_U)$$

with the incident dose K_E, a scaling between skin and uterus depth, the Mass absorption coefficient twa and the tissue to air ratio T_a, to calculate the Uterus dose. The incident dose is the product of attenuation coefficients, the fluoroscopy time and the image receiver performance. It turns out that the reference-dose values from the report include a safety buffer of around 40% to take the worst conditions into account.
Materials and Methods: After the theoretically determined doses, experimental measurements are carried out, in which the conditions are reproduced from the report with a water equivalent phantom. The measured and calculated

values for the uterine dose are significantly smaller than the reference values. The measured values are between 45 and 93% smaller than the reference-dose values. It could be expected that a reason for the deviating doses from the reference values is, that the devices used at the time of the report cause a higher dose load than devices of today's development level. However, during continuous fluoroscopy, this assumption is rejected, since the reference values take account of the individual image receiver performance. Yet there are tremendous differences between the dose rate of the newer and the older C-arm.

Results: The decisive factor is that a continuous fluoroscopy at the new C-arm is not possible and that the measurements have been approximated with a high pulsation. In 2002 most of the C-arms only had the function of continuous fluoroscopy. However, nowadays pulsed fluoroscopy achieves considerable dose reduction, which the report does not consider. That is why the phantom measurements are repeated under the same conditions, with the difference that pulsed fluoroscopy is applied. The radiation load for the embryo with pulsed fluoroscopy is significantly lower than with continuous. This, in turn, corresponds to a reduction of the reference dose values from the report of 59-92%. For innovative reference dose values consideration should be given to pulsed fluoroscopy.

Discussion: The results of this study show that concepts for dose calculations like the image receiver concept are still accurate. Yet, it is advisable to extend reference dose values with different pulse frequencies, since there are devices that does not have the option of pulsed fluoroscopy anymore. For those the reference values are invalid.

P-183

CONE BEAM COMPUTED TOMOGRAPHY IMAGE QUALITY AND DOSE OPTIMIZATION

Gaurav Trivedi[1,2], C. K. Dixit[2], Arun Oinam[1], Ranjit Singh[1], Ngangom Robert[1], Amanjot Kaur[1]

[1]Department of Radiotherapy & Oncology PGIMER, Postgraduate Institute of Medical Education and Research, Chandigarh, [2]Department of Physics, Dr. Shakuntala Misra National Rehabilitation University, Lucknow,
Uttar Pradesh, India. E-mail: gauravtrivedi25@gmail.com

Imaging is prerequisite for positional setup correction of the patient before radiation dose delivery. Imaging can either be obtained by MV source detector system or by the help of kV source detector system. Three dimensional Cone beam computed tomography imaging is possible using latter mode of imaging. CBCT imaging delivers lesser dose to the patient compare to MV imaging. But as the unnecessary radiation exposure to any part of the body other than target site can become potential site for secondary malignancy. The dose due to CBCT imaging needs to monitor. The aim of this study was to estimate and optimize the doses due to kV CBCT imaging of Head & neck and pelvis region of the patient. The study was done to evaluate the effect of different filters on patient doses without much affecting the image quality. Imaging Dose to the patient was estimated using CTDI phantom. Both H&N as well as Pelvic CTDI Phantom were used to measure Cone Beam Dose Index (CBDI). A system for imaging the Patient on treatment couch using kV source (G242) and flat pannal detector system (PaxScan4030CB) added on Trilogy linear accelerator by varian medical system, Inc, Palo Alto, California was used. This system known as On Board Imager (OBI) has an active area of 397 mmX298 mm and it is capable to provide good quality 2D radiograph and 3D Cone Beam Computed tomography (CBCT) image. For pelvis, single protocol of 125kV-80mA was used with half bow tie filter whereas for H & N region three protocols of High quality head (100kV-80mA), low dose head (100kV-10mA) and standard dose head (100kV-20mA) were used with full bow tie filters. The dose delivered in a CBCT procedure was assessed using a cylindrical Perspex phantom (diameter, 32 cm body phantom and 16 cm Head and Neck phantom) with a calibrated Farmer type cylindrical ionization chamber (10 cm active length) in conjunction with a DOSIMAX plus A, iba dosimetry, Germany electrometer. Maximum Dose reduction of 7.1 % was observed in Pelvis protocol with additional brass alloy filter. The maximum dose reduction was observed in High quality head protocol and that was 25% for the same brass filter. Different factors to define image quality likes special resolution, contrast to noise ratio and uniformity was assessed on CATPHAN-500 with the no of filters to monitor the stability of the imaging quality. Acceptable image quality was observed with the brass and copper filters with reduced imaging dose.

P-184

SCATTERING, ABSORPTION AND EXTINCTION CHARACTERISTICS OF ELECTROMAGNETIC WAVE BY A SPHERICAL PARTICLE

S. M. Kurawa, M. M. Kashimbila[1]

Sa'adatu Rimi College of Education, Kumbotso, [1]Bayero University Kano, Kano, Nigeria.
E-mail: sabuwalle@gmail.com

The scattering of electromagnetic wave by a spherical particle was presented using the Mie formulation. The parameters needed to describe the characteristics of the radiation scattered by the particles were derived. The parameters include the Mie coefficient a_n and b_n, the scattering, absorption and extinction efficiencies, the cross section for radiation pressure and the asymmetry factor $<\cos\theta>$. The behavior of these parameters was investigated as functions of the dimensionless size of the particle ($2\pi r/\lambda$). Experimental value was obtained from radiation pressure measurements on a levitated oil droplet with refractive index of m= 1.29. It was found that the various efficiency factors are related to the optical property of the scattering. For pure dielectric, the efficiency factors for scattering and extinction are equal, since there was no absorption. Superimposed on the extinction curves are the minor oscillations called ripple structures. When the particles were absorbing, the refractive index became complex, it was found that the amplitude of the extinction curve decreased, and the ripple structures gradually disappeared. Similarly, the distance between resonances, also called the period of resonances was found to be related to the refractive index of the particle. Using the Mie theory, the period calculated was 0.750, which was in good agreement with the experimentally quoted value of 0.671.

P-185

DOSIMETRIC COMPARISON BETWEEN NOMEX MULTIMETER AND RAD CAL ION CHAMBER IN NUCLETRON SIMULIX EVALUATION SIMULATOR

C. Senthamil Selvan, C. S. Sureka, Raghavendra Holla[1]

Department of Medical Physics, Bharathiar University, Coimbatore, Tamil Nadu, [1]Department of Medical Physics and Radiation Safety, Amrita Institute of Medical Sciences and Research, Kochi, Kerala, India. E-mail: surekasekaran@buc.edu.in

Introduction: X-ray tube performance is considered as one of the most important issues in medical imaging science and radiation protection. Hence, all necessary measures should be taken to maintain an effective performance of the X-ray machine through regular calibration and maintenance. Based on this, quality assurance tests of diagnostic x-ray tube are carried out periodically because poor performance of the equipment will directly lead to poor image quality and increase the dose to the patients. Therefore, the selection of an appropriate instrument for dosimetry should be done very carefully.

Objectives: The objective of this study is to evaluate the X-ray tube voltage (kVp), current (mA), exposure time (milliseconds), half value layer (HVL), leakage radiation and compare the radiation output in Nucletron Simulix Evolution using semiconductor based NOMEX multimeter (D-1) and ion chamber based detector Rad Cal 9095 (D-2).

Materials and Methods: This measurement includes 50 selected parameters with stranded experimental setup includes gantry, collimator and couch rotation angle at 0^0, and the focus to couch distance was 100 cm. Both the detectors were placed very close to the isocentric point and the collimator opened for 30×30 $cm^{2,}$. The operating parameters were varied from 60 kVp to 120 kVp at 10 kVp interval at 50 mA, 100 mA and 200 mA with respect to different exposure time in the range of milliseconds for the measurements of kVp, mA and exposure time. The HVL measurement was performed with added aluminium filters at the operating parameter of 120 kVp, 100 mA and1000 mSec. The leakage radiation was measured using the pressurized μR ion chamber survey meter (451P-RYR) at 1 meter distance from the X-ray tube focus to with the set parameters of 130 kVp, 100 mA and 1000 mSec.

Results and Discussion: The measured kVp in D-1 and D-2 values were compared, the maximum kVp error from ±2.2 kVp to ±11.1 kVp and the practical peak voltage (PPV) is 0 to ±11.3 kVp and mean kVp errors is ±0.2 kVp to ±11.6 kVp. The measured exposure time varied in D-1 is 0 to 4.5 msec and D-2 is 0 to 1 msec. The measure HVL values were within the acceptable limit as per the AERB guidelines. In output measurements, more deviation observed in D-2, the values from 18.78 mR to 588 mR compared to D-1. The maximum leakage radiation is 1.68 mR/hrs. From this data, it is observed that the semiconductor based detector D-1 gives more reliable data than ion chamber based detector D-2 for all the selected parameters and for output measurement.

P-186

CT DOSES ESTIMATION WITH THE DOSIMETRIC QUANTITIES CTDI AND DAP TO DEFINE DIAGNOSTIC REFERENCE LEVELS IN INTERVENTIONAL RADIOLOGY

Jyoti Bisht, S. P. Mishra, Sonal Vashnerya[1], Raj Kumar Tyagi[2]

Department of Radiation Oncology, Dr. Ram Manohar Lohia Institute of Medical Sciences, Lucknow, Uttar Pradesh, [1]Department of Radiotherapy, All India Institute of Medical Sciences, Jodhpur, Rajasthan, [2]Government Post-Graduation College, Kotdwar, Uttarakhand, India. E-mail: jyoti797bisht@gmail.com

Introduction: CT simulation provides a graphic display of the 3D anatomy of both normal tissue and cancerous tissue and it is capable of interactive three-dimensional (3D) volumetric treatment planning this allows radiation oncology departments to operate without conventional x-ray simulators. Current computed tomographic (CT) scanners generate patient dose indexes of the volume CT dose index ($CTDI_{vol}$) and the dose length product (DLP).

Method: $CTDI_{vol}$ is an index that quantifies the relative intensity of the radiation that is incident on the patient. CT scanners that have patient size– specific scanning protocols would likely select lower $CTDI_{vol}$ values for pediatric patients but higher ones for oversized patients. The total amount of radiation delivered to the patient at a given examination, however, is also dependent on the CT scan length. The product of $CTDI_{vol}$ and scan length is the DLP, which can be used to quantify the total amount of radiation patients receive during a given scan. The DLP is directly related to the patient (stochastic) risk and may be used to set reference values for a given type of CT examination to help ensure patient doses at CT are as low as reasonably achievable. In CT examinations, the CT dose index (CTDI), the Dose Length Product (DLP) and the effective dose are the most common used dosimetric quantities for DRLs.

Discussion: In comparison to conventional radiography, CT is a high-dose imaging modality, although doses are generally well below the threshold dose for the induction of deterministic effects. CT imaging is now the dominant contributor to the population dose from medical x-rays, where the latter is the major source of radiation exposure from man-made sources. Results of one study estimated that although CT accounted for only 10% of diagnostic examinations in US hospitals in 2000, this imaging modality accounted for nearly 70% of the corresponding medical dose. Because the CTDI is an averaged dose to a homogeneous cylindrical phantom, the measurements are only an approximation of patient dose. Another limitation is that CTDI overestimates dose for scans where the patient table is not incremented, such as in interventional and perfusion CT. For these CT applications, the CTDI can overestimate peak dose by a factor of two.

Conclusion: Several actions are to be undertaken to limit the irradiation of patients: lowering the high voltage (kV) and the tube current (mAs), reducing the scanning length and the tube rotation time, increasing slice thickness or pitch, using auto-exposure control or dose reduction software, and the training of staff. Regular awareness of medical imaging professional on radiation protection during staff, meetings and national and international meetings/workshops would also disseminate best practice and harmonize the best CT-scan protocols. There is also need for quality control of CT Equipment and audit of CT practices to alert professional in case of inappropriate practice.

P-187

RADIATION LEAKAGE TEST FOR LEAD APRONS OUR EXPERIENCE

R. Pichumani
Jawaharlal Nehru Hospital & Research Centre, Bhilai Steel Plant, Bhilai, Chhattisgarh, India.
E-mail: rpichumani@sail-bhilaisteel.com

Introduction: Lead aprons are used in various departments of our hospital. We have a routine test for lead aprons at our Institute for cracks using fluoroscopic procedures once in 6-8 months.
Materials and Methods: This poster describes our experiences with the lead aprons and testing of lead aprons (with images). This poster demonstrates the importance of lead apron testing using fluoroscopic procedures. On an average of 50-60 lead aprons are tested every time. The poster also describes the importance of testing the lead aprons before accepting it for regular usage.
Results and Discussion: It is very important to have leakage test for lead aprons atleast once a year if it is regularly used and also before accepting it for use. This ensures radiation safety to radiation workers.

P-188

MODERN IMAGING IN ONCOLOGY: PRESENT CHALLENGES AND FUTURE EXPECTATIONS

Deboleena Mukherjee, Kirti Tyagi, Partha Brata Mukherjee[1], Arti Sarin[2]
Radiation Oncology Centre, INHS Asvini, [1]Nuclear Medicine and PET/CT Centre, INHS Asvini, [2]Department of Radiodiagnosis and Radiotherapy, INHS Asvini, Mumbai, Maharashtra, India. E-mail: deboleena.rso@gmail.com

Introduction: Imaging plays an important role in Oncology; presently Positron Emission Tomography (PET) has been integrated with Computed tomography (PET/CT) or Magnetic Resonance (PET/MR) imaging, for hybrid (combined) imaging. These hybrid systems are used to evaluate extent of disease, to detect occult lesions and monitor treatment response in respect of its metabolic activity and anatomical and functional details as well as its invasion into surrounding normal tissues before and after treatment with surgery, chemo or radiation therapy. In the last few years, there has been significant advances in radiation treatment planning (RTP) software of the treatment planning system (TPS) calculation algorithms and it is able to combine the biologically guided PET data or MR data and anatomic CT data with five registrations methods, Manual approach (MA), Landmark, Identity, Surface Matching, and Mutual Information (MI) for precise three dimensional (3D) computer based dose calculation. Hybrid imaging based treatment planning has an advantage over CT alone in the standardization of target volume delineation (Gross tumour volume (GTV), Clinical target volume (CTV), and Planning target volume (PTV) margins), in reduction of risk for geometric misses and in minimizing radiation dose to the non-target organs. The most commonly used PET radio tracer is ^{18}F-fluorodeoxyglucose (FDG), others like ^{18}F-FMISO (fluoromisonidazole), ^{64}Cu-diacetyl-bis (N^{4}-methylthiosemicarbazone) and ^{64}Cu-ATSM have also been used to demonstrate “hypoxia” and ^{18}F-FLT (flouro-3-deoxythymidine) as a marker of “cellular or sub-cellular” proliferation and ^{11}C-MET (Methionine) in brain imaging. Also, PET/MR is an exciting new modality for cardiovascular applications and recently ^{68}Ga-DOTATAC has been used for RTP in meningioma patients. A new field of “theragnostics” has emerged where image fusion of PET or MR data with CT data shall be used to localize tumour sites more precisely, with other suitable tumour targeting agents labelled with ^{124}I (half life 4.2 days) as they are not taken up by inflamed and infected tissues. Present challenges are procurement of radiotracers from a cyclotron facility, high cost, and degradation of PET image quality due to photon attenuation in tissues and quantitative accuracy and optimal integration of the DICOM images obtained in the treatment position into TPS software. The use of 4D PET/CT imaging with respiratory compensation in the thorax improved the partial volume effect and accuracy of SUV (standard uptake value) measurements. However, some limitations have also been well documented like false-negative results with ^{18F}FDG PET/CT may occur if a patient is scanned too early after completion of chemotherapy or radiation therapy, if there is recurrent disease; if malignancy is present in structures with a physiologically elevated metabolism (e.g., tonsillar carcinoma); or if the tumor is not FDG-avid. “Attenuation-correction” artifact results from erroneous overcorrection of PET emission data by software that uses CT transmission data for attenuation correction. This occurs in areas that have a high attenuation on corresponding CT images (e.g., enhancing blood vessels, metallic implants) and can be easily detected by evaluating the uncorrected emission PET data. Mis-registration artifact from involuntary activity is not as much a problem in head and neck ^{18F}FDG PET/CT as in imaging the chest or abdomen. Adequate patient instruction and immobilization during scanning prevents artifact due to voluntary movements. These hybrid imaging systems also vary in terms of sensitivity, spatial and temporal resolution. Technological developments to increase imaging speed to match with physiological processes of tumour sites and use of other therapeutic agents for targeted imaging shall be the future expectations of these hybrid systems.
Conclusion: Thus, today in cancer therapy, these modern imaging hybrid systems is probably superior for more accurate diagnostic PET/CT & MRI and RTP CT scan in a single session for a variety of cancers with better visualization and detection of distant metastases.

P-189

DOSE ESTIMATION IN WATER EQUIVALENT PHANTOM USING GEANT4 SIMULATION TOOLKIT

Sachin Dev[1,5], B. S. Rana[2], Davinder Siwal[3], Sanjeev Kumar[4]

Departments of [1]Radiotherapy and [2]Radiology, PGIMER, [3]Department of Physics, Panjab University, [5]Centre for Medical Physics, Panjab University, [4]Department of Physics, GGDSD College, Chandigarh, India.
E-mail: ss09731@gmail.com

Introduction: In radiological examinations radiation dose calculations are essential to understand the relationship between risk and benefiets of medical examination. Radiological investigations use X-ray in kV range for which absorbed dose measurement in phantom is somewhat difficult process as all the energy is deposited on surface. With the help of computer simulation, various physical process can be modeled and used for absorbed dose calculation. A versatile Monte Carlo based ; Geant4 (Geometry ANd Tracking), toolkit[1] can be used for the fundamental particle interaction simulation including electron and X-ray transport. A simple Monte Carlo algorithm consists in repeating similar process but with randomised starting conditions or events. In our case, photons emission direction is randomized isotropically, in Geant4. All the possible photons interactions are considered in simulation while allowing them to fall over water phantom. The incident X-Ray energy spectrum has been obtained using SpekCalc software[2] and fed in Geant4. Spectra obtained for Tungsten anode at tube potential of 100 KVp with 12 anode angle at air thickness of 1000 mm.
Objectives: Proposed work aimed to investigate the spatial distribution of radiation dose in water equivalent phantom induced by a diagnostic X-Ray unit and organ dose measurement so that diagnostic technique can be properly justified.
Materials and Methods: Geant4 (version 4.9.6.p02)[3] has been used for simulation which takes into account coherent and incoherent scattering, photoelectric effect, Compton effect, bremsstrahlung for photon transport. Geant4 is a set of libraries providing tools to perform simulations. It is programmed in C++ and follows an object-oriented philosophy. For data analysis, in scientific framework ; ROOT (version 5.36/34)[4,5] has been used and integrated with Geant4. Geometeric construction of water equivalent phantom is constructed in Geant4 along with material information. For the dose calculation, X-ray spectra obtained by SpekCalc is fed in Geant4 as a energy generator of RADspeed X-Ray unit.
Results and Discussion: Absorbed dose at various positions in phantom has been calculated. It is to be verified with experimental data which is future prospective of our study. A close match between simulated and actual dose deposition is expected, results will be presented in conference.

P-190

HIGH TERRESTRIAL GAMMA RADIATION DOSE RATE MEASURED IN GRANITE GEOLOGICAL TYPES; A CASE STUDY IN DISTRICT OF KUALA PILAH, MALAYSIA

Nor Eliana Norbani[1], Nazaratul Ashifa Abdullah Salim[2], Amin Aadenan[1], Ahmad Taufek Abdul Rahman[1,3]
[1]Faculty of Applied Sciences, Universiti Teknologi MARA, [3]Institute of Science, Universiti Teknologi MARA, Shah Alam, [2]Malaysian Nuclear Agency, Bangi, Selangor, Malaysia. E-mail: ahmadtaufek@salam.uitm.edu.my

Naturally-occurring radioactive materials (NORM) are all minerals and raw materials that contain radioactive nuclides of natural origin. These elements have always been presence in the Earth's crust and atmosphere. NORM concentrations can be altered through industrial activities such as coal, metal and mineral mining, fertiliser's production and usage, oil and gas production, building construction and recycling process. Some of these activities discarded the waste to water streams and alter the NORM concentration, known as the technologically-enhanced NORM (TENORM). It is important to have a fundamental baseline data for the radiation exposure of human to NORM across a geographical area to estimate dose received by the population. We have measured terrestrial gamma radiation dose-rates (TGRD) from surface soils throughout accessible areas in the district of Kuala Pilah, Malaysia. Dose rate measurements were carried out using a NaI (Tl) scintillation survey meter, encompassing 214 locations, covering about 71% of the 1047 km^2 of the land area Kuala Pilah district. This has allowed development of a TGRD contour map, plotted using WinSurf software. TGRD measured in the district of Kuala Pilah varies from 143 $\pm$ 7 nGy h^{-1} to 857 $\pm$ 15 nGy h^{-1}. Higher TGRD were found at the area covered by soil type is *Riverine-Local Alluvium Association*. These soil types of high TGRD level are underlay by Undifferentiated Granit Rocks geological formations. The lowest TGRD measured was found in *Acrisols* and *Ferralsols* soil family which were underlay by Permian geological structure. The mean TGRD measured is 458 $\pm$ 13 nGy h^{-1} compared to a mean value of 92 nGy/h and 59 nGy/h for Malaysia and the world, respectively. The average annual dose from such TGRD to an individual in Kuala Pilah district, assuming a tropical rural setting is estimated to be 0.93 mSv y^{-1}, which is considered to be within the normal range for doses from natural sources. The results can be considered as base values for distribution of natural radionuclides in the region and will be used as reference information to assess any changes in the radioactive background level due to geological processes and industries activities.

P-191

MONTE CARLO SIMULATION OF CONCRETE ACTIVATION IN MEDICAL CYCLOTRON VAULT

Biju Keshav Kumar, Anil Anant Shanbhag, Deepak Sakharam Joshi, Tapas Bandyopadhyay
Division of Health Physics, Bhabha Atomic Research Centre, Mumbai, Maharashtra, India.
E-mail: bijusivolli@gmail.com

Introduction: Medium energy proton accelerators are used for the production of PET and SPECT radioisotopes. 30 MeV proton cyclotron for medical use is being commissioned in VECC, Kolkata for this purpose. The secondary radiations, neutrons and gammas needs to be shielded adequately to protect the personnel working around and the public. In addition to this, the induced activity of the accelerator components and the concrete structure by neutrons is also one of the major safety concerns during maintenance and decommissioning of the installation. The build-up of induced radioactivity in the structural material over the years and the resulting gamma dose rates exposes the workers during maintenance operations.

Objective: This study aims to simulate build up of the long lived radionuclides induced in the Portland concrete walls and dose rates with 10 ppm of trace elements of Cobalt and Europium of a typical 30 MeV cyclotron vault over a period of 4 years of operation. It is assumed that the accelerator operates for two shifts (16 h) followed by one shift (8 h) shutdown in a day.

Materials and Methods: This study makes a Monte Carlo simulation of a virtual medical cyclotron vault of dimensions 8 m x8 m x 6 m with 100 cm thick walls of Portland concrete. A trace level of 10 ppm of Cobalt and Europium is assumed in the Portland concrete composition. A pencil beam of protons of 30 MeV, 1 microampere falling on the thick stopping target is modelled at the centre of the vault with the proton irradiation profile, as mentioned in the objective. Copper and aluminium are two important materials commonly used for beam line fabrication and slit holders. Tantalum is used for beam current measurements in proton accelerators. These are the beam loss materials considered in the simulations. Simulations are made using a validated Monte Carlo code FLUKA2011.2C.5. Fluka is capable of making predictions about residual nuclei produced in hadronic and electromagnetic showers and time evolution of the radionuclide inventory calculations online. The isotope production and decay as a function of irradiation time and cooling time is calculated analytically using the Bateman equations by the code.

Results and Discussions: The neutron yield from the target material obtained by this study is 2.13E-2 per proton of the beam. This value is agreeing well with the value 2.0E-2, reported in the IAEA TRS-283 report.2 m x 2m slab of 10 cm thick layers of concrete along the depth are the scoring volumes. The centre of the scoring slabs coincides with the beam direction. It is observed that the major long lived gamma emitting radionuclides produced by the (n, gamma) reactions in the concrete are Co-60, Eu-152, Eu-154, Na-24 and Na-22. Individual concentrations of the above mentioned radionuclides in the front wall are presented in Table 1 respectively after 4 years. The gamma dose rate at 1 m from the wall at the end of irradiation is 743 microSv per hour. This dose rate comes down to 10 microSv per hour after one week cooling, due to the decay of Na-24 isotope. The production and build-up of these long lived radionuclides and dose rates are studied as a function of irradiation time as well as the depth in the concrete.

Table 1: Induced radioactivity of long lived gamma emitting radionuclides

Radionuclide	*Half life*	*Mode of production in concrete*	*Gamma energy (MeV)*	*Induced activity after 4 years (Bq/cm^3/ microampere)*
Co-60	5.27 years	(*n*, gamma) on naturalcobalt	1.17, 1.33	0.2
Eu-152	13.3 years	(*n*, gamma) on natural europium	0.122, 1.458	2.3
Eu-154	8.8 years	(*n*, gamma) on natural europium	0.123, 1.597	0.2
Na-24	15 h	(*n*, gamma) on natural sodium	1.369, 2.754	38.4
Na-22	2.6 years	(*n*, 2*n*) on natural sodium	0.55, 1.275	0.1

P-192

QUALITY MANAGEMENT OF RADIOTHERAPY DEPARTMENT USING FAILURE MODES AND EFFECT ANALYSIS

P. Nagendran, V. Poopathi, Jibak Bhattacharya, Saibal Mukherjee

Department of Radiation Oncology, Apollo Gleneagles Hospitals, Kolkata, West Bengal, India.

E-mail: vpnagendran@yahoo.com

Introduction: Hospital is one where defects and mistakes are not and cannot be tolerated. A mistake could cost a patient their life. This means processes need to be in place and followed exactly how they are set forth to eliminate mistakes. In our radiotherapy department we have implemented Six Sigma project work using FMEA and avoid some issues and improved quality of treatment and new procedure. FMEA is a systematic method of identifying and preventing procedure and process problems before they occur.

Purpose: Improvement of Treatment Quality.

Aim and Objectives: Aim of the FMEA is avoid prevention of tragedy and doesn't require previous bad experience. Six Sigma certification is the best requirement in a healthcare environment for employees dealing with critical patient information. Quality improvement methods are more difficult to implement in a healthcare institute. The comprehensive approach offered by a Six Sigma Certification allows for the methodologies to be successfully implemented with positive results.

Materials and Methods: There are five steps of FMEA below mentioned here.

Step 1: Definition of Process: This FMEA is focused on Radiotherapy process and we have chosen only 11 Topics with team members. The radiotherapy treatment process is complex and involves multiple transfers of data between professional groups and across work areas for the delivery of radiation treatment. A minimum of three professional groups are needed for successful and safe treatment.

Step 2: FMEA Team: FMEA Number: 01; Date: Jan 2016 to December 2016; Team Members: 05.

Step 4: Hazard Analysis and Step 5: Actions and Outcomes are tables and graphically defined and analyzed errors.

Result and Discussion: We have collected all data, analysed and rectified in our department and compared with FMEA 2011, 2014 and 2016 years.

Conclusions: Improvements made in the department:

1. Introduced HIS and the patient name and UIHID are printed out on stickers. The stickers are pasted on file
2. Introduced workflow management software in Radiation therapy (Varian Medical System ARIA 11 ie version ECLIPSE 11) to do all the steps in radiation treatment from CT scan to treatment approval through the software. This has enabled a smooth workflow and reduced the chance of missing any step in the course of simulation and planning with periodically.

3. Patient prescription is part of the workflow and is done through the software. Only approved prescriptions will go to the Physicist for planning
4. Introduced time out form to reduce the probability of any wrong site radiation therapy
5. Barcode scanner is used for scanning of patient card to open an approved plan so that the correct patient and the correct procedures are done automatically without manual intervention.
6. Repeat CT scan reduced (wrong site avoid, mould fitting correctly)
   Etc……

Future Goals: We are planning to improve the current year data error rectify and so many new plans to implement in our department. Etc…

P-193

MEDICAL PHYSICS EDUCATION AND CLINICAL TRAINING PROGRAM IN BANGLADESH

Kamila Afroj Quadir

Bio-Science Division, Bangladesh Atomic Energy Commission, Bangladesh. E-mail: q.kamila@gmail.com

Introduction: The number of medical physicist working in diagnostic and therapeutic facilities requiring medical physicists is disproportionately low in Bangladesh. There are around 30 hospitals that have radiotherapy department and 20 hospitals having nuclear medicine department. The number of medical physicists in oncology is 35 and 14 in nuclear medicine. There are no medical physicists working in diagnostic radiology. Two universities, one public and the other private, have medical physics degree program. These degree programs include B.Sc., M.Sc. and Ph.D. However, university programs are not coupled with adequate clinical training.

Objective: Medical Physicists in their specializing field who can confidently work unsupervised within a multi-disciplinary team with safety and high professional standard need clinical training.

Approach: International Atomic Energy Agency (IAEA) under the project "Strengthening of Medical Physics through Education and Training" developed guidebooks for clinical training for medical physics working in, Radiation Oncology (TCS-37) Diagnostic Radiology (TCS-47) and Nuclear Medicine (TCS-50). These clinical training guidebooks were designed to be relevant for all modalities irrespective of the level of equipment complexity in use in the RCA member countries. Bangladesh started its first clinical training program in nuclear medicine in 2011 by following IAEA TCS-50. This 2 years structured clinical training program was completed successfully. The medical physicists, (4 Residence), who qualified in the clinical training program were evaluated by IAEA expert by written, practical and oral examination. These qualified Residents were subsequently tested and certified by the Bangladesh Medical Physics Association. Clinical training program for medical physicists commenced again in 2016 organized by IAEA/RCA project "Strengthening the Effectiveness and Extent of Medical Physics Education and Training" through the e learning platform (AMPLE) and with medical physicists from both radiotherapy and nuclear medicine discipline. Ten (10) medical physicists working in radiotherapy and six (6) medical physicists working in nuclear medicine are taking part in this program. The radiotherapy Residents are following IAEA guide book TCS-37 while the nuclear medicine Residents are following the IAEA guide book TCS-50.

Conclusion: It is expected that in future accreditation will become a basic requirement for all medical physicist operating in a clinical environment.

P-194

MICRODOSIMETRIC MEASUREMENTS IN BHABHATRON TELECOBALT INSTALLATION

Arghya Chattaraj, T. Palani Selvam, Vandana Srivastava, Sandipan Dawn, Kishore Joshi[1], A. K. Bakshi, D. Datta

Division of Radiological Physics and Advisory, Health, Safety and Environment Group, Bhabha Atomic Research Centre, Mumbai, [1]Advacned Centre for Treatment, Research and Education in Cancer, Navi Mumbai, Maharashtra, India. E-mail: arghyachattaraj@ymail.com

Introduction: Radiation quality can be described by macrodosimetric quantities LET and absorbed dose. LET and absorbed dose are volume average quantity and does not consider random nature of energy loss along the track. LET cannot express energy deposition in a small volume where average number of interactions is of the order of one or less. Radiations which differ in the number of energy deposits, their magnitude and spatial distribution may cause different effects for the same absorbed dose. All these drawbacks are taken care in microdosimetry. Microdosimetry is a technique for measuring the microscopic distribution of energy in cellular or sub-cellular level. Tissue Equivalent Proportional Counter (TEPC) is widely used for microdosimetric measurements in radiations field to characterize the radiation quality in radiation protection and radiotherapy environment. In microdosimetry, a lineal energy distribution is related to Relative Biological Effectiveness. Lineal energy, y is defined as the quotient of the energy imparted (ε) to the matter in a volume by single energy-deposition event, by the mean chord length $\bar{l}$ through that volume. The number of events with event size between y and $y + dy$ is denoted by $f(y)$ and the expectation value of y is frequency mean lineal energy, $\bar{y}_F$ $d(y) = yf(y)/\bar{y}_F$ .is dose probability density and the expectation value of y is dose mean lineal energy, $\bar{y}_D$ which describes variance of energy deposition in a sensitive volume.

Objectives: This study was aimed at measuring microdosimetric lineal energy distributions at different locations of a Bhabhatron telecobalt installation as a function of field size. From the measured microdosimetric distributions, and were determined.

Materials and Methods: Indigenously developed Bhabhatron telecobalt machine was used for microdosimetric measurements. A 20 x 30 x 30 cm^3 water phantom was kept at source-to-surface distance (SSD) of 80 cm. 10 cm x 10 cm and 25 cm x 25 cm field size were opened at SSD = 80 cm. 10 cm x 10 cm and 25 cm x 25 cm field size were opened at SSD

Table 1: Measurement of microdosimetric lineal energy at different locations of a Bhabhatron-II TAW Telecobalt installation as a function of field size using TEPC

Location of TEPC	*Field size*	*Water phantom*	*Gantry angle (°)*	$\bar{y}_F$ *(keV/μm)*	$\bar{y}_D$ *(keV/μm)*
Behind maze wall	10 cm × 10 cm	Present	0	1.19	1.75
Behind maze wall	10 cm × 10 cm with 30° wedge	Present	0	1.66	2.74
Behind maze wall	25 cm × 25 cm	Present	0	1.67	2.74
Above ceiling	25 cm × 25 cm	Absent	180	1.27	2.67

TEPC: Tissue equivalent proportional counter

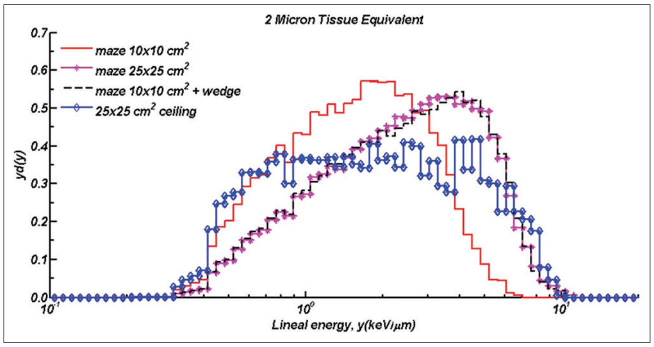

Figure 1:Graphical representation of variation in Lineal energy for different field size and location

= 80 cm. Walled spherical TEPC filled with tissue equivalent propane gas and capable of simulating 2 μm site was used in the measurements. The measurements were carried out at the locations: (a) Behind Maze Wall for 10 cm x 10 cm (open and wedge field) and 25 cm x 25 cm open fields, and (b) above ceiling for 25 cm x 25 cm field size.

Results and Discussion: The measured microdosimetric lineal energy distributions are shown in Figure 1. The peak of the lineal energy spectra for 10 cm x 10 cm wedged field and 25 cm x 25 cm open field are shifted towards higher *y* value compared to 10 cm x 10 cm open field. Depending upon the location of measurements, variations in and are observed as shown in Table 1. Such variation is attributed to beam quality and angular distribution of scattered photons present at the location. The measured and values are expected to be affected due to the thresholds of TEPC in the range of 0.3 - 0.5 keV/μm. Whereas for photons, the threshold value of *y* could be up to 0.01 keV/μm.

P-195

DIURNAL VARIATION OF INDOOR RADON CONCENTRATION IN WAYANAD DISTRICT, KERALA

Reshma Bhaskaran[1,2], C. D. Ravikumar[1]

[1]Department of Physics, University of Calicut, Thenhipalam, [2]Department of Radiotherapy, Government Medical College, Kozhikode, Kerala, India.
E-mail: bhaskaran_reshma@yahoo.co.in

Introduction and Aim: Among all the natural sources of radiation dose to mankind, inhalation of radon (^{222}Rn), thoron (^{220}Rn) and their progeny contribute about 50% of global effective dose. The concentration of radon indoors depends on the ventilation conditions. The present work studies the diurnal variation of indoor radon concentration in the mud houses of Wayanad district of Kerala.

Materials and Methods: The region of study is Bathery in Wayanad district. The active measurements were done using the state of the art equipment, the Portable Radon Monitor (SMART RnDuo), developed by BARC (Bhaba Atomic Research Center, Mumbai). The detector works on the principle of scintillation counter by scintillation with ZnS (Ag).

Result and Discussion: The active measurements were done for a period of five days in ten houses to study the diurnal variation. The indoor radon concentration varies from 22.47 Bq/m3 to 386.5 Bq/m3. The active measurements showed very good correlation with the passive indoor measurements (R = 0.99). It is seen that the concentration of radon reduces during the day time as compared to the night. The concentration keeps fluctuating. The maximum concentration of radon is found after midnight and in the early morning hours. In the house showing the highest concentration of radon, the value increased to as high as 1533 Bq/m^3 at night. However, the concentration dropped to levels shown during the day time when the room had increased ventilation by keeping the door of the room open overnight. The maximum concentration of radon decreased by a factor of 5 when the door was kept open along with the window opposite to it in the corridor which opens to the outside environment. The diurnal variation shows that the concentration of radon builds up at night when the ventilation in the houses is significantly reduced. The maximum concentration was found in the early mornings. Another room in the house was also studied using active measurements to check whether the concentration is the same in all the rooms. However, this room showed lesser concentration (average 161 Bq/m3). The room showing the highest concentration of radon had very large cracks in the floor. Due to the closed room, at night the temperature inside the room will be higher as compared to the outside environment. This results in stack effect, drawing the radon inside the room. The large cracks on the floor further assists in the flow of radon from soil gas to the indoor atmosphere due to the pressure variation between the indoor areas and the soil gas. Besides this the room has only one door giving entry to another room and not the outside environment. Hence lack of air circulation from the outdoor environment may also be contributing to accumulation of radon at night when the door was kept closed. As the second room has intact floors and the door of the room faces the outside environment the concentration of radon was not as high as seen in the first room. This shows that in spite of the source (concentration of radon in the soil gas) being the same, cracks and openings in the floor and walls contribute significantly to increase the radon concentration and hence the inhalation dose to the residents. It was found that the radon concentration in the houses in Wayanad district is higher as compared to the high background areas of Kerala.

P-196

PRACTICAL PHANTOM STUDY USING SMALL-TYPE OSL DOSIMETER TOWARD DIRECT DOSE MEASUREMENT DURING PEDIATRIC CT EXAMINATION

Tohru Okazaki[1], Hiroaki Hayashi[2], Emi Tomita[2], Sota Goto[2], Keiji Tada[3], Yoshiki Mihara[2], Natsumi Kimoto[2], Ryosuke Kasai[4], Yuki Kanazawa[2], Vergil LE Cruz[1], Takuya Hashizume[1,5], Cheng Wei Hsin[1], Ikuo Kobayashi[1]

[1]Nagase Landauer Ltd., Tsukuba, Ibaraki, [2]Tokushima University, Tokushima, [3]Faculty of Medicine, Shimane University, Shimane, [4]Tokushima University Hospital, Tokushima, [5]SOKENDAI, Shonan Village, Hayama, Kanagawa, Japan.
E-mail: okazaki@nagase-landauer.co.jp

Clinical diagnosis using X-rays is a useful tool in finding abnormalities in organs noninvasively. However, radiation exposure raises the risk of cancer; thus, it is preferable to manage the exposure dose of each patient. The management of exposure dose is important especially for neonates and infants because their cancer risk is relatively high. A small-type OSL dosimeter, called nanoDot, has a small energy and angular dependences in diagnostic X-ray region and its detection efficiency is extremely low. We expected to use it for direct measurement of the surface dose on patients during Computed Tomography (CT) examinations. Our previous study using the neonate phantom showed that the nanoDot does not interfere with the CT image. Furthermore, the lower detection limit of a nanoDot was estimated to be less than 10 μGy, and it indicates the possibility to be used for the surface dose evaluation of exposure doses caused by scattering radiation. For example, the doses around the eye lens and the gonads during a chest CT examination can be evaluated. Therefore, we plan to use nanoDots for a clinical study in measuring surface doses. The aim of this study is to estimate the uncertainty of the directly measured surface dose related to the pediatric CT examinations in a phantom study. We used a volumetric scan mode of a 320-detector row CT (Toshiba Medical Systems), in which a scan length is 160 mm in one rotation of X-ray tube. The tube voltage was set to 80 kV and rotational speed was set to 0.275 s with the current 100 mA. For the CT examination, 13 annealed nanoDots were placed symmetrically on a neonate phantom (Kyoto Kagaku Co. Ltd.) from the head to the feet. First, we evaluated the influence of phantom positions on measured doses. One phantom placement is $\pm$1 cm off-centered position from the center of scanning bed, and another is $\pm$10 degrees rotated position. Second, the influence of wearing clothes on the exposure dose was examined. Exposed nanoDots were read with a portable-type OSL reader, called microStar (Landauer, Inc.). In the experiment, in which the phantom without clothes was placed at the center, the averaged measured dose of 6 nanoDots placed inside of the irradiation area was 2.7 mGy. On the other hand, the doses of nanoDots placed outside of the irradiation area concerning the gonads and the eye lens were estimated to be 0.27 mGy and 0.2 mGy respectively; these doses were less than or equal to 1/10 of the measured dose inside the irradiation area. We estimated the effect of wearing clothes, and the correction factor was estimated to be approximately 5% when nanoDots were placed on the clothes to measure surface doses. This result was caused by the decrease of scattered X-ray incident to nanoDots. From the experiments in off-centered positions, dose distribution of 6 nanoDots was evaluated. Although the position of the phantom was varied, the measured doses of nanoDots placed in a symmetric position and the averaged measured doses of each condition did not show a significant difference. These results show that the position of the phantom does not affect the measured dose during a pediatric CT examination. In conclusion, during a CT examination the surface dose of patients can be measured directly using the small-type OSL dosimeters. The OSL dosimeter can measure exposure doses both inside and outside the irradiation area. Additionally, we estimated the measurement uncertainty depending on the variation of the phantom settings and the presence of clothes. Based on the results, we will start a clinical study of directly measuring patient doses using nanoDots.

P-197

POLYMER COMPOSITES FOR RADIATION PROTECTION

R. Ambika, N. Nagaiah

Department of Physics, Bangalore University, Bengaluru, Karnataka, India. E-mail: nagaiahn@rediffmail.com

X/Gamma rays find their increased applications in several areas of Science and Technology, for the benefit of mankind. From the past few decades, the nuclear techniques are being utilised for early diagnosis and treatment of several diseases. Radiation therapy (Internal and external) is one which uses X/Gamma rays, electron beam or proton to kill cancerous cells. Exposure to high energy radiations such as X/Gamma rays beyond certain limit, will definitely affect the normal tissues resulting in several radiation hazards. Hence, protecting from radiation exposure plays a crucial role in the radiation environment through proper shielding with the knowledge of shielding parameters. The common shielding material in use is lead, which is toxic, heavy and lack in usage flexibility. While, polymer composites have now added an advantage of being light weight in addition to their shielding ability. The present study deals with evaluation of shielding efficiency of polyester based composites filled with oxides of bismuth and tungsten for 80, 662, 1170 and 1332 keV gamma photons. The polymer composites with two different fillers Bi_2O_3 and WO_3 were prepared by open mould cast technique by varying the additive weight %. The filler dispersability was confirmed through scanning electron microscopy technique. Gamma shielding measurements were performed using a gamma ray spectrometer with a narrow beam geometry set up. The shielding parameters such as attenuation coefficient, half value layer thickness, effective atomic number (Z_{eff}) and electron density (n_e) were evaluated. The results reveal the dependency of linear attenuation coefficient on density, Z_{eff}, n_e and energy of the gamma photons. Density, Z_{eff}, n_e of the polymer composites have been increased due to the addition of filler concentration to the polymer matrix. Upon increasing the filler weight % in both the composites, the linear attenuation coefficient was found to increase considerably. Of which, 50 wt% filled composites possess maximum attenuation

coefficient. This may be attributed to the presence of high metal oxide Bi_2O_3 and WO_3 in the matrix, as high Z metal is responsible for the photon interaction in the material medium. Further, the probability of photon interaction with the medium is also dependent on incident photon energy. It is clear from the present study that, as the energy increases, interaction cross section decreases resulting in decrease in the attenuation coefficient. The attenuation coefficient is high at low photon energy say 80 keV when compared to high energy, as the probability of photoelectric absorption is high for the energy less than 100 keV. The shielding parameter, mass attenuation coefficient is very important to evaluate and assess any material as an excellent radiation shield, as it is density independent. It was found to be high for the tungsten oxide filled composite for 80 keV gamma photons when compared to bismuth oxide filled composite. In the case of Bi_2O_3 filled composite, the formation of absorption edge at 90.5keV, where complete absorption takes place may be the reason for the decrease in the attenuation coefficient at 80 keV. Further, half value layer thickness which is required for the practical appliance was found to be very low for both the composites and is 0.32 cm and 0.11 cm respectively for Bi_2O_3 and WO_3 filled composites at 50 Wt %. Both the composites are appreciable in terms of shielding ability. However, the shielding efficiency of the 50 wt% Bi_2O_3 filled polymer composite is almost comparable to barite at 662 keV, whereas, 50 wt% WO_3 filled polymer composite perform better than lead at low energy. Hence, these composites can be used in different forms by the medical radiation practitioners/professionals for protecting themselves and the patients from the exposure of X/Gamma rays.

P-198

STRUCTURAL RADIATION SHIELDING DESIGN OF GAMMA KNIFE FACILITY

Smriti Sharma, G. Sahani, Pankaj Tandon, A. U. Sonawane

Division of Radiological Safety, Atomic Energy Regulatory Board, Mumbai, Maharashtra, India.
E-mail: sharmasmriti.24@gmail.com

Introduction: Gamma knife equipment used to deliver a single high dose fraction of radiation, from 192/201 cobalt-60 sources which are distributed over a hemisphere. Centre of the hemisphere where radiation beams from these sources are focused is called focal point. Gamma knife equipment is designed for maximum capacity of total activity ~6000 Ci of Co-60. Bunker housing Gamma Knife equipment need to be provided adequate radiation shielding so that radiation exposures to members of the public and occupational worker not exceeding stipulated radiation dose limits. In order to achieve the goal, this paper focused on shielding calculation of bunker housing Gamma Knife equipment. Institutions desirous to start Gamma knife facility required to obtain layout plan approval from Atomic Energy Regulatory Board (AERB), national regulatory body, prior to construction. This work will be useful in preparing standard layout drawing which will further guide user institutions for preparing layout drawing for Gamma Knife facility to obtain layout approval from AERB. Hence, it may be helpful to avoid multiple rejection of layout plan application.

Objectives: The objective of this paper is to work out shielding thickness of a bunker having minimum required inner dimension to house gamma knife equipment.

Materials and Methods: Manufacturer of Gamma Knife is Elekta Instrument AB Stockholm, Sweden. The Gamma knife model Type B/C/4C and Perfexion are available in the country and one model is upcoming. Out of these, Type B/C/4C models are obsolete and no longer available for new installation and commissioning. Shielding calculation for Gamma knife installation is complex due to highly anisotropic radiation around the unit. Hence, dose map around the equipment is primarily required for shielding calculation. Manufacturer has provided dose map for Perfexion and new upcoming model for the Beam ON/OFF condition and with/without phantom. Dose map was provided in both horizontal and vertical plane at grid spacing of 0.5 m (along x, y, z directions). As per the manufacturer, radiation level was measured and then rescaled for maximum design capacity. For determining shielding thickness, workload is key factor to be first determined. Workload is defined as total dose delivered per week at isocenter or weekly Beam ON time considering maximum number of patient treated in a week. In this study, we have considered weekly Beam ON time as workload of the facility. Workload of the facility was determined by assuming 6 min/target, 5 average number of targets/patient, 5 patients treated/day and 5 working days/week. Based on above assumption, estimated workload comes out to be 12.5 hrs/week. Use factor and occupancy factors were taken to unity. Minimum inner dimension of the treatment room provided by manufacturer is 6.5m (L)×4.6m (W)×2.5m (H). However, considering the futuristic approach e.g. to house other radiotherapy equipment (Telecobalt, Accelerator etc.), inner dimensions 7.0m (L)×6.0m (W)×3.0m (H) were considered for shielding calculation of Gamma Knife facility and it was used for preparation of standard layout. Minimum distance between the unit focal point and the wall back side of the Gamma Knife was taken 2 m and that of opposite wall at 5m. Minimum distances of the walls along width were taken 2m and 4m on either side of focal point.

Results and Discussion: Using the dose map and optimizing parameters such as beam ON time, use factor and occupancy factor, radiation shielding thickness of the walls/ceiling comes out to be less than that of the required for earlier models of Gamma Knife. Moreover, manufacturer standard plan stated the shielding thickness around 60 cm of concrete. Hence, to prepare standard layout plan it was decided to keep the shielding thickness 60 cm of concrete depending upon near future extension for another type of equipment.

*Authors are thankful to Elekta Medical System, Sweden for support for the study.

P-199

RADIOIODINE I131 PATIENTS RELEASE CRITERIA IN DUBAI HEALTH AUTHORITY

N. A. Boshara, M. M. Zakaria, L. G. Albalooshi

Medical Physicist, Dubai Health Authority, Dubai, UAE.
E-mail: nabahmed@dha.gov.ae

Radioiodine therapy is well established as a treatment for thyroid cancer because of its radioactive proprieties; radioiodine decay by emitting high energy Beta particles that interact with mater in short distance. This interaction results in depositing energy locally within the patient tissues. From a radiation safety perspective, this radiological practice should be optimized to ensure radiation safety of staff, the public and care providers during handling excretions and patient's body fluids. A total of 391 Patients in Dubai Hospital, Dubai Health Authority, United Arab of emirates, received I-131 high therapy doses for thyroid cancer treatment from January 2010 until December 2016. This study was conduct to review the patient release criteria in Dubai Health Authority. The study classified the obtained data into groups according to the administered dose as: Group A patient received I131 capsules with activities below than 100 mCi, Group B patient received activities between 100-150 mCi and Group C patient received activities above 150 mCi. For each group, administered dose, remaining activities and dose rate were calculated and recorded for an average age of 40 years old ranged between (16 and 73) years old. Approximately 80% of patients were females and 20% were males. More or less, 39% of these patients received up to 100 mCi (3700 MBq), I-131 Oral Doses, where the minimum and the maximum doses were 60 mCi and 97 mCi respectively. 42.7% of these patients received I-131 Oral Doses from 100 to 150 mCi. Minimum and maximum doses activity were 101.57 mCi and 137.54 mCi respectively. Moreover, 61% of patients received I-131 doses up to 150 mci (5550 MBq) fluctuated between 102 and 138 mCi. Both the NRC and the NCRP recommend releasing I131 patients from hospitals following the administrated activities and radiopharmaceuticals criteria. some of the neighboring Gulf countries that having the same social culture as UAE such as Oman releasing I131 patients with dose rate $\leq$ 70 μSv/hr. On the other hand, a number of international countries depend on the criteria of discharging I-131 patients, according to residual activity in the patient body since the patients released for discharge with residual activities less than 33 mci (1221 MBq). However, Dubai Hospital- DHA in UAE following IAEA recommended criteria for releasing patients with radiation dose rate at defined distance, the applicable radiation dose rate for discharge I-131 patients in DHA – UAE is 50 μSv/hr at 1 meter. The emitted radiation dose rate detected by ceiling-mounted detector (DLMon (Dose Rate Monitoring) System) fixed at one meter from the patient's bed. An average of three readings every two hours obtained and recorded in the system. Remaining Activity in patient's body estimated by using the below equation:

Remaining Activity (MBq) = A *EXP ((-0.693/T1/2)*T)

Patients released for discharge from Dubai Hospital-DHA with an average of 35 μSv/hr at one meter. Hence, this dose rate is equivalent to an average of 17 mci (633 MBq) as residual activities in the body. Accordingly, the applied criteria in DHA tolerate releasing of I131 patients with radiation dose rate lower than a number of other countries and within the recommended international limits (70 μSv/hr recommended by IAEA and 50 μSv/hr recommended by NRCO & NRC). Nevertheless, the common lifestyle and social culture in UAE may contribute in enhancing radiation protection for patient family and public.

P-200

PEDIATRIC INTERVENTIONAL CARDIOLOGY: A LITERATURE REVIEW ON RADIATION DOSES

A. Ploussi, K. Platoni, E. P. Efstathopoulos

2nd Department of Radiology, University General Hospital "Attikon", School of Medicine, National and Kapodistrian University of Athens, Athens, Greece.
E-mail: aplousi@gmail.com

Introduction: The increased frequency of interventional cardiology procedures in recent years, the radiation-related cancer risks, the high radiation doses delivered during interventional procedures as well as the increased radiosensitivity of children have raised serious concerns regarding the exposure of pediatric population to ionizing radiation. Moreover, as pediatric patients with congenital diseases often undergo multiple interventional cardiology procedures during their life, cumulative radiation dose may reach high levels.

Objectives: The purpose of the current study is to provide a literature review concerning radiation doses to pediatric patients undergoing interventional cardiology procedures.

Materials and Methods: A thorough literature search was conducted using the database PubMed for studies published between January 2000 and April 2017 with the following keywords: [children or paediatric] and [doses or exposure] and [nterventional cardiology or catheterization or angiography]. Only articles in the English language were included.

Results: The literature search identified a total of 39 relevant articles: 38 originals articles and 1 review article. The studies included diagnostic as well as therapeutic interventioanl cardiology procedures. Radiation dose measurements were performed either with physical measurements using pediatric anthropomorphic phantoms or using Monte Carlo simulation techniques. The articles included information regarding DAP, effective dose, organ dose and fluoroscopy time. Effective dose values ranged from 0.16 to 27.8 mSv for diagnostic and from 0.38 to 66.7 mSv for therapeutic interventional cardiology procedures. The highest radiation doses received by the heart, lungs, breast, esophagus and thyroid gland. The fluoroscopy time ranged between 0.3 and 47.8 min for diagnostic and between 7 and 75.1 min for therapeutic interventional cardiology procedures.

Discussion: The overview revealed large variations in the values of radiation dose even for the same type of interventional procedure. This can be attributed to three main reasons: i) the different technology of imaging equipment (eg. image intensifier vs flat panel detectors), ii) the wide range of body size in pediatric patients even for children of the same age and iii) the education of medical staff on radiation protection issues as well as the physician's experience. Reliable estimation of radiation dose and cancer risk faces many challenges in pediatrics. It requires standardization of the recorded dosimetric quantities, optimization of the clinical protocols, follow-up of the patients during their life and studies in larger cohort of patients.

P 201 ABS0291

P-201

CATEGORIZATION OF RADIATION SOURCES AND APPLICABLE SECURITY MEASURES FOR RADIATION SOURCES USED IN RADIOTHERAPY

B. Mishra, M. Mahesh, G. Sahani, Pankaj Tandon

Division of Radiological Safety, Atomic Energy Regulatory Board, Mumbai, Maharashtra, India.
E-mail: m.bibek@gmail.com

Introduction: The technologies that make use of ionising radiation sources (i.e. radioactive material and radiation generating equip.) continue to spread around the world as well as in our country. They are used in multifarious applications in various fields such as medicine, industry, agriculture, research, military, mining, academic applications, etc. This technology has been playing remarkable role in enhancing quality of life and plays significant role in improving or saving life by treatment of cancer and diagnosis of various diseases. Safety record of this technology is generally good, however, However, while attempting to address the threats from malevolent acts involving radioactive sources, it is clear that sources of certain magnitudes and types are more vulnerable to such acts than others. Therefore, it is felt that there is a need to adopt different security approach based on the potential hazard associated with the source and hence there is need of stringent regulatory control for security of radioactive sources.

Objective: Sources with high activity, if not managed safely and securely, could cause severe deterministic effects to individuals in a short period of time. The categorization provides an internationally harmonised basis for risk informed decision making. Based on these values different security measures has been considered.

Materials and Methods: A dangerous source is defined as a source whose activity is high enough to deliver a radiation dose which would result in severe deterministic effects in the exposed individual. The activity of a source, which can deliver this dose, is termed its “D value”. Both external and internal exposures are therefore considered in the derivation of D values and which is already established in the IAEA safety guide No. RS-G-1.9 and AERB safety guide on security of radioactive material i.e. AERB/RF-RS/SG-1 . There are five different categories based on the calculated value of the ratio i.e. “A/D” (Activity of the source” A” in Ci) value. For example Co-60, D value is 0.8 Ci and for a telecobalt source of the order of activity A~12000 Ci. The A/D> 1000 which falls under Category1 source. No categorization for radiation generating equipments. Considering security different security scenarios associated with radioactive sources, four security levels - A, B, C and D have been defined. These levels provide a systematic way of categorising the graded performance objectives required to cover the range of security measures that might be needed. The performance objectives for the four security levels of a security system are detailed below:

- Security Level A: Prevent unauthorised removal
- Security Level B: Minimise the likelihood of unauthorised removal
- Security Level C: Reduce the likelihood of unauthorised removal
- Security Level D: Measures should be established to ensure safe use of the source.

Conclusion: While addressing the threats associated with radioactive materials with respect to malevolent act/terrorist act and potential exposure with the source loss the principles of security measures: detection, delay, response and security management need to be implemented. During our review on the submitted security plans, it is revealed that there is a need to strength the security measures at Radiation Facilities (RFs). User need to design the security infrastructure based on perceived security threat addressing the issues in the security plan and register it with the Law & Enforcement Authority. Additional measures need to be augmented by establishing information exchange procedure with the Law & Enforcement authority. There should be separate detection system such as CCTV, intrusion systems, passive infrared systems integrated with response mechanism for 24×7 days instead of considering the CCTV which is available for patient monitoring during treatment. Access control systems must be implemented such as biometric, PIN based systems, swipe card systems etc. All security devices/systems need to be maintained periodically and quality control system need to be in place. The physical security system must address the detection time, delay time, and time required to initiate response and defeating the adversary. Administrative procedure must be in place defining clear role and responsibility. There should be a layout diagram indicating the access point, entry/exist to the facility and security infrastructure etc. Security measures shall be implanted at RFs to address the security threats and malevolent acts.

P-202

SOURCE ON POSITION LEAKAGE MEASUREMENT FROM SOURCE HOUSING OF TELEGAMMA UNIT OVER THE PERIOD OF 36 MONTHS – A RETROSPECTIVE ANALYSIS

N. Balasubramanian, V. Kaushal, Yogesh Kumar, N. P. Patel, Anil K. Dhull

Department of Radiation Oncology, Pt. B.D. Sharma PGIMS, Rohtak, Haryana, India.
E-mail: baluwda@yahoo.com

Introduction: The aim of this study is to evaluate and analyze the on position leakage in-patient plane and radiation safety compliance of telegamma unit over the period of 36-months. RMM (Roentgen per minute at 1 meter) measurements and leakage radiation measurements in-patient plane are the part of the Quality assurance programme. Both measurements were repeated at regular intervals. These recorded values have been taken up to assess the shielding adequacy of source housing of telecobalt unit over the period of years. Measured values at 69.0 cm and 156.0 cm from the beam axis 8 points located in-patient plane ranges from 0.027% to 0.081% and 0.0045% to 0.0062% respectively, which were well below the specified tolerance limit of 0.1% RMM.

Materials and Methods: A new cobalt-60 source from BRIT (Board of Radiation Isotope and Technology) has been loaded on telecobalt machine and commissioned for patient treatment in the Department of Radiotherapy, Pt. B. D. Sharma PGIMS, Rohtak in the year 2014 after receiving authorization from the competent authority. As per the literature, the defined age of the 780E Teletherapy machine is 13 years. The recorded values for the years 2015, 2016 and 2017 have been taken up and evaluated. The gantry of telegamma machine was stationary at 0º and the collimator was closed fully with shielding blocks supplied by manufacturer during entire leakage measurements. For this leakage measurement, calibrated large volume pressurized ionization chamber based radiation survey meter from fluke biomedical model 451P-DE-SI-RYR with integrated mode was used. The great care must be taken to position the survey meter in such a way that patient plane is parallel to GM detector axis and perpendicular to radiation beam axis. During the measurement, chamber was positioned at 69.0 cm and 156.0 cm radius from the isocentre of the machine. The couch has been rotated carefully and the readings were recorded for different angular positions. Figure 1 shows the measurement positions in the patient plane at two different radii. Calibrated Secondary Standard Fluke dosimeter coupled with 0.6cc ion chamber was used to carry out RMM measurement. The measured source strength was 169.233 RMM as on 29.09.2014. Percentage of source head leakage at various points were calculated[1] using RMM value measured at 1 meter along the radiation beam axis for 20 cm × 20 cm field size.

Results and Discussion: Table 1 shows the measured percentage leakage radiation from the treatment head of telegamma machine at different angular positions in the patient plane at 69.0 cm and 156.0 cm away from the isocentre. As per national protocol,[1] the measured exposure rate at 1 meter from the source with collimator jaws closed completely blocked with appropriate lead thickness should be less than or equal to 0.1% of RMM of the loaded source. The recorded values are less than the tolerance limit 0.1% specified by the competent authority.[1] The source housing shielding is adequate for the cobalt telegamma unit installed in our center.

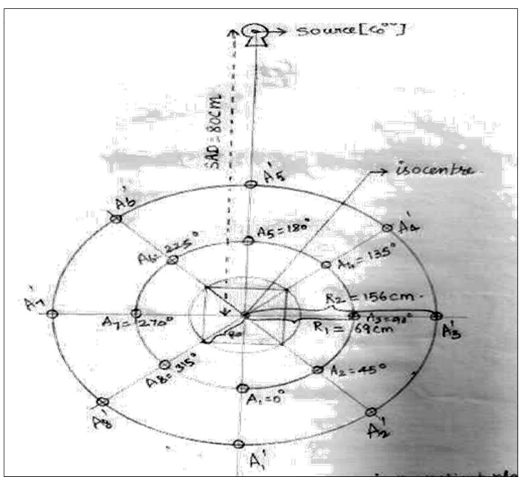

Figure 1: Measurement position in the patient plane at two different radius R_1 = 69 cm and R_2 = 156 cm

Table 1: On-position leakage from the source head of telecobalt machine (theratron 780E) in the patient plane for the last 3 years

Table positions (°)	*Percentage of source head leakage in a patient plane*					
	69 cm from the isocentre of telecobalt machine			*156 cm from the isocentre of telecobalt machine*		
	2015	*2016*	*2017*	*2015*	*2016*	*2017*
0	0.073	0.067	0.044	0.0048	0.0051	0.0054
45	0.081	0.075	0.029	0.0045	0.0050	0.0043
90	0.075	0.068	0.058	0.0053	0.0062	0.0054
135	0.077	0.075	0.029	Not done	Not done	Not done
180	0.076	0.068	0.040	Not done	Not done	Not done
225	0.076	0.067	0.057	Not done	Not done	Not done
270	0.065	0.069	0.027	0.0053	0.0050	0.0045
315	0.070	0.075	0.027	0.0053	0.0050	0.0054

The radii 69.0 cm and 156.0 cm have been derived from IEC equation.
IEC: International Electromechanical Commission

Conclusions: From this retrospective analysis, the percentage on-position leakage from the source head of telegamma unit at various points was less than the tolerance limit recommended by the competent authority. The study results shows that the shielding adequacy of the source head over the period of time is adequate and improve the safety of the patient during the treatment and the telecoblat machine can be used for patient treatment safely.

P-203

ESTIMATION OF RADIATION EXPOSURE TO TECHNOLOGIST DURING ^{18}F-FDG PET/CT PROCEDURES AT OUR CENTRE

M. S. AL-Aamri, N. K. AL-Balushi

Department of Nuclear Medicine, Molecular Imaging Center, Royal Hospital, Muscat, Sultanate of Oman.
E-mail: marwasulei@gmail.com

Introduction: Positron Emission Tomography (PET) is the imaging modality of choice in oncology. In addition, there are several indications for using PET in cardiology and neurology. The main radiotracer used is the radiolabeled glucose analog ^{18}F-FDG (Fluro Deoxy Glucose). The high-energy annihilation radiation from positron emission may leads to significant radiation exposure to professionals, patients and their relatives.

Objectives: In this cross sectional observational study, we have assessed the effective dose to workers in Molecular Imaging Center (MIC) from patients injected with ^{18}F-FDG.

Materials and Methods: Dose rates were estimated by calibrated (Ludlum14 C model, pancake GM external detector, USA), portable gamma ray survey meter at 0.300, 0.500, 1.000 and 2.000 m from 70 patients who undergo whole body ^{18}F-FDG PET/CT procedure immediately and 2 hours' post injection. Electronic Personnel Dosimeters (EPD) (*Rados)* were used to determine the radiation doses per PET/CT imaging for the five staff involved in and directly handing the injected patients; two technologists, two staff nurses and one medical physicist.

Results: The mean dose rates from patients after injection and standard deviation for the four distances were 98.120 ± 24.000, 55.263 ± 15.000, 28.234 ± 10.500 and 10.806 ± 5.000 μSv/h respectively. After 2 hours, the measurements significantly dropped to 45.734 ± 13.000, 23.649 ± 10.000, 9.934 ± 4.000 and 3.749 ± 1.000 μSv/h.

Conclusion: The average effective dose values for workers from injected patients throughout the procedure of PET/CT study were less than 20 mSv/year which is the limit recommended by the International Commission on Radiological Protection (ICRP).

P-204

OPERATIONAL EXPERIENCE WITH E-LICENSING OF RADIATION APPLICATION FOR RADIOTHERAPY PRACTICE

B. Mishra, G. Sahani, Pankaj Tandon, A. U. Sonawane

Division of Radiological Safety, Atomic Energy Regulatory Board, Mumbai, Maharashtra, India.
E-mail: bibek@aerb.gov.in

Introduction: eLORA is a web-based I&CT (Information and Communication Technology) application establishing communication between Atomic Energy Regulatory Board and its stakeholders (i,e Radiation Facilities, Supplier, Manufacturer etc.) for exchange of information and communication for delivering its regulatory services.

Objectives: The eLORA system is designed to automate the regulatory submissions, to achieve transparency and better efficiency in regulatory system. The components of eLORA are chosen to ensure Security, Performance, Availability, Scalability, Manageability and Maintainability.

Materials and Methods: The objective of eLORA is to reengineer the paper application forms to electronic submissions. Periodic update at institutional level (such as details of staff members, safet/QA instruments etc.) which affects application submission/process has been separated out for simplicity and better efficiency. System is constructed with more business logic for regulatory activities. On the same platform during the design phase the scalability has been consider significantly to construct all regulatory practice. Various regressive test such as factory acceptance test, pre-user acceptance test, user acceptance test are carried out before implementing the system.

Results and Discussion: Table 1 represents data for more than 4 years in this analysis for efficiency, productivity and reliability of the eLORA system. It is noted that, during the paper based regulatory process, RSD, AERB used to receive ~18,000 submissions annually. From the Table-1 it is clear that the submission has reached almost four fold. In the same time, there is no enhancement in staff members at the Division. Some of the application details are considered for representation as below.

Institute Registration: This is a new step introduced in eLORA for registering the authenticated information about the institution. During the initial phase, there is a tremendous increase of these

applications as all existing RFs are switching to eLORA system. Around 32,000 institutes are now under regulatory purview through eLORA. The rejections of the submitted applications are due to the data inconstancy, inappropriate documents. The approval ration can be enhanced by referring the guidelines before submission.

Radiological Safety Officer (RSO): The trend of RSO applications were maximum during 2015-16 as existing approved RSOs getting migrated to the system and more number of institutes started using the system. The rejection shows the lower trend with respect to the preceding years and mainly attributing for PMS availability and appropriately updating the qualifications of registered Radiation Professional.

Regulatory Applications for all practices: It is noted that 234,006 number of applications has been submitted in the system, which clearly indicates the consistency and reliability of the system. The rejection indicates a decreased trend. It is mainly attributing in easy submission process, simplified regulatory procedure and further it can be drastically reduced by verifying the application submission through different tabs as provided in the in the application page.

Regulatory Applications for Radiotherapy (RT) Practice: Regulatory form submission as applicable to RT practice has shown reduced rejection over the preceding years. Typically it is noted that the major rejections are in response to non-compliance and inconstancy in transport applications.

Table 1: Analysis for efficiency, productivity and reliability of the eLORA system using data of 4 years online application submission

Nature of application	*Year*				
	2013	*2014*	*2015*	*2016*	*2017 (till 12th July)*
Institute registration					
Total submission*	1016	9069	12,987	16,736	11,889
Approved	712	5872	9898	9673	5873
Rejected	357	3197	3088	7063	5718
RSO					
Total submission	10	1925	4432	3868	1844
Approved	3	761	2408	2361	1215
Rejected	7	567	1337	1195	481
Regulatory applications: All practices					
Total submission*	1712	27,015	60,039	89,756	53,605
Approved	1606	23,425	48,196	68,358	41,614
Rejected	106	3590	11340	17687	7614
RT-regulatory submissions					
Total submission*	43	1404	3002	5999	3207
Approved	19	743	1855	4173	2128
Rejected	24	661	1131	1429	593
RT-layout plan					
Total submission*	33	528	514	637	287
Approved	12	195	186	269	138
Rejected	21	333	328	368	121
RT-procurement (equipment/source)					
Total submission*	7	479	735	648	348
Approved	4	249	463	533	277
Rejected	3	230	272	115	43

Total submission: Number of application submitted through the system which may be approved/rejected/pending/in progress etc. Therefore the total submission is not equal to the sum of approved and rejected application. Radiotherapy related applications are considered here form the user perspective. RT: Radiotherapy, RSO: Radiological safety officer

RT-Layout Plan: In the site and layout plan submission for radiotherapy practice has shown an increasing trend in the preceding years because of regularisation process for the existing bunkers. It was further observed that the rejection is more in comparison to the approvals. It can be reduced by referring the guidelines specially prepared for preparation of site and layout purpose and can downloaded from the help menu.

RT-Procurement: The source and equipment application shows a clear trend in decreased rejection. It is mainly attributed toward the clear understanding of regulatory requirements from the user end as the regulatory process

built in eLORA are simplified. Further, it can bereduced by re verifying the institute details for availability of adequate staff members, availability of adequate QA/Safety/Measuring and Monitoring tools before submission.
Recently, performance level upgrades are going on which will ensure the availability of the system 24x7 days.

P-205

QUANTITATIVE ANALYSIS OF AYURVEDA DRUG BY COMPARATIVE STUDY OF KASISA BHASMA USING ATOMIC ABSORBPTION SPECTROMETRIC TECHNIQUE

A. Ashwini, S. S. Teerthe, B. R. Kerur
Department of Physics, Gulbarga University, Kalaburagi, Karnataka, India. E-mail: kerurbrk@yahoo.com

Introduction: In Ayurveda bhasma (calx) is a drug used for therapeutic purpose by different practitioners since centuries. Preparation of bhasma includes various processing steps like purification, levigation, calcinations cycle, improving quality and removing blemishes etc, processing of bhasma aims at formation of herbo-mineral complex molecule which can act in minimal dosage, palatable, easy for assimilation, highly efficacious with minimal or no complication. Now a day different brands bhasma are commercially prepared and available in market being used by patients, but contamination of ayurvedic drugs with trace elements is major concern and the poor quality of these medicines causes health hazards. Hence is necessary to know the levels of major, minor and trace elements present in the ayurvedic drugs. In this direction in present work studied the elemental concentrations of Kasisa bhasma manufactured by four branded firms and analysis is carried out using AAS.
Materials and Methods: In the present study four brand Kasisa bhasma (drug) selected and labeled such as AKB, BKB, PKB, and DKB. The drug sample solution is prepared as per standard solution preparation for Atomic Absorption Spectroscopic technique. Elemental analysis is carried out by the Thermo Scientific range of ICE 3000 series Atomic Absorption Spectrometer (AAS). Atomic Absorption Spectrometer is an analytical instrumentation technique used in determination of metal concentration in sample which is in solid or liquid form. Atomic Absorption (AA) occurs when a ground state atom absorbs energy in the form of light of a specific wavelength and is elevated to an excited state. The amount of light energy absorbed at this wavelength will increase as the number of atoms of the selected element in the light path increases. The relationship between the amount of light absorbed and the concentration of analytes present in known standards can be used to determine unknown sample concentrations by measuring the amount of light they absorb.
Result: Presented in Table 1 and Figure 1.
Discussion: The estimated concentrations of Mg, Al, K, Ca, Mn, Fe, Cu and Zn are presented in Table 1. From the Table 1 and Figure 1 observed that Kasisa bhasma is iron rich drug in ayurveda which is used in anemia treatment and in treatment of eye diseases, leucoderma, primary and secondary amenorrhea. All four brand drug showing little variations in the concentrations of all elements.
Conclusion: This result revealed that the Kasisa bhasma is rich in iron. Ca, Mg, Mn, Zn and other element are found, though the drug of all brand are shows small variation in elemental concentrations but these elements found within the rate of Recommended Daily intake of minerals and vitamins in food as recommended by WHO. Thus present work is comparative study will reflect quantitative analysis of Kasisa bhasma.

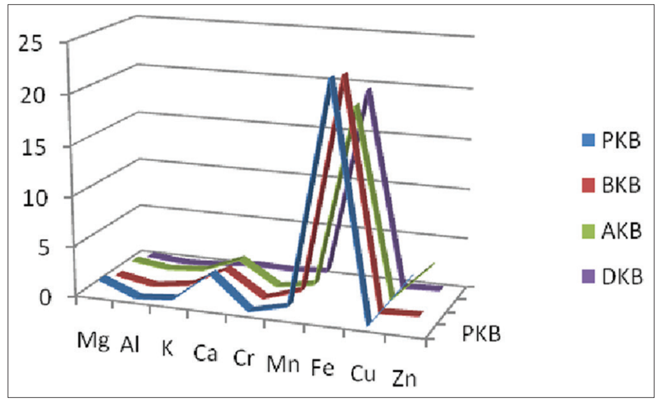

Figure 1: Elements concentration in mg/l versus elements in the Kasisa bhasma

Table 1: Quality Management of Radiotherapy Department Using FMEA

SN	Sample code	ELEMENTS CONCENTRATION IN mg/l								
		Mg	Al	K	Ca	Cr	Mn	Fe	Cu	Zn
1	PKB	1.452	ND	0.344	3.293	0.061	0.992	23.094	ND	5.064
2	BKB	0.693	ND	0.536	2.538	0.091	1.297	22.620	0.011	0.206
3	AKB	1.021	0.527	0.864	2.369	0.052	0.672	18.895	0.029	3.814
4	DKB	0.338	ND	0.218	0.625	0.512	0.794	19.640	0.039	0.214

* ND: not detected.

Acknowledgment: The authors express their sense of gratitude to UGC-BSR for providing financial support.

P-206

'MOCK TRIAL' ON PATIENT RELEASE DURING 'SOURCE STUCK' IN A CLINICAL TELECOBALT RADIOTHERAPY MACHINE AND ESTIMATES OF STRAY RADIATION EXPOSURES

Ramamoorthy Ravichandran
Cachar Cancer Hospital and Research Centre, Silchar, Assam, India. E-mail: ravichandranrama@rediffmail.com

Radioactive cobalt-60 teletherapy machines still find a place in radiation therapy departments, in more populated and developing countries. Radiation safety text books and protection safety guides of different nations give guidelines how to react at a situation, but so far, there are no reports how these are executed practically. There is no documented method, how a technologist will approach problems of this nature, when the patient wears an immobilization shell. The Radiological Safety Officer (RSO) has to display sufficient warning instructions and the actions to be followed in terms of emergency situations, such as "source drawer stuck ON position" or "not going fully back to OFF position." A "mock trial" "source stuck" was simulated by keeping the machine is in OFF condition. A human dummy model (Medical Mannequin) was kept on the treatment table for demonstration. Two radiation technologists carried out the above exercise to release the clamp on the "Orfit" Base Board, table top operations, and the actual duration is recorded with an electronic stop watch as a mean of two attempts. A condenser chamber type "calibrated pocket dosimeter" (Model 909, chamber 242952) (Arrow-Tech Inc., USA) was used to estimate the doses at known location inside the room. Cumulated doses were estimated at a position 1.45 m radially away from "source," which corresponded to the location of a technologist standing and operating the hand control. The pocket dosimeter had a water can to provide back scatter. Stray doses with and without scatter water phantom at 0°,90°, and 270° positions of the gantry. For lateral beam, the recorded dose rates were 72.4–37.2 μGy/min with and without water phantom. Same lateral beam with machine head on the opposite side had 35% increased exposure rate due to forward scatter, i.e., 98 μGy/min against previous value of 72.4 μGy/min. It reveals the presence of more forward scatter in the gamma beam. In this position, when the phantom is not there, the exposure rate at the radial location increases from 98 μGy/min to 114.0 μGy/min (increase of about 16%). This implies that unattenuated primary initiates increased scatter from the opposite concrete barrier wall, thereby increasing the stray radiation dose level. Effect in the vertical beam results in an exposure rate of 147.2 μGy/min with phantom present, which reduces to 86.8 μGy/min (a reduction of about 41%) when phantom removed. From above measurements, if we normalize the values for a nominal source activity of 333 TBq (9000 Ci) and 30 s duration (assumed as patient releasing time by technologist), the resultant personnel dose in these situations vary from 63 μGy to 267 μGy (6.3–26.7 mR). As part of the time in these estimations is for "presence of primary" and later only scatter, the actual exposures will be nearer to 63 μGy (6.3 mR). CD dosimeter estimated a leakage of 2.2 cGy/h at 89 TBq, which will correspond to 1.8 mGy/min if the collimator is totally closed (as in the case of Bhabhatron machine) when the technologist will be exposed to only leakage radiations as the primary is shut off. In this present report, the true situation encountered in a cobalt-60 teletherapy installation is simulated, and a possible management strategy is arrived at. This work is likely to remove the apprehensions on the use of telecobalt machine, and might continue give preference as a practical solution in addition of armamentarium for cancer radiotherapy in busy centres.

P-207

AN ENHANCED IONISING RADIATION MONITORING AND DETECTING TECHNIQUE IN RADIOTHERAPY UNITS OF HOSPITALS USING WIRELESS SENSOR NETWORKS

Peter Ali

Department of Physics, Ebonyi State College of Education, Ikwo, Nigeria. E-mail: petera754@gmail.com

In this paper, a solution of ionising radiation monitoring based on the concept of Wireless Sensor Network (WSN), is presented. Radiation dose rate measured by the sensor node is sent to the monitoring station through ZigBee wireless network operated on 2.4 GHz unlicensed Industrial Scientific Medical (ISM) band. The system is calibrated for use for ionizing radiation dose rate range of between amount of ionising radiation observed in radiotherapy unit of a hospital and 1.02 mSv/h. Power consumption of the sensor node is kept low by operating the node ZigBee radio with low duty cycle: i.e. by keeping the radio awake only during data transmission/reception. Two *ATmega8* microcontrollers, one each for sensor node and the monitoring station, are programmed to perform interfacing, data processing, and control functions. The system range of coverage is 124m for outdoor (line of site) deployment and 56.8m for indoor application where 5 brick walls separated the sensor node and the monitoring station. Range of coverage of the system is extendable via the use of ZigBee router(s).

P-208

NUCLEAR EMERGENCY PREPAREDNESS IN ATERTIARY CARE HOSPITAL

Deboleena Mukherjee, Arti Sarin[1], Sachin Taneja, Kirti Tyagi

Radiation Oncology Centre, INHS Asvini, [1]Department of Nuclear Medicine, INHS Asvini, Mumbai, Maharashtra, India. E-mail: deboleena.rso@gmail.com

Introduction: Disasters are mainly classified into two types natural and man-made. Natural disasters are weather or earth related namely floods, cyclones, hurricanes, landslides, earthquakes, drought, famines and volcano eruptions etc caused due to natural impact on the environment. Man-made disasters are nuclear, biological and chemical nature either caused by accidents or by terrorist activity. Worldwide, there is an increased use of radioactive materials in industrial, medical, agricultural and other scientific research activities leading to a measurable increase in natural background radiation levels. Accidents in nuclear power plants (NPP), medical or industrial facilities that use radiation or nuclear weapons and constant threats by militants of "dirty bomb" are always a cause of concern and therefore a comprehensive "nuclear emergency preparedness" is of utmost importance. Being a tertiary care hospital, this need is further enhanced for safeguarding the human and animal life in sea, land and air of our country in case of any such disasters. In this paper we will discuss the response plan in case of "nuclear emergency" by this hospital.

Materials and Methods: To handle mass casualties, as per the guidelines a Nuclear Biochemical Cell (NBC) comprising of medical super specialist officers cum RSO, nursing staff and trained personnel has been formed to monitor, decontaminate, cleanse and treat the causalities in case of any emergency related to Chemical, Biological, Radiological and Nuclear (CBRN) disasters. A wide range of NBC protection materials and equipment like NBC suits, protecting gloves, masks, respirators, medicines, radiation survey meters, contamination monitors, gamma zone monitors and personal monitoring devices are procured (available). All protection instruments are periodically checked and calibrated at Defence Research Laboratory (DRL), Jodhpur. As per AERB guidelines, a local committee on radiation safety has been appointed and frequent mock drills and meetings related to emergency preparedness are carried out at this hospital.

Results and Discussion: A comprehensive emergency preparedness procedure and response plan is a necessity in our country. The main role of CBRN decontamination centre is to detect contamination, monitor, and segregate and to carry out the decontamination and treatment of casualties due to toxic agents (chemical, biological, radiological and nuclear) using appropriate means as per IAEA, AERB and National disaster management guidelines. Such procedures have to rely on extensive instrumentation support for efficient and viable counter measures. Every individual should act like a responsible citizen during any emergency and a strict security system and alertness should be followed in our country to avoid such an emergency.

P-209

ANALYSIS OF EXCESSIVE EXPOSURE CASES OF RADIATION WORKERS IN MEDICAL FIELD

Kirti Tyagi, Deboleena Mukherjee, P. B. Mukherjee

Department of Nuclear Medicine, INHS Asvini, Colaba, Mumbai, Maharashtra, India. E-mail: callkirti@yahoo.com

Introduction: The main objectives of monitoring radiation workers is to ensure that exposure are kept as low as reasonably achievable (ALARA). In India Atomic Energy Regulatory Board (AERB) is the national regulatory body and as per their directives the lifetime cumulative effective dose constraint for five years shall be 100mSv i.e average 20 mSv / year - five year block, however, whole body equivalent dose shall not exceed 30mSv in any one year.

Objectives: The purpose of this study is to analyse the cause of reported excessive exposure cases in various department dealing with radiation units and radiation sources.

Materials and Methods: Medical X-ray facilities avail Personnel Monitoring Service (PMS) for their radiation workers from Bhabha Atomic Research Centre (BARC) accredited laboratories on quarterly basis. The institutions and radiation workers are registered with National Occupational Dose Registry System (NODRS). The accredited labs send the dose data of these radiation workers to the dose registry after each monitoring period. In Armed Forces hospital, all radiation workers of the hospital receive TLD badges on quarterly basis from Defence Research Laboratory (DRL), Jodhpur, Rajasthan. If measured dose exceeds investigation level, accredited laboratory informs to AERB for further action. Subsequently AERB directs the institution to investigate possible causes of reported excessive exposure using questionnaires pertaining to individual work profile, type of procedure and workload in the reported period, availability of radiation protective accessories, procedure of handling of TLD badge. In case the reported dose is 100 mSv, the employer of the institute is directed to keep the radiation worker concerned away from radiation work till the investigations are completed satisfactorily. In addition the concerned radiation worker is called for Chromosome Aberration (CA) test at Radiological Physics & Advisory Division (RP & AD), BARC. In this study the overexposure cases reported from year 2006 to 2016 are presented. These cases relates to different X-ray modalities such as interventional Radiology, Radiography, Computed Tomography, Mammography, Nuclear Medicine and Cardiology.

Results and Discussion: From 2006-2016, four cases of overexposure were reported in the hospital. These cases pertained to Nuclear Medicine (02 in no.), Radiology (01 in no.) and Cardiology department (01 in no.). In all these overexposure cases after investigation it was found that all of them were non-genuine cases. The excessive exposure in these cases resulted due to improper handling and inappropriate storage of TLD badges, wrong placement of TLD badge while using (above lead apron) and unknown accidental exposure of TLD badge. In one case the worker (Equivalent Dose =301 mSv (G), 546 mSv (B)) left the badge in the radiation area. Hence the non- genuineness was quite obvious from the information obtained. In another case it was not traceable how badge get exposed as radiation worker (Dose =108.8 mSv) denied any misplacement of badge as well as undergoing any medical examination wearing the TLD badge. Subject was called for CA test at BARC also, but nothing came out of report. Last incidence (Dose = 14.85mSv) happened with a doctor (cardiologist) who placed TLD badge above lead apron during multiple procedures.

Conclusion: The non-genuine exposures are mainly due to carelessness in handling the badge (kept/dropped in radiation field), improper storage when the badge is not in use and negligence by radiation workers. To minimize the non-genuine cases of over exposure in medical X-ray facilities, proper training for the staff operating the x-ray equipment regarding proper use of TLD badge has been given.

P-210

INTRODUCTION TO MONTE CARLO SIMULATION THROUGH MICROSOFT EXCEL

A. K. Pandey

Department of Nuclear Medicine, All India Institute of Medical Sciences, New Delhi, India.
E-mail: akpandeyaiims@gmail.com

Introduction: The Monte Carlo technique has become ubiquitous in medical physics in the last 60 years. Monte Carlo techniques have played many roles in medical physics and its use is increasing day by day. The increased use of Monte Carlo techniques is partially due to the massive increases in computing power per unit cost and partially due to the increasing availability of many powerful software tools. The range of applications is very broad in medical physics, for example, there are commercial treatment planning systems for external beam radiotherapy which employ Monte Carlo techniques. Hence, it is important for young medical physicist to grasp the concept of Monte Carlo Simulation (MCS). There can be a variety of ways (as many ways as the number of instructors) “the concept of MCS” can be delivered to the students. Still, young medical physicist undergoing undergraduate and postgraduate courses often find difficult to grasp the concept of MCS.

Objectives: To introduce the concept of MCS through Microsoft Excel taking one example.

Materials and Methods: The Monte Carlo methodology for simulation, requires the following: (a) develop a complete definition of the problem, (b) determine the elements of the model that are uncertain and the nature of the uncertainty in terms of a probability distribution that represents its behavior,

(c) implement the uncertain elements by using the RAND () or other Excel functions, (d) replicate a number of experiments sufficient in size to capture accurate behavior, (e) collect data from experiments, (f) analyze the result. The RAND ( ) function in Excel is used to perform sampling in MCS. The key characteristic of the RAND () is that each time it is used in a cell, it yields a random value which is independent of other cells containing the RAND () function. An interactive spreadsheet model for teaching introduction to MCS has been developed using Microsoft Excel under Microsoft windows operating system. This tool consists of the MCS of radionuclide decay and radiation detection. The tool will be used for illustration of the MCS concept during talk.

Results and Discussion: This tool is suitable for both students and teachers who are interested in the basic concepts of MCS in a simple manner. It offers ease of use and a shorter learning curve than theother method of illustrating the same concept (say: using computer programming languages). It is intended to complement rather than replace existing approaches to learning, such as lectures and assignments. The instructor can use them with some sort of projection facilities in lecture presentations for quick simulations and enhance the classroom environment. Students can use them as a self-studying framework to help them to grasp quickly.

P-211

THE ROLE OF INTERNATIONAL COMMUNITY IN THE DOMESTICATION OF THE GAINS OF MEDICAL PHYSICS PRACTICES IN THE WEST AFRICAN SUB-REGION

Peter Ali, Kelechi Nwifior

Department of Physics, Ebonyi State
College of Education, Ikwo, Ebonyi, Nigeria.
E-mail: petera754@gmail.com

This paper is aimed at bringing to the limelight the current situation of medical physics practices in the West African sub region. Medical Physics in Africa has evolved over the last half a century from the Republic of South Africa in the southern tip of the continent to Ghana and Nigeria in the Western half and also Kenya, Uganda and United Republic of Tanzania in the Eastern sphere of the region and unto Algeria, Egypt, Morocco and Sudan in the Northern part. There is however a wide disparity in terms of educational infrastructure and availability of equipment across this very wide geographical landscape to provide the required medical physics services particularly in the health establishments as well as the other areas where the expertise of this cadre of professionals are needed. In terms of human resources capability, the continent can only boast of a slightly more than 300 personnel employed in and around her health facilities and about 60% of these staff are domiciled in just three countries – Egypt, Morocco and Republic of South Africa. The West African sub region has been noted to be still far behind in assessing the gains of medical physics practices. The learning objectives of the paper include identifying the medical physics infrastructure in terms of equipment and manpower, the status of education and training in the West African sub region, the gaps in the medical physics profession that should be addressed in the region, and the role expected of the international community.

P-212

STATUS OF RADIOTHERAPY TREATMENT IN LEBANON

Ibrahim Duhaini

Department of Radiation Oncology, Rafik Hariri University Hospital, Beirut, Lebanon. E-mail: duhaini@yahoo.com

Lebanon is located in the heart of the Middle East Region with a population of 4.5 million and is considered one of the best places of Medical Hot Spot destination that attracts many of the neighboring Arab countries to seek medical treatment. This is due to the fact of the highly skilled medical professionals and advanced health infrastructure in the country. Radiotherapy started in the early 70's with Cobalt Machines and has developed tremendously thought the years to include the highly technological and advanced Linac Systems. Now, there are 11 Hospitals that offer Radiotherapy Treatment with 17 Linacs equipped with the state of the art technology using 3-D Conformal, IMRT, Stereotactic Radiosurgery, IGRT and other modalities. In this presentation, an overview of the current cancer treatment in these 11 hospitals will be revealed. Detailed information will be unwrapped for the newly opened Radiotherapy Center at Nabih Berry Governmental University Hospital (NBGUH) in South Lebanon, which covers one third of the Lebanese population in that region. Also, detailed information will be exposed for the newly Upgraded Radiotherapy Department at Rafik Hariri University Hospital.

P-213

THE EFFECTS OF ELECTROMAGNETIC FIELDS ON HUMAN HEALTH

Ibrahim Duhaini

Department of Radiation Oncology, Rafik Hariri University Hospital, Beirut, Lebanon. E-mail: duhaini@yahoo.com

Since The beginning of the 20th century, we are overwhelmed by the increasing sources of the Electromagnetic Field (EMF) that is coming from telecommunication, electricity, appliances, medical equipment, and many other apparatus that we use in our daily life. Although these new technologies became inevitable and indispensable, the EMF they produce may cause health risks and hazards to human. Some studies show a link between exposure to EMF and increased rate of Leukemia, cancer, brain tumors and other health problems. Also, there is some uncertainty remains as to the actual mechanisms responsible for these biological hazards and which type of fields magnetic or electric or both are of great concern. It is needless to say that no matter the effects of these EMF be trivial or catastrophic, we should take all the necessary precautions to reduce our exposure to EMF as low as reasonably attainable. For this to occur, all those involved or affected by this exposure should follow the RF safety standards and guidelines set forth by the regulatory authorities like the IEEE, WHO, ICNIRP, and other likewise organizations. Any failure in taking immediate actions to the above guidelines, the public would be at a high epidemic risk of potentially fatal diseases in the future.

P-214

CHALLENGES FACED WHILE ROLLING OUT E-LORA IN AN ARMED FORCE HOSPITAL

Kirti Tyagi[1,2], Sachin Taneja[1], Deboleena Mukherjee[1,2], P. B. Mukherjee[2]

[1]Radiation Oncology Centre, INHS Asvini, [2]Nuclear Medicine Centre, INHS Asvini, Colaba, Mumbai, Maharashtra, India. E-mail: callkirti@yahoo.com

Introduction: In India Atomic Energy Regulatory Board (AERB) looks after the medical and industrial radiation facilities. All institutions dealing any type of equipments/ units related to radiation have to be in sync with rules and regulations stipulated by AERB. Before 2014, dealings with AERB were done on hard copies, but after 2014 AERB aimed to become paperless and to improve transparency, AERB followed ONLINE wagon via e-Licensing of Radiation Applications (e-LORA) platform. This is a web based system which deals with regulatory processes associated with different practices using ionizing radiation in India.
Objective: We experienced few hiccups while carrying out the e-LORA drive in our hospital. In this paper we are summarizing how we tackled those challenges.
Materials and Methods: INHS Asvini is a super- specialty naval hospital, with 895 bed capacity. It has fully functional Radiotherapy, Nuclear medicine and Radiology departments. In 2013, AERB started e-LORA with radiotherapy first, then they opened up Diagnostic Radiology portal and later on Nuclear Medicine was also introduced. In AERB's e-LORA portal, medical facilities are divided into main categories (1) Radiotherapy, (2) Nuclear Medicine and (3) Diagnostic Radiology.
Result and Discussion: Radiotherapy: RT dept has a dual energy Linear accelerator and remote afterloading HDR brachytherapy unit. These machines have been installed after obtaining licenses from AERB. While transferring required data to e-LORA portal, a problem surfaced in arranging a computer with Internet access, scanner and printer attached to it. The computer at our electronic data processing centre came handy to us. Later on computers with internet access were made available to all heads of the departments. Small problems were encountered and debugged immediately. The transition to ONLINE for radiotherapy happened quite smoothly. Nuclear Medicine: This dept houses a SPECT, a PET-CT and it also has two bedded high dose radio Iodine ablation therapy ward. In Nuclear Medicine as our documentation was all up to the mark so no hindrance was there from shifting to e-LORA portal for obtaining NOC's. Diagnostic Radiology: Radiology department houses fixed and mobile radiography units, mammography unit, a CT scanner and an interventional DSA X-ray unit. The maximum work needed to be done during e-LORA was in Diagnostic Radiology as all X-ray units housed in a hospital were made to be registered under Diagnostic Radiology Portal. X- ray units with Dept of Radiology and Cardiology were all registered and licensed way before e-LORA. The main hindrance was the educational qualification of radiographers. In our naval institution the courses run by the institution are recognised by institutional academic body. This is due to different structure for fulfilling armed forces requirement. This part has been taken care as now radiographers course has been recognised by MUHS, Nashik. Other departments like Cardiology, Endocrinology, and Urology all were informed regarding e-LORA guidelines and regulations. These departments have started availing TLD services from Defence Lab, Jodhpur. The process of getting the layout plans of the rooms and performing quality assurance tests are all in progress.
Conclusion: It was a huge challenge in facilitating the transition of OFFLINE to ONLINE for becoming e-LORA competent. e-LORA has been introduced to all radiation related departments within the hospital. Updating all radiation workers on e-LORA is also a mammoth task, keeping in mind that all service personnel are bound to undergo transfers within a span of 3-5 years. Presently Nuclear Medicine, Radiology, Radiotherapy, Cardiology & RIA are harnessing benefits of this electronic licensing system.

P-215

BRAIN TUMOR SEGMENTATION AND TEXTURE ANALYSIS BY MAGNETIC RESONANCE IMAGING

Akbar Gharbali, Mir Hojjatollah Mousavi Maleki, Hossein Aghdasi[1]
Department of Medical Physics, Faculty of Medicine, Urmia University of Medical Science, [1]Department of Medical Imaging Centre, Arefian Hospital, Urmia, Iran. E-mail: Gharbali@yahoo.com

Introduction: Since the radiologist interpretation is often the clinicians guide for brain tumor treatment, differentiating malignancy from benign and detecting the tumor site and knowing its shape perfectly are important. So, automated brain image segmentation and texture analysis for determination precise form of the brain tumor and discrimination of benign and malignant brain tumors are critical to achieve the best results of treatment in comparison with radiologist visual texture analysis and or radiotherapist handy segmentation.
Objective: The goal of the present study is to explore detection and diagnostic potential of computer aided segmentation and texture analysis methods in precise determination of tumor shape and differentiation benign and malignant brain cancers by Magnetic Resonance Imaging (MRI).
Materials and Methods: In this study, the T2 weighted -MRI images of 50 patients with brain tumors were used. Firstly, the image segmentation was done by utilizing Mat lab software via Ant and Fuzzy clustering methods. Detection performance of the applied segmentation methods were evaluated by Dice Metric and ROC cure analysis. Secondly, the image texture analysis was done for differentiation of benign and malignant brain tumors by using the MaZda software via uploading two slice MRI- T_2 weighted HASTE sequence images and up to 270 texture feature parameters were computed as a descriptor per ROI (Region of interest) per applied options. Then, extracted features parameters eliminated to 10 most effective texture feature parameters for describing texture patterns of the benign and malignant brain tumors. Optimal feature parameters were used for texture analysis by PCA (Principle component analysis), LDA (Linear discriminate analysis) with first nearest – neighbor (1- NN) classifier and NDA (Non-linear discriminate analysis) with Artificial neuralnetwork (A-NN) classifier. At the end, the discrimination performance of each of applied methods was evaluated by ROC cure analysis.
Results and Discussion: The better results of the segmentation phase were related to Ant algorithm with Dice Metric 85%, sensitivity of 89% and accuracy of 99%. In comparison with PCA and LDA, The best discrimination performance results for differentiation benign from malignant

brain tumor was obtained by NDA analysis with sensitivity of 96% specificity 95% and accuracy of 95% respectively.

Conclusion: The results of this study show that the computerized segmentation and texture analysis of the brain tumor has potential to increase confidence of radiologist and radiotherapist in precisely segmenting and correctly discriminating brain tumors in Brain MRI.

P-216

INVESTIGATE THE EFFECT OF IONIZING IRRADIATION ON THE ELASTICITY ON HUMAN ERYTHROCYTES AT CLINICAL DOSES

E. Spyratou, M. Gazouli[1], M. Dilvoi, M. Makropoulou[2], A. Serafetinides[2], E. P. Efstathopoulos, K. Platoni

2nd Department of Radiology, Medical School, National and Kapodistrian University of Athens, [1]Department of Basic Medical Science, Laboratory of Biology, School of Medicine, University of Athens, [2]Department of Physics, Faculty of Applied Mathematical and Physical Sciences, National Technical University of Athens, Zografou Campus, Athens, Greece.

E-mail: info@theotokistravel.gr

Introduction: The biomechanical behavior of the erythrocyte's membrane skeleton is an important predictor of circulation efficiency and cell's health. The roughness of the cytoskeleton membrane is correlated with any redistribution of lipid molecules or proteins in the membrane bilayer and can indicate any rearrangement of the bilayer structure induced by external factors such as ionizing irradiation.

Objectives: In this work, we studied the effect of ionizing radiation on the morphology and the elastic properties of human erythrocytes after X-ray irradiation at clinical doses. The erythrocyte's changes were probing by using the advanced microscopic techniques of Atomic Force Microscopy and optical tweezers which is ideally suited for single cell measurements providing simultaneously information about the mechanical properties of the cells.

Materials and Methods: Whole human blood was drawn by venipuncture and subjected to the minimum possible treatment which can be induced morphological alterations. The blood samples were irradiated in the range of 0.2Gy -2.0 Gy doses and with a dose rate of 240 cGy/min. The morphology and the elastic modulus of the erythrocytes were examined in comparison with non-irradiated erythrocytes by using AFM and optical tweezers, and just few drops of whole blood without any special preparation.

Results and Discussion: No morphological changes appeared according to the shape of the erythrocytes. However, the roughness of the erythrocyte cytoskeleton was increased as the irradiation dose was increased according to AFM measurements. The elasticity modulus of the irradiated sample was reduced with the increasing of radiation dose. AFM and optical tweezers appears powerful nanotools and accurate techniques for probing the biomechanical properties of the erythrocytes. The elastic modulus and the membrane roughness of the erythrocytes could be an index to assess the damage caused by irradiation.

Acknowledgment: The authors would like to thank the "IKY fellowships of excellence for postgraduate studies in Greece"

P-217

BIOCHEMICAL CHANGES IN TESTES OF SWISS ALBINA MICE EXPOSED TO 2.45 GHZ MICROWAVES RADIATION

C. L. Jonwal[1,2], Rashmi Sisodia[1], V. K. Saxena[3]

Departments of [1]Zoology and [3]Physics, University of Rajasthan, Jaipur, Rajasthan, [2]Department of Zoology, Hindu College, University of Delhi, Delhi, India.

E-mail: rashsisodia@yahoo.co.in

Background: A number of studies have reported that male reproductive system is susceptible to electromagnetic fields (EMFs).

Objectives: The objectives of this study were to explore the changes in biochemical parameters of testes exposed to 2.45 GHz microwave radiations.

Materials and Methods: 6-8 weeks old male Swiss albino mice, weighing 35.0 ±3.0 grams were procured from inbred colony. Total 16 mice were divided into two groups; 1) Sham exposed, and 2) microwave exposed group. Microwave radiation experimental bench was used for the exposure to mice. Exposure was given in plexiglas cages. Mice were exposed to 2.45 GHz for 2 hrs/day for 30 days with power density 0.25 mW/cm^2 and SAR 0.09 W/kg.

Results: Results revealed that 2.45 GHz radiations resulted in significant increase ($P < 0.001$) in catalase (CAT), malondialdehyde (MDA), reactive oxygen species (ROS) and decreased ($P < 0.001$) levels of glutathione peroxidase (GPx) and superoxide dismutase (SOD) ($P < 0.05$) in exposed group in comparison to control group.

Conclusion: We conclude that microwaves at 2.45 GHz frequency causes oxidative stress mediated cellular toxicity and it leads to adverse and detrimental biochemical changes in testis.

P-218

THE EFFECTS OF CO-60 GAMMA RADIATION ON HUMAN LYMPHOCYTES BY MICRONUCLEI ASSAY

K. Mayakannan, S. K. Grace Mercy, V. Prabhakaran, C. S. Sureka

Department of Medical Physics, Bharathiar University, Coimbatore, Tamil Nadu, India.

E-mail: surekasekaran@buc.edu.in

Introduction: The study of radiation induced damage on chromosome is an essential part of genetic toxicology. The Cytokinesis-block micronucleus (CBMN) assay was well developed, radiation sensitive and widely used technique for assessing chromosome damage because they can measure both chromosome loss and breakage reliably. CBMN assay offer the various DNA damage analysis on genotoxicity and cytotoxicity such as chromosome rearrangement (nucleoplasmic bridges), cell division inhibition, necrosis and apoptosis.

Objective: To analyze the effects of Co-60 Gamma radiation induced DNA damage on human lymphocytes by Cytokinesis-block micronuclei assay.

Materials and Methods: The Peripheral blood was obtained in a 4 ml tube containing lithium heparin (BD Franklin Lakes NU

USA). The blood was then divided into ten separate samples. The first sample was used as a control sample and other nine samples were irradiated with Co-60 Gamma irradiation dose of 0.5 Gy, 1 Gy, 2 Gy, 3 Gy, 4 Gy and 5 Gy. The blood samples were irradiated under Theratron 780c cobalt unit. The institutional human ethical committee of Bharathiar University approved all of the experimental procedure used in this study. After irradiation the cultures were set according to the most widely accepted method of French and Morley (1986), 5 ml of PB- Max Karyotyping medium (255703, Gibco,) and 0.5 ml of irradiated blood was added to the sterile 15 ml culture vial. All the procedure was carried out inside the Class-II Bio Safety Cabinet. Then the culture vial was placed inside the Co2 incubator with 37° C and 5% Co2 atmosphere. Cytochalasin B was added to the culture at a final concentration of 6 g/ml after 44 h to arrest cells at cytokinesis stage. At the end of incubation time (72 h), cells were harvested and supernatant were discarded by centrifugation and hypotonic solution (0.075M KCl) was added then left undisturbed for 20 minutes and supernatant were discarded by centrifugation. The cells were fixed in fresh fixative solution (methanol: acetic acid, 3:1) and this fixation step was repeated twice. About more than 200 cells were scored from each subject.

Results and Discussion: To find whether the micronuclei frequency followed poisson distribution the dispersion index σ^2/**y** were calculated and it's close to 1 and indicated conformity with poisson distribution. Among the entire sample analyzed, the MN yield is found to be 1 for control sample, 5 at 0.5Gy, 14 at 1 Gy, 29 at 2 Gy, 37 at 3 Gy, 54 at 4 Gy and 90 at 5 Gy and data presented in Table 1. From the obtained result it is concluded that the yield of average micronuclei varied from 2-90 were found for doses ranging from 0-5Gy. As the dose increases, the micronuclei yield is also increased linearly. *In-vitro* irradiation of assay in Co60 beam at various dose levels. The induced cytokinesis blocked micronuclei are shown in Figure 1.

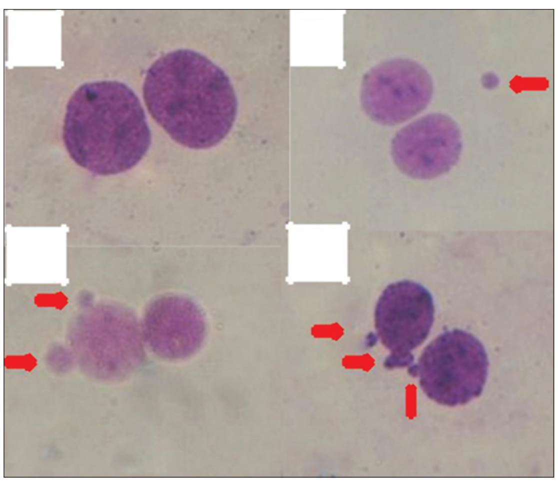

Figure 1: Co-60 beam induced cytokinesis blocked micronuclei from *in vitro* irradiation; (a) normal binucleated lymphocyte without micronuclei, (b) binucleated lymphocytes with one micronuclei, (c) binucleated lymphocytes with two micronuclei and (d) binucleated lymphocyte with three micronuclei

Table 1: Frequencies and distribution of micronuclei in human lymphocytes after acute Co-60 gamma irradiation with 0–5 Gy dose

Dose (Gy)	*Number of cells scored*	*Number of MN*	*D0**	*D1**	*D2**	*D3**	*σ^2/y*
0	228	1	226	0	0	0	0.999981
0.5	360	5	355	5	0	0	0.988858
1	297	14	284	10	2	0	1.242601
2	223	29	192	20	3	1	1.28543
3	285	37	256	26	4	1	1.253864
4	238	54	200	30	9	2	1.337143
5	306	90	244	44	17	4	1.357647

σ: Variance, y: Mean, MN: Micronuclei, D: Differential doses

P-219

ENHANCEMENT OF RADIATION EFFECT BY CETUXIMAB ON COLON CANCER CELL LINES

Takamitsu Hara, Takeo Aoki, Yu Shinozaki, Hiro Sato[1], Tomoo Funayama[2], Tomoaki Tamaki[3], Yoshiyuki Suzuki[3], Atsushi Okazaki[4], Takashi Nakano[1]

Department of Radiological Technology, School of Radiological Technology, Gunma Prefectural College of Health Sciences, [1]Department of Radiation Oncology, Gunma University, [2]Department of Radiation Applied Biology, Takasaki Advanced Radiation Research Institute, National Institutes for Quantum and Radiological Science and Technology, Gunma, [3]Department of Radiation Oncology, Fukushima Medical University, School of Medicine, Fukushima, [4]Department of Radiation Oncology, Tsuboi Cancer Center Hospital, Koriyama, Japan. E-mail: thara@gchs.ac.jp

Chemoradiotherapy is considered as an enhanced effective therapy on colon cancers. It has already been reported improved outcome by combination of cetuximab, a molecular EGFR-targeted drug, and radiotherapy which has synergistic effect in head and neck cancers. Therefore, we hypothesized that combination of cetuximab and radiotherapy on colon cancers would be an effective therapy. First, radiation sensitivities of 8 human colon cancer cell lines were examined by colony formation method. Next, radiosensitizing effect of cetuximab on each cell lines were examined by colony formation method. Radiosensitizing effect of cetuximab was observed in 3 of the 8 cell lines.

P-220

CALCULATION OF ATTENUATION COEFFICIENTS FOR BIOLOGICAL SUBSTANCES AT VARIOUS GAMMA ENERGIES USING THE GEANT4 MONTE CARLO CODE

C. S. Sureka, Francesco Longo[1]

Department of Medical Physics, Bharathiar University, Coimbatore, Tamil Nadu, India, [2]University of Trieste and INFN, Science Park Area, Padriciano, Trieste, Italy. E-mail: surekasekaran@buc.edu.in

Introduction: The attenuation of gamma rays in tissues that are present between the organs of interest and the detector is one of the most important subjects in nuclear medicine and in radiation dosimetry as well. Hence, calculation of half-value thickness, linear, and mass attenuation coefficient of biological substances such as soft tissue, adipose tissue, compact bone, cortical bone, brain, lung, normal kidney, cancerous kidney, and water are important.

Objective: Calculate the half-value thickness, linear, and mass attenuation coefficient of different biological substances at various gamma ray energies using the Geant4 (**Ge**omery **an**d **T**racking) Monte Carlo code.

Materials and Methods: The testem example of the Geant4 code was modified to study the attenuation of 122 (Co-57), 140 (Tc-99m), 356 (Ba-133), 364 (I-131), 662 (Cs-137), 893 keV (Na-22), and 1.25 MeV (Co-60) gamma rays through various biological substances such as soft tissue, adipose tissue, compact bone, cortical bone, brain, lung, normal kidney, cancerous kidney, and water of thickness ranging from 1 to 10 cm in 1 cm steps. The attenuating substance was constructed as a box defined by three parameters such as the material, thickness, and its transverse size of 10 cm. The standard EM physics was chosen to track 10 million gamma rays and its secondary particles. By knowing the number of gamma rays incident on the substance (I_0), and transmitted (I_t) through the substance, a graph was drawn between the thickness of substance and ln (I_t/ I_0). Then, the linear attenuation coefficient was calculated as it is the slope of the graph. The mass attenuation coefficient was calculated by dividing the linear attenuation coefficient by its density. Further, the thickness of the materials to transmit 50% of gamma rays (ie. half-value thickness) was calculated.

Results and Discussion: Calculated half-value thickness, linear, and mass attenuation coefficient of those biological substances at various gamma ray energies are reported and data presented in Tables 1-3 respectively. To validate the present results, the half value thickness, linear, and mass attenuation coefficient of water was compared with the calculated and measured data of published report. The calculated and measured half-value thickness of water at 662 keVis 8.095 cm and 9.096 cm +/- 0.291 respectively and it is comparable with the present value of 8.052 cm. The calculated and measured linear attenuation coefficient of water at 662 keV is0.085 cm^{-1} and 0.076+/- 0.002 respectively and it is also comparable with the present value of0.086 cm^{-1}. The calculated and measured mass attenuation coefficient of water at 662 keV is0.0848 cm^{-1} and 0.0777+/- 0.002 respectively and it is also comparable with the present value of0.0861 cm^{-1}. From this study, it is observed that the attenuation coefficients are different among biological

Table 1: Half-value thickness (cm) of various biological substances

Energy	*Water*	*Soft tissue*	*Adipose tissue*	*Bone compact*	*Bone cartical*	*Brain*	*Lung*	*Kidney normal*	*Kidney cancer*
122 keV	4.4605	3.9766	4.6929	2.4335	2.3511	4.3042	4.3125	4.2836	4.2838
140 keV	4.6377	4.1474	4.8707	2.5673	2.5046	4.4800	4.4884	4.4610	4.4615
356 keV	5.3276	5.6761	6.6494	3.5913	3.5607	6.1071	6.1173	6.0860	6.0876
364 keV	6.2757	5.6302	6.5955	3.5619	3.5315	6.0557	6.0663	6.0339	6.0356
662 keV	8.0515	7.2279	8.4698	4.5702	4.5344	7.7844	7.7972	7.7593	7.7613
893 keV	9.2226	8.2774	9.6974	5.2277	5.1842	8.9098	8.9233	8.8805	8.8830
1.25 MeV	>10	9.8381	>10	6.2097	6.1594	>10	>10	>10	>10

Table 2: Linear attenuation coefficient of various biological substances

Energy	*Water*	*Soft tissue*	*Adipose tissue*	*Bone compact*	*Bone cartical*	*Brain*	*Lung*	*Kidney normal*	*Kidney cancer*
122 keV	0.1560	0.1743	0.1482	0.2888	0.2989	0.1616	0.1613	0.1624	0.1624
140 keV	0.1499	0.1675	0.1425	0.2734	0.2805	0.1553	0.155	0.1560	0.1560
356 keV	0.1107	0.1234	0.1053	0.1957	0.1975	0.1146	0.1144	0.1150	0.1149
364 keV	0.1098	0.1224	0.1045	0.1941	0.1958	0.1136	0.1134	0.1140	0.1140
662 keV	0.0861	0.0960	0.0819	0.1523	0.1535	0.0892	0.0890	0.0895	0.0894
893 keV	0.0752	0.0838	0.0715	0.1329	0.1340	0.0778	0.0777	0.0781	0.0781
1.25 MeV	0.0632	0.0705	0.0601	0.1118	0.1127	0.0655	0.0654	0.0657	0.0651

Table 3: Mass attenuation coefficient of various biological substances

Energy	*Water (ρ=1.0 g/cm³)*	*Soft tissue (ρ=1.127 g/cm³)*	*Adipose tissue (ρ=0.95 g/cm³)*	*Bone compact (ρ=1.85 g/cm³)*	*Bone cartical (ρ=1.92 g/cm³)*	*Brain (ρ=1.04 g/cm³)*	*Lung (ρ=1.04 g/cm³)*	*Kidney normal (ρ=1.05 g/cm³)*	*Kidney cancer (ρ=1.05 g/cm³)*
122 keV	0.1560	0.1964	0.1408	0.5343	0.5739	0.1681	0.1678	0.1705	0.1705
140 keV	0.1499	0.1888	0.1354	0.5058	0.5386	0.1615	0.1612	0.1638	0.1638
356 keV	0.1107	0.1391	0.1000	0.3620	0.3792	0.1192	0.1190	0.1208	0.1206
364 keV	0.1098	0.1379	0.0993	0.3591	0.3759	0.1181	0.1179	0.1197	0.1197
662 keV	0.0861	0.1082	0.0778	0.2818	0.2947	0.0928	0.0926	0.0940	0.0939
893 keV	0.0752	0.0944	0.0679	0.2459	0.2573	0.0809	0.0808	0.0820	0.0820
1.25 MeV	0.0632	0.0795	0.0571	0.2068	0.2164	0.0681	0.0680	0.0690	0.0684

substances due to the variation in its density and atomic composition. As the energy increases, the linear, and mass attenuation coefficient of these biological substances are decreased but its half-value thickness is increased significantly.

P-221

ESTIMATION OF PERCENTAGE SCATTERING CONTRIBUTION IN ACTIVITY MEASUREMENT OF ^{60}CO TELETHERAPY SOURCES

R. S. Vishwakarma, T. M. Ashraf[1], S. A. Tariq[1], S. P. Gupta[1], P. Baral[1], D. Paul[1], T. Palani Selvam, L. N. Bandi[2]

Radiological Physics and Advisory Division, Bhabha Atomic Research Centre, Mumbai, [2]Board of Radiation and Isotope Technology, Navi Mumbai, Maharashtra, [1]Regional Centre (RAPPCOF), Board of Radiation and Isotope Technology, Kota, Rajasthan, India. E-mail: viswakarma_ram@yahoo.com

Introduction: High intensity ^{60}Co sources are used in various healthcares, agricultural and industrial applications. The ^{60}Co activity in the form of slugs and capsules is recovered at Regional Centre, Kota of Board of Radiation and Isotope Technology (BRIT) from the various Pressurized Heavy Water Reactors in the country and sent for further processing to sealed sources fabrication facility. These sources are fabricated from ^{60}Co pellets and slugs in shielded enclosure called as hot-cell.

Objective: The effect of scattered radiation during activity measurements in a hot-cell may lead to an over-estimation of the actual activity. In the present work, we have measured the scattering contribution from ^{60}Co Teletherapy Sources produced in the hot-cell of Regional Centre-Kota of BRIT. The work also includes Monte Carlo-based calculations of scattering contribution.

Materials and Methods: The hot-cell has room dimensions of 2.4 m (length) x 2.4 m (width) x 4.8 m (height) with approximately 1.9 m thick high density reinforced cement concrete enclosure walls. The source strength measurements having nominal activities of 1 kCi - 10 kCi were carried out inside the hot-cell by using a 0.6 cm^3 PTW-make ionization chamber which is calibrated at Secondary Standard Dosimetry Laboratory, BARC, Mumbai. The distance between source and ionization chamber is 2.575 m. Meter reading obtained by dosimeter system was corrected for temperature and pressure corrections and multiplied by air-kerma calibration coefficient, $N_{k,air}$. Using conversion factors and correcting for distance, the source strength is measured in unit of roentgen per minute at 1 meter (RMM). The measured RMM values include contributions from primary radiation from the source and scattered radiation from walls, floor, ceiling and other objects present in the hot-cell. The measurements of scatter contribution are carried out by blocking the primary radiation beam by a truncated conical lead block of 30 cm height without altering the source-detector geometry. The scattering contribution was calculated from ratio of measured RMM with and without lead cone. RMM values were also calculated using the MCNP (version 3.1) Monte Carlo code by modeling the experimental setup. Photon fluence spectrum was scored which was converted to Roentgen per initial photon (R/photon) by using the mass-energy-absorption coefficients of air[2].

Results and Discussion: The measured and Monte Carlo-based estimated percentage scattering contributions are about 12% and 13%, respectively. Measurement was also carried by removing the transport flask present inside the hot cell. Such measurement did not change the scatter contribution which suggests that the structural materials around the source contribute to the scatter. The investigation concludes that there is an improvement in the RMM value by about 12% while accounting for scatter contribution.

P-222

DETECTION OF MINERALS USING SEM-EDX IN SAME FAMILY MEDICINAL PLANT LEAVES

Santoshkumar S. Teerthe, A. Ashwini, B. R. Kerur, S. Narayana Kalkura[1]

Department of Physics, Gulbarga University, Gulbarga, Karnataka, [1]Crystal Growth Centre, Anna University, Chennai, Tamil Nadu, India.
E-mail: stp.santosh4@gmail.com

Natural plants have been used as potential source of therapeutic medicine, home remedies and also primary health care throughout the history. Medicinal plants are considered safe for human health, it is known that certain organic and inorganic elements or metals played important role in plants as well as human body for secondary metabolites. Elements or metals were uptake from soil to roots, from environment dry deposition or by contamination during processing. Plant materials may contain high major/minor and trace amounts of essential elements along with high content of elements which are exceeds the permissible limits of intake. The essential elements such as Magnesium, Aluminum, calcium, phosphorous, vanadium, chromium, nickel, Iron, copper, zinc, Arsenic, Cadmium, molybdenum, antimony, mercury, Lead etc. The World Health Organization (WHO) has established maximum concentration limits for these elements in order to ensure the safe consumption and use of herbal medicinal plants. Therefore, it is important to determine the concentrations of these elements in different parts of herbal medicinal plants. In present research work two different families viz., Apocynaceae and Myrtaceae herbal medicinal plants samples were collected from Yadgir district of North-East Karnataka region. The study of structural morphology and detection of elemental concentration were carried out by using SEM-EDX method. The elements likes C, O, Mg, Si, S, Cl, K, Ca, Mn, Fe, are found in effective concentrations and the crystalline and cylindrical shaped election image impact within 20μm and the value of elements Na, Al, Cu, Zn, Br and As were found in 1wt% of concentration. The quantitative elemental concentration analysis was identified with x-ray energy which is observed in between 1 KeV to 16 KeV. Further the present investigation suggests that the collected herbal medicinal plants have good alignments of secondary metabolites, functional groups and trace elements. The present data gives good information on antioxidant, anti informant and Physiochemical study, and useful for treatment

Table 1: Details of elemental concentration analyzed by scanning electron microscopy-energy dispersive X-ray spectroscopy method in (wt%)

Coding	*C*	*O*	*Mg*	*Si*	*S*	*Cl*	*K*	*Ca*	*Mn*	*Fe*
YCr1	46.41	37.53	0.86	4.33	0.24	1.14	1.57	5.42	0.01	0.72
YCg2	54.69	28.75	0.60	0.85	0.94	4.75	5.42	2.80	ND	0.06
YPr3	58.75	36.59	ND	ND	ND	1.05	ND	2.87	0.23	ND
YNi4	72.22	21.56	0.39	1.57	0.19	ND	0.39	2.08	0.30	0.38
YEo5	59.79	36.38	0.31	0.02	ND	0.77	1.23	1.07	0.13	0.06
YGu6	73.45	23.17	0.96	0.08	0.80	ND	1.00	0.32	0.08	ND

ND: Not detected

Table 2: Structural morphology, energy spectra and quantitative analysis

Plant name: Catharanthus roseus		
SEM – image structural morphology	*EDX - spectra*	*Quantitative results*
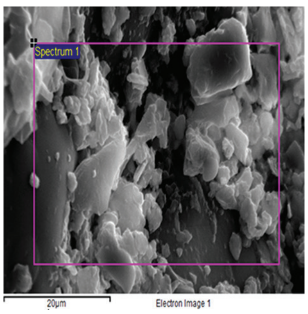	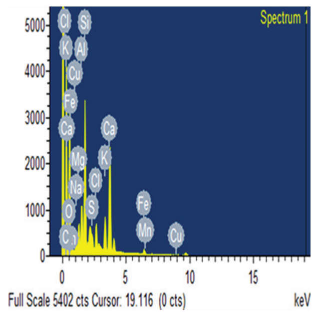	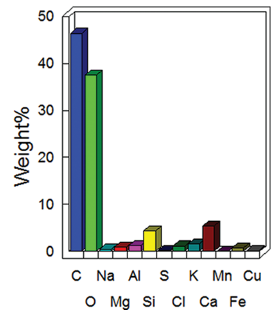

SEM: Scanning electron microscopy, EDX: Energy dispersive X-ray spectroscopy

and preparation of new herbal medicinal drugs for Cancer, HIV-AIDS, Diabetes, brain tumor etc. The given Tables 1 and 2 presents the percentage variations of elemental content in different plant and the study of morphology surface structure with energy- spectra.

P-223

INVESTIGATION OF MASS ATTENUATION COEFFICIENTS OF DOSIMETRIC MATERIALS USING FLUKA MONTE CARLO CODE

Amandeep Sharma, Bhajan Singh[1], B. S. Sandhu[1]
Department of Physics, Akal University, Talwandi Sabo,
[1]Department of Physics, Punjabi University, Patiala,
Punjab, India. E-mail: adsphy@gmail.com

Introduction: The use of radiation in health physics, medical physics, radiation dosimetry, radiation protection and radiobiology require knowledge of radiation interaction with the materials for shielding and dose measurement. When a beam of X or gamma rays pass through matter, the removal of photons from the beam is called attenuation. The linear attenuation coefficient is defined as the fraction of photons removed from a monoenergetic beam of X or gamma rays per unit thickness of material. The simulation to estimate the mass attenuation coefficient can be done with the use of well-known simulation program such as FLUKA. This tool is based on the Monte Carlo (MC) methods to simulate the interaction of particles with their traversing medium. In medical imaging, such as PET, an attenuation correction for gamma photons is fulfilled to enhance the spatial resolution, i.e., image quality. This correction is performed by taking into consideration the mass attenuation coefficients of the related parts of the human body. In this regard, mass attenuation coefficients of the related biological materials have great importance in this process. For this reason, MC method (FLUKA) was utilized to determine the coefficients for some dosimetric material and obtained results are compared with the WinXCom.

Objectives: (i) Introduction to FLUKA Monte Carlo code for the beginners

1. Application of FLUKA code to calculate essential parameter, mass attenuation coefficient, for medical physics

Materials and Methods: In this work, we have estimated the mass attenuation coefficients of some dosimetric materials like LiF, $CaCO_3$, $CdSO_4$, $BaSO_4$, water (H_2O), ethylene (C_2H_4), bakelite (C_9H_9O) and PMMA etc. for the photons with energy of 661.6 keV by using the FLUKA Monte Carlo code due to its event-by-event tracking feature. The applications of dosimetric materials in radiation physics and radiobiology are essential for exposure monitoring and estimation of the dose. FLUKA input data cards have been arranged in sequential order. A simple cylindrical geometry with the axis along the z-direction was described in the input file. A beam of $1x10^5$ gamma-rays was directed towards the materials in the z-direction and attenuated in cylindrical samples. The results of photon transmission were obtained from output files for each of the material thicknesses using the USRBDX score card. By plotting $\ln(I_o/I)$ versus thickness, the slope was calculated. The linear attenuation coefficients were calculated by using Lambert-Beer's law.

Results and Discussion: Monte Carlo simulation is a powerful tool for studying the interaction of photons in any material. The mass attenuation coefficient, an essential parameter, of some dosimetric materials with potential applications in dosimery, medical and radiation protection have been investigated using the FLUKA Monte Carlo simulation code. The special feature of FLUKA, probably not found in any other Monte Carlo program, is its double capability to be used in a biased mode as well as fully analogue code. The simulated results, for attenuation coefficient of dosimetric material/ biological substitutes, obtained by FLUKA agree well with WinXCom prediction. It is observed that the mass attenuation coefficients of the selected dosimetric materials are small when low atomic number elements are predominant, whereas large for high atomic number elements. The results of this preliminary study demonstrate that FLUKA Monte Carlo simulations can be applied to estimate mass attenuation coefficients for various attenuators and energies especially when it is hard to set up an experiment.

P-224

RADIATION ONCOLOGY FACILITIES: CURRENT STATUS AND FUTURE PERSPECTIVES IN THE COUNTRIES MEMBERS OF THE MEFOMP

Rabih Hammoud, Tarraf Torfeh, Satheesh Paloor, Noora Al-Hammadi

Department of Radiation Oncology, National Center for Cancer Care and Research, Hamad Medical Corporation, Doha, Qatar. E-mail: rhammoud2@hamad.qa

Introduction: As a part of the International Organization for Medical Physics (IOMP), the Middle East Federation of Medical Physics (MEFOMP) is a regional organisation that includes the medical physics societies and associations of the following countries: Bahrain, Iraq, Jordan, Kuwait, Lebanon, Oman, Qatar, Saudi Arabia, Syria, United Arab Emirates and Yemen. The socio-economic and political factors are known to influence healthcare facilities in general and radiation oncology in particular. In view of the different socio-economic and political status in these countries, the aim of this work is to share the current status of the Radiation Oncology resources in these countries.
Materials and Methods: A detailed description of the current status of the radiation oncology facilities will be presented for each country. Furthermore, some of the state of the art projects will be highlighted and discussed such as the implementation of proton radiation therapy. The latest advancement in the sate of Qatar as well as an overview of the future perspectives in the radiation oncology facilities will also be presented. This study will cover all the areas of the radiation oncology including the simulation, treatment planning, the delivery and the personnel with an emphasis on some of the projects such as MR guided Brachytherapy and CyberKnife.
Results: The diversity of the socio-economical and political status in the countries that are members of the MEFOMP resulted in a wide range of technological advancement in the radiation oncology facilities and resources. Ranging from primitive facilities with low qualified staff observed in the some countries to a very advanced technology and qualified personnel in other countries.
Discussion: This study allowed having an overview of the current and future status of the development in the radiation oncology in the countries members of the MEFOMP. This study allowed also identifying the areas of weakness and strength in the radiation oncology for each country which represents an important step for identifying development and improvement areas.

P-225

ASSOCIATION OF PROTON PUMP INHIBITORS WITH HYPOMAGNESEMIA: A CROSS SECTIONAL STUDY AT A TERTIARY HEALTH CARE CENTRE

Sejal Sejwani, Pramod Jha, Garvit Garg, Ronak Shah[1]

Department of Medicine, [1]Department of PSM, Dhiraj Hospital, Sumandeep Vidyapeeth, Baroda, Gujarat, India. E-mail: sejal.sejwani.p@gmail.com

Introduction: Proton Pump Inhibitors (PPIs) are one of the most common class of drugs that are used in almost all alternative prescription. Few studies have shown that PPIs are responsible for hypomagnesemia.
Aim and Objective: To analyse whether prolonged use of Proton Pump Inhibitor is associated with hypomagnesmia.
Methodology: It is a cross sectional, single centred study of 3 months duration, at a tertiary health centre in Baroda. 80 patients were enrolled in the study with non critical illness and divided them in two arms viz 'PPI group' (n=40) and 'non PPI' group (n=40). Patients with history of PPI consumption of 3 months or more duration were enrolled in 'PPI group' while patients with no history of PPI use in last 3 months were in 'non PPI group'. Serum Magnesium (S. Mg) levels were estimated and data was collected and analysed.
Outcome: This study revealed that mean S. Mg in PPI group was 1.69 mg/dL while in non PPI users mean S. Mg was 1.93 mg/dL, the difference being statistically significant (p = 0.00). However, female PPI users had slightly lower S. Mg levels in comparison to male PPI users. S.Mg levels were analysed in age groups also which revealed lower S. Mg in PPI users patients with age above 40 years i.e 1.65 mg/dL while slightly higher in patients below 40years of age. Also duration of PPI was analysed which showed low level of S.Mg in patients with PPI use of more than 7months. Analysis of pantoprazole, rabeprazole and omeprazole depicted that pantoprazole users had less S.Mg levels as compared to other two drugs.
Conclusion: This study revealed that S.Mg levels were low in PPI users. To avoid fatal complications of hypomagnesemia rational use of PPI should be done specially in elderly group.

P-226

DEVELOPMENT OF GREEN LEDS BASED OPTICAL BLEACHING SETUP FOR THERMOLUMINESCENCE DOSIMETRY APPLICATION

Mukesh Uke, L. Paliwal, S. Kadam, A. K. Singh, D. K. Koul, D. Datta

Division of Radiological Physics and Advisory, Bhabha Atomic Research Centre, Mumbai, Maharashtra, India. E-mail: mukeshmu@barc.gov.in

Introduction: $CaSO_4$: Dy based thermoluminescence dosimetry programme is being used in the country wide personnel monitoring program in India. The TL glow curve of $CaSO_4$: Dy consists of a dosimetric peak at 220°C and a low temperature peak at 120°C, which is unstable at room temperature. The TL integral counts reduces by

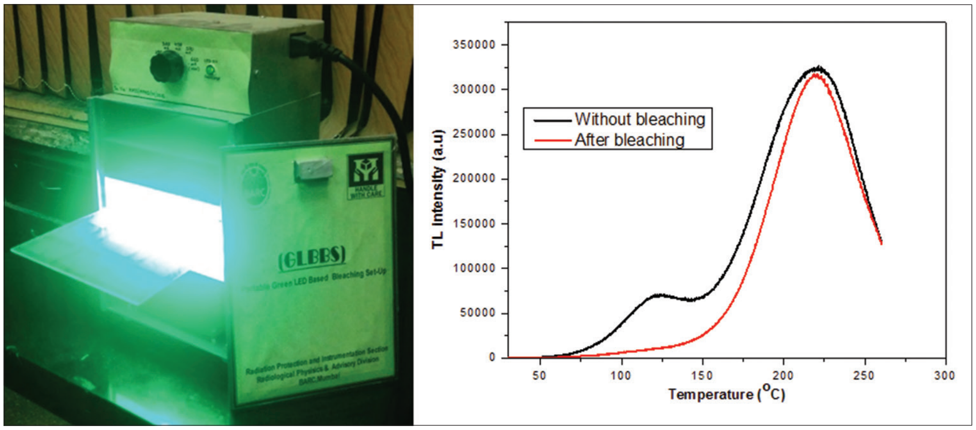

Figure 1: TL glow curve of CaSO4: Dy disc with and without bleaching. Discs were irradiated for 100 mGy dose and TL were recorded at the heating rate of 5°C/s.

Table 1: Comparison of dose delivered to CaSO4: Dy TLD and dose evaluated

Dose	*Set-A*	*Set-B*	*Set-C*
Dose delivered (mGy)	0.6	4	9
Dose evaluated (mGy)	0.61±0.04	4.04±0.24	8.97±0.51

15% in 7 days after irradiation due to the thermal fading of 120°C TL peak at room temperature. So, if TLD cards are processed immediately after the exposure the conventional dose evaluation protocol will yield un-reliable results due to presence of low temperature peak at 120°C. In order to overcome this difficulty an alternative technique based on optical bleaching was developed for the urgent processing of TLD cards. Optical bleaching with green LED (555 nm photons) was observed to remove the low temperature TL peak without affecting the dosimetric peak.[1] This setup has the facility of selecting the desired intensity and time period of bleaching.

Experimental Method: The bleaching setup consists of 3023 Buck Puck LED power module, green high power LEDs, glass sheet, rotary switch, etc. A 3023 module is a current regulated driver for powering LEDs with high efficiency. A rotary switch is used in 5 modes of intensity control of the green LEDs string. The light intensity of LEDs is ~25000 lux which is measured by light meter (LX-101A). TLD cards were prepared using personnel monitoring discs of $CaSO_4$:Dy. These cards were annealed and sensitivity variations within 6% were selected for the experiment. Three sets of TLD badges were exposed to various fractionated doses on different days. Each TLD cards were bleached for 1 hr 30 minutes having an intensity of 25000 lux at the sample position before TL readout. The TL was recorded in semi automatic TLD badge reader.

Results and Discussions: The CaSO4: Dy based discs (5 mm Dia.) were exposed to 20mSv and kept at the centre on the bleaching glass plate. These were bleached for 1 hr 30 minutes and TL readings were taken in semi automatic TLD badge reader. Peak intensities of dosimetric peaks were compared. The variation was found to be within 6%. Figure 1 shows that the low temperature TL peak which is responsible for fading is bleached out. Doses were estimated immediately after the last irradiation and compared with actual delivered dose. The dose delivered and dose estimated in this study are compared in Table 1.

Conclusion: The results shows that optical bleaching technique makes it possible to evaluate dose immediately after exposure. This might be a requirement for urgent dose evaluation in case of personnel monitoring using CaSO4: Dy TLDs. This setup has been working satisfactorily for the last one year in RPAD, BARC, CT&CRS, Anushaktinagar, Mumbai.

P-227

INDIGENOUS TECHNOLOGY FOR RADIOACTIVITY MEASUREMENT IN FOODSTUFF AND DRINKS

P. Narayan, R. M. Sahani, S. L. Damor, G. L. Baheti
Defence Laboratory, DRDO, Jodhpur, Rajasthan, India.
E-mail: pradeep_narayan@rediffmail.com

Natural radioactivity concentration in food items has been reported internationally in the range of 40-600 Bq/kg with ^{40}K as major isotope with typical activity 50, 420, 165, and 125 Bq/kg in milk, milk powder, potato and beef respectively. Due to variation in radiotoxicity, IAEA has stipulated different consumption limit for different radioisotopes (^{134}Cs, ^{137}Cs, ^{103}Ru, ^{106}Ru, and ^{89}Sr) produced during nuclear detonation and accident. This is the reason to have dedicated technology for rapid radioactivity measurement and identification of isotopes presence in foodstuff and drinks for controlling internal exposure especially during nuclear emergency. An indigenous technology for radioactivity measurement in edible items has been developed using NaI (Tl) gamma detector (Size:75 mm x 75 mm). It is based on the detection of gamma rays emitted from the materials under investigation through conversion of scintillation light into electrical signal. The electrical signal is fed to 1k Multichannel Analyzer (MCA) for its further processing and identifying the type and level of contamination in the sample under examination. The system compares the sample count data with natural background and generates the visual warning and subsequently computes the activity concentration. The system has been facilitated with three size sample containers (100, 500 and 1000 ml) for accommodating radioactive samples of wide activity range. It is provided with adequate radiation shielding (30 lead) for reducing unwanted signal due to cosmogenic and terrestrial radiation, which helps in reducing MDA (minimum detection activity) in high radiation background area. The system has capability for correcting the signal

loss due to self-attenuation of radiation through the sample under measurement depending upon its matrix and density. The system has three point energy calibration facility using standard reference sources. The system was subjected to various radiological and physical quality tests and the results found to be in agreement with the internationally available technology. At typical PMT settings (HV: 750 V and Gain: 15%), there has been linear relationship between energy (60 to 1460 keV) and channel number within 0.1% with calibration factor 2.37 keV/channel. The system efficiency has been found to vary inversely with the photon energy, which decreases from 17% to 2% with increase in the energy from 80 keV to 1.46 MeV. It gives reproducible results within ±2.5% with measurement repeatability ±2%. It can measure radioactivity concentration in food samples within activity range 50 to 10^6 Bq/kg in 60s data acquisition time. This development is "First of its kind" in India, which utilizes raw food samples and drinks for radioactivity measurement. It generates visual warnings (Green, Yellow & Red) depending upon the level of radioactivity presence in the item under investigation. It identifies the radioisotope/s and computes gross as well as individual isotope activity. At a time it can identify 10 radioisotopes and compute their respective activity concentration. The system finally generates sample contamination analysis report and save it for future record and application. This technology is useful for military, civilian and research applications involving low level radioactivity measurement in any types of samples restricted with density up to 3 g/cc. The equipment may be helpful in controlling the radioactivity spread and restricting the contaminated food consumption. This paper reports the scientific and technical work carried out for development of the indigenous technology for food radioactivity measurement.

P-228

ESTIMATION OF MID POINT DOSE FOR CANCER CERVIX PATIENTS USING EPID BASED IN VIVO DOSIMETRY

B. Gowri[1,2], C. Anu Radha[1], V. Ramasubramanian[1], N. Surendran[2], A. Gopiraj[2]

[1]School of Advanced Sciences, VIT University, Vellore,
[2]Department of Medical Physics, Government Arignar Anna Memorial Cancer Hospital and Research Institute, RCC, Kanchipuram, Tamil Nadu, India.
E-mail: gowrisandhyabalan@gmail.com

Aim: To estimate the midpoint dose delivered to cancer cervix patients treated by conventional technique using Electronic Portal Imaging Device (EPID) based in vivo dosimetry.

Materials and Methods: Clinac 2100C equipped with aS500 EPID was used in this study. Phantom study was carried out using 0.6 cc chamber to establish a relationship between the EPID measured CU values and ion chamber measured midpoint dose in Gy. A Gy/CU look up table was generated and was used in the estimation of midpoint dose of patients. The look up table was validated using phantom for rectangular fields and for different separations. 25 patients of cancer cervix was included in this study and the delivered dose to the midpoint of the patients was estimated using EPID. The deviation between the prescribed and the measured dose was calculated and analysed.

Results and Discussion: EPID showed a linear response with increase in Monitor unit. The validation of the Gy/CU table for rectangular fields and other than measured separation showed minimal deviation in the range of 0.00 to 0.40 % for equivalent field sizes from 6.85 cm^2 to 16.94 cm^2 and from 0.12 to 0.24 % for 15.0 cm separation. 250 fields were measured for 25 patients, 10 measurements per patient, weekly once and for 5 weeks. The results show that out of 250 measurements, 98% of the measurements are within ±5% and 83.2% are within ±3% of the prescribed dose with a standard deviation of 1.66%.

Conclusion: EPID can be effectively used as an in vivo dosimeter for any busy radiotherapy department with minimal effort, time and without any inconvenience to the patients unlike other in vivo dosimeters.

P-229

COMPARING AND EVALUATING THE POST IRRADIATED EBT-3 GAFCHROMIC FLIM USING COMMERCIAL FLATBED SCANNER AND DENSOQUICK 2 DENSITOMETER

S. Nilavarasu, G. Bharanidharan, P. Aruna, J. Velmurugan, P. Thamilkumar[1], R. R. Rai[1], S. Ganesan

Department of Medical Physics, Anna University,
[1]Department of Radiotherapy, Dr. Rai Memorial Cancer Institute, Chennai, Tamil Nadu, India.
E-mail: nilavarasu@hotmail.com

Introduction: The emerging technologies in the field of radiotherapy increase the planning and delivery complexities hence, there is need for entire verification of treatment. Due to the sharp dose gradient around the normal critical structures which enhances the volume effect for almost all the detectors and due to the low energy contribution to the absorbed dose, there is difficulty in dose measurement hence, Radiochromic film is appropriate for entire dose verification due to its high spatial resolution, tissue equivalency and low energy dependence. Recently gafchromic EBT3 film is independent of inhomogines dose response post irradiation colouration and low sensitivity. There are several types of densitometer in use for 2D film dosimetry and each of them has its own specific characteristics. The aim of the current study is examine the characteristics of EPSON Expression 11000XL and Densoquick 2 densitometer in combination with gafchromic EBT3 film and to compare the results between the two densitometers.

Materials and Methods: To examine the characteristics of EPSON Expression 11000XL (EPSON-Japan) and Densoquick 2 densitometer (PTW- Germany). Gafchromic EBT3 film were used after irradiating in Varian LINAC true beam Long stand with 6MV and 10MV without FFF.

Result and Discussion: All the films were scanned before irradiation in order to subtract the OD of unirradiated film from irradiated film. Gafchromic EBT3 film was irradiated for various field sizes such as 2x2 cm^2, 3x3 cm^2, 5x5 cm^2 , 10x10 cm^2, 15x15 cm^2, 20x20 cm^2 with various dose rates ranging from 200 to 600 MU/minute for 6MV and 10MV photon beam without

FFF. The irradiated film were measured for the absorbed dose after 24 hours and scanned using a commercially available EPSON Expression 11000XL flat bed scanner and optical densities for various filed sizes and dose rates were calculated using verisoft software and the OD were also calculated using desoquick2 densitometer manually at various points in the central axis towards the off-axis of the field size. The absorbed Optical density shows that densoquick 2 is more accurate than commercially available flatbed scanner, Since the optical density observed in EPSON Expression 11000XL shows fluctuation initially due to the warm up of the lamp of the scanner later after performing more than two or three scans. The optical density observed in the flat bed scanner is comparable with densoquick2 densitometer which was within ±5%.

Conclusion: Both densoquick2 densitometer and EPSON Expression 11000XL densitometer is an excellent device to perform accurate two dimensional film dosimetry with gafchromic EBT3 However, some precautions and corrections have to be carried out in the flat bed scanner which needs to be taken in to account with the result. In case of densoquick2 although it was accurate than flat bed scanner the processing time required to get the result is more and tedious because everything need to be done manually henceforth from the results, it is concluded that both the devices can be used to perform accurate two dimensional film dosimetry.

P-230

UTILIZATION OF OSLD AS THE QUALITY CONTROL INDICATOR FOR IN-VIVO MEASUREMENTS IN TOTAL BODY IRRADIATION

V. Karthik, Salih Osman, Sandeep Singh, Kanan Jassal, Biplab Sarkar, T. Ganesh, Upendra Kumar Giri

Department of Radiation Oncology, Fortis Memorial Research Institute, Gurgaon, Haryana, India. E-mail: karthivittal@gmail.com

Objective: The In vivo dosimetry involves a measurement of the dose delivered to the patient in the treatment conditions to detect a possible deviation between the prescribed and the delivered dose. The advent of the optically stimulated luminescence dosimeters (OSLD), particularly in the Nano Dots form, is a very appropriate tool for its size, ease of handling, accurate and fast reading. This study investigate the application of OSLD for the quality control of Total Body Irradiation (TBI) treatment.

Introduction: Special techniques of radiation treatments generally require a quality control very thorough because in general tend to be high risk techniques of complications due to imparting high doses in a small volume or involve a very large volume of the patient are the techniques of TBI either photons or electrons. In these techniques a moderate error in the given dose can mean a very significant variation in tumor control probability (TCP) or the likelihood of complications in normal tissues has happened in known published accidents and can be deduced from the typical sigmoid curve of response vs. dose. The technique invivo dosimetry has proved useful a final tool to detect any possible error in the chain of procedures to which is subjected prior to radiation treatment. This study evaluate the feasibility of OSLD for in-vivo dosimetry of patients undergoing TBI.

Materials and Methods: In-vivo dose measurements using OSLD nanoDots (LANDAUER, Glenwood, Illinois) were done in a total of 24 patients who treated with 6 MV & 15 MV. To provide a uniform dose to the entire patient length, the treatment was split into 2 lateral fields. In this technique, the patient is kept inside the TBI box which is filled with rice filled muslin bags and irradiated using bilateral parallel opposed beams of 40×40 cm^2 size with 45° collimator rotation at an SSD of 333.5 cm in an Elekta Synergy Platform linear accelerator (Elekta AB, Stockholm, Sweden). All patients received a dose of 2 Gy in single fraction as conditioning regimen. The beams were equally weighted at the centre of the box which lies exactly at mid-line plane of the patient. The nanoDots were placed at both medially and laterally including forehead, right and left neck, right and left lung, umbilicus, right and left abdomen, upper right of thigh, and right knee.

Results: Measurement values of doses with nanoDots were found for medial sites forehead, umbilicus, and knee were, 2.19±9.66, 2.12±6.35, 2.16±8.1 Grey respectively. Lateral sites right and left neck, right and left lung, right and left abdomen were 2.17±8.75, 2.12±6.37, 2.15±7.81, 2.16±8.42, 2.21±5.35, and 2.17±8.66 Grey respectively. For medially placed nanoDots measurement Dmean was 2.16±9.66 Grey and laterally Dmean was 2.16±8.75 Grey.

Discussion: The characterization of the nanoDots dosimeters in terms of dose response, dose rate, angulation and other parameters in measuring conditions is the essential step before beginning the ultimate goal. The nanoDots showed their capacity for use invivo dosimetry, after tests on phantoms for both characterization and for treatment simulation. Finally, in clinical practice results in the three irradiation techniques raised they showed highly satisfactory results with acceptable deviations and comparable with existing previous techniques, proving the feasibility of conducting invivo dosimetry with OSL easily and efficiently.

Conclusion: The results demonstrate that nanoDot can be potentially used for TBI verification in various levels on Patients body, with a high degree of accuracy and precision. In addition OSLD exhibit better dose reproducibility with standard deviation of 0.6%. The dose response was also linear for both medial and lateral fields. This can help with time saving and work efficiency in the clinic.

P-231

DOSIMETRIC EFFECT OF BRASS MESH BOLUS ON SURFACE DOSE DISTRIBUTIONS

Zakiya S. Al-Rahbi[1,2], Dean L. Cutajar[1,3], Peter Metcalfe[1], Anatoly B. Rosenfeld[1]

[1]Centre for Medical Radiation Physics, University of Wollongong, Wollongong, [3]St. George Cancer Care Centre, St. George Hospital, Kogarah, Australia, [2]Department of Radiotherapy, National Oncology Center, The Royal Hospital, Muscat, Oman.
E-mail: z.alra7bi@gmail.com

Purpose: To investigate the feasibility of using the Brass Mesh Bolus as an alternative to tissue-equivalent Bolus for post mastectomy chest wall cancer by characterizing the spatial distribution (beam profile) using 2-mm fine Brass Mesh Bolus during chest wall PMRT.

Materials and Methods: Transmission surface dose data were acquired for a 6 MV photon beam in a solid water phantom using MO*Skin*™ dosimeter. Data were measured under the case of: full hole Face-up Brass, empty hole Face-up Brass Bolus, full hole Face-down Brass and empty hole Brass Bolus. The same steps were done to measure the exit dose.

Gafchromic EBT3 film strips were used to plot dose profile at surface and 10 cm depth for Face-up Brass, Face-down Brass, double brass, 0.5 cm and 1.0 cm of Superflab TE bolus.

Results: Generally, the Face-up Brass Bolus produced more surface dose than the Face-down Brass Bolus. The enhanced dose to the skin at the skin-mesh interface is due primarily to secondary charged particles produced in the mesh Brass.

The surface dose measured via MO*Skin*™ dosimeter increased from 19.2 $\pm$ 1.0% to 63.1$\pm$ 2.1% under full hole Face-up Brass, 51.2 $\pm$ 1.2% under empty hole Face-up Brass, 61.5 $\pm$ 0.5% under full hole Face-down Brass Bolus, and 41.3 $\pm$ 2.1% under empty hole Face-down Brass Bolus.

The percentage difference in the dose measured under full holes between face-up versus Face-down Brass was less than 2% for entrance dose and 10% for exit dose, whereas the percentage difference under empty holes was approximately 3% for entrance dose and about 5% for the exit dose.

For Face-up Brass Bolus, the dose measured under full holes versus empty holes was around 12%, whereas it was 20% for Face-down Brass Bolus. For exit dose, the dose measured under full holes versus empty holes was around 2% and 10% for Face-up and Face-down Brass Bolus, respectively.

Gafchromic EBT3 film strip measurements show that the mesh bolus produced ripple beam profiles and these oscillations are expected due to the mesh brass construction which results in inhomogeneous attenuation. The profiles for Face-up Brass Bolus oscillated from -58.8% to 48.8% and 61.6% - 50.3% under empty and full holes, respectively. For Face-down Brass Bolus, the profiles fluctuated from 56.3% to 41.5% under empty holes and from 59.3% to 43.3% under full holes.

Conclusions: Face-up Brass mesh has been successfully introduced into clinical practice in several institutions as an alternative to tissue-equivalent bolus, although usually for a percentage of treatment fractions. However, the effect of the mesh on surface and superficial dose when used in conjunction with tangential irradiation geometries is complicated and requires careful consideration before clinical use.

P-232

COMPARISON OF ITO, FTO AND GOLD COATED CATHODE OF THE PCB TECHNOLOGY BASED 3D POSITIVE ION DETECTOR

P. Venkatraman, C. S. Sureka

Department of Medical Physics, Bharathiar University, Coimbatore, Tamil Nadu, India.

E-mail: surekasekaran@buc.edu.in

Introduction: Nanodosimetry is a natural extension of microdosimetry, developed by H.H. Rossi and his colleagues more than 40 years ago, into the nanometer domain. Many of the concepts that were originally developed for micro dosimetry have been applied directly to nanodosimetry. One of these concepts is that, the geometrically well-defined regions in which the energy absorbed or the number of energy transfers is studied. There is a growing interest to study the interaction of ionizing radiation with matter/gas at nanometer level as it simulates the damage on DNA. Further in the field of nanodosimetry, the appropriate selection of cathode materials of its sensitive detector plays a more significant role in order to improve the performance of the detector.

Objective: To compare the Indium Tin Oxide (ITO), Fluorine Tin Oxide (FTO) and Gold coated cathode materials of the PCB technology based detector in order to optimize the cathode of the detector.

Materials and Methods: To find the suitable cathode material of the newly fabricated PCB technology based detector, the signal captures using three different cathode coated materials such as Indium Tin Oxide (ITO), Fluorine Tin Oxide (FTO) of 7 ohm resistivity, and gold of 0.1 ohm resistivity were studied as conducting layer over the ceramic insulator using Co-60 source under methane medium at an applied cathode voltage of -470 V. Further, variations in amplitude and efficiency of those signals at various pressure ranging from 0-10 Torr were analyzed.

Result and Discussion: It is observed that the signal amplitude and efficiency were found to be 785% and 67.27%, and 646% and 15.48% higher for gold than ITO, FTO and gold respectively. From this data, it is inferred that gold coated cathode showed better performance than ITO and FTO coated cathode. This may be due to the fact that the mobility of electrons in gold is higher than ITO and FTO materials. Further, it is observed that the signal efficiency gets decreased when the pressure is increased and its amplitude is almost constant throughout the range of pressure for all the materials. From these results, it is concluded that the gold coated cathode can improve the performance of the PCB technology based 3D positive ion detector.

P-233

AN *IN-VITRO* STUDY OF BREAST CANCER DIAGNOSIS AT ALL STAGES USING THE PCB TECHNOLOGY BASED NANODOSIMETER

P. Venkatraman, C. S. Sureka

Department of Medical Physics, Bharathiar University, Coimbatore, Tamil Nadu, India.

E-mail: surekasekaran@buc.edu.in

Introduction : In the modern field of nanodosimetry, the Printed Circuit Board (PCB) technology based positive ion detector has been identified as a device to detect cancer at all stages. The specific volatile organic compounds (VOCs) such as alkanes, alkenes, ketones, halogenated hydrocarbons, aldehydes, alcohols, esters, unsaturated hydrocarbons, terpenes, siloxanes, and aromates exhaled by breast cancer cells in the nano environment are the source biomarkers of to diagnose breast cancer. It also serves as direct evidence that the diagnosis of breast cancer through exhaled air without disturbing the patient is possible. **Objective:** The objective of the present paper is to analyse the normal and breast cancer tissues of all stages using the Nanodosimeter in order to confirm the suitability of this technique for breast cancer detection.

Materials and Methods: Multilayer PCB technology based Nanodosimeter was designed to capture positive ions produced by the interaction of ionizing radiation with low pressure gas medium. In order to confirm the signal, the present signal captured under methane and nitrogen medium at 1 to 10 Torr pressure was compared with the signal published by M. Casiraghi et al (Radiation protection dosimetry, 2015). After the validation, the normal breast tissues were placed inside the chamber and it was evacuated in order to remove all molecules present in the chamber. Then, it is allowed to exhale molecules at various pressures in order to measure the amplitude, rise time, fall time, and number of pulses of the signal. Later, these normal tissues were replaced with breast cancer tissues of all stages (Stage 0, 1, 2, 3a, 3b, and 4) in the evacuated medium and the same was allowed to exhale Volatile Organic Compounds (VOCs) to capture signal at various pressure ranging from 1 to 10 Torr. Those signals were captured for 5 sets of both normal and cancerous tissues at each stage.

Results and Discussion: When comparing the present signal with published signal under methane and nitrogen medium, it is confirmed that the present detector is well suited with higher efficiency to proceed further. When comparing the signal captured for both normal and breast cancer tissues, it is observed that the signals of normal and cancerous breast tissues gets varied in terms of amplitude, rise time, fall time, and number of pulses at all pressures and it showed maximum strength at 1 Torr pressure. It is observed that the signal amplitude, rise time, fall time and number of pulses of normal breast tissues was found to be 74.1±0.08 Volts, 2.4±0.005 ms, 480±0.0 μs, and 581±40.5 respectively. The signal amplitude, rise time, fall time and number of pulses at Stage 0, 1, 2, 3a, 3b, and 4 of breast cancer tissues are 76.8±0.28 Volts, 1.6±0.005 ms, 460 ± 0.02 μs and 1008±231.125; 79.3±0.15 Volts, 1.8±0.001 ms, 450 ±0.025 μs and 1546±364.5; 86.3 ±0.01 Volts, 480±0.0 μs, 480±0.0 μs and 2596±420.5; 88.5±0.03 Volts, 2.1±0.005 ms, 480±0.0 μs, and 3434±200; 90.7±0.01 Volts, 1.9±0.012 ms, 480±0.0 μs, and 3795±2.53; and 91.5±0.03 Volts, 470±0.2 μs, 480±0.0 μs, and 4077±210.12 respectively. From this data, it is inferred that the amplitude, rise time and number of pulses are gradually increased when the tissue became cancer and developed into various stages. Based on these, it is concluded that the PCB technology based 3D positive ion detector can be used a device to diagnose breast cancer.

P-234

ASSESSMENT OF THYROID DOSES FROM SUPRACLAVICULAR FIELD IRRADIATION OF POST-OP BREAST CANCER PATIENTS USING NANO DOT-OSLD

R. Gomathi, Mary Joan, K. Ananth[1], Arun Chougule

Department of Radiological Physics, SMS Medical College and Hospital, [1]SEAROC Linear Accelerator Center, SMS Medical College and Hospital, Jaipur, Rajasthan, India. E-mail: arunchougule11@gmail.com

Objective: The assessment of surface dose to critical organs or organs at risk in the treatment or close to treatment field is essential in radiotherapy to avoid deterministic effect or to reduce the severity of side effects from radiation treatment. The objective of this study was to investigate the absorbed dose to thyroid of Post operative breast cancer patients undergoing Supra clavicular Field (SCF) irradiation by Conformal External Beam Radiation Therapy (3DCRT). Optically Stimulated Luminescence Dosimeters (OSLDs) were used for the measurements.

Materials and Methods: In this study measurement of thyroid dose received by 10 female patients undergoing conformal external beam radiotherapy for breast cancer with supraclavicular lymph node involvement were done. For each measurement the OSLD disc was placed on the surface of the thyroid gland and Surface Dose (SD) to thyroid from supraclavicular field irradiation was measured. The measurements were performed for three treatment fractions and averaged. The total dose to thyroid was estimated by multiplying it with the total number of fractions. The relationship of the OSLD measured dose and the radiotherapy treatment field was analyzed.

Results and Discussion: Thyroid is a radiosensitive organ and the most common radiation-induced thyroid dysfunction, affects 20–30% of patients undergoing curative radiotherapy to the neck region, with approximately half of the events occurring within the first 5 years after radiotherapy. Wartofsky et al. have reported that a dose about 400 mGy can increase benign and malignant thyroid tumors. Hancock et al. reported that doses to the thyroid gland that exceeded 26 Gy produce hypothyroidism. Turner et al. reported that vascular damage and follicular cell damage followed radiation doses as low as 2.25 Gy. In the present study the mean maximum thyroid dose observed was almost 300-400cGy so it is possible that some patients will develop thyroid disorders after irradiation.

Conclusion: According to Radiation Therapy Oncology Group (RTOG) protocols, the maximum thyroid absorbed dose should be less than 3% prescribed dose, but in this study, the thyroid absorbed dose was about 6%. Doses to organ at risk such as thyroid which is in the supraclavicular field should be carefully evaluated and measures should be taken to minimize the dose. Accurate surface dose estimation could also help to avoid unnecessary skin reactions such as erythema, desquamation and necrosis.

P-235

A SIMPLE AND ECONOMIC TECHNIQUE FOR ANNEALING OSLD NANO DOTS

C. Senthamil Selvan, C. S. Sureka, U. Selvaraj[1]

Department of Medical Physics, Bharathiar University, [1]Department of Radiation Oncology, Sri Ramakrishna Hospital, Coimbatore, Tamil Nadu, India.
E-mail: surekasekaran@buc.edu.in

Introduction: The Optically Stimulated Luminescence (OSL) technique has been used extensively in personnel monitoring, dosimetry of radiation accidents and dating. Optically stimulated luminescence dosimeters (OSLDs) offers many advantages include faster readout of OSLDs, re-evaluation of the detectors and better signal to noise ratio using the pulsed OSL technique, etc., over Thermo Luminescence Dosimeters (TLD) that are used widely in radiotherapy and radiology. The most commonly used material in OSL dosimetry is Al_2O_3:C. These nanoDots are reusable and need to be annealed effectively prior to its usage.

Objectives: To analyze the suitability of Light Emitting Diode (LED) of various color to anneal OSLD nanoDots and find the best wavelength of LED and required time for effective annealing.

Materials and Methods: A Primus linear accelerator (Siemens Medical Systems, Concord, CA, USA) was used for irradiation and InLight microStar reader (Landauer, Inc., Glenwood, USA) was used to read the OSLDs signals with the reader warm up time of 10 min. The nanoDots were irradiated at various doses include 50, 100, 150, 200, 300, 500 and 1000 cGy. For each exposure 8 nanoDots were placed at the Dmax of 100 cm SSD, field size 10 × 10 cm^2 and 10 cm thickness of PMMA slab were used for backscatter in all irradiation. Then, the nanoDots were read by the OSLD reader to note the initial value. Then, these irradiated nanoDots were annealed using the LED (24 W) of Red, Green, Blue and white colors for analysis.

Results and Discussion: The PMT counts measured just before annealing the nanoDots those were irradiated to 50, 100, 150, 200, 300, 500 and 1000 cGy dose was 37287, 74590, 111684, 152637, 239007, 395893 and 847262 respectively. Then, the PMT counts after annealing those nanoDots using Red, Green, Blue and white LEDs over 45 minutes are (183, 195, 211, 227, 231, 250 and 294), (148, 159, 164, 182, 197, 225 and 243), (126, 145, 153, 172, 184, 193 and 217) and (153, 168, 181, 204, 221, 257 and 283) respectively. From this data, it is observed that the order of annealing efficiency of various LEDs is blue, green, red and white. This is due to the higher wavelength and energy of blue photons than others. Even though the trace PMT counts remained with LED based annealing are doubled than the conventional annealing setup, the LED based annealing has many advantages such as shorter time for annealing (6 hrs for commercially available annealing device), lesser heat production, lesser risk to nanoDots, more comfortable and highly economic (the total cost of LED setup is ~Rs. 500 /- and of commercially available annealing device is Rs. 0.5 Lakhs).

P-236

MONTE CARLO SIMULATION OF ELECTRON BEAM USING GEANT4

Nitin Garg, Parsee Tomar, Arun S. Oinam, Vivek Kumar[1]

Department of Radiation Therapy, Regional Cancer Center, Postgraduate Institute of Medical Education and Research, [1]Centre for Medical Physics, Panjab University, Chandigarh, India. E-mail: nitingarg6252@gmail.com

Introduction: Monte Carlo simulation is a technique used to model the probability of different outcomes in a process that can-not be easily predicted due to intervention of random variables. So it is assumed that Monte Carlo can provide both accurate and detailed calculations of the particle fluence from the treatment head of a radiotherapy linear accelerator. GEANT4 Software helps in simulation of treatment head with the same configuration provided by the Varian Medical Systems Inc., Palo Alto, CA, which is under confidential agreement. Monte Carlo simulation is performed to calculate the dose distribution in the water phantom of size 30 ×30 ×30 cm^3 for different field sizes 10 ×10 cm^2, 15 ×15 cm^2, 20 ×20 cm^2, 25 ×25 cm^2 and for energies 6 MeV, 9 MeV, 12 MeV, 15 MeV, 18 MeV, with electron applicator. The Other parameters like the Range of the Electron beam, Mean energy, Most probable energy are also calculated and compared with the measured which is obtained from the Clinac iX, Trilogy STX installed in our facility.

Objective: The aim of the study is to verify the deviation in the percentage depth dose distribution curve, the beam profile and all the other parameter related to the range of the electron derived from the R50 as obtained by the GEANT4 simulation and the actually measured in the water phantom.

Materials and Methods: A computer with processor speed 2.2GHz, RAM 4Gb and Geant4 software version 10.02 is used for the simulation. Medical Linear accelerator Varian Medical Systems Inc., Palo Alto, CA, is simulated. For dose calculation a simulated water phantom is used which is placed at SSD = 100 cm and phantom is divided into voxel size of 0.1 x 0.1 ×0.1 cm^3 which acts as the sensitive detector and record the events. For the verification of the dose distribution Blue Phantom, IBA and Trilogy STX is used. Percentage Depth dose distribution and Beam profiles are obtained using the software OmniPro I'mrt System Version 1.7b. The data recorded was analyzed using the ROOT software and analysis is done for the number of points satisfying the criterion 3% in 3 mm.

Results and Discussion: Simulation process has been started. More the number of particles run more accurate is the result. As it is time taking due to system limitation and all other parameters. The results are expected to be comparable with measured data.

P-237

BASIC CHARACTERISTICS IN DOSIMETRY OF THE SURFACE RADIOACTIVE SOURCE

Hiroki Ohtani, Takao Kono[1], Takahiro Hirayama[1]

Teikyo University, [1]Japan Shield Technical Research Co. Ltd., Tokyo, Japan. E-mail: ohtani@med.teikyo-u.ac.jp

Introduction: Three general rules of a radiation protection are the distance, time and shelter. The attenuation of radiation is based on inverse square law of the distance in theory, but this is a thing by a point source. Since it's necessary to treat as the surface radioactive source in the medical treatment for which many radioactive sources are used, and it influences the value of the leak dose distribution in a radiation irradiation room. When using several kinds of radioisotope, radiation exposure by radiation from which the energy is different in wide range shows. The purpose of this research is to make the basic characteristics necessary to a dose assessment of the surface radioactive source clear.

Materials and Methods: Radiation dosimetry every size of the surface radioactive source and distance between the radioactive source and the detector. It was made the surface radioactive source by arranging 8 of 60-Co sealed up in a circle each 45 °. A detector was installed on the circular center where the radius was set to 20 cm from 4 cm and dosimetry was performed. Used detectors are the HDS-101G which arranged CsI scintillator and a semiconductor detector (million technology company) and a NaI scintillator (Hitachi ALOKA company). The degree of radiation incidence angle to the detector was considered and the distance between the radioactive source-detector was set to at most 46 cm. Radiation dosimetry of 60-Co-137-Cs mix area radioactive source That installs 60-Co and 137-Cs alternately, and is the surface radioactive source. A detector was installed on the circular center where the radius was set to 20 cm from 4 cm and dosimetry was performed. The detector is same as the previous method. The distance between the radioactive source-detector was set to 25 cm.

Results and Discussion: The dose decreased so that the radius of the surface radioactive source became long. The ratio which decreased most was 9.46%. This is for decrease by the radiation incident on a detector slantingly. When the distance between the radioactive source-detector became short, it was increase of the radiation dose. This reason is decrease of the radiation dose escaping to detector outside. The radiation dose by the point source isn't based on inverse square law of the distance. The tendency of the measure by the Sievert unit and the tendency by the cps unit were different in a result of measurement of 60-Co-137-Cs mix area radioactive source. The factor by the difference in the energy influences this.

Conclusion: The basic characteristics of dosimetry were made clear about inverse square law of the distance and a mix radioactive source as basic characteristics necessary to a dose assessment of the surface radioactive source in this research. The radiation dose of the surface radioactive source isn't based on inverse square law of the theoretical distance. It's also same to the size of the lateral direction of the surface radioactive source. A dose assessment by a mix radioactive source was affected by the energy of the radioactive source and arrangement.

P-238

THE EFFECT OF SILDENAFIL ON PERSISTENT PULMONARY ARTERIAL HYPERTENSION IN PATIENTS POST BALLOON MITRAL VALVULOPLASTY

Garvit Garg, Krunal, Sejal Sejwani, Jayesh Rawal[1]

Department of General Medicine, [1]Department of Cardiology, Sumandeep Vidyapeeth University, Baroda, Gujarat, India. E-mail: justgarvit@gmail.com

Introduction: Pharmacological means of treating pulmonary arterial hypertension includes various drug groups like pulmonary vasodilators and diuretics, although their role is under clinical scrutiny. However, they cause potential adverse effects in the form of systemic hypotension and hypoperfusion of vital organs. Various studies are going on for the efficacy of oral sildenafil in treating secondary pulmonary hypertension. In this study we tried to evaluate the efficacy of oral sildenafil in patients who underwent balloon mitral valvuloplasty (BMV).

Aim: To see the effect of sildenafil on persistent pulmonary arterial hypertension in patients post balloon mitral valvuloplasty.

Materials and Methods: This is a prospective cohort study in which we enrolled cases that underwent Balloon mitral valvuloplasty (BMV) from June 2014 to December 2015. Total 31 patients, 11 were males and 20 were females, with mean age of 26 years. These patients were evaluated for the level of symptoms, echocardiography (ECHO), 6 mins. walk test (6MWT) and Tricuspid Annular Plane Systolic Excursion (TAPSE). These study parameters were assessed in OPD at 6, 12 and 18 months of follow-up after the procedure. The average period of starting Tab. Sidenafil was 6 months in our study group. Patients in the study group were given oral Sildenafil 25 mg once daily for 1 week followed by 50 mg once daily after the 18 months evaluation post procedure.

Results: Out of these 31 patients, 8 were in NYHA class II, 17 patients in NYHA class III and 6 patients were in NYHA class IV. All of these 31 patients who had no improvement in WHO functional class received Sildenafil. Average pulmonary artery systolic pressure (PASP) was 51 mmHg. Out of total 31 patients, 58.1% of patients in NYHA class II showed improvement, 35.5% NYHA class III patients showed improvement and in NYHA class IV show 6.4% after 18 month from the baseline. Mean value of TAPSE at baseline was 8.96 mm which increased to 14.6 mm after 18 months follow up ($P=0.002$), and average 6MWT was 217.7 meters at baseline which increased to 370.9 meters at the end of 18 months from the baseline.

Conclusion: In this study we conclude that there is significant role of sildenafil in improvement of PAH in patient which are gone BMV on the basic of improvement in our assessment parameters like NYHA class, TAPSE, 6MWT.

P-239

MONTE CARLO SIMULATION OF THE PHOTON BEAM QUALITY USING GEANT4 AND COMPARISON WITH THE ACTUAL LINEAR ACCELERATOR

Amanjot Kaur, Gaurav Trivedi, Arun S. Oinam, Vivek Kumar[1]

Department of Radiotherapy, Regional Cancer Center, Postgraduate Institute of Medical Education and Research, [1]Centre for Medical Physics, Panjab University, Chandigarh, India. E-mail: aman22jot@gmail.com

Introduction: Monte Carlo simulation is a technique used to model the probability of different outcomes in a process that can-not be easily predicted due to intervention of random variables. So it is assumed that Monte Carlo can provide both accurate and detailed calculations of the particle fluence from the treatment head of a radiotherapy linear accelerator. GEANT4 Software helps in simulation of treatment head with the same configuration provided by the Varian Medical Systems Inc., Palo Alto, CA, which is under confidential agreement. Monte Carlo simulation was performed and the dose distribution in water phantom along the central axis was calculated.

Objective: The aim of the study was to observe the deviation in the TPR20/10 simulated by GEANT4 Software to the TPR20/10 calculated from commissioned data of linear accelerator installed in the department.

Materials and Methods: A computer with processor speed 2.2GHz, RAM 4GB and Geant4 software version 10.02 was used for the simulation of the Medical Linear accelerator Varian Medical Systems Inc., Palo Alto, CA. Dose distribution (PDD) and photon beam quality (TPR20/10) will be calculated in this simulated water phantom using simulated gantry head.

This calculated beam quality will be compared with the beam quality measured using the ionization chamber in the actual water phantom and commissioned data of the machine.

Results and Discussion: The results are expected to be good in accordance with allowed variation in TPR20/10 and the same will discussed later on.

P-240

RADIATION INDUCED HEMATOLOGICAL ALTERATIONS IN MICE AND THEIR PREVENTION BY *DELONIX REGIA* EXTRACT

Itisha Vijayvargiya, Jaimala Sharma

Department of Zoology, Radiation and Cancer Biology Laboratory, University of Rajasthan, Jaipur, Rajasthan, India. E-mail: itisha410@gmail.com

Introduction: The ionizing radiation has been exploited in various aspects of human life such as in medical and for industrial purposes. *Delonix regia* (plant), commonly known as Gulmohur, consists of a variety of free radical scavenging phyto-constituents like sterols, phenolic compounds, triterpenoids and flavonoids.

Aims and Objectives: The present study was focused to on investigation of the anti-oxidative and antiradiation potential of *Delonix regia* flower extract (DRE) giving orally on before ionizing irradiation.

Materials and Methods: Swiss albino mice were exposed to 3.0 Gy gamma radiation to serve as the irradiated control (Group I), while the other group received DRE (200 mg/kg b. wt./day) orally for 7 consecutive days half an hour before 3.0 Gy gamma irradiation (Group II). Animals were autopsied at different intervals between 24 hrs to 30 days after irradiation.

Results: Irradiated animals were found to have decreased hematological constituents like erythrocyte count, total leucocyte count, hemoglobin content and hematocrit value at various autopsy intervals. It was observed that DRE pretreatment effectively prevented radiation-induced alterations in blood.

Conclusion: Based on the results obtained in the present study it can be concluded that *Delonix regia* flower extract have the protective effect on hematological alterations caused by gamma radiation.

P-241

EVALUATION OF CYTOLOGICAL CHANGES DURING RADIOTHERAPY FOR ORAL CAVITY CANCERS

Rajni Verma, Maryem Abid[1], Mary Joan, Gurvinder Singh, Gourav Jain, Suresh Kumar Akula, Arun Chougule

Departments of Radiological Physics and [1]Pathology, SMS Medical College and Hospitals, Jaipur, Rajasthan, India. E-mail: 1989vermarajni@gmail.com

Aim: The study was designed to analyze various Cytological changes with radiation doses in patients treated with Radiotherapy for oral cancers. Also, the present study radio biologically verified the planned and expected treatment outcomes of Radiotherapy by cell cytology.

Materials and Methods: 70 Male cancer patients in the age group 35-50 years with oral cavity cancers are observed in the study. 10 normal samples were kept as controls. All patients were treated with conventional radiotherapy. Serial scrape smears are collected three times per patient; before treatment, middle of treatment and on completion of treatment. These smears were analyzed after Giemsa staining with the help of microscope with digital imaging facility.

Results and Conclusions: The cytological parameters such as Cytoplasmic Vacuolation, Leucocytic Infilteration, Micronuclei, Karyorrhexis, Multinucleation and Nuclear Budding were observed and evaluated with dose. It was found that all the parameters increases with dose given but increment in first half of the treatment process (pre to middle fraction of treatment) was linear with steep slope and after that it started to saturate. This nature of cell response to radiation dose indicates that accelerated radiotherapy may be a better option to treat these malignancies. 49 patients observed in this study were histo pathologically proven squamous cell carcinoma and shown considerable increase in various cytological parameters with radiation. This demonstrated that radiation treatment response is better in well differentiated cancers in comparison to poorly differentiated cancers. Increased chance of recurrence is indicated by presence of dysplastic cells, hyper-chromatic nuclei, irregular nuclear outline, small dark tumor cells or large naked ovoid nuclei. All the patients observed in this study are having an addiction to either tobacco chewing or smoking or both which shows a strong correlation between tobacco use and these malignancies. In this study the selected patients were treated with chemotherapy simultaneously. Out of the 70 patients, 47 patients were treated with 3 cycles of chemotherapy, 13 patients with 4 cycle of chemotherapy and 10 patients with 5 cycle of chemotherapy. This was a limitation of this study. The study needs to be continued to eliminate this limitation.

P-242

THE EFFECT OF ELECTROMAGNETIC RADIATION FREQUENCIES OF 900 MHZ FROM MOBILE PHONE ON THE BLOOD OF SWISS ALBINO MICE

Niharika Sharma, Jaimala Sharma

Department of Zoology, Radiation and Cancer Biology Laboratory, University of Rajasthan, Jaipur, Rajasthan, India. E-mail: jaimalauor@gmail.com

Aim: To evaluate effect of electromagnetic radiation from mobile phones on Swiss albino mice.

Introduction: Cellular wireless telephones are based on widespread networks of base stations that connect the users through Radio Frequency (RF) signals, which expose to RF in general and radiations from base stations become great deal of concern about possible consequent health effects in human beings.

Materials and Methods: Animals (Swiss albino mice) of 6-8 weeks of age from an inbred colony were selected and were divided into two groups- (i) Sham irradiated (without mobile phone radiation) (ii) Mobile phone irradiated (for 60 days - 2hours/day). The mice were exposed to mobile phone radiation daily for 2 hours per day for 60 days with CDMA Mobile phone (Group II). After the exposure period the animals were sacrificed at different intervals between, 1-60days and blood was collected to estimate various hematological parameters.

Results: in Group II (Radiation exposed), total leucocytes counts (TLC), differential leucocytes counts (DLC), erythrocyte (RBC) counts and hemoglobin percentage, were significantly declined as compared to Group I (Shame exposed). In Group I no remarkable change was observed.

Conclusions: On the basis of the results obtain in this study it can be concluded that EMR frequency of 900 MHz emitted from CDMA mobile phone decreased TLC, DLC, RBC and hemoglobin percentage in the exposed mice.

P-243

PROTECTIVE EFFECT OF *CARISSA CARANDAS* EXTRACT AGAINST DMBA/TPA INDUCED SKIN CARCINOMA IN SWISS ALBINO MICE

Tanuja Jain, Jaimala Sharma

Department of Zoology, Radiation and Cancer Biology Laboratory, University of Rajasthan, Jaipur, Rajasthan, India. E-mail: tanujajain52@gmail.com

Aim: The current study was designed to elucidate preventive effect of orally administered *Carissa carandas* extract (CCE) at a dose rate of 50 mg/kg b.wt./day on a two-stage skin carcinogenesis model in Swiss Albino mice against 7,12 dimethylbenz[a] anthracene (DMBA)/12-O-tetradecanoylphorbol-13-acetate (TPA) induced squamous cell carcinoma.

Introduction: *Carissa carandas*, belongs to Apocynaceae family and popularly known as Karaunda, possess various pharmacological properties.

Materials and Methods: The mice were divided in two groups. Topical application of DMBA (100nmol/100μl of acetone) for two weeks, followed by TPA application (1% in acetone/ thrice in a week) throughout the experiment i.e. 16 weeks, induced skin lesions, on the depilated back of mice (Group I). Oral administration of CCE (Group II) at the dose rate of 50mg/kg body weight at the peri-initiational stage (i.e., 7 days before & 7 days after DMBA application). Histopathology of tumors was evaluated in the treatment groups.

Results: Treatment of animals in Group II (oral administration of CCE of 50 mg/kg b.wt./day) reduced the skin papillomas, also delayed tumor formation and tumor growth in CCE treated experimental group (Group II). Histopathological study revealed that epidermal hyperplasia, keratinized pearl formation, and acanthosis in skin and tumors were observed in carcinogen treated animals whereas these were found to be reduced after CCE administration.

Conclusions: These results proved that CCE protected against DMBA/TPA induced skin carcinogenesis by reducing adverse histopathological alterations during skin carcinogenesis process in Swiss albino mice of Group II as compared to carcinogen treated animals (Group I).

P-244

DOSIMETRIC ANALYSIS OF UNFLATTENED (FFFB) AND FLATTENED (FB) PHOTON BEAM ENERGY FOR GASTRIC CANCERS USING IMRT AND VMAT – A COMPARATIVE STUDY

Manindra Bhushan[1,2], Girigesh Yadav[1], Deepak Tripathi[2], Kothanda Raman[1], Lalit Kumar[1], Munish Gairola[1]

[1]Medical Physics Division & Department of Radiation Oncology, Rajiv Gandhi Cancer Institute & Research Centre, New Delhi, [2]Amity Institute of Applied Sciences, Amity University, Uttar Pradesh, India.
E-mail: manindra.mishra@rediffmail.com

Introduction: Gastric carcinomas contribute a large patient population worldwide. Evolution of megavoltage accelerators has provision of photons of desired energy. IMRT has ability to cover the target and spare the nearby critical organs. Advancement in technology has introduced VMAT which allows continuous treatment delivery with modulated intensity map. Usually 6MV_FFB energy is used for the treatment planning in abdominal malignancies; however flattening filter free (FFF) 6MV beam is gaining momentum for the treatment of such cases, due to their advantage of higher dose rate than 6MV beam.

Objectives: The aim of present study is to evaluate the feasibility of flattening filter free beam (FFFB) for the treatment of gastric tumors and to review their benefits over 6MV flatten beam (6MV_FFB).

Material and Methods: 15 patients with Gastric carcinoma were selected for the study. CT scans of thickness of 0.3 cm. were acquired in supine position. PTV and OAR's were delineated. All the plans were made retrospectively for each patient for the prescription dose of 45 Gy/25 fractions to the PTV. Four isocentric plans were compared in the present study on Varian TrueBeam Linear accelerator (Varian Medical Systems, Palo Alto, California, USA).

Results: PTV $D_{98\%}$ was 44.41 ± 0.12 Gy, 44.38 ± 0.13 Gy, 44.59 ± 0.14 Gy and 44.49 ± 0.19 Gy for IMRT 6MV_FFB, IMRT 6MV_FFFB, VMAT 6MV_FFB and VMAT 6MV_FFFB respectively. 6MV_FFFB beam minimizes the mean Heart dose D_{mean} (P=0.001). It was observed for Spinal cord that VMAT reduces D_{max} (P=0.002) and $D_{<2cc}$ (P=0.001) significantly as well as for Liver, VMAT plans have reduced the mean dose D_{mean} (P=0.022) and $D_{>700cc}$ (P=0.001). VMAT dominates over IMRT when it came to kidney doses V_{12Gy} (P=0.02), V_{23Gy} (P=0.015), V_{28Gy} (P=0.011) and D_{max} (P<0.01). VMAT has significantly reduced the doses to kidneys. It was analyzed that 6MV_FFFB significantly reduces the dose to normal tissues (P=0.006 & P=0.018). VMAT significantly reduces the TMU, required to deliver the similar dose by IMRT (P<0.01).

Discussion: Simultaneously changing multi-leaf position and dose-rate helps to achieve the optimum solution in VMAT. This study demonstrated that 6MV_FFB and 6MV_FFFB provided similar dose coverage, homogeneity and conformity whether they are used with IMRT or VMAT. Daniel *et al* found similar results while using hypo-fractionated VMAT using flattening filter free beam in prostate cancers. Cold-spots were reduced with VMAT due to rotational nature of the treatment. For the critical structures like common lung, heart, liver and kidneys; mean dose reduced significantly with VMAT unflattened beam. This may be possible due to non-deposition of un-necessary dose to the area outside the PTV. Reduced low-dose region of kidney and bowel with 6MV FFF lowers the risk of secondary cancers. Although TMU increased slightly in FFF, yet unfiltered beam made it possible with availability of higher dose rate. Our data demonstrated that the time required to deliver the same dose is 5.62 times higher in IMRT 6MV, 2.93

times higher in IMRT 6MV FFF and 1.95 times higher in VMAT 6MV when compared with VMAT 6MV FFF.

Conclusion: Unflattened beam spares the organs at risk significantly to avoid the chances of secondary malignancies and reduces the intra-fraction motion during treatment due to provision of higher dose rate. Hence, we conclude that 6MV unflattened beam can be used to treat gastric carcinoma.

Reference

1. Daniel RZ, Stephanie L, Jan H *et al*. Use of photon beam of a flattening filter-free linear accelerator for hypofractionated volumetric modulated arc therapy in localized prostate cancer. Int J Radiat Oncol Biol Phys 2012; Vol.83,No.5, pp.1655-1660.

P-245

SYNTHESIS AND THERMOLUMINESCENCE PROPERTIES OF RARE EARTH DOPED (TB, DY) DOPED FLUOROPEROVSKITE NAMGF3

Aayushi Jain, Pooja Seth, Shruti Aggarwal
University School of Basic and Applied Sciences,
GGSIPU, New Delhi-110078, India.
E-mail: aayushi3jain@gmail.com

Introduction: Thermoluminescence dosimetry (TLD) is a potential method for the measurement of absorbed dose in the field of medical physics, personal dosimetry and environmental monitoring. This has encouraged the search for new sensitive thermoluminescent (TL) material with good dosimetric properties. A worldwide progress has been made in this direction for the development of TL dosimeter by applying different preparation route and dopant ions. Fluoroperovskite, $NaMgF_3$ is one of the important material due to its interesting properties such as non toxicity, less hygroscopicity, high thermal durability and wide band gap. $NaMgF_3$ is a tissue equivalent (tissue equivalent $Z_{eff} \sim 10.32$) material and its mass attenuation coefficient is similar to that of water for photon energies above 0.1 MeV. These useful properties allow its potential application in the field of radiation therapy and radiodiagnostics for the dose monitoring and measurement.

Objectives: To synthesize fluoroperovskite, $NaMgF_3$ doped with rare earth ions Tb and Dy using solid state diffusion method. To investigate the effect of dopant ion (Tb and Dy) on thermoluminescence (TL) properties of $NaMgF_3$.

Materials and Methods: Powder samples of $NaMgF_3$, $NaMgF_3$:Tb (0.5 mol%) and $NaMgF_3$:Dy (0.5 mol%) were prepared by solid state diffusion method. Starting materials NaF and MgF_2 were taken in equimolar stoichiometric ratio. Dopants Tb in the form of $TbCl_3.6H_2O$ & Dy in the form of $DyCl_3.xH_2O$ were used. The mixture was heated in an alumina crucible at 1043 K for 12h. The solid formed was then crushed to obtain powder of $NaMgF_3$, $NaMgF_3$:Tb (0.5 mol%) and NaMgF3:Dy (0.5 mol%). XRD pattern were taken from model Rigaku Ultima IV. The assynthesized samples were annealed at 400˚C for 15 min and irradiated with a gamma dose of 15 Gy from 60Co source. A Harshaw Q TLD reader model 3500 was used for recording of TL glow curves.

Results and Discussion: X-Ray Diffraction: Powder XRD pattern of assynthesized $NaMgF_3$, NaMgF3:Tb3+ and $NaMgF_3$:Dy_3+ matches well with standard JCPDS data (No.

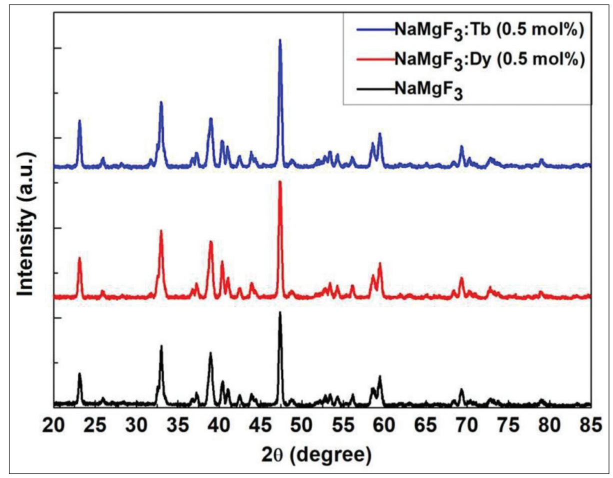

Figure 1: XRD pattern of $NaMgF_3$, $NaMgF_3$:Tb (0.5 mol%) and $NaMgF_3$:Dy (0.5 mol%)

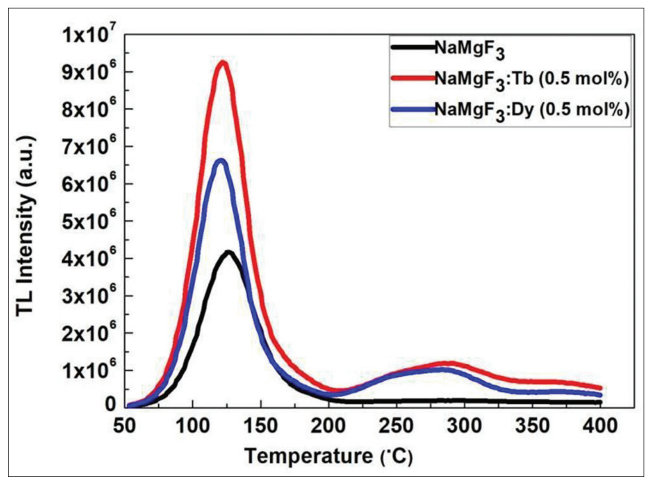

Figure 2: TL glow curve of $NaMgF_3$, $NaMgF_3$:Tb (0.5 mol%) and $NaMgF_3$:Dy (0.5 mol%)

82-1224) as shown in Figure 1. XRD pattern confirms the formation of NaMgF3. Addition of dopant Tb and Dy does not change the host lattice. Themoluminescence (TL): $NaMgF_3$ showed a simple glow curve structure with a single peak at 127˚C. The glow curve structure changes after doping with Tb and Dy, a new high temperature peak appears at 292˚C and 279˚C with Tb and Dy, respectively as shown in Figure 2. However, main TL peak position was approximately same in all the samples. From the glow curve structure, it is observed that with Tb dopant, TL intensity is increased by a factor of 2.2 and with Dy dopant, TL intensity is increased by a factor of 1.6 in comparison to undoped $NaMgF_3$.

Conclusion: In this paper, $NaMgF_3$, $NaMgF_3$:Tb and $NaMgF_3$:Dy were successfully synthesized by solid state diffusion method. A preliminary investigation of thermoluminescence properties such as glow curve structure, peak intensity and peak position were done. From the glow curve structure, it is found that doping of Tb showed better results in comparison to Dy as it increases the TL sensitivity of $NaMgF_3$ by a factor of 2.2. Encouraged by these results, further investigations on dosimetric properties of $NaMgF_3$ and related kinetic parameters will be made.

P-246

BIOCHEMICAL CHANGES IN BRAIN OF SWISS ALBINA MICE EXPOSED TO 2.45 GHz MICROWAVES RADIATION

Rajendra Jat, Najendra Singh, Rashmi Sisodia, Deepak Bhatnagar[1]

Department of Zoology, University of Rajasthan, Jaipur, [1]Department of Physics, University of Rajasthan, Jaipur, India.
E-mail: rashsisodia@yahoo.co.in

Objectives: Exploration of the changes in biochemical parameters of brain exposed to 2.45 GHz microwave radiations.

Material and Methods: 6-8 weeks old male Swiss albino mice, weighing 25.0 ±2.0 grams were procured from inbred colony. Mice were divided into two groups (6 mice in each group). Group 1) Sham exposed, and group 2) microwave exposed group. Microwave radiation experimental bench was used for the exposure to mice. Exposure was given in plexiglas cages. Mice were exposed to 2.45 GHz microwaves radiations for 2 hrs/day for 15 days with power density as 0.25 mW/cm^2 and specific absorption rate (SAR) to be 0.072 W/kg. Catalase (CAT), Lipid per oxidation (LPO), Glutathione (GSH) and superoxide dismutase (SOD), assays were performed to observe biochemical changes.

Results: A significant increase ($P < 0.001$) in Catalase (CAT) and in Lipid per oxidation (LPO) and a significant decrease ($P < 0.001$) in Superoxide dismutase (SOD), Glutathione (GSH) were observed in exposed group in comparison to control group

Conclusion: It may be concluded that microwaves at 2.45 GHz frequency cause oxidative stress mediated cellular toxicity which leads to adverse and detrimental biochemical changes in brain.

Keywords: Microwave radiations, CAT, SOD, LPO, GSH

P-247

BIOCHEMICAL CHANGES IN BLOOD OF SWISS ALBINA MICE EXPOSED TO 2.45 GHZ MICROWAVES RADIATION

Najendra singh, Rajendra Jat, Rashmi Sisodia, V. K. Saxena[1]

Department of Zoology, University of Rajasthan, Jaipur, [1]Department of Physics, University of Rajasthan, Jaipur.
E-mail: rashsisodia@yahoo.co.in

Objectives: The objectives of this study were to explore the changes in biochemical parameters of Blood exposed to 2.45 GHz microwave radiations.

Material and Methods: 6-8 weeks old male Swiss albino mice, weighing 25.0 ±2.0 grams were procured from inbred colony. Mice were divided into two groups; (6 mice in each group) 1) Sham exposed, and 2) microwave exposed group. Microwave radiation experimental bench was used for the exposure to mice. Exposure was given in Plexiglas cages. Mice were exposed to 2.45 GHz for 2 hrs/day for 15 days with power density as 0.25 mW/cm^2 and SAR to be 0.072 W/kg. Blood sugar, Total protein, Acid phosphatase, and alkaline phosphatase (ALP) assays were performed to observe biochemical changes.

Results: A significant decrease ($P < 0.001$) in Blood sugar, Total protein, and Acid phosphatase (ALP) and increase ($P < 0.001$) levels of Alkaline phosphatase (ALP) were observed in exposed group in comparison to control group.

Conclusion: It may be concluded that microwaves at 2.45 GHz frequency causes oxidative stress mediated cellular toxicity which leads to adverse and detrimental biochemical changes in Blood.

Keywords: Microwave radiations, Blood sugar, Total protein, Acid phosphatase, ALP.

P-248

LUNG SBRT – DOSIMETRY AND DELIVERY COMPARISON OF ROTATIONAL IMRT TECHNIQUE FROM LINEAR ACCELERATOR AND TOMOTHERAPY.

Rajesh Kinhikar[1], Priyadarshini Sahoo[1], Naveen Mummudi, Deepak Deshpande[1], Jai Prakash Agarwal

Departments of Radiation Oncology and [1]Medical Physics, Tata Memorial Hospital, Parel, Mumbai, India.
E-mail: rosy3468@gmail.com

Introduction: Stereotactic body radiation therapy (SBRT) for lung demands high precision dose delivery technique to minimize the doses to organs at risk (OARs), while simultaneously enabling dose escalation to target. These techniques employ either intensity modulated radiation therapy (IMRT) or volumetric modulated arc therapy (VMAT). Aim of this study was to evaluate the plans based on dosimetric indices for rotational IMRT delivered with tomotherapy and VMAT (RapidArc) with Linac for SBRT in early stage non-small cell lung cancer (NSCLC).

Materials and Methods: Fifteen Patients (stage I NSCLC with peripherally located lesion) treated with Rapid Arc SBRT using 6 MV X-rays with one/two partial-arc plan (180˚) in Linac (with maximum dose rate of 600 MU/Min) were included. To determine the optimal treatment modality, a new treatment plan was generated using IMRT with HT for each patient for comparative purpose. For HT plans, the field width of 2.5 cm, pitch as 0.1 and modulation factor as 2.5 was used. Dosimetric indices compared were conformity index, homogeneity index, D_{2cm} and R50% for PTV. For Lung-PTV and Heart- V20, V5, mean dose were evaluated and for other OARs (Esophagus, trachea and spinal cord), Dmax was compared. Dosimetric accuracy was assessed using gamma index (3% dose difference, 3 mm DTA, 10% threshold) and point dose measurement for HT plans (3% tolerance).

Results and Discussion: Mean volume of PTV was 84 cc (range 24cc-158cc). Mean CI, HI, $R_{50\%}$ for PTV with HT plan were1.16 (SD 0.18), 1.02 (SD 0.01) and 5.65 (SD 0.98) respectively. With Rapid Arc, mean CI, HI and R50% were found to be 0.83 (SD 0.35), 1.14 (SD 0.08) and 4.6 (SD 1.1) respectively. D_{2cm} was comparable with both the technologies. R50 was slightly on higher side in HT plan. MU for HT is around 8-9 times more than RA. Delivery of a 7.5 Gy fraction required an average of 19.97 min (HT) and 3.2 min (Rapid Arc). All verification plans were well within tolerance dosimetrically. Isodose distribution (90%) for RapidArc (RA) Isodose distribution(90%) for TOMO are shown in Figure 1.

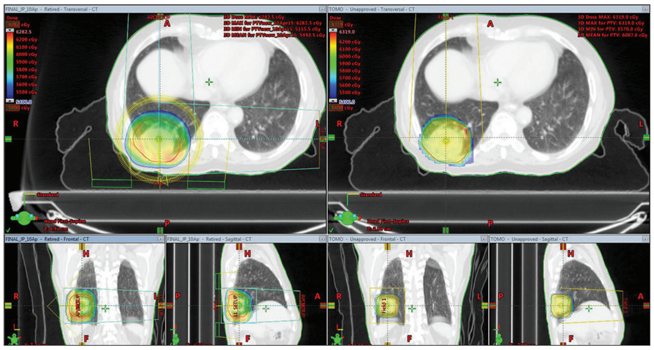

Figure 1: Isodose distribution(90%) for RA, Isodose distribution(90%) for TOMO

Conclusions: Both high precision radiotherapy techniques with Helical Tomotherapy and Linac were capable of achieving the desired goals. However, HT plans showed relatively better conformity compared to Rapid Arc. Doses to OARs were minimal with Rapid Arc. Shorter treatment time with Rapid Arc may have the patient comfort.

P-249

DOSIMETRIC DEPENDENCE ON COLLIMATOR ANGLE IN VOLUMETRIC MODULATED ARC THERAPY OF HEAD AND NECK CANCERS

Resmi K. Bharathan, Arya Devi, Silpa Ajaykumar, Suja C. A, Soumya N. M, Geetha M

Department of Radiation Oncology, Malabar Cancer Centre, Thalassery, Kerala, India.
E-mail: resmikbharathan@gmail.com

Introduction: Multileaf collimators (MLC) are the best tool for beam shaping, and an important way to minimize the absorbed dose to healthy tissue and critical organs. They have moveable leaves arranged in pairs that can block a certain part of beam. Owing to its ability to control leaf position and with a large number of controlled leaves, it can be used to shape any desired field. During VMAT the linear accelerator (LINAC) control system changes the dose rate and the multi leaf collimator (MLC) positions while gantry is rotating around the patient. Collimator angle is usually rotated in the plans of VMAT to reduce radiation leakage between MLC leaves. At a zero angle, the leakage between MLC leaves accumulates during the gantry rotation and the summed leakage results in unwanted dose distributions, which cannot be controlled by optimization. At different collimator angles, the unwanted doses can be controlled by dose constraints in the optimization procedure so that we can reduce the unwanted doses. The optimal collimator angle for VMAT plan is thus required to be determined.

Objective: The purpose of this study is to investigate the dose-volume variations of planning target volume (PTV) and organs-at-risk (OARs) in prostate volumetric modulated arc therapy (VMAT) while varying the collimator angle.

Methods and Materials: The key study variables include the coverage of the PTV and doses to the OARs in the plans with different collimator angles (10, 20 and 45 degree) of 30 patients. The dosimetric comparison was carried out using the following parameters such as dose to 98% of the PTV (D98%), dose to 50% of the PTV (D50%), dose to 2% of the PTV (D2%), maximum dose (Dmax), mean dose (Dmean), Conformity Index (CI), Homogeneity Index (HI), Gradient index (GI) and Monitor Units (MU) for the PTV for each of the collimator angle.30 patients who were already treated for head and neck cancers were selected for this study. Plans were created by changing the collimator angle. Eclipse planning system was used for creating the plans. For each change of collimator angle, a new plan was re-optimized for that angle. The treatment plan not changed for each angle, only repeated by changing the collimator angles. A 30-degree collimator angle is used in the already approved plans. The dosimetric parameters was compared across each plans using t-test and annova.

Results and Disussion: This work explores the impact of different collimator angles on VMAT plans. Collimator angle selection could play vital role in improving the quality of treatment plans. It is concluded from the results that the dose variations with the change of collimator angle are significant. VMAT plans with said collimator angles do not play a substantial role in PTV coverage but for more accuracy, a 30˚ collimator angle provides superior PTV dose distribution than all other studied collimator angles as shown by a better value of CI and HI. It was observed that a 45˚ collimator angle is appropriate for sparing of OARs. The results of our study set the groundwork for guiding the collimator angle selection with regards to PTV dose distribution and sparing of OARs in VMAT planning of Ca larynx and Ca hypopharynx cases. This work can be extended with more number of patients. This work also can be extended to other treatment sites using VMAT.

P-250

EVALUATION OF INTRAFRACTIONAL SETUP ERRORS IN FRAMELESS SRS COMPUTED USING OPTICAL SURFACE MONITORING SYSTEM & CBCT

P. T. Patwe, V. Mhatre[1], A. Nachankar, P. Dandekar

Sir HN Reliance Foundation Hospital & RC, Girgaum, [1]Kokilaben Dhirubhai Ambani Hospital & RC, Andheri, Mumbai, India. E-mail: parimal19@gmail.com

Purpose or Objective: The aim of study was to evaluate setup accuracy and intrafraction errors of patients treated with single fraction intracranial stereotactic radio surgery using the Optical Surface Monitoring System and Perfect pitch Six Degree of Freedom (DoF) couch. We compared the patient positioning shifts (translational and rotational set up error) computed by OSMS against the shifts given Cone Beam CT (CBCT).

Material and Methods: During August 2016 and May 2017, 3 patients were treated with single fraction frameless stereotactic radio surgery (SRS) at our institution. Patients were immobilized using Q fix immobilization system and Perfect Pitch 6 DoF couch platform. Q-fix immobilization system consists of Q-fix Aquaplast mask, Portrait Head & Neck base plate, MOLDCARE® Cushion & Silverman head support. MOLDCARE® Cushion used on Silverman head support provides customized head support. The cushion is composed of a soft fabric bag containing polystyrene beads. When water is sprayed over pillow, it becomes rigid conforming to the contours of patients head & neck. The OSMS is a video-based 3D surface imaging system used to detect and reconstruct the skin surface of a patient in 3D before and during the radiotherapy treatment. As shown in Figure 1, it consists of 3 ceiling camera units positioned, two laterally to the treatment couch, and the third centrally located at the foot of the couch. A projector unit projects a red light speckle pattern onto the patient. Overall, 2 image sensors located on either side of the projector acquire the image of the patient and the speckle pattern. With the images from the 3cameras,the system reconstructs the 3D surface for all the gantry positions, even in the cases where the linac head interposes between one of the cameras and the isocenter, obscuring the image projection for that camera. The OSMS system was used to position the patient immediately prior to treatment & to 6 dimensionally track the patient during treatment. The Cone-Beam computed tomography (CBCT) were acquired before and after treatment to asses for set up errors. Translational and rotational set up errors were obtained in Right-Left (RL), Antero -Posterior (AP),Cranio-Caudal (CC) directions. The shifts were applied in accordance with the CBCT match results. The shifts given by CBCT match were compared with the shifts given by OSMS. Means and one standard deviation of the Intrafractional errors in all six directions were analyzed. The rotational & translational shifts given by OSMS were compared with shifts given by CBCT.

Results: A total of 06 CBCT scans were analyzed & compared with the shifts computed by OSMS. The couch was shifted as per the shifts given by CBCT. The OSMS computed shifts were compared with CBCT shifts. The mean & standard deviation in the shifts computed by OSMS as compared to CBCT (in mm for translation and degrees for rotation) were 0.2 ± 0.10 (RL), 0.10 ± 0.20 (PA), 0.2 ± 0.10 (CC), 0.15 ± 0.30 (Roll), 0.08 ± 0.2 (Pitch), 0.2 ± 0.3 (Rotation).

Conclusion: OSMS guided frameless SRS utilizing immobilization system like Q Fix open mask , Perfect Pitch 6DoF couch platform is precise and reproducible technique. The accuracy of shifts computed by OSMS is comparable to CBCT data.

Figure 1: True Beam STx with 6DoF Perfect Pitch Couch & OSMS System

P-251

MEASUREMENT OF ENTRANCE SKIN DOSES IN COMMON DIGITAL RADIOGRAPHY EXAMINATIONS & PROPOSED LOCAL DIAGNOSTIC REFERENCE LEVELS

Bhupendra Singh Rana, Sanjeev Kumar[1], I. S. Sandhu[2], (CC) P. Singh[3], N. Khandelwal

Department of Radiodiagnosis, PGIMER, Chandigarh, [1]Department of Physics, G. G. D. S. D. College, Chandigarh, India, [2]Chitkara University, Punjab, [3]I. K. Gjural P. T. U., Jalandhar, India. E-mail: bhupendrasrana@gmail.com

Introduction: In radiology, collective radiation doses resulting from the use of X- rays in radiography, computed tomography (CT) scans and interventional procedures has maximum contribution to the medical exposures.[1] In diagnostic x ray procedures radiation doses to the patients are usually low and of the order of few μGy to tens of mGy. The low dose exposures in the radiological examinations increase the risk of stochastic effects, mostly cancer induction in exposed patients. The risk of stochastic effects primarily depends on the magnitude of radiation dose as well as on the anatomical structure irradiated.[2-4] Therefore, all the radiation exposures need to be monitored and optimized to limit the associated radiation risk to the patient without limiting the clinical utility of the diagnostic examinations.

Objective: The aim of the present work is to measure the ESDs for common radiographic examinations of adult and pediatric patients for 12 diagnostic examinations *viz*. chest (AP and PA), lumbo sacral spine (AP and LAT), thoracic spine (AP and LAT), cervical spine (AP and LAT), abdomen (AP), pelvis (AP), hip joints (AP), skull (AP and LAT)), knee joint (AP and Lat), wrist (AP), upper extremity (AP) and lower extremity (AP) in digital radiography (DR) setup and propose LDRL for DR.

Materials and methods: The assessment of the patient doses in present work was done in accordance with International Atomic Energy Agency (IAEA) recommended protocol[5] for radiographic exposures. We have utilized thermoluminescent dosemeters TLDs (LiF: Mg, Ti) for dose measurement to evaluate the ESDs in adult patients. For pediatric patients, ESDs were estimated from exposure parameters and tube output measurement with appropriate back scatter factor (BSF). The examinations were performed in X-ray machines installed in Department of Radiodiagnosis, Post Graduate Institute of Medical Education and Research (PGIMER), Chandigarh, India. Information on type of examination, sex, age, height, weight of the patient, focus to table top distance (FTD), field size along with set KVp and mAs were recorded during data collection.

Results and Discussions: The measured minimum, maximum and average values of the ESD along with their third quartile values proposed as LDRLs for adult and pediatric patients. LDRL values obtained in this study were compared with published values of Health Protection Agency, UK in its report HPA-CRCE-034 (2012)[6], Italian DRL values[7] and values reported by Sonawane et al.[8]. In this study, pediatric patients are arranged into five age groups of <1months, 1-12 months, 13-60 months, 61-120 months and 121 months and above. LDRLs of this study were also compared with DRLs published by NRPB-R318 (2000)[9], Billinger et al. (2010)[10] and Wambani et al. (2013)[11]. In addition, LDRL values of this study were also compared with earlier reported DRLs for chest, abdomen (AP), skull (AP) and skull (Lat) of pediatric patients. The present study has demonstrated that use of DR technology reduces the patient's radiation exposure and helps in maintaining the ALARA principle.

References

1. National Council on Radiation Protection and Measurements. Ionizing radiation exposure of thepopulation of the United States. NCRP Report No. 160 (2009).
2. United Nations. Sources and Effects of Ionizing Radiation. Report to the General Assembly, with Scientific Annexes Volume II Effects: United Nations Scientific Committee on the Effects of Atomic Radiation, UNSCEAR 2000 Report. United Nations publications Sales No. E.00.IX.3, New York (2000).
3. Hall, E. J. and Brenner, D. J. Cancer risks from diagnostic radiology. Br. J. Radiol. 81, 362–78 (2008).
4. Pearce, M. S., Salotti, J. A., Little, M. P., McHugh, K., Lee, C., Kim, K. P., Howe, N. L., Ronckers, C. M., Rajaraman, P., Craft, S. A. W., Parker, L. and De González, A. B.Radiation exposure from CT scans in childhood and subsequent risk of leukaemia and brain tumours:a retrospective cohort study. The Lancet 380, 499-505 (2012).
5. International Atomic Energy Agency. Dosimetry in diagnostic radiology: an international code of practice. Technical reports series No 457 (2007a).
6. Hart, D., Hillier, M. C. and Shrimpton, P. C. Doses to patients from medical x-ray examinations in the UK–2010 review. Health Protection Agency, HPA–CRCE-034, London. (2012).
7. Compagnone, G., Pagan, L. and Bergamini, C. Local diagnostic reference levels in standard X-ray examinations. Radiat. Prot. Dosim. 113(1), 54-63-94 (2005).
8. Sonawane A U, Shirva V K, Pradhan A S. Estimation of skin entrance doses (SEDs) for common medical X ray diagnostic examinations in india and proposed diagnostic reference lenels (DRLs). Radiat. Prot. Dosimetry 138(2), 129-136 (2010).
9. Hart, D., Wall, B. F., Shrimton, P. C., Bungay, D. R. and Dance, D. R. Reference doses and patient sizes in pediatric radiology. National Radiological Protection Board, NRPB-R318, London. (2000).
10. Billinger, J., Nowotny, R. and Homolka, P. Diagnostic reference levels in pediatric radiology in Austria. Eur. Radiol. 20, 1572-79 (2010).
11. Wambani, J. S., Korir, G. K., Korir, I. K. and Kilaha, S. Establishment of local diagnostic reference levels in pediatric screen film radiography at a children's hospital. Radiat. Prot. Dosim. 154(4), 465-76 (2013).

P-252

THE PROTON COMPUTED TOMOGRAPHY WITH VIPMAN PHANTOM: A SIMULATION STUDY

D.Q.Huy[1,2], D.T.Manh[1], T.C.Chao[2], C.C.Lee[2]

[1]Oncology Center, 175 Military Hospital, Ho Chi Minh City, Viet Nam, [2]Department of Medical Imaging and Radiological Sciences, College of Medicine, Chang Gung University, Taiwan. E-mail: huybv175@yahoo.com

Introduction: The proton therapy dramatically is increasing in the world. Because the range proton is a finite in matter, this treatment modality permits a comparable superiority with conventional external beam X-ray therapy. In current clinical particle, proton therapy treatment are made with pre-treatment X-ray the patient's CT scans. To convert the X-ray CT Hounsfield to proton relative stopping powers used a derived calibration function. However, the relationship between Hounsfield units and relative stopping power is not bilinear which be able to lead range uncertainties at planning timely treatment. The Proton Computed Tomography can be directly applied to treatment planning system in order to mitigate a range uncertainty. Objectives: The first, to apply the Discrete Range Modulate (DRM) method that could convert E80(energy 80%) to Water Equivalent Thickness (WET) of various simulated Proton Radiography projections. The second, developing feasibility of both Ray Tracing and Monte Carlo simulation code MCNPX/DRM method, being a simultaneous reconstruction of VIP-Man model. Material and method: Both Ray Tracing which was used to Water Equivalent Ratio (WER) as characteristic material organ in order to replace voxel by voxel of VIP-Man model and MCNPX/DRM method will be approaching similarly to set up experiment geometries. After that collecting Proton Radiography by cone-beam source that rotated VIP-Man phantom from 0 to 180 degree with step angle 4 degree. It means, 45 image projections will be carried out both methods. Finally, (Feldkamp–Davis-Kress) FDK algorithm approaches reconstructed slices of VIP-Man model. Result: Gamma index (GI) was evaluated through the Proton Radiography of Ray Tracing (WER) and MCNPX/DRM method. The pass-rate (GI) = 0.9846 with image projections at 0 degree. X-profile and Y-profile Proton Radiography also were estimated. The reconstructed slices of 45, 90, 180 projections that reconstructed by Ray Tracing method were comparable each other and the cavity hole and bone-jaw also observe clearly in the reconstructed slices, respectively. Finally, the reconstructed slice of Ray Tracing and MCNPX/DRM method with 45 projections which will be comparable with original slice VIP-Man (WER). Conclusion: No difference significant of reconstructed slice between two methods. Developed successfully Ray Tracing (WER) and MCNPX/DRM method to create the reconstructed image of Proton Computed Tomography.

Keywords: The Proton Computed Tomography, VIP-Man Phantom, Ray Tracing, MCNPX

P-253

SMALL FIELD AND SABR AUDITS BY THE AUSTRALIAN CLINICAL DOSIMETRY SERVICE (ACDS)

S Manktelow, M Shaw[1], S Keehan[2], A Alves[3], J Lehmann[4], J Lye[5]

Australian Clinical Dosimetry Service, ARPANSA, Yallambie VIC Australia Sophie.Manktelow@arpansa.gov.au, [1]Australian Clinical Dosimetry Service, ARPANSA, Yallambie VIC Australia RMIT University, Melbourne VIC Australia, Maddison.Shaw@arpansa.gov.au, [2]Australian Clinical Dosimetry Service, ARPANSA, Yallambie VIC Australia, Stephanie.Keehan@arpansa.gov.au, [3]Australian Clinical Dosimetry Service, ARPANSA, Yallambie VIC Australia, Andrew.Alves@arpansa.gov.au, [4]Calvary Mater Hospital, Newcastle NSW Australia RMIT University, Melbourne VIC Australia, Joerg.Lehmann@calvarymater.org.au, [5]Australian Clinical Dosimetry Service, ARPANSA, Yallambie VIC Australia, Jessica.Lye@arpansa.gov.au

Introduction: Stereotactic radiosurgery (SRS) and stereotactic ablative/body radiotherapy (SABR) are complex

techniques in modern radiotherapy, with inherently higher risk to patients than conventional radiotherapy. Integrated within these techniques are the challenges involved with accurate small field dosimetry. A research project to develop small field and SABR dosimetry audits was undertaken by the Australian Clinical Dosimetry Service in order to meet this challenging area of clinical work.

Objectives: To provide information regarding the development of the ACDS small field and SABR field trials. Initial results will be discussed, including a small field chamber intercomparison undertaken at the ACDS.

Materials & Methods: The ACDS included field trials of small fields in the Level Ib audits as of September 2016. Output factors were measured with the PTW 60019 microDiamond and compared to the facility stated output factors. Profile scans and output measurements were taken for the facility defined field sizes in categories Medium (2.0-2.9 cm), Small (1.0-1.9 cm) and Very small (0.4-0.9 cm). The ACDS used SABR principles from existing literature, together with common practice observed in the Australian context, to design a SABR dosimetry audit that would meet the needs of Australian Radiotherapy facilities. An end-to-end dosimetry audit was developed using a customised CIRS® humanoid thorax phantom as shown in Figure 1. The audit planning cases replicate the most common tumour sites treated with SABR: lung, spine and soft tissue. Tumour shaped volumes located inside the phantom were planned by the facility for delivery with modality of choice: 3DCRT, IMRT, VMAT, DCAT, FFF. The audit planning guidelines follow current SABR clinical trials: SAFRON II [1], NIVORAD [2] and RTOG 1112 [3]. The planning cases were designed to ensure compatibility with all TPS/Linac equipment combinations currently used for SABR across Australia. Gafchromic EBT3 film, PTW 60019 microDiamond and various other small field detectors were investigated for use in the Level III audit.

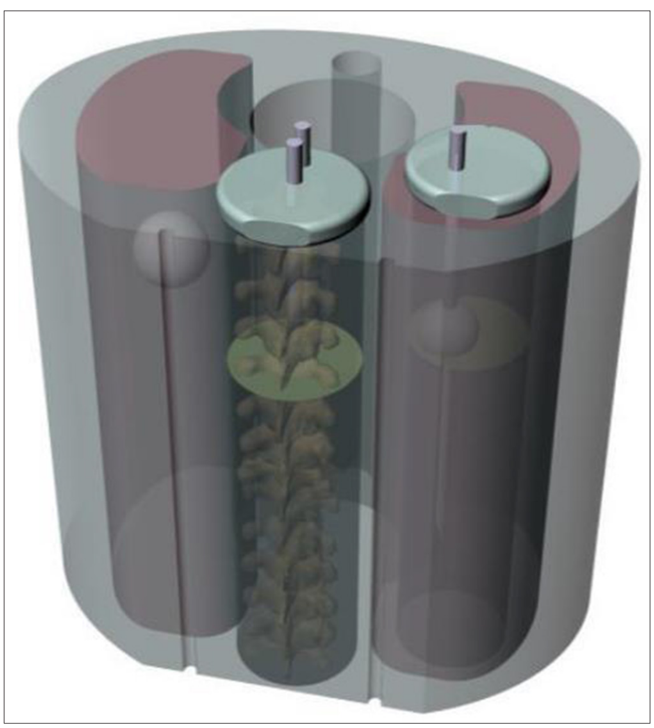

Figure 1: ACDS custom CIRS thorax phantom for SBRT

Results: Initial results for the ACDS Level Ib small field and Level III SABR field trials will be discussed.

Discussion: Small field dosimetry will be incorporated into the existing Level Ib and Level III audits offered by the ACDS. The ACDS is a nation-wide dosimetry auditing service, supporting standardisation of SABR practice across Australia.

References/ Acknowledgements:

1. Trans-Tasman Radiation Oncology Group, Australasian Lung Cancer Trials Group. Amendment 4 (2016). SAFRON II – Stereotactic Ablative Fractionated Radiotherapy versus Radiosurgery for Oligometastatic Neoplasia to the Lung: A Randomised Phase II Trial (TROG 13.01/ ALTG 13.001).
2. NHMRC Clinical Trials Centre, Australasian Lung Cancer Trials Group, Trans-Tasman Radiation Oncology Group. Version 1.1 (2015). NIVORAD – A randomised phase 2 trial of nivolumab and stereotactic ablative body radiotherapy in advanced non-small cell lung cancer, progressing after first or second line chemotherapy (ALTG 14/002/CTC 0135).
3. NRG Oncology, National Clinical Trials Network, National Cancer Institute. RTOG 1112 – Randomized phase III study of sorafenib versus stereotactic body radiation therapy followed by sorafenib in hepatocellular carcinoma.

P-254

IMPROVEMENT OF MEASUREMENT ACCURACY OF LATERAL DOSE PROFILES USING SCINTILLATOR FOR CARBON PENCIL BEAM

Takumi Narusawa[1], Katsunori Yogo[2], Tatsuaki Kanai[3], Akihiko Matsumura[3], Hikaru Souda[3], Yosuke Kano[4], Kohei Kamada[1], Yuya Tatsuno[1], Masami Torikoshi[3], Kazushige Hayakawa[1,5]

[1]Graduate School of Medical Sciences, Kitasato University, [2]Hiroshima High-Precision Radiotherapy Cancer Center, [3]Gunma University Heavy Ion Medical Center, [4]Accelerator Engineering Corporation, [5]School of Medicine, Kitasato University.

Email: mm16032@st.kitasato-u.ac.jp

Introduction: Scanned carbon ion pencil beams, with small fields and sharp penumbras, require accurate dosimetry, with high spatial resolutions, for clinical use. One such use includes lateral dose profiles at low-dose envelopes, which are conventionally measured with ionization chambers. We previously reported the development of an easy-to-use dose measurement tool that employed a ZnS:Ag scintillator and a CCD camera. However, one issue with the tool was the need to improve the signal-to-noise ratio of the lateral brightness profile at low-dose envelopes (down to ~0.01% of the central dose). To overcome this issue, we tested two methods: irradiating the scintillator system beam with a saturated central dose and central masking. We tested the tool's performance for these methods and compared the collected data with data obtained from conventional methods.

Materials and Methods: A sheet of the ZnS:Ag scintillator was placed perpendicular to the beam axis, in a dark box, to eliminate any background light. The water level of the tank above the dark box was remotely controlled to adjust measurement depth. The scintillation light, produced by irradiation with a carbon ion beam, was reflected with a mirror and recorded with a CCD camera. Spatial resolution of this tool was ~0.24 mm. Measurements were performed using 290 MeV/nucleon mono-energetic carbon ion pencil beams at Gunma University's Heavy Ion Medical Center. Reference depth and lateral dose profiles were measured with a plane-parallel ionization chamber (PTW TN34045), a PinPoint chamber (PTW TN31014, ~2 mm diameter), and a p-type silicon diode detector (PTW PR60020, ~1.1 mm diameter). Lateral dose and brightness profiles were measured at the depth of entrance and the Bragg peak with varying beam dose rates. To measure lateral brightness profiles at low-dose envelopes with high signal-to-noise ratios, a metal cylindrical bar (12 mm or 20 mm diameters) supported with an acrylic plate (t = 10 mm) was used as a masking central beam to avoid saturation of brightness.

Results and Discussion: Relative depth dose profiles, measured with the scintillator, were underestimated by approximately 23%, at the Bragg peak, compared with those measured with the chamber. These data indicate that the scintillation light depends on the linear energy transfer (LET) of the beams. The beam spot sizes, determined by the Gaussian fitting at the Bragg peak, were sigma = 2.6 mm for the scintillator, 3.2 mm for the chamber, and 2.6 mm for the diode. Lateral brightness profiles, measured with the scintillator at the peak, generally agreed with those measured with the diode, however, the discrepancy became larger at the low-dose envelope due to data scattering. The signal-to-noise ratios of lateral brightness profiles at low-dose envelopes were improved by irradiating the beam with a saturated dose and with central masking. The lateral brightness profile, created using the beam with a saturated dose, was overestimated by about 3 times at low-dose envelopes, presumably due to scattering of saturated scintillation light. In contrast, the profile created using the beam with central masking showed good agreement with dose profiles measured with the diode. These data suggest that scintillation measurements using the beam with central masking were suitable for the measurement of lateral profiles at low-dose envelopes.

P-255

THE EFFECT OF DIFFERENT IMAGING RECONSTRUCTION METHODS IN ACCURACY OF QUANTITATIVE PARAMETERS AT 4DMSPECT, QGS AND ECTB SOFTWARE

Habibeh Vosoughi[1,2], Farshad Emami[1], Farzad Dehghani Sani[1]

[1]Nuclear Medicine Department, Research and Education Department, Razavi Hospital, Mashhad, Iran, [2]Medical Physics Department, Faculty of Medicine, Mashhad University of Medical Sciences, Mashhad, Iran.
E-mail: vosoughih941@mums.ac.ir

Introduction: Quantitative factors like LVEF, ESV, EDV plays a great role in decision making in era of myocardial perfusion gated SPECT. Evaluating the accuracy of these factors, which are influenced by reconstruction parameters, are of upmost importance.

Materials and Methods: Using a dynamic heart phantom filled with 185 MBq of 99mTc-Pertechnatate capable of producing different ejection fractions, SPECT images were obtained with EF values of 45% to 70% in 5% intervals. Images were reconstructed with OSEM (with flash3d) with 28 different combinations of iterations (I) (2, 4, 6, 8, 10, 12, 16) and subsets (S) (2, 4, 8, 16). Mean difference of calculated LVEF with actual EF for each reconstruction and for each quantitative software packages (4DMSPECT, QGS, ECTB) were calculated. Using Kruskal-Wallis test performance of each software package was compared.

Results: Best combination for 4DMSPECT with 0%±1% was 4Ix4S. When subset was 2 increasing iterations from 6 to 16 also difference was not high. In QGS 2 combinations of 2Ix4S and 4Ix2S with mean difference of 0%±1% were the best combinations. Other reconstruction combinations made large difference between phantom and calculated EFs. Using I=2 in ECTB made a small mean difference but with a considerable standard deviation for subsets of 4-16 and by increasing the number of iterations mean difference was also increased. Generally in most combinations QGS and ECTB underestimate LVEF.

Conclusion: 4DMSPECT made the most realistic EF value in comparison with the QGS and ECTB. The best reconstruction combination in the current study was 4Ix4S while in the other studies which were used in patients not by phantom 2Ix12S and 2Ix10S were best combinations. Concordantly for evaluation of BMI on reconstruction parameters 4Ix4S was the best combination for all BMI values.

Keywords: Iterative reconstruction, OSEM, Flash3D, Dynamic heart phantom, 4DMSPECT, QGS, ECTB

P-256

DEVELOPMENT OF INDIGENOUS 2D AND 3D GAMMA EVALUATION SOFTWARE TOOL FOR IMRT PATIENT SPECIFIC QA

Abhilasha Saini, Reena Sharma[1], Gaganpreet Singh, Arun S. Oinam[1]

Panjab University and [1]Post Graduate Institute of Medical Education and Research Chandigarh, India.
E-mail: abhilashasaini1992@gmail.com

Introduction: With the wide clinical implementation of intensity- modulated radiation therapy, software tools for quantitative dose (or fluence) distribution comparison are required for patient-specific quality assurance. The technique known as the 'Gamma evaluation method' is the most widely used and incorporates pass–fail criteria for both distance-to-agreement and dose difference analysis of dose distributions and provides a numerical index (*Gamma*) as a measure of the agreement between two datasets.

Objective: Based on the concept of Low et al. a MATLAB based indigenous software tool for patient specific IMRT QA using 2D and 3D Gamma evaluation method is developed. Results of 2D Gamma are compared with commercially available software (OmniPro I'mRT). The program is a preliminary approach for 3D Gamma Index evaluation. Further, the developed software tool uses search distance that efficiently reduces the computation time. The effect of noise is studied by implementing different signal thresholds.

Materials and Method: Eclipse planning system (version 11.0.3) was used to make IMRT plans and corresponding verification plans. 40 IMRT cases, 10 of each site (Head & Neck, Esophagus, Prostate, Cervix & Vault) with segmental MLC delivery technique were selected. Ion MatriXX was used to give measured distribution in 2D. The dataset1 was picked from the TPS (termed as evaluation distribution) and the dose matrix from the IBA Omnipro software was used as dataset 2 (measured distribution). These datasets were compared in terms of Gamma Index using OmniPro I'mRT software and In-house developed software tool such that each measured point is evaluated to determine if both the dose difference and DTA exceed the selected tolerances (e.g., 3% and 3 mm, respectively). Points that fail both criteria are identified on a composite distribution. For testing of 3D Gamma Evaluation tool, a hypothetical 3D dose matrix is created by adding an intentional error of 1mm in the 3D dose matrix to be evaluated. Gamma Index for the resultant dose cubes is calculated. Plans were also evaluated with Incremental error of 1-4mm to verify if the index falls. Gamma Index of 14 cases was studied without and with 20% signal threshold.

Results and Discussion: The developed 2D Gamma evaluation tool shows good agreement between measured and calculated fluences (dose planes). Mean of differences of 2D Gamma Index between commercially used OmniPro I'mRT software and In-house developed software for all sites is found to be within 1%. 3D Gamma Index for all cases is above 97%. The mean increment in Gamma Index with 20% threshold with respect to no threshold is (2.637±2.615) %. Due to lack of information of signal thresholding, it is difficult to choose best thresholding value. In this study we choose 20% signal thresholding with shows better consistency with the commercial tool.

P-257

PROCESS OF STEREOTACTIC BODY RADIATION THERAPY FOR LIVER CANCER AT HUE CENTRAL HOSPITAL

Le Trong Hung, Pham Nhu Hiep[1], Pham Nguyen Tuong[2], Phan Canh Duy[2], Nguyen Van Thanh, Nguyen Huu Minh Tuan

Medical Physicist, Hue Central Hospital, Vietnam, [1]Surgeon, Director of Oncology Center, Director of Hue Central Hospital, Vietnam, [2]Radiation Oncologist, Hue Central Hospital, Vietnam.
E-mail: hunghue73@gmail.com

Introduction: Stereotactic body radiation therapy (SBRT) for liver is a radiotherapy technique, which uses several fractions with high dose of radiation for liver tumors with proper volumes and sites. Oncology center of Hue central hospital is the pioneer in Vietnam applying successfully Linac-based SBRT with imaging guide radiotherapy (IGRT). The aim of this study is to survey and assess treatment planning quality of SBRT for hepatocellular carcinoma (HCC).

Materials and Methods: There were 15 HCC patients underwent SBRT technique at Oncology center - Hue central hospital from August 2015 to August 2016. We applied volumetric arc therapy technique (VMAT) with 5 fractions (prescribed doses depended on sites and size of tumors). Radiation treatment was given on LINAC of Elekta AXESSE, planned by Monaco 5.11 version, IGRT by daily conebeam CT/XVI device and assured quality by Verisoft software, 1500 detectors, OCTAVIUS 4D/PTW system. CT Similation 4D of PHILIPS with breathing compressor, Orfit immobilization devices.

Results and Discussion: Mean age was 50 (32-78). All patient was Child-Pugh A classification, the average tumor size was 4.5cm. Prescribed doses ranged from 27.5Gy to 50.0Gy (depended on sites and size of tumors). Requiring percentages of planning target volume were not lower than 95%, maximum hotspots were 150% of prescribing dose. Normal tissues and remnant liver tissues were in allowed limits.

Conclusion: SBRT technique requires high accuracy and synchronous facilities. SBRT entails precise delivery of high-dose in few fractions, with tumor ablation and maximal normal-tissue sparing. SBRT is a non-invasive, well-tolerated and effective treatment for HCC patients not suitable to others local ablation treatment. SBRT is as an alternative ablation treatment of HCC with promising results. It may concern using SBRT for oligometastatic patients. Prospective randomized clinical trials are required to confirm clinical evidence and long term results.


Reject
Accept

International Advisory Committee

Dr. Agnetta Peralta, Philippines
Dr. Alan Nahum, UK
Dr. Ali Binesh, Iran
Dr. Anchali Krisanachinda, Thailand
Dr. Bhudatt R Paliwal, USA
Dr. Brendan Healy, Australia
Dr. Chaurasia P.P, Nepal
Dr. David W Townsend, Singapore
Dr. Donald McLean, Australia
Dr. Franco Milano, Italy
Dr. G. Ramanathan, Australia
Dr. Geoffrey Ibbott, USA
Dr. Harrie Mol, Belgium
Dr. Ho-Ling Anthony Liu, Taiwan
Dr. James Lee, Singapore
Dr. Jenia Vassileva, Austria
Dr. John Damilakis, Greece
Dr. Joshi CP, Canada
Dr. Kehwar T, USA
Dr. Kiyonari Inamura, Japan
Dr. L S Arun Kumar, Oman
Dr. M. M. Rehani, USA
Dr. Maria Brandan, Mexico
Dr. Mohammad Toosi, Iran
Dr. Mustafa Majali, Jordan
Dr. Napapong Pongnapang, Thailand
Dr. Pirunthavany Muthuvelu, Malaysia
Dr. R. Rangacharyulu, Canada
Dr. S Fukuda, Japan
Dr. M. Saiful Huq, USA
Dr. Satish Jaywant, USA
Dr. Simone K Renha, Brazil
Dr. Stelios Christofides, Cyprus
Dr. Virendra Patel, Australia
Dr. Wamied Abdel-Rahman, Dammam
Dr. William Rae, South Africa
Dr. Yakov Pipman, USA
Dr. Youngyih Han, South Korea
Dr. Akbar Gharbali, Iran
Dr. Alejandro Mazal, France
Dr. Ali Mehdipour, Iran
Dr. Belal Moftah, Saudi Arabia
Dr. Bilal Jalal, Saudi Arabia
Dr. Carmel J Caruana, Malta
Dr. Colin Orton, USA
Dr. Dario Sanz, Argentina
Dr. Ferid Shannoun, Austria
Dr. Fujio Araki, Japan
Dr. Gavin Cranmer Sargison, Canada
Dr. Habib Zaidi, Switzerland
Dr. Hafiz M Zin, Malaysia
Dr. Hema Vaithianathan, Australia
Dr. Ibrahim Duhaini, Lebanon
Dr. Jeffrey F. Williamson, USA
Dr. Jeong Woo Lee, South Korea
Dr. John Drew, Australia
Dr. K Y Cheung, Hong Kong
Dr. Kitagawa A, Japan
Dr. Kwan Hoong Ng, Malaysia
Dr. Lakshmi Santhanam USA
Dr. Magdalena Stoeva, Bulgaria
Dr. Masahiro Endo, Japan
Dr. Mosa Matsumoto, Japan
Dr. Nand K Relan, USA
Dr. Nasaa Nagi, Iraq
Dr. Pradip Deb, Australia
Dr. Raymond K Wu, USA
Dr. S Sivanesan, Singapore
Dr. Salahuddin Ahmad, USA
Dr. Shinichi Wada, Japan
Dr. Slavik Tabakov, UK
Dr. Tae Suk Suh, South Korea
Dr. Virginia Tsapaki, Greece
Dr. Wilbroad E Muhogora, Tanzania
Dr. Xiance Jin, China
Dr. Yimin Hu, Republic of China
Dr. Yuri Dekhtyar, Latvia

National Advisory Committee

Dr. A K Bansal, Delhi
Mr. A M Pendse, Mumbai
Dr. Abhijit Mandal, Varanasi
Mr. Agarwal S P, Mumbai
Dr. Ajay Shrivastava, New Delhi
Dr. AnujTyagi, Agra
Dr. Apurba Kabasi, Kolkata
Dr. Arun S Oinam, Chandigarh
Dr. Atul Tyagi, New Delhi
Mr. Balasubramanian N, Rohtak
Dr. B S Rao, Mumbai
Dr. Baskaran Pillai, Kochi
Dr. C S Sureka, Coimbatore
Mr. Choubey Vijay, Nagpur
Dr. D Dutta, Mumbai
Dr. Dash Sharma P K, Mumbai
Dr. D Deshpande, Mumbai
Dr. G Sahani, Mumbai
Dr. Ganesan S, Chennai
Dr. Gopi Shankar N,New Delhi
Dr. Govindarajan K N, Coimbatore
Dr. Hota P K, Odisha
Mr. Jibon Sharma, Guwahati
Dr. K Krishna Murthy, Hyderabad
Dr. K Muthuvelu, Chennai
Dr. Kaliappan P, Chennai
Dr. Kamlesh Passi, Ludhiana
Mr. Karthikeyan S, Bangalore
Dr. Lakshmanan A V, Chennai
Dr. M S Kulkarni, Mumbai
Dr. Madhu Bala,New Delhi
Dr. Manoj Semwal, Delhi
Dr. Maria Das, Lucknow
Mr. M P Singh Mann, New Delhi
Mr. Munjal R K, New Delhi
Dr. Muralidhar K R, Hyderabad
Dr. Negi P S, Delhi
Dr. Nirmal Kumar Penuley, Lucknow
Dr. Om Prakash Gurjar, Indore
Dr. Palani Selvam, Mumbai
Dr. Paneer Selvam S, Chennai
Dr. PankajTandon, Mumbai
Dr. Paul B Ravindran, Vellore
Dr. Pradhan A S, Mumbai
Mr. Poopathi V, Kolkatta
Dr. R N L Srivastava, Kanpur
Dr. Rabi Raja Singh , Vellore
Dr. Radhakrishnan B Nair, Pathanamthitta
Dr. Raghavendra Holla, Kochin
Dr. Raghukumar P, Trivandrum
Mr. Ritu Raj Upreti, Mumbai
Dr. Rajesh Kumar, Mumbai
Dr. Ramakrishna Rao C, Hyderabad
Dr. Rath A K, Bhubaneshwar
Dr. Ravi Kumar M, Bangalore
Dr. Ravichandran R, Bangalore
Dr. S H Panwar, Kolhapur
Dr. S J Supe, Mumbai
Mr. S.N. Sinha, Mathura
Dr. S P Mishra, Lucknow
Dr. Sai Subramanian, Hyderabad
Dr. Saji Oommen, New Delhi
Dr. Saju Bhasi, Trivandrum
Dr. Saraswathi Chitra, Chennai
Dr. Sathish Pelgade, Ahmedabad
Dr. Satish Rao, Manipal
Dr. Senthil Kumar S, Madurai
Mr. Sharma P K, Delhi
Dr. Shukla A K, Lucknow
Mr. Subhash Kheruka,Lucknow
Mr. Suresh Pangam, Hyderabad
Dr. T Ganesh, New Delhi
Dr. Thayal Singh Elias, Trivandrum
Dr. Thayalan K, Chennai
Dr. Varadarajan E, Chennai
Dr. Varatharaj C, Bangalore
Mr. V Satyanarayan, Pune
Dr. Velmurugan J, Chennai
Dr. Vinod Kumar Dangwal, Patiala
Mr. Vinod Pandey, Haldwani

Registered with Registrar of Newspapers in India
Vide RNI No. MAHENG/2012/44833, Rs 20 for AMPI Members

AOCMP - AMPICON 2017
Jaipur, India

Editor Dr. A. S. Pradhan. Printed and published by Wolters Kluwer India Private Limited on behalf of Association of Medical Physicists of India, Mumbai and printed at Dhote Offset Technokrafts Pvt. Ltd., Jogeshwari (E), Mumbai - 400 060, India, and published at A-202, 2nd Floor, The Qube, C.T.S. No.1498A/2 Village Marol, Andheri, Mumbai, India